15th Central European Symposium on Pharmaceutical Technology

»Where the Future Challenges in Pharmaceutical Technology Meet 30+ Years of Experience«

Book of Abstracts

25th-27th September 2025, Bled, Slovenia

UNIVERSITY OF LJUBLJANA | FFA Faculty of Pharmacy

SLOVENSKO FARMACEVTSKO DRUŠTVO
SLOVENIAN PHARMACEUTICAL SOCIETY

Impressum

The 15th Central European Symposium on Pharmaceutical Technology

Where the Future Challenges in Pharmaceutical Technology Meet 30+ Years of Experience: Book of Abstracts

Editors: Mirjana Gašperlin, Rok Dreu, Alenka Zvonar Pobirk, Barbara Sterle Zorec

Reviewers: Zrinka Abramović, Petra Kocbek et al.

Authors: Peter Kleinebudde, Adam Haimhoffer, Maja Kus et al.

Prepress design: Barbara Sterle Zorec, Alenka Zvonar Pobirk, Anže Zidar

Design: Sebastjan Jenko

Cover photo: Lake Bled (Aleš Krivec, www.bled.si)

Publisher: Slovensko farmacevtsko društvo in Univerza v Ljubljani, Fakulteta za farmacijo

URL address: The book of abstracts will be pdf format, available at:
https://www.sfd.si/cespt2025/programme/scientific-programme/

Ljubljana, 2025

Kataložni zapis o publikaciji (CIP) pripravili v Narodni in univerzitetni knjižnici v Ljubljani
COBISS.SI-ID **249007107**
ISBN 978-961-97122-0-7 (Slovensko farmacevtsko društvo, PDF)

Welcome letter

Dear Colleagues,

The 15th Central European Symposium on Pharmaceutical Technology (CESPT) returns to its original venue, Bled, Slovenia, where the symposium was first established in October 1995 under the patronage of EUFEPS. Since that time, CESPT has been successfully hosted in a number of cities across Europe, including Portorož (Slovenia, three times), Vienna and Graz (Austria), Ljubljana (Slovenia, twice), Siófok and Szeged (Hungary), Dubrovnik (Croatia), Belgrade (Serbia), Gdańsk (Poland), and Ohrid (North Macedonia).

This year's symposium carries special significance as we celebrate the 30th anniversary, so *t*he title *"Where the Future Challenges in Pharmaceutical Technology Meet 30+ Years of Experience,"* reflects both our tradition and our forward-looking perspective. The program will address five major thematic areas:

- Pharmaceutical Manufacturing and Engineering
- Delivery of Biopharmaceutics and Nanomedicine
- Strategies for Optimizing Pharmacotherapy: Addressing Clinical Outcomes and Patient-Friendly Drug Delivery
- Current Trends in Pharmaceutical Analytics
- Biorelevant Methods of Assessment

Across these areas, key topics include the evolving landscape of drug manufacturing such as continuous manufacturing, 3D printing, process intensification and automation — the design and delivery of advanced biopharmaceuticals, including peptides, proteins, and nucleic acid-based therapeutics as well as innovative delivery systems, such as nanoparticulate carriers. Further focus will be placed on bridging science with clinical practice, exploring strategies to enhance outcomes while supporting patient adherence and quality of life. The final section highlights innovations in analytical sciences, focusing on biorelevant dissolution testing and bio-predictive testing.

The scientific program comprises 5 plenary lectures, 10 invited lectures, 21 oral presentations, and over 120 poster presentations, providing a comprehensive overview of today's pharmaceutical challenges and opportunities. With more than 250 participants from 20 countries, CESPT 2025 promises to be an inspiring international forum for scientific exchange, collaboration, and innovation.

We extend our sincere thanks to all sponsoring and supporting organizations and societies whose contributions have strengthened the visibility of this symposium within the international scientific community.

We look forward to welcoming you to Bled, 25–27 September 2025.

Prof. dr. Mirjana Gašperlin
President of the symposium

Prof. dr. Rok Dreu
Co-president of the symposium

OUR KNOWLEDGE FOR **YOUR HEALTH**.

We contribute to effective treatment through our research and development, innovative procedures and state-of-the-art products.

- 10% of total sales revenues invested in research and development
- Advanced pharmaceutical dosage forms and technologies
- Patent-protected innovations

KRKA

Living a healthy life.

www.krka.biz

SARTORIUS

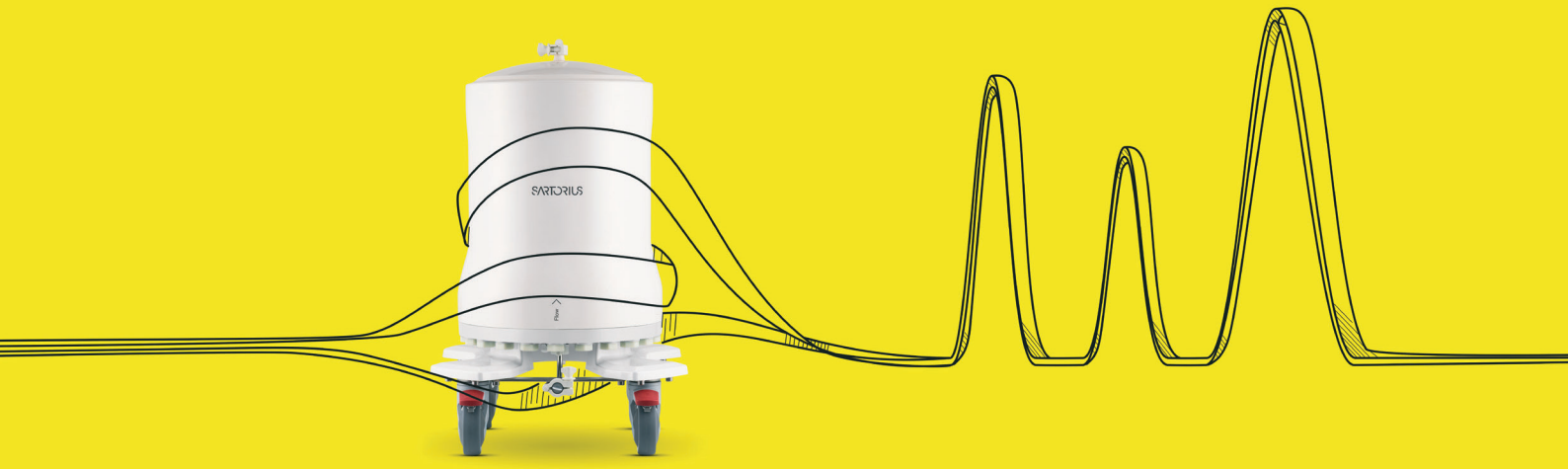

Sartorius BIA Separations

Monolithic chromatography columns and bioprocessing solutions for production, purification and analysis of large biomolecules for gene therapy and vaccines.

www.biaseparations.com

Strategic Location:

Slovenia, offers stunning landscapes and prime location for biotech business. Slovenia combines a rich tradition in pharmacy with cutting-edge innovations, making it an ideal location for biopharma partnerships.

Biopharmaceutical Excellence:

Sartorius BIA Separations leads in the next-gen biopharmaceutical processes, collaborating with business partners from the USA (80%) and abroad, such as AstraZeneca, Arcturus, Sanofi, BioNet Asia, Avexis/Novartis and many more.

Innovative Campus:

The campus features state-of-the-art facilities and highly skilled workforce with close to 30 years' experience in gene therapy processes and products development to meet biopharma manufacturing needs.

Advanced Therapies:

At Sartorius BIA Separations we are strong in the field of mRNA vaccines, LNP formulation, gene therapy, CAR-T, bacteriophages, human plasma fractionation and more, driving the present and the future of medicine. Our products and expertise were utilized in the development and manufacture of gene therapy product Zolgensma and many others—some not disclosed and many still in trials.

Partner organisations

EUFEPS European Federation for Pharmaceutical Sciences

APV MAKING SCIENCE WORK

hfd 1858 HRVATSKO FARMACEUTSKO DRUŠTVO CROATIAN PHARMACEUTICAL SOCIETY

Magyar Gyógyszerésztudományi Társaság Budapest, Alapítva: 1924

MPA IMFD

POLSKIE TOWARZYSTWO FARMACEUTYCZNE

SFUS Savez farmaceutskih udruženja Srbije

SITELF Società Italiana di Tecnologia e Legislazione Farmaceutiche

(Photo: Jošt Gantar, www.bled.si)

CONTENT

(Photo: Jošt Gantar, www.bled.si)

COMMITTEES

Honorary Committee
- Dominique Duchêne, France
- Atilla Hincal, Turkey
- Franc Kozjek, Slovenia
- Julijana Kristl, Slovenia
- Aleš Mrhar, Slovenia (president)
- Fulvio Rubessa, Italy
- Stanko Srčič, Slovenia
- Jelka Šmid Korbar, Slovenia

International Scientific committee
- Zrinka Abramovič, Slovenia
- Ildikó Bácskay, Hungary
- Carla Caddeo, Italy
- Ildikó Csóka, Hungary
- Jelena Filipović-Grčić, Croatia
- Nikola Geskovski, N. Macedonia
- Svetlana Ibrić, Serbia
- Albin Kristl, Slovenia
- Jasmina Lovrić, Croatia
- Janina Lulek, Poland
- Jelena Parojčić, Serbia
- Luka Peternel, Slovenia
- Beatrice Perissutti, Italy
- Eva Roblegg, Austria
- Maja Simonoska Crcarevska, N. Macedonia
- Malgorzata Sznitowska, Poland
- Zvone Simončič, Slovenia
- Edina Vranić, Bosnia and Hercegovina

Organizing Committee
- Katarina Bolko Seljak
- Miha Homar
- Mojca Kerec Kos
- Petra Kocbek
- Peter Molek
- Odon Planinšek
- Barbara Sterle Zorec
- Jurij Trontelj
- Natalija Škrbina Zajc
- Tomaž Vovk
- Anže Zidar

President of the Symposium
Mirjana Gašperlin

Co-President of the Symposium
Rok Dreu

General Secretary of the Symposium
Alenka Zvonar Pobirk

Secretary of the Symposium
Andrijana Tivadar

(Photo on the right: Statue of the Genius (sculptured by Dane Zajc, 1935) located above the entrance to the University of Ljubljana Faculty of Pharmacy)

The 1st CESPT Symposium took place in October 1995 in Bled, Slovenia, under the patronage of EUFEPS. Since then, the event has been successfully organized in several locations across different countries, including Portorož (Slovenia, twice), Vienna and Graz (Austria), Ljubljana (Slovenia), Siofok and Szeged (Hungary), Dubrovnik (Croatia), Belgrade (Serbia), Gdansk (Poland), and Ohrid (North Macedonia). After 30 years, 15th CEPST Symposium is returning to its original venue – Bled. Over the past three decades, CESPT has been recognized as a well-established platform for promotion of new scientific, professional and business collaborations. Today it is a renowned international event regularly attracting more than 200 experts from industry, academia and regulatory authorities worldwide and in particular from Central and Eastern Europe.

GENERAL INFORMATION

CONFERENCE VENUE: Rikli Balance Hotel, Cankarjeva cesta 4, SI–4260 Bled.
The ARNOLD congress center, in the ground floor.

PRE-EVENT WORKSHOP VENUE: University of Ljubljana, Faculty of Pharmacy,
Aškerčeva cesta 7, SI–1000 Ljubljana
Meeting point in the faculty lobby.

THE EXHIBITION is located in SONCE – ZRAK congress center in the ground floor of Rikli Balance Hotel.

REGISTRATION AND INFORMATION is located in SONCE – ZRAK congress center in the ground floor of Rikli Balance Hotel.
Opening hours:
Thursday, September 25, 12.00–18.30
Friday, September 26, 8.00–18.30
Saturday, September 27, 8.00–13.30

BADGES
Each participant will receive a badge. All participants are required to carry the badges during the conference and social events.

FOOD AND DRINKS
Coffee breaks (coffee, tea and water & sweet and fruit snacks) will be served in the SONCE – ZRAK congress center during breaks.
On Friday lunch will be served during lunch break in the dining hall of the Rikli Balance Hotel (included in the registration fee for participants).

INTERNET
A wireless internet connection is provided free of charge.

(Photo: Faculty of Pharmacy, University of Ljubljana (left), and Arnold Hall, Rikli Balance Hotel Bled (right))

KEY INFORMATION – SCIENTIFIC PRESENTATIONS

If you are **a session chairperson**, you are kindly asked to arrive at the ARNOLD lecture hall at least 15 minutes before the start of the session to meet with the speakers.
There are three types of lectures at the 15th CESPT:
- plenary lectures – 40 minute and 5 minutes for discussion,
- invited lectures – 25 minutes and 5 minutes for discussion,
- oral presentations – 10 minutes and 5 minutes for discussion.

The chairs are kindly requested to **adhere strictly to the scheduled times of sessions**.

As a speaker, you are kindly asked to arrive in the ARNOLD lecture hall at least 15 minutes prior to the start of the session to meet with the chairpersons and the technician in charge of projection.
The standard format for presentations is MS-PowerPoint. Please use the "embedded fonts" to avoid certain problems when projecting files prepared on a different computer. For all other types of video presentations, a laptop of the speaker must be used.
Authors may keep their presentation on a USB flash drive. Files must be uploaded to the central computer in the ARNOLD lecture hall before the session begins. It is recommended that the presentation be uploaded before 8.45 a.m. for the morning sessions and during the lunch break for the afternoon sessions. Preview of presentations is available during breaks in the ARNOLD lecture hall.

If you are **a poster presenter**, please refer to the poster list at the website **https://www.sfd.si/cespt2025/programme/poster-session/** for the number. Authors are asked to hang their posters on the display boards on Thursday and remove them at the end of the Saturday session. Some mounting materials are available at the information desk.
Posters will be on display throughout the 15th CESPT Symposium.
The main poster session is scheduled for: Friday, September 26, 2025.

SOCIAL PROGRAM

All social events are included in the symposium fee. All participants will be asked to present their conference badge and admission ticket before being admitted.

Welcome Reception

Date: Thursday, September 25, 2025
Time: 19.00
Venue: Rikli Balance Hotel Lobby
You will enjoy meeting colleagues and friends in the unique atmosphere of the lake Bled.

Conference Dinner

Date: Friday, September 26, 2025
Time: 19.30
Venue: Grand Hotel Toplice, Cesta svobode 12, Bled
Program: Dinner and Musical entertaining program

HARKE
Academy

Technological Expertise
Always Available for You

HARKE Pharma stands for more than 40 years of expertise in supporting the **development and optimization** of innovative pharmaceutical and nutraceutical dosage forms, offering a broad range of excipients.

With offices across many European countries and in India, we serve the industry locally and keep expanding our **international presence.**

Technology is in our DNA.
Get a glimpse on our services and learn about functionalities of excipients and their influence on different formulations in our **HARKE Academy:**

www.harke.com/academy

HARKE Pharma GmbH
Business Unit Pharma
Xantener Straße 1
45479 Mülheim an der Ruhr
Germany

+49 (0)208 3069-0
pharma@harke.com
www.harke.com

HARKE GROUP

Our purpose is to reimagine medicine **to improve and extend people's lives.**

We use innovative science and technology to address some of society's most challenging healthcare issues.

Fostering a culture of being inspired, curious, unbossed, and guided by integrity is essential to driving our strategy and fueling innovation.

This foundation empowers us to develop breakthrough treatments and transform the future of healthcare.

NOVARTIS | Reimagining Medicine

SCIENTIFIC PROGRAMME

15th Central European Symposium on Pharmaceutical Technology

Program with topics presented at the Symposium

September 24–25, 2025		
Pre-Event: CEEPUS Workshop for PhD Students: Introduction to Electrospinning University of Ljubljana, Faculty of Pharmacy, Ljubljana and Rikli Balance Hotel, Bled		

	September 25, 2025	
Afternoon sessions	Opening of the 15th CESPT	14.00 – 14.30
	Session title: **Pharmaceutical Manufacturing & Engineering**	
	Plenary lecture: **Some learnings about roll compaction** (Peter Kleinebudde)	14.30 – 15.15
	Invited lectures	16.15 – 16.45
	Coffee break	16.10 – 16.45
	Invited lectures & oral presentations	16.45 – 18.45
	Welcome reception	19.00
	September 26, 2025	
Morning sessions	Session title: **Delivery of Biopharmaceutics**	
	Plenary lecture: **Understanding the formulation challenges of protein drugs** (Wolfgang Frieß)	9.00 – 9.45
	Invited lectures & oral presentations	9.45 – 11.00
	Coffee break	11.00 – 11.30
	Session title: **Nanomedicine**	
	Plenary lecture: **Nanomedicine for the treatment of childhood cancer** (María Blanco-Prieto)	11.30 – 12.15
	Invited lectures & oral presentations	12.15 – 13.45
	Luncheon & Poster session	13.45 – 15.15
Afternoon sessions	Session title: **Strategies for Optimizing Pharmacotherapy Addressing Clinical Outcomes and Patient Friendly Drug Delivery**	
	Plenary lecture: **Patient-centric drug product development acceptability across patient populations - Science and evidence** (Jörg Breitkreutz)	15.15 – 16.00
	Invited lectures & oral presentations	16.00 – 17.00
	Coffee break	17.00 – 17.30
	Invited lectures & oral presentations	17.00 – 18.30
	Conference dinner	19.30

September 27, 2025		
Morning sessions	Session title: **Strategies for Optimizing Pharmacotherapy Addressing Clinical Outcomes and Patient Friendly Drug Delivery (cont.)**	
	Invited lectures & oral presentations	9.00 – 10.30
	Coffee break	10.30 – 11.15
	Session title: **Current Trends in Pharmaceutical Analytics and Biorelevant Methods of Assessment**	
	Plenary lecture: **Personalized Biorelevant Dissolution Testing: Addressing the Impact of Population & Disease Variability on Oral Drug Performance** (Grzegorz Garbacz)	11.15 – 12.00
	Invited lectures & oral presentations	12.00 – 13.30
	Closing of the Symposium	13.30

Conference floor plan

Exhibitors

1. Krka
2. Asahi KASEI
3. MICRO+POLO
4. Anton Paar
5. Lek
6. LabTim
7. Analysis Adria
8. RED EYE MONKEY
9. AstrinexLab
10. Hamilton
11. ABL&E-JASCO
12. Mettler Toledo
13. Novartis
14. Harke Pharma

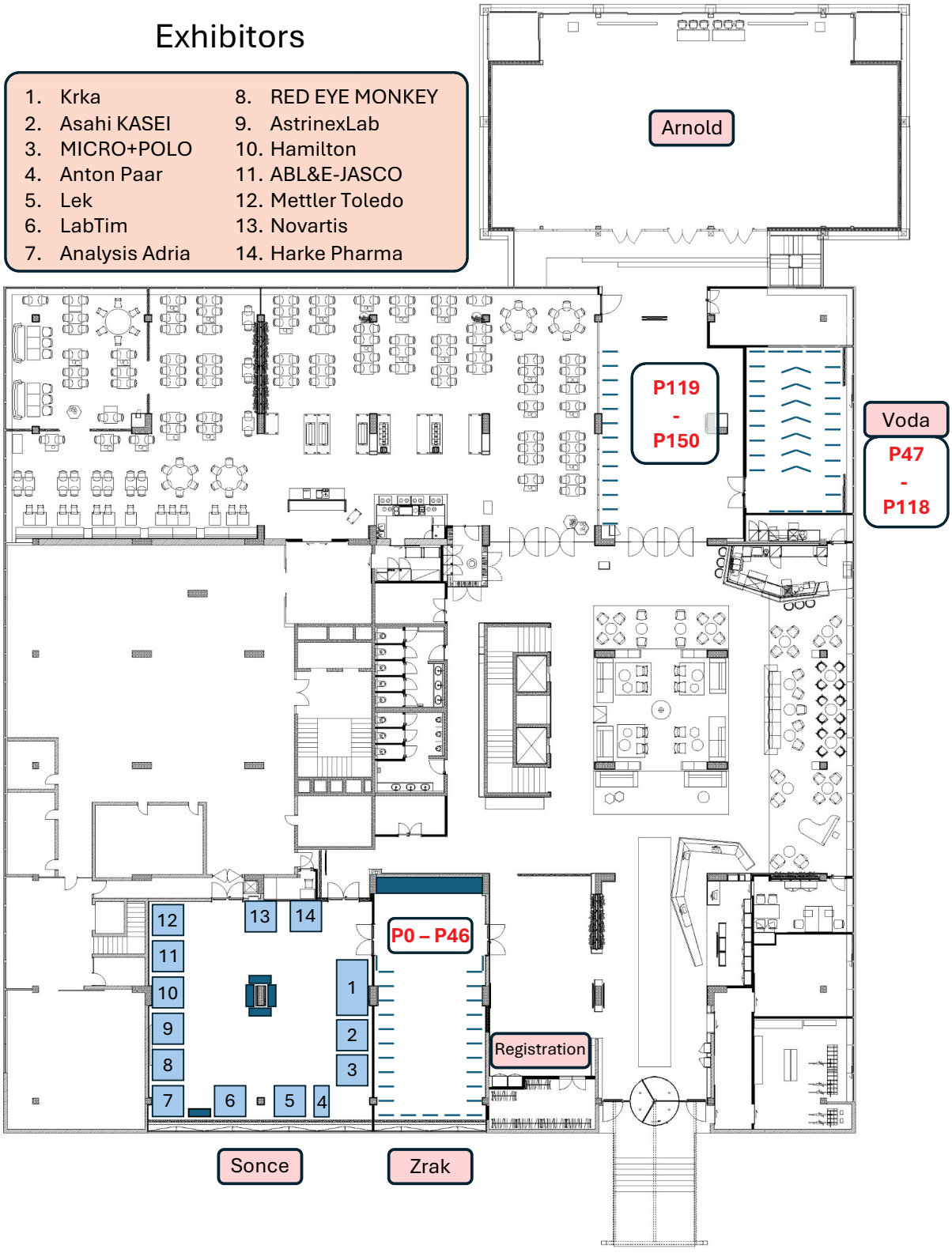

CEEPUS Workshop for PhD Students

September 24–28, 2025

Wednesday, September 24, 2025 (University of Ljubljana, Faculty of Pharmacy)	
16:00 – 17.00	**Registration for the CEEPUS Workshop**
17:00 – 17.30	Welcome and Introduction to workshop
17:30 – 18.15	Karin Kogermann, University of Tartu, Estonia *Nanofibers in Biomedicine with a Focus on Tissue Regeneration and Drug Delivery*
18:15 – 19.00	Špela Zupančič, University of Ljubljana, Slovenia *Nanofibers with Probiotics*
19.00	Participant gathering and networking
Thursday, September 25, 2025 (University of Ljubljana, Faculty of Pharmacy)	
9:00 – 12.00	Practical part of the workshop, including • Demonstration of nanofiber electrospinning using different devices • Presentation of how selected parameters affect the process • Introduction to basic methods for characterizing the prepared samples
	Organised transport to Bled and participation in the 15th CESPT

15th Central European Symposium on Pharmaceutical Technology

Where the Future Challenges in Pharmaceutical Technology Meet 30+ Years of Experience

Detailed Programme

Thursday, September 25, 2025 (Rikli Balance Hotel, Bled)	
12.00 – 18.00	**15th CESPT Registration**
14:00 – 14.30	**Opening ceremony** **Chairpersons:** Mirjana Gašperlin, Rok Dreu
	Aleš Mrhar, 30 years of CESPT Symposium (Opening lecture)
	Section 1 – Pharmaceutical Manufacturing & Engineering Chairpersons: Rok Dreu, Jelena Parojčić
14:30 –15:15	**[PL]** Peter Kleinebudde, Heinrich Heine University Düsseldorf, Germany *Some learnings about roll compaction*
15:15 – 15:45	**[IL]** Adam Haimhoffer, University of Debrecen, Hungary *Development of hormone-containing vaginal film and applicator using QbD approach*
15.45 – 16.15	**[IL]** Maja Kus, Novartis d.o.o., Slovenia *Innovation in Pharma: Development and Implementation of Continuous Manufacturing for Commercial Production*
16.15 – 16.45	Coffee break

Plenary lecture (PL), Invited lectures (IL), Oral Presentations (OP), Poster Presentations (PP)

	Section 1 – Pharmaceutical Manufacturing & Engineering (cont.) Chairpersons: Peter Kleinebudde, Malgorzata Sznitowska
16.45 – 17.15	**[IL]** Klemen Korasa, Krka d.d., Novo Mesto, Slovenia *Process Analytical Technology: Cases and Insights from the Pharmaceutical Industry*
17.15 – 17.30	**[OP]** Teodora Tasevska, Ss. Cyril & Methodius University in Skopje, R North Macedonia *Predicting 3D printability of semi-solid extrusion formulations using rheological data and machine learning models*
17.30 – 17.45	**[OP]** Paola Šurina, Research Center Pharmaceutical Engineering & Graz University, Austria *From Powder to a Personalized Tablet: Optimizing Direct Powder Extrusion 3D Printing for Tablet Manufacturing*
17.45 – 18.00	**[OP]** Magdalena Urbanowicz, National medicine institute, Warsaw, Poland *Pre-formulation studies of SLS 3D printed tablets*
18.00 – 18.15	**[OP]** Hadi Shammout, University of Szeged, Hungary *Laser marking of tablets for anti-counterfeiting and its effect on coating integrity*
18:15– 18.30	**[OP]** Lukas Vergeiner, University of Graz, Austria *Dehydration and Purification of Microparticle Suspensions via Vibro® TFF*
18.30 - 18.45	**[OP]** Karoliina Inno, University of Tartu, Estonia *The effect of tablet design and excipients on drug release from 3D printed tablets*
19:00 – 22:00	**Welcome reception at Rikli Balance Hotel**

Friday, September 26, 2025	
08.00 – 18.00	**15th CESPT Registration**
	Section 2 – Delivery of Biopharmaceutics Chairpersons: María Blanco-Prieto, Eva Roblegg
9.00 – 9.45	**[PL]** Wolfgang Frieß, Ludwig-Maximilians-University Munich, Germany *Understanding the formulation challenges of protein drugs*
9.45 – 10.15	Rok Sekirnik, Sartorius BIA Separations d.o.o, Slovenia *In-Process Analytics in Manufacturing of mRNA Therapeutics (promotion lecture)*
10.15 – 10.30	**[OP]** Monika Prašnikar, University of Ljubljana, Slovenia *Monoclonal antibody formulation optimization using novel viscosity-reducing and stabilizing excipients*
10.30 – 10.45	**[OP]** Martin Deak, University of Szeged, Hungary *Optimization of solid self-emulsifying drug delivery systems to achieve oral peptide therapy*
10.45 – 11.00	**[OP]** Ágnes Rusznyák, University of Debrecen, Hungary *Cyclodextrin polymers: Formulation and investigations of new RNA delivery systems*
11.00 – 11.30	Coffee break
	Section 3 – Nanomedicine Chairpersons: Petra Kocbek, Karin Kogermann
11.30 – 12.15	**[PL]** María Blanco-Prieto, University of Navarra, Spain *Nanomedicine for the treatment of childhood cancer*

Plenary lecture (PL), Invited lectures (IL), Oral Presentations (OP), Poster Presentations (PP)

12.15 – 12.45	**[IL]** Jasmina Lovrić, University of Zagreb, Croatia *Innovative aspects in the development of drug delivery platforms for the treatment of dry eye disease*
12.45 – 13.00	**[OP]** Luka Casula, University of Cagliari, Italy *Phospholipid vesicle-based topical formulation to unlock the potential of a biosynthetic melanin*
13.00 – 13.15	**[OP]** Ivana Ruseska, University of Graz, Austria *The role of protein corona in enhancing microRNA delivery via nanostructured lipid carriers*
13.15 – 13.30	**[OP]** Nina Katarina Grilc, University of Ljubljana, Slovenia *Sticky business: Investigating the role of nanofiber encapsulation in Lactobacilli surface adhesion and biofilm formation*
13.30 – 13.45	**[OP]** Imren Esenturk-Guzel, University of Health Sciences, Istanbul, Turkey *Development and in vivo evaluation of haemostatic silk fibroin-based nanofiber formulations*
13.45 – 15.15	Luncheons / Poster session
	Section 4 – Strategies for Optimizing Pharmacotherapy Addressing Clinical Outcomes and Patient Friendly Drug Delivery Chairpersons: Odon Planinšek, Ildikó Bácskay
15.15 – 16.00	**[PL]** Jörg Breitkreutz, University of Düsseldorf, Germany *Patient-centric drug product development acceptability across patient populations - Science and evidence*
16.00 – 16.30	**[IL]** Tomasz Osmałek, Poznan University of Medical Sciences, Poland *Tiny needles, big possibilities – microneedle systems in modern drug delivery*
16.30 – 16.45	**[OP]** Mercedes Vitek, University of Ljubljana, Slovenia *In situ forming liquid crystals for peptide drug delivery: From gelation dynamics and sustained release to biocompatibility assessment*
16.45 – 17.00	**[OP]** Rabia Ashfaq, University of Szeged, Hungary *Nanolipid gel-based local therapy for periodontal diseases: A dual-action anti-inflammatory and antibacterial strategy*
17.00 – 17.30	Coffee Break
	Section 4 - Strategies for Optimizing Pharmacotherapy Addressing Clinical Outcomes and Patient Friendly Drug Delivery (cont.) Chairpersons: Jelena Filipović-Grčić, Maja Simonoska Crcarevska
17.30 – 18.00	**[IL]** Odon Planinšek, University of Ljubljana, Slovenia *Buccal films and Granules-in-straw as patient friendly dosage forms*
18.00 – 18.15	**[OP]** Ilenia D'Abbrunzo, University of Trieste, Italy *Assembling three anthelmintic molecules in a single solid: A praziquantel/niclosamide/acetic acid cocrystal solvate*
18.15 – 18.30	**[OP]** Ana Krese, Sandoz, Lek d.d., Ljubljana, Slovenia *Assessing the performance of ophthalmic gel: IVRT methodology*
19.30 – 00.00	**Conference dinner at Grand Hotel Toplice**

Plenary lecture (PL), Invited lectures (IL), Oral Presentations (OP), Poster Presentations (PP)

Saturday, September 27, 2025	
	Section 4 - Strategies for Optimizing Pharmacotherapy Addressing Clinical Outcomes and Patient Friendly Drug Delivery (cont.) Chairpersons: Tomaz Vovk, Grzegorz Garbacz
9.00 – 9.30	**[IL]** Katarina Vučičević, University of Belgrade, Serbia *Optimizing Dosing Regimen of Vedolizumab in Patients with Inflammatory Bowel Disease: Choosing the Right Pharmacokinetic Model for Routine Therapeutic Drug Monitoring*
9.30 – 10.00	**[IL]** Lea Knez, University Clinic Golnik & University of Ljubljana, Faculty of Pharmacy, Slovenia *Immunocheckpoint Inhibitors in Cancer Immunotherapy: Optimizing Drug Therapy to Improve Treatment Outcomes*
10.00 – 10.15	**[OP]** Jadwiga Paszkowska, Physiolution Polska, Poland *From in vitro to in vivo: How reliable are our bioequivalence predictions?*
10.15 – 10.30	**[OP]** Jiri Zeman, Masaryk University, Czech Republic *Are original and generic extended-release metformin tablets truly interchangeable?*
10.30 – 11.15	Coffee break
	Section 5 - Current Trends in Pharmaceutical Analytics and Biorelevant Methods of Assessment Chairpersons: Jurij Trontelj, TBC
11.15 – 12.00	**[PL]** Grzegorz Garbacz, Physiolution, Wroclaw, Poland *Innovative methods and software tools for biopredictive testing of oral medicines*
12.00 – 12.30	**[IL]** Sandra Cvijić, University of Belgrade, Serbia *Personalized Biorelevant Dissolution Testing: Addressing the Impact of Population & Disease Variability on Oral Drug Performance*
12.30 – 13.00	**[IL]** Tomasz Bączek, Medical University of Gdańsk, Poland *Profiling of phytocannabinoids in medicinal cannabis plant material via solid-phase microextraction approach*
13.00 – 13.15	**[OP]** Andrej Grobin, University of Ljubljana Slovenia *A useful method for monitoring of antibiotics in wastewaters by SPE_LC_MS/MS*
13.15 – 13.30	**[OP]** Ewelina Baran, Pedagogical University of Cracow, Poland *In situ characterization of 3D printed pharmaceuticals using magnetic resonance imaging and relaxometry methods*
13.30	**Closing of the Symposium**

Plenary lecture (PL), Invited lectures (IL), Oral Presentations (OP), Poster Presentations (PP)

POSTER SESSION

The list of posters with assigned numbers is available here:

NOTES

SPONSORS

PLATINUM SPONSORS

KRKA

At Krka, our dedication lies in producing high quality products, and keeping people healthy is what motivates us. From start to finish, everything we do revolves around our patients and our attempts to help them preserve and improve their health. Each day, more than 100 million patients in 70 markets are treated with our medicines, which are marketed under our own brand names. This is possible because of our innovative products, investments, and market expansion. Stable sales growth, multiple research projects, and sound business performance have seen us grow into a multinational pharmaceutical business group with almost 13,000 employees.

SARTORIUS BIA SEPARATIONS

Sartorius BIA Separations develops and manufactures leading CIM® monolithic chromatographic columns for purifying and analyzing large biomolecules like viruses, plasmids, and mRNA, used in cell and gene therapies. With over 25 years of experience, their Cornerstone® Biomanufacturing Development Services offer integrated process development solutions and novel technology to enhance the robustness and yield of biomolecule production while ensuring product safety. Their technology is pivotal in manufacturing-scale purification for advanced therapeutics and novel drug candidates in clinical trials.

GOLD SPONSOR

HARKE

HARKE Pharma & Nutra is your technology driven distributor for innovative excipients. Our technical team provides R&D support and gives periodical online seminars. Our customers can count on a good quality, using special warehousing and transport partners following GDP guidelines. We are able to support our customers to be fully compliant with legal and regulatory requirements. We support with a comprehensive range of products for applications including coating, tableting, sustained-release dosage forms, solubility enhancement, granulation, pelletization, semi-solids and capsules.

NOVARTIS

In Novartis in Slovenia, we develop, manufacture, and market innovative medicines, supporting over half of Novartis's priority treatments across various stages. Leveraging cutting-edge technology, we address diseases with unmet needs and play a key role in strengthening Slovenia's healthcare. With locations in Ljubljana, Mengeš, and Slovenj Gradec, we employ over 3,800 skilled professionals. Our purpose is to reimagine medicine to improve lives, driven by research, innovation, and advanced manufacturing to enhance treatment accessibility …

SILVER SPONSOR

LEK

Lek, a Sandoz company, is the first and oldest pharmaceutical company in Slovenia. It develops, manufactures, and markets effective, safe and high-value generic and biosimilar medicines for patients around the world. Their work is guided by high ethical standards, innovative thinking, and breakthrough achievements of their top experts. With more than 3,700 employees, they have been actively contributing to the Slovenian, European, and global research and development landscape for decades. They foster a culture of open dialogue and proudly and responsibly hold the title of the most reputable employer in Slovenia.

LABTIM

Labtim provides complete solutions for analytical laboratories, with a strong focus on the pharmaceutical and biopharmaceutical industries. As an official distributor for leading manufacturersincluding Waters Corporation, Wyatt Technology, Sotax, TA Instruments, and Merck Millipore—we combine world-class technologies with expert local support. Our services span sales, application support, technical maintenance, education, and IT consultations. With expertise in LC, LCMS, SFC, tablet testing, sample prep, columns, water purification systems, and our own GMP lab, we ensure accuracy, compliance, and confidence at every step.

BRONZE AND OTHER SPONSORS

We are grateful to our sponsors who support pharmaceutical technology and drug delivery science and add value to the 15th CEPST. Many of the symposium events are made possible only through the generosity of sponsors.

Pioneering access for patients.

We are Sandoz, the world's leading generic and biosimilar pharmaceutical company. And we are Lek, the pioneers of the pharmaceutical industry in Slovenia.

Our passion lies in delivering excellence and high quality medicines. We are inspired by cutting-edge biotech processes in the development and production of biosimilars and the highest pharmaceutical production standards.

SANDOZ | lek

Lek Pharmaceuticals d.d.
Verovškova ulica 57
1526 Ljubljana, Slovenia
www.lek.si

Are you ready for absolute answers in an uncertain world?

Waters™ | WYATT TECHNOLOGY

GMP data analysis in Astra™ or Empower™

Achieve absolute molecular weight, size, and aggregation status

Premier MaxPeak™ HPS for metal-sensitive analytes

Characterize mAbs, oligonucleotides, ADCs, AAVs, PEGylated proteins

Arc™ Premier LC System + Wyatt MALS Detection

Labtim

Complete solutions for analytical laboratories.

Application Support, Technical Support, Educational Training, Sales, IT Consultations and our in-house GMP Laboratory.

Plenary lectures

PL1

SOME LEARNINGS ABOUT ROLL COMPACTION

Peter Kleinebudde

Institute of Pharmaceutics and Biopharmaceutics, Heinrich Heine University, Germany

1. ROLL COMPACTION/ DRY GRANULATION

Direct compaction (DC) is the simplest method for producing tablets [1]. However, DC is often not possible due to various issues, such as insufficient flowability, wettability, tabletability, de-mixing or dust production. Granulation is a process of increasing particle size whereby smaller particles are converted into larger agglomerates. Various granulation methods are available that can overcome some or all of the aforementioned DC problems. One method that does not require binding liquids is roll compaction/dry granulation. In this method, the raw materials are first pressed into ribbons by a roll compactor and then granulated in a second step by grinding. Advantages include the absence of liquids, which avoids the need for further drying, environmental friendliness, ease of scaling up, and the fact that it is an inherently continuous process that can easily be integrated into a continuous manufacturing line. The main disadvantages are the high fines content compared with other granulation processes and the reduced tabletability of some materials [2].

2. PROCESS UNDERSTANDING AND PROCESS CONTROL

Johanson [3] performed fundamental work regarding the understanding of the roll compaction (RC) process in the 1960s. Based on his work, numerous modifications were published in the following decades. The most important intermediate critical quality attribute is the solid fraction of the ribbon. The solid fraction (SF) is important for the subsequent processes and determines the ribbon's strength and grinding behaviour, as well as the particle size distribution, flowability, and tabletability of the granules. Therefore, a key objective is to control the SF and keep it as consistent as possible.

The work of Johanson and subsequent researchers has enabled us to understand the interdependence of equipment parameters such as roll diameter and width, process parameters such as compaction force and gap width, and material parameters such as the compressibility coefficient. Meanwhile, some simplified approaches are available which are valid under certain conditions [4]. This forms the basis for process transfer and scaling up in RC. The measured specific compaction force can be related to the peak pressure, which is important for determining the solid fraction of the ribbon.

Modern roll compactors are designed to control both the specific compaction force and the gap width simultaneously. Several control circuits work simultaneously and quickly. This enables the SF of the ribbon to be kept constant. Several approaches have been published for measuring the ribbon SF in real time.

The mean solid fraction of the ribbon can be controlled over time. However, there is variation within the ribbon. Approaches to improve the homogeneity of the SF within the ribbon have been proposed.

3. MATERIAL ASPECTS

One of the main disadvantages is the partial loss of tablettability following RC. This is particularly evident in plastically deforming materials. This phenomenon has been extensively studied in the context of microcrystalline cellulose (MCC), but it is also relevant to many other excipients and APIs. Several reasons have been suggested for this partial loss of tablettability, with particle size enlargement and granule hardening being the most significant mechanisms [5].

Several approaches can help to overcome the partial loss of tablettability. Using starting materials of the same type, but with smaller initial particle sizes, can compensate for the loss in tablettability. A second approach is to use suitable binders. This has been demonstrated numerous times. Both approaches can be combined.

For materials that stick to the rolls, it has been proposed that a lubricant be added prior to rolling compression (RC). While this may prevent sticking, it also reduces the friction

required to reach the desired nip angle. This can be problematic, particularly at the start of the process. As with the addition of any lubricant, the amount added, as well as the mixing time and intensity, are important factors in determining the outcome.

4. CONCLUSION

RC is well understood, modern equipment is available to control the process, the scale up and process transfer is easy. RC can be incorporated into continuous manufacturing lines. “Golden rules” have been proposed to overcome the disadvantages [5].

5. REFERENCES

1. Leane, M. et al., *A proposal for a drug product Manufacturing Classification System (MCS) for oral solid dosage forms.* Pharmaceutical Development and Techology. 2015. 20: 12-21.
2. Kleinebudde, P. *Roll compaction/dry granulation: pharmaceutical applications* European Journal of Pharmaceutics and Biopharmaceutics. 2004. 58: 317-326.
3. Johanson, J.R. *A Rolling Theory for Granular Solids.* Journal of Applied Mechanics. 1965. 32: 842.
4. Kleinebudde, P. *Improving Process Understanding in Roll Compaction.* Journal of Pharmaceutical Sciences. 2022. 111: 552-558.
5. Sun, C.C. and Kleinebudde, P. *Mini review: Mechanisms to the loss of tabletability by dry granulation.* European Journal of Pharmaceutics and Biopharmaceutics. 2016. 106: 9-14.

ACKNOWLEDGMENT

This work would not have been possible without the help and engagement of numerous PhD students, postdoctoral researchers and partners. It is not possible to mention them all individually. I am deeply grateful to all of them. Collaboration is key to generating new knowledge.

PL2

UNDERSTANDING THE FORMULATION CHALLENGES OR PROTEIN DRUGS

Wolfgang Friess

Department of Pharmacy; Pharmaceutical Technology and Biopharmaceutics; Ludwig-Maximilians-Universität, Germany

1. INTRODUCTION

Protein drugs are characterized by an inherent chemical, colloidal, and conformational instability. This multitude of potential changes upon processing and storage are critical both from quality, and safety and efficacy perspective. Thus, products have to be characterized and understood at a highly detailed level. Furthermore, the interplay has to be considered and methods with enable different view angels at different stages of development and stability testing are mandatory. This generates a formulation space in which the different critical instabilities and the target product profile have to be considered and balanced. The protein itself as well as formulation, processing and packaging materials affect stability. Furthermore, aspects such as solution viscosity for subcuteneous application of higher doses have to considered.

To this end, the presentation will highlight different formulations challenges and explain underlying mechanisms, analytical tools and appropriate stabilization methods considering

a) Protein Self Interaction
b) Protein Interaction with various Interfaces
c) Computational Models
d) Bulk Freezing
e) Stabilization by Lyophilization

2. REFERENCES

1. Koepf E., Eisele S., Schroeder R., Brezesinski G., Friess W., Notorious but not understood: How liquid-air interfacial stress triggers protein aggregation. International Journal of Pharmaceutics, 2018. 537: 202-212.
2. Marschall C., Witt M., Hauptmeier B., Friess W., Powder suspensions in non- aqueous vehicles for delivery of therapeutic proteins. European Journal of Pharmaceutics and Biopharmaceutics, 2021. 161:37-49.
3. Deiringer N., Friess W., Proteins on the Rack: Mechanistic Studies on Protein Particle Formation During Peristaltic Pumping. Journal of Pharmaceutical Science, 2022. 111: 1370-1378.
4. Isaev N., Lo Presti K., Friess W., Insights into Folding and Molecular Environment of Lyophilized Proteins Using Pulsed Electron Paramagnetic Resonance Spectroscopy. Molecular Pharmaceutics, 2025. 22: 424-432.
5. Binder J., Zalar M., Huelsmeyer M., Siedler M., Curtis R., Friess W., Enhancing Martini 3 for protein self-interaction simulations. European Journal of Pharmaceutical Sciences, 2025. 209: 107068

PL3

NANOMEDICINE FOR PEDIATRIC CANCER THERAPY AND TISSUE REGENERATION

María J. Blanco-Prieto

Pharmaceutical Sciences Department, Faculty of Pharmacy and Nutrition, University of Navarra, Pamplona, Navarra, Spain; Instituto de Investigación Sanitaria de Navarra (IDISNA), Pamplona, Navarra, Spain

This lecture will present the development of advanced therapeutic strategies to address two critical medical challenges: pediatric cancer treatment and brain tissue regeneration.

The first part will focus on the design and application of lipid nanoparticles loaded with antitumor agents for the treatment of osteosarcoma, a highly aggressive pediatric cancer. These nanoparticles are specifically engineered for oral administration, offering a non-invasive, patient-friendly approach that enhances drug stability and bioavailability while minimizing systemic toxicity. Preclinical studies have demonstrated their remarkable efficacy in reducing primary tumor burden and preventing metastatic spread, positioning them as a promising therapeutic strategy for osteosarcoma. Moreover, the oral delivery method is anticipated to significantly improve patient compliance, a crucial factor in pediatric oncology.

The second part of the lecture will explore advancements in brain tissue repair within the context of Parkinson's disease. Specifically, it will discuss how the development of delivery systems based on biodegradable polymers, combined with neurotrophic factors such as glial cell-derived neurotrophic factor (GDNF), can promote the regeneration of dopaminergic neurons and restore motor function in non-human primate models of Parkinson's disease. These systems have shown great potential in regenerating dopaminergic pathways and overcoming challenges related to protein delivery to specific brain regions, offering new therapeutic avenues for the treatment of neurodegenerative disorders.

Together, these examples underscore the transformative potential of innovative drug delivery systems to address complex challenges in oncology and regenerative medicine through multidisciplinary approaches.

References

1. Rodríguez-Nogales C, et al., ACS Nano. 12 (2018) 7482-7496.
2. Lasa-Saracibar B, et al., Cancer Lett 334:2 (2013) 302-310.
3. Aznar MA, et al., Int J Pharm, 454:2 (2013) 720-726
4. González-Fernández Y et al., Cancer Let,. 388 (2017) 262–268.
5. González-Fernández Y et al., Cancer Lett, 430 (2018) 193-200.
6. Garbayo E et al., Biomaterials, 110 (2016) 11-23.
7. Garbayo E et al., WIREs Nanomedicine and Nanobiotechnology, (2020), 10.1002/wnan.1637.
8. Torres-Ortega et al., Biomacromolecules, 629 (2022), 122356.

PL4

PATIENT-CENTRIC DRUG PRODUCT DEVELOPMENT AND ACCEPTABILITY ACROSS PATIENT POPULATIONS – SCIENCE AND EVIDENCE

Jörg Breitkreutz

Institute of Pharmaceutics and Biopharmaceutics, Heinrich Heine University Düsseldorf, Universitätsstr. 1, 40225 Düsseldorf, Germany

1. INTRODUCTION

Patient-centric medicinal products are a recent demand from competent authorities and foster various trends in pharmaceutical development, medical treatment and new drug applications. The Center for Drug Evaluation and Research (CDER) at the United States´ Food Drug Administration (U.S.FDA) has introduced a systematic approach called "Patient-focused drug development (PFDD)" [1].
Its primary goal is to "better incorporate the patient's voice in drug development and in the evaluation process, including but not limited to facilitating and advancing use of systematic approaches to collect and utilize robust and meaningful patient and caregiver input that can better inform medical product development and regulatory decision-making, best practices to facilitate patient enrolment and minimize the burden of patient participation in clinical trials, enhancing appropriate use of methods to capture information on patient preferences and the potential acceptability" [1].
U.S.FDA procedural guidance for industry on "methods to identify what is important to patients" comprises qualitative, quantitative and mixed research methods to understand what matters most to the patients suffering from a specific disease or condition [2].
Acceptability of oral drug dosage forms has been thoroughly investigated in children before in order to identify the best drug administration strategy for unmet needs of this vulnerable patient subpopulation ranging from pre-term neonates to adolescents [3]. Similar concepts have been also proposed for patients in adulthood, especially for elderly [4]. In late 2023, the European Medicins Agency (EMA) filed a Letter of Support for the most advanced methodology, the "Composite endpoint method for acceptability evaluation" developed by a public-private partnership including the Novartis company and the Children's University Hospital of our university [5].
The applicants have conducted various clinical studies on the swallowability and palatability, combined as indicators for acceptability, of various advanced paediatric dosage forms including liquid preparations, mini-tablets (uncoated and coated), orodispersible films and others [3, 5, 6]. The results of these studies have been ground-breaking in the area of paediatric formulations and paved the way for innovative products such as the recently introduced product Aqumeldi®, an Enalapril maleate containing orodispersible mini-tablet (ODMT) by Proveca Ltd.

The presentation will report the science and the evidence of investigations connected with the product Aqumeldi® as an example for modern patient-focused drug development from the idea to the market.

2. RESULTS AND DISCUSSION

2.1. Immediate-release minitablets

Drug-free minitablets of different diameters, coated or not, as monolithic and multiparticulate form, have been broadly investigated regarding the swallowability and palatability, revealing the acceptability of the medication. In a prospective exploratory cross-over study [8], it was shown that an uncoated 2 mm, immediate-release minitablet was equally or even better accepted than the former gold standard in paediatric therapy, a sweet syrup (glucose syrup) of 5 ml volume. The following confirmatory study using 306 children (from 6m to 6y) demonstrated even overall favourable acceptance for the minitablet vs. the syrup, irrespectively whether they have been film-coated or not [9]. The uncoated minitablets were successfully administered even to neonates [10], including pre-term neonates by moving them into a breast-feeding position.

2.2. Minitablets as multiparticulates

Film-coated minitablets can be used as multiparticulate drug carriers in children and show no inferiority to a syrup even up to 25 for children of less than 2 y and up to 100 for 6 y old ones [7]. The dimensions can be even enlarged to 2.5 mm, still the composite end-point method demonstrate suitability between 1 m and 6 y.

2.3. Orodispersible minitablets

Orodispersible minitablets have been first proposed in 2011 [11]. In the EU funded project LENA which was completely accompanied by delegates of the Childrens` Heart Federation two types of orodispersible minitablets (0.25 and 1.00 mg enalaprilat maleate) were successfully developed at our university and transferred to the contracting manufacturer Nextpharma. ODMTs were produced under GMP conditions and used for a comparative bioavailability study using healthy (adult) volunteers. The minitablets showed pharmacokinetic profiles similar as Renitec® from MSD and no transmucosal absorption [12]. Based on these results, we initiated three clinical studies in paediatric patients with heart failures in various European Countries in order to apply for a Paediatric Use Marketing Authorisation (PUMA) at the EMA. EMA requested further in-vitro studies on food interactions and use of nasogastral tubes. We found the Enalapril ODMTs to be precisely dosed, stable, and fully accepted by all paediatric subpopulations. Children *and* caretakers found them better suitable than former extemporaneously compounded medicines. Both products were transferred to Proveca Ltd., Ireland, who recently received the marketing authorisation for both dose strength for Europe and introduced the new PUMA product in some EU member states already. Other countries will follow soon.

3. CONCLUSION

Drug-free minitablets have been shown in patient-centricity studies to be suitable dosage forms in the paediatric population. From the basic idea of an ODMT in 2011, the market entry of a product was realized 14 years later by following a consistent patient-focused pathway.

4. REFERENCES

1. FDA/CDER, *Patient-focused drug development*, ww.fda.gov/drugs/development-approval-process-drugs/cder-patient-focused-drug-development.
2. FDA/CDER, *Patient-focused drug development: methods to identify what is important to patients*, Guidance, 2022.
3. V. Klingmann, C.E. Pohly, T. Meissner et al., *Acceptability of an orodispersible film compared to syrup in neonates and infants: A randomized clinical trial*, Eur J Pharm Biopharm 2020, 151: 239-245.
4. S. Stegemann, V. Klingmann, S. Reidemeister, J. Breitkreutz, *Patient-centric drug product development acceptability across patient populations - Science and evidence.* Eur J Pharm Biopharm, 2023. 188: 1-5.
5. S. Reidemeister, B. Nafria Escalera, D.Marín et al., *Young patients' involvement in a composite endpoint method development on acceptability for paediatric oral dosage form.* Research Involvement and Engagement, 2023, 9: 108.
6. J. Münch, I. Sessler, H.M. Bosse et al., *Evaluating the acceptability, swallowability, and palatability of film-coated mini-tablet formulatio in young children: results from an open-label, single-dose, cross-over study,* Pharmaceutics, 2023. 15: 1729.
7. V. Klingmann, M. Hinder, T.H. Langenickel et al., *Acceptability of multiple coated mini-tablets in comparison to syrup in infants and toddlers: a randomised controlled study,* Arch Dis Child 2023, 108: 730-735.
8. N. Spomer, V. Klingmann, I. Stoltenberg et al., *Acceptance of uncoated mini-tablets in young children – Results from a prospective exploratory cross-over study*, Arch Dis Child 2012, 97: 283-286.
9. V. Klingmann, N. Spomer, C. Lerch et al., *Favourable acceptance of mini-tablets compared with syrup: a randomised controlled trial in infants and preschool children,* J. Pediatr. 2013, 163:1728-1732.
10. V. Klingmann, A. Seitz, T. Meissner et al., *Acceptability of uncoated minitablets in neonates – a randomized controlled trial,* J. Pediatr. 2015, 167: 893-896.
11. I. Stoltenberg, J. Breitkreutz, *Orally disintegrating mini-tablets (ODMTs) – A novel solid dosage form for paediatric use,* Eur J Pharm Biopharm 2011, 78: 462-469.
12. S. Läer, W. Cawello, B.B. Burckhardt et al., *Enalapril and enalaprilat pharmacokinetics in children with heart failure due to dilated cardiomyopathy and congestive heart failure after administration of an orodispersible enalapril minitablet (LENA-studies),* Pharmaceutics 2022, 14: 1163.

PL5

INNOVATIVE METHODS AND SOFTWARE TOOLS FOR BIOPREDICTIVE TESTING OF ORAL MEDICINE

Grzegorz Garbacz[1], Marcela Staniszewska[1], Jadwiga Paszkowska[1], Justna Dobosz[1], Michał Smoleński[1], Michał Romański[1], Dorota Danielak[1]

[1]Physiolution, Piłsudskiego 74, 50-020 Wrocław, Poland

1. INTRODUCTION

The only constant in the gastrointestinal (GI) tract is the variability of its physiological conditions. This seemingly paradoxical observation carries significant implications for the development and evaluation of oral drug products, and to this day remains an intriguing scientific challenge. One of the most pressing tasks in this context is the design and construction of test devices capable of realistically simulating the dynamic environment of the GI tract. Equally important is the selection of test conditions that enable meaningful prediction of a drug's delivery performance already at the preclinical stage.

In this presentation, I will focus on the simulation of variability in the key physiological parameters that govern the dissolution of orally administered drugs, including the peristaltic forces of the GI tract, pH fluctuations, and temperature gradients. I will outline the physiological variability ranges of these parameters and introduce the simulation strategies we have developed, which employ dedicated, abstract models. These include:

pHysio-grad®, a dynamic pH control system capable of simulating high-resolution pH gradients using both liquid and gaseous titrants; the AMP® device platform, designed to replicate the mechanical and physicochemical conditions of the gastrointestinal tract;

and PhysioCell®, a flow-through system dedicated to the testing of immediate-release (IR) formulations, which mimics pH gradients, flow rates, and mechanical stresses encountered during GI transit.

Once properly parameterized, these models enable the simulation of physiological variability within a well-defined Physiological Design Space.

These advanced biopredictive models play a pivotal role throughout the entire R&D cycle of oral drug products. They support the rational, physiology-driven characterization of drugs, facilitate formulation optimization, assist in the preparation for clinical trials, and contribute to the evaluation of post-approval changes. Moreover, these tools are specifically designed to generate high-quality datasets suitable for absorption simulations and pharmacokinetic (PK) modeling, thereby bridging the gap between in vitro experimentation and in vivo drug performance.

The practical applicability of these approaches for predicting the drug delivery of oral medicines will be demonstrated.

ACKNOWLEDGMENT

The work has been partially financed by Polish National Centre for Research and Development (POIR.01.02.00-00-0011/17 and POIR.04.01.04-00-0142/17).

Invited lectures

IL1

DEVELOPMENT OF HORMONE-CONTAINING VAGINAL FILM AND APPLICATOR USING QBD APPROACH

Réka Révész[1,2,3], Dóra Nick[2], Tamás Görbe[2], Ádám Haimhoffer[2]

[1]Doctoral School of Pharmaceutical Sciences, University of Debrecen, Hungary
[2]Department of Pharmaceutical Technology, Faculty of Pharmacy, University of Debrecen, Hungary
[3]Department of Industrial Pharmaceutical Technology, Faculty of Pharmacy, University of Debrecen, Hungary

1. INTRODUCTION

The symptoms of menopause and postmenopausal are caused by a change in hormonal balance. The balance of the hormones oestrogen and progesterone is altered because of a decrease in the amount of oestrogen. These hormonal changes can cause cardiovascular disease and osteoporosis. One of the most common and most frequent primary symptoms, along with hot flushes, is the appearance of vaginal dryness and loss of libido. This period takes its toll on women not only physically but also mentally, so there are now several therapeutic options available as hormone replacement, but none of them are a complete solution to menopause [1]. In modern medicine, there is an increasing need to develop new or modified forms of medicines that are safe, have adequate bioavailability and patient compliance. In addition to transdermal, oral drug delivery, there is a need for an innovative and attractive alternative form of medicine that is capable of systemic action while providing an appropriate solution for local changes. Vaginal films provide a solution for estrogen replacement and the polymers and excipients used reduce the degree of vaginal dryness that develops.

Our aim is to develop a new vaginal film that can replace the lack of estrogen during menopause as a complex with a cyclodextrin polymer and also provide a solution to the most common physical change that women experience, which is also a major psychological burden. We also aim to develop a prototype film applicator that could become a potential product on the market, helping thousands of women.

2. MATERIALS AND METHODS

2.1. Materials

β-CD polymer was purchased from Cyclolab Kft. (Budapest, Hungary). All other reagents were purchased from Sigma Aldrich Kft. (Budapest, Hungary) in analytical grade.

2.2. Methods

The development of the formulation was QbD-based, with the first step being to assess patient needs and the competitive advantages of products on the market using a questionnaire. The critical parameters of the product (tensile strength, pH, moisture content) were then determined and the formulations and manufacturing processes were optimised using factorial experimental design. The effect of oestradiol was enhanced with a cyclodextrin polymer. The efficacy of the developed formulation was tested both *in vitro* and *ex vivo*.

3. RESULTS AND DISCUSSION

3.1. Vaginal applicator development considering patient needs

The needs assessment revealed that a large proportion of women have experienced vaginal problems and have used products that require an applicator to apply them. For the applicators, the characteristics shown in Figure 1. were identified as the characteristics to be improved. Thus, our applicator was designed and developed accordingly, and its prototype was 3D printed.

IL1

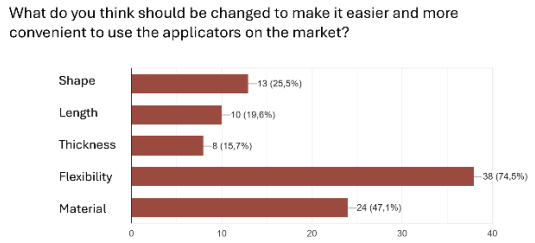

Figure 1. illustrates which features respondents think should be changed for existing vaginal applicators.

3.2. Vaginal film development

We optimised the formulation and production process using Box-Behnken design of experiments. The final composition has a pH between 3.5 and 4.5, which is within the vaginal range. It also has sufficient tensile strength to be used with an applicator. Its low moisture content ensures adequate stability. The film disintegrates in vaginal fluid in less than 15 minutes. The formulation's ability to regenerate cells has been demonstrated in vitro using a cell model. The absorption of oestradiol was characterised further *ex vivo*.

4. CONCLUSION

In conclusion, we have developed an applicator that meets the needs of patients and is suitable for administering hormone-containing films. The developed film can be used to alleviate the symptoms of menopause for thousands of women.

5. REFERENCES

1. Rozenberg, S. Postmenopausal hormone therapy: Risks and benefits. Nat. Rev. Endocrinol. 2013, 9, 216–227,

ACKNOWLEDGMENT

Project no. TKP2021-EGA-18 has been implemented with the support provided by the Ministry of Culture and Innovation of Hungary from the National Research, Development and Innovation Fund, financed under the TKP2021-EGA funding scheme. Supported by the EKOP-24-4 University Research Scholarship Program of the Ministry for Culture and Innovation from the source of the National Research, Development and Innovation Fund.

IL2

INNOVATION IN PHARMA: DEVELOPMENT AND IMPLEMENTATION OF CONTINUOUS MANUFACTURING FOR COMMERCIAL PRODUCTION

Maja Kus

Novartis farmacevtska proizvodnja d.o.o. (Novartis Pharmaceutical Manufacturing LLC), TechOps Ljubljana, Slovenia

1. INTRODUCTION

Continuous manufacturing (CM) is a relatively new technology within the pharmaceutical industry. It is increasingly being recognized for providing benefits over conventional batch manufacturing processes. When talking about CM in scope of solid dosage oral forms the most commonly applied technology is so-called "direct compression".

In Novartis we have developed continuous manufacturing line that includes complete technological procedure – from wet granulation, drying, compression and coating, therefore combining three otherwise separate manufacturing steps into a continuous train that brings from starting materials to a final film-coated tablet in less than an hour. With this innovative technology Novartis has joined a group of four pharmaceutical companies using this technology for commercial manufacturing.

The Continuous Manufacturing Project in Ljubljana started in 2020. The CM Line was built in TechOps Ljubljana, Slovenia, as part of like-to-like concept. Ljubljana CM Line is therefore a copy of Continuous Manufacturing Line in Technical Research and Development (TRD) Basel. Both lines have the same equipment and use NovaControl (Novartis' proprietary control system) for automation and control over the manufacturing process. The CM line in TechOps Ljubljana was qualified and handed over to production in beginning of 2024.

2. CM LINE AT TechOPS LJUBLJANA

The CM line is divided into four quadrants that are controlled via NovaControl. First quadrant consists of feeding the API and internal phase into continuous blender and feeding the blend intro twin screw granulator. Second quadrant consists of granulation and drying. Water granulation with product specific twin-screw design is carried out, the granules are continuously dried in fluid-bed drier. Dried granules are milled using specially designed rotary mill and are fed to special hopper above the tablet press. In quadrant three granules, outer phase and lubricant are fed into continuous blender and the final blend is fed into tablet press. In quadrant four the tablet cores are produced and fed into heated deduster. Tablet cores are stored in three heated hoppers that are alternately emptied into continuous coater using a robot arm. The cores are coated simultaneously in two coaters that each have three compartments. In each compartment coating spray rate can be adjusted.

In-line PAT tools enable enhanced process insight. Current line set-up allows for three PAT controls: moisture content after fluid-bed drying, blend uniformity prior compression and 100% drug content on each and every tablet during compression. Product specific modules are in development.

The CM line has five rejection ports that are initiated if the process is in "start-up" mode or if it exceeds set alarm limits in the "production" mode. The rejection of material is possible after twin screw granulation, after drying, before compression, after compression and after coating.

The CM line can be adjusted to operate with only some quadrants, therefore, it can be used only for continuous granulation, direct compression or continuous compression and coating.

The throughput of the line is from 5 to 50 kg/h, depending on the CM set-up.

3. LIKE-TO-LIKE CONCEPT

The like-to-like concept means that all critical equipment is identical to both Development and Commercial site. Therefore, it allows us simpler process transfer from development (TRD) to production without scale-up. As the continuous manufacturing lines in Basel and Ljubljana use the same equipment and control

system, the process can be developed in Basel and then transferred to TechOps Ljubljana using the same process parameters, which minimise transfer risk and transfer efforts. Using the same overlying control software (NovaControl) on both sites also enables site-to-site support and recipe transfer.

The first technical trial at TechOps Ljubljana where we transferred the knowledge from TRD to commercial line in TechOps Ljubljana took place at the end of 2024. This was the first time we produced active final product. Within the technical trials that involved separate quadrant-by-quadrant tests, partially continuous runs and finally full continuous manufacturing, we have successfully run the entire continuous line for 10 hours for one dosage strength and 6 hours for another dosage strength. The technical run and analytical results confirmed the like-to-like concept as products produced at TechOps and at TRD with the same process parameters are comparable and meet the specification requirements.

Activities on Continuous Manufacturing Line are on-going with further planned technical runs that will confirm some process improvements to be affective. The timeline for submission for first Novartis' continuously manufactured product is in place.

4. CONCLUSION

With installing and qualifying Continuous Manufacturing Line we have brought a development, launch and supply platform into Novartis Technical Operations Ljubljana.

There are many benefits of CM in comparison with conventional "batch" technology, which is why Novartis is actively expanding CM project portfolio. Like-to like installation in TRD and TechOps enables accelerated and smooth transfers and early clinical supplies already from commercial production site. CM decreases process time from several days to few hours and allows production of larger batch sizes at the same equipment size only by prolonging the run time. Moreover, the CM is also a green line, as due to smaller footprint we reduce energy consumption by 64 %, which means 46 tons less of CO_2 emissions.

ACKNOWLEDGMENT

The author would like to thank all the colleagues in TechOps Ljubljana Small Molecules that were actively involved with the Continuous Manufacturing Project and helped establish a working CM Line.

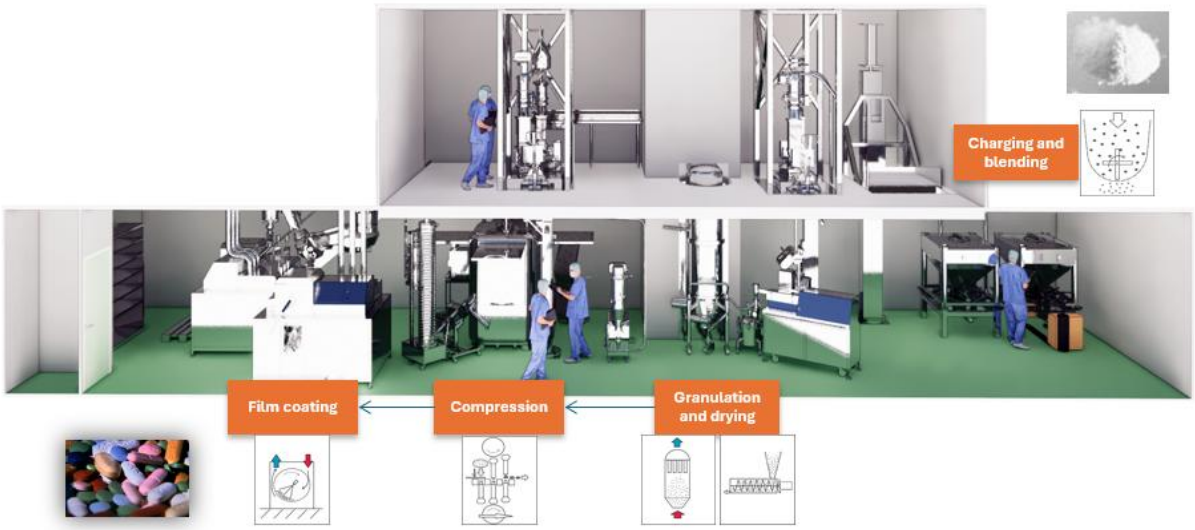

Figure 1. Schematic presentation of Continuous Manufacturing Line at TechOps Ljubljana.

IL3

PROCESS ANALYTICAL TECHNOLOGY: CASES AND INSIGHTS FROM THE PHARMACEUTICAL INDUSTRY

Klemen Korasa[1,2]

[1]*Krka, d. d., Novo mesto, Šmarješka cesta 6, 8501, Novo mesto, Slovenia*
[2]*University of Ljubljana, Faculty of Pharmacy, Aškerčeva 7, 1000, Ljubljana, Slovenia*

1. INTRODUCTION

More than 20 years have passed since the U.S. FDA introduced its *Process Analytical Technology (PAT)* guidance for industry [1]. Over this period, numerous studies and industrial applications have demonstrated the high relevance and effectiveness of PAT as a framework for real-time process monitoring and control, aimed primarily at ensuring consistent product quality. Today, virtually every pharmaceutical academic institution, regulatory agency, and manufacturer use some of the PAT tools. However, the widespread implementation of fully integrated PAT solutions across the pharmaceutical industry remains limited.

2. DISCUSSION

The use of PAT in the pharmaceutical industry has been well documented in both scientific and industrial literature. Studies confirm that PAT is applicable for monitoring various technologies and dosage forms, including oral solids, sterile products, and both simple and complex formulations [2]. The literature also shows that PAT process analyzers have evolved into sophisticated and reliable tools for process monitoring. By using different probes, it is possible to monitor a range of process and material attributes at different stages, leading to improved process understanding. Additionally, some studies demonstrate that a single analyzer can measure multiple product attributes, contributing to even greater process knowledge and resource-related benefits [3].

The application of multivariate statistical tools has enhanced the benefits derived from process data. Additionally, employing design tools like DoE has improved and facilitated the process and formulation development stage. In addition to process monitoring and design, PAT also supports effective process control [4]. The literature already reports early proof-of-concept examples of integrated continuous medicine manufacturing, allowing the production of both the active pharmaceutical ingredient and the final dosage form in a single stream [5]. Recently, there has been a growing trend in the use of process simulation tools, such as CFD-DEM (Fig. 1). Such simulations can help to define optimal process parameters, reduce costs and environmental impact of technology transfer, and prevent potential future process deviations.

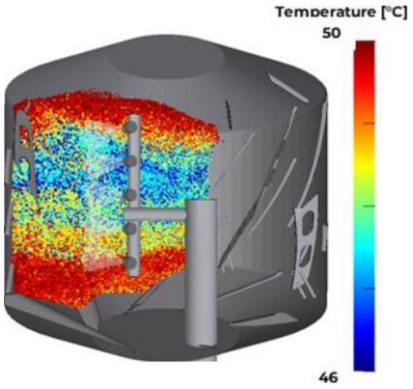

Figure 1: Example of industrial film coating CFD-DEM simulation.

The PAT tools have become well-recognized and frequently applied across the broader pharmaceutical industry. However, more than two decades after the introduction of the PAT guidance, the framework is still not incorporated in the industry as primarily expected. Individual tools are applied regularly, but examples of routine PAT applications or the comprehensive industrial PAT solutions remain rare. There are several factors that contributed to the current PAT status. The costs and resources required for the implementation and maintenance of such system remain high. Therefore, manufacturers tend to be cautious regarding the implementation of the PAT and typically adopt such systems only when no other feasible solutions are available. Regulatory barriers are also a contributing factor. The perspectives of different medicine agencies are often not synchronized, posing a risk when implementing PAT solutions. While individual agency may accept the rationale,

others may not, potentially resulting in the establishment of two separate systems for process and quality control. This could consequently lead to increased costs for the manufacturer. Even though one of the main scopes of the PAT guidance in the beginning of the century was to reduce the regulatory uncertainty, hesitancy to implement such novel solutions from regulatory perspective remains. Implementing a new PAT system voluntarily necessitates additional justifications, potentially extending the regulatory approval process. Furthermore, resources are required post-approval to ensure regulatory compliance throughout the product's lifecycle. Regulatory tightening of PAT demands could lead to its faster adoption. However, mandatory PAT requirements may result in higher medicine costs, raising questions about the alignment with public health interests.

3. CONCLUSION

PAT tools are becoming an increasingly important part of the development, manufacturing, and quality control of medicines. However, the use of comprehensive PAT solutions in the pharmaceutical industry remains limited. It would be valuable to review the key benefits of PAT tools for manufacturers, regulatory authorities, and for the public health and based on the insights redefine the future role of PAT. Commercially available integrated PAT solutions along with recent AI advancements could accelerate broader and faster adoption within the pharmaceutical industry.

IL4

INNOVATIVE ASPECTS IN THE DEVELOPMENT OF DRUG DELIVERY PLATFORMS FOR THE TREATMENT OF DRY EYE DISEASE

Jasmina Lovrić

Department of Pharmaceutical Technology, University of Zagreb Faculty of Pharmacy and Biochemistry, Croatia

1. INTRODUCTION

Dry eye disease (DED) is a multifactorial, symptomatic disease characterized by a loss of homeostasis of the tear film and/or ocular surface [1]. It is a growing public health concern caused by ophthalmic and other medications, digital device use, environmental factors, nutrition, cosmetics, contact lenses, and general lifestyle. The development of safe, effective, and patient-acceptable topical ophthalmic drug products tailored to the severity of DED is a necessity to control the cumulative burden of DED symptoms on overall quality of life. A structured approach to preclinical formulation development is essential to create ophthalmic formulations that offer multiple therapeutic modalities to improve the treatment of DED. This approach should be based on *in vitro* biomimetic tools that consider the key physiological and anatomical aspects of the ocular surface.

2. MATERIALS AND METHODS

2.1. Materials

Loteprednol etabonate and latanoprost were generously donated by JGL d.d. The following excipients were used: castor oil (Fagron), Capryol® 90 (Gattefosse), Kolliphor® EL (BASF), Kolliphor® RH40 (BASF), Soluplus® (BASF), sodium hyaluronate (Contipro Ltd.), glycerol, sodium dihydrogen phosphate monohydrate, disodium phosphate anhydrous, sodium chloride. All the components for artificial tear solution (ATS) of different levels of complexity were purchased from Sigma-Aldrich. HCE-T cell line was obtained from RIKEN Cell Bank and Cytion.

2.2. Ophthalmic formulation development

For the preparation of nanoemulsions, the oil and water phase were premixed with Ultra-Turrax® (IKA-Werke GmbH & Company) and obtained coarse emulsions were subjected to a microfluidizer LM20 (Microfluidics). Latanoprost formulations were prepared by simple dissolution of drug and excipients.

2.3. Development of innovative in vitro biomimetic tools

For the analysis of formulation stability in the tear fluid, formulations were subjected to a biorelevant dilution simulating tear turnover (16 % min^{-1}, 34°C) with ATS of different levels of complexity according to the components present [2]. Another level of complexity was added by exposing the diluted formulations to a series of simulated eye blinks using rheometer (MCR102, Anton Paar).

For the analysis of biocompatibility of a large number of formulations as developed by design of experiments, an improved biocompatibility screening model with higher throughput was developed, namely a 3D HCE-T cell model grown on 96-well insert plates [3,4].

To investigate the effect of biorelevant dilution on drug release from the nanoemulsion, the successive dilution was simulated by mixing the formulation with release medium [3]. Afterwords, diluted formulations were centrifuged in centrifuge tubes with ultrafilter (Microcon®) and drug content in the oil phase was determined indirectly based on the content of drug quantified in the filtrate (aqueous phase).

For testing the anti-inflammatory effect, a simple DED *in vitro* model was developed by exposing 3D HCE-T cell-based model to osmotic stress.

3. RESULTS AND DISCUSSION

This study focuses on the development of ophthalmic formulations with high clinical potential for effective DED treatment, guided by *in vitro* biomimetic tools. Several topical glucocorticoids and NSAID have been shown to modulate ocular surface inflammation, with multiple studies demonstrating their clinical benefit in short-term DED management. Nanoemulsions, which are ultrafine oil-in-water dispersions stabilized by an amphiphilic surfactant, hold significant promise for

effective DED treatment. In addition to supplementing and stabilizing the tear film, nanoemulsions efficiently deliver active pharmaceutical ingredients with limited water solubility, such as glucocorticoids and NSAIDs, into the corneal tissue.

In this study, nanoemulsions loaded with loteprednol etabonate and ibuprofen were successfully developed. For loteprednol etabonate which is poorly soluble in water and oils, quality-by-design approach enabled the identification of formulation and process parameters with the most significant influence on drug content.

A method for evaluating the stability of nanoemulsions on the ocular surface under biorelevant dilution conditions using artificial tear solution was successfully established.

An extended-throughput corneal epithelial model was successfully developed to assess the biocompatibility of the nanoemulsions, and the developed nanoemulsion demonstrated excellent biocompatibility.

Furthermore, an innovative method combining dilution and ultrafiltration was developed to investigate the distribution of drug between the oil and aqueous phases under biorelevant dilution conditions.

The anti-inflammatory effect of loteprednol etabonate loaded nanoemulsion was evaluated using a developed *in vitro* dry eye model.

Developed *in vitro* biomimetic tools were further employed for the selection of lead formulation of latanoprost improved in terms of diminishing negative latanoprost effect on ocular surface leading to DED symptoms.

IL5

TINY NEEDLES, BIG POSSIBILITIES – MICRONEEDLE SYSTEMS IN MODERN DRUG DELIVERY

Tomasz Osmałek

Chair and Department of Pharmaceutical Technology, Poznań University of Medical Sciences, Poznań, Poland

Microneedle (MN) systems are an innovative drug delivery platform that bridges the gap between transdermal administration and injectable formulations. These minimally invasive systems enable efficient transport of active pharmaceutical ingredients through the skin, while reducing pain, avoiding bleeding, and improving patient adherence.

MNs can be fabricated in various forms—solid, coated, dissolving, hollow, or hydrogel-forming—each offering unique advantages in terms of drug release profiles, loading capacity, and ease of application.

Recent advances in manufacturing techniques, including micromolding, laser ablation, and 3D printing, have enabled precise control over microneedle geometry, size, and material composition, tailoring them to specific therapeutic or diagnostic goals.

Research in the field has demonstrated the potential of MNs for delivering substances through the skin, mucosal surfaces, and even ocular tissues. Their ability to bypass biological barriers, enhance bioavailability, and eliminate the need for cold chain storage makes them highly attractive for a wide range of medical applications.

Additionally, microneedles have shown promise in diagnostic use, such as sampling interstitial fluid for real-time biomarker monitoring.

The flexibility of design, combined with a favorable safety profile and potential for self-administration, positions MN technology as a key contributor to the future of patient-centered, non-invasive therapy and diagnostics.

References

1. Kordyl O, Styrna Z, Wojtyłko M, Michniak-Kohn B, Osmałek T. *Microneedle-based arrays - Breakthrough strategy for the treatment of bacterial and fungal skin infections. Microbes Infect. 2025 Feb;27(2):105426. doi: 10.1016/j.micinf.2024.105426*
2. Monika Wojtyłko, Anna Froelich, Barbara Jadach, Mirosław Szybowicz, Ariadna Nowicka, Tomasz Osmałek, *Chapter 8 - 3D printed microneedle patches for painless drug delivery, Fundamentals and future trends of 3D printing in drug delivery, Academic Press, 2025, Pages 185-206, https://doi.org/10.1016/B978-0-443-23645-7.00008-8.*

IL6

BUCCAL FILMS AND GRANULES-IN-STRAW AS PATIENT FRIENDLY DOSAGE FORMS

Odon Planinšek

Department of Pharmaceutical Technology, Faculty of Pharmacy, University of Ljubljana, Slovenia

Patient-friendly dosage forms in pharmaceutical technology are designed to improve ease of administration, taste, convenience, and overall patient compliance compared to traditional solid tablets or capsules. These dosage forms address issues such as difficulty swallowing, unpleasant taste, and the need for flexible dosing, especially for populations like children and the elderly. The two of such dosage forms are discussed in the following text.

1. Buccal fims

Buccal films offer numerous advantages that make them highly acceptable and convenient for patients. Buccal films are thin, flexible strips that adhere to the mucosal lining inside the cheek, allowing the drug to be absorbed directly into the bloodstream, bypassing the digestive system and first-pass metabolism. This leads to rapid onset of action and enhanced bioavailability.

Key patient-friendly features of buccal films include:

- No need for chewing or swallowing, reducing choking risk, which is especially beneficial for pediatric and geriatric patients.
- Convenient and discreet administration without water.
- Taste-masking capabilities and good mouth feel improve patient adherence.
- Accurate dosing compared to liquid forms.
- Reduced side effects due to localized release and rapid absorption.
- Cost-effective, stable, and easy to manage and transport.

Bilayer buccal films are an advanced formulation designed to enhance drug delivery and patient experience, including improved taste masking. Typically, the layer facing the oral mucosa contains mucoadhesive polymers for strong attachment, while the outer layer controls drug release away from taste buds, minimizing bitter taste perception. It is reasonable to estimate that approximately 20-30 distinct buccal film products are currently marketed globally with therapeutic doses from 0.075 for Buprenorphine to 17,5 mg for Diazepam. Today a dose adjustment is made by prescribing different strengths or numbers of films, however cutting buccal films in a pharmacy for dose adjustment as a form of personalized medicine could theoretically be a future solution.

2. Granules in a straw

Granules in a straw as another patient-friendly dosage form offer several distinct advantages:

- Improved Swallowing and Taste Masking: The granules enclosed in a straw can be coated with taste-masking polymer, making them nearly tasteless when ingested with a beverage. This is particularly beneficial for children and elderly patients who have difficulty swallowing tablets or dislike the bitter taste of medicines. Patients sip a beverage through the straw while simultaneously taking the medication.
- Ease and Convenience: The dosage is pre-measured and pre-dosed by the manufacturer, eliminating the risk of dosing errors. The straw device is easy to use and can be combined with a drink of choice, increasing patient compliance.
- Dose Flexibility and Accuracy: Dosing is accurate due to the pre-filled, measured granules in the straw and the control filter/valve, ensuring the entire dose is ingested.
- Stability and Storage: The straw packaging with granules often uses hermetically sealed components, ensuring no special storage conditions are required, which is convenient for patients and caregivers.

In the future, a pharmacy could use a digital dispenser to precisely count and combine

granules of different medications—each granule a pre-measured dose—into a single straw, creating a custom, multi-drug dose tailored to a patient's specific prescription. This allows for accurate, personalized combinations that are impossible to achieve by splitting pills, making complex regimens much simpler and safer for the patient to take.

Both of the described dosage forms offer promising, patient-friendly features but must overcome significant formulation, stability, and manufacturing challenges to realize their full potential as convenient and effective future therapies.

References

1. Shipp L, Liu F, Kerai-Varsani L, Okwuosa TC. Buccal films: A review of therapeutic opportunities, formulations & relevant evaluation approaches. J Control Release. 2022; 352: 1071-1092.
2. Subramanian, P. Mucoadhesive Delivery System: A SmartWay to Improve Bioavailability of Nutraceuticals. Foods. 2021; 10: 1362.
3. Grilc, B.; Planinšek, O. Evaluation of Monolayer and Bilayer Buccal Films Containing Metoclopramide. Pharmaceutics. 2024; 16: 354.
4. Simšič T, Nolimal B, Minova J, Baumgartner A, Planinšek O. A straw for paediatrics: How to administer highly dosed, bitter tasting paracetamol granules. Int J Pharm. 2021; 602: 120615.

IL7

OPTIMIZING DOSING REGIMEN OF VEDOLIZUMAB IN PATIENTS WITH INFLAMMATORY BOWEL DISEASE: CHOOSING THE RIGHT PHARMACOKINETIC MODEL FOR ROUTINE THERAPEUTIC DRUG MONITORING

Katarina Vučićević

Department of Pharmacokinetics and Clinical Pharmacy, University of Belgrade – Faculty of Pharmacy, Republic of Serbia

1. INTRODUCTION

Vedolizumab (VDZ) is a monoclonal antibody approved for the treatment of inflammatory bowel disease (IBD). Model-informed precision dosing (MIPD) is a powerful approach to individualize drug dosing and optimize therapeutic outcomes. It can integrate therapeutic drug monitoring (TDM) data and advance TDM-based dosing individualization. *A priori* dose individualization is guided by pharmacometric model-derived covariates, whereas *a posteriori* individualization incorporates both model covariates and one or more observed concentrations to refine dosing predictions. A critical component of MIPD is the selection of the most appropriate population pharmacokinetic (PopPK) model for predicting optimal dosing regimen based on individual demographic and clinical patient characteristics with highest probability of reaching target drug concentrations. The number of published VDZ PopPK models remains limited [1-3], and their clinical applicability has not yet been systematically evaluated. To determine the most suitable models for VDZ dosage individualization, we conducted an external evaluation of available models and developed our model using routine TDM samples.

2. MATERIALS AND METHODS

2.1. Materials

A cohort of 106 IBD patients treated at the University Medical Center "Zvezdara" in the Republic of Serbia provided on average 1-2 VDZ trough concentrations. Demographic, disease, laboratory and prior/current treatment characteristics were available as well [4,5].

2.2. Methods for Monte Carlo Simulations and Predictive Performance of Existing PopPK Models

A comprehensive review identified several published PopPK models of VDZ [1-3], each incorporating similar or distinct covariates in varying ways. The models were utilized for Monte Carlo simulations to generate PK profiles based on covariate combinations specified within the models and the standard dosing regimen. In addition, these models were externally evaluated using TDM measurements and population predictions based on characteristics of our cohort of patients. Range of prediction error metrics were employed to determine bias and precision. Additionally, simulation-based diagnostics, were utilized to evaluate model performance.

2.3. Development of VDZ PopPK Model

VDZ concentrations were analyzed using a nonlinear mixed-effects modeling approach implemented in NONMEM® software (Icon Development Solutions, version 7.5) utilizing PopPK model developed by Rosario et al. [1] within the $PRIOR block. The association between VDZ clearance (CL) and demographic, treatment, and clinical characteristics was investigated using an automated stepwise covariate modeling approach.

3. RESULTS AND DISCUSSION

3.1. Simulations and Prediction Parameters based on VDZ PopPK models

We have evaluated all existing PopPK models, while Fig. 1 presents simulations based on Rosario et al. model [1].

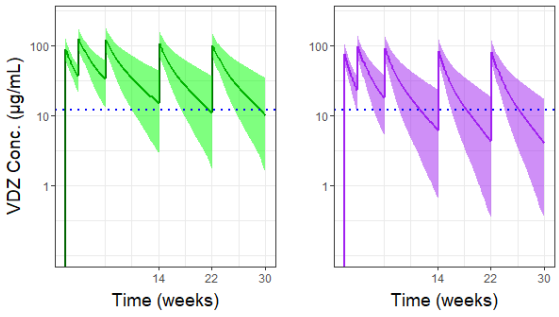

Figure 1. Simulated PK profile based on model by Rosario et al. [1] following 8-week dosing during maintenance in Crohn's disease population characterized by: (left) no previous biologic treatment, body weight 70 kg, no anti-VDZ antibodies detected, albumin 40 g/L and (right) previous biologic treatment, body weight 100 kg, detected anti-VDZ antibodies, albumin 30 g/L. Blue dotted line represents level of 12 μg/mL.

Median prediction error (MDPE) and median absolute prediction error (MAPE) for *a priori* predictions based on the patients' covariates and Rosario et al. model [1] and calculated by comparing predictions with measurements resulted in values of 25.57% and 47.56%, respectively [4].

3.3. Characterization and Clinical Implications of Developed VDZ PopPK Model

A high degree of interindividual variability in VDZ concentrations was observed. A systematic evaluation of covariates revealed a significant difference in VDZ CL in patients with *prior* exposure to infliximab or adalimumab therapy, with CL being, on average, 26.4% higher in previously treated patients compared to anti-TNFα-naïve individuals [5]. In our final model, the variance of the interindividual random effects associated with CL was estimated at 0.0269 [5]. Based on our PopPK model, the median trough VDZ concentration during the maintenance phase following an 8-week treatment regimen was predicted to be 11.6 ng/mL in anti-TNFα-naïve patients and 6.82 ng/mL in those with *prior* anti-TNFα exposure [5]. Our model can be used to predict VDZ concentration-time profiles across different dosing regimens, both in the presence and absence of TDM data, for patients with and without prior anti-TNFα treatment.

4. CONCLUSION

These findings underscore the challenges in selecting appropriate PopPK model(s) for VDZ dosing in IBD patients. While tested models exhibit limitations in predictive performance, certain models may still offer value in specific clinical contexts. Prospective validation and potential model refinement are essential before their implementation in clinical practice.

5. REFERENCES

1. Rosario, M., et al., *Population pharmacokinetics-pharmacodynamics of vedolizumab in patients with ulcerative colitis and Crohn's disease*. Alimentary Pharmacology & Therapeutics, 2015. 42: 188-202.
2. Okamoto, H., et al., *Population pharmacokinetics of vedolizumab in Asian and non-Asian patients with ulcerative colitis and Crohn's disease*. Intestinal Research, 2021., 19: 95-105.
3. Hanzel, J., et al., *Pharmacokinetic-pharmacodynamic model of vedolizumab for targeting endoscopic remission in patients with Crohn disease: Posthoc analysis of the LOVE-CD study*. *Inflammatory Bowel Diseases*, 2022. 28: 689-699.
4. Jovanović, M., et al., *Review and External Evaluation of Population Pharmacokinetic Models for Vedolizumab in Patients with Inflammatory Bowel Disease: Assessing Predictive Performance and Clinical Applicability*. Biomedicines, 2024. 13(1): 43.
5. Marković, S., et al., *Vedolizumab Clearance as a Surrogate Marker for Remission in Inflammatory Bowel Disease Patients: Insights from Real-World Pharmacokinetics*. Pharmaceutics, 2024. 16(12): 1629.

ACKNOWLEDGMENT

This research was supported by the Science Fund of the Republic of Serbia, through grant agreement No. 6777, Improving Clinical Outcomes with Precision Dosing in Patients with Inflammatory Bowel Disease Through Investigating Variability of Monoclonal Antibodies Based on Population Pharmacokinetic-Pharmacodynamic Modeling-optYmAb. I would like to acknowledge the support and collaboration of all optYmAb team members from University of Belgrade – Faculty of Pharmacy and University Medical Center "Zvezdara", Belgrade, Serbia.

IL8

IMMUNE CHECKPOINT INHIBITORS IN CANCER IMMUNOTHERAPY: OPTIMIZING DRUG THERAPY TO IMPROVE TREATMENT OUCTOMES

Lea Knez[1, 2]

[1]*Faculty of Pharmacy, University of Ljubljana, Slovenia*
[2]*Pharmacy, University Clinic Golnik, Slovenia*

1. INTRODUCTION

Immunotherapy with immune checkpoint inhibitors (ICI) has dramatically changed the treatment of numerous cancers, achieving long-term responses alluding to the possibility of cure also in traditionally poor prognosis cancers as metastatic melanoma or advanced non-small cell lung cancer (aNSCLC). As ICI have been entering the treatment arena of various types of cancers, various disease settings and medicine combinations, it is imperative to assess and streamline drug therapy to improve treatment outcomes in everyday clinical practice. Some of the efforts undertaken by researchers from the University Clinic Golnik and Faculty of Pharmacy, University of Ljubljana will be presented within this lecture.

2. THE EFFICACY - EFFECTIVENESS GAP OF IMMUNOTHERAPY

Translating the encouraging results achieved in the highly defined frame of randomised clinical trials (RCT) into the variable and unpredictable situations in routine clinical practice may be challenging. The efficacy-effectiveness gap may be informed only by real-world studies, which are imperative in the case of introduction of new treatment modalities with a very peculiar mode of action and unique toxicities as ICI immunotherapy.

Thus we conducted an observational study with 176 consecutive patients with aNSCLC, treated with first-line ICI, either as monotherapy (mono-IT; 118 patients) or in combination with chemotherapy (chemo-IT; 58 patients), at a single academic institution [1]. The observed median overall survival (mOS) was 19.4 months and 21.3 months in the mono-IT and chemo-IT, respectively. These results largely compare with those from the pivotal RCTs of ICIs, despite our cohort includes patients with poorer performance and more comorbidities than those included in RCTs.

Severe adverse events of grade 3 or 4 according to the Common Toxicity Criteria for Adverse Events were recorded in 18% and 26%, and treatment discontinuation in 19% and 9% of patients in the mono-IT and chemo-IT group, respectively. No treatment-related death was recorded. The observed safety profile compares favorably with data from RCTs, possibly also due to earlier treatment discontinuation of ICI and underreporting of adverse events within routine clinical practice.

These data are reassuring and especially important as firsts among those originated from the Central Eastern European area, characterized by a lack of healthcare resources resulting in a gap in cancer control compared to Western Europe.

3. THE HARM OF HARMLESS DRUGS

Treatment with ICI roughly doubled the survival of patients with a NSCLC. Still, only a third of patients respond to treatment, thus research efforts are directed towards understanding the mechanisms of intrinsic and extrinsic resistance to ICI therapy to identify ways to overcome it. Among others, medicines that alter gut microbiota may interfere ICI effectiveness. In post-hoc analyses of RCTs and observational studies exposure to proton pump inhibitors (PPI), antibiotics (atb) and other medicines were associated with worse survival in patients treated with ICI. As medicine use may differ in various healthcare systems and geographic regions, we assessed the impact of selected concomitant medicines on ICI outcomes in a cohort of nearly 400 consecutive patients with aNCLC, treated with ICI in any setting or combination.

Within this aim we assessed the use of atb within the year prior and until the end of ICI treatment [2]. Most patients (70%) were prescribed an atb, most often a penicillin (57%), receiving a median of 2 exposures and 23 daily

defined doses (DDD) within the observation period. Prescription of atb within one year prior to ICI was associated with shorter mOS (atb vs non-atb: 17.0 vs 25.4 months; HR=1.20; 95% CI: 1.00-1.67) in uni- but not multivariate analysis. Use of atb is common in patients with aNSCLC and may hamper ICI treatment, thus strategies to minimize unnecessary atb use should be explored in future research.

Further on we assessed the impact of the timing and intensity of PPIs treatment on survival outcomes [3]. Expectedly, nearly 75% of patients had access to PPIs within 1 year prior to 30 days after start of ICI. PPI exposure within 30 days of ICI start (PPI vs no PPI: 15.4 vs 21.9 months; aHR= 1.373; 95% CI: 1.007-1.873) and being exposed to over 159 DDD within the entire observation period (high vs low exposure: 13.4 vs 21.9 months; aHR=1.454; 95% CI: 1.023-2.067) was associated with worse survival in multivariate analysis. Overprescribing of PPIs is common [4], and the detrimental effect of PPIs may be largely avoided by simply implementing deprescribing activities. However, as shown by our research and as supported by the known lag time between PPI discontinuation to the restoration of gut microbioma, PPI deprescription should be done well in advance of start of ICI, possibly implying actions on a population level. And that is the direction of our further research activities.

4. CONCLUSION

Immunotherapy with ICI has significantly improved the outcomes of patients with numerous cancers, including aNSCLC. Future efforts should be directed towards understanding the challenges of their use within routine clinical practice. A preventive approach to avoid medicines, that may hamper ICI effectiveness, should be prioritised over reactive approaches adding more medicines to overcome the harm impose by medicines, often presumed as harmless as PPIs.

5. REFERENCES

[1] Pelicon, V., *et al*., *Real-world outcomes of immunotherapy with or without chemotherapy in first-line treatment of advanced non-small cell lung cancer*. Front Oncol, 2023, 13: doi: 10.3389/fonc.2023.1182748.

[2] Knez, L., *et al*., *Antibiotic prescription patterns and their association with outcomes in patients with advanced non-small cell lung cancer (aNSCLC) treated with immune checkpoint inhibitors (ICI)*. *J Thorac Oncol*, 2025, 20:S244.

[3] Japelj, N., *et al., Association of the timing and intensity of proton pump inhibitor exposure with overall survival in patients with immune checkpoint inhibitors: a retrospective cohort study.* Article under Revision.

[4] Ravbar, N., *et al., Deprescribing proton pump inhibitors: A study in hospitalized patients in Slovenia.* Int J Clin Pharmacol Ther, 2023, 61:306–14.

ACKNOWLEDGMENT

The author would like to acknowledge the contribution of researchers from the University Clinic Golnik and Faculty of Pharmacy University of Ljubljana, participating patients and treating oncologist from the University Clinic Golnik.

IL9

PERSONALIZED BIORELEVANT DISSOLUTION TESTING: ADDRESSING THE IMPACT OF POPULATION & DISEASE VARIABILITY ON ORAL DRUG PERFORMANCE

Sandra Cvijić

Department of Pharmaceutical Technology and Cosmetology, University of Belgrade-Faculty of Pharmacy, Serbia

1. INTRODUCTION

Dissolution testing remains a cornerstone of pharmaceutical development, ensuring consistent drug release profiles and predicting in vivo drug performance, especially for solid oral dosage forms. While traditional methods rely on standardized conditions defined by pharmacopeia and regulatory guidelines, emerging research highlights the need for personalized approaches that account for population-specific physiological variability and disease-driven gastrointestinal (GI) alterations [1,2]. This presentation explores current practices, challenges, innovations and needs in designing biorelevant dissolution tests tailored to diverse patients' demographic and (patho)physiological data.

2. CURRENT PRACTICES AND REGULATORY FRAMEWORKS

Regulatory recommendations prioritize dissolution methods that discriminate between critical formulation and manufacturing changes. Consequently, for most formulations, testing under standardized conditions, including conventional buffer media in a paddle or basket apparatus, is considered sufficient. On the other hand, recent trends highlight the need for dissolution testing under biorelevant conditions (e.g., in fasted/fed state simulating media) to better predict oral drug clinical performance [3]. However, these approaches do not specifically address population- or disease-specific GI barriers for drug dissolution.

3. DESIGNING A PERSONALIZED BIORELEVANT DISSOLUTION TEST

3.1. Challenges in Dissolution Test Design

The selection of biorelevant dissolution test conditions is guided by multiple factors, including drug physicochemical properties, formulation type, (pato)physiological characteristics of the GI tract (which may also be influenced by concomitant intake of food, drugs or dietary supplements), and the specific purpose of the study.

Compendial dissolution tests fail to capture diverse GI environment of specific population or disease groups, risking underestimation of a drug in vivo performance. Therefore, the key challenges in designing personalized biorelevant dissolution test include identifying and mimicking the specific GI conditions of the target patien groups (Fig. 1). This is not an easy task considering that robust GI physiological data for certain patient groups are often lacking. In additions, in vitro dissolution test findings may be difficult to interpret in terms of clinical significance [3,4].

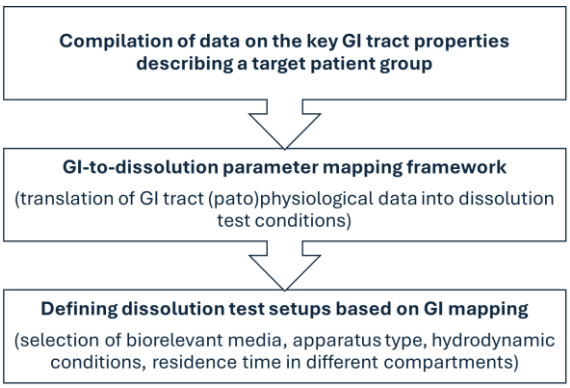

Figure 1. Selection of a target population/disease-specific dissolution test conditions.

3.2. Population and Disease Specific Variability

Although distinct physiological characteristics, influenced by factors such as age, genetics, and comorbidities, define each population, the critical GI parameters governing drug dissolution are alterations in luminal pH and GI motility (including gastric emptying rates). Furthermore, variations in media composition (e.g., enzyme and surfactant concentrations), luminal volume and viscosity are important determinants of drug dissolution [3]. Some examples of population/disease-specific GI alterations affecting drug dissolution are noted in Table 1.

Table 1. Examples of GI parameters informing personalized dissolution test design.

Population/ Disease/Condition	Key considerations (GI parameters)
Paediatric patients	Reduced stomach volume; Altered gastric pH, gastric emptying, GI motility pattern and luminal viscosity; Reduced bile salts concentration
Geriatric patients	Reduced saliva excretion; Altered gastric pH; Decreased GI motility; Reduced bile salts concentration
Hypochlorhydria/Achlorhydria	Reduced gastric acidity (increased stomach pH)
Diabetes	Delayed gastric emptying; Altered intestinal pH
Crohn's disease	Reduced gastric acidity (increased stomach pH); Reduced gastric and increased small intestine transit time; Reduced bile salts concentration
Parkinson's disease	Delayed gastric emptying; Increased gastric pH; Reduced GI fluid volume; Increased intestinal viscosity; Altered motility pattern
Bariatric patients	Reduced stomach volume; Increased gastric pH; Decreased gastric transit time; Altered gastric contractility

3.3. Efforts Toward Patient-Centric Dissolution Methods

Contemporary research initiatives have made significant progress in developing biorelevant dissolution methods tailored to mimic population or disease-specific GI conditions. This presentation will address some of the examples documented in literature. While these studies demonstrate proof of concept, further standardization and validation are needed to fully integrate personalized dissolution testing into routine practice and regulatory evaluation.

4. CONCLUSION

Patient-specific GI conditions can profoundly affect drug dissolution and, consequently, therapeutic outcomes. This highlights the need for personalized dissolution testing that aligns in vitro models with patient-specific GI (patho)physiology. In parallel, regulatory frameworks must evolve to accommodate these innovations, ensuring equitable drug efficacy across diverse populations/disease groups.

5. REFERENCES

1. Masada, T., et al., *Bioequivalence of oral drug products in the healthy and special populations: Assessment and prediction using a newly developed in vitro system "BE Checker".* Pharmaceutics, 2021. 13(8): 1136.
2. McAllister, M., et al., *Developing clinically relevant dissolution specifications (CRDSs) for oral drug products: Virtual webinar series.* Pharmaceutics, 2022. 14(5): 1010.
3. de Lemos, H., et al., *Use of biorelevant dissolution media in dissolution tests as a predictive method of oral bioavailability.* Brazilian Journal of Pharmaceutical Sciences, 2022. 58(3): e19759.
4. Mire-Sluis, A., et al., *Patient-Centric Quality Standards.* Journal of Pharmaceutical Sciences, 2024. 113(4): 837-855.

ACKNOWLEDGMENT

This presentation was prepared within the framework of two Grant Agreements between the University of Belgrade-Faculty of Pharmacy and Ministry of Science, Technological Development and Innovation, Republic of Serbia (grants No 451-03-136/2025-03/ 200161 and No 451-03-137/2025-03/ 200161).

IL10

PROFILING OF PHYTOCANNABINOIDS IN MEDICINAL CANNABIS PLANT MATERIAL VIA SOLID-PHASE MICROEXTRACTION APPROACH

Anna Roszkowska[1,2], Katarzyna Woźniczka[1], Václav Trojan[3,4], Joanna Bogusiewicz[5], Krzysztof Urbanowicz[6], Patrik Schreiber[3], Barbara Bojko[5], Ryszard Tomasz Smoleński[6], Janusz Pawliszyn[2], Tomasz Bączek[1]

[1]Department of Pharmaceutical Chemistry, Medical University of Gdańsk, Gdańsk, Poland
[2]Department of Chemistry, University of Waterloo, Waterloo, Canada
[3]Cannabis Facility, International Clinical Research Centre, Czech Republic
[4]Department of Natural Drugs, Masaryk University, Czech Republic
[5]Department of Pharmacodynamics and Mol. Pharmacology, Nicolaus Copernicus University, Bydgoszcz, Poland
[6]Department of Biochemistry, Medical University of Gdańsk, Gdańsk, Poland

1. INTRODUCTION

Solid-phase microextraction (SPME) is a non-exhaustive sample preparation technique that enables the extraction of low molecular weight compounds from complex biological matrices [1-3]. In this study, SPME was optimized and applied for direct isolation of phytocannabinoids (PCs) from growing *Cannabis spp.* plants (*in vivo* conditions) and also from dried plant material [4].

2. MATERIALS AND METHODS

In vivo SPME utilizing biocompatible C18 probes along with liquid-chromatography coupled with quadrupole time-of flight mass spectrometry (LC-Q-TOF-MS) facilitated the extraction and analysis of acidic forms of PCs in growing medicinal cannabis plants [4].

3. RESULTS AND DISCUSSION

SPME probes were statically inserted into the inflorescences of two varieties of *Cannabis spp.* plants (*i.e.*, CBD-dominant and Δ9-THC-dominant) cultivated under controlled conditions. The results confirmed that the developed method is a precise and efficient tool that enables direct and rapid isolation and analysis of PCs under *in vivo* conditions without the need for collection of plant material. In addition, SPME probes were used for monitoring of the content and composition of PCs (acidic and neutral forms) at different stages of cannabis plant material handling, from harvest of plants to final decarboxylated product. Extracts obtained by SPME technique were analysed according to the recommendations of US Pharmacopeia utilizing high performance liquid chromatography (HPLC) with UV detection and with liquid-chromatography coupled with quadrupole time-of flight mass spectrometry (LC-Q-TOF-MS) [4].

4. CONCLUSION

The proposed SPME-based methodologies can be used as an additional quality tool for monitoring the content of particular PCs in the medicinal cannabis plant cultivation facilities and during cannabis plan material production [4].

5. REFERENCES

1. Leszczyńska, D., et al., *Recent advances in the use of SPME for drug analysis in clinical, toxicological, and forensic medicine studies*. Talanta, 2024. 270: 125613.
2. Woźniczka, K., et al., *SPME as a green sample-preparation technique for the monitoring of phytocannabinoids and endocannabinoids in complex matrices*. Journal of Pharmaceutical Analysis, 2023. 13: 1117.
3. Roszkowska, A., et al., *Monitoring of age- and gender-related alterations of endocannabinoid levels in selected brain regions with the use of SPME probes*. Metabolomics, 2023. 19(40): 1.
4. Woźniczka, K., et al., *In vivo profiling of phytocannabinoids in Cannabis spp. varieties via SPME-LC-MS analysis*. Analytica Chimica Acta, 2024. 1306: 342621.

Oral presentations

OP1

PREDICTING 3D PRINTABILITY OF SEMI-SOLID EXTRUSION FORMULATIONS USING RHEOLOGICAL DATA AND MACHINE LEARNING MODELS

Teodora Tasevska[1], Nikola Geskovski[1], Katerina Goracinova[1], Riste Popeski Dimovski[2], Maja Simonoska Crcarevska[1]

[1]Faculty of Pharmacy, Ss. Cyril & Methodius University in Skopje, R North Macedonia
[2]Faculty of Natural Sciences and Mathematics, Ss. Cyril & Methodius University in Skopje, R North Macedonia

1. INTRODUCTION

Rheological properties are essential in determining the printability of pharmaceutical inks in 3D printing, affecting both filament formation (FF) and layer stacking (LS). A balance of elastic, viscous, and capillary forces control filament formation, while rapid structural recovery after extrusion is crucial to prevent layer deformation [1].

The aim of the study was to assess the 3D printability potential of semi-solid extrusion formulations by applying machine learning models, using rheological data as input variables and FF and LS results as output variables.

2. MATERIALS AND METHODS

2.1. Preparation of hydrogels for 3D printing

Twenty-four hydrogel formulations were prepared using different polymers. Eighteen P407 formulations (BASF, Germany) (16.08–45.81% m/V) were made by the cold method, and additional formulations with tragacanth (7% and 10%) and chitosan (10%) (Sigma-Aldrich, USA) by direct dispersion in distilled water. Sixteen P407 formulations included active substances: cefixime (ten) and probiotic, Diastop® (six) (Alkaloid AD, N. Macedonia).

2.2. Rheology, filament, layer stacking test

The rheology was analyzed using a modular compact rheometer (MCR 92, Anton Paar, Austria) with a Peltier temperature control. The amplitude sweep method [2], was used to measure shear stress, storage modulus (G′), loss modulus (G″), loss factor (tan δ), torque and complex viscosity (η*) (CP50-1 cone geometry, zero gap 0.104 mm, 25 ± 0.1 °C, angular frequency 10 rad s^{-1}, shear strain 0.1–100%, 31 data points over 500 seconds).

Hydrogels were loaded into 3 mL pneumatic cartridges and placed on the 3D bioprinter (BioX, Cellink, Sweden). The hydrogels were extruded through a 22G nozzle for 3 seconds, and FF morphology was assessed. Filaments were classified as 0 (drop), 1 (curved), or 2 (straight >5 mm), with straight string-like filaments considered printable [3]. For LS two perpendicular lines from each formulation were extruded through a 22G nozzle onto a microscope slide, forming a cross, and analyzed under stereomicroscope (ZEISS Stemi 305). Based on layer definition and structural integrity, formulations were scored as: 0 (complete fusion), 1 (unclear boundary), or 2 (distinct layers with clear separation) [3].

2.3. Machine learning model training and evaluation

Features were extracted and standardized using StandardScaler. For 1D Convolutional neural network (CNN) models, categorical targets were one-hot encoded with Keras' to_categorical function, and inputs were reshaped into 3D arrays (input variables, shear strain steps, output variables). For the Random Forest Classifier (RFC) model, targets were encoded using scikit-learn's OrdinalEncoder, and the data was retained in its original tabular format. A basic CNN model (1D convolution, 32 filters, kernel size 2, max-pooling, dropout, softmax output), a deeper CNN model (two convolutional layers with 64 and 128 filters), and an advanced CNN model (convolutional blocks with Batch Normalization, LeakyReLU, dropout, trained for 150 epochs with early stopping) were developed. RFC model (100 trees) was also trained on standardized features to predict FF and LS scores. The data were split 80/20 for training and testing. Model performance was evaluated using confusion matrices, and per-class accuracy. Additionally, for CNNs, loss and accuracy curves were used. Feature importance was calculated for the RF model to assess the contribution of each rheological parameter. The analysis was conducted with Python libraries: pandas,

numpy, scikit-learn, Keras (TensorFlow), matplotlib, and seaborn.

3. RESULTS AND DISCUSSION

The study analyzed 24 polymer formulations characterized by six rheological parameters measured at 31 shear points, to predict 3D printability, assessed through FF and LS scores (0–2). The dataset comprised 4,464 input data points. CNNs were chosen for their ability to capture temporal dependencies, while the RFC was selected for multi-class classification and feature importance insights.

The basic CNN model accurately predicted low printability (Class 0: FF 0.92, LS 0.88 per-class accuracy) but struggled with high-quality prints (Class 2), particularly in FF (0.35), while performing better in LS (0.80). It also showed moderate performance for intermediate prints (Class 1), with better accuracy for FF (0.74) but poor performance in LS (0.00). The deeper CNN model improved the prediction for high-quality prints (Class 2) in FF (0.81), although accuracy in LS decreased (0.64). It also handled extremes better (Class 0: FF 0.92, LS 0.98) but showed lower accuracy for Class 1 (FF 0.56), though LS improved (0.78). The advanced CNN model further enhanced Class 0 prediction (FF 0.97, LS 0.94), but faced difficulties with Class 2 (FF 0.32, LS 0.53). For Class 1, it performed slightly better than the deeper CNN (FF 0.58, LS 0.83). The RFC excelled at predicting high-quality prints (Class 2) in LS (0.97) but showed lower performance for FF (0.48) compared to the deeper CNN. It achieved strong performance for Class 1 (FF 0.94) but was slightly lower in LS (0.73) compared to the deeper and advanced CNN models. For Class 0, the RFC model was consistent (FF 0.88, LS 0.88), demonstrating the highest overall reliability and providing valuable feature importance insights. For FF prediction, the top features influencing printability include η^* (0.22 value of feature importance) dictating flow during extrusion, G' (0.20) ensuring shape retention, and torque (0.16), reflecting the force required for material processing. For LS, the most significant features were η^* (0.21) (crucial for material flow and layer formation), torque (0.19) (vital for extrusion), and G' (0.19) (good adhesion and structural integrity of layers).

4. CONCLUSION

The deeper CNN performed best for predicting high-quality prints (Class 2) in FF. Although the RFC showed weaker performance for Class 2 in FF compared to the deeper CNN, it demonstrated strong performance in LS. Taking all results into account and considering the RFC's capability for feature importance analysis, it can be considered as more suitable for assessing and explaining the 3D printability potential of semi-solid extrusion formulations.

5. REFERENCES

1. Barrulas, R.V., et al., *Rheology in product development: an insight into 3D printing of hydrogels and aerogels*. Gels, 2023. 9: 986.
2. Dutta, S.D., et al., *Electromagnetic field-assisted cell-laden 3D printed poloxamer-407 hydrogel for enhanced osteogenesis*. RSC Advances, 2021. 11(33): 20342–20354.
3. O'Connell, C., et al., *Characterizing bioinks for extrusion bioprinting: printability and rheology*. Methods in Molecular Biology, 2020. 2140:111-133.

ACKNOWLEDGMENT

The authors appreciate the project “Improving the technical competence of the Center for pharmaceutical nanotechnology by introducing standard analytical procedures in rheometry and 3D bioprinting” (2021-2023). Additionally, the authors would like to express their gratitude to Alkaloid AD Skopje, N. Macedonia, for their generous donation of cefixime.

OP2

FROM POWDER TO A PERSONALIZED TABLET: OPTIMIZING DIRECT POWDER EXTRUSION 3D PRINTING FOR TABLET MANUFACTURING

Paola Šurina[1,2], Simone Eder[1], Andreas Kottlan[1], Ivan Raguž, Josip Matić[1], Amrit Paudel[3], Patrizia Ghiotti[3], Thomas Quinten[3], Laura Martinez Marcos[3], Martin Spoerk[1,2]

[1]Research Center Pharmaceutical Engineering GmbH, Inffeldgasse 13, 8010 Graz, Austria
[2]Institute for Process and Particle Engineering, Graz University of Technology, Inffeldgasse 13/3, 8010, Austria
[3]Janssen Pharmaceutica, Pharmaceutical Companies of Johnson & Johnson, Turnhoutseweg 30, 2340 Beerse, Belgium

1. INTRODUCTION

Although fused filament fabrication (FFF) is the most widely explored material extrusion-based 3D-printing technology in the pharmaceutical field, its applicability is limited by the filament's mechanical properties, which prevents the processing of brittle polymers such as Soluplus®. To overcome this limitation, Direct Powder Extrusion (DPE) was utilized as an alternative approach, allowing direct 3D-printing of powder blends without the need for filament fabrication.

DPE is an emerging 3D-printing technology for manufacturing pharmaceutical tablets, offering precise dosage control and formulation flexibility [1]. While the process eliminates the need for filament preparation, it introduces new challenges. Powder blends may exhibit significant differences in bulk densities and cohesion, often leading to flowability issues which can cause inconsistent extrusion or even clogging. This study aims to optimize the DPE process by compensating powder flow issues through technical and formulation adjustments to ensure a stable material flow and consistent tablet production.

2. MATERIALS AND METHODS

2.1. Materials

A BCS class II model API and Soluplus® were supplied by Johnson & Johnson Innovative Medicine (Belgium). Kollidon® CL was kindly provided by BASF and Aerosil® 200 Pharma was purchased from Evonik.

2.2. Powder (blends) characterization

Particle size and shape were characterized for both Soluplus® and the API using the QICPIC dynamic picture analyzer. Bulk and tapped density were measured and the Carr's Index calculated as an indicator of powder flowability. Melt rheology was conducted at temperatures above the glass transition (T_g) of the excipient and below the degradation temperature (T_{deg}) of the API to assess optimal viscosity, as viscosity requirements for DPE have not yet been identified.

2.3. Printing process

A Direct3D single screw pellet based printhead with an in-house built building platform was used (Fig. 1A). Besides adapting the barrel (165–170 °C) and build platform temperature (55 °C), nozzle size (0.8 mm), extrusion multiplier (EM; 5-15), and infill (50 and 70% rectilinear and 100% concentric), the following adaptations were performed: incorporation of a printhead motor with increased power to address increased friction in the extruder due to the use of powder instead of pellets and attaching an agitator onto the screw to further improve powder flow through the gravity-fed hopper system. To assess flow behavior and process stability, tablets were printed consecutively and weighed. Additionally, Aerosil® (4 w%) as a flow aid, and Kollidon® CL (4 w%) as a disintegrant were added.

2.4. Tablet characterization

Tablets were evaluated for mass uniformity, disintegration and in-vitro dissolution. Solid-state characteristics were assessed using differential scanning calorimetry (DSC) starting from 20°C to below the API's T_{deg}.

3. RESULTS AND DISCUSSION

3.1. Powder (blends) characterization

The spherical Soluplus® particles showed good flowability with a Carr's index (Fig. 1B) of 15.2 ± 1.4. Yet, the addition of 30% API significantly increased the Carr´s index to 46.4 ± 1.4 due to non-spherical API particles, rendering the blend a poorly flowable powder. The optimal viscosity was identified at ~50 Pa·s at 165 °C (Fig. 1C),

since the blend revealed ideal printability at this barrel temperature.

3.2. Printing process

Due to the decrease in bulk density of the powder blend in contrast to filaments, the EM as a crucial factor for avoiding under-extrusion had to be increased 5-7 times compared to FFF [2]. Initial printing trials revealed a significant decrease in tablet mass (Fig. 1D) with the tablet printed fourth showing a mass loss of 57.56 ± 0.16% compared to the tablet printed first, indicating inconsistent powder feeding. To improve flowability, Aerosil® (4 w%) was added. However, minimal improvement was observed (mass loss of 48.60 ± 2.93 %). Further, an agitator was integrated onto the screw, leading to a further reduction in mass variation. After agitator modifications, mass consistency was given, while increased motor power prevented screw twitching from cohesive powder clogging the printhead before complete melting.

3.3. Tablet characterization

DSC confirmed the API was in an amorphous state and exhibited interactions with Soluplus®. The addition of only 4 w% Kollidon CL as a disintegrant promoted disintegration and correspondingly increased the in-vitro drug release.

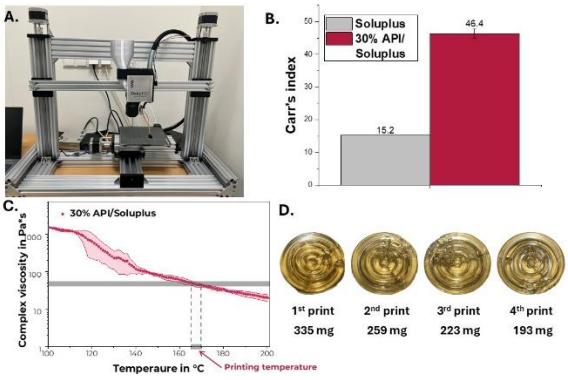

Figure 1. A. DPE printer, **B.**, Carr's Index results **C.** Temperature sweep **D.** Consecutively printed tablets with corresponding mass variations.

4. CONCLUSION

DPE was investigated as an alternative to FFF for processing brittle formulations. Adding 30% API caused flow and feeding issues, requiring motor power increase, an agitator, and EM adjustments to improve feeding, extrusion stability, and tablet uniformity, while Aerosil® had limited impact. These results emphasize the impact of mechanical adaptations in optimizing the DPE process, making it a viable technique for precise dosage control and enhanced tablet manufacturability.

5. REFERENCES

1. Aguilar-de-Leyva, Á., et al., *3D Printing Direct Powder Extrusion in the Production of Drug Delivery Systems: State of the Art and Future Perspectives., Pharmaceutucs, 2024. volume: 16.*

2. Samaro, A., et al., *Can filaments, pellets and powder be used as feedstock to produce highly drug-loaded ethylene-vinyl acetate 3D printed tablets using extrusion-based additive manufacturing?;* International Journal of Pharmaceutics, 2021, volume: 607

ACKNOWLEDGMENT

This work was funded through the "Johnson & Johnson Innovative Medicine" as part of the "WAVE" project. The Research Center Pharmaceutical Engineering (RCPE) is funded within the framework of COMET - Competence Centers for Excellent Technologies by BMK, BMAW, Land Steiermark, and SFG. The COMET program is managed by the FFG.

OP3

PRE-FORMULATION STUDIES OF SLS 3D PRINTED TABLETS

Urbanowicz Magdalena[1], Łaszcz Marta[1], Ewelina Baran[2], Kulinowski Piotr[2]

[1]Falsified Medicines and Medical Devices Department, National Medicines Institute, Warsaw, Poland
[2]Institute of Technology, Pedagogical University of Cracow, Cracow, Poland

1. INTRODUCTION

The growing interest in additive manufacturing for pharmaceutical applications has opened new possibilities for personalized drug delivery systems [1]. In this study, we explored the potential of Selective Laser Sintering (SLS) 3D printing tablets using a formulation composed of polyamide 12 (PA12) and metronidazole (Met). The raw Met, PA12, as well as their physical mixtures, were extensively characterized using Differential Scanning Calorimetry (DSC), High Performance Liquid Chromatography (HPLC) and Nuclear Magnetic Resonance (NMR) to assess their thermal and structural stability [2, 3].

The goal of the study was to investigate the feasibility of using SLS 3D printing in pharmaceutical applications, focusing on the thermal properties of polymers and APIs, as well as the potential for powder recycling to reduce waste.

2. MATERIALS AND METHODS

2.1. Materials

Met - Hubei Hongyuan Pharmaceutical Technology Co., Ltd. Fengshan, China; PA12 - carbon-stained powder, Sintratec AG, Brugg, Switzerland.

2.2. DSC

The Mettler-Toledo system DSC 3+ with IntraCooler and STARe software was used. Samples were weighed as received into aluminum crucibles then heated from 25 to 200 °C at 10 °C/min under a nitrogen atmosphere.

2.2. HPLC analysis

The HPLC Shimadzu system with LabSolution software was used. HPLC analysis was performed with a Phenomenex Gemini 5 µm, 250 × 10 mm column using a mobile phase of CH_3CN/aqueous 0.1% HCOOH, a flow rate of 1 mL/min and a gradient of 20% CH_3CN at 10 min, to 50% CH_3CN at 20 min, χ=260 nm.

2.3. NMR analysis

The NMR spectra of dissolved materials were recorded using a Varian VNMRS-500 spectrometer with a 5 mm Z-SPEC Nalorac IDG500-5HT probe and VnmrJ 3.1A software. The NMR spectra were recorded at 298 K. As an internal reference, TSPA-*d*4 was used.

2.4. Measurement protocol

Following the initial raw material characterization, the powders were subjected to SLS 3D printing [2]. After the printing process, the remaining powders were again analysed using DSC, HPLC, and NMR techniques to determine the impact of the printing process on the physicochemical stability of both PA12 and Met. Then, powders were reused for 2-5 printing process and again analysed, assessing the possibility of their repeated use without loss of structural and chemical integrity.

3. RESULTS AND DISCUSSION

3.1. Thermal analysis

DSC profiles of fresh and recycled PA12 powders demonstrated consistent thermal behaviour, with no observable shifts in melting points, melting enthalpy and crystallinity changes, or the appearance of new thermal events (Fig. 1). An endothermic peak corresponding to water loss was detected in the unprocessed powders, which was absent in powders that had undergone at least one printing cycle, indicating that moisture was effectively removed during the 3D printing process.

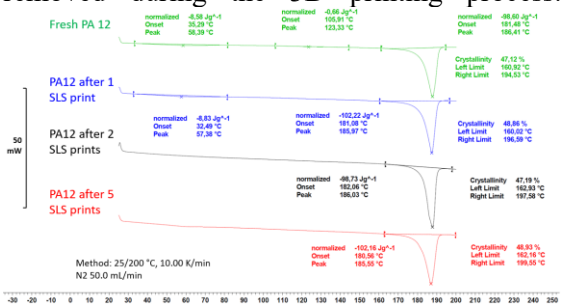

Figure 1. PA 12 thermal profiles: a) fresh powder, b) after 1 cycle, c) after 2 cycles, d) after 5 cycles.

OP3

3.2. HPLC analysis

To simulate the SLS printing process, we investigated the effect of repeated rapid heating/cooling cycles on metronidazole. Met samples were heated from 25 to 220 °C and back to 25 °C, with 200, 100, or 50 °/min step using DSC. Then samples were analysed by HPLC. Obtained chromatograms revealed the presence of a new, unidentified signal at approximately 8.5 minutes retention time. Notably, the intensity of this signal increased with the slower heating rates (100 and 50 °C/min), while when fast heating its concentration was significantly lower (Fig. 2).

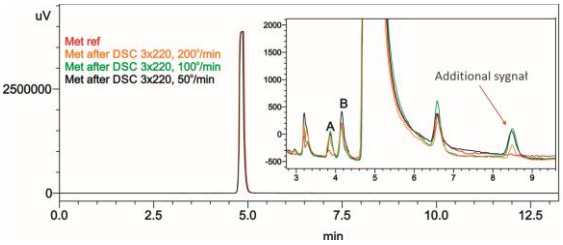

Figure 2. Comparison of chromatograms of reference Met and after 3x220 cycles.

This observation suggests that the degradation or transformation of Met is kinetically favoured under extended exposure to high temperatures. A longer exposure to high temperature likely provides sufficient time for thermally induced reactions, resulting in the formation of stable degradation products.

3.2. NMR analysis

To elucidate the identity of the compound corresponding to the newly emerged peak at 8.5 minutes in the HPLC chromatogram, the NMR analysis was performed. Obtained spectra revealed a distinct proton signal at 4.57 ppm, which was absent in the spectra of untreated metronidazole (Fig. 3).

Based on the chemical shift and signal characteristics, the observed spectra were consistent with a known degradation product, *Impurity D*. This compound is associated with thermal decomposition pathways of Met and is known to form under high-temperature conditions. This finding confirms that slower heating rates promote the formation of this impurity.

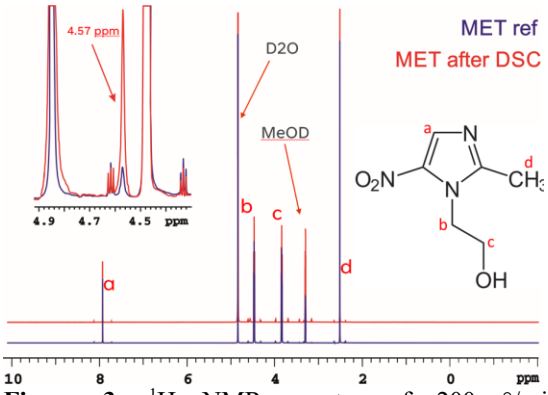

Figure 3. ^{1}H NMR spectra of 200 °/min heated/cooled Met vs reference Met.

4. CONCLUSION

Performed studies suggest that SLS printing may be a useful tool for pharmaceutical applications. PA12 is stable under the studied conditions, and its recycling for up to the 5th cycle is possible. The degradation studies of Met indicate that fast heating, which is present during the SLS printing process, does not cause a significant increase in the impurities profile. The only one observed impurity was the *Imp. D*, a degradation product, and its concentration increases only when a heat exposure is greater. The results indicate overall good formulation stability under SLS process conditions and the potential for reusing the material in the production of personalized drugs.

5. REFERENCES

1. Norman, J., et al., *A new chapter in pharmaceutical manufacturing: 3D-printed drug products. Advanced Drug Delivery Reviews, 2017: 108, 39–50.*

2. Kulinowski P., et al. *Development of Composite, Reinforced, Highly Drug-Loaded Pharmaceutical Printlets Manufactured by Selective Laser Sintering—In Search of Relevant Excipients for Pharmaceutical 3D Printing. Materials 2022: 15 (6), 2142.*

3. U. Holzgrabe, et al., *Quantitative NMR spectroscopy—Applications in drug analysis, J. Pharm. Biomed. Anal, 2005: 38 (5): 806-81.*

ACKNOWLEDGMENT

Research financed by grant 2022/45/B/NZ7/04081 from the National Science Centre, Poland.

OP4

LASER MARKING OF TABLETS FOR ANTI-COUNTERFEITING AND ITS EFFECT ON COATING INTEGRITY

Hadi Shammout[1], Krisztina Ludasi[1], Orsolya Jójárt-Laczkovich[1], Béla Hopp[2], Tamás Smausz[2], Tamás Sovány[1]

[1]Institute of Pharmaceutical Technology and Regulatory Affairs, University of Szeged, Szeged, Hungary
[2]Department of Optics and Quantum Electronics, University of Szeged, Szeged, Hungary

1. INTRODUCTION

Laser marking technology has become an essential tool in the pharmaceutical domain, especially for packaging and solid dosage forms (SDFs). This technology offers several advantages over traditional marking methods. For example, in contract with inkjet printing, the marks are usually free of cosmetic defects and resistant to environmental conditions. Furthermore, this type of marking is considered a non-contact process, reducing the risk of contamination and avoiding the need to use environmentally risky chemicals [1]. Laser marking technology may help to identify medications by creating a unique fingerprint code for the product. Furthermore, this code can also prevent drug counterfeiting and maintain its security. Not to mention the high-speed production of this technique, and its compliance with regulatory requirements [2].
This research aims to create a quick response (QR) code on the surface of the coated tablets with laser, which can be used to track and prevent drug counterfeiting. At the same time, the evaluation of the impact of this type of marking on the performance of the coatings was attempted.

2. MATERIALS AND METHODS

2.1. Materials

Ibuprofen DC 85 (BASF, Ludwigshafen, Germany) was used as a model drug in this study beside specific excipients for the tablet formulation. In addition, Acryl-EZE® MP (white) and Opadry® (brown and blue both with/without titanium dioxide TiO_2 all from Colorcon (Budapest, Hungary) were employed as film-forming polymers.

2.2. Methods

Ibuprofen tablets were directly compressed with a Korsch EK0 eccentric tablet press (E. Korsch Maschienenfabrik, Berlin, Germany) after homogenization of the materials (Turbula mixer, Willy A. Bachofen Maschienenfabrik, Basel Switzerland). Later, these tablets were coated at specific conditions as recommended by the suppliers using a perforated drum coater (ProCepT 4M8, Zelzate, Belgium). The aqueous coating dispersions were prepared with Acryl-EZE® MP (20% w/w solids) and Opadry® (15% w/w solids). In addition, a double film coating was applied to the tablets: an inner layer to obtain modified release and an outer one for laser marking.
QR codes were drawn onto the surface of the tablets by laser ablation (THz Pump #2, ELI-ALPS Research Institute). The hardness and geometry of the tablets were checked before/after coating and lasering with a MT50 tablet tester, (Sotax AG, Aesch, Switzerland). Furthermore, the readability of the QR code was evaluated. Analytical methods, including scanning electron microscope (SEM, Hitachi, Japan S4700), profilometry studies (Veeco, Dektak 8 Advanced Development Profiler®), Raman spectroscopy (Thermo Fisher Scientific Inc., MA), and *in-vitro* disintegration tests (Erweka, ZT71 apparatus) were used to investigate the coatings after marking.

3. RESULTS AND DISCUSSION

The current formulators focus on omitting/replacing TiO_2 in pharmaceuticals due to toxicity concerns after it was proven in food. Based on the above, there were no significant differences between tablets containing TiO_2 and its alternatives (e.g., $CaCO_3$). The laser marking process for one tablet did not exceed a maximum of 6 seconds, which provides a cost-effective benefit to pharmaceutical companies. In addition, each coating type has a specific range of lasering parameters for which the QR code is readable (1)/unreadable (0) by the smartphone. For example, Table 1. shows that readability with Opadry® brown was easily achieved under most conditions studied. However, it was unreadable with Acryl-EZE®

MP at all, and Opadry® blue was in the middle of the two previous cases.

Table 1. Some of laser parameters applied to the film-coated tablets with the readability results.

Laser parameters		Acryl-EZE® MP	Opadry® Brown	Opadry® Blue
energy (μJ)	number of pulses			
400	80	0	1	1
350	50	0	1	1
300	30	0	1	0
250	65	0	1	0

Furthermore, some physical properties of the tablets differed after laser treatment, such as disintegration behaviour in gastric media. From a morphological perspective, the profilometry results revealed that both the energy and the number of used laser pulses clearly affect the depth of ablation to the tablet surface. Moreover, SEM analysis for the cross-sectional part of the same tablets shows that the coating thickness plays a critical role in protecting the expected release pattern of the drug. It can be observed from Fig. 1 that the coating thickness was insufficient to protect the core from the laser processing. This was clearly confirmed by the results of Raman analysis and *in-vitro* disintegration test.

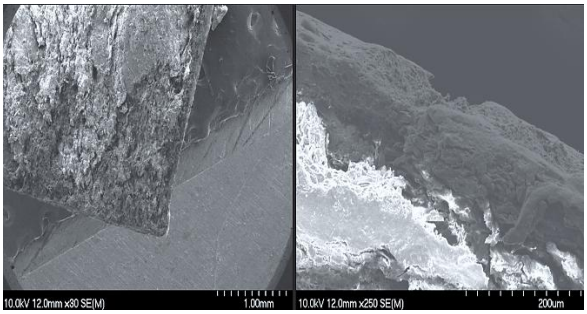

Figure 1. SEM micrographs of laser-treated tablets: The tablet's cross-section surface at different magnifications of 30× & 250× respectively.

4. CONCLUSION

Laser marking appears to offer a package of advantages for the design of SDFs. However, it may affect the performance of these dosage forms. Therefore, the potential effects of this type of marking should be considered, particularly when applied to the modified-release ones.

5. REFERENCES

1. Ludasi, K., et al., *Anti-counterfeiting protection, personalized medicines− Development of 2D identification methods using laser technology. International Journal of Pharmaceutics, 2021. 605(74): 120793.*

2. Shaurya, A., *Enhancing Efficiency and Accuracy in Food Packaging and Pharmaceutical Labeling: An Analysis of UV Laser Printing Technology. International Journal of Science and Research, 2022. 13(2): 1359-1362.*

ACKNOWLEDGMENT

We would like to thank ELI-ALPS Research Institute for providing lasers, and Colorcon, Inc. for supplying the coating polymers. Project no TKP2021-EGA-32 has been implemented with the support provided by the Ministry of Culture and Innovation of Hungary from the National Research, Development and Innovation Fund, financed under the TKP2021-EGA funding scheme.

OP5

DEHYDRATION AND PURIFICATION OF MICROPARTICLE SUSPENSIONS VIA VIBRO® TFF

Lukas Vergeiner[1], Ramona Jeitler[1], Marie-Christin Wiesler[1], Anke Schuster[2], Karoline Bechtold-Peters[3], Eva Roblegg[1]

[1]University of Graz, Institute of Pharmaceutical Sciences, Pharmaceutical Technology & Biopharmacy, Graz, Austria
[2]Technical Research and Development, Novartis Pharmaceutical Manufacturing GmbH, Austria
[3]Technical Research and Development, Novartis Pharma AG, 4002 Basel, Switzerland

1. INTRODUCTION

Parenteral suspensions have their place within the spectrum of dosage forms, particularly for achieving highly concentrated preparations for injection [1, 2]. Various particle generation techniques are available, although they may require a concentration step.
The steps from particle generation onwards to achieve sufficient purification and higher concentrations can be carried out by membrane filtration, for instance. Tangential flow filtration (TFF) is a continuous, scalable process in which the dispersion flows parallel to the membrane surface. However, robust operation depends on an appropriate system design [3]. Hence, in this study, the scalable vibro® technology, a TFF system in which turbulence is generated by vibration of the membrane relative to the feed flow, was tested. SorboLac® 400 was used as a surrogate to evaluate key TFF parameters, focusing on microparticle properties (e.g., size and shape) and formulation characteristics (e.g., solid content). Particle generation aid exchange efficiency was monitored via refractive index (RI) measurements, with the process optimized to minimize reagent consumption and maximize final solid content.

2. MATERIALS AND METHODS

In this study, diafiltration and concentration was performed by a Vibro-Lab35P TFF apparatus (SANI Membranes, Denmark) with a 35 cm^2 0.2 µm PVDF membrane (Synder Filtration, USA). To reflect the characteristics of microparticles produced via a particle generation method, SorboLac® 400 was chosen as a surrogate because of its comparable particle size (>90% <32 µm) and poor solubility. Due to the expected low concentration after particle generation, an initial concentration step was included to increase the solid content without compromising the performance of the TFF. Both continuous and mixed diafiltration modes were investigated while maintaining a maximum solid content of 20% (w/v). In the continuous mode, the vehicle was fed constantly via a syringe pump to achieve a balanced ratio between particle generation aid removal and the addition of the suspension vehicle. In the mixed mode, the dispersion was diluted 1:20 (v/v) with suspension vehicle and then reconcentrated and diafiltered until complete removal of the particle generation aid. Particle generation aid removal was monitored at-line via RI measurements of the filtrate (Abbemat 500, Anton Paar, Austria), while feed flow rates and transmembrane pressure (TMP) were controlled using peristaltic pumps (BT600M, GrossEnCon, Germany) (see Fig. 1).

Figure 1. Vibro® TFF set-up consisting of a syringe pump, sample reservoir, peristaltic pumps, vibration unit, TFF-membrane cassette and filtrate collection vessle (created with BioRender).

3. RESULTS AND DISCUSSION

Initially, vibro® TFF conditions were optimized to enable efficient and time-effective diafiltration. To this end, the maximum solid content allowing high filtration rates at low TMP was determined. At approximately 20% (w/v) solid content, a high flux was maintained with low TMPs, indicating rapid and efficient filtration (see Fig. 2). At higher solid contents, filtrate rates declined markedly, with the concentration step reaching its endpoint at 63 % (w/v) solid content. Based on these results, a solid content of 20 % (w/v) was selected for the subsequent diafiltration studies (i.e., dehydration and generation aid removal).

OP5

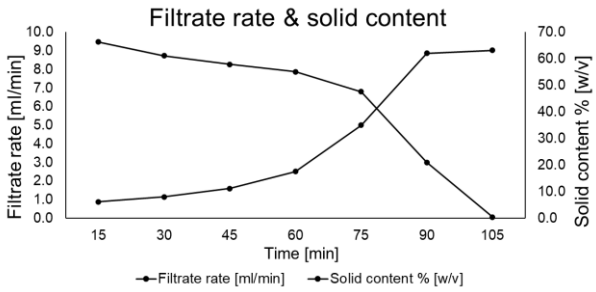

Figure 2. Filtrate rate [ml/min] and solid content [%] over time during the vibro® TFF concentration step.

In the continuous mode, no significant increase in TMP surpassing 0.35 bar was observed. Over time, a constant filtrate rate was maintained. Within 60 minutes a residual particle generation aid fraction of 1.40 % (v/v) was reached; within 120 minutes complete aid exchange was achieved. In the mixed mode, fluctuations in TMP were noted due to the preceding concentration step. However, the TMP never exceeded 0.6 bar. A residual aid fraction of 1.43% (v/v) was examined within a total purification time of 40 minutes.
The vehicle consumption was 1165 ml for the mixed mode and 1200 ml for the continuous method. Due to the dilution step in the mixed mode, the necessary process time to reach a fraction of aid under 1.5% (v/v) was reduced by 33%. In this mode, however, fluctuations in the filtrate rate occurred more frequently.

4. CONCLUSION

The vibro® TFF strategy represents a promising approach for the continuous and scalable exchange from particle generation aid to suspension vehicle and up-concentration of dispersions obtained from the particle generation processes. With a clear understanding of critical process parameters and formulation characteristics, this method enables time- and cost-efficient downstream processing of stable solid microparticle suspensions. Future studies will focus on evaluating the applicability of this approach to relevant biological candidates and assessing its impact on bioactivity and long-term stability.

5. REFERENCES

1. Kowsari K, Lu L, Persak SC, Hu G, Forrest W, Berger R, et al. *Injectability of high concentrated suspensions using model microparticles.* J Pharm Sci. 2024;113:3525–37. doi:10.1016/j.xphs.2024.09.026.
2. Marschall C, Graf G, Witt M, Hauptmeier B, Friess W. P*reparation of high concentration protein powder suspensions by milling of lyophilizates.* Eur J Pharm Biopharm. 2021;166:75–86. doi:10.1016/j.ejpb.2021.04.023.
3. Agrawal P, Wilkstein K, Guinn E, Mason M, Serrano Martinez CI, Saylae J. *A Review of Tangential Flow Filtration: Process Development and Applications in the Pharmaceutical Industry.* Org. Process Res. Dev. 2023;27:571–91. doi:10.1021/acs.oprd.2c00291.

OP6

THE EFFECT OF TABLET DESIGN AND EXCIPIENTS ON DRUG RELEASE FROM 3D PRINTED TABLETS

Karoliina Inno[1], Ivo Laidmäe[1,2]

[1]Institute of Pharmacy, University of Tartu, Estonia
[2]Institute of Biomedicine and Translational Medicine, University of Tartu, Estonia

1. INTRODUCTION

3D printing is a novel approach in pharmaceutical technology for personalised medications. It enables tailoring both the dose and shape of the dosage form to the patient's individual needs [1]. One of the most-researched printing technologies in pharmacy is fused deposition modelling (FDM), where one of the main concerns is achieving consistent drug release at different doses of the active pharmaceutical ingredient (API) [2].
The aim of this study was to assess the effect of tablet design and used excipients on drug release from the FDM 3D printed tablets.

2. MATERIALS AND METHODS

2.1. Materials

The base polymer used was hydroxypropyl cellulose (HPC), solid plasticizer was xylitol (Xyl) and the disintegrant was Kollidon CL or sodium croscarmellose (Ac-Di-Sol®). The model API used was caffeine (CAF).

2.2. Hot melt extrusion and 3D printing

Filaments of six different formulations (Table 1) were hot melt extruded in a single-screw extruder at 120°C. The filaments were FDM 3D printed at 165°C in three designs with a different surface area to volume ratio.

Table 1. Compositions of the used formulations.

No.	CAF	HPC	Xyl	Kollidon CL	Ac-Di-Sol
F_1	10%	90%			
F_2	10%	75%	15%		
F_3	10%	65%	15%	10%	
F_4	10%	65%	15%		10%
F_5	10%	55%	15%		20%
F_6	10%	62.5%	7.5%		20%

2.3. Characterisation of filaments and tablets

Content uniformity in the filaments was studied by UV-Vis spectrophotometry at 273 nm on five samples of formulations F_1 and F_5.

All raw materials, and the physical mixtures, filaments and tablets of formulations F_1, F_3 and F_5 were characterised in FTIR measurements at 600…4000 cm^{-1}.
XRD analysis was performed on all raw materials, and the physical mixtures and tablets of formulations F_1, F_3 and F_5.

2.4. Drug release

Drug release from the printed tablets was assessed in a dissolution study for two hours at pH=2 at 37±0.5°C. The concentration of CAF was measured every 5 minutes with a flow-through apparatus and UV-Vis spectrophotometer at 273 nm.

3. RESULTS AND DISCUSSION

3.1. Extrusion and 3D printing

Filaments of all formulations were successfully extruded. The filaments were collected from extrusion manually, therefore the diameter of them was uneven and the thinnest filaments were not used for 3D printing.
3D printing of all formulations was successful. However, the printing of F_1 led to the print head clogging repeatedly and the results of printing were uneven in quality on visual inspection. All tablets were printed in triplicate, except for the largest surface area design of F_1, where there were only two successfully printed tablets.

3.2. Characteristics of the filaments and tablets

CAF content in all tested samples was 10±1% and there were no differences between samples from the beginning, midsection, and end of the filament batch.
FTIR showed no changes in the solid-state form of CAF. However, it showed likely larger changes in the structures of Kollidon CL and Ac-Di-Sol, likely due to the repeated heating.
XRD showed a twin diffraction peak characteristic of the metastable II polymorph of CAF at 27° 2θ in tablets of all three tested formulations.

OP6

3.3. Drug release

No combination of formulation and tablet design led to the complete release of CAF. In several formulations and designs, there was large variability in the results, possibly due to small differences in printing density.
The drug release was faster from tablets with a larger surface area to volume ratio in all formulations (Fig. 1).
Drug release from all six formulations was similar in all three designs and there was no clear order from slowest to fastest dissolution between the formulations. The formulations containing sodium croscarmellose (F_4, F_5 and F_6) showed the three slowest release profiles in two of the three designs. Sodium croscarmellose was unsuitable as a disintegrant with the used materials and process parameters. Formulations with Kollidon CL showed similar drug release to the control formulation (F_1). Therefore, at the used concentration and process parameters it did not improve drug release. However, different grades of Kollidon could be investigated further for this purpose.

4. CONCLUSIONS

The excipients used in this study were suitable for hot melt extrusion and 3D printing at the used concentrations and temperatures. The solid plasticizer improved the 3D printability of the filaments.
The disintegrants did not significantly improve drug release in the used concentrations. Drug release was faster from the 3D printed tablets with a larger surface area. This demonstrates the applicability of the technique to a personalised formulation approach.

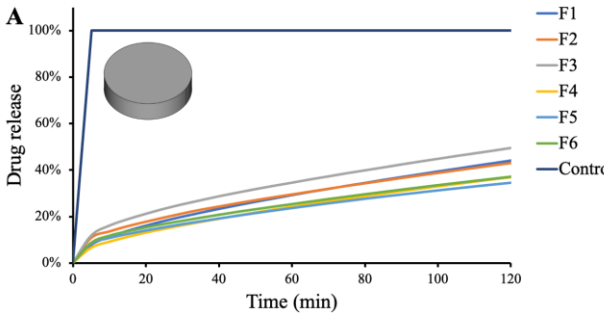

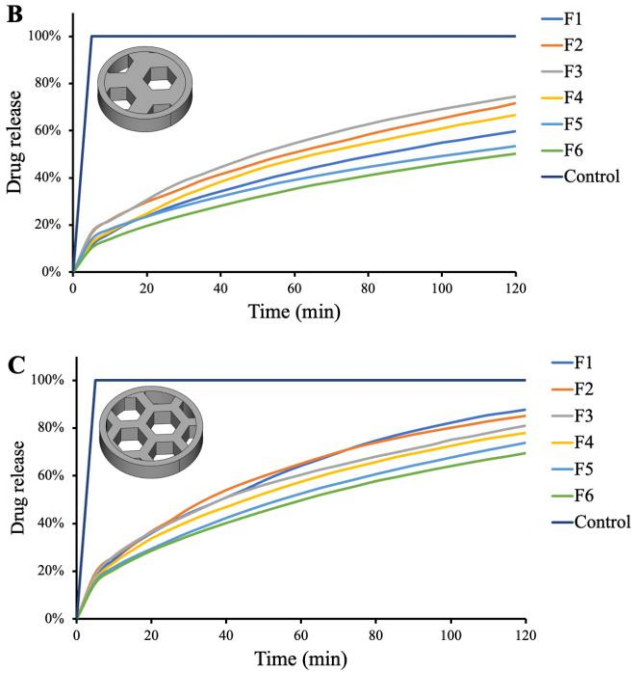

Figure 1. Drug release from tablets of six formulations in three different designs (N=3). A) cylindrical tablets, B) small honeycomb tablets, C) large honeycomb tablets.

5. REFERENCES

1. Araújo, M., et al. *The Digital Pharmacies Era: How 3D Printing Technology Using Fused Deposition Modeling Can Become a Reality.* Pharmaceutics, 2019. 11(3): 128.

2. Gorkem Buyukgoz, G., et al. *Exploring tablet design options for tailoring drug release and dose via fused deposition modeling (FDM) 3D printing.* International Journal of Pharmaceutics, 2020. 591: 119987.

ACKNOWLEDGMENT

The authors would like to thank Jaan Aruväli for conducting the XRD measurements

OP7

MONOCLONAL ANTIBODY FORMULATION OPTIMIZATION USING NOVEL VISCOSITY-REDUCING AND STABILIZING EXCIPIENTS

Monika Prašnikar[1], Maja Bjelošević Žiberna[1], Iztok Grabnar[1], Aleš Žula[2], Pegi Ahlin Grabnar[1]

[1]Department of Pharmaceutical Technology, Faculty of Pharmacy, University of Ljubljana, Slovenia
[2]Biologics Drug Product, Technical Research and Development, Global Drug Development, Novartis, Slovenia

1. INTRODUCTION

Subcutaneous administration of therapeutic monoclonal antibodies (mAbs) is advantageous over intravenous due to faster administration and reduced injection pain, improving patient adherence and reducing treatment cost [1,2]. However, to achieve the therapeutic effect, mAbs are often formulated at high concentrations, leading to increased viscosity and reduced protein stability. Viscosity above 20 mPas can limit production and administration and mAb instability leads to reduced efficacy and safety [1, 3]. Viscosity-reducing excipients offer a potential solution, but only a few are known and their effect often depends on the mAb properties [3]. This study aims to evaluate proline analogs and their combinations regarding their effect on the viscosity of a highly concentrated mAb formulation and the protein stability.

2. MATERIALS AND METHODS

2.1. Materials

The model mAb was provided by Novartis, d. o. o.. Common reagents and laboratory materials were purchased from Merck, Thermo Fisher Scientific, and other commercial vendors. Test compounds S05–S36 ((2S,4S)-pyrrolidine-2,4-dicarboxylic acid (S05), H-Pro-Pro-OH (S09), H-Pro-Tyr-OH (S11), nicotinic acid (S32), 1H-pyrrole-3-carboxylic acid (36)) were obtained from BLD Pharmatech, Chem Impex, AA BLOCKS, Acros Organics, CARLO ERBA, and Fluorochem.

2.2. Sample preparation

Samples were prepared by mixing the protein solution with test compound solutions and concentrating them using ultracentrifugal filter units. The final formulations contained 200 mM sucrose, 20 mM histidine buffer, 0.02 mg/mL polysorbate 80, and 170 ± 10 mg/mL mAb at pH 6.0, with varying amounts of test compounds added. Protein concentration was measured using a UV-Vis spectrophotometer at 280 nm (Nanodrop ONEc, USA).

2.4. Viscosity and stability measurement

Viscosity was measured using a viscometer-rheometer (RheoSense VROC (Viscometer/ Rheometer-On-a-Chip) or m–VROC, Initium One Plus, USA). Viscosity reduction was calculated as a relative decrease in viscosity (%) of the sample containing the test compound compared to the starting formulation without the test compound at the same mAb concentration. Size exclusion chromatography (SEC) was used to assess the physical stability of mAb, with samples first analyzed after preparation and then stored in glass vials at 4 and 40 °C and reassessed after 4 and 12 weeks.

3. RESULTS AND DISCUSSION

3.1. Combination of test compounds

The study shows that increasing the concentration of viscosity-reducing excipients or combining them can effectively reduce the viscosity of a concentrated mAb formulation without promoting mAb aggregation. Individual test compounds at 25 mM reduced the viscosity of the mAb formulation by more than 30%, but not below the critical 20 mPas threshold. Furthermore, combinations of test compounds were evaluated, namely S32 and S36 with an aromatic moiety (S32 and S36) were combined with other test compounds. The most effective combinations were S36-S05, S36-S09, and S36-S11, which reduced the viscosity of the formulation by up to 58%, exceeding the effect of S36 at 50 mM. Other combinations did not prove as effective and the combination S32-S31 even increased the viscosity of the formulation (Fig. 1).

OP7

Figure 1. Viscosity reduction of the mAb formulation with two test compounds (25 mM each). Dashed reference lines present S32 (orange) and S36 (blue) at 50 mM for comparison. Error bars represent 95% confidence intervals.

3.2. Concentration-dependent viscosity-reducing effect of test compounds

Decreasing viscosity of the formulation was observed with increasing concentration (25–200 mM) of selected test compounds (S09, S32, and S36). At 170 mg/mL mAb concentration, the viscosity of the formulations containing Arg, S32 and S36 at concentrations above 50 mM did not fall below 15 mPas. This suggests that further viscosity reduction beyond this point may not have been achievable through reducing protein–protein interactions. In contrast, at 200 mg/mL mAb concentration, a concentration-dependent viscosity-reducing effect was observed for Arg and the test compounds S32 and S36, which can form aromatic interactions with the mAb (Fig. 2).

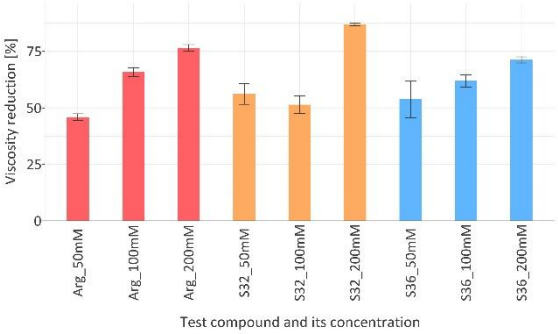

Figure 2. Viscosity reduction of formulations at 200 mg/mL mAb with test compounds at 50, 100, and 200 mM. Error bars represent 95% confidence intervals.

3.3. Physical stability of mAb formulations

In most formulations with test compounds or their combinations the physical stability of mAb was maintained or improved. Less than 5% aggregates were observed in most samples after 12 weeks at 40 °C, except in the sample with S36 at 200 mM, which promoted aggregation (>8%).

4. CONCLUSION

Overall, the study highlights that increased concentrations or combinations of viscosity-reducing excipients can reduce viscosity more efficiently than an individual excipient at 25 mM concentration, while preserving the physical stability of mAb formulations. However, a deeper understanding of which specific combinations yield additive effects is essential for rational excipient selection. Further research of the test compounds with various mAb formulations could confirm if the observed effects are broadly applicable and help excipient selection in development of new mAb formulations.

5. REFERENCES

1. Bittner B., et al., *Subcutaneous Administration of Biotherapeutics: An Overview of Current Challenges and Opportunities*. BioDrugs, 2018. 32:425–40.

2. McCloskey C., et al., *A Systematic Review of Time and Resource Use Costs of Subcutaneous Versus Intravenous Administration of Oncology Biologics in a Hospital Setting.* PharmacoEconomics Open, 2023. 7:3–36.

3. Prašnikar M., et al., *Additive effects of the new viscosity-reducing and stabilizing excipients for monoclonal antibody formulation*. International Journal of Pharmaceutics, 2025. 674:125451.

ACKNOWLEDGMENT

The authors acknowledge financial support by the Slovenian Research and Innovation Agency, research core funding No. P1-0189 and grant L1-3160 co-financed by Novartis d.o.o., and colleagues for their various contributions.

OP8

OPTIMIZATION OF SOLID SELF-EMULSIFYING DRUG DELIVERY SYSTEMS TO ACHIEVE ORAL PEPTIDE THERAPY

Martin Deak[1], Nur Aslan[2], Katalin Kristo[1], Tamas Sovany[1]

[1]Institute of Pharmaceutical Technology and Regulatory Affairs, University of Szeged, Hungary
[2]Department of Pharmaceutical Technology, Ege University, Turkey

1. INTRODUCTION

The medicinal use of biologic therapeutics such as peptides, proteins, and antibodies is rapidly expanding. These biopharmaceuticals are typically administered by parenteral injection or infusion due to poor oral bioavailability. This method poses a great challenge to patient adherence because of the invasive nature of injections their high cost, and the frequent need for medical personnel to administer, all of which limit the widespread use of these drugs.
Therefore, extensive research is ongoing to deliver proteins via alternative routes of administration, including the oral, nasal, ophthalmic, pulmonary, buccal, and transdermal way. [1] However, oral drug delivery is the most preferred and has the highest compliance due to ease and simplicity of medication. [2] Unfortunately, biologics are highly susceptible to degradation in the gastrointestinal system and their large size limit the absorption through the intestinal epithelium. For this reason, a drug delivery method which can provide substantial protection for the carried protein and facilitate its transport across the intestinal barrier needs to be utilized. [3]
Various strategies have been used to overcome this challenge such as structural drug modifications, co-administration of excipients and development of nanocarriers. Considering the latter, SEDDS show a promising approach for oral delivery since it can provide enhanced bioavailability and stability for macromolecules. In comparison with other nanocarriers for instance, liposomes, micelles or carbon nanotubes its preparation is simpler and more cost efficient. Furthermore, it can be combined with solid nano and microcarriers such as mesoporous silica to develop a convenient solid dosage form, including tablets or capsules. [4]

In present research a lysozyme containing optimized solid-SEDDS was developed, to study the potential of this drug delivery system.

2. MATERIALS AND METHODS

2.1. Materials

Surfactants used in the SEDDS formulations were Tween 20 and 80 (Merck KGaA, Darmstadt, Germany) and Span 20 and 80 (TCI Co. Tokyo, Japan). Miglyol 810 (Sasol Chemicals GmbH, Witten, Germany) was used as oil phase. Lyophilized powder of lysozyme (LYZ) from chicken egg white was purchased from MedChemExpress (Monmouth, NJ, USA) and sodium dodecyl sulfate (SDS) used in hydrophobic ion pair formation was received from EGIS Pharmaceuticals Plc. (Budapest, Hungary). Neusilin UFL2 mesoporous silica used in the solidification process and carrier was kindly gifted by Fuji Chemical Industries Co. (Toyama, Japan).

2.2. Hydrophobic ion pairing (HIP)

HIP complexes were formed from lysozyme and the anionic surfactant SDS with a 1:8 molar ratio at pH 8 in order to provide sufficient stability and solubility for the peptide in the oil phase. After complexation, the samples were centrifuged (15,000 RPM, 15 min) and drying was carried out in a ventilated oven. (25°C, 50% fan speed, 3 hours) [5]

2.3. Preparation of the SEDDS

Liquid SEDDS were formulated according to a three-factor-constrained mixture experimental design using the aforementioned oil and surfactants. The surfactants were combined based on a 2^2 full factorial design. Dependent variables regarding the stability of SEDDS mixtures determined as CQAs, droplet size, PDI, zeta potential and encapsulation efficiency were measured by photon correlation spectroscopy, using a Malvern Nano ZS Zetasizer (Malvern Instruments Ltd., Malvern, UK)

2.4. Compressibility tests

Solid SEDDS were obtained by adsorbing SEDDS mixtures in an increasing ratio onto

Neusilin UFL2 (1:10 to 2:1). The influence of oil and surfactant components on the compressibility and tabletability of the solid carrier was investigated according to Kawakita's and Walker's equations by performing tests with an eccentric tablet press (Korsch EK0, E. Korsch Maschinenfabrik, Berlin, Germany). The acquired results were analyzed using an artificial neural network (ANN) model where the correlation between the physico-chemical properties of the liquids and the measured compressibility parameters were examined.

3. RESULTS AND DISCUSSION

3.1. Stability studies of liquid SEDDS

Based on the statistical analysis of the results and using ternary diagrams, design spaces were created for each batch. (Fig. 1) The acceptance criteria of the design space were droplet size smaller than 200 nm, PDI smaller than 0.4, and zeta potential below -10 mV. Thus, making it possible to prepare optimized SEDDS formulations.

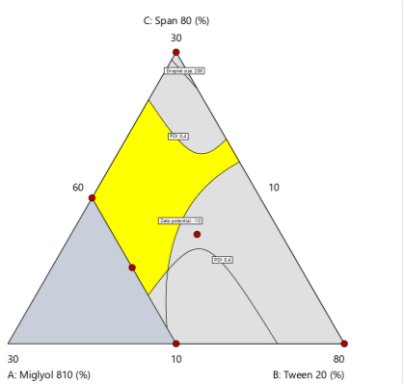

Figure 1. Design space of the SEDDS prepared with the combination of Tween 20 and Span 80.

3.2. Compressibility of solid SEDDS

According to the conducted tests, the best compressibility values were observed with the 1:1 SEDDS:Neusilin ratio and Tween 20 had the most advantageous influence on compressibility. ANN modelling was performed for a dual purpose: to be able to predict the compressibility values of new compositions (Table 1), and to estimate the effect of various factors on the compressibility of the loaded mesoporous carriers.

Table 1. Prediction performance of compressibility parameters

Parameter	Train	Test	Validation
a	0,912222	0,982060	0,904582
1/b	0,511458	0,887350	0,811414
W	0,498027	0,927834	0,867117
L	0,711899	0,049460	0,631419

Regarding the effect of the tested factors on the compressibility results, the global sensitivity analysis of the system revealed the surface tension of the loaded liquid had the highest influence on the compressibility, followed by liquid density while the load percent and the liquid viscosity had smaller, and approximately same sized influence on the system behavior.

4. CONCLUSION

This systematic investigation on this innovative and complex drug delivery system can contribute to better understanding the role and behaviour of the individual components in the formulation, enable to predict their effect on compressibility which is substantial for further development into tablets, and overcome the challenge of oral bioavailability of peptides and proteins.

5. REFERENCES

1. Drucker J. D., *Advances in oral peptide therapeutics.* Nature Reviews Drug Discovery, 2020. 19: 277-289 .
2. Verma S., et al., *Challenges of peptide and protein drug delivery by oral route: Current strategies to improve the bioavailability.* Drug Development Research, 2021. 82(7): 927-944.
3. Anselmo C. A., et al., *Non-invasive delivery strategies for biologics.* Nature Reviews Drug Discovery, 2019. 18: 19-40.
4. Mahmood A., et al., *SEDDS: A game changing approach for the oral adminsitration of hydrophilic macromolecular drugs.* Advanced Drug Delivery Reviews, 2019. 142: 91-101.
5. Hassan, A.A.A.; et al. *Hydrophobic Ion-Pairing Complex of Lysozyme with Sodium Dodecyl Sulphate to Enhance Stability in Lipid-Based Carriers.* Pharmaceutics 2024, 16: 589.

ACKNOWLEDGMENT

Project no TKP2021-EGA-32 has been implemented with the support provided by the Ministry of Culture and Innovation of Hungary from the National Research, Development and Innovation Fund, financed under the TKP2021-EGA funding scheme.

OP9

CYCLODEXTRIN POLYMERS: FORMULATION AND INVESTIGATION OF NEW RNA DELIVERY SYSTEMS

Virág Dajka[1], Ildikó Bácskay[2], Ferenc Fenyvesi[1], Ágnes Rusznyák[1]

[1]Department of Molecular and Nanopharmaceutics, University of Debrecen, Hungary
[2]Department of Pharmaceutical Technology, University of Debrecen, Hungary

1. INTRODUCTION

Nowadays, RNA-based therapies play an increasingly important role in the treatment of various diseases. siRNA is mainly used in the maintenance of different genetic diseases, while the mRNA also used in the development of vaccines. Due to the large molecular size and polyanionic nature of RNA, the intracellular delivery of these molecules are difficult [1]. To solve this problem several delivery systems are available or under development, which are usually based on liposomes and cationic polymers, such like cyclodextrin polymers [2]. Cyclodextrins are widely used excipients in the pharmaceutical and cosmetic industries to increase the solubility and bioavailability of lipophilic molecules, but there polymer derivatives are able to carry macromolecules.

In the present study we aimed to investigate and to compare the siRNA and mRNA carrying capacity of a cationic cyclodextrin polymer (Q polymer) and the polyethylenimine (P polymer), which is used in the practice.

2. MATERIALS AND METHODS

2.1. Materials

The soluble cationic cyclodextrin polymer and its fluorescein-labelled derivative were the products of CycloLab Ltd. (Budapest, Hungary). The predesigned human GAPDH siRNA, the branched polyethylenimine were derived from Sigma-Aldrich Ltd. (Budapest, Hungary), while the CleanCap EGFP mRNA was the product of Tebubio (Le Perray-en-Yvelines, France).

2.2. Methods

The cytotoxicity effect of the applied polymers was examined using the MTT method. The siRNA and mRNA polyplexes were formulated in different nitrogen/phosphate (NP) ratios from 1 to 24. The formulated polyplexes were characterized based on their size distribution using dynamic light scattering (DLS) and their zeta potential. In the case of siRNA polyplexes their cellular internalization was investigated by confocal microscopy after 30 min, 4 and 24 h treatment with polyplexes formulated with fluorescently labelled GAPDH siRNA. The intracellular effect of these delivery systems was investigated via the expression of GAPDH protein after 48 h treatment by fluorescence microscopy. In the case of the mRNA polyplexes the examination of the cellular internalization was no relevant, so the intracellular effect of these was investigated via the expression of green fluorescent protein (GFP) after 48 h treatment by fluorescence microscopy and flow cytometry.

3. RESULTS AND DISCUSSION

The P polymer was more cytotoxic than the cationic cyclodextrin polymer. According to the DLS and zeta potential measurements both polymer were able to form polyplexes with siRNA and mRNA, but based on the gel electrophoresis, the cyclodextrin polymer is able to form a stronger polyplex with mRNA molecule. Polyplexes formulated with Q polymer were able to enter the cells, while these formulated with P polymer were bound to the cell membrane. Polyplexes were influenced both the GAPDH and green fluorescent protein (GFP) expression, but the increasing concentration of P polymer was cytotoxic.

4. CONCLUSION

In summary, we have successfully formulated cyclodextrin polymer-based RNA delivery systems. Polyplexes formulated with different polymers showed different cellular internalization. The formulated polyplexes are able to influence the expression of different proteins and the cationic cyclodextrin polymer is more suitable for gene or protein expression than for gene silencing.

OP9

5. REFERENCES

1.Kanasty, R.; Dorkin, J.R.; Vegas, A.; Anderson, D. *Delivery materials for siRNA therapeutics. Nat. Mater. 2013, 12, 967–77, doi:10.1038/nmat3765.*

2.Chaturvedi, K.; Ganguly, K.; Kulkarni, A.R.; Kulkarni, V.H.; Nadagouda, M.N.; Rudzinski, W.E.; Aminabhavi, T.M. *Cyclodextrin-based siRNA delivery nanocarriers: A state-of-the-art review. Expert Opin. Drug Deliv. 2011, 8, 1455–1468, doi:10.1517/17425247.2011.610790.*

ACKNOWLEDGMENT

Project no. TKP2021-EGA-18 has been implemented with the support provided by the Ministry of Culture and Innovation of Hungary from the National Research, Development and Innovation Fund, financed under the TKP2021-EGA funding scheme.

OP10

PHOSPHOLIPID VESICLE-BASED TOPICAL FORMULATION TO UNLOCK THE POTENTIAL OF A BIOSYNTHETIC MELANIN

Luca Casula[1], Simona Demuro[1], Rita Argenziano[2], Francesca Pintus[1], Alessandra Napolitano[2], Carla Caddeo[1]

[1]Dept. of Life and Environmental Sciences, University of Cagliari, Italy
[2]Dept. of Chemical Sciences, University of Naples Federico II, Italy

1. INTRODUCTION

Melanins are known to exert a protective action to the skin thanks to UV-vis absorption and reactive oxygen species scavenging properties. Exploitation of such properties for dermocosmetic purposes by use of easily accessible synthetic melanins prepared from biosynthetic precursors, particularly methyl ester of 5,6-dihydroxyindole-2-carboxylic acid (MeDHICA), has so far been hampered by the marked insolubility of the melanins.

In this study, a melanin obtained from MeDHICA via peroxidase/H_2O_2 oxidation was incorporated into phospholipid vesicles with the aim of increasing its solubility and producing an aqueous-based formulation that could be safely applied onto the skin. The nanoformulation contained glycerol, which was key to producing stable, small, homogeneous vesicles. The antioxidant activity of the MeDHICA melanin glycerol-liposomes was studied via DPPH and FRAP assays, and the biosafety was assessed *in vitro* in immortalized keratinocytes.

2. MATERIALS AND METHODS

2.1. Materials

LipoidS75 (soybean phospholipids) was purchased from Lipoid GmbH (Ludwigshafen, Germany); glycerol was purchased from Galeno (Carmignano, Italy); phosphate buffered saline (PBS, pH 7.4) was purchased from Merck (Milan, Italy). MeDHICA melanin was obtained via enzymatically promoted oxidation of MeDHICA. After 24 h, the maximum absorption of the starting MeDHICA shifted bathochromically becoming broad and featureless. Reverse-phase HPLC confirmed the complete consumption of MeDHICA. Upon full monomer conversion, the reaction mixture was acidified to induce precipitation of the melanin, which was recovered by centrifugation and lyophilization.

2.2. Vesicles' production and characterization

To produce glycerol-liposomes, LipoidS75 (200 mg/ml) and glycerol (200 mg/ml) were dispersed in PBS, in presence or absence of MeDHICA melanin (1 mg/ml), and sonicated with an ultrasound disintegrator. The mean diameter, polydispersity index, and zeta potential of the vesicles were measured via dynamic/electrophoretic light scattering. The MeDHICA melanin in glycerol-liposomes was quantified via UV-vis spectrophotometry at 330 nm and the entrapment efficiency was calculated. The ultrastructure of the glycerol-liposomes was studied via cryogenic-Transmission Electron Microscopy (cryo-TEM). The antioxidant activity of MeDHICA melanin was tested via the DPPH and FRAP assays. MeDHICA melanin (in DMSO or in glycerol-liposomes) or the empty glycerol-liposomes were added to *i*) DPPH reagent and analysed spectrophotometrically at 517 nm; *ii*) FRAP reagent and analysed spectrophotometrically at 593 nm. The cytotoxicity of MeDHICA melanin was assayed in human keratinocytes (HaCaT) exposed to MeDHICA melanin in DMSO or in glycerol-liposomes, or to empty glycerol-liposomes for 24 h. Cell viability was determined by the MTT assay and expressed as a percentage of control untreated cells (NT).

3. RESULTS AND DISCUSSION

With the aim to exploit the favorable properties of MeDHICA melanin and resolve the insolubility issue, a nanotechnology-based approach was explored. Glycerol-liposomes, which combine the ability of liposomes to enhance solubility and bioavailability of their cargo with the penetration enhancing ability of glycerol, were developed. The incorporation of MeDHICA melanin into glycerol-liposomes significantly affected their mean diameter (90 nm), while polydispersity and surface charge

OP10

were unaltered (Table 1). The glycerol-liposomes displayed high entrapment efficiency (77%; Table 1).

Table 1. Mean diameter (MD), polydispersity index (PI), zeta potential (ZP), and entrapment efficiency (E) of glycerol-liposomes. *p<0.01.

Formulation	MD (nm)	PI	ZP (mV)	E (%)
Empty gly-lip	82±5.0	0.25±0.02	−9±0.4	--
MeDHICA melanin gly-lip	*90±2.6	0.25±0.01	−9±0.5	77±3.8

Cryo-TEM micrographs (Fig. 1) showed that glycerol-liposomes were spherical, predominantly unilamellar, below 100 nm, and slightly larger when loaded with MeDHICA melanin, in alignment with size data (Table 1).

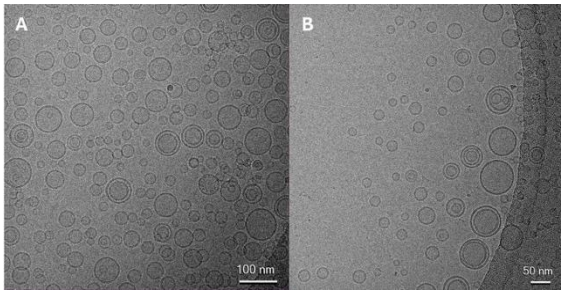

Figure 1. Cryo-TEM micrographs of MeDHICA melanin glycerol-liposomes (A) and empty glycerol-liposomes (B) at 73,000× magnification.

The antioxidant activity of MeDHICA melanin was high (87% - 323 µg TE/ml; Table 2) and remained unchanged when nanoformulated. Similarly, the same reducing power was found for MeDHICA melanin in solution as in glycerol-liposomes (~ 1.7 mg FE/ml; Table 2). This indicates that the nanoformulation process had no impact on MeDHICA melanin's antioxidant activity.

Table 2. Antioxidant activity of MeDHICA melanin. AA (Antioxidant Activity %); TE (µg Trolox Equivalents/ml solution); FE (µg Fe^{2+} Equivalents/ml solution).

Formulation	DPPH		FRAP
	AA (%)	TE (µg/ml)	FE (µg/ml)
MeDHICA melanin solution	87±1.5	323±11	1744±136
MeDHICA melanin gly-lip	84±4.0	316±14	1749±146
Empty gly-lip	47±2.4	172±9.6	600±54

The cell viability tests showed that the MeDHICA melanin solution was not cytotoxic (93% at the higher concentration tested; Fig. 2), as well as the MeDHICA melanin glycerol-liposomes (87%; Fig. 2).

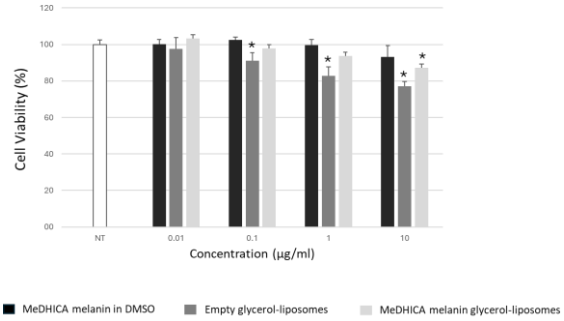

Figure 2. Viability of HaCaT cells incubated for 24 h with MeDHICA melanin in DMSO or in glycerol-liposomes (0.01–10 µg/ml). Empty glycerol-liposomes were tested as a control. *p<0.05 *vs.* NT.

4. CONCLUSION

The results showed the successful incorporation of MeDHICA melanin in phospholipid vesicles, characterized by small size, stability, antioxidant capabilities and non-toxicity, encouraging further investigation to validate their effective and safe use on the skin.

ACKNOWLEDGMENT

This study was funded by European Union - Next Generation EU, Mission 1 Component 1, CUP F53D23011650001. The authors acknowledge CF CEITEC/Brno (Czech Republic), supported by MEYS CR (LM2023042) and European Regional Development Fund-Project No. CZ.02.01.01/00/23_015/0008175, and EDUC-WIDE project funded by the European Union under Grant Agreement No. 101136533 for cryo-TEM measurements.

OP11

THE ROLE OF PROTEIN CORONA IN ENHANCING MICRORNA DELIVERY VIA NANOSTRUCTURED LIPID CARRIERS

Ivana Ruseska[1], Amina Tucak-Smajić[2], Edina Vranić[2], Andreas Zimmer[1]

[1]Department of Pharmaceutical Technology and Biopharmacy, Institute of Pharmaceutical Sciences, University of Graz, Graz, Austria

[2]Department of Pharmaceutical Technology, Faculty of Pharmacy, University of Sarajevo, Sarajevo, Bosnia and Herzegovina

1. INTRODUCTION

Cationic nanostructured lipid carriers (cNLCs) have been described as suitable delivery systems for microRNA (miRNA), by forming complexes (so-called NLCplexes) that improve its stability and enhance its cellular uptake. However, despite their favourable physicochemical properties and efficacy as delivery systems, the presence of protein corona significantly reduced their stability and cellular uptake [1]. Therefore, we investigated the possibility of modulating the protein corona by using human serum albumin (HSA) as a dysopsonin, to potentially develop a more stable and efficient system.

2. MATERIALS AND METHODS

2.1. Materials

Octadecylamine, Precirol ATO 5, Miglyol 812, Tween 80, Poloxamer 188, amd Mili-Q (MQ) water were used to produce cationic nanostructured lipid carriers (cNLCs). For in vitro studies, a miRNA mimic (Dharmacon, Horizon, Vienna, Austria) labelled with Cy3 was used. Human serum albumin (HSA) was obtained from Sigma Aldrich Chemie GmbH (Steinheim am Albuch, Germany). As a cell model, 3T3-L1 murine-derived fibroblasts were used.

2.2. NLCplex preparation and HSA coating

cNLCs were prepared using high-pressure homogenization. NLCplexes were prepared by mixing aqueous solutions of miRNA and cNLC in ratio 1:5 (w/w). These NLCplexes were coated using HSA to obtain the so-called abluplexes in ratio 1:5:1500 (w/w). The albuplexes were characterized in using DLS and ELS, as well as CD and UV/Vis spectroscopy.

2.3. Stability studies

To evaluate the stability of albuplexes in serum conditions, 1:5 albuplexes were incubated in MQ water, serum-free medium (SFM) and medium supplemented with 10% FBS (10 % DMEM). The protein corona effect was evaluated using SDS-PAGE, DLS and ELS.

2.4. Uptake studies

The uptake of 1:5 albuplexes was evaluated in 3T3-L1 cells. The uptake was evaluated in the span of 8 hours by measuring the fluorescence intensity of the internalized particles at concentrations of 100 and 200 nM using a CLARIOstar® plate reader (BMG LABTECH, Germany). The uptake was also traced using CLSM (Leica Microsystems, Germany). In this case, the albuplexes were labelled using Cy3 (red), the actin skeleton was labelled using AlexaFluor™ Phalloidin (green), whereas the nuclei were stained using DAPI (blue).

To analyse the endocytic mechanism involved in the uptake of albuplexes, we pre-treated 3T3-L1 cells with various inhibitors of endocytosis: chlorpromazine, EIPA, genistein, dynasore, and nystatin. Furthermore, to determine the effect of protein corona of the uptake, the internalization was evaluated after incubating the albuplexes in cell culture medium supplemented with 10% FBS.

3. RESULTS AND DISCUSSION

3.1. NLCplex preparation and HSA coating

Coating NLCplexes with HSA increased the hydrodynamic diameter of the complexes. 1:5 NLCplexes had a diameter of 123 ± 4 nm, whereas the size of 1:5 albuplexes was 225.4 ± 2 nm. Furthermore, the charge of the complexed was changed from highly positive (42.3 ± 1 mV for NLCplexes) to negative (-13.6 ± 0.7 mV), indicating that HSA was indeed adsorbed on the surface of the NLCplexes. CD and UV/Vis data also confirmed the HSA coating and the intactness of the protein's structure. What is more, CD data demonstrated and increase in the protein's helicity.

OP11

3.2. Stability studies

Incubating the 1:5 albuplexes in SFM led to a minimal change in hydrodynamic diameter – the observed size was 191.9 ± 9 nm, with a charge of -15.7 ± 1 mV. On the other hand, NLCplexes had a diameter of 172.8 ± 21 nm, and a charge of -12.9 ± 1 mV. In the presence of serum proteins, the hydrodynamic diameters of 1:5 albuplexes and NLCplexes were 232.9 ± 9 nm and 269.6 ± 21 nm, respectively. Both formulations kept their negative charge. Furthermore, in all cases, the PdI values suggested improved colloidal stability of albuplexes. The enhanced stability can be attributed to electrostatic repulsion and steric hindrance provided by the surface-bound HSA.

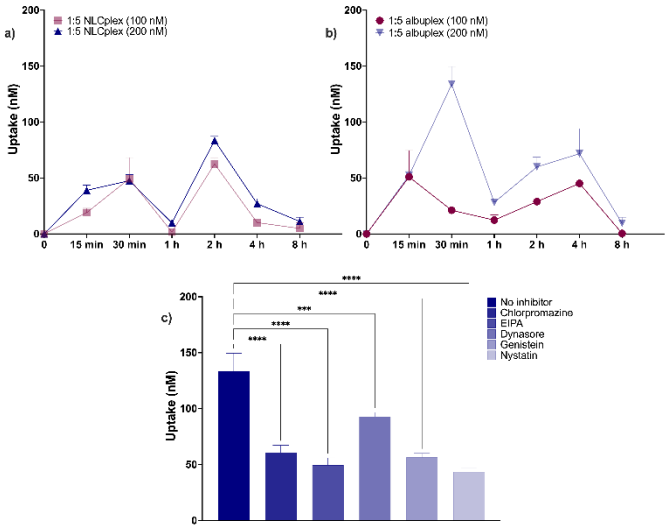

Figure 1. Uptake of 1:5 NLCplexes (a) and 1:5 albuplexes (b) in 3T3-L1 cells. Metabolic inhibition data are presented under (c).

3.3. Uptake studies

Coating the 1:5 NLCplexes with HSA led to improved cellular uptake, especially at a concentration of 200 nM. The albuplexes were taken up by cells in 30 min, similarly to NLCplexes (Fig. 1). What is more, the uptake of 200 nM 1:5 albuplexes was characterized by a higher rate constant compared to that of 200 nM 1:5 NLCplex. Metabolic inhibition data demonstrated that more than one uptake mechanisms (clathrin- and caveolae-mediated endocytosis, as well as macropinocytosis) were involved in the uptake. This observation is likely due to the activation of gp30 and gp18 receptors by albumin [2].

Images obtained by CLSM demonstrated that albuplexes were internalized in serum-free conditions, as well as in the presence of 10% FBS, confirming that the HSA-coat increased the serum stability of the particles and led to improved cellular uptake (Fig. 2).

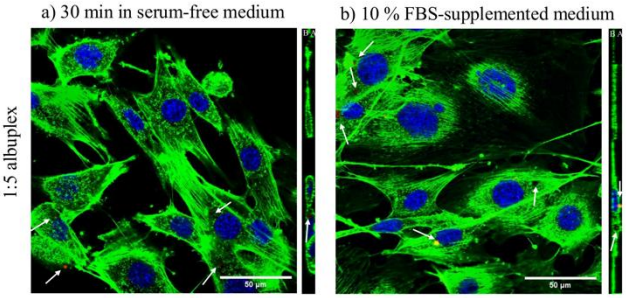

Figure 2. CLSM images of 3T3-L1 cells treated with 1:5 albuplexes in a) serum-free conditions, and b) medium supplemented with 10% FBS. The albuplexes are labelled using Cy3 (red) and pointed out using white arrows.

4. CONCLUSION

By coating 1:5 NLCplexes using HSA we obtained abluplexes which demonstrated superior serum stability and improved cellular uptake in serum-conditions. Furthermore, by modulating the protein corona, albuplexes demonstrated superior efficacy compared to NLCplexes.

5. REFERENCES

1. Ruseska, I. et al., *Elucidating the uptake and trafficking of nanostructured lipid carriers as delivery systems for miRNA.* European Journal of Pharmaceutical Sciences, 2025. 204: 106973.

2. Ji, Q. et al., *GP60 and SPARC as albumin receptors: key targeted sites for the delivery of antitumor drugs.* Frontiers of Pharmacology, 2024. 15.

ACKNOWLEDGMENT

The authors would like to acknowledge the Doctoral Academy Nano Graz at the University of Graz, the CEEPUS network RS-1113-06-2223—Central European Knowledge Alliance for Teaching, Learning & Research in Pharmaceutical Technology (CEKA PharmTech).

OP12

STICKY BUSINESS: INVESTIGATING THE ROLE OF NANOFIBER ENCAPSULATION IN LACTOBACILLI SURFACE ADHESION AND BIOFILM FORMATION

Nina Katarina Grilc[1], Samo Jeverica[2,3], Miha Lučovnik[4], Julijana Kristl[1], Špela Zupančič[1],

[1]*Faculty of Pharmacy, University of Ljubljana, Slovenia*
[2]*National Laboratory of Health, Environment and Food, Department of medical microbiology, Slovenia*
[3]*General Hospital Izola, Slovenia*
[4]*University Medical Center Ljubljana, Division of Gynaecology, Ljubljana, Slovenia*

1. INTRODUCTION

The ability to adhere to mucosal surfaces and form biofilms or multicellular structures like microcolonies is a desirable trait of probiotic strains as it enhances their capacity to colonize mucosal surfaces. However, not all probiotic strains are efficient biofilm formers. Encapsulation, including into nanofibers, is a widely explored strategy for improvement of mucosal colonization by probiotics [1,2]. Current *in vitro* studies of nanofibers with probiotics focus on short-term bacterial retention on epithelial models or mucosal surfaces, limiting the insight into the impact of nanofibers on probiotic growth or biofilm formation. This study investigates the effects of nanofiber encapsulation of four strains of vaginal lactobacilli on biofilm formation.

2. MATERIALS AND METHODS

2.1. Materials

Potential vaginal probiotic strains (*L. jensenii* LJE6, *L. gasseri* LGA13, *L. crispatus* LCR6, *L. crispatus* LCR13) were isolated from vaginal microbiota of volunteers without clinical signs of vaginal dysbiosis. Other materials (all from Sigma, unless otherwise stated): poly(ethylene oxide) (PEO) 800 kDa, crystal violet (CV), porcine mucin type III, de Man, Rogosa, and Sharpe (MRS) broth, MRS-agar, convertible flow cells, TPP 24-well plates, sodium alginate (ALG) (138 kDa, LF 10/60, Protanal.

2.2. Lactobacilli culturing and encapsulation into nanofibers

Lactobacilli obtained by overnight culturing in in MRS were washed and re-suspended in ultra-pure water. Such bacterial suspensions were added to PEO or PEO/ALG (75:25) solutions, yielding polymer-bacterial dispersions with the final total polymer concentration of 4 % (w/v). The dispersions were electrospun (Fluidnatek LE-100, Bioinicia) at 12-14 kV and flow rate of 425 µL/h or 300 µL/h for PEO and PEO/ALG dispersion, respectively.

2.3. Determination of biofilm biomass

In static conditions, biofilms were grown in MRS or modified simulated vaginal fluid (MVSF) by incubation of varying length at 37 °C in non-coated or mucin-coated 24-well microtiter plates. CV staining was used to determine the biomass of biofilms grown by incubating dispersed, non-encapsulated lyophilized lactobacilli alone (LYO) or in the presence of dissolved polymers (LYO-P) or lactobacilli encapsulated into nanofibers (NF).

Biofilms of *L. jensenii* LJE6 (LYO or NF) were also grown in dynamic conditions in a flow cell to mimic the *in vivo* conditions of constant washout of bacteria. Incubation of varying length was performed at 37 °C under a constant MVSF flow of 150 µL/h and the biofilm biomass was determined by CV staining.

3. RESULTS AND DISCUSSION

3.1. Determination of lactobacilli biofilm-forming ability

Preliminary experiments showed that the different strains exhibited varying biofilm-forming abilities in the rich MRS medium. LGA13 emerged as a good biofilm former capable of producing superior biofilm biomass compared to other strains ($p < 0.05$) which were established to be poor biofilm formers (Fig. 1).

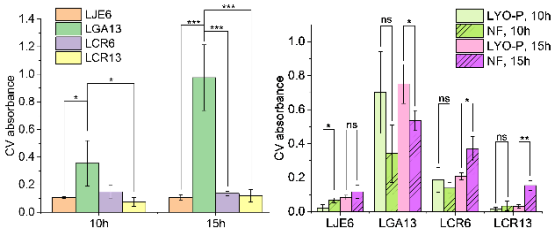

Figure 1. Left – biofilm formation in MRS on uncoated plates by four strains of vaginal lactobacilli; Right – biofilm formation in MVSF on mucin-coated plates by PEO nanofiber encapsulated lactobacilli (NF) and non-encapsulated lyophilized lactobacilli in the presence of dissolved polymers (LYO-P).

3.2. Effect of encapsulation in PEO nanofibers on biofilm formation by different strains

The effect of lactobacilli encapsulation into PEO-only nanofibers on biofilm formation depended on the individual strain. Encapsulation into nanofibers resulted in minor or no improvements of biofilm-forming properties of the poor biofilm formers. These effects were dependent on the phase of growth. Strain LJE6 benefitted from encapsulation in the earlier stages of biofilm formation, while similar effects on both *L. crispatus* strains were only observed at later stages. Meanwhile, nanofibers significantly decreased the biofilm-forming ability of *L. gasseri* LGA13 ($p < 0.05$), indicating that encapsulation of nanofibers impedes biofilm formation of an already strong biofilm-former (Fig. 1).

3.3. Effect of encapsulation of poor biofilm former *L. jensenii* LJE6 in PEO/ALG nanofibers on biofilm formation

Strain LJE6 was chosen for further studies. Nanofiber formulations were improved by addition of alginate, a polymer with known mucoadhesive properties which also exhibited a nutrient role for the chosen strain LJE6, evidenced by improved parameters of its growth kinetics (increased optical density yield and growth rate and decreased lag time, $p < 0.05$, data not shown). Encapsulation of LJE6 into PEO/ALG nanofibers resulted in significant improvement of biofilm formation in static conditions of growth in microplate wells when compared to non-encapsulated lyophilized bacteria ($p < 0.05$ for time-points 10 and 15 hours). This improvement could be observed on both uncoated (data not shown) and mucin-coated plates (Fig. 2)), however, the biomass of the adhered biofilm after washing was higher on mucin-coated surfaces, indicating specific mucin-binding. The increase in biofilm biomass could not be attributed to encapsulation into nanofibers, but rather the presence of polymers themselves, as similar results to nanofiber samples could also be observed for biofilms grown from lyophilized bacteria in medium supplemented with dissolved PEO/ALG ($p > 0.05$). This can be attributed to ALG growth-promoting activity.

Encapsulation into nanofiber membranes proved beneficial in dynamic conditions of constant medium flow. Here, nanofibers improved retention of bacteria on mucin-coated surfaces which enabled biofilm formation, resulting in higher biofilm biomass compared to samples of bacteria lyophilized in the presence of polymers producing a highly porous and rapidly dissolving matrix (Fig. 2).

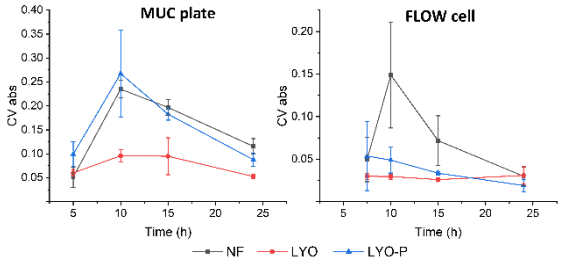

Figure 2. Biofilm formation in MVSF on mucin-coated surfaces (left – microtiter plate wells, right – flow cell) by various dry formulations of *L. jensenii* (NF – PEO/ALG nanofibers; LYO – lyophilizates without any polymer addition; LYO-P – lyophilizates with addition of PEO/ALG).

4. CONCLUSION

Encapsulation of lactobacilli into nanofibers affects their ability to form adherent biofilms in a strain-specific manner. Nanofibers can improve adhesion and biofilm formation of poor biofilm formers.

5. REFERENCES

1. Salas-Jara MJ, et al. *Biofilm Forming Lactobacillus*: *New Challenges for the Development of Probiotics*. *Microorganisms*, 2016; 4(3):35.

2. Heumann, A., et al. *Intestinal release of biofilm-like microcolonies encased in calcium-pectinate beads increases probiotic properties of Lacticaseibacillus paracasei*. npj Biofilms Microbiomes, 2020;6(44).

ACKNOWLEDGMENT

This work was supported by the Slovenian Research Agency [grants P1-0189, J7-4418, J4-4556] and University of Ljubljana [gr. SN-ZRD/22-27/0510].

OP13

DEVELOPMENT AND *IN VIVO* EVALUATION OF HEMOSTATIC SILK FIBROIN-BASED NANOFIBER FORMULATIONS

Imren Esenturk-Guzel[1], Oksan Karal-Yilmaz[2], Ozlem Ayşe Tosyali[3], Burcin Izbudak[4], Ayca Bal-Ozturk[4,5,6], Luceyn Abdo[1], Beyza Nur Ozkan[7], Eray Metin Güler[7,8]

[1]University of Health Sciences, Hamidiye Faculty of Pharmacy, Department of Pharmaceutical Technology, Istanbul, Turkey

[2]İstanbul Beykent University, Faculty of Engineering&Architecture, Department of Chemical Engineering, Istanbul, Turkey

[3]İstanbul Beykent University, Faculty of Engineering&Architecture, Department of Biomedical Engineering, Istanbul, Turkey

[4]Istinye University, Institute of Graduate Education, Department of Stem Cell and Tissue Engineering, Istanbul, Turkey

[5]Istinye University, Stem Cell and Tissue Engineering Application and Research Center (ISUKOK), Istanbul, Turkey

[6]Istinye University, Faculty of Pharmacy, Department of Analytical Chemistry, Zeytinburnu, Istanbul, Turkey

[7]University of Health Sciences, Hamidiye Faculty of Medicine, Department of Medical Biochemistry, Istanbul, Turkey

[8]University of Health Sciences, Haydarpasa Numune Health Application and Research Center, Department of Medical Biochemistry, Istanbul, Turkey

1. INTRODUCTION

Uncontrolled bleeding is a major cause of death and severe injury, particularly in combat scenarios. In such critical situations, the availability of fast-acting hemostatic agents is essential in modern first aid practices. Conventional methods like bandages and gauze often fall short, especially in complex wounds. As a result, there is an increasing demand for advanced hemostatic solutions that are user-friendly, lightweight, cost-effective, safe, and capable of rapid blood clotting, whether applied by the injured individual or a first responder [1]. Electrospun nanofibers are promising drug carrier systems. Their structure closely resembles the extracellular matrix (ECM), which is critical for supporting cellular processes such as attachment, growth, movement, and differentiation [2]. This makes electrospun nanofibers an excellent candidate for next-generation wound care applications.

Silk fibroin (SF) is a protein fiber produced by the silkworm (Bombyx mori). SF is a natural biopolymer in protein structure used in treatment with physical properties such as excellent biocompatibility, biodegradability, water vapor permeability, and mechanical strength. SF supports collagen synthesis and re-epithelialization. Chitosan (CS) exhibits antibacterial activity due to its amino groups and cationic structure. In addition, it induces type III collagen production in the wound environment and supports the proliferation and migration of fibroblasts which support the degree of healing. In addition, forming a complex structure with heparins that prevent blood clotting in wound applications and accelerating the healing process are among the superior features of this polymer [3].

In this study, SF was blended with CS to add hemostatic activity besides its wound healing properties. Nanofibers composed of SF, CS, and polyethylene oxide (PEO) were electrospun and then loaded with vancomycin (VAN) or in combination with antibacterial agent of zinc nanoparticles (ZNP) for the first time in the literature. Then, the prepared formulations were characterized in terms of morphology and fiber size using SEM and drug loading efficiency. Then, *in vitro* cytotoxicity was determined using MTT, and the hemostatic activity of the nanofibers was evaluated *in vivo* using Sprague-Dawley rats.

2. MATERIALS AND METHODS

2.1. Materials

Silkworm cocoons were from Koza Birlik (Bursa, Türkiye). Low molecular weight chitosan (MW: 50-190 kDa, 75-85% deacetylated), poly(ethylene oxide) (PEO, MW:

1,000 kDa), ZNP (<100 nm particle size), MTT, formic acid (≥98%), glutaraldehyde solution (25% aqueous), and RPMI-1640 medium were purchased from Sigma-Aldrich (St. Louis, USA). VAN was gifted by VEM İlaç (Türkiye). All chemicals used were of analytical grade and used as received.

2.2. Preparation of Nanofiber Formulations

The formic acid solutions of the polymers of SF, CS, and PEO were mixed and 20% (w/w) VAN was added to the polymer blend. ZNP was integrated into the polymer blend at 2% (w/w). The mixtures were stirred at 300 rpm overnight, at room temperature, to get a homogeneous solution. Then, an electrospinning device (NE-100, Inovenso, Türkiye) was used to obtain electrospun nanofiber formulations. The distance was 24 cm between the needle tip and the collection plate, the voltage was 24 kV, and the flow rate was 1 ml/h as electrospinning conditions.

Following electrospinning, the obtained nanofiber mats were crosslinked with glutaraldehyde. The CS to SF ratio was 1:1 by weight in the final nanofibers.

2.3. Characterization of Nanofiber Formulations

The surface morphology and average fiber diameters of the nanofibers were determined by SEM (FESEM; SU7000, Japan). The study on drug loading efficiency was conducted.

2.4. *In Vitro* Cytotoxicity Study

To evaluate the cytotoxicity of the nanofiber mats, an indirect MTT assay was conducted using the human dermal fibroblast cell line (CCD-1136Sk).

2.5. *In Vivo* Hemostatic Activity Study

The “rat tail amputation model” was used to determine the hemostatic activity of nanofiber formulations. Sprague-Dawley rats were used for the experimental groups. Ethical approval for the study was obtained from the Bezmialem Vakıf University Animal Experiments Local Ethics Committee, Istanbul, Türkiye.

3. RESULTS AND DISCUSSION

3.1. Characterization of Nanofiber Formulations

Drug loading efficiencies of the formulations were between 95-98%. The nanofibers were homogenous and non-beaded. Also, the fiber sizes of the formulations ranged between 442 and 506 nm.

3.2. *In Vitro* Cytotoxicity Study

All of the prepared nanofibers not only supported cell survival but also promoted cell proliferation.

3.3. *In Vivo* Hemostatic Activity Study

Both the bleeding time and the bleeding amount of the formulations applied on the hemostasis model created on the tail were compared with the commercial product HemCon. Among the formulations, the plain nanofiber formulation reduced bleeding time the most, while the nanofiber formulation containing the combination of VAN and ZNP was the group that reduced bleeding amount the most.

4. CONCLUSION

As a result, it can be stated that the developed plain, VAN alone, or combined with ZNP loaded nanofiber formulations are innovative drug carrier systems that can be used in bleeding control as hemostatic formulations.

5. REFERENCES

1. Huang, W., et al., *Strong and rapidly self-healing hydrogels: Potential hemostatic materials.* Advanced Healthcare Materials, 2016. 5, 2813–2822.

2.Zhang, X., et al., *Advances in wound dressing based on electrospinning nanofibers.* Journal of Applied Polymer Science, 2024. 141.

3. Bombin ADJ., et al., *Electrospinning of natural polymers for the production of nanofibres for wound healing applications*. Materials Science and Engineering, 2020. 114.

ACKNOWLEDGMENT

This study was supported by Health Institutes of Türkiye (TUSEB, Project No: 28428). This study was supported by TUBITAK 2224-A - Grant Program for Participation in Scientific Meetings Abroad.

OP14

IN SITU FORMING LIQUID CRYSTALS FOR PEPTIDE DRUG DELIVERY: FROM GELATION DYNAMICS AND SUSTAINED RELEASE TO BIOCOMPATIBILITY ASSESSMENT

Mercedes Vitek[1], Robert Roškar[2], Alenka Zvonar Pobirk[1], Mirjam Gosenca Matjaž[1]

[1]*Department of Pharmaceutical Technology, University of Ljubljana, Faculty of Pharmacy, Slovenia*
[2]*Department of Biopharmaceutics and Pharmacokinetic, University of Ljubljana, Faculty of Pharmacy, Slovenia*

1. INTRODUCTION

Patient adherence remains a critical challenge in pharmaceutical care, particularly in the management of chronic diseases, where consistent dosing regimen is required. This is especially relevant for peptide-based therapeutics, which are limited by inherent poor stability and short plasma half-lives, requiring frequent parenteral administration. Long-acting subcutaneous (SC) depot drug delivery systems offer a promising strategy to address these issues by reducing dosing frequency and enabling patient self-administration [1].

Among important advancements in this field are *in situ* forming lyotropic liquid crystals (LLCs), which are formed by the spontaneous self-assembly of precursor formulations into nanostructured mesophases upon contact with aqueous fluids. These LLC systems typically consist of ordered hexagonal or cubic mesophases that enable sustained drug release through aqueous nanochannels, making them an attractive platform for the prolonged delivery of labile biopharmaceuticals such as peptides [2].

Novel *in situ* forming LLCs were developed and evaluated by our research group for the SC delivery of thymosin alpha 1 (Tα1), a 28-amino-acid immunomodulatory peptide with a short plasma half-life requiring twice-weekly dosing. The systems demonstrated high potential for SC administration [3]. Encouraged by the gelation kinetics induced by water uptake and the *in vitro* release of Tα1, these results are now further upgraded by biocompatibility testing using the MTS assay and morphological assessment by inverted phase-contrast microscopy. The obtained findings offer valuable insights into the development of patient-friendly peptide drug delivery systems that enhance therapeutic outcomes.

2. MATERIALS AND METHODS

2.1. Materials

The precursor formulations consisted of either glycerol monooleate type 40 (Go, Peceol®) or glycerol monolinoleate (Gl, Maisine® CC) (both from Gattefossé SAS, Saint-Priest, France), in combination with ethanol (Pharmachem, Slovenia) and lecithin (Lipoid S-100®, Lipoid GmbH, Germany) as presented in Table 1.

Table 1. Composition of the studied precursor formulations (m/m, %).

	Go	Gl	Ethanol	Lecithin
(E/L)Go50	50	-	25	25
(E/L)Gl50	-	50	25	25
(E/L)Go60	40	-	30	30
(E/L)Gl60	-	40	30	30
(E/L)Go70	30	-	35	35
(E/L)Gl70	-	30	35	35
(E/L)Go80	20	-	40	40
(E/L)Gl80	-	20	40	40

2.2. Water uptake evaluation

Water uptake was evaluated gravimetrically at set time points. 0.5 g of each precursor formulation was injected into a 10 mL vial containing 5 mL of preheated PBS to 37 °C.

2.3. *In vitro* release testing

Precursor formulations (1.6 mg/g of Tα1) were injected into 15 mL of release medium preheated to 37 °C. A membraneless model was used.

2.4. Biocompatibility assessment

Biocompatibility was assessed on fibroblast (BJ-5ta) and keratinocyte (NCTC 2544) cells by 24 h exposure to samples, followed by MTS assay and morphological evaluation using an inverted phase-contrast microscope (Olympus CKX41, Tokyo, Japan).

3. RESULTS AND DISCUSSION

OP14

3.1. Water uptake evaluation

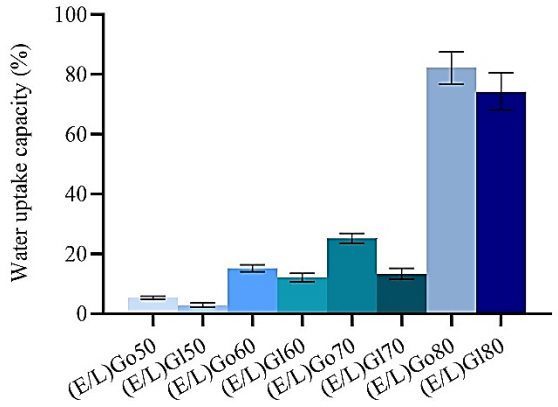

Figure 1. Results of water uptake evaluation of the studied precursor formulations.

Gelation of all the studied precursor formulations was quick and convenient. Water uptake studies (Fig. 1) showed that *in situ* gels with higher Go or Gl content had lower water uptake capacity due to dominant hexagonal mesophases [3].

3.2. *In vitro* release testing

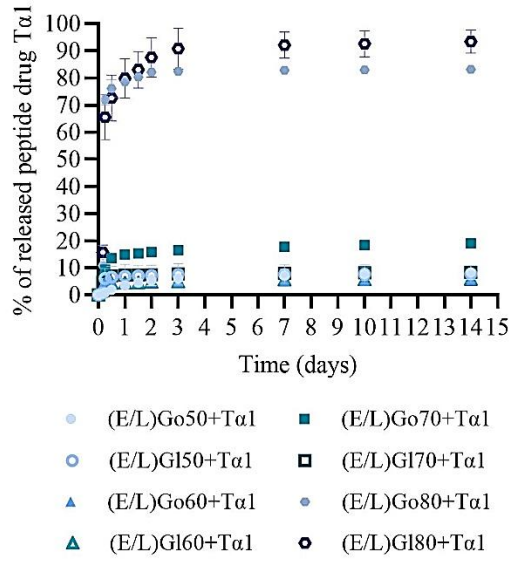

Figure 2. *In vitro* release profiles of the studied precursor formulations.

All *in situ* gels showed sustained Tα1 release (Fig. 2), with (E/L)Go80 and (E/L)Gl80 achieving the highest levels due to the coexistence of lamellar phases and high water uptake. The release was slower for LCCs with predominant hexagonal mesophases, except for (E/L)Go70, where increased free water enabled moderately higher diffusion [3].

3.3. Biocompatibility assessment

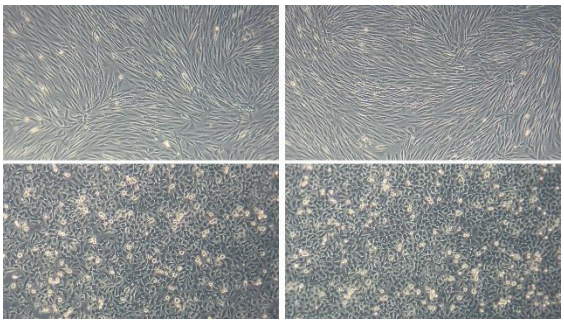

Figure 3. Representative morphology of fibroblasts (top panels) and keratinocytes (bottom panels). Untreated control cells (left) are compared with cells following 24-hour treatment with the tested samples (right).

MTS assay results on both cell lines showed excellent biocompatibility, comparable between the formulations. Cell proliferation in fibroblasts was ≥94.7% and in keratinocytes ≥86.9%, both comparable across samples. No visible changes in cell morphology were observed under inverted optical microscopy after exposure to the samples (Fig. 3).

4. CONCLUSION

Novel *in situ* forming LLCs demonstrate strong potential for SC delivery of Tα1, with favorable gelation dynamics, sustained release, and excellent biocompatibility in fibroblasts and keratinocytes.

5. REFERENCES

1. Sharma, R., et al., *Recent advances in lipid-based long-acting injectable depot formulations.* Advanced Drug Delivery Reviews, 2023. 199: 114901.

2.Chavda, V.P., et al., *Lyotropic liquid crystals for parenteral drug delivery*. Journal of Controlled Release, 2022. 349:533-549.

3. Vitek, M., et al., *Exploiting the potential of in situ forming liquid crystals: development and in vitro performance of long-acting depots for peptide drug thymosin alpha 1 subcutaneous administration.* Drug Delivery, 2025. 32(1): 2460708.

ACKNOWLEDGMENT

This work was supported by the Slovenian Research and Innovation Agency under Research core Funding No. P1-0189 and Grant No. L1-3160.

OP15

NANOLIPID GEL-BASED LOCAL THERAPY FOR PERIODONTAL DISEASES: A DUAL-ACTION ANTI-INFLAMMATORY AND ANTIBACTERIAL STRATEGY

Rabia Ashfaq[1], Nóra Tóth[1], Anita Kovács[1], Szilvia Berkó[1], Gábor Katona[1], Rita Ambrus[1], Tamás F. Polgár[2, 3], Mária Szécsényi[3], Katalin Burián[3], Mária Budai-Szűcs[1]*

[1]Institute of Pharmaceutical Technology and Regulatory Affairs, Faculty of Pharmacy, University of Szeged, , Hungary
[2]Core Facility, HUN-REN Biological Research Centre, Hungary
[3]Theoretical Medicine Doctoral School, University of Szeged, Hungary
[4]Department of Medical Microbiology, University of Szeged, Hungary

1. INTRODUCTION

Periodontitis is a common inflammatory disease of the gums caused by microbial infection and immune responses, posing significant clinical challenges. Traditional treatments like mechanical cleaning and antibiotics often fail to address the disease's complexity fully [1]. Advanced drug delivery systems are being developed to improve therapeutic outcomes. Syringeable semisolid bioadhesive gels with injectable flow properties, strong mucoadhesion, and sustained drug release show promise for treating periodontal pockets more effectively. Meloxicam (Melox), a selective COX-2 inhibitor, is known for its potent anti-inflammatory and analgesic effects with fewer gastrointestinal side effects compared to traditional NSAIDs [2]. Combined with clove oil (CO) as liquid lipid, which offers antibacterial and anti-inflammatory benefits, to manage periodontitis. CO is also reported to enhances formulation stability and therapeutic efficacy [3]. Nanostructured lipid carriers (NLCs) provide a stable, controlled-release system for delivering these drugs effectively to the treatment site. This study aims to develop mucoadhesive gel systems incorporating Melox-loaded NLCs using polymers like hypromellose (HPMC) and hyaluronic acid (HA), including its zinc salt (ZnHA) and sodium salt, sodium hyaluronate (NaHA), known for their biocompatibility, mucoadhesion, and healing properties. These formulations were evaluated for their physicochemical characteristics, drug release profiles, and *in vitro* therapeutic effects. Overall. the goal is to identify an optimal delivery system that offers prolonged retention, enhanced healing, and targeted treatment for periodontitis.

2. MATERIALS AND METHODS

2.1. Materials

Compritol® 888 ATO, clove oil (76.8% eugenol), Miglyol® 812N, and Kolliphor® RH40, Mucin, Meloxicam, Hypromellose, Zinc hyaluronate, Sodium hyaluronate, Bovine serum. All chemicals were of analytical grade.

2.2. Methods

2.2.1. NLC preparation
2.2.2. Dynamic Light Scattering
2.2.3. Morphological Analysis
2.2.4. Entrapment Efficiency, Drug Loading
2.2.5. Rheological Analysis
2.2.6. *In Vitro* Release Study
2.2.7. *In Vitro* Anti-inflammatory Activity
2.2.8. Antibacterial Study (Agar plate methods, MIC, MBC)
2.2.9. Stability study

3. RESULTS AND DISCUSSION

The study successfully developed and evaluated NLCs loaded with Melox, a selective COX-2 inhibitor, and CO.

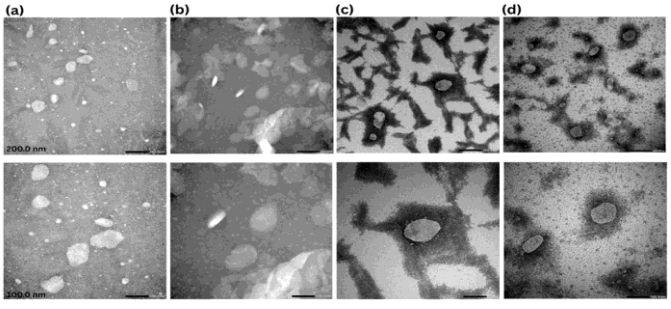

Figure 1. TEM images of Melox-loaded nanoparticles and gel formulations at 25,000 and 50,000x magnifications with scale bars 200 (1st row) and 100 nm (2nd row). (a) NLC-Melox, (b) NLC-HPMC gel, (c) NLC-NaHA gel, and (d) NLC-ZnHA gel.

OP15

The optimized NLCs exhibited favorable physicochemical properties with an average particle size of 183 nm, low polydispersity (PDI = 0.26), and improved zeta potential (−24.7mV). TEM confirmed intact nanoparticles with uniform distribution (Fig 1), even after 3 months of storage (Fig 2).

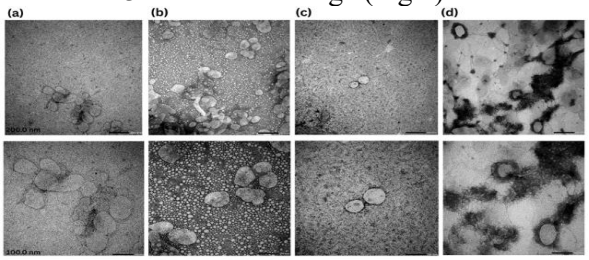

Figure 2. TEM images of Melox-loaded nanoparticles and gel formulations after 3 months. (a) NLC-Melox, (b) NLC-HPMC gel, (c) NLC-NaHA gel, and (d) NLC-ZnHA gel.

High entrapment efficiency (>91%) and amorphous drug dispersion were validated through DSC (Fig. 3) and XRD analyses, supporting enhanced solubility and stability.

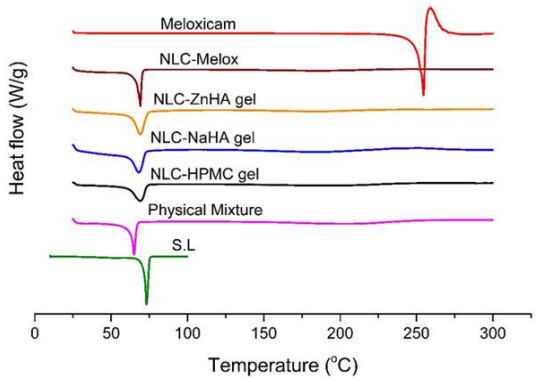

Figure 3. DSC thermograms of the Melox, lipid, physical melt, Melox-loaded NLC, and polymeric gel systems.

Raman spectroscopy confirmed no chemical incompatibility among components. Rheological and mucoadhesion tests identified ZnHA gel as the most structurally stable and adhesive, making it highly suitable for periodontal application. *In vitro* release studies revealed sustained drug release over 24 hours across all gel types. Biological evaluation demonstrated that the NLC–Melox gels effectively inhibited protein denaturation (anti-inflammatory activity: 81 ± 5% inhibition) and showed strong antibacterial effects against two bacterial strains due to presence of antibacterial liquid lipid (Table 1).

Table 1. Antibacterial activity of formulations.

Formulations	**Zone of Inhibition for 48 hrs**	
	A actinomyce-temcomitans	***S. mutans***
NLC-ZnHA gel	30.7 ± 0.6	N.A
NLC-NaHAgel	24.3 ± 1.2	N.A.
NLC-HPMC gel	30.0 ± 0.0	N.A
ZnHA blank gel	24.7 ± 1.2	14.2 ± 0.3
NaHA blank gel	N.A.	N.A.
HPMC blank gel	N.A.	N.A.
NLC-Melox	34.3 ± 2.9	14.4 ± 1.1

4. CONCLUSION

In conclusion, the developed NLC-based mucoadhesive hydrogels demonstrated enhanced drug delivery, sustained release, and effective antibacterial and anti-inflammatory properties for periodontitis treatment. ZnHA-based formulations emerged as the most promising, offering a novel and effective approach for localized periodontal therapy.

5. REFERENCES

[1] R. Ashfaq, B. Sisa, A. Kovács, S. Berkó, M. Szécsényi, K. Burián, P. Vályi, M. Budai-Szűcs, Factorial design of in situ gelling two-compartment systems containing chlorhexidine for the treatment of periodontitis, Eur. J. Pharm. Sci. Off. J. Eur. Fed. Pharm. Sci. 191 (2023)106607. https://doi.org/10.1016/j.ejps.2023.106607.

[2] H. Toker, I. Marakoglu, O. Poyraz, Effect of meloxicam on gingival crevicular fluid IL-1beta and IL1 receptor antagonist levels in subjects with chronic periodontitis, and its effects on clinical parameters, Clin. Oral Investig. 10 (2006) 305–310. https://doi.org/10.1007/s00784-006-0062-3.

[3] K. Banerjee, H. Madhyastha, R. Sandur V., M. N.t., T. N., P. Thiagarajan, Anti-inflammatory and wound healing potential of a clove oil emulsion, Colloids Surf. B Biointerfaces 193 (2020)111102. https://doi.org/10.1016/j.colsurfb.2020.111102

ACKNOWLEDGMENT

Project no TKP2021-EGA-32 by the Ministry of Culture and Innovation of Hungary from the National Research, Development, and Innovation Fund, financed under the TKP2021-EGA funding scheme. This work was supported by the János Bolyai Research Scholarship of the Hungarian Academy of Sciences (M. Budai-Szűcs, BO/00244/24). Rabia Ashfaq was supported by the University Research Scholarship Program (EKÖP) of the Ministry for Culture and Innovation from the source of the National Research, Development and Innovation Fund. Funding number: EKÖP-24-3 - SZTE-200.

OP16

ASSEMBLING THREE ANTHELMINTIC MOLECULES IN A SINGLE SOLID: A PRAZIQUANTEL/NICLOSAMIDE/ACETIC ACID COCRYSTAL SOLVATE

Ilenia D'Abbrunzo[1], Lara Gigli[2], Nicola Demitri[2], Chiara Sabena[3], Carlo Nervi[3], Michele R. Chierotti[3], Serena Bertoni[4], Irena Škorić[5], Cecile Haberli[6,7], Jennifer Keiser[6,7], Dritan Hasa[1], Dario Voinovich[1], Beatrice Perissutti[1].

[1]Department of Chemical and Pharmaceutical Sciences, University of Trieste, Italy;
[2]Elettra-Sincrotrone Trieste, Basovizza–Trieste, Italy;
[3]Department of Chemistry and NIS Centre, University of Torino, Italy;
[4]Skolkovo Institute of Science and Technology, Moscow, Russia
Department of Pharmacy and Biotechnology, University of Bologna, Italy
[5]Department of Organic Chemistry, Faculty of Chemical Engineering and Technology, University of Zagreb, Croatia
[6]Department of Medical Parasitology, Swiss Tropical and Public Health Institute, Switzerland.
[7]University of Basel, Switzerland.

1. INTRODUCTION

Cocrystallization of two or more active pharmaceutical ingredients (APIs) has recently gained attention as an innovative strategy for the development of multi-drug solids. A major advantage of this approach is the co-administration of multiple APIs within a single dosage form, which can simplify treatment regimens, mitigate side effects and drug resistance, and ultimately improve patient compliance [1-2].
In a previous study, we reported the successful formation of a binary antiparasitic cocrystal of praziquantel (PZQ) and niclosamide (NCM), demonstrating enhanced anthelmintic activity [3]. Building upon these findings, we aimed to develop a ternary cocrystal solvate by incorporating acetic acid (AA), a compound recently identified for its anthelmintic potential [4].

2. MATERIALS AND METHODS

2.1. Materials

PZQ, NCM and AA were provided from Fatro S.p.a. (Bologna, Italy), Sigma-Aldrich (St. Louis, USA) and Carlo Erba (Rodano-Milan, Italy), respectively. All three components were used without further purification.

2.2. Synthetic strategies for preparing the ternary cocrystal solvate

- *Mechanochemical routes:*

Mechanochemical grinding (25 Hz, 400 mg total load) was carried out using a Retsch MM400 mill. Each strategy was tested at 30, 60, and 120 minutes, with 160 µL of AA added to each experiment. Five different synthetic strategies were explored using both individual coformers and preformed binary solids as starting materials:

1. From individual coformers;
2. From preformed PZQ-NCM binary cocrystal, raw PZQ and AA;
3. From preformed PZQ-AA monosolvate, raw NCM and AA;
4. From preformed PZQ-NCM coamorphous and AA;
5. From individual coformers with preformed ternary cocrystal seeds.

- *Slurry bridging routes*

2.3. Characterization analyses

1. PXRD and Synchrotron X-ray diffraction;
2. Thermal analyses (DSC and TGA);
3. Spectroscopic analyses (SS-NMR, ^{1}H-NMR and FT-IR);
4. DFT calculations;
5. SEM analysis;
6. Physical stability test;
7. *In vitro* and *in vivo* activity.

3. RESULTS AND DISCUSSION

The new phase was only accessible via mechanochemistry, as slurry experiments failed to yield the desired product. Although the ternary solid was synthetized through all five routes, a pure phase was obtained by milling a preformed PZQ-AA monosolvate with raw NCM in a 1:1 molar ratio for 60 minutes in the presence of 160 µL of AA, which served both as a solvate-forming agent and a liquid-assisted grinding additive. The purity of the new phase was confirmed by SS-NMR spectrum, which

OP16

suggested the presence of one independent molecule of each of PZQ, NCM and AA, a finding further corroborated by ^{1}H-NMR spectroscopy. Structure elucidation via Synchrotron powder X-ray pattern and DFT optimization revealed a triclinic *P*-1 space group, with the three components linked by hydrogen bonding (Fig. 1), as supported by FT-IR spectroscopy.

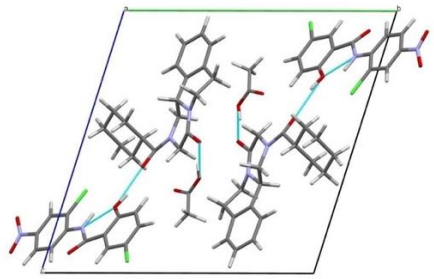

Figure 1. Capped-stick representation of the crystalline structure of PZQ-NCM-AA viewed along *a* axis. H-bonds showed with dashed blue lines.

Morphological analysis by SEM revealed the formation of small plate-like agglomerates. Thermal analysis indicated a desolvation event at approximately 107 °C (TGA weight loss: 9.77%). The multicomponent crystal demonstrated excellent physical stability, remaining unchanged after 24 months at room temperature and under high humidity conditions (75% RH), effectively suppressing the formation of NCM monohydrate, typically observed after one month of air exposure [5].
Importantly, the ternary cocrystal exhibited markedly enhanced anthelmintic activity against *in vitro* Schistosoma *mansoni* adults and, notably, Newly Transformed Schistosomula, outperforming both the pure APIs (i.e., PZQ and NCM) and the binary solids (i.e., PZQ-NCM cocrystal and PZQ-AA monosolvate).

4. CONCLUSION

Mechanochemistry was key to unlocking a novel ternary solid form, enabling the precise assembly of three bioactive components otherwise inaccessible by conventional methods. This study reinforces the power of multicomponent cocrystallization as a successful strategy in crystal engineering to boost drug performance. The significant reduction in IC_{50} highlights the critical impact of the ternary system on bioactivity, fully justifying the challenge of incorporating more than two components into a single crystalline phase.

5. REFERENCES

1. Port A. et al., *Cryst Growth Des* **2019**, 19, 3172–3182.
2. Thipparaboina R. et al., *Drug Discov Today* **2016**, 21(3), 481-490.
3. D'Abbrunzo I. et al., *Int J Pharm* **2023,** 644, 123315.
4. Tan X. et al., *Aquac.* **2023**, 577, 739993.
5. Sanphui P. et al., *Cryst Growth Des* **2012**, 12, 4588–4599.

ACKNOWLEDGMENT

Authors acknowledge Paolo Pengo for FT-IR analysis support and funding from CH4.0 (MUR "Dipartimenti di Eccellenza 2023–2027", CUP D13C22003520001), FLIPPER (PRIN2022, CUP D53D23010020006), and NICE (PRIN2020, CUP D13C22000440001), supported by EU – Next Generation EU, Mission 4, Component 1.

OP17

ASSESSING THE PERFORMANCE OF OPHTHALMIC GEL: IVRT METHODOLOGY

Ana Krese[1], Sara Žaberl Majcenovič[1], Biljana Janković[1]

[1]Sandoz, Lek d.d., Development center Ljubljana, Slovenia

1. INTRODUCTION

The development of in vitro release testing (IVRT) methods for ophthalmic gels must consider the unique physiological conditions of the anterior eye segment. Drug delivery to this area is particularly challenging due to rapid clearance mechanisms such as blinking, tear turnover, and nasolacrimal drainage, which limit drug residence time to approximately 5–6 minutes. Furthermore, only about 5% of a topically applied ophthalmic drug reaches intraocular tissues. To simulate precorneal conditions, IVRT methods must employ low-volume dissolution media, short testing durations, and dynamic flow conditions. Despite the lack of standardized IVRT protocols for ophthalmic products, adapting semisolid performance tests (e.g., USP <1724>) offers a viable path toward developing biorelevant methods that reflect ocular physiology.

2. MATERIALS AND METHODS

2.1. Materials

Test formulation and reference listed drug were used for comparative evaluation. Various dissolution media and surfactants were assessed to optimize drug solubility and release conditions. Analytical-grade reagents and analytical methods were employed throughout the study**.**

2.2. Methods

Multiple compendial and non-compendial apparatuses were evaluated, including paddle, basket, immersion cell, and flow-through cell systems. The method development focused on identifying suitable dissolution media, surfactants, flow rates, and sample positioning strategies. The final method was selected based on its ability to provide reproducible, biorelevant, and discriminatory drug release profiles.

3. RESULTS AND DISCUSSION

3.1. Method Screening and Selection

Initial evaluations of various compendial apparatuses revealed that USP Apparatus 4 (flow-through cell) provided the most biorelevant and reproducible results for ophthalmic gel formulations. Other systems, such as paddle, basket, and immersion cells, exhibited limitations including overly rapid release, membrane-related variability, or poor simulation of ocular conditions.

3.2. Optimization of Test Parameters

Key parameters such as dissolution medium composition, surfactant type and concentration, flow rate, and sample positioning were systematically optimized. A phosphate-buffered saline medium with non-ionic surfactant was selected to balance solubility and physiological relevance. A flow rate of 8 mL/min and a low sample dose placed on a glass bead layer provided consistent and complete drug release within 45 minutes.

3.3. Discriminatory Capability

The method demonstrated sensitivity to critical quality attributes (CQAs), particularly viscosity (Fig.1) and particle size distribution (Fig.2). Batches with altered polymer content or drug substance PSD showed distinct release profiles, confirming the method's discriminatory power. However, PSD and viscosity measurements exhibited even greater sensitivity, suggesting their primary role in quality control.

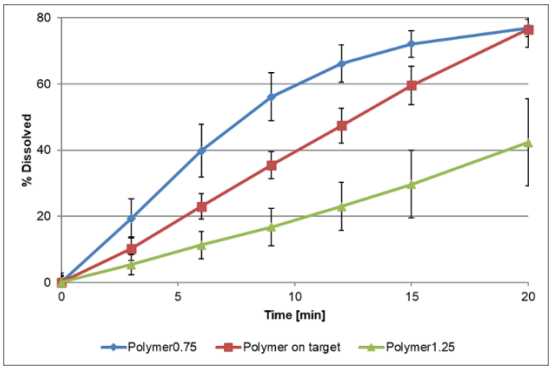

Figure 1. Influence of viscosity on drug release profile (variation of polymer content).

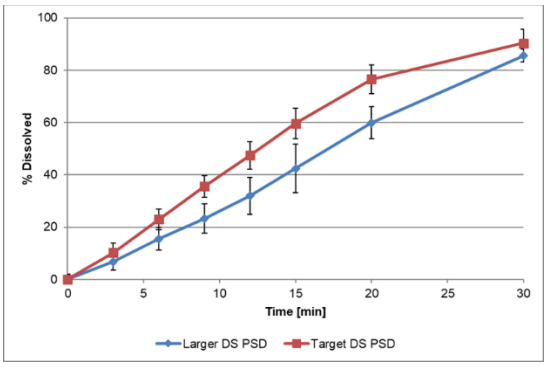

Figure 2. Influence of drug particle size on drug release profile.

4. CONCLUSION

A robust and biorelevant IVRT method using USP Apparatus 4 was developed for ophthalmic gel. While the method provides valuable insights into drug release kinetics, PSD and viscosity remain more sensitive indicators of formulation performance. The method supports regulatory expectations and complements a quality-by-design approach.

ACKNOWLEDGMENT

The authors acknowledge the support of the Sandoz development and analytical teams for their contributions to this work.

OP18

FROM IN VITRO TO IN VIVO: HOW RELIABLE ARE OUR BIOEQUIVALENCE PREDICTIONS?

Jadwiga Paszkowska[1], Marcela Staniszewska[1], Justyna Dobosz[1], Michał Smoleński[1], Dorota Danielak[1], Michał Romański[2], Jarosław Pieczuro[3], Michał Kątny[3], Dagmara Roznerska[3], Janusz Szczepański[3] , Michał Schraube[3], Monika Renn-Hojan[3], Ewa Puk[3] , Oksana Hrem[3], Grzegorz Garbacz[1]

[1]Physiolution Polska, Poland
[2]Department of Physical Pharmacy and Pharmacokinetics, Poznan University of Medical Sciences, Poland
[3] Biofarm, Poland

1. INTRODUCTION

Physiologically-based biopharmaceutics modeling (PBBM) is a valuable tool in modern oral drug development, offering the potential to streamline formulation optimization while reducing both the cost and risk associated with clinical trials. The reliability of PBBM depends heavily on the quality of in vitro dissolution data used for simulation, as well as the robustness of the prediction model, which must be grounded in a thorough understanding of the active pharmaceutical ingredient's (API) behavior following oral administration.

In our previous work, we reported PBBM-based simulations for immediate-release (IR) tablets containing vortioxetine, utilizing dissolution testing in PhysioCell - a novel biopredictive apparatus [1]. In this study, we confront our findings with the results of bioequivalence trials conducted for selected formulations.

2. MATERIALS AND METHODS

2.1. Materials

IR tablets with 20 mg of vortioxetine as a hydrobromide: Brintellix (Comparator) LOT 2706755 was purchased from a local pharmacy; Vortioxetine (Test) LOT 224501 was manufactured by Biofarm (Poland).

2.2. Dissolution testing

Dissolution tests were performed using the PhysioCell [2] in an open-loop configuration. Gastric fluid was simulated with a HCl solution (pH 2.0), and intestinal fluid with a 50 mM phosphate buffer (pH 6.5), both containing physiological levels of bile salts and lecithins. The test protocol reflected fasted intake gastric conditions also in terms of a temperature gradient, variable flow rate, an intragastric stress event (15 min, 300 mbar), and gastric emptying (30 min, 3 × 300 mbar, with an elevated flow rate). Samples were withdrawn independently from the Stress Cell ("gastric" compartment) and the Collection Vessel ("intestinal" compartment). Tests were performed in triplicate. A detailed description of the test conditions is presented elsewhere [1].

2.3. PK modeling

The modeling was performed in Python 3.8. PK simulations were based on a semi-mechanistic approach combined with a two-compartmental popPK model. The model incorporated age and CYP2D6 metabolic status as covariates influencing total clearance, while body height was included as a covariate affecting the volume of the central compartment. All other parameter estimates were adopted from the original reference study by Areberg et al. [3].

2.4. Bioequivalence trial

An open label, randomized, single-dose, monocenter, crossover, PK bioequivalence trial included 32 healthy volunteers of both sexes. The trial was approved by a local ethics committee.

3. RESULTS AND DISCUSSION

3.1. Dissolution test results

Figure 1 presents the API concentration over time in the Stress Cell, while Figure 2 shows the cumulative percentage released over time in the Collection Vessel for both the Test and Comparator products. The in vitro dissolution profiles reveal notable differences between the two formulations. The Test product dissolved faster, reaching complete release within 20 minutes, whereas the Comparator required approximately 30 minutes to fully dissolve.

OP18

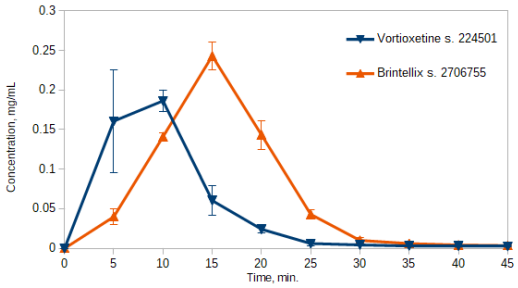

Figure 1. Mean (n=3) dissolution profiles obtained in the Stress Cell.

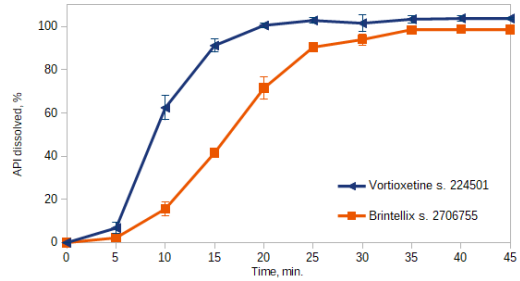

Figure 2. Mean (n=3) cumulative dissolution profiles obtained in the Collection Vessel.

3.2. PK simulations

Despite in vitro differences, the simulated PK profiles were nearly identical (Fig. 3). Moreover, calculated endpoint parameters, such as C_{max} and AUC were similar for Test and Comparator products, indicating high probability of being bioequivalent.

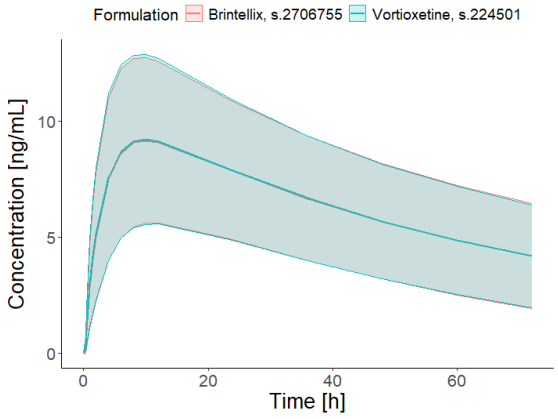

Figure 3. Plasma concentrations (mean with one standard deviation) simulated for the Comparator and Test products in 12 subjects.

3.3. Bioequivalence trial

The results presented in Table 1 show that the 90% confidence intervals $AUC_{(0\text{-}72h)}$ and C_{max} were within 80-125%, proving the bioequivalence of both products.

Table 1. Bioequivalence results: 90% confidence intervals of vortioxetine end point PK parameters (ratio Test vs. Comparator)

Variable	Point estimator	Confidence intervals
$AUC_{(0\text{-}72h)}$	100.34%	96.52%-104.32%
C_{max}	101.82%	97.77%-106.05%

4. CONCLUSION

The bioequivalence study results for the vortioxetine IR tablets confirmed the accuracy of our predictions. This case highlights that the direct comparison of in vitro dissolution profiles alone may be insufficient for reliably forecasting in vivo behavior. Instead, successful prediction requires a comprehensive understanding of the API's physicochemical and PK properties, as well as careful consideration of the target patient population.

5. REFERENCES

1. Romański, Michał, et al., *Application of a novel PhysioCell apparatus for biopredictive dissolution tests of oral immediate release formulations - A case study workflow for in vitro-in vivo predictions.* International Journal of Pharmaceutics, 2023. 641: 123061.
2. Staniszewska, Marcela, et al., *PhysioCell - a Novel, Bio-relevant Dissolution Apparatus: Hydrodynamic Conditions and Factors Influencing the Dissolution Dynamics.* AAPS PharmSciTech,2023. 24(65).
3. Areberg, Johan, et. al., *Population Pharmacokinetic Meta-Analysis of Vortioxetine in Healthy Individuals*, Basic & Clinical Pharmacology & Toxicology, 2014. 115(6), 552-559.

ACKNOWLEDGMENT

This work was supported by the Polish National Centre for Research and Development [POIR.01.02.00-00-0011/17-01]

OP19

ARE ORIGINAL AND GENERIC EXTENDED-RELEASE METFORMIN TABLETS TRULY INTERCHANGEABLE?

Jiri Zeman, Jakub Vyslouzil, Jan Elbl, Sylvie Pavlokova

Department of Pharmaceutical Technology, Faculty of Pharmacy, Masaryk University, Czech Republic

1. INTRODUCTION

Metformin is the first-choice drug for the treatment of type 2 diabetes, with extended-release (XR) tablets being preferred as they reduce adverse effects and improve patient compliance [1]. Since metformin is absorbed primarily in the duodenum and jejunum, gastroretention (prolonged stomach retention) is essential for the proper functioning of extended-release tablets [2]. This can be achieved through various mechanisms; original formulations use a hydrogel-based system that enlarges the tablet so it cannot pass through the pylorus while also controlling drug release [3]. With the increasing number of generic products on the market, the question arises whether these products use the same gastroretentive principles as the original. Despite bioequivalence testing, generics may not have the same properties. Therefore, the study's main aim is to compare the gastroretentive properties of selected products and their dissolution profiles at different pH values, which may occur in comorbidities or treatment with drugs that increase gastric pH.

2. MATERIALS AND METHODS

2.1. Materials

Three samples of XR tablets containing 500 mg of metformin, which are registered and available on the market in the Czech Republic, were used. For this study, the names of the products were anonymized – these included an original medicinal product (original) and two generic products (generic 1 and generic 2). Buffer solutions with pH 1.2 and 6.8 were prepared according to the Ph. Eur. 11. The buffer solution with pH 4.0 was prepared by neutralizing the pH 1.2 buffer solution with sodium hydroxide (Penta Chemicals, Czech Republic).

2.2. Evaluation of tablet physical properties

Tablet weight (n = 5) and dimensions (n = 10) were measured using a WHT-1 Tablet Testing Instrument (Pharma Test, Germany). Hardness (n = 10) was measured using a C50 Tablet Hardness and Compression Tester (Engineering Systems, UK). Tensile strength (Ts) was calculated using the known methodology [4].

2.3. Gel layer analysis

For gel layer analysis, tablets inserted in 3D-printed stabilization cells were immersed in a pH 1.2 buffer. Thickness and time to reach the dry core were measured after 60, 120, 180, 240, and 300 min using a Texture Analyzer CT3 (Brookfield, UK) equipped with a TA39 probe.

2.4. Dissolution test

Dissolution profiles were determined in pH 6.8, 4.0, and 1.2 media (n = 6) using a dissolution apparatus SOTAX AT7 Smart (paddle method, 50 rpm; Sotax, Switzerland) with UV/Vis spectrophotometer Lamda 25 (PerkinElmer, Germany). Difference and similarity factors were calculated to compare the original and generics.

2.5. Data analysis

Statistical analysis used MS Excel paired t-tests for gel layer properties and unpaired t-tests for hardness and tensile strength. The resulting p-values indicate statistical significance ($p < 0.05$) or insignificance ($p > 0.05$). Results are presented as mean ± standard deviation.

3. RESULTS AND DISCUSSION

This study examined the gastroretentive mechanisms of original and generic metformin XR tablets. Rapid gastrointestinal passage could significantly reduce treatment efficacy since metformin is primarily absorbed in the upper small intestine [2]. While physical properties showed similarities among samples, with generics exhibiting greater tablet strength than the original product (Table 1), the critical difference appeared in gel layer formation testing. The original and generic 1 created comparable gel layers at all evaluated times ($p < 0.326$), enabling effective gastroretention through hypromellose matrix swelling.

OP19

However, generic 2 failed to demonstrate similar swelling properties (Fig. 1), nor did it show signs of flotation or high density, which are other gastroretention mechanisms. The dissolution revealed further differences, with generic 1 showing significantly altered dissolution profiles at higher pH values (Fig. 2), potentially affecting therapy when used concurrently with antacids or in conditions that increase gastric pH.

Table 1. Tablet weights (n = 5), dimensions, hardness (n = 10), and calculated tensile strength.

Sample	Original	Generic 1	Generic 2
Weight (mg)	727.90 ± 10.40	845.10 ± 9.00	714.90 ± 8.40
Length (mm)	12.09 ± 0.01	16.50 ± 0.03	15.05 ± 0.02
Width (mm)	12.09 ± 0.01	8.23 ± 0.02	8.58 ± 0.02
Height (mm)	6.95 ± 0.03	6.63 ± 0.02	6.96 ± 0.02
F (N)	151.97 ± 6.69	299.81 ± 15.47	247.07 ± 8.48
Ts (N/mm^2)	1.15 ± 0.05	2.45 ± 0.12	n/a

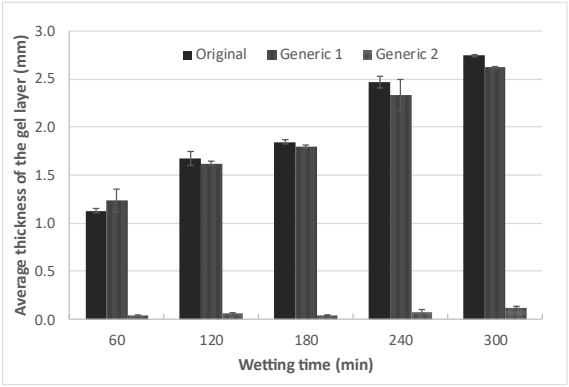

Figure 1. Thickness of the gel layer during swelling in a buffer solution at pH 1.2 (n = 3).

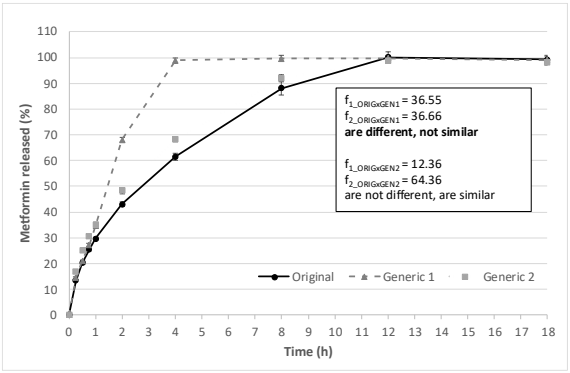

Figure 2. Dissolution profiles of tablets at pH 6.8 with similarity evaluation (n = 6).

4. CONCLUSION

This study compared the original formulation with two generics, focusing on gastroretention and dissolution characteristics. A pronounced difference was observed in the gastroretentive mechanism: the original formulation and generic 1 utilized matrix swelling and mucoadhesion for retention, whereas generic 2 lacked these properties and also did not float. Based on these findings, generic 2 may transit through the stomach more rapidly, potentially reducing metformin absorption in the upper gastrointestinal tract. Regarding dissolution, generic 1 exhibited a faster release at pH 6.8, which could increase the risk of adverse effects under specific conditions, such as pathological states or elevated gastric pH. These findings indicate that generic formulations may not exhibit identical *in vivo* properties despite meeting bioequivalence criteria, highlighting the need for caution in generic substitution.

5. REFERENCES

1. Blonde, L., et al., *Gastrointestinal tolerability of extended-release metformin tablets compared to immediate-release metformin tablets: results of a retrospective cohort study.* Current Medical Research and Opinion, 2004. 20(4): 565–572.

2.Graham, G.G., et al., *Clinical pharmacokinetics of metformin.* Clinical Pharmacokinetics, 2011. 50(2): 81–98.

3. Timmins, P., et al., *Steady-state pharmacokinetics of a novel extended-release metformin formulation.* Clinical Pharmacokinetics, 2005. 44(7): 721–729.

4. Yohannes, B., et al., *Determination of tensile strength of shaped tablets.* Powder Technology, 2021. 383: 11–18.

OP20

A USEFUL METHOD FOR MONITORING OF ANTIBIOTICS IN WASTEWATERS BY SPE-LC-MS/MS

Andrej Grobin[1], Robert Roškar[1], Jurij Trontelj[1]

[1]*Department of biopharmaceutics and pharmacokinetics, University of Ljubljana, Faculty of Pharmacy, Slovenia*

1. INTRODUCTION

The presence of antibiotics in environmental waters is a significant health issue because it contributes to the development and spread of antibiotic-resistant bacteria. When antibiotics enter surface waters through wastewater discharge, they create selective pressure that enables populations of resistant microbes to spread [1]. These resistant strains are making infections harder to treat and are increasing the risk of disease outbreaks, prolonged illnesses, and higher medical costs. Such infections could lead to over 39 million direct deaths and 169 million indirect deaths globally between 2025 and 2050 [2]. Therefore, addressing this contamination is crucial to safeguarding both environmental and public health.

2. MATERIALS AND METHODS

2.1 Materials

Analytical standards of amoxicillin, azithromycin, ciprofloxacin, erythromycin, sulfamethoxazole, trimethoprim (Sigma-Aldrich) and clarithromycin (EDQM) were used.

2.2. LC-MS/MS Analysis

Chromatographic separation was performed using an Agilent Infinity 1290 II system with an Agilent InfinityLab Poroshell 120 EC-C18, 100 × 3,0 mm, 2,7 µm column at 40 °C. 0.05% acetic acid in MQ water and acetonitrile were used as a mobile phase in a gradient method. A Sciex 5500+ was used for MS/MS analysis.

2.3. Sample Preparation

The extraction was performed on a Horizon technologies SPE-DEX 4790 semi-automated extraction system using Atlantic HLB H disks provided by Waters corporation. 250 mL of unfiltered wastewater samples were combined with 250 mL of 50 mM KH_2PO_4 buffer with a pH value of 7.0, loaded onto the disks and eluted. The eluates were treated with magnesium sulphate for excess water removal, centrifuged and dried in a Turbovap LV solvent evaporator (Biotage). The dried samples were then reconstituted in 200 µL of reconstitution solvent, thus achieving a concentration factor of 100.

3. RESULTS AND DISCUSSION

3.1. Method Validation

The developed method was validated in terms of selectivity (no crosstalk of analytes at representative retention times), linearity (R^2>0,99 for the combined procedure), limits of quantitation (as low as 5 ng/L), accuracy (98-108% for most analytes), precision (up to 6,0% RSD) and recovery (over 75% for most analytes). The method is sensitive and calibrated at environmentally relevant concentrations, achieves high repeatability and is accurate. The chromatogram of the analytes is presented in Fig 1.

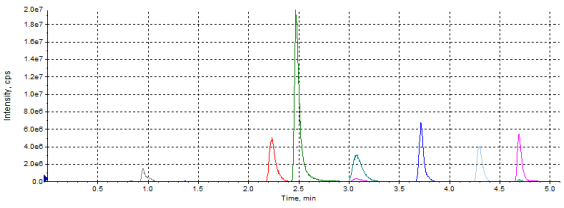

Figure 1. A combined MRM chromatogram of analytes in the method. Retention times for peaks in minutes as follows: amoxicillin 1.0, trimethoprim 2.2, ciprofloxacin 2.5, azithromycin 3.1, sulfamethoxazole 3.7, erythromycin 4.3 and clarithromycin 4.7.

3.2. Method Application

The method was applied to wastewater samples from a communal wastewater treatment plant to determine the occurrence of antibiotics and the effectiveness of their removal with conventional techniques. The results are presented in Fig. 2. All antibiotics except amoxicillin were successfully quantified in samples in concentrations of up to 640 ng/L in influents and up to 760 ng/L in effluents with removal rates of up to 83%.

OP20

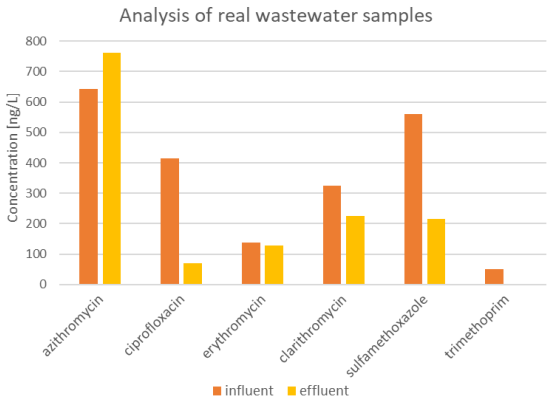

Figure 2. Concentrations of antibiotics in wastewater influent and effluent samples in ng/L

4. CONCLUSION

The developed method is based on a simple semi-automatic SPE extraction and a quick LC-MS/MS method, which was extensively validated. Combining the environmentally relevant LOQ values with good accuracy and precision, the method provides a reliable tool for the routine monitoring of important antibiotics in wastewaters to provide relevant information on their presence and risks in the environment.

5. REFERENCES

1. Mohsen N., et al., *Global burden of bacterial antimicrobial resistance 1990–2021: a systematic analysis with forecasts to 2050.* The Lancet, 2024. 404(10459): 1199 – 1226.

2. Wengenroth, L., et. al. *Antibiotic Resistance in Wastewater Treatment Plants and Transmission Risks for Employees and Residents: The Concept of the AWARE Study*. Antibiotics, 2021. 10(5): 478.

ACKNOWLEDGMENT

This research was financially supported by the Slovenian Research Agency (ARRS) [P1-0189 and J2-4480] and European Partnership for the Assessment of Risks from Chemicals (PARC) [101057014].

OP21

IN SITU CHARACTERIZATION OF 3D PRINTED PHARMACEUTICALS USING MAGNETIC RESONANCE IMAGING AND RELAXOMETRY METHODS

Ewelina Baran[1], Piotr Kulinowski[1], Magdalena Urbanowicz[2], Marta Łaszcz [2]

[1]Institute of Technology, Pedagogical University of Cracow, 2 Podchorążych St., 30-084, Kraków, Poland
[2]Falsified Medicines and Medicinal Materials, National Medicines Institute, Poland

1. INTRODUCTION

3D printing opens new possibilities for the pharmaceutical industry, such as on-demand manufacturing of medicines for individual patients [1,2]. The selection of the appropriate 3D printing method for manufacturing the desired dosage form depends on the desirable drug release pattern, properties of the active pharmaceutical ingredients (APIs) and polymers, as well as the risk of APIs degradation during the printing process with high printing temperature or using UV light/beams [3]. Particularly promising techniques seem to be those based on printing from photopolymers and powders (selective laser sintering - sls). 3D printed drug delivery systems can be characterized in situ during drug release using NMR/MRI techniques in terms of describing mass transport phenomena, especially in the case of systems dealing with two mobile phases (e.g. water and polymer). The studies allow to determine how interfacial mass transport phenomena affect the functional properties of the 3D printed material [4,5]. They complement very well the standard measurements performed during release studies.

2. MATERIALS AND METHODS

2.1. DLP 3D-printing

The basic composition consisted of a photopolymer - PEGDA, API and a photoinitiator DPPO (1%). Additives were added to the mixtures, which were intended to modify the release profiles. The matrices were printed using a Sonic Mini 8K LCD printer (Phrozen, Hsinchu City, Taiwan). Under appropriate printing conditions, the tablets produced showed sufficient hardness, retained their shape, were not too friable and had a smooth surface.

2.2. SLS 3D-printing

Metronidazole (Met) (Hubei Hongyuan Pharmaceutical Technology Co. Ltd. Fengshan, China) and commercial, carbon-stained nylon for 3D printing (PA12 Powder, Sintratec AG, Brugg, Switzerland), sodium chloride (Merck KGaA, Darmstadt, Germany) were used in the study. All other materials were applied in analytical grade. SLS of initially homogenized through sieve 150 mesh, powders of fine, pure crystals of Met, PA12 or sodium chloride was performed using Sintratec Kit 3D (Sintratec AG, Brugg, Switzerland) 3D printer equipped with a blue laser (2.3 W, 445 nm wavelength), operating under Sintratec Central v. 1.2.5 software.

2.3. Drug release

API release studies were performed using USP Apparatus 2, Apparatus 3 and Apparatus 4, according to The European Pharmacopoeia.

2.4. Magnetic resonance imaging

MRI was performed using a 9.4 T MRI research scanner (Biospec 94/20, Bruker BioSpin MRI GmbH, Ettlingen, Germany). Two imaging sequences were used: multi-echo spin-echo (MSME) and a three-dimensional version of UltraShort Echo Time (UTE3D).

2.5. LF TD NMR relaxometry

LF TD NMR relaxometry was performed using a 23 MHz NMR Rock Core Analyzer under PROSPA 4.26 software (Magritek, New Zealand and Germany). Three pulse sequences were used: FID, CPMG (Carr-Purcell-Meiboom-Gill) for obtaining 1D T2 relaxation times spectra Inversion-Recovery CPMG (IR-CPMG) for obtaining 2D T1-T2 relaxation time maps

3. RESULTS AND DISCUSSION

3.1. DLP - printlets

Figure 1 shows the sample (PEGDA to PEG ratio = 30/70) printed using the DLP method and the measurement results: the T_1-T_2 relaxation time correlation map and the image obtained using the MSME method along with the

parametric profiles. Across this formulation in an as-printed state, two components related to PEG presence were detected with T_2 of the component of higher intensity lower than 100 ms. Also, the sample was spatially homogeneous. At 0 h, two components in the profile coexisted; however, the first originated from PEG, and the second from water diffusing from the surrounding bulk medium. The matrix changed its properties in terms of A and T_2 immediately after immersion in water. The T_1-T_2 map allows additional separation of various proton pools in terms of signal components using the T_1 relaxation time scale. In MRI T2/A profiles, the shortest fitted T2 relaxation times were about 10 ms, and only highly mobile fractions were detected and quantified .

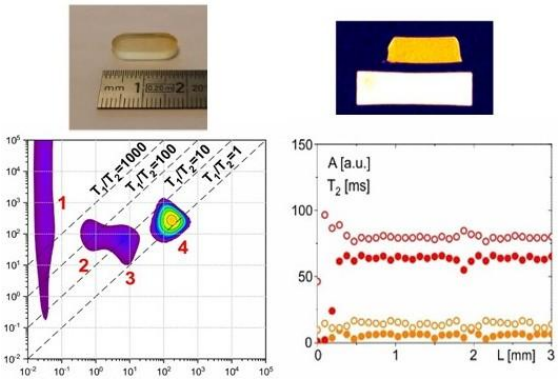

Figure 1. The example of printlet, T_1-T_2 maps for as-printed sample, image obtained at the first echo (3.5 ms); T_2 and amplitude profiles across the tablet's for PEGDA to PEG ratio = 30/70.

3.2. SLS - printlets

The resulting printlets were of good quality with an internal porous structure, which assured flotation. Laser speed and the addition of an osmotic agent in low content influenced drug release changing release profiles. The time required to release 80% of the drug substance ranged from 13 hours to 21 hours depending on the formulation. Met release in USP apparatus 3 was substantially faster than in USP4 for all formulations due to different hydrodynamic conditions. X-ray microtomography shows interesting aspects of matrix porosity and a plethora of features when performer on printlet immersed in a dissolution medium (porous zone, water penetration zones, macro cracks, air bubbles). The T1-T2 obtainded using LF TD NMR map allows separation of various proton pools. Based on UTE3D MRI analysis, areas with different water mobility were distinguished based on signal intensity.

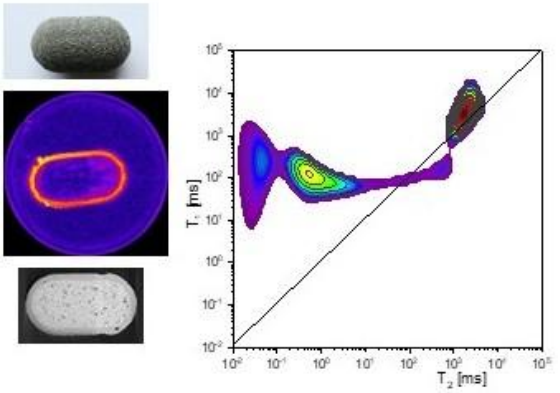

Figure 2. The example of printlet, longitudinal sections obtained using the microCT and UTE3D methods after 24 h hydration, T_1-T_2 correlation maps for formulation Met to Pa12 ratio = 80/20 after removal from water after 3 h of hydration.

4. CONCLUSION

3D printed tablets could be characterized using MRI techniques including mass transport phenomena description, in particular for systems dealing with mobile phases and how these phenomena could influence their functional properties. MRI measurement results were compared with drug release studies.

5. REFERENCES

1. Mathur, S., Sutton, J., *Personalized medicine could transform healthcare*, Biomedical Reports, 2017, 7: 3–5.
2. Redekop, W. K., Mladsi, D. *The Faces of Personalized Medicine: A Framework for Understanding Its Meaning and Scope.* Value in Health, 2013, 16: 4.
3. Abdella, S., et al., *3D Printing of Thermo-Sensitive Drugs*, Pharmaceutics,2021, 9: 13.
4. Baran et al., *3D Printed Drug Delivery Systems in Action–Magnetic Resonance Imaging and Relaxometry for Monitoring Mass Transport Phenomena,* ACS Appl. Mater. Interfaces, 2024, 16, 31, 40714–40725.
5. Kulinowski, P., et al., *Development of Composite, Reinforced, Highly Drug-Loaded Pharmaceutical Printlets Manufactured by Selective LaserSintering—In Search for Relevant Excipients for Pharmaceutical 3D Printing,* Materials, 2022, 15: 2142.

ACKNOWLEDGMENT

The work was supported by the National Science Centre Poland grants number UMO-2022/45/B/NZ7/04081 and UMO-2018/31/B/NZ7/03238.

Poster presentations

P001

MATERIAL MATTERS: HOW RAW MATERIAL PARTICLE PROPERTIES INFLUENCE OPHTHALMIC SUSPENSION CQAs

Željko Agić[1], Nina Popović[1], Kristina Žuža[1], Ivona Pečurlić[1], Andrea Roje[1]

[1]Jadran-Galenski Laboratorij d.d., Rijeka, Croatia

1. INTRODUCTION

Loteprednol etabonate (LE) 0.5% eye drops suspension is a topical corticosteroid solution used to treat post-surgical ocular inflammation [1]. In addition, LE shows promising results in the treatment of dry eye disease [2]. Ophthalmic suspensions are commonly used for formulating poorly soluble active pharmaceutical ingredients (APIs), enhancing drug delivery by extending ocular residence time. Suspended API particles remain in the fornix and dissolve slowly, improving bioavailability [3]. API's particle size is a key factor affecting both physical stability and therapeutic efficacy of suspensions. Therefore, particle size distribution (PSD) is a critical quality attribute (CQA) of such drug products.

The goal of this work was to evaluate how the critical material attributes of sterile and non-sterile LE, such as particle size, shape, and surface characteristics, influence the PSD in the drug product, with the aim of optimizing the physical stability of LE 0.5% eye drops suspension.

2. MATERIALS AND METHODS

Several batches of sterile (Universal Farma, Spain) and non-sterile (Industriale Chimica Srl, Italy) LE were used for preparation of laboratory and scale-up batches of the drug product. The size and morphology of LE particles were analysed using both laser diffraction method (Mastersizer 3000 with Hydro MV unit, Malvern Panalytical Ltd., UK) and morphology directed Raman spectroscopy (MDRS; Morphologi 4-ID system, Malvern Panalytical Ltd., UK). The X-Ray Powder Diffractometry (XRPD) patterns were obtained using an X'Pert Pro diffractometer (model PW3050/60, Malvern Panalytical Ltd., UK). PSD in the drug product was measured by the laser diffraction method (Mastersizer 3000, Hydro MV unit, Malvern Panalytical Ltd., UK). To screen for potential changes in PSD over time, measurements were performed immediately after drug product preparation and at different time points. The following parameters were analysed and compared: D_{10}, D_{50}, D_{90}, D_{98}, D_{100}, and span. An increase in PSD was a sign of poor suspension stability and an indicator of agglomeration.

3. RESULTS AND DISCUSSION

3.1. Raw material analysis

MDRS analysis revealed differences in particle size and morphology of sterile and non-sterile LE. The non-sterile API contains a significantly higher portion of particles smaller than two micrometres (D_{50}=1.4 µm), while the sterile API has larger individual particles (D_{50}=2.8 µm).

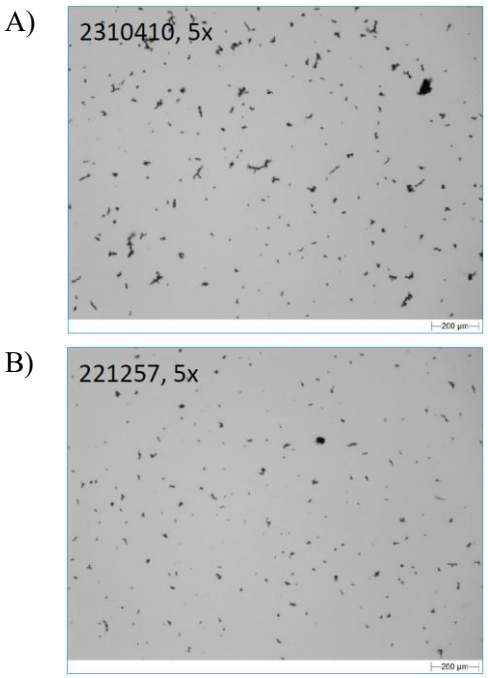

Figure 1. Optical micrograph of sterile (A) and non-sterile (B) LE.

The non-sterile material contains more round particles (higher circularity), whereas the sterile LE particles are elongated (Fig. 1).
XRPD analysis showed no difference in crystal structure between sterile and non-sterile LE. No

P001

change in crystal structure was observed during the manufacturing process of suspensions.

3.2. Laboratory batches

Several laboratory batches containing sterile and non-sterile LE were prepared, and their PSD analysed. All batches containing sterile LE, had greater PSD than batches containing non-sterile LE. Even though D_{10}, D_{50}, and D_{90} were somehow similar, the difference was more pronounced in the D_{98} and D_{100} PSD parameters (Fig. 2), suggesting the presence of agglomerates in the batches containing sterile API.

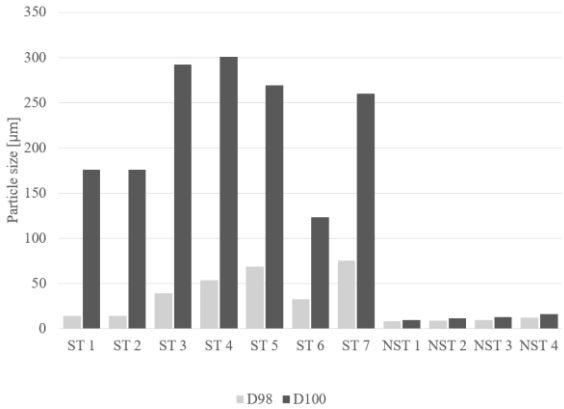

Figure 2. PSD parameters D_{98} and D_{100} for laboratory batches containing sterile (ST) and non-sterile (NST) LE.

3.3. Scale up batches

Two scale-up batches, one with sterile and the other with non-sterile LE were manufactured. PSD was measured for both batches immediately upon bulk preparation (T0), after one month (T1), and after six months (T6) at 25°C and 60% relative humidity (RH). PSD results at T0 showed no significant differences in D_{10}, D_{50}, and D_{90} between batches containing sterile and non-sterile LE. The difference in PSD was only noticeable in parameters D_{98} and D_{100}, confirming the results of laboratory phase. T1 analysis revealed an increase in particle size of batches containing sterile LE, while the same phenomenon was not observed for batches containing non-sterile API. This increase in size was more pronounced over time, resulting in out-of-specification results for D_{90} in T6 (Fig. 3). On the other hand, the batch containing non-sterile LE showed no increase in any of the PSD parameters.

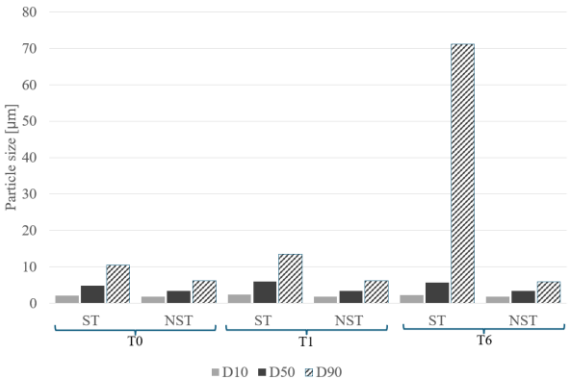

Figure 3. PSD parameters $D_{10,}$ D50 and D_{90} for scale-up batches containing sterile (ST) and non-sterile (NST) LE. PSD measured at three time points, stored at 25°C and 60% relative humidity (RH).

4. CONCLUSION

Even though the sterilization process did not result in structural changes, it does evoke morphological differences between sterile and non-sterile raw material. Particle size and morphology of raw material influence the drug product PSD - one of the main CQAs of a drug product in the form of suspension. Drug products formulated with sterile API exhibited generally larger particles compared to those containing non-sterile API, with a tendency to increase over time, i.e. to form agglomerates. In this work we have shown that PSD parameters D_{98} and D_{100}, can be predictive of the suspension stability. These parameters are often not included in the drug product or raw material specification and are not in the scope of regulatory guidance. Regardless, they can be a helpful tool for formulation screening in the early stage of development.

5. REFERENCES

1. Amon, M., et al., *Loteprednol etabonate ophthalmic suspension 0.5 %: efficacy and safety for postoperative anti-inflammatory use*. International Ophthamology, 2012. 32(5): 507-517.

2. Beckman, K., et al., *Loteprednol Etabonate for the Treatment of Dry Eye Disease*. Journal of Ocular Pharmacology and Therapeutics, 2020. 36(7): 497-511.

3. Vo, A., et al., *Factors affecting the particle size distribution and rheology of brinzolamide ophthalmic suspensions*. International Journal of Pharmaceutics, 2020. 586: 119495

P002

A NOVEL APPROACH TO LIQUISOLID FORMULATION FOR LORNOXICAM

Alaa Gamiel[1], Csilla Balla-Bartos [1], Rita Ambrus[1]

[1]Institute of Pharmaceutical Technology and Regulatory Affairs, University of Szeged, Szeged, Hungary

1. INTRODUCTION

Lornoxicam is a potent nonsteroidal anti-inflammatory drug (NSAID) belongs to the oxicam group. It is commonly used for pain conditions musculoskeletal disorders and postoperative pain. Its major problems are the formulation challenges due to poor water solubility and the potential gastric side effects and ulcerogenesis. Conventional liquisolid systems represent an innovative and promising approach for creating solid dosage forms that incorporate a significant amount of liquid, specifically by dispersing the drug within an appropriate hydrophilic and non-volatile liquid medium or a liquid drug. This technology boasts several benefits, most notably: ease of use, affordability, suitability for large-scale manufacturing, and eco-friendliness. In our study, we aimed to employ the core principle of this technique with modifications pertaining to the usage of a coating material.

2. MATERIALS AND METHODS

2.1. Materials

The model drug was lornoxicam (LXM) (6-Chloro-4-hydroxy-2-methyl-N-(pyridin-2-yl)-2H-thieno[2,3-e] [1,2] thiazine-3-carboxamide 1,1-dioxide) (Tokyo Chemical Industry, Japan). Polyvinylpyrrolidone K90 (PVP K90) (Sigma-Aldrich, China), Tween 80® (Sigma-Aldrich Chemie GmbH, Darmstadt, Germany), sodium bicarbonate and Avicel PH 102 were chosen as excipients based on our previous work [1] and purified water was used to prepare the aqueous solutions.

2.2. Solubility studies

Solubility of LXM was studied in different solvent: distilled water (pH 6.8), a buffer at pH 1.2, Tween 80, a 15% w/v aqueous $NaHCO_3$ solution with Tween 80, and a 15% w/v aqueous $NaHCO_3$ solution.

2.3. Sample preparation

Figure 1 represents the steps of sample preparation.

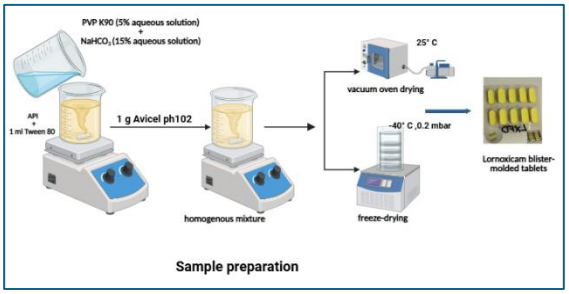

Figure 1. Preparation of sample formulation.

2.4. Sample characterization

Physico-chemical properties of pure LXM, physical mixture, vacuum-dried sample and freeze-dried sample were investigated. Surface morphology was analyzed via scanning electron microscopy (SEM). Thermal behaviour was accessed by Differential scanning calorimetry (DSC) Thermogravimetric Analysis (TGA). X-ray powder diffraction (XRPD) analysis was employed to examine the physical structure. Surface free energy and polarity of were calculated for evaluation of powder wettability.

2.5. In vitro dissolution

In Vitro dissolution testing was performed at pH 1.2, and a comparative analysis was conducted between our sample and the commercial product using the pairwise similarity factor model (f_2)[2].

3. RESULTS AND DISCUSSION

3.1. Solubility studies

LXM exhibited limited solubility at pH 1.2. The integration of and Tween® 80 was observed to enhance solubility improves solubility, while incorporation of sodium bicarbonate aqueous solution yielded the optimal solubility outcome

3.2. Sample characterization

LXM Images obtained via (SEM) revealed geometric crystal structures demonstrating a wide size distribution. Conversely, the formulations exhibited a porous matrix structure, indicating the potential amorphization of the active ingredient. When comparing vacuum drying (VD) with freeze drying (FD), the FD samples exhibited a more porous surface. The LXM DSC curve exhibited a

distinct exothermic peak at 225.48 °C, signifying its decomposition, which is corroborated by Thermogravimetric Analysis (TGA). This peak was absent in the sample powders, suggesting the formation of an amorphous state. The crystallinity indices calculated from sample diffractograms revealed reduction crystallinity of the drugs (Figure 2). Results of calculated polarity and the surface free energy suggested that the formulated samples exhibit greater wettability and hydrophilic properties compared to the pure drug.

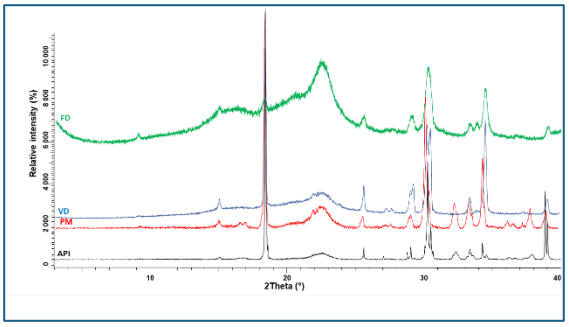

Figure 2. XRPD diffractograms of API, physical mixture (PM), vacuum-dried powder (VD), and freeze-dried powder (FD).

3.3. In vitro dissolution

The dissolution profiles of the API and various formulations are depicted in Figures 3. Our formulations, which were subjected to freeze-drying and vacuum drying techniques, demonstrated complete dissolution within 15 minutes, in contrast to the less than 10% dissolution observed with the pure drug (after 60 minutes). This enhancement in solubility may be attributed to the influence of excipients chosen. Furthermore, there is a significant positive correlation between this finding and the formulation techniques employed. Both drying methods positively affect dissolution; however, the freeze-drying method yields notably superior results (f_2 = 42). This aligns with the findings of Taldaev et al. as reported in their review [3], which may be explained by the increased surface area of the freeze-dried powder, the amorphous structure of LXM, and the high porosity of the lyophilizate. Additionally, our freeze-dried product was evaluated in comparison to both simple and rapid commercial tablets containing LXM. The dissolution characteristics of the freeze-dried product were analogous to those of the rapid-acting commercial tablet (f_2 = 66).

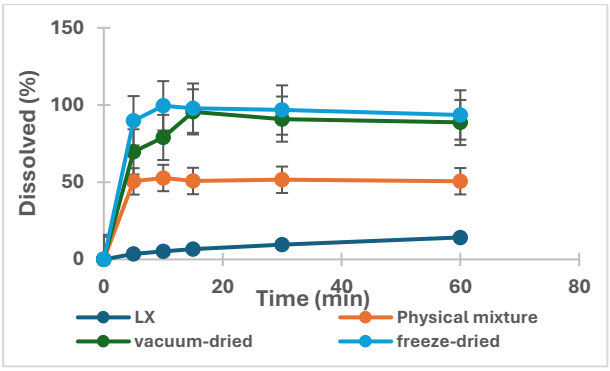

Figure 3. Dissolution rate profiles at pH 1.2.

4. CONCLUSION

The modified liquisolid technique has demonstrated efficacy in enhancing the solubility of lornoxicam in acidic environments. Structural analysis indicates a reduction in the crystallinity of lornoxicam alongside increased hydrophilicity. Freeze-drying significantly impacts the structural integrity and dissolution rate of lornoxicam, yielding promising outcomes for the formulation of an advanced oral dosage form with rapid dissolution, utilizing a minimal quantity of effective excipients. Our future endeavours include conducting stability studies and further investigations to extend the application of this technique to various drug models.

5. REFERENCES

1. El-Setouhy, D.A.; Gamiel, A.A.-R.; Badawi, A.A.E.-L.; Osman, A.S.; Labib, D.A. *Comparative Study on the in Vitro Performance of Blister Molded and Conventional Lornoxicam Immediate Release Liquitablets: Accelerated Stability Study and Anti-Inflammatory and Ulcerogenic Effects. Pharmaceutical Development and Technology* **2017**, *22*, doi:10.1080/10837450.2016.1221423.
2. Moore, J.W.; Flanner, H.H. Mathematical Comparison of Dissolution Profiles. *Pharm. technol* **1996**, *20*, 64–74.
3. Taldaev, A.; Pankov, D.I.; Terekhov, R.P.; Zhevlakova, A.K.; Selivanova, I.A. *Modification of the Physicochemical Properties of Active Pharmaceutical Ingredients via Lyophilization*. *Pharmaceutics* **2023**, *15*, 2607, doi:10.3390/pharmaceutics15112607.

ACKNOWLEDGMENT

This work was supported by the NKFI OTKA K_146148 project.

P003

GREEN FLUIDIZED BED GRANULATION: INVESTIGATION OF THE INFLUENCE OF WATER CONTENT AND POVIDONE GRADE

Ivana Aleksić[1], Teodora Glišić[1]

[1]*Department of Pharmaceutical Technology and Cosmetology, University of Belgrade, Faculty of Pharmacy, Serbia*

1. INTRODUCTION

The pharmaceutical industry has recently been identified as one of the main contributors to climate change [1]. In recent years, pharmaceutical companies have been working hard to reduce their environmental footprint, but the changes are still negligible in relation to the use of carbon-intensive traditional manufacturing technologies. It is well known that wet granulation, which is the most commonly used method in tablet production, contributes significantly to greenhouse gas emissions. Green fluidized bed granulation (GFBG) has recently been introduced as an environmentally friendly alternative to wet granulation, characterized by the absence of a drying phase [2]. The aim of the present study was to investigate the influence of the water content and the type of povidone (PVP) used as a binder on the flowability and tableting properties of granulates prepared by GFBG.

2. MATERIALS AND METHODS

2.1. Materials

Lactose monohydrate (Sigma-Aldrich, Germany) was used as filler and povidone K12 or K25 (Plasdone^{TM}, Ashland, Switzerland) as binder. Microcrystalline cellulose (Vivapur 102, JRS Pharma, USA) and colloidal silicon dioxide (Aerosil 200, Evonik Industries AG, Germany) were used as moisture absorbents, while crospovidone (Polyplasdone XL-10, GAF Chemicals Corporation, USA) was used as a disintegrant and magnesium stearate (Dr. Paul Lohman, Germany) as a lubricant.

2.2. Preparation of tableting mixtures

Granulation was carried out in the Mycrolab fluid bed processor (OYSTAR Hüttlin, Germany) according to the method described by Takasaki et al. [2]. The inlet air flow rate was 25 m^3/h, and the inlet air temperature was 25 °C. The amount of water used was 3 or 5%. The water feed rate was 5 g/min, the spray air pressure was 1.2 bar and the microclimate pressure was 0.4 bar.

2.3. Particle size analysis, density and flowability testing

The particle size distribution was evaluated by sieve analysis using a set of standard sieves in the range of 63–500 μm. The flow properties of tableting mixtures prepared were evaluated by the powder flow rate (Erweka flowmeter type GDT, Erweka GmbH, Germany) and by calculating the Carr index based on the determined bulk and tapped density (STAV 2003, J. Engelsmann AG, Germany). The true density was determined using a helium pycnometer (AccuPyc 1330, Micromeritics, USA).

2.4. Preparation of compacts and tableting properties evaluation

The compacts were prepared on an instrumented single-punch tablet press (GTP D series, Gamlen Tableting Ltd, UK) with 6 mm flat faced punches. The compacts (100 mg) were compressed under compression loads in the range of 300 to 500 kg and a compression speed of 60 mm/min. The detachment stress and the ejection stress were calculated from the force-displacement curves obtained. The compact tensile strength was calculated from the tablet crushing force determined using the Erweka TBH 125D tablet hardness tester (Erweka GmbH, Germany). Elastic recovery (24 h after compression) was also determined. The compressibility, compactibility and tabletability profiles were constructed, as well.

2.4. Disintegration testing

The disintegration time of the compacts prepared was determined using the disintegration tester (Erweka ZT52, Germany).

3. RESULTS AND DISCUSSION

3.1. Particle size distribution and flowability

The investigated samples showed a similar particle size distribution, with the main particle size fraction being 63–125 μm. The influence of the amount of water or povidone viscosity grade

on the particle size distribution was not pronounced, although a slightly higher proportion of particles in larger particle size fractions was observed in the samples prepared with PVP K12. The influence of the investigated factors on the flow properties of the tested samples was also not pronounced. All tableting mixtures tested showed acceptable flow properties with Carr index values between 20 and 23%.

3.2. Tableting properties

Good mechanical properties of the compacts prepared by GFBG were observed, with higher compression pressure leading to higher tensile strength (Fig. 1). It can be observed that the use of PVP K12 leads to a somewhat higher tensile strength than PVP K25, which is characterized by its higher viscosity in aqueous solution. This is consistent with literature data supporting the use of PVP K12 for this low water content granulation method [2]. For the samples prepared with the same type of PVP, a higher water content led to a slightly higher tensile strength.

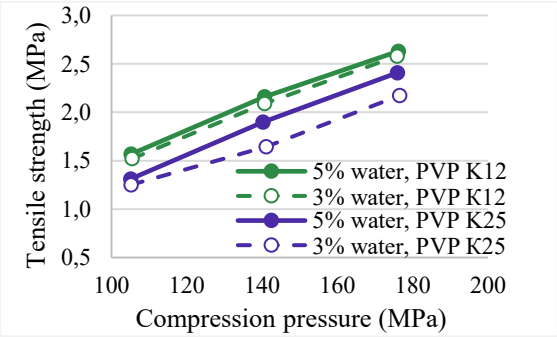

Figure 1. Tabletability profiles of the investigated samples.

The values determined for the detachment and ejection stress were rather low (< 1.5 MPa) regardless of the applied compression pressure, indicating good lubricating properties of the investigated samples. The elastic recovery of the investigated samples was between 17 and 28% and increased at higher compression pressures.

The compression characterization of the tableting mixture prepared with PVP K12 and 3% water revealed favorable compressibility and compactibility profiles. In the compression pressure range tested, the tensile strength values were between 1.5 and 2.5 MPa and the solid fraction values were in the range of 0.85±0.05, which corresponds to the values recommended in the literature [3].

3.3. Disintegration time

The investigated samples showed rapid disintegration. The disintegration time varied between 14 and 77 s, depending on the formulation factors and the applied compression pressure. In general, factors that led to a higher tensile strength also led to a longer disintegration time.

4. CONCLUSION

The results presented show that a novel, green fluidized bed granulation can ensure excellent tableting properties combined with rapid tablet disintegration. It was found that the type of povidone and the water content moderately influence the properties of the investigated tableting mixtures.

5. REFERENCES

1. Belkhir L, Elmeligi A. *Carbon footprint of the global pharmaceutical industry and relative impact of its major players*. Journal of Cleaner Production, 2019. 214: 185-194.

2. Takasaki, H., et al., *Novel, lean and environment-friendly granulation method: Green fluidized bed granulation (GFBG).* International Journal of Pharmaceutics 2019. 557: 18-25.

3. Leane, M., et al., *A proposal for a drug product Manufacturing Classification System (MCS) for oral solid dosage forms.* Pharmaceutical Development and Technology, 2015. 20(1): 12-21.

ACKNOWLEDGMENT

This research was funded by the Ministry of Science, Technological Development and Innovation, Republic of Serbia through two Grant Agreements with University of Belgrade-Faculty of Pharmacy No 451-03-136/2025-03/ 200161 and No 451-03-137/2025-03/ 200161.

P004

PROCESS OPTIMIZATION OF NANOEMULSION CONTAINING A LIPOPHILIC PEPTIDE FOR OPHTHALMIC USE: DESIGN OF EXPERIMENTS APPROACH

Antonela Baćac[1], Karla Dubaić[1], Ivana Poropat[1], Maria Tadić[1], Drago Špoljarić[2], Ivo Ugrina[2]

[1]Research and Development, Jadran – Galenski laboratorij d.d., Rijeka, Croatia
[2]Intellomics d.o.o., Split, Croatia

1. INTRODUCTION

Nanoemulsions (NEs) are dispersions of nanosized droplets of one immiscible liquid in another, typically oil in water, stabilized by surfactants. NEs are widely studied in ophthalmic pharmaceuticals to improve the solubility, bioavailability, and targeted delivery of drugs. The formulation of innovative drug delivery systems, such as NEs, requires a deep understanding of pharmaceutical principles and manufacturing processes - especially in selecting process parameters that ensure the desired properties and stability of the formulation [1].

Considering the complexity of the developed formulation, the Design of experiment (DoE) approach was chosen for process optimization. DoE is used to plan investigations and solve experimental problems that arise across a variety of areas [2].

The effect of critical process parameters (CPPs) on the critical quality attributes (CQAs) of the emulsion was systematically assessed using the DoE approach. CPPs with potential influence on the CQAs were identified based on understanding of the formulation and process, supported by preliminary experiments.

2. MATERIALS AND METHODS

2.1. Design of Experiment

As part of the DoE screening, 22 formulations were prepared by modifying CPPs as follows: the temperature of the oily and water phases, the quantity of water in the water phase, the mixing time of the oily phase, the mixing time and mixing speed of the oily and water phases, homogenization pressure, and total homogenization time (Fig. 1).

The formulations' qualitative and quantitative composition was kept constant throughout the study. Each formulation was tested on relevant physical parameters (pH, osmolality, surface tension, mean droplet size, polydispersity index, zeta potential) (Fig. 1). Obtained results were statistically evaluated.

Definitive screening experimental design was performed using JMP® 14.0 statistical software (SAS Institute Inc., Cary, NC,1989–2007).

2.2. Formulations preparation

The oily and water phases were mixed with an Ultra-Turrax® mixer (IKA-Werke) resulting in a coarse emulsion. The coarse emulsion was homogenized using a high-pressure homogenizer, PandaPlus 2000 (GEA Niro Soavi) to obtain a NE. The final NE product was sterilized by heat.

2.3. Formulations analysis

The pH of the NEs was measured using a SevenExcellence™ pH Meter (Mettler Toledo). The osmolality was measured using Osmomat 3000 D (Gonotec). For measuring surface tension of NEs, optical tensiometer Attention Theta Flex (Biolin Scientific) was used.

The droplet size and polydispersity index (PDI) of NEs were measured at 25 °C by dynamic light scattering (DLS) using a Zetasizer Ultra (Malvern Panalytical). The zeta potential was determined by electrophoretic light scattering (ELS) using a Zetasizer Ultra.

P004

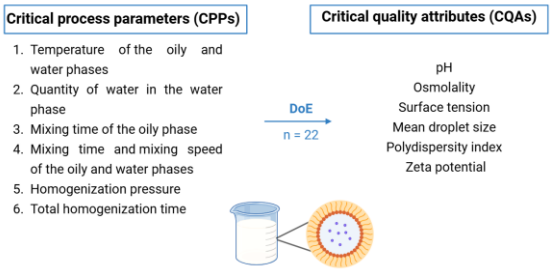

Figure 1. CPPs set by experimental design with potential influence on the CQAs of nanoemulsion.

3. RESULTS AND DISCUSSION

The measured values of osmolality (240–270 mOsmol/kg), pH (6-7) and surface tension (36 - 37 mN/m) for the formulated NEs are within the acceptable physiological range. According to literature data, tear film osmolarity ranges typically range from 231 to 446 mOsmol/kg, while pH values between 3.5 and 8.5 are tolerated due to the buffering capacity of the lacrimal fluid [1].

The mean droplet size of the NEs is between 130 and 150 nm, which is suitable for ophthalmic administration (Fig. 2). The PDI of all NEs was below 0.2, confirming a narrow size distribution of the droplets in the NEs. The zeta potential of NEs is between 25 and 35 mV (Fig. 3), indicating the stability of the NEs and their potential for enhanced interaction with the negatively charged surface of the cornea [1].

The only outliers were two formulations (no. 14 and 22), having zeta potential and mean droplet size values outside the expected range (Fig. 2, Fig. 3).

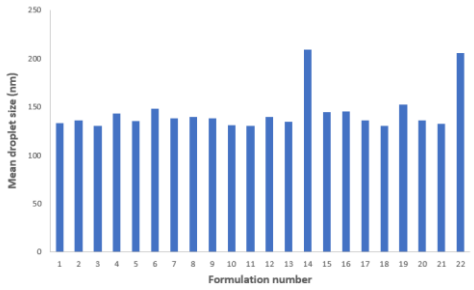

Figure 2. Mean droplet size of the DoE formulations.

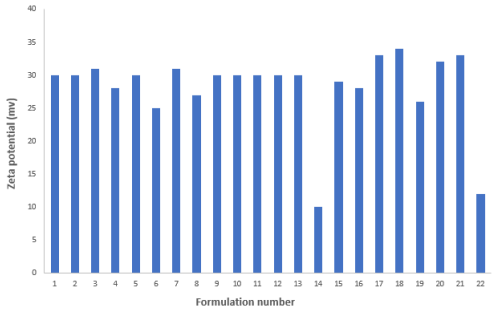

Figure 3. Zeta potential of the DoE formulations.

The obtained statistical data, including two outliers, was evaluated with the aim of defining CPPs for the further development of the NE.

4. CONCLUSION

Performed DoE screening showed that the developed method of preparation of formulation (a NE containing a lipophilic peptide for ophthalmic use) is robust and that tested variations of CPPs did not affect relevant physical parameters. Based on a detailed evaluation of the obtained statistical data, optimal process parameters were selected and will be used in further development of a stable nanoemulsion containing a lipophilic peptide for ophthalmic use.

5. REFERENCES

1. Gawin-Mikołajewicz, A., et al., *Ophthalmic Nanoemulsions: From Composition to Technological Processes and Quality Control.* Molecular Pharmaceutics, 2021. 18(10):3719-3740.

2. European Pharmacopoeia. *Design of experiments.* 11th Ed.: European Directorate for the Quality of Medicines & Healthcare; 2025. Chapter 5.33.

P005

FORMULATION AND EVALUATION OF ORALLY DISINTEGRATING TABLETS (ODTs) OF POORLY SOLUBLE API CELECOXIB USING AMORPHOUS SOLID DISPERSION (ASD) TECHNIQUES

Oxana Brante[1], Paula Kaufelde[1], Baiba Mauriņa[2] Konstantins Logviss[1]

[1]Laboratory of Finished Dosage Forms, Faculty of Pharmacy, Rīga Stradiņš University, Latvia
[2]Department of Applied Pharmacy, Faculty of Pharmacy, Rīga Stradiņš University, Latvia

1. INTRODUCTION

Celecoxib (CLX), a selective COX-2 inhibitor traditionally used to relieve pain and treat inflammation in conditions such as osteoarthritis and rheumatoid arthritis, is now being repurposed in groundbreaking clinical trials in oncology and neurology (11 clinical trials in the EU) [1]. As a class II drug in the Biopharmaceutical Classification System (BCS) with poor solubility and high permeability, it is an active pharmaceutical ingredient (API) that can be used for orodispersible tablets (ODTs) utilizing solubilizing formulation strategies. CLX has a pKa of 11.1, meaning that its solubility improves as the pH of the medium increases. A poorly soluble crystalline substance can be formed into an amorphous solid dispersion (ASD) with a polymer and made into an ODT. A tablet that can rapidly disintegrate in saliva is a patient-oriented dosage form [2, 3], as many patients have difficulty swallowing tablets, capsules, or powders. To alleviate this problem, ODTs are designed to dissolve in the oral cavity without water.

2. MATERIALS AND METHODS

2.1. Materials

Materials: Celecoxib (BLDpharm), polymer PVPVA64 (Vivapharm), excipients for ODT formulation: dextrose, sodium croscarmellose, talc, magnesium stearate. Hot-melt extruder Thermo Scientific Pharma 11. Tablet press Medelpharm Style One Nano. DSC Linseis CHIP-DSC 100, tablet tester Sotax ST50, disintegration tester Erweka ZT732, dissolution apparatus USP 2 Sotax ATXtend.

2.2. Methods

Preparation of ASDs: CLX was mixed with polymer in a specific ratios and processed using hot-melt method in hot-melt extruder (HME) to create ASD. Formulation and preparing of ODTs: the milled ASD and crystalline API (control) were blended separately with the same excipients and compressed into tablets using a direct compression method. Characterization: the tablets were characterized for physical characteristics, disintegration time, and dissolution profile.

3. RESULTS AND DISCUSSION

3.1. Physical characteristics of tablets.

Table 1. Physical characteristics of tablets.

Tablets	Weight, mg	Diameter, mm	Hardness, N (n 10)	Disintegr. time, s (n 6)
CLX ASD	500	11	68	52
CLX cryst.	500	11	28	54

3.2 Dissolution

The dissolution results showed significant differences in the dissolution profiles of ASD tablets vs the crystalline form of the API. The amorphous form dissolved >2 times more than the crystalline form. (Fig.1.)

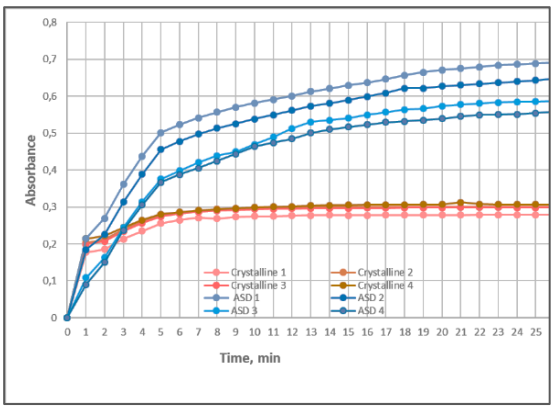

Figure 1. Dissolution rate: crystalline vs ASD.

P005

3.3. Stability

Ongoing stability studies have confirmed by DSC analysis that the ASDs have retained their amorphous state over time, with no recrystallization observed so far (6 months in 40C° temperature and 75% RH chambers).

4. CONCLUSION

The formulation of ODTs using CLX and PVPVA amorphous solid dispersion techniques significantly improved celecoxib's solubility characteristics. This research underscores the potential of ODTs to optimize the applications of ASD formulations, leading to improved bioavailability and therapeutic efficacy for patients. Further studies are recommended to investigate clinical implications and refine formulation strategies.

5. REFERENCES

1. Register, E.C.T. *Clinical trials for Celecoxib*. [cited 2025 02.05.]; Available from: https://www.clinicaltrialsregister.eu/ctr-search/search?query=Celecoxib&status=ongoing
2. Desai, N., et al., *How Do Orodispersible Tablets Behave in an In Vitro Oral Cavity Model: A Pilot Study.* Pharmaceutics, 2020. **12**(7).
3. FDA, *Guidance for Industry: Orally Disintegrating Tablets;*, F.a.D.A.C.f.D.E.a. Research, Editor. 2008, Silver Spring.

P006

SUSTAINABLE SIMPLICITY IN WOUND CARE: FUNCTIONAL FILMS MADE OF A VISCOSE-TYPE CARBOXYMETHYLCELLULOSE WITH DEXPANTHENOL

Kateřina Brückner[1], Ruta Masteiková[1]

[1]*Department of Pharmaceutical Technology, Faculty of Pharmacy, Masaryk University Brno, Czech Republic*

1. INTRODUCTION

Wound healing is a complex process requiring a balanced environment to retain moisture, prevent infection, and support tissue repair. While advanced systems, such as nanotechnologies, offer strong therapeutic potential, their clinical use is often restricted by high costs, regulatory challenges, and technical complexity. This has led to increased interest in simpler, sustainable materials that are easier to produce and suitable for practical applications. Viscose-derived carboxymethylcellulose (CMC) is a biodegradable and biocompatible polymer with excellent film-forming properties. When combined with dexpanthenol, a well-established agent that supports skin regeneration, the resulting films present a practical, efficient, and eco-conscious approach to modern wound care. This study aimed to prepare and evaluate films made from materials well-established in wound therapy, which offer promising potential when combined. The films were assessed with a focus on their practical applicability to the wound [1].

2. MATERIALS AND METHODS

2.1 Materials

The partially modified (DS 0,604) viscose-type sodium carboxymethylcellulose (NaCMC) in the fibrous form was obtained from Holzbecher, spol. s.r.o. (CZ). Dexpanthenol, glycerin and macrogol 300 (Ph. Eur. grade) were purchased from Fagron, a.s. (Olomouc, CZ).

2.2 Film preparation

The films were prepared using the solvent casting method. A dispersion of NaCMC (cut viscose-type textile fibers) was formulated with purified water and plasticizer, thoroughly homogenized and left to swell for 1 hour. The concentration of CMC was 0.0035 g/cm². The dispersion was acidified to pH 3 using hydrochloric acid under continuous mixing. Subsequently, a 50% dexpanthenol solution was added to achieve a final concentration of 4 mg/cm². The finished dispersion was poured onto trays and dried in a hot air oven at 60 °C for 3 hours. After drying, the films were carefully peeled off and stored in closed plastic bags to await testing. The composition of the prepared films is summarized in Table 1.

Table 1. Composition of casting dispersions (100 g)

Sample	CMC (g)	Plasticizer (g)	Dexpanthenol (g)
V-G-1-D	1.736	glycerin 1.736	0.4
V-G-2-D	1.736	glycerin 3.472	0.4
V-M-1-D	1.736	macrogol 1.736	0.4
V-M-2-D	1.736	macrogol 3.472	0.4

2.3 Evaluation of the films

Swelling properties. The measurement was carried out using an artificial wound model [2]. Film samples (2.5 × 2.5 cm) were weighed on an analytical scale (KERN 870–13, Gottl. KERN & Sohn GmbH, Balingen, GER) in dry conditions (Wd) and placed in the wound model. At certain time intervals (1, 3, 8, 24 h), swollen films were weighed (Ws). The degree of swelling (Sw) was calculated using the equation: $Sw = (Ws - Wd)/Wd$. *Surface pH.* Film squares (2.5 × 2.5) cm were cut and put on the artificial wound model. The lid was used to cover the Petri dish to prevent the evaporation of the liquid. At determined time intervals (1, 3, 8, 24 h), surface pH was measured. *Mechanical properties – tensile testing*. Tensile strength was measured in both dry and wet state using a CT3 Texture Analyzer (Brookfield, Middleboro, MA, USA) and TexturePro CT software. Film strips (40 × 10 mm) were stretched at 0.5 mm/s until break. Force and elongation at break point were recorded and recalculated for a thickness of 100 µm.

3. RESULTS AND DISCUSSION

The films with dexpanthenol were successfully prepared by the solvent evaporation method (Figure 1). All the samples were flexible and cohesive even after wetting, which is necessary for the intended wound application. Utilization of viscose-type NaCMC in the fibrous form and additional acidification of the dispersion led to the strengthening and improvement of the

P006

mechanical properties of the films as was also confirmed in our previous studies [3].

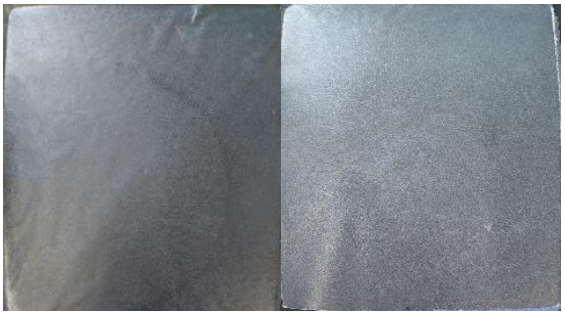

Figure 1. The films (V-G-1-D, V-M-2-D)

Swelling properties indicate the ability of the dressing to provide a moist environment in the wound and absorb exudate. Films exhibited a mild degree of swelling (Figure 2). The degree of swelling of all films increased gradually up to 24 hours. Samples with a higher amount of plasticizer showed a slightly lower degree of swelling.

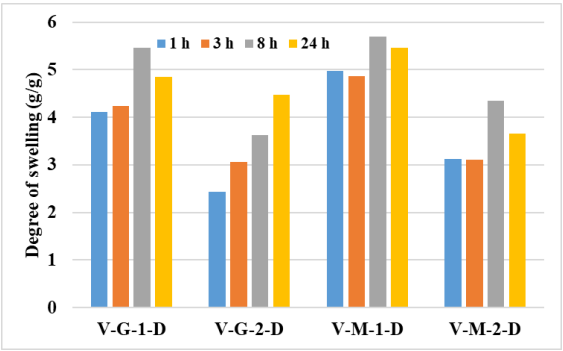

Figure 2. Swelling properties of the films

pH evaluation shows the dressing's ability to maintain an acidic environment that supports wound healing. Table 2 demonstrates that, although the pH increased within the time intervals, all the films retained acidic pH values even after 24 h, achieving pH values from 6.26 ± 0.15 (V-G-2-D) to 6.34 ± 0.50 (V-M-2-D), respectively.

Table 2. pH alterations in time

Sample	1 h	3 h	8h	24 h
V-G-1-D	4.20 ± 0.70	4.76 ± 0.44	5.52 ± 0.88	6.32 ± 0.29
V-G-2-D	4.09 ± 0.38	4.22 ± 0.95	5.32 ± 0.32	6.26 ± 0.15
V-M-1-D	4.35 ± 0.61	4.30 ± 0.17	4.74 ± 0.39	6.27 ± 0.41
V-M-2-D	3.99 ± 0.49	4.09 ± 0.72	5.37 ± 0.58	6.34 ± 0.50

This indicates the ability of the films to keep their pH in the acidic range, so we can consider them as pH-modulating wound dressings.

Mechanical properties of the films are essential not only in a dry state but also after contact with wound exudate (wetting). Films must be cohesive and durable but flexible for better adaptation to the wound. Figure 3 shows the mechanical properties results. Films with glycerol exhibited greater mechanical strength compared to those with macrogol; however, increasing the plasticizer concentration led to a reduction in strength. Upon hydration, the mechanical properties of the films decreased markedly, while high flexibility was retained, as indicated by increased deformation values in comparison with the dry state.

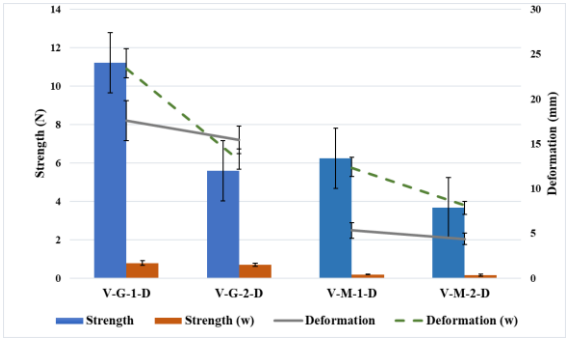

Figure 3. Mechanical properties of the films

4. CONCLUSION

This study aimed to develop effective wound dressings using a simple method and sustainable materials that are already well-established in wound care. Based on preliminary evaluation for practical application, the films appear promising due to their pH-modulating effects and favorable organoleptic and mechanical properties, even under moist conditions. However, further testing is required.

5. REFERENCES

1. Verma, D. et al., *A sustainable and green approach towards the utilization of biopolymers for effective wound dressing applications: A detailed review. Nano-Structures & Nano-Objects,* 2024. 37: 101086.

2. Vinklárková, L. et al., *Film wound dressing with local anesthetic based on insoluble carboxymethylcellulose matrix*. Journal of Applied Biomedicine, 2017. 15:313-320.

3. Tenorová, K. et al. *Formulation and Evaluation of Novel Film Wound Dressing Based on Collagen/Microfibrillated Carboxymethylcellulose Blend.* Pharmaceutics, 2022. 14:782.

P007

POLYOLS AS SUSTAINABLE SOLUTION IN ORAL DRUG DELIVERY SYSTEMS

Elzbieta Maria Buczkowska, Zoltan Mark Horvath, Kirils Kukuls, Alina Jaroslava Frolova, Liga Petersone, Valentyn Mohylyuk

[1]Leading Research Group, Faculty of Pharmacy, Riga Stradiņš University, Riga, Latvia

1. INTRODUCTION

Polyols are excellent green chemistry solution to pharmacy, regarding they functionality, they could be utilized not only as excipients and active ingredients, but also as innovative components of drug delivery systems (DDS). Innovative controlled release formulations using polyols as components are part of the topic of drug delivery, currently revolutionizing the pharmaceutical industry.

In this research we experimentally investigated physicochemical properties and intrinsic dissolution profiles of 4 commercially available polyols. The aim of the research was the characterization of physicochemical properties of commercially available polyols in order to use them in DDS with controlled release.

2. MATERIALS AND METHODS

2.1. Materials

Spray dried grades of mannitol – Mannogem XL Opal SD (Roquette, Lestrem,France) and Sorbitol (MP22004640, Merck KGaA, Darmstadt, Germany); Isomalt - LM-PF(#L121294100, Südzucker AG, Obrigheim, Germany) and Xylitol (D) Xylisorb 300 (#737201;Roquette, Lestrem,France).

2.2. Methods and Intrinsic Dissolution Rate (IDR)

The description of used methods could be found at RSU published datasets (Gniazdowska, E. M. et al.2025; Frolova, A. J. et al 2025; Horvath, Z. M. et al 2025)

3. RESULTS AND DISCUSSION

The studies included isomalt and xylitol, which are frequently used ingredients in sugar-free drug delivery systems, as well as two diastereoisomers (mannitol and sorbitol), which have nearly identical chemical structures but very different physicochemical properties (Fig.1.).

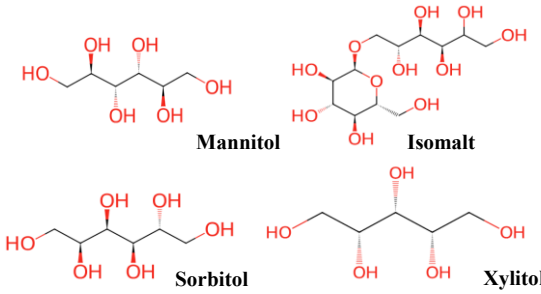

Figure 1. Chemical structures of polyols.

3.1. Physicochemical Characterization

The polyols contain absorbed water (bound water) trapped by the polyol and bulk water (free water) (Table.1.). All polyols analysed were high polar and hydrophilic (LogP ≥3).

Table 1. Physical and chemical properties of polyols.

Polyol	Mannitol	Isomalt	Sorbitol	Xylitol
KF	0.03	0.78	0.41	0.02
LOD	0.80	1.01	0.58	0.19
Mw (g/mol)	182.172	344.313	182.17	152.15
HBD/HBA	6/6	9/11	6/6	5/5
LogP	-3.73	-5.50	-3.73	-3.10
pKa	12.59	12.06	12.59	12.76

All polyols showed the same distinctive peaks. Peaks in the 1049–1269 cm^{-1} range are caused by C-O stretching consistent with esters, ethers, and hydroxyl groups, whereas peaks at 3427 cm^{-1} and 1747 cm^{-1} are attributed to OH groups and carbonyl groups, respectively. Additional bands are ascribed to the CH_3 and CH_2 groups' stretching (2880–2990 cm^{-1}) and bending (1379, 1454 cm^{-1}) (Fig.2.).

P007

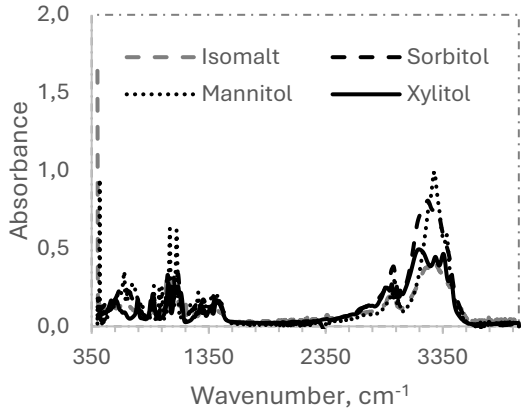

Figure 2. FTIR spectrum of polyols.

The high peak intensities of polyols in XRD spectra indicates a high degree of crystallinity (Fig.3.).

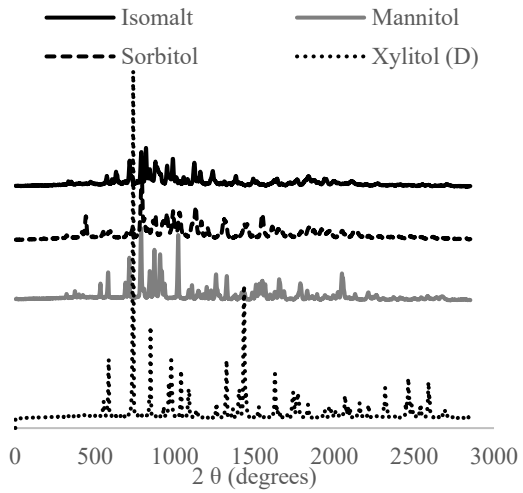

Figure 3. Results of XRD analysis of polyols

The obtained intrinsic dissolution profiles of polyols are rapid, complete and polyol-controlled (Fig.4.).

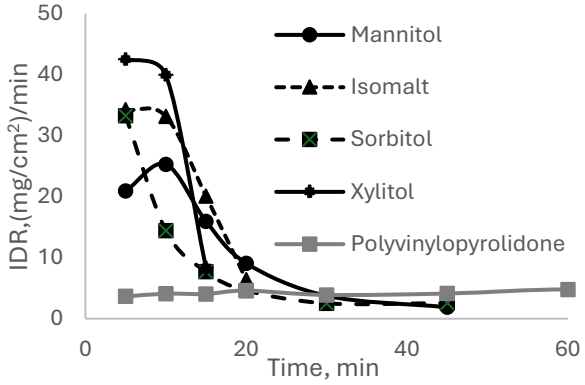

Figure 4. IDR profiles of polyols and polyvinylopyrolidone

Despite the fact that molecular weights tend to release quicker and to crystallize more easily than the lower molecular weight polyols in most cases. In our case no correlation between molecular weight and intrinsic dissolution rate was found.

3.2. Schematic overview of polyols in oral drug delivery systems

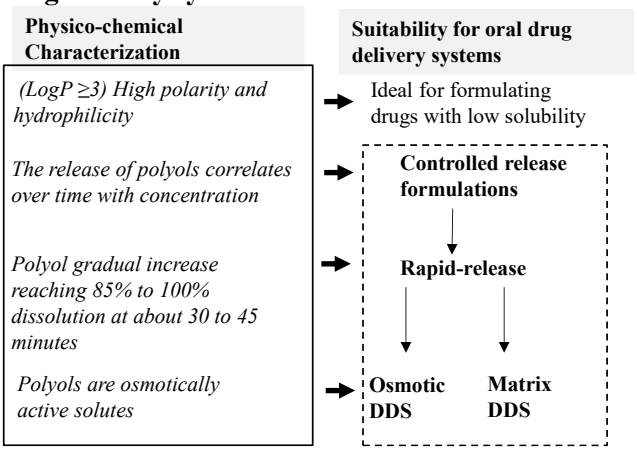

Figure 5. Proposed overview of polyols in oral drug delivery systems

4. CONCLUSION

Physicochemical properties could be used as a tool for the first choice of polyols in drug delivery systems. Polyols could help to increase the dissolution rate of poorly water-soluble drugs.

REFERENCES

Gniazdowska, E. M. et al (6 Feb 2025). Intrinsic Dissolution Rate (IDR) of Polyols. Riga Stradins University. 10.48510/FK2/BJPEC8

Frolova, A. J. et al (21 Jan 2025). Loss on Drying (LoD) of Polyols. Riga Stradins University. 10.48510/FK2/XILW3Z

Frolova, A. J. et al (17 Mar 2025). Karl Fischer (KF) Titration of Polyols. Riga Stradins University. 10.48510/FK2/4AREIO

Horvath, Z. M. et al Fourier-Transform Infrared (FTIR) Attenuated Total Reflectance (ATR) Spectroscopy Profiles of Polyols. Riga Stradins University. 10.48510/FK2/PTJHF7

ACKNOWLEDGMENT

The project ‘‘Internal consolidation of RSU and external consolidation of RSU with LSPA” Grant ‘‘Suitability of sugar alcohols (polyols) as binders in twin-screw melt granulation for preparation of high-drug-loaded immediate-release tablets with superior mechanical properties” (No. RSU-PAG-2024/1-0004).

P008

FORMULATION AND CHARACTERIZATION OF INDOMETHACIN-CONTAINING MICROCAPSULES

Paula Cermakova[1], Miroslava Spaglova[1], Patricia Jackuliakova[1], Juraj Piestansky[1,2]

[1]Comenius University Bratislava, Faculty of Pharmacy, Department of Galenic Pharmacy, Bratislava, Slovakia
[2]Institute of Neuroimmunology, Slovak Academy of Sciences, Bratislava, Slovakia

1. INTRODUCTION

The development of innovative drug delivery systems plays crucial role in the pharmaceutical industry by enabling effective, safe and controlled administration of active substances. One such system is microencapsulation, which offers significant benefits in enhancing bioavailability, stability and controlled drug release [1]. This study focuses on the formulation and characterization of indomethacin (IND)-loaded microcapsules (MCPs). IND, a commonly used non-steroidal antiphlogistic drug is often associated with gastrointestinal side effects. We designed optimal formulation method, analysed physical and chemical properties of MCPs and assessed the drug release behaviour under simulated gastrointestinal conditions.

2. MATERIALS AND METHODS

2.1. Materials

MCPs were prepared from: sodium alginate (Biochemica Applichem, DE), $CaCl_2$ (Sigma-Aldrich Chemie, DE), indomethacin (Jozef Valuch, SK), deionized water (Biosan, LV). Artificial gastric fluid (AGF) was prepared from: HCl, NaCl (Centralchem s.r.o., SK), deionized water (Biosan, LV). Nicotinamide (SERVA Feinbiochemica, DE) was used for content determination of IND.

2.2. Formulation of Ca^{2+} alginate microcapsules

We prepared an aqueous sodium alginate solution (1.6 % w/v) which exhibited characteristics of a viscous gel. Subsequently, IND was dissolved in this solution. Separately, we prepared $CaCl_2$ solution (2 % w/v) by dissolving $CaCl_2$ in deionized water. The IND-containing alginate solution was extruded through a needle into the $CaCl_2$ solution, which was continuously stirred using a magnetic stirrer [2]. For the MCPs formulation we used an automated process with a custom-built apparatus. A Terumo Sterican needle (I.D. – 0.84 mm) was used for extrusion. Excess liquid was decanted, and MCPs were washed twice with deionized water. Obtained MCPs were spread into an even layer on watch glasses and left to dry in room temperature. We formulated two samples of MCPs, F1 and F2, with the F2 containing twice the amount of the drug.

2.3. Determination of physical properties

Physicochemical properties of IND-containing MCPs were characterized to evaluate their quality and performance. Particle size distribution was determined by sieve analysis, providing the size range of the prepared samples. The bulk volume and bulk density were measured to evaluate their packing properties for further processing. Mechanical resistance was analysed both, by standard methods and by texture analyser. Flow rate was determined to characterize the flowability. The loss on drying (LOD) was measured to establish the moisture content. Swelling ratio (SR) was evaluated to understand the swelling behaviour in different media - water and AGF.

2.4. IND content determination

The content of IND encapsulated within the MCPs was quantified to ensure the accuracy and reproducibility of the encapsulation process using nicotinamide for its hydrotropic effect. Calibration curves of IND in water and IND in AGF were created. UV-VIS spectrophotometry (λ = 320 nm) was used to determine the concentration of IND.

2.5. Dissolution test

Dissolution tests were conducted to study release profile of IND from the MCPs in different pH conditions – water and AGF. The test was performed using basket method at 37 ± 0.5°C and a rotation speed of 50 rpm in two various dissolution media – H_2O and AGF within 6 hours.

3. RESULTS AND DISCUSSION

3.1. Sieve analysis of microcapsules

Table 1. Sieve analysis of microcapsules

P008

	Sieve size [µm]	%	S.D.
F1	1250	45.4	0.2
	900	19.1	0.9
	710	34.1	0.9
F2	1250	50.8	0.3
	900	22.6	0.4
	710	25.6	0.3

MCPs in both F1 and F2 were mostly retained on sieves with mesh size of 1250, 910, and 710 µm. Based on the specification of the needle (I.D. – 0.84 mm) a particle size greater than 840 µm was anticipated. Approximately 50% of produced MCPs exhibited anticipated size (Table 1).

3.2. Physical properties of microcapsules

Table 2. Overview of physical characterisation results for F1 and F2

Method	Measured parameter	F1	F2
Determination of BV and BD	Bulk volume	1.08	1.12
	Bulk density	0.93	0.89
Determination of mechanical resistance	Average residue [%]	99.96 ± 0.06	99.82 ± 0.21
Texture analysis	Force [N]	26.21 ± 3.63	28.95 ± 6.19
Determination of flowability	Flow rate [g/s]	4.24	3.83
Loss on Drying (LOD)	LOD [%]	17.06	14.31
Content determination of IND	c [µg/ml]	12.09 ± 0.02	17.42 ± 0.07

Table 2 presents the summarized results of physical properties. BV and BD indicated minimal differences between samples. Mechanical resistance tests showed excellent durability for both F1 and F2. Excellent flowability results were demonstrated. LOD was more significant in F1 due to higher proportion of hydrophilic material. IND content determination showed that F2 incorporated ± 1.44 times more IND than F1, although we expected a twofold increase.

3.3. Determination of swelling ratio

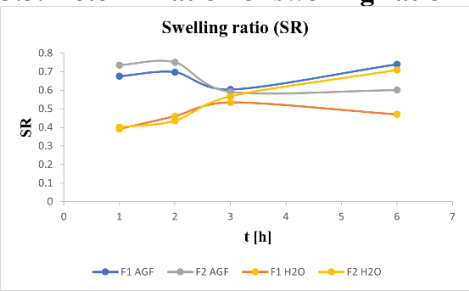

Figure 1. Swelling ratio for F1 and F2

Swelling ratio (SR) of alginate-based MCPs was evaluated in two media: AGF and water (Fig. 1) The results demonstrated more pronounced swelling in the acidic environment starting from the 1st hour. In water, which exhibits higher pH values, the swelling was initially slower. The use of higher concentration of $CaCl_2$ solution likely resulted in more tightly crosslinked structure, thereby reducing the swelling capacity.

3.4. Dissolution testing

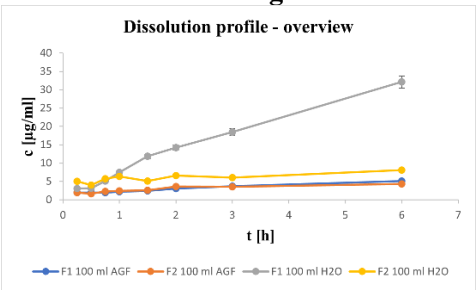

Figure 2. Dissolution profile for F1 and F2 in aqueous medium and AGF

The dissolution profiles of IND from MCPs are presented in the Fig. 2. It can be observed that the highest amount of drug was released from F1 into the water (pH ≈ 7). This behaviour is advantageous, considering that IND is associated with numerous adverse effects in acidic environment of stomach.

4. CONCLUSION

Two IND-loaded microcapsule samples were successfully formulated, differing in drug content, along with placebo microcapsules to validate the method. The physical properties of F1 and F2 were satisfactory, comparable and consistent with expectations. The assay of IND content did not demonstrate a twofold drug content in F2. F1 sample showed superior drug release characteristics in higher pH values and was identified as the more promising formulation.

5. REFERENCES

[1] BAH, M.G. et al. Fabrication and application of complex microcapsules: a review. In *Soft Matter*. 2020. Vol. 16, no. 3, p. 570–590.
[2] PAPADAKOS, M. et al. A Multiple Unit Abuse-deterrent Dosage Form Based on Sodium Alginate. In *European Pharmaceutical Journal*. 2023. Vol. 70, no. s1, p. 75–79.

ACKNOWLEDGMENT

Research was funded by Grant of Comenius University UK/1021/2025 and VEGA 1/0302/24.

P009

TOPICAL TADALAFIL HYDROGEL: A PROMISING APPROACH FOR ERECTILE DYSFUNCTION THERAPY

Rafal Chiczewski[1], Zaneta Sobol[1], Dorota Wątróbska-Świetlikowska[1]

[1]*Department of Pharmaceutical Technology, Pomeranian Medical University in Szczecin, Poland*

1. INTRODUCTION

Carbopol is bioadhesive and pharmaceutically inert polymer, was selected for its favorable physicochemical and rheological properties. The formulation aims to enhance cutaneous absorption using penetration enhancers, enabling improved drug delivery while preserving safety. The study evaluated tadalafil release from the hydrogel matrix and assessed its physicochemical characteristics, confirming its suitability as a transdermal delivery vehicle for ED therapy.

Figure 1. Hydrogels with tadalafil for transdermal

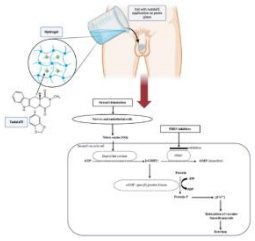

drug delivery directly to the penis glans.

2. MATERIALS AND METHODS

2.1. Materials

Tadalafil and its reference standard, Carbopol ***(Noveon® AA-1 Polycarbophil)*** and *β*-Cyclodextrin was purchased from Sigma-Aldrich (Steinheim, Germany). A *Strat-M®* membrane was purchased from Merck

Millipore (Darmstadt, Germany). HPLC grade sodium dihydrogen phosphate, disodium hydrogen phosphate and acetonitrile, were procured from POL-AURA (Morąg, Poland). High pure water was prepared by using the HLP demineralizer, (*Hydrolab apparatus DH-0004-00 purification system*). All other chemicals were of USP or reagent grade and used without further purification.

2.2. Methods

Each formulation was prepared in duplicate, and the resulting hydrogels were stored in a refrigerator (T= 4°C). Physicochemical analysis of the gels included: pH measurement, rheological property assessment, quantitative analysis (using HPLC), release studies (Franz diffusion cell).

2.3. Gel preparation

The formulations and composition of tadalafil gel are shown in Table 1. Briefly, Carbopol 940 was dispersed into distilled water under stirring to form homogeneous solution. Subsequently, auxiliary substances were added sequentially, each requiring a 15-minute mixing period, until a homogeneous mixture was obtained. Tadalafil was added last, before initiating the gelling process by adjusting the pH. All tadalafil gels were stored in a fridge at 4°C prior to use [1,2].

Table 1. Composition of the Tadalafil hydrogels

Formulation number	Composition of the gel	CB [g]	TD [g]	OE [g]	P400 [g]	T80 [g]	E [g]	GL [g]	Parabens [g]	H_2O [g]	NaOH [g]
01A0923	1% CB + TD + 2% E	0,2	0,08	0	0	0	0,4	0	0,04	19,28	q.s.
01B0923	1% CB + TD + 2% E	0,2	0,06	0	0	0	0,4	0	0,04	19,3	q.s.
01C0923	1% CB + TD + 2% E	0,2	0,04	0	0	0	0,4	0	0,04	19,32	q.s.
02A0923	1% CB + TD + 15% P400 + 15% T80 + 2% E	0,2	0,08	0	3	3	0,4	0	0,04	13,28	q.s.
02B0923	1% CB + TD + 15% P400 + 15% T80 + 2% E	0,2	0,06	0	3	3	0,4	0	0,04	13,3	q.s.
02C0923	1% CB + TD + 15% P400 + 15% T80 + 2% E	0,2	0,04	0	3	3	0,4	0	0,04	13,32	q.s.
03A0923	1% CB + TD + 15% P400 + 15% T80 + 1% OE + 2% E	0,2	0,08	0,2	3	3	0,4	0	0,04	13,08	q.s.
03B0923	1% CB + TD + 15% P400 + 15% T80 + 1% OE + 2% E	0,2	0,06	0,2	3	3	0,4	0	0,04	13,1	q.s.
03C0923	1% CB + TD + 15% P400 + 15% T80 + 1% OE + 2% E	0,2	0,04	0,2	3	3	0,4	0	0,04	13,12	q.s.
04A0923	1% CB + TD + 20% P400 + 10% T80 + 2% E	0,2	0,08	0	4	2	0,4	0	0,04	13,28	q.s.
04B0923	1% CB + TD + 20% P400 + 10% T80 + 2% E	0,2	0,06	0	4	2	0,4	0	0,04	13,3	q.s.
04C0923	1% CB + TD + 20% P400 + 10% T80 + 2% E	0,2	0,04	0	4	2	0,4	0	0,04	13,32	q.s.
05A0923	1% CB + TD + 15% P400 + 10% T80 + 2% E	0,2	0,08	0	3	2	0,4	0	0,04	14,28	q.s.
05B0923	1% CB + TD + 15% P400 + 10% T80 + 2% E	0,2	0,06	0	3	2	0,4	0	0,04	14,3	q.s.
05C0923	1% CB + TD + 15% P400 + 10% T80 + 2% E	0,2	0,04	0	3	2	0,4	0	0,04	14,32	q.s.
06A0923	1% CB + TD + 10% P400 + 10% T80 + 10% GL + 2% E	0,2	0,08	0	4	2	0,4	2	0,04	11,28	q.s.

Legend: CB - Carbopol, OE - Sodium Oleate, TD - Tadalafil, P400 - PEG400, T80 - Tween80, E - Ethanol 96%, Parabens - MethylParaben+PropylParaben in a total concentration of 0,2%

formulations

3. RESULTS AND DISCUSSION

3.1. pH determination

The pH of the hydrogel samples were determined, and were monitored using a digital pH meter. All of the gels had value of pH=7.10±0.55.

3.2. Spreadability

Table 2. pH values of tadalafil hydrogels

P009

Formulation	Firmness	Shear	Stickiness	Adhesion
01A0923	350.40±18.39	347.25±15,20	-404.3±13.21	-77.64±7.72
02A0923	824.69±14.94	775.3±33,15	-600.91±9.33	-190.18±2.61
03A0923	817.58±18.48	895.10±43.40	-594.16± 14.06	-178.98±6.76
04A0923	1165.09±14.23	1008.09±27.41	-619.00±9.92	-232.52±6.69
05A0923	872.59±13.67	877.70±36.06	-749.37±13.86	-174.42±9.72
06A0923	1147.01±0.88	1256.00±53.66	-811.98±7.47	-325.53±11.49

3.3. Rheological measurements

Table 3. The Mechanical Properties of Hydrogels

Formulation	Hardness (g)	Adhesiveness (g·sec)	Cohesion	Resilience (%)	Springiness (%)
01A0923	10.185 ± 1.219	-35.372 ± 8.234	0.885 ± 0.005	14.506 ± 2.581	89.355 ± 0.980
02A0923	20.854 ± 1.637	-63.600 ± 0.392	0.810 ± 0.052	9.975 ± 0.945	92.147 ± 2.149
03A0923	36.819 ± 0.904	-65.927 ± 10.080	0.816 ± 0.035	20.041 ± 0.624	91.816 ± 1.559
04A0923	51.292 ± 1.360	-67.759 ± 15.066	0.823 ± 0.016	11.715 ± 1.973	93.811 ± 1.306
05A0923	34.450 ± 0.180	-62.477 ± 13.674	0.864 ± 0.019	18.370 ± 2.286	90.552 ± 1.662
06A0923	53.496 ± 3.824	-53.961 ± 2.062	0.752 ± 0.112	14.218 ± 0.158	93.846 ± 1.248

3.4. In-vitro drug diffusion Study using franz diffusion cells

Franz-type diffusion cells with an effective diffusion area of 1.81 cm^2 with the diameter of 16 mm and a receptor volume of 11.8 mL were used to assess in vitro drug permeation. The receptor compartment was kept at 37°C. The receptor fluid was selected as pH 7.4 phosphate buffer solution containing 1% tween 80 and stirred continuously with magnetic stirrer at 500 rpm. Permeation experiments were carried out until 24 h after application. Samples were taken from the receiver compartment at scheduled time intervals (0, 1, 2, 4, 6 h) and immediately replaced with the same volume of fresh receptor fluid. The amount of tadalafil in the samples was determined by HPLC [2,3].

Table 4. Permeation parameters of tadalafil from different tadalafil gels.

Formulation number	Flux (mg/cm^2 /h)	Accumulative amount (mg/cm^2)
01A0923	0.125	0.75
01B0923	0.085	0.51
01C0923	0.022	0.132
02A0923	0.154	0.924
02B0923	0.101	0.606
02C0923	0.056	0.336
03A0923	0.335	2.01
03B0923	0.224	1.344
03C0923	0.124	0.744
04A0923	0.221	1.326
04B0923	0.152	0.912
04C0923	0.101	0.606
05A0923	0.169	1.014
05B0923	0.106	0.636
05C0923	0.069	0.457
06A0923	0,225	1.350

3.5. HPLC analysis

The column is a reversed-phase column (*Kinetex C_{18} 150 mm × 4.6 mm, 5μ*). The mobile phase system consisting of sodium dihydrogen phosphate (pH=±6.0) and acetonitrile (50:50 V/V). Temperature was set at 30°C, the retention time was found to be 3.21 minute at flow rate of 1.2 mL/min. The detection wavelength was 285 nm [3].

4. CONCLUSION

Transdermal drug delivery system of tadalafil was studied through the improvement of solubility of tadalafil using the mixed solution of many enhancer like HPCD, PEG 400, or tween 80. Based on the conducted studies, formulations containing tadalafil were selected as potential alternatives to oral administration. The most promising release results were observed for formulations containing cyclodextrin.

5. REFERENCES

1. Çağlar, E. Ş., Karaotmarlı Güven, G., & Üstündağ Okur, N. (2023). Preparation and characterization of Carbopol based hudrogels containing dexpanthenol. Journal of Faculty of Pharmacy of Ankara University, 47(3), 770-783.

2. Baek, J. S., & Cho, C. W. (2015). Transdermal delivery of tadalafil using a novel formulation. *Drug Delivery*, *23*(5), 1571–1577.

3. Atipairin, A.; Chunhachaichana, C.; Nakpheng, T.; Changsan, N.; Srichana, T.; Sawatdee, S. Development of a Sildenafil Citrate Microemulsion-Loaded Hydrogel as a Potential System for Drug Delivery to the Penis and Its Cellular Metabolic Mechanism. *Pharmaceutics* 2020, *12*, 1055.

ACKNOWLEDGMENT

I sincerely thank Dr. Dorota Wątróbska-Świetlikowska for his invaluable guidance throughout this research.

P010

MONITORING CRYSTALLINITY CHANGES IN AMORPHOUS SOLID DISPERSION DURING ACCELERATED STABILITY TESTING

Sandi Svetič [1,2], Boštjan Jerman [1], Matjaž Pajk [1], Franc Vrečer [2], Klemen Korasa [1,2]

[1]KRKA, d. d., 8501 Novo Mesto, Slovenia
[2]Faculty of Pharmacy, University of Ljubljana, 1000 Ljubljana, Slovenia

1. INTRODUCTION

Amorphous solid dispersions (ASDs) are widely used to improve the solubility and dissolution rate of poorly soluble active pharmaceutical ingredients (APIs). However, physical stability remains a key concern, as recrystallization during storage can compromise performance and bioavailability.

Raman spectroscopy is particularly sensitive to differences in molecular order, making it a valuable method for distinguishing between crystalline and amorphous forms of API, as well as for detecting early stages of recrystallisation. Previous studies have demonstrated its effectiveness for solid-state characterisation, including monitoring transformations in ASDs during processing and storage [1].

Raman spectroscopy, combined with partial least squares (PLS) regression, was applied as process analytical technology (PAT) tool for monitoring crystallinity in ASDs during stability testing.

2. MATERIALS AND METHODS

2.1. Materials

Amlodipine maleate (AM) was kindly supplied by Krka, d. d. (Novo Mesto, Slovenia). Polyvinylpyrrolidone, grade K-30 (PVP, marketed as Kollidon 30), was sourced from BASF SE (Ludwigshafen, Germany). Ethanol was supplied by Krka, d. d. (Slovenia).

2.2. Spray drying

A solution containing 3.3% AM and 1.1% PVP in ethanol (96 % v/v) was spray-dried using Mini Spray Dryer B-290 (BÜCHI Labortechnik AG, Switzerland). The process was performed at an inlet air temperature of 90 °C, with an air flow rate of 30 m^3/h and liquid feed rate of 3 g/min. This procedure yielded an ASD with AM:PVP ratio of 3:1.

2.3. Sample preparation

Eight samples were prepared by blending the spray-dried ASD with a crystalline AM (CAM) and PVP mixture in a 3:1 ratio, to obtain CAM contents of 0%, 10%, 20%, 30%, 40%, and 50% relative to the total AM content in each sample (Figure 1).

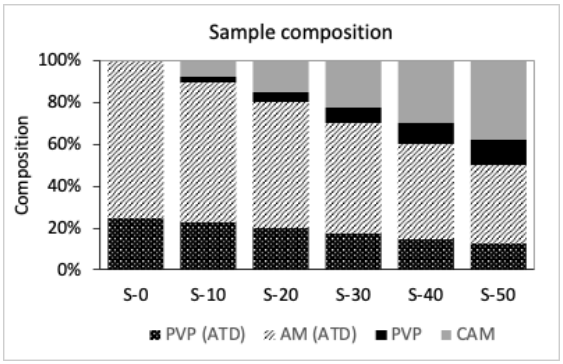

Figure 1. Composition of ASD samples with added mixture of CAM and PVP in a 3:1 ratio.

2.4. Accelerated stability testing

Samples were subjected to accelerated stability conditions at 50 °C and 75 % relative humidity. Analyses were performed before exposure (t_0) and after 2, 4, and 8 weeks.

2.5. Sample analysis

Raman measurements were conducted using PhAT probe (Kaiser Optical Systems, Inc., USA), connected to Raman RXN1TM Spectrometer (Kaiser Optical Systems, Inc., USA). Spectral range was 1762-644 cm^{-1}. The 'Integrating Sphere' channel was used. Two acquisitions were averaged to obtain a single spectrum, with integration time of 10 s.

The X-ray powder diffraction (XRPD) analysis was performed on an X'Pert PRO MPD instrument (Malvern Panalytical, UK), using CuKα radiation (λ = 1.5406 Å), 45 kV and 40 mA. Data were collected in step-scan mode with a step size of 0.033° in 2θ over an angular range of 4–30 ° in 2θ, using an X-Celerator detector.

P010

2.6. Multivariate analysis

Spectra were pre-processed using OPUS 7.5 software (Bruker Optik GmbH, Germany). PCA and PLS models were built with Aspen Unscrambler® 12.2 (Aspen Technology, Inc., USA). The PLS model was created using t_0 samples with known CAM concentrations and was then applied to predict CAM content in samples exposed to accelerated stability conditions.

3. RESULTS AND DISCUSSION

3.1. PCA analysis

PCA score plot of the collected Raman spectra showed that t0 samples differed from those exposed to accelerated stability conditions (Figure 2). This suggests that t_0 spectra may not represent the stressed samples well, which could reduce the reliability of predictions made by the PLS model.

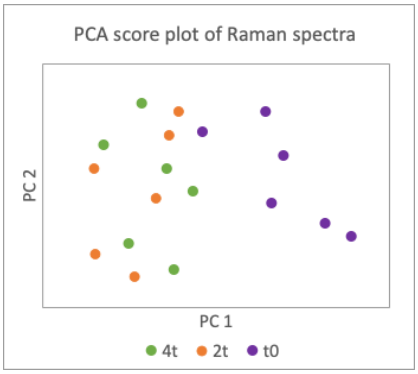

Figure 2. PCA score plot of Raman spectra.

3.2. PLS model

The developed PLS model includes two factors. The first factor explains 47 % of the data variability, and the second adds another 42 %, giving a total of 89%. The model exhibits an RMSEC of 2.6 %, RMSECV of 6.7 %, with an R^2 value of 0.97 and a Q^2 value of 0.89.

PLS loadings showing largest weights at wavelengths 1700 cm^{-1} (corresponds to AM), 1640 cm^{-1} (corresponds to AM), 1490 cm^{-1} (corresponds to PVP and AM) and 1200 cm^{-1} (corresponds to PVP and AM).

3.3. Prediction of crystalline AM

Predictions indicate an increase in CAM after two weeks, followed by stable or slightly decreasing concentrations.

Table 1. Prediction of CAM concentration in samples exposed to accelerated stability testing.

Initial CAM:	Prediction:		
	2w	4w	8w
0,0%	27,2%	26,2%	24,6%
10,0%	34,2%	34,6%	30,2%
20,0%	42,5%	41,8%	43,6%
30,0%	54,1%	49,1%	48,8%
40,0%	56,5%	58,6%	52,7%
50,0%	60,7%	65,7%	63,1%

3.4. XRPD

In Figure 3, the sample without added CAM at t_0 displays an XRPD pattern characteristic of an ASD. After 8 weeks under accelerated stability conditions, the diffractogram reveals the emergence of crystalline reflections, indicating recrystallization. These reflections are less sharp and less defined compared to the pure CAM diffractogram, suggesting the formation of less-ordered crystalline domains.

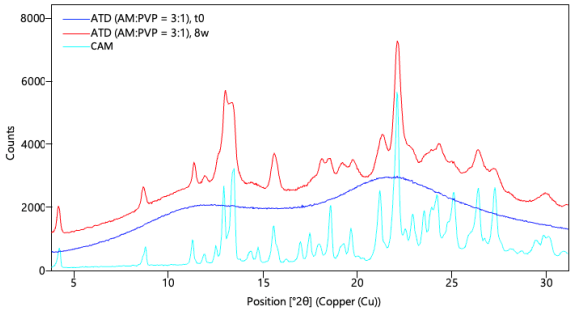

Figure 3. XRPD diffractograms of CAM and the sample without added CAM, recorded at t_0 and after 8 weeks.

4. CONCLUSION

The developed PLS model can serve as a useful tool for qualitative detection of AM recrystallization from ASD. However, observed spectral differences and XRPD diffractograms indicate that t_0 spiked samples may not adequately represent stressed samples. As a result, they may not form a fully appropriate calibration set for reliable quantitative predictions.

5. REFERENCES

1. Svetič S. et al., *Quantifying crystallinity of amlodipine maleate in amorphous solid dispersions produced by fluidized bed granulation using PAT tools.* Eur. J. Pharm. Sci., 2025. 206: 107018.

P011

DEVELOPMENT OF EMULSION CARRIERS FOR TREHALOSE AND EVALUATION OF THEIR MOISTURIZING PROPERTIES

Anna Czajkowska-Kośnik, Paulina Perkowska, Katarzyna Winnicka

Medical University of Bialystok, Department of Pharmaceutical Technology, Bialystok, Poland

1. INTRODUCTION

Emulsions are one of the pharmaceutical dosage forms used for skin care and as drug carriers in topical treatment. In the care and treatment of the dry skin symptoms, emulsions as **water-based moisturizers are** routinely **u**sed. Lighter texture and more comfortable application of emulsions affect their advantages over other skin products (ointments, oils) [1,2]. Trehalose is a naturally occurring disaccharide composed of 2 glucose units with hydrating (moisturizing) properties. This sugar is widely used in the food, cosmetic and pharmaceutical industries [3].
The aim of this study was to develop emulsions composition based on the bioadhesion and stability evaluation, and then to assess transepidermal water loss (TEWL) and hydration values (HV) of selected emulsions containing various concentrations of trehalose.

2. MATERIALS AND METHODS

2.1. Emulsions preparation

In the preliminary study, placebo emulsions (without trehalose), containing an oily phase (liquid paraffin, jojoba seed oil and avocado oil), a preservative (GSB - gluconolactone and sodium benzoate), an antioxidant (vitamin E), a humectant (glycerol), emulsifiers (GSC - glyceryl stearate citrate; cetyl alcohol; Olivem 1000 – cetearyl olivate and sorbitan olivate**)**, water and a gelling agent (xanthan gum) were prepared (Table 1).

For the moisturizing assessment, emulsions with the recommended concentrations of trehalose (up to 5%) were prepared [4,5].

Table 1. Composition of placebo emulsions.

Components	E1	E2	E3	E4	E5	E6
Liquid paraffin	10.0					
Jojoba oil	5.0	10.0	0	5.0	10.0	0
Avocado oil	5.0	0	10.0	5.0	0	10.0
GSB	1.0					
Witamin E	0.1					
Glycerol	10.0					
GSC	0	0	0	2.0	2.0	2.0
Cetyl alcohol	0	0	0	3.0	3.0	3.0
Olivem	5.0	5.0	5.0	0	0	0
Xanthan gum	0	0.5	0	1.0	0.5	0.5
Water up to	100.0					

2.2. Evaluation of bioadhesiveness

Adhesion behaviour of the placebo emulsions was tested using a TA.XT Plus texture analyzer (Stable Micro Systems, Godalming, UK). Gelatin membrane, porcine skin and mice skin were utilized as adhesive layers.

2.3. Stability test

Stability study was carried out by centrifugation method. Emulsions were centrifuged at 4000 rpm for 10 min and observed for possible phase separation.

2.4. Moisturizing assessment

TEWL and HV tests were approved by the Bioethics Committee at the Medical University of Bialystok (bioethical per mission number APK.002.364.2024).

The assessments were performed by instrumental techniques (Corneometer CM825 and Tewameter TM300, Courage-Khazaka, Köln, Germany) to measure the amount of water present in the stratum corneum (corneometry) and the skin barrier condition (evaporimetry). The prepared emulsions were applied to the forearms of the respondents, twice a day.

3. RESULTS AND DISCUSSION

Among the prepared placebo emulsions, emulsions E3 and E4 presented the highest adhesive properties (Figure 1). They showed strong adhesion and required more effort to separate from the applied adhesive layers. Emulsion E3, containing avocado oil and Olivem, was characterized by better stability than emulsion E4 (mild phase separation), thus was selected as the emulsion carrier for trehalose.

P011

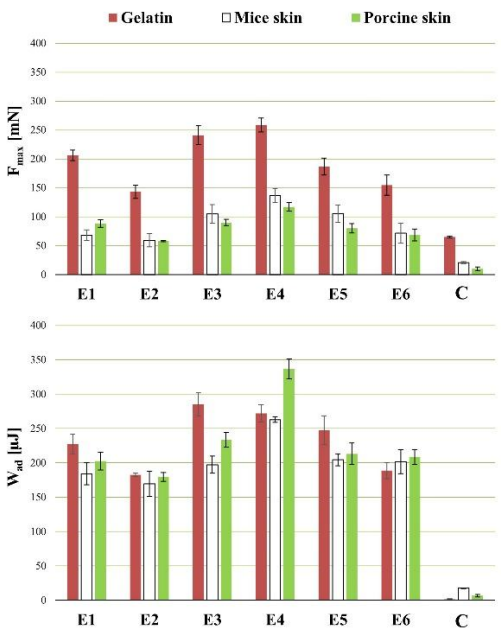

Figure 1. Adhesive force (F_{max}) and work of adhesion (W_{ad}) of the designed emulsions and control (C, cellulose paper). Mean ± SD, n = 6.

The highest reduction of TEWL and increase of HV was noted after 30 days of emulsions application (Figure 2). However, both moisturizing parameters were changed – TEWL increased and HV decreased on the 14th day after the last application. This highlights the necessity of daily application of emulsions to maintain the moisturizing effect. No significant differences ($p > 0.05$) were observed between placebo emulsion and emulsions with trehalose (1-5%). Additionally, it can be supposed that emulsion base containing moisturizing components (avocado oil and Olivem) significantly improved the skin hydration level.

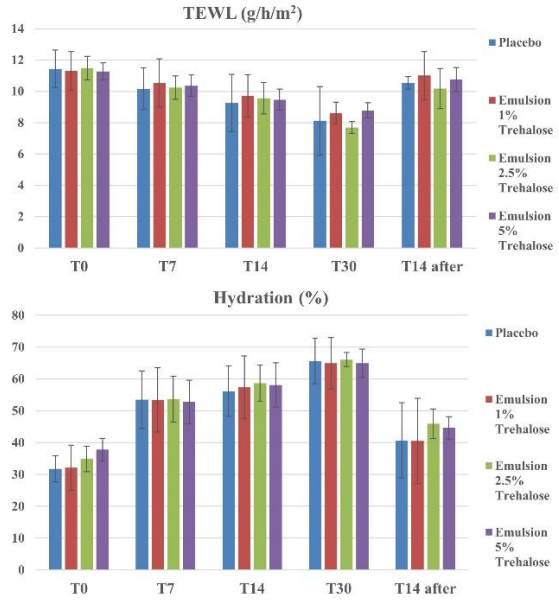

Figure 2. TEWL and HV before the 1st application (T0), on the 7th, 14th and 30th day of the application (T7, T14, T30) and 14 days after the last application (T14 after). Mean ± SD, n = 4.

4. CONCLUSION

The emulsion composed of liquid paraffin and avocado oil as an oily phase and Olivem 1000 as an emulsifier possessed high bioadhesive properties, satisfying stability and it significantly improved the skin hydration.

The research was funded by the Medical University of Bialystok (grant number B.SUB.25.347).

5. REFERENCES

1. Thakur R., Sharma A., Verma P., Asha D. A review on pharmaceutical emulsion. AJPRD 2023, 11 (3).
2. Madawi E.A., Manaa H.M., Alattrach D.G., et al. Dry emulsions as a promising adaptation in pharmaceutical dosage formulations: A review of recent developments and biopharmaceutical significance. J. Drug Deliv. Sci. Technol. 2024, 96, 105712.
3. Kuczyńska-Wiśnik D., Stojowska-Swędrzyńska K., Laskowska E. Intracellular protective functions and therapeutical potential of trehalose. *Molecules* 2024, *29*, 2088.
4. Greco L., Ullo S., Rigano L., et al. Evaluation of the filming and protective properties of a new trehalose and ceramides based ingredient. Cosmetics 2019, 6, 62.
5. https://cosmetics.specialchem.com/_/media/production/cosmetics/dksh/tds/trehalose-100brochurepim000000309.pdf

P012

POTENTIAL OF SOY PROTEIN CONCENTRATE AND PUMPKIN OIL CAKE AS DISINTEGRATION ENHANCERS FOR 3D PRINTED HPC MINI TABLETS

Jelena Čanji Panić[1], Nemanja Todorović[1], Aleksandra Ćoškov[1], Dušica Bosiljčić[2], Senka Popović[3], Mladena Lalić-Popović[1,4]

[1]Department of Pharmacy, Faculty of Medicine Novi Sad, University of Novi Sad, Serbia
[2]Pharmacy Institution Benu, Galenic Laboratory, Novi Sad, Serbia
[3]Department of Food Preservation Engineering, Faculty of Technology Novi Sad, University of Novi Sad, Serbia
[4]Center for Medical and Pharmaceutical Investigations and Quality Control (CEMPhIC), Faculty of Medicine Novi Sad, University of Novi Sad, Serbia

1. INTRODUCTION

Hot-melt extrusion (HME) coupled with fused deposition modeling (FDM) 3D printing has been excessively researched in the past decade for production of pharmaceuticals. However, this technology still faces many difficulties, such as lack of suitable pharmaceutical-grade materials [1], slow disintegration and therefore slow drug-release [2]. Due to good safety profile and biocompatibility, biopolymers are increasingly used as pharmaceutical excipients [3]. In this study we researched possibility of applying biopolymer food product, soy protein concentrate (SPC) and by-product of the food production process, pumpkin oil cake (PuOC) as environmentally friendly pharmaceutical excipients, in FDM 3D printing. The aim was to investigate the possibility of formation of filaments for 3D printing containing selected biopolymers and to determine the influence of SPC and PuOC on the disintegration of the 3D printed mini tablets (printlets).

2. MATERIALS AND METHODS

2.1. Materials

For the filament formulation, hydroxypropyl cellulose (HPC) (donation of Galenika A.D., Serbia) was used as thermoplastic polymer, sodium-starch glycolate (NaSG) (donation of Galenika A.D., Serbia) as conventional superdisintegrator and mannitol (Farmalabor, Italy) as plasticizer. Biopolymers, SPC and PuOC (donation of Faculty of Technology Novi Sad, Serbia) were added as potential disintegration enhancers.

2.2. Filament extrusion

Five filament formulations were prepared by HME on a single-screw extruder (NoztekTouch, UK) with nozzle diameter 3 mm. The masses of the powders of each individual component were weighed on an analitical balance (Radwag, Poland) and mixed in a powder mixer (Pharmalabor, Italy). The powder mixtures were dried for 24 h at 40 °C (Memmert, Germany) before extrusion. The composition of the formulations F1-F5 is shown in Table 1. Extrusion temperature was 115-125˚C, and the screw rotation was 10 rpm.

Table 1. Formulation composition in w/w %.

Component [w/w %]	F1	F2	F3	F4	F5
SPC	/	/	/	10	20
PuOC	/	10	20	/	/
Mannitol	25	25	25	25	25
NaSG	10	10	10	10	10
HPC	65	55	45	55	45

2.3. FDM 3D printing

A cylindrical model (printlet/mini tablet) measuring 3x5 mm was designed in 3D Builder software 20.0.4.0 (Microsoft Corporation, USA) and processed in Ultimaker Cura 3.2.1 software (Ultimaker, The Netherlands). FDM 3D printer Ultimaker S3 (Ultimaker, The Netherlands) was used to produce the printlets. Printing temperature was 135˚C, build plate temperature 60˚C and 0.8BB Core was used.

2.4. Disintegration test

The disintegration of printlets was tested in a thermostatic bath with a shaker (Witeg, Germany). The movement speed of the device

P012

was set at 50 rpm at the temperature of physiological 37°C. The test was done in triplicate. The printlets were transferred to a 10 ml beaker filled with distilled water, previously thermostatted in the water bath. Every 15 min for the total of 90 min, the printlets were taken out of the beaker and the mass was measured on an analytical balance. The printlet mass change was expressed as a percentage of the mass change in relation to its initial mass. Statistical calculations were performed in SPSS software, version 23 (SPSS, USA). The differences were considered significant for $p<0.05$.

3. RESULTS AND DISCUSSION

Both SPC and PuOC were successfully incorporated into HPC filaments via HME in two mass proportions, 10% and 20%. All of the obtained filaments were printable, and five formulations of printlets were produced.

Figure 1. shows the speed of disintegration of the printlets. In the initial phase of the test, all printlet formulations had an increase in mass, due to swelling. Formulations with SPC and PuOC, especially in higher proportions, showed accelerated disintegration. After 45 min, formulations with higher proportion of PuOC (F3) and SPC (F5) started to show statistically significantly lower mass than F1, indicating faster disintegration. After 60 min, F3 was the first formulation to completely disintegrate, followed by F5 after 75 min of the test. Statistically significant difference between F1 and formulation with lower proportion of SPC (F4) started to occur after 75 min and between F1 and formulation with lower proportion of PuOC (F3) only after 90 min. Within 90 min of the test all formulations except F1 have completely disintegrated.

.

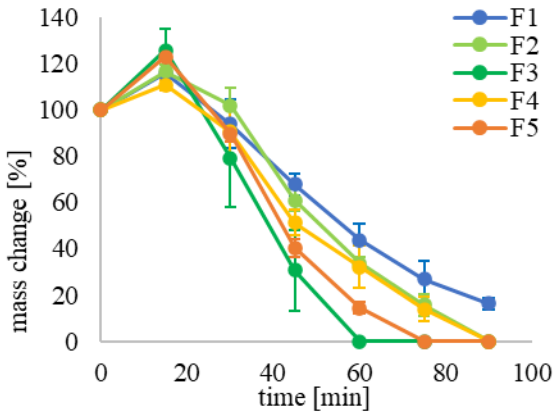

Figure 1. Printlets disintegration

4. CONCLUSION

SPC and PuOC can be successfully employed in filament formulations preparation by HME for FDM 3D printing. These biopolymers showed potential as pharmaceutical excipients that can enhance the disintegration of pharmaceutical solid dosage forms obtained by FDM 3D printing, especially when used in higher proportions.

5. REFERENCES

1. Shi, K., et al., *Role of release modifiers to modulate drug release from fused deposition modelling (FDM) 3D printed tablets.* Internation Journal of Pharmaceutics, 2021. 597:120315.

2. Đuranović, M., et al., *The evaluation of the effect of different superdisintegrants on the drug release from FDM 3D printed tablets through different applied strategies: In vitro-in silico assessment.* Internation Journal of Pharmaceutics, 2021. 610:121194.

3. Aguilar-de-Leyva, Á., et al., *3D Printed Drug Delivery Systems Based on Natural Products*. Pharmaceutics, 2020. 12(7): 620.

ACKNOWLEDGMENT

This study was supported by the Ministry of Science, Technological Development and Innovation, Republic of Serbia (grant: 451-03-136/2025-03/ 200114).
Authors would like to thank Galenika A.D. for the donation of pharmaceutical excipients

P013

DEVELOPMENT OF HYPOALLERGENIC OIL-IN-WATER CREAM USING HYDROGENATED PHOSPHATIDYLCHOLINE: A QUALITY BY DESIGN APPROACH

Beata Denisa[1], Oxana Brante[1], Baiba Mauriņa[2], Konstantīns Logviss[1]

[1]Laboratory of Finished Dosage Forms, Faculty of Pharmacy, Rīga Stradiņš University, Latvia
[2]Department of Applied Pharmacy, Faculty of Pharmacy, Rīga Stradiņš University, Latvia

1. INTRODUCTION

Patients with various skin disorders have dry skin that needs to be moisturised.[1] Often used emulsifiers such as cetyl and stearyl alcohols are known to cause contact allergy in some patients.[2,3] Widespread use of these emulsifiers narrows treatment availability for patients with sensitive skin. An alternative emulsifier, hydrogenated phosphatidylcholine, can be used to develop a hypoallergenic cream formulation. However, this excipient is not widely used as a main emulsifier in creams. Therefore, the aim of this work was to develop creams using the hydrogenated phosphatidylcholine, while applying Quality by Design (QbD) principles to study the effects of excipient concentration in formulation on the product characteristics.

2. MATERIALS AND METHODS

2.1. Materials

The materials used for cream preparation were *prunus amygdalus dulcis* (sweet almond) oil, penthylene glycol, glycerin, caprylic/capric triglyceride, hydrogenated phosphatidylcholine, *butyrospermum parkii* butter, xanthan gum and aqua (purified water).

2.2. Method of cream preparation

The materials were categorized into two phases based on their solubility properties. Each phase was heated to 80 ± 10 °C. Phases were mixed together and continuously stirred, ensuring the formation of a uniform and homogeneous cream.

2.3. Methods of cream evaluation

Product Critical Quality Attributes were established. Prepared formulations were analysed for organoleptic characteristics, microscopic appearance, cream type and pH.

3. RESULTS AND DISCUSSION

3.1. Formulation compositions

8 cream formulations with varying concentrations of sweet almond oil (10%, 15%, 20%, 30%), hydrogenated phosphatidylcholine as an emulsifier (1.5%, 3%, 6%) and caprylic/capric triglyceride as a second emulsifier (1.5%, 3% and 6%) were produced.

3.2. Cream evaluation

All formulated creams exhibited an oil-in-water (O/W) emulsion structure (Fig.1), with a measured pH of 5.

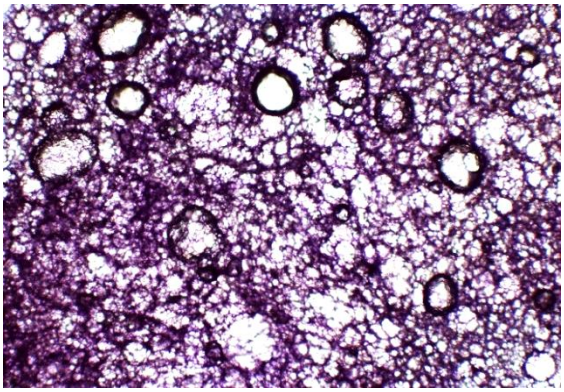

Figure 1. Cream type determination under microscope, cream E*, x10 magnification

Phase separation was observed in five formulations (A, B, C, D, E, Fig.2) under normal storage conditions, and in sample G following stress conditions (40°C ± 2°C/75% RH ± 5%).

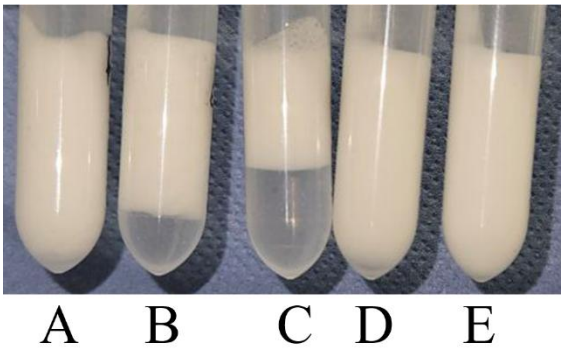

Figure 2. Visual observation of creams, phase separation

Analysis of microscopic appearance indicated appropriate structural integrity for three batches under normal storage conditions (F, G, H), however appropriate microscopic appearance upon stress exposure (40°C ± 2°C/75% RH ± 5%) was maintained only in sample H.

3.3. Design Space

Based on the results of the cream evaluation, a Design Space was established (Fig. 3), utilizing a color scale ranging from green to red to visually represent the compatibility of each formulation with the predefined Critical Quality Attributes (CQA), where green indicates compatibility.

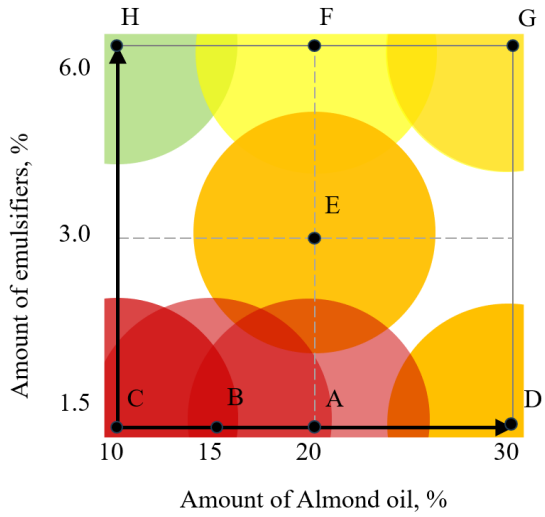

Figure 3. Established Design Space

4. CONCLUSION

Hydrogenated phosphatidilcholine can be used as a main emulsifier in oil-in-water creams at concentration of 6% in the proposed formulation but cannot be used at concentration of 3% or below. A higher amount of emulsifiers results in better product homogeneity, absence of phase separation and satisfactory microscopic structure.

5. REFERENCES

1. Ahmed, I. A. and Mikail, M. A. 2024. Diet and skin health: The good and the bad. *Nutrition*. 119(3), 112350. Elsevier Inc. Available from: https://doi.org/10.1016/j.nut.2023.112350 [viewed 26.12.2024.]

2. González-Muñoz, P., Conde-Salazar, L. and Vañó-Galván, S. 2014. Allergic Contact Dermatitis Caused by Cosmetic Products. *Actas Dermosifiliogr.* 105(9), 822-832. Available from: doi: 10.1016/j.ad.2013.12.018. [viewed 30.11.2024.]

3. Hamann, C, R,, Bernard, S., Hamann, D., Hansen, R and Thyssen, J. P. 2015. Is there a risk using hypoallergenic cosmetic pediatric products in the United States? *Journal of Allergy and Clinical Immunology*. 135(4),1070–1071. Available from: https://doi.org/10.1016/j.jaci.2014.07.066 [viewed 30.11.2024.]

ACKNOWLEDGMENT

This research is a part of the Master's thesis conducted within the Industrial Pharmacy program at Rīga Stradiņš University (RSU).

P014

COMPARATIVE ANALYSIS OF CIPROFLOXACIN HYDROCHLORIDE PARTICLE SIZE AND METHODS OF PRODUCTION IN TABLET FORMULATION

Natalija Dimovska[1], Maja Todeska[1], Dobrinka Dimova[1]

[1]Research and Development Department, Replek, North Macedonia

1. INTRODUCTION

Ciprofloxacin hydrochloride is a fluoroquinolone antibiotic widely used for treating bacterial infections. Its formulation as film-coated tablets enhances stability, improves patient compliance, and ensures appropriate drug release.

According to some research ciprofloxacin hydrochloride is classified as a BCS Class IV drug, indicating low solubility and low permeability. [1] This classification suggests that this active pharmaceutical ingredient (API) exhibits poor aqueous solubility, which can lead to poor dissolution and hence poor bioavailability.

This study aims to compare different particle sizes of ciprofloxacin hydrochloride and different methods of production and evaluate their impact on dissolution and disintegration.

2. MATERIALS AND METHODS

2.1. Materials

Ciprofloxacin hydrochloride with varying particle sizes (d_{90}<850 µm and d_{90}<1700 µm) was obtained from Aarti Drugs. Excipients included: Microcrystalline cellulose from JRS (Vivapur® 101), Maize starch from Roquettes Freres, Povidone and Copovidone from BASF (Kollidon® 30 and Kollidon® CL-F, accordingly), Silica, colloidal anhydrous from Cabot (Cab-o-sil®), Magnesium stearate from Mosselman and hypromellose-based film coating system from Colorcon (Opadry®).

2.2. Methods of Production

Two different methods of production were applied: direct compression (DC) and wet granulation (WG). In the DC method, mixing was performed in a bin blender. WG was performed in a high shear granulator with ciprofloxacin hydrochloride, maize starch, microcrystalline cellulose and povidone (binder) intragranularly, and all other excipients included extragranularly. The tablets were compressed into an oval tablet, 18 x 8 mm in diameter on a rotary tablet press (Manesty, UK) and subsequently coated in a coating machine (O-Hara Labcoat, Canada).

2.3. Disintegration Testing

Disintegration tests followed Ph.Eur. guidelines. The time required for complete tablet breakdown was recorded.

2.4. Dissolution Testing

Dissolution studies of the film-coated tablets were performed using USP apparatus II (paddle method). Samples were collected at 30 minutes and analyzed using UV spectrophotometry.

2.5. Particle Size Analysis

Particle size distribution of ciprofloxacin hydrochloride was analyzed using laser diffraction method (provided by manufacturer of API) and by sieve analysis.

3. RESULTS AND DISCUSSION

Different production methods and different API particle size didn't seem to affect disintegration, since all film-coated tablets disintegrated for less than 7 minutes.

The correlation of the methods of production, the particle size of the API and dissolution of film-coated tablets is presented in the following table (Table 1).

Table 1. Methods of production, API particle size and dissolution results.

Production method	API particle size	Dissolution (%)
WG	d_{90}<850 µm	89.73
WG	d_{90}<1700 µm	79.06
WG	d_{90}<1000 µm*	81.12
DC	d_{90}<1000 µm*	89.50

*API with particle size d_{90}<1700 µm milled through 1.0 mm sieve using a rotor mill.

3.1. Effect of Particle Size in Wet Granulation

The dissolution is higher (89.73%) for tablets produced using wet granulation with API particle size d_{90}<850 µm compared to larger particle sizes (d_{90}<1700 µm, 79.06%). This suggests that smaller particle size API forms smaller granules with larger surface area available for dissolution, leading to better performance.

Tablets produced with wet granulation of API milled through a 1.0 mm sieve show only slightly higher dissolution (81.12%), compared to API particle size d_{90}<1700 µm (79.06%).

3.2. Comparison of Production Methods

Tablets produced with direct compression of API milled through a 1.0 mm sieve achieved dissolution of 89.50%, which is comparable to wet granulat**ion with smaller particle size API** (d_{90}<850 µm, 89.73%). This demonstrates that direct compression, when applied to API with particle size d_{90}<1000 µm, can maintain effective dissolution performance, similar to the wet granulation process with API with particle size d_{90}<850 µm.

Wet granulation, while offering enhanced mechanical properties of the granules, appears to have reduced dissolution for API milled through a 1.0 mm sieve (81.12%) compared to direct compression (89.50%). This difference might be attributed to the compact nature of granules formed during wet granulation, which could limit immediate exposure to the dissolution medium.

3.3. Comparison of Milled and Unmilled API

In this study, milling of the API with larger particle size was applied before wet granulation. The results show that milling had only a minimal effect on dissolution (79.06% vs 81.12%). Wet granulation itself may override the influence of milling, as the API undergoes agglomeration, altering its dissolution behaviour. Another explanation for this case is that using a rotor mill is not a suitable way to reduce API particle size.

4. CONCLUSION

The study highlights the critical role of particle size and production methods in optimizing dissolution profiles for challenging APIs. Tablets produced using wet granulation with smaller particle size API (d_{90}<850 µm) achieved the highest dissolution (89.73%), emphasizing the importance of increased surface area for enhanced dissolution. Conversely, larger particle sizes (d_{90}<1700 µm) and wet granulation of milled API showed reduced dissolution, likely due to decreased porosity and compact granule formation. Direct compression of API milled through a 1.0 mm sieve produced comparable dissolution (89.50%) to wet granulation with smaller particles (89.73%), suggesting that larger particle size of the API is suitable for direct compression, while smaller is suitable for wet granulation. These findings underscore the need to carefully select both the particle size and production method to improve the bioavailability of ciprofloxacin hydrochloride.

5. REFERENCES

1. Olivera, M. E., et al., *Biowaiver monographs for immediate release solid oral dosage forms: ciprofloxacin hydrochloride.* Journal of pharmaceutical sciences, 2011. 100(1): 22–33.

ACKNOWLEDGMENT

The authors express their gratitude to Replek for funding and support, as well as to their colleagues for their contribution.

P015

ADVANCED DRUG DELIVERY: VORICONAZOLE-LOADED MICROEMULSION HYDROGELS

Gackowski Michał[1,2], Froelich Anna[1], Schneider Raphaël[2], Osmałek Tomasz[1]

[1]Chair and Department of Pharmaceutical Technology, Poznań University of Medical Sciences, Poznań, Poland
[2]CNRS, LRGP, Université de Lorraine, F-54000 Nancy, France

1. INTRODUCTION

Dermatophytoses, particularly those affecting deeper skin layers, pose a significant therapeutic challenge due to the need for prolonged systemic antifungal treatment, often associated with severe adverse effects [1]. Voriconazole (VRC) has demonstrated high efficacy in topical applications, offering a promising alternative for difficult-to-treat infections [2,3]. However, its bioavailability remains limited by the skin's natural barrier, necessitating advanced drug delivery strategies [4]. Nanocarrier-based systems, such as microemulsions (ME), have gained increasing attention due to their ability to enhance drug solubility, improve skin penetration, and enable controlled release [5]. Additionally, incorporating absorption enhancers into ME formulations may further optimize drug bioavailability and therapeutic outcomes. In this study, we designed and evaluated novel ME-based hydrogels for the topical delivery of VRC, aiming to improve therapeutic efficacy.

2. MATERIALS AND METHODS

2.1. Materials

VRC was used as a model drug. The following oil phases prepared the ME systems: triacetin, Neobee M5, isopropyl palmitate, ethyl oleate, oleic acid, and isopropyl myristate. Surfactants used included Tween 80, Etocas 35, Brij 05-SS-(RB), Ludox HS-30 Coll., and Tween 85, while the co-surfactants were PEG E400 and Transcutol®. ***In vitro*** release and permeation studies were conducted using SnakeSkin™ (Thermo Scientific™) and Strat-M® (MERCK) membranes. Also, the study used PBS pH 7,4, acetonitrile, ethanol absolute, NaCl, Carbopol EZ-3, and triisopropanolamine (TIPA).

2.2. Construction of pseudoternary phase diagrams

The surfactant, co-surfactant, and oil phase mixture was titrated with the polar phase – DI water – to achieve turbidity at a temperature of 32°C ± 0.5°C, which indicated that the ME system had broken. Phase diagrams of Gibbs were then constructed.

2.3. Electrical conductivity studies

The tests used 0.05% NaCl(aq) as the polar phase along one dilution line. The FiveEasy™ conductivity meter (Mettler Toledo, Greifensee, Switzerland) was used for the test.

2.4. Dynamic light scattering (DLS) analysis

The average size and size distribution (Polydispersity Index, PDI) of the dispersed phase were measured by DLS (Zetasizer Nano-S, Malvern Panalytical, Westborough, MA, USA) for the ME system that provided the best VRC release.

2.5. *In vitro* drug release and permeation

Release and permeation studies were conducted using SnakeSkin™ membrane for the screening phase and Strat-M® for the final product. The studies were performed using Franz diffusion cells (Teledyne Hanson Research, Chatsworth, CA, USA) at 32°C ± 0.5°C, with a rotation speed of 200 RPM, in PBS buffer pH 7.4:ethanol 90:10 (%V/V). Six replicates were performed for each formulation.

2.5. Preparation of ME-based gels

VRC was dissolved in the surfactant-co-surfactant mixture with the oil phase, and water was added to form the ME. Carbopol EZ-3 was added to the ME, and the mixture was stirred (RPM 800) until a milky white dispersion was obtained. The pH of the mixture was then adjusted to the desired level using TIPA.

2.5. Rheological and texture profile analysis

Rheological analysis was performed at 25.0 ± 0.5 °C using a HAAKE™ RheoStress™1 rotational rheometer (Thermo Scientific™) with plate-plate geometry. Textural profile analysis was conducted using a Shimadzu AGS-X tetrameter. All tests were performed in triplicate.

P015

2.5. UHPLC-UV analysis

Chromatographic analysis was performed using a Shimadzu LC-10AT VP liquid chromatograph with an SPD-10A VP UV-Vis detector (λ = 256 nm), Equipped with Luna™ Omega 5 µm C18 100 Å column (250 × 4.6 mm) was used at 30°C. The mobile phase was a 60:40 (v/v) mixture of acetonitrile and DI water, with a 1 mL/min flow rate and an injection volume of 10 µL. The method was validated for linearity, accuracy, precision, and sensitivity, with a concentration range of 1 to 200 µg/mL (r = 1).

3. RESULTS AND DISCUSSION

Screening studies of ingredients for ME systems led to the construction of 46 phase diagrams, identifying combinations that provided the largest ME area. The solubility profiles of VRC in the most promising ingredients were then determined. Based on these results, five oil phases were selected and tested with surfactants and co-surfactants through conductometric studies to determine the emulsion type (w/o, lamellar, o/w) depending on the volume of the polar phase added. The optimized systems were tested for VRC release to identify the oil phase that yielded the best results. The release profiles are displayed in Figure 1. The chosen oil phase was further tested with three surfactants to evaluate their influence on VRC release. The semi-solid form was then assessed for VRC permeation using Strat-M™, a synthetic model for transdermal diffusion. The formulation exhibited non-Newtonian, shear-thinning behavior and was analyzed for texture and spreadability.

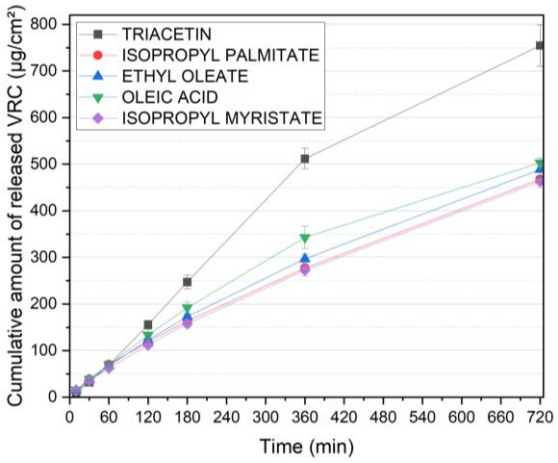

Figure 1. Cumulative release of VRC from ME over time, depending on the composition of the oil phase. Formulations contained Brij 05-SS-(RB) as the surfactant and Transcutol® as the co-surfactant. Data are presented as mean ± SD (n=6).

4. CONCLUSION

In this study, ME-based hydrogels loaded with VRC were successfully prepared and evaluated for drug release, permeation, and physio-chemical properties. The experiments that were conducted enabled optimization of both the preparation method and the composition of the systems investigated. The resulting formulations exhibited favorable mechanical properties, indicating their potential for application on the skin surface. These findings provide a foundation for further developing transdermal delivery systems for VRC.

5. REFERENCES

[1] Garg, A.; et.al. Heliyon 2020, 6, e04663, doi:10.1016/j.heliyon.2020.e04663.

[2] Gueneau, R.; et.al. Int. J. Antimicrob. Agents 2022, 60, 106677, doi:10.1016/j.ijantimicag.2022.106677.

[3] Khurana, A.; et.al. J. Med. Mycol. 2022, 32, 101306, doi:10.1016/j.mycmed.2022.101306.

[4] Paccoud, O.; et.al. Acta Derm. Venereol. 2023, 103, adv9590, doi:10.2340/actadv.v103.9590.

[5] De Almeida Campos, et.al. Pharmaceutics 2023, 15, 266, doi:10.3390/pharmaceutics15010266

ACKNOWLEDGMENT

Poznan University of Medical Sciences Doctoral School grant number (02/05/DGB/2024) financed from the statutory funds.

P016

EFFECT OF SPRAY DRYING PROCESS VARIABLES ON THE AERODYNAMIC PROPERTIES OF MICROPARTICLES FOR LUNG ADMINISTRATION

Jan Gajdziok[1], Andrea Peštálová[1], Sylvie Pavloková[1]

[1]Department of Pharmaceutical Technology, Faculty of Pharmacy, Masaryk University, Brno, Czech Republic

1. INTRODUCTION

Inhalation therapy is commonly used to treat respiratory diseases. The importance of this targeted delivery is growing, especially for conditions affecting specific lung regions, like primary ciliary dyskinesia or lung cancer [1]. Solid microparticles with customized aerodynamic properties, such as size, shape, porosity, and surface characteristics, enable efficient delivery to specific lung areas [2]. Aerosol performance, often measured by the fine particle fraction (FPF), can be enhanced with excipients like L-leucine, which improve the dispersibility of powders and porogens that decrease particle density, boosting deep lung deposition. Spray-drying conditions play a crucial role in determining the properties of particles, especially aerodynamic diameter, and their aerosolization efficiency [3]. Porous and large porous particles (LPPs) can maintain a low aerodynamic diameter, even with a larger geometric size, improving lung deposition and bioavailability [4]. Therefore, the combination of suitable excipients and spray drying conditions provides a complete picture of the physical and structural properties of the microparticles. The findings of this study offer valuable insights for designing more effective drug delivery systems for targeted lung deposition.

2. MATERIALS AND METHODS

2.1. Materials

D-mannitol (Penta s. r. o., Prague, CZ) was chosen as the carrier of microparticles. Adding L-leucine (My protein, Manchester, UK) as an enhancer of aerosolization properties and ammonium bicarbonate (Penta s. r. o., Prague, CZ) as porogen. Isopropanol (Penta s. r. o., Prague, CZ) was used as the dispersion medium for laser diffraction measurements, and purified water was used as a solvent. (Rodem 4, Aqua Osmotic, Prague, CZ).

2.2. Particles' preparation by spray drying

Microparticles were prepared using a LabPlant SD-06 spray dryer (Huddersfield, UK). A 10% w/v dispersion of D-mannitol (8.4%), L-leucine (1.5%), and ammonium bicarbonate (0.1%) was stirred in distilled water. The solution was atomized through a two-fluid nozzle (0.5 or 1.0 mm) with a medium-speed deblocker. The powder was collected via cyclone and stored in a desiccator before analysis.

2.3. Evaluation methods

The morphology of the microparticles was examined using SEM (Mira 3, Tescan, Brno, CZ), focusing on shape, surface texture, and porosity. Aerodynamic properties were characterized by an Aerodynamic Particle Sizer (APS 3321, TSI Inc., Minnesota, USA), providing real-time data on the particle size distribution and enabling calculation of MMAD and FPF. Complementary size distribution analysis was carried out by laser diffraction (Partica LA-960, HORIBA, Kyoto, Japan), offering rapid and accurate determination of mean size, GSD, and D-values (D_{10}, D_{90}). This multimodal approach ensured robust characterization of both geometric and aerodynamic properties critical to inhalation performance.

2.4. Design of experiment and data analysis

A two-phase design of experiment (DoE) approach was applied to evaluate the effects of key process parameters on microparticle properties. In Experiment I, a full factorial design tested the influence of three factors (X_1, X_2, X_3) using samples 1–8. Air flow rate strongly affected aerodynamic outcomes, improving MMAD and FPF at higher levels. Experiment II built on these findings, integrating a reduced nozzle diameter (0.5 mm) and modifying the factor set (X_1, X_2, X_4) in samples 5–8 and 5a–8a. Both phases employed two-level full factorial designs. The influence of individual factors was evaluated using ANOVA, while data analysis was conducted via software R.

P016

3. RESULTS AND DISCUSSION

3.1. Particle morphology

According to SEM images (Fig. 1), elevated drying temperatures (160 °C) produced smaller, more spherical particles with smoother surfaces, improving aerodynamic behavior. A lower pump speed (~900 mL/h) proved optimal, but a higher speed led to irregular structures. Increased air flow rates (4.3 m/s) enhanced droplet breakup, yielding smaller, more uniform particles, though overly high rates could induce deformation. Reduced nozzle diameter (from 1.0 to 0.5 mm) generated finer droplets that solidified into smaller, denser, and more uniform particles with improved sphericity and aerosol performance. Overall, formulations combining high air flow, smaller nozzle diameter, elevated temperature, and lower pump speed (samples 5a–8a) showed the most favorable properties for lung deposition.

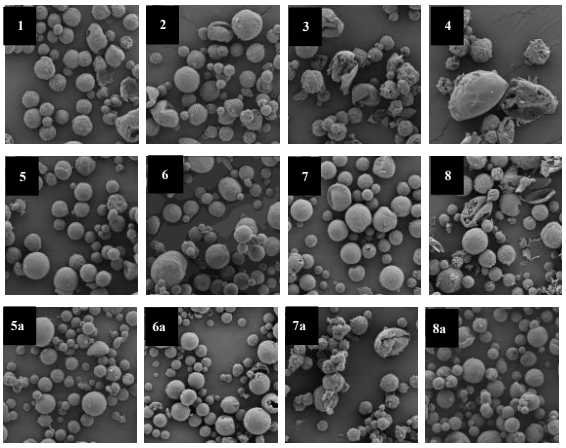

Figure 1: SEM images of microparticles at 5000× magnification

3.2. Particle size distribution

Among spray drying parameters (Table 1), air flow rate was identified as the dominant factor, as its increase led to a notable decrease in MMAD and an increase in FPF, primarily due to enhanced atomization and improved particle dispersion. Smaller nozzle diameters intensified this effect by producing finer droplets and ensuring a more uniform particle size distribution, enhancing aerosolization performance. Additionally, lower pump speeds contributed to a narrower size distribution (↓ GSD), likely due to extended drying times that enabled more consistent particle formation. In contrast, although drying temperature has been associated with changes in particle size and moisture content, it did not significantly influence MMAD, FPF, or GSD under the tested conditions.

Table 1. Output average values of aerodynamic properties depending on the DoE parameters.

Sample	X_1 (°C)	X_2 (ml/h)	X_3 (m/s)	X_4 (mm)	Y_1 (µm)	Y_2	Y_3 (%)
1	120	900	3.0	1.0	8.11	1.37	6.62
2	160	900	3.0	1.0	7.52	1.34	8.23
3	120	1665	3.0	1.0	7.46	1.34	9.28
4	160	1665	3.0	1.0	7.65	1.35	8.69
5	120	900	4.3	1.0	7.10	1.37	13.00
6	160	900	4.3	1.0	6.46	1.34	19.00
7	120	1665	4.3	1.0	6.74	1.36	16.90
8	160	1665	4.3	1.0	7.12	1.37	13.30
5a	120	900	4.3	0.5	5.84	1.34	31.70
6a	160	900	4.3	0.5	4.91	1.34	52.20
7a	120	1665	4.3	0.5	5.53	1.39	39.02
8a	160	1665	4.3	0.5	5.76	1.36	34.11

X_1 = Drying temperature; X_2 = Pump speed; X_3 = Air flow rate; X_4 = Nozzle diameter; Y_1 = MMAD; Y_2 = GSD; Y_3 = FPF

4. CONCLUSION

This study examined the effects of spray-drying parameters on microparticle properties using a DoE approach. SEM, laser diffraction, and APS data showed that the best performance was achieved with sample 6a by drying temperature (160 °C), higher air flow rate (4.3 m/s), lower pump speed (900 ml/h), and smaller nozzle diameter (0.5 mm). Using these conditions, particles with lower MMAD (4.91 µm) and higher FPF (52.20 %) were obtained. The optimized parameters yielded particles with MMAD < 5 µm and FPF > 50 %, suitable for deep lung delivery and enhancing the therapeutic efficacy of inhaled formulations.

5. REFERENCES

1. Athanazio R. *Airway disease: similarities and differences between asthma, COPD and bronchiectasis*. Clinics, 2012. 67: 1335-1343.
2. Borghardt J. M., et al., *Inhaled therapy in respiratory disease: the complex interplay of pulmonary kinetic processes*. Canadian Respiratory Journal, 2018. 1: 1-11.
3. Akdač Ç. Y. *Development of dry powder inhaler formulations for drug delivery systems*. Journal of Research in Pharmacy, 2019. 23(6): 973-987.
4. Munir M., et al., *Development of a spray-dried formulation of peptide-DNA nanoparticles into a dry powder for pulmonary delivery using factorial design*. Pharmaceutical Research, 2022. 39(6): 12151232.

P017

DEVELOPMENT OF A MULTIMODAL RELEASE DICLOFENAC SODIUM TABLET USING SEMI-SOLID EXTRUSION 3D PRINTING

Anastas Dimoski, Teodora Tasevska, Lina Livrinska, Maja Simonoska Crcarevska, Dushko Shalabalija, Katerina Goracinova and Nikola Geskovski

Ss. Cyril and Methodius University in Skopje, Faculty of Pharmacy, Skopje N. Macedonia

1. INTRODUCTION

Three-dimensional (3D) printing has emerged as a promising technology in pharmacy as evidenced by the increasing number of scientific publications addressing its application [1]. Despite certain limitations, this technology offers significant advantages, among which is the potential for personalized drug production. Considering the physicochemical and biopharmaceutical properties of diclofenac sodium and the therapeutic profile of chronic NSAID treatment, this study aimed to develop a bilayer solid oral dosage form with a multimodal drug release profile using three-dimensional semi-solid extrusion (SSE) 3D printing technology. The primary objective was to achieve a dual-phase release system, in which one fraction of the active pharmaceutical ingredient (50 mg) would be released at a pH above 6.8 - representing the enterosolvent layer, while the remaining 25 mg would be continuously released in a pH-independent manner (sustained-release layer).

2. MATERIALS AND METHODS

2.1. Materials

Diclofenac sodium was kindly donated by ReplekFarm LTD, Skopje. Eudragitl L-100 was purchased from Evonik, while PEG-DA, DPPO, Tragacanth and HPMC were purchased from Merck-Milipore. All other chemical were of reagent grade and used as received.

2.2. Preparation procedure

2.2.1. Sustained release (bottom) layer

The bottom layer was prepared by dissolving 0.2g HPMC in solution of PEG-DA (0.3g) and DPPO (0.005g) in 2.71g distilled water at 60°C, using a heated magnetic stirrer. It was 3D-printed through a 0.4 mm nozzle with UV exposure (10s every other layer), a pressure of 80-90 kPa, and a speed of 4-5 mm/s on a BioX 3D printer (Cell-ink, Sweden). Printing conditions included a substrate temperature 25°C, syringe temperature 30°C, 30% rectilinear infill.

2.2.2. Enterosolvent (top) layer

Microspheres containing diclofenac sodium were prepared using a spray-drying technique. An ethanolic solution of the copolymer Eudragit L-100 was used as the coating matrix, with triethyl citrate as a plasticizer. Diclofenac sodium was dissolved in this solution along with 0.1 M NaOH to enhance solubility. The ratio Diclofenak sodium : Eudragit L-100 was optimized to obtain favourable drug release profile. The upper tablet layer was prepared by dispersing 0.21g tragacanth in 3ml 5% acetic acid, followed by the addition of diclofenac sodium microspheres. It was 3D-printed on top of the bottom layer at 40-50 kPa and 5-7 mm/s, with a substrate temperature of 25°C, syringe temperature of 30°C, and 30% rectilinear infill. Immediately after printing, the tablets were frozen at -20°C and then freeze dried at -40°C and 0.01 mBar for 12 hours. The upper tablet layer matrix polymer and concentration were chosen based on printability criteria (filament collapse and shape fidelity tests) described by O'Connell et al., and the matrix pH (≤5) [2]. A total of 32 matrix compositions were tested.

2.3. Characterization methods

The resulting microspheres and printed tablets were characterized using FTIR and Raman spectroscopy to assess possible interactions between drug and excipients. Particle size distribution was measured using a laser diffraction technique, and morphological analysis was conducted via optical microscopy. Dissolution tests were conducted using a closed loop flow-through cell method simulating gastrointestinal pH transition from 1.2 (0.1M HCl) to 6.8 (phosphate buffer) (the medium change was initiated at 2h) at 37°C, volume=500ml, flow rate=10ml/min. Samples were collected over 6 hours, filtered, and analyzed via UV/VIS spectroscopy to determine the release profile**.** Quantification of diclofenac sodium was performed via UV/VIS spectroscopy at 276 nm, using calibration

curves in both 0.1M HCl and phosphate buffer (pH 6.8).

3. RESULTS AND DISCUSSION

The sustained-release layer was designed to consist of diclofenac sodium dissolved in a cross-linked PEG-DA matrix, while the delayed-release layer was formulated in such a way that diclofenac sodium, in the form of enteric-coated microspheres with Eudragit L-100, would be dispersed in a fast-disintegrating carrier. The ratio of Eudragit L-100: Diclofenac sodium of 2.5:1 was found optimal in regards to the desired dissolution profile. While the 10% tragacanth gel in 5% acetic acid presented the best matrix properties for dispersing the prepared microparticles and printing the upper layer in regards to the printability and pH. The dimensions and weight of the printed tablets (Fig. 1 right panel) were consistent with the computer aided design (Fig. 1 left panel). The tablets exhibited good mechanical strength and structural integrity after freeze-drying.

The FTIR and Raman spectroscopy confirmed the successful encapsulation of diclofenac in the gastroresistant microspheres, and its effective dispersion within the carrier—tragacanth, as well as the successful crosslinking of the PEG-DA matrix dispersion of pure diclofenac in the.. The microspheres incorporated into the formulation exhibited uniform size distribution (d50= 4.75 µm ± 0.19) with spherical morphology.

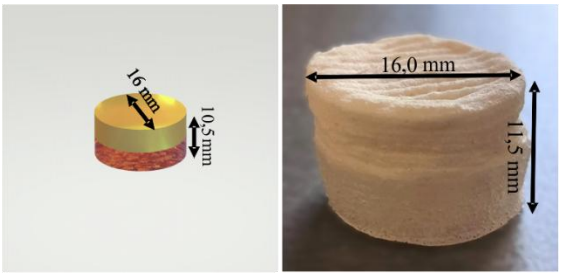

Figure 1. Tablet model designed in Tinkercad (left panel), actual printed tablet (right panel)

Dissolution tests showed that the 3D-printed tablets exhibited the expected dual release profile of diclofenac sodium. This profile was characterized by a sustained release from the bottom layer throughout the dissolution period, punctuated by a burst release from the top layer upon the pH change in the dissolution medium from 1.2 to 6.8.

4. CONCLUSION

This study confirms the potential of using SSE 3D printing for the preparation of advanced solid dosage forms. The dual-release bilayer tablet of diclofenac sodium effectively combines pH sensitive rapid and prolonged release phases to improve therapeutic efficiency and patient safety. The results pave the road for further research into the possibilities of implementing 3D printing technologies in personalized medicine, offering customized and safer treatments for chronic diseases.

5. REFERENCES

1. Wang, S, et al. A Review of 3D Printing Technology in Pharmaceutics: Technology and Applications, Now and Future. *Pharmaceutics* 2023. *15:* 416.

2. O'Connell C, et al. Characterizing Bioinks for Extrusion Bioprinting: Printability and Rheology. *Methods in Molecular Biology*, 2020.114: 111–33.

P018

SPRAY-DRIED PLGA MICROPARTICLES FOR EXTENDED DRUG DELIVERY: IMPACT OF FORMULATION PARAMETERS ON DRUG RELEASE KINETICS

Iva Erak[1], Mirna Perkušić[2], Biserka Cetina Čižmek[1], Jelena Filipović-Grčić[2], Anita Hafner[2]

[1]R&D, PLIVA Croatia Ltd., TEVA Group Member, Croatia

[2]Department of Pharmaceutical Technology, University of Zagreb Faculty of Pharmacy and Biochemistry, Croatia

1. INTRODUCTION

Poly(lactide-co-glycolide) (PLGA) has been widely used for injectable long-acting formulations for more than three decades. During this time, the influence of formulation components and processing conditions on the properties of the microparticles has been thoroughly investigated. Nonetheless, the underlying mechanisms are still not fully understood, with release kinetics remaining the most critical factor for formulation efficacy [1]. This study investigates the formulation of melatonin-loaded PLGA microparticles prepared by spray drying and evaluates the *in vitro* release behavior. The aim is to explore the influence of the drug-to-polymer (D/P) ratio on the physicochemical properties of the microparticles and the release kinetics of the drug.

2. MATERIALS AND METHODS

2.1. Materials

Melatonin was purchased from Biosynth Ltd (Slovakia), and PLGA (Resomer® RG 756 S, L/G ratio 75/25, ester-terminated, Mw 76–115 kDa) from Evonik (Germany). Dichloromethane (DCM) was purchased from Merck (Germany). Float-A-Lyzer®G2 (0.5-1 kDa molecular weight cutoff, cellulose ester dialysis membrane) was purchased from Repligen (CA, USA).

2.2. Preparation of microparticles

Melatonin loaded PLGA microparticles were prepared by spray drying of drug/polymer solutions in dichloromethane (Table 1) using Büchi Mini Spray Dryer B-290 equipped with an ultrasonic nozzle (Büchi, Switzerland) and the Inert Loop B-295, with nitrogen as the drying gas. The process parameters were as follows: inlet temperature at 55 °C, feed pump at 10 %, nitrogen flow 414 L/h, aspirator rate at 100 % and ultrasonic nozzle power at 90 %.

Table 1. The composition of spray dried solutions.

Sample #	Melatonin conc. (g/mL)	PLGA conc. (g/mL)	Drug: polymer ratio (*w/w*)
1	1.25	1.25	1:1
2	2.22	2.22	1:1
3	0.63	1.26	1:2
4	0.25	2.50	1:10

2.3. Microparticles characterization

Drug loading (DL) and encapsulation efficiency (EE) were analysed by high performance liquid chromatography (HPLC, Agilent Technologies, USA). Thermal properties of the polymer, the drug, their physical mixture and microparticles were determined using differential scanning calorimetry (DSC, TA Instruments, USA). Scanning electron microscopy (SEM, Jeol, Japan) was employed to examine morphology of microparticles.

2.4. *In vitro* release study

Sample containing about 1 mg of melatonin was transferred to the Float-A-Lyzer, suspended in 1 mL of phosphate buffered saline (PBS) pH 7.4, and placed into a well closed glass bottle containing 200 mL PBS. The bottle was constantly agitated in water-bath shaker set at 37 °C and 100 rpm. At predetermined intervals 1 mL of outer medium was withdrawn followed by PBS replacement. The released melatonin content was determined by HPLC.

3. RESULTS AND DISCUSSION

3.1. Powder yield, drug loading and encapsulation efficiency

Powder yield (PY) was highest for microparticles obtained from solutions with lower polymer concentrations (#1 and #3; Table 2). The yield decreased with increasing polymer concentration, especially when the relative ratio to drug content was higher.

The EE was high for all tested samples (Table 2).

P018

Table 2. PY, DL and EE of PLGA microparticles, results are presented as mean ± s.d., n=3.

Sample #	PY (%)	DL (%)	EE (%)
1	24.2	48.4±0.1	96.9±0.3
2	15.8	48.2±0.5	96.5±1.0
3	29.2	31.9±0.2	96.2±0.5
4	3.9	9.1±0.0	99.7±0.4

3.2. Differential scanning calorimetry

Melatonin was characterized by an endothermic peak appearing at the midpoint temperature of about 118 °C, that was attributed to the melting point (T_m). PLGA analysis confirmed the glass transition temperature (T_g) of about 57 °C. In case of spray dried microparticles, a T_m shifted to about 112 °C and 51 °C for melatonin and PLGA, respectively, indicating drug-polymer interaction that was not observed in the physical mixture. However, the outlet temperatures were maintained well below 51 °C throughout the spray-drying process (40–43 °C).

3.3. Scanning electron microscopy

SEM images (Figure 1A-C) showed similar morphology for samples #1-3. The high drug content in these microparticles may have caused a slightly rough surface and a few distinct craters in the otherwise spherical microparticles [1]. In contrast, the microparticles with higher polymer content (Figure 1D) had a smoother surface but often had pronounced deflated depressions. All samples showed a tendency to aggregate.

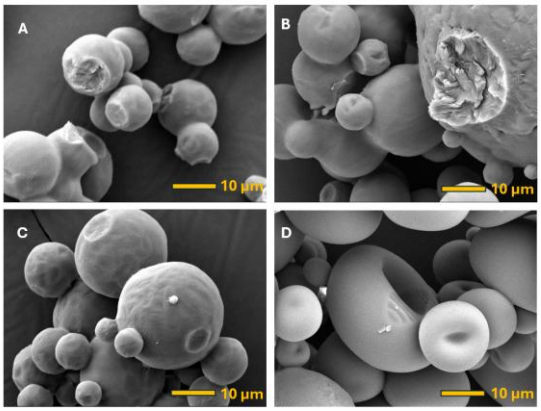

Figure 1. SEM images (M=2200×) of microparticles: A. #1; B. #2, C. #3; D. #4.

3.4. *In vitro* release

The prolonged release of melatonin up to 60 days was achieved (Figure 2). Microparticles with higher D/P ratios (1:1 and 1:2) showed similar biphasic drug release kinetics. The initial release phase was relatively high (Figure 2, enlarged) - about 50 % and 20 % in the first 24 h of release for D/P ratios of 1:1 and 1:2, respectively. After the initial burst, the drug was released continuously over the next 2 months. The sample with a lower D/P ratio (1:10) had a completely different release profile: the initial release was less than 10% in the first 24 h. After the third day the release started to accelerate, reached the first two formulations after about 20 days and continued to release at the same rate.

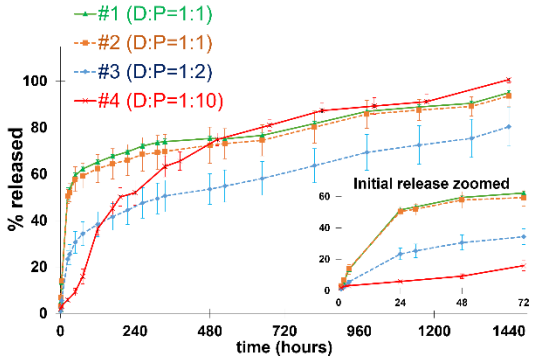

Figure 2. *In vitro* release of melatonin from PLGA microparticles up to 1440 h (60 days); Insert: Initial release up to 72 h (mean ± s.d., n = 3).

4. CONCLUSION

The study showed that the drug and polymer concentrations in the feed solution have an impact on the process yield. The drug to polymer ratio significantly affects the microparticle morphology and drug release kinetics.

ACKNOWLEDGMENT

This work has been supported in part by the University of Zagreb Faculty of Pharmacy and Biochemistry, Croatia, and R&D, PLIVA Croatia Ltd. (Contract No. 251-62-01-15-27), and project FarmInova (KK.01.1.1.02.0021) funded by the European Regional Development Fund. The authors thank Nikol Bebić, Mateja Prpić, and Jelena Torić from Teva R&D for their assistance with SEM and DSC analysis.

5. REFERENCES

1. Park, K., et al., *Formulation composition, manufacturing process, and characterization of poly(lactide-co-glycolide) microparticles*. Journal of Controlled Release, 2021. 329: 1150–1161.

P019

TABLETING-RELEVANT POLYOLS' PROPERTIES COMPARISON

Zoltan Mark Horvath, Kirils Kukuls, Alina Jaroslava Frolova, Liga Petersone, Elzbieta Maria Buczkowska, Valentyn Mohylyuk

Leading Research Group, Faculty of Pharmacy, Riga Stradiņš University, Riga, Latvia

1. INTRODUCTION

Polyols are widely used as excipients in pharmaceutical and nutraceutical formulations. Tablets comprise a major part of these formulations; thus, the effect of formulation ingredients on the properties of the formulation upon tableting is very important during pre- and formulation. In the market of pharmaceutical excipients, polyols are represented by a variety of chemical substances and their grades.

This research aimed to compare the tableting-relevant properties of available polyols.

2. MATERIALS AND METHODS

2.1. Materials

Dextrin – Nutriose FM06, FM10, and FM15S (Roquette Frères, Beinheim, France); inulin – Orafti GR, HP, HPX (BENEO-Orafti N.V., Oreye, Belgium); isomalt – galenIQ 720, 721, 800, 810, 960, and LM-PF (BENEO-Palatinit GmbH, Neuoffstein, Germany); mannitol – Mannogem XL Opal SD and Ruby GR (SPI Pharma, Grand Haven, MI, USA), Parteck M 100 and M 200 (Merck KGaA, Darmstadt, Germany), Pearlitol 200 SD (Roquette Frères, Beinheim, France); oligofructose – Orafti P95 (BENEO-Orafti N.V., Oreye, Belgium); PEG 8000 – Kollisolv PEG 8000 (BASF SE, Ludwigshafen, Germany); sorbitol – Parteck SI 150, SI 200, and SI 400 (Merck KGaA, Darmstadt, Germany); xylitol – Xylisorb 90 and 300 (Roquette Frères, Beinheim, France), xylitol (Sigma Aldrich/Merck KGaA, Darmstadt, Germany); sucrose (Maxima Int. Sourcing, Vilnius, Lithuania).

2.2. Characterisation methods

Powder X-ray Diffraction (pXRD) [1], optical microscopy [2], particle size distribution (PSD) [3], densification [4], loss on drying (LoD) [5], mean yield pressure (Py) and strain rate sensitivity (SRS) [6].

3. RESULTS AND DISCUSSION

Dextrin (Nutriose FM06, FM10, and FM15S), inulin (Orafti GR and HP), and oligofructose (Orafti P95) were found to be pXRD-amorphous while the rest of polyols were crystalline (**Fig. 1**) [1].

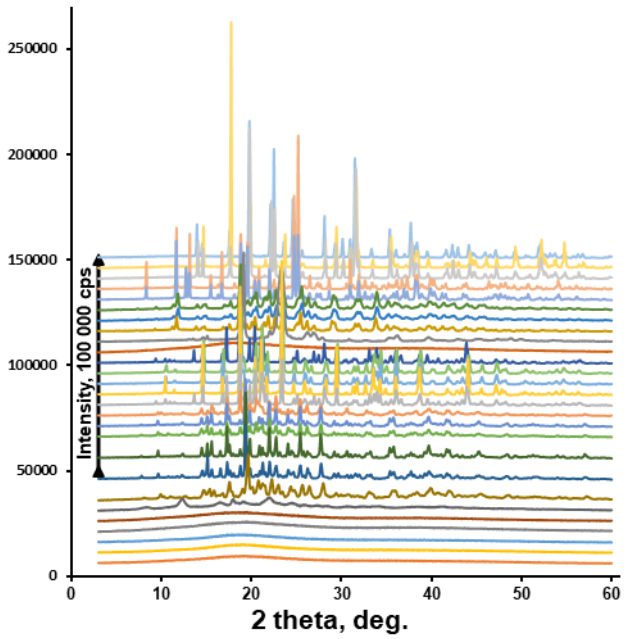

Figure 1. pXRD profiles of polyols [1].

Differences of particle shape and size were observed by optical microscopy [2]. Every grade of available polyols demonstrated a specific PSD profile (**Fig. 2**), which can be described in terms of $D_{10\%}$, $D_{50\%}$, and $D_{90\%}$ [3].

Polyols have different true densities. For example: dextrin, xylitol, sorbitol, mannitol, isomalt, inulin, and sucrose have 1.54, 1.52, 1.51, 1.51, 150, 1.35, and 1.60 g/cm^3. True density, together with solid state, particle shape, particle size, and PSD influences the densification profiles of polyols [4]. The last one can be used for the description of powder properties upon mixing, conveying, and tableting precompression.

P019

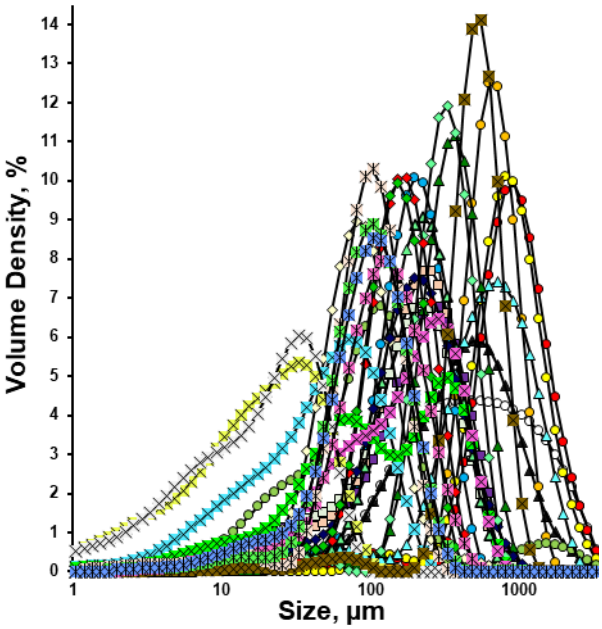

Figure 2. PSD profiles of polyols [3].

Even in small amounts, moisture content can drastically change the mechanical properties of excipients upon tableting [7]. Thus, the LoD of commercially available polyols was determined before their characterisation in terms of Py and SRS. Average Py values of polyols were found in the range of 55-300 MPa, while the SRS were between 0 and 38 % (**Fig. 2**) [6]. It means that increasing the tableting speed, the differences in deformation behaviour of polyols upon tableting will increase in accordance with the SRS increase.

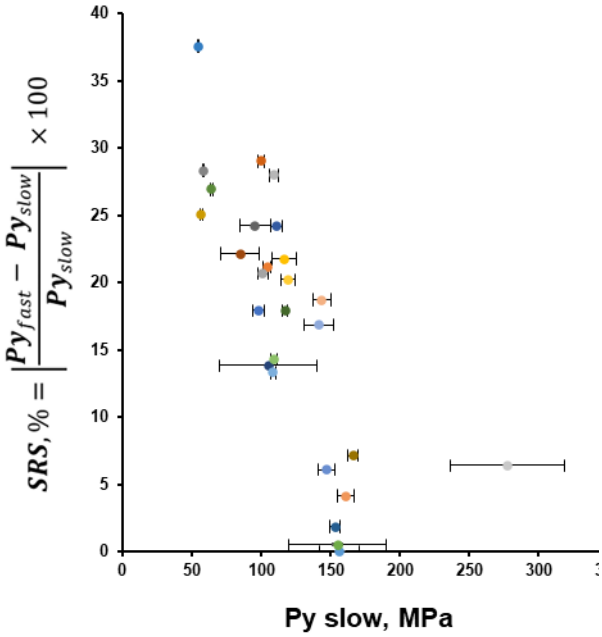

Figure 3. Py at slow tableting speed vs. SRS [6].

4. CONCLUSION

Being represented with different chemical compounds and different commercially available grades, a specific grade of polyols can be chosen for the formulation of nutraceutical and pharmaceutical products based on the desired solid state, particle size, PSD, densification and flowability propensity, as well as mean yield pressure and strain rate sensitivity.

5. REFERENCES

1. Horváth, Z.M., et al., *Dataset: Powder X-ray Diffraction (pXRD) Profiles of Polyols*. 2025.01: Riga Stradins University, Riga, Latvia; DOI: 10.48510/FK2/TDBOKG.
2. Kukuls, K., et al., *Dataset: Optical microscopy of polyols*. 2025.01: Riga Stradins University, Riga, Latvia; DOI: 10.48510/FK2/RBPONG.
3. Kukuls, K., et al., *Dataset: Particle size distribution (PSD) profiles of polyols*. 2025.01: Riga Stradins University, Riga, Latvia; DOI: 10.48510/FK2/GDGHY6.
4. Frolova, A.J., et al., *Dataset: Densification Profiles of Polyols*. 2025.01: Riga Stradins University, Riga, Latvia; DOI: 10.48510/FK2/SLQKI9.
5. Frolova, A.J., et al., *Dataset: Loss on drying (LoD) of polyols*. 2025.01: Riga Stradins University, Riga, Latvia; DOI: 10.48510/FK2/XILW3Z.
6. Kukuls, K., et al., *Dataset: Mean yield pressure (Py) and strain rate sensitivity (SRS) of polyols*. 2025.01: Riga Stradins University, Riga, Latvia; DOI: 10.48510/FK2/KMWDO6.
7. Paulausks, A., T. Kolisnyk, and V. Mohylyuk, *The Increase in the Plasticity of Microcrystalline Cellulose Spheres' When Loaded with a Plasticizer.* Pharmaceutics, 2024. **16**(7), DOI: 10.3390/pharmaceutics16070945.

ACKNOWLEDGMENT

The project "Internal consolidation of RSU and external consolidation of RSU with LSPA" (No. 5.2.1.1.i.0/2/24/I/CFLA/005) grant "Suitability of sugar alcohols (polyols) as binders in twin-screw melt granulation for preparation of high-drug-loaded immediate-release tablets with superior mechanical properties" (No. RSU-PAG-2024/1-0004) is financed within the framework of the European Union Recovery and Resilience plan and the state budget.

P020

FORMULATION AND CHARACTERIZATION OF LIDOCAINE-LOADED MICROEMULSION GELS

Patricia Jackuliakova[1], Miroslava Spaglova[1], Paula Cermáková[1], Juraj Piestansky[1,2]

[1]*Comenius University Bratislava, Faculty of Pharmacy, Department of Galenic Pharmacy, Slovak Republic*
[2]*Institute of Neuroimmunology, Slovak Academy of Sciences, Bratislava, Slovak Republic*

1. INTRODUCTION

Microemulsion-based gels (MEGs) are advanced topical drug delivery systems that combine the benefits of microemulsions-nanoscale droplets with high drug-loading capacity-with the structural stability of gels [1]. These formulations typically consist of oil, water, surfactants/ co-surfactant, and a gelling agent [2]. They enhance skin permeation while maintaining adhesion to the dermal surface. For lidocaine (LID), a widely used local anesthetic, MEGs provide sustained release, reduced systemic side effects, and improved patient compliance.

2. MATERIALS AND METHODS

2.1. Materials

Oleic acid (Centralchem, Bratislava SVK) and isopropyl myristate (Sigma-Aldrich, DE) as an oleic phase, distilled water and 20% solution of Poloxamer 407 (Sigma-Aldrich, St. Louis, USA) as a water phase, Polysorbate 80 (Centralchem, Bratislava SVK), Cremophor RH40 (BASF, Ludwigshafen, DE), Poloxamer 188 (Merck, Darmstadt, DE) as a surfactant, Transcutol Sigma-Aldrich, St. Louis, USA) and ethanol (Centralchem, Bratislava SVK) as a co-surfaktant, Carbopol 940 (Thermo scientific, Geel, BE) as a gelling substance, lidocaine (SOLUPHARM, Melsungen DE) as the active pharmaceutical ingredient.

2.2. Preparation of microemulsion-based gels

Microemulsions were prepared by a phase titration. A water phase was titrated in an oil phase containing also surfactant and co-surfactant (see in Table 1). In the process of preparing microemulsions, there was noticed self-gelling process, so in this case no other gelling agent have to be used. For the physical characterization of the MEGs, rheometry (Anton Paar, RheolabQC), and texture analysis (Stable Micro System TA-XT plus) was used. Additionally, *in vitro* drug release test through semi-permeable membrane using Franz cell (JM Glass, s.r.o.) was performed.

Table 1. The composition of MEGs

Materials	MEG 1 [%]	MEG 2 [%]	MEG 3 [%]
Polysorbate 80	35,54		
Transcutol	17,72		
Oleic acid	17,72		5
Water	29,03	37,74	
Izopropyl myristate		8,79	
Cremophor RH40		44,03	
Ethanol 96%		9,44	25,5
Poloxamer 188			25,5
20% solution of Poloxamer 407			45

2.3. The comparison: gels *versus* MEGs

For comparative evaluation of liberation from gels and MEGs, reference gels with similar composition as MEGs, but without the oil phase were prepared.

3. RESULTS AND DISCUSSION

3.1. Physical characterization

The rheological measurements were realized under 25°C and for formulation MEG1 and MEG3 it showed thixotropic behavior. For formulation MEG2 graphical representation showed rheopexy (Fig. 1). Texture analysis demonstrated that addition of LID does not change the structure of MEG, except for MEG3, where the addition of LID significantly increased the negative area above the curve in the first measurement cycle corresponding to the adhesiveness of the sample (Fig. 2).

P020

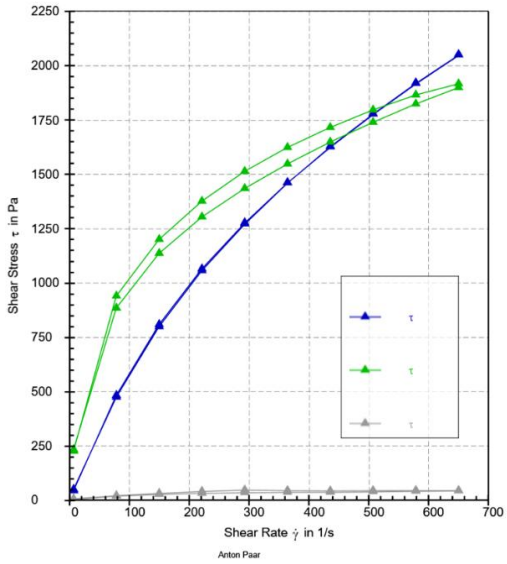

Figure 1. Rheograms of MEGs: MEG1 (with Polysorbate 80, grey), MEG2 (with Cremophor RH40, blue), MEG3 (with Poloxamer 188, green)

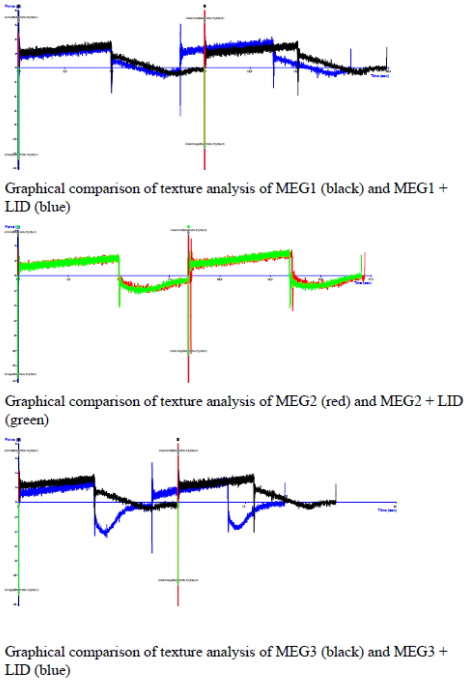

Figure 2. Texture profiles of MEG1-MEG3 influenced by the addition of LID

In vitro drug release studies demonstrated a linear release profile over 6 hours. Comparison of the total drug released after 6 hours (Fig. 3) indicates that MEG formulations containing Polysorbate 80 or Cremophor RH40 achieved greater drug release than their corresponding comparative gels. In contrast, for poloxamer-based formulations, the comparative gel facilitated higher LID (lidocaine) release than the MEG3 formulation. It should also be noted that no detectable drug release was observed from the comparative gel of formulation 1 during the 6-hour study period; therefore, its data are not included.

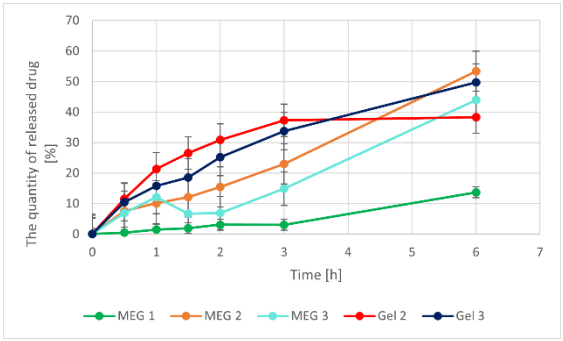

Figure 3. *In vitro* LID release study from MEGs *versus* gels

4. CONCLUSION

The study presents an innovative dermal formulation for administration of LID. The prepared formulations showed typical physical characteristics for gels, which did not change even after incorporation of LID. Addition of LID did not affect texture of prepared MEGs significantly. The study confirmed that MEGs may improve *in vitro* drug release from the dosage form.

5. REFERENCES

1. Daryab, M, et al., *Preparation and Characterization of Lidocaine-Loaded, Microemulsion-Based Topical Gels*. Iranian Journal of Pharmaceutical Research, 2021; 21(1):e123787.

2. Mehta, DP, et al., *A Review on Microemulsion Based Gel: A Recent Approach for Topical Drug Delivery System.* Research Journal of Pharmacy and Technology, 2015; 8(2):118-26.

ACKNOWLEDGMENT

This research was funded by Faculty of Pharmacy, Comenius University Bratislava FaF/1/2025 and Slovak Academy of Sciences VEGA 1/0302/24.

P021

CAN ANTISOLVENT CRYSTALLISATION BE USED FOR API CO-PROCESSING WITH COMMON DIRECT COMPRESSION EXCIPIENTS? A CASE STUDY WITH AMLODIPINE BESYLATE

Emilia Jakubowska[1,2], František Štěpánek[1]

[1]*Department of Chemical Engineering, University of Chemistry and Technology Prague, Czech Republic*
[2]*Chair and Department of Pharmaceutical Technology, Poznan University of Medical Sciences, Poland*

1. INTRODUCTION

The transition from batch to continuous manufacturing in pharmaceutical industry has been intensively discussed in recent years, with much focus on continuous direct compression (DC). However, many APIs are unsuitable for this process due to poor powder flow and/or compression properties. Their manufacturability can be improved by co-processing (CP) with excipients, resulting in engineered composite particles which behave in a similar way to bulk excipient [1]. Crystallisation processes are a promising area to be explored for this purpose. Relying on the phenomenon of templated heteronucleation on a solid surface, they are designed to promote the crystallisation of an API directly on excipient particles, as opposed to free bulk crystals. So far, co-processing studies employing cooling crystallisation with a limited range of excipients have been described (e.g. [2]).

The aim of this screening work was to test the feasibility of antisolvent crystallisation for co-processing amlodipine besylate as model API with a wide variety of common DC excipients as heteronucleation templates. The goal was to identify a promising combination of solvent and excipient type for further method optimisation.

2. MATERIALS AND METHODS

Various chemical types and grades of excipients from different suppliers (Table 1) were screened in combination with water-miscible organic solvents (MeOH, EtOH, IPA, acetone, ACN, DMF, NMP, DMSO, dioxane). Antisolvent crystallisation was performed in a milifluidic T-mixer (I.D. 1 mm, tubing I.D. 3.2 mm). Water was used as antisolvent (AS), while API solution phase (S) contained 40-70% organic, depending on amlodipine solubility curves in respective binary water-organic mixtures [3].

Table 1. Excipient types used in the study.

Excipient *(suppliers)*	**Grades**
MCC *(Asahi Kasei, JRS Pharma, Chemfield)*	PH 101,102,301, 302, 12; UF 702,711; KG802,1000
Low-substituted HPC *(Shin-Etsu)*	L-HPC: LH-11, LH-21, NBD-021
Pre-gelatinized starch *(Roquette)*	Lycatab: C, CT
Lactose (monohydrate spray dried or agglomerated; lactose anhydrous) (*DFE Pharma, Kerry)*	Lactopress Granulated; SuperTab: 11SD, 22AN, 24AN 30GR; Sheffield: Spray dried Foremost 315, Spray dried FastFlo 316, Anhydrous 60M, Anhydrous Impalpable
Mannitol (granulated, spray-dried) *(Freund, Roquette)*	Granutol: F, R, S Pearlitol: 100SD, 200 SD
Maltose *(SPI Pharma)*	Advantose 100

Supersaturation ratio (1.1-1.4, depending on the solvent) was chosen in preliminary excipient-free crystallization experiments. The goal was to ensure operation in metastable zone, where heteronucleation may occur. For co-processing, excipients were suspended in the solution phase for theoretical drug load of 25%. In the case of soluble excipients, both phases contained pre-dissolved excipient at suitable concentration to avoid its dissolution in the S and simultaneously target its saturation after phase mixing. S phase was fed at the maximum operating flow rate of the peristaltic pump (peRISYS Cetoni): 33 mL/min. For each type of solvent, AS flow rate was adjusted for target SR (total Q: 51-62 mL/min). Optical microscopy was used to

detect the presence of free and/or co-processed amlodipine crystals.

3. RESULTS AND DISCUSSION

Among the systems screened so far, successful co-processing of amlodipine besylate occurred in acetone-based crystallisation with lactose monohydrate of different grades. The appearance of composite particles varied. With Lactopress Granulated and SuperTab 11SD (Fig. 1), several amlodipine plates, typically smaller than 10-20 µm, were attached to the surface of lactose particle.

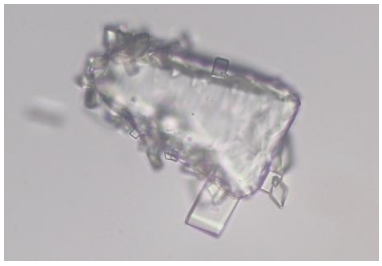

Figure 1. CP-particle, acetone x SuperTab 11 SD.

On the other hand, with SuperTab 30GR (Fig. 2) and Sheffield Foremost Spray-Dried 315, amlodipine grew into thick, large plates (500-900 µm), interconnecting several clusters of lactose particles. Nevertheless, free bulk amlodipine crystals were also present apart from the few observed co-processed particles.

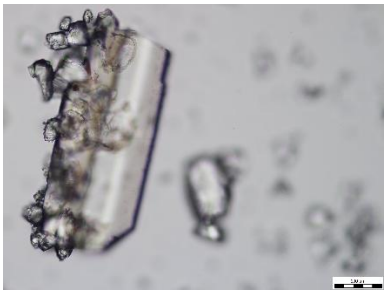

Figure 1. CP-particle, acetone x SuperTab 30GR.

Moreover, it could not be reliably verified if excipients based on anhydrous lactose or maltose monohydrate are a suitable heteronucleation template for amlodipine. In every tested solvent system, the sugar underwent phase transition, as the observed morphology of excipient particles in the processed samples differed from raw materials.

The use of insoluble excipients (MCC, L-HPC, pregelatinized starch) did not result in successful co-processing with any of the tested solvents. In some instances, bulk nucleation of amlodipine rod- and plate-shaped crystals occurred erratically, without correlation to excipient type or grade.

4. CONCLUSION

Antisolvent crystallisation of amlodipine besylate from acetone in the presence of lactose monohydrate produced co-processed API-excipient particles. Further optimisation work with respect to supersaturation, hydrodynamic conditions etc. is necessary to improve CP yield and reduce the occurrence of bulk nucleation.

5. REFERENCES

1. Schenck, L., et al., *Recent Advances in Co-processed APIs and Proposals for Enabling Commercialization of These Transformative Technologies*. Mol. Pharmaceutics, 2020. 17(7): 2232–2244.

2. Yazdanpanah, N., et al., *Continuous Heterogeneous Crystallization on Excipient Surfaces.* Cryst Growth Des., 2017. 17(6): 3321–3330.

3. Jakubowska, E., *Solubility of amlodipine besylate in binary water-organic solvent mixtures*. Zenodo dataset. 2025. https://doi.org/10.5281/zenodo.14771033

ACKNOWLEDGMENT

The project has received funding from the European Union's Horizon Europe programme under the Marie Skłodowska-Curie grant agreement no. 101152117, ManCoProc. Funded by the European Union. Views and opinions expressed are however those of the author(s) only and do not necessarily reflect those of the European Union. Neither the European Union nor the granting authority can be held responsible for them.

Funded by the European Union

Excipient suppliers and their regional representatives are gratefully acknowledged for kindly providing samples. Amlodipine besylate was donated by Zentiva k.s.

P022

CYCLODEXTRIN COMPLEXATION BY GRINDING AS A SUSTAINABLE STRATEGY TO ENHANCE *IN VITRO* DISSOLUTION OF CINNARIZINE

Mario Jug[1], Lorena Pažameta[1], David Klarić[2], Nives Galić[2]

[1]*Department of Pharmaceutical Technology, University of Zagreb Faculty of Pharmacy and Biochemistry, Croatia*
[2]*Chemistry Department, University of Zagreb Faculty of Science, Croatia*

1. INTRODUCTION

Cinnarizine (CNZ) is a lipophilic drug with limited oral bioavailability caused by its insolubility at a pH above 4.5. It is used to prevent motion sickness and to treat tinnitus, nausea, vomiting, and vertigo associated with Meniere's disease. Several approaches have been employed to address CNZ's limited bioavailability, and cyclodextrins (CDs) appear as a promising approach [1].

Conventional, solution-based methods of CD complexation present several challenges. CNZ may degrade in acidic conditions, or organic solvents may be needed to dissolve the drug. However, these solvents can be difficult to remove and remain in the final product, impairing its biocompatibility and safety. Grinding presents a fast, highly efficient, convenient, versatile, sustainable, and eco-friendly alternative for preparing CD complexes in the solid state without using any solvent [2].

In this study, grinding in high-energy mills was optimized by adjusting grinding times and frequencies to prepare CNZ/CD complexes with enhanced dissolution properties.

2. MATERIALS AND METHODS

2.1. Materials

Cinnarizine (CNZ) was obtained from Biosynth. Hydroxypropyl-β-cyclodextrin (HP-β-CH, with an average degree of substitution 4.5) was obtained from Cyclolab. All other chemicals used were of analytical grade.

2.2. Complex preparation by grinding

Complexes were prepared by grinding the equimolar CNZ/HPβCD mixtures in a Retch Mixer Mill MM 500 control at 20 and 30 Hz.

2.3. Differential scanning calorimetry (DSC)

DSC analysis was performed on a Discovery DSC 250 calorimeter employing a heating rate of 10 °C/min. The relative drug crystallinity (*RDC*) was calculated using the standardised CNZ melting enthalpy (Δ*H*) from the sample and the pure compound, respectively, according to the equation (1):

$$RDC = \frac{\Delta H_{sample}}{\Delta H_{drug}} \times 100\ \% \quad (1)$$

2.4. Drug content determination

Ten mg of the co-ground products were weighed into 10 mL flasks, dissolved in 1 mL of acetonitrile and brought up to volume with 0.1 M HCl. The drug quantity in the samples was assessed spectrophotometrically at 253 nm.

2.5. *In vitro* dissolution test

The test was performed on samples containing 37.5 mg of CNZ using a mini paddle apparatus at 37 °C with 125 mL of phosphate buffer pH 4.5 as the medium, stirred at 75 rpm. Aliquots were collected at predetermined time points, filtered and assayed spectrophotometrically at 253 nm. The volume of the dissolution medium was kept constant during the experiment. The dissolution efficiency (*DE*) was calculated from the amount of the dissolved drug (*Q*) at a given time (*t*) according to equation (2):

$$DE_{60\ min} = \frac{\sum_0^t Q dt}{Q_{100\%} \times t} \times 100 \quad (2)$$

P022

3. RESULTS AND DISCUSSION

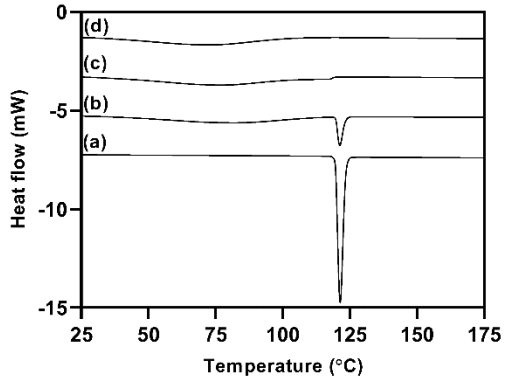

Figure 1. DSC thermograms of CNZ (a), CNZ/HPβCD physical mixture and the products ground at 20 Hz (c) and 30 Hz (d).

CNZ presented a sharp exothermic peak at 119.7 °C, corresponding to the drug melting. In the physical mixture before the grinding, the drug melting peak was reduced in accordance with its content in the sample. In the sample co-ground at 20 Hz, even after processing for 120 min, the drug melting peak still can be observed (Fig. 1, Table 1). However, when grinding was performed at 30 Hz, the amorphous product was obtained after 40 min of processing time. Sample amorphisation demonstrates the effective solid-state interaction between CNZ and HPβCD brought up by grinding [2].

Table 1. Grinding time, residual drug crystallinity (RDC) and dissolution enhancement factor (DE) for the co-ground products prepared.

Sample	Grinding time (min)	RDC (%)	DE
CNZ	-	100	-
CNZ/HPβCD GR 20 Hz	120	9.21	10.91
CNZ/HPβCD GR 30 Hz	40	0	22.13

Prolonged grinding at elevated frequencies provides high energy input to the treated system, potentially triggering the drug degradation. However, the relative drug content in the co-ground samples was around 100%, demonstrating no drug degradation irrespective of the grinding parameters employed.

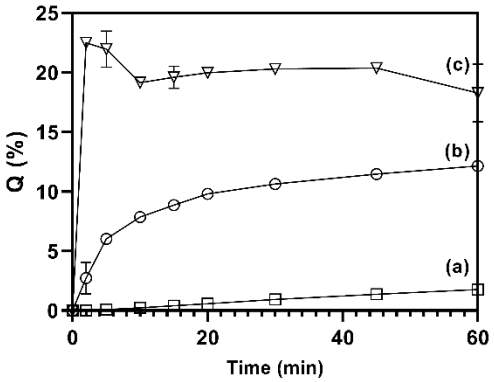

Figure 2. *In vitro* dissolution profiles of CNZ (a), CNZ/HPβCD products ground at 20 Hz (b) and 30 Hz (c) in phosphate buffer solution pH 4.5 at 37 °C.

Finally, *in vitro* dissolution test demonstrated that co-grinding with HPβCD efficiently enhanced CNZ dissolution even at elevated pH. The observed enhancement in dissolution is directly related to the obtained drug amorphization degree (Table 1). However, a supersaturation phenomenon was observed for product co-ground at 30 Hz.

4. CONCLUSION

Grinding with HPβCD was demonstrated as an efficient approach for enhancing the dissolution properties of CNZ. Further studies are required to address the suitability of such a co-ground product for further formulation development.

5. REFERENCES

1. Tanaka, Y., et al., *In vivo evaluation of supersaturation/precipitation/re-dissolution behavior of cinnarizine, a lipophilic weak base, in the gastrointestinal tract: The key process of oral absorption*. European Journal of Pharmaceutical Sciences, 2017, 96: 464-471.

2. Jug, M. et Mura, P., *Grinding as solvent free green chemistry approach for cyclodextrin inclusion complex preparation in the solid state*. Pharmaceutics, 2018. 10: 189.

ACKNOWLEDGMENT

Financial support from the IP-2022-10-6033 project of the Croatian Science Foundation and the basic funding of the University of Zagreb are greatly acknowledged.

P023

UNDERSTANDING THE VISCOSITY PROPERTIES AND THEIR ROLE IN PREDICTING HOT MELT EXTRUSION PARAMETERS FOR AMORPHOUS SOLID DISPERSIONS OF CELECOXIB AND PVPVA64

Paula Kaufelde[1], Rita Maria Soares[2], Oxana Brante[1], Konstantins Logviss[1]

[1]Laboratory of Finished Dosage Forms, Faculty of Pharmacy, Rīga Stradiņš University, Latvia
[2]Faculty of Pharmacy, Universidade de Lisboa (FFUL), Portugal

1. INTRODUCTION

Celecoxib (CCX), a selective cyclooxygenase-2 (COX-2) inhibitor, is a nonsteroidal anti-inflammatory drug (NSAID) classified under the Biopharmaceutics Classification System (BCS) Class II [1]. Due to its poor aqueous solubility, strategies such as amorphous solid dispersions (ASDs) have been widely adopted in the pharmaceutical industry. Notably, approximately 30% of marketed products requiring solubility enhancement between 2000 and 2020 utilized ASD technology [2].

Among the various methods for ASD production, hot-melt extrusion (HME) is particularly advantageous due to its solvent-free nature, scalability, efficient drug-polymer mixing, and ability to enhance drug solubility and stability in a continuous and reproducible manner [3].

Viscosity is a critical parameter in HME processing, and its preliminary determination can optimize the process by facilitating the identification of ideal processing conditions (e.g., temperature, T). Rheometry can be employed to measure viscosity and extrapolate relevant data, enabling the estimation of optimal processing temperature.

2. MATERIALS AND METHODS

2.1. Materials

The materials used in this study included *celecoxib* (batch CLP734, BLD Pharmatech Ltd., Telangana, India) with 99.92% purity and *PVP/VA 6:4* (Vivapharm® PVP/VA 64, batch 031017006, JRS Pharma, Rosenberg, Germany).

2.2. Methods

Preparation of physical mixtures (PM): PMs of CCX and PVP/VA64 were prepared by individually weighing each compound using an Ohaus PX323M scale (New Jersey, United States) and mixing them manually.

Flowability: Tapped density, Hausner ratio (HR), and Carr Index (CI) were determined using a 100 ml graduated cylinder with the USP2 method at a 250 taps/min speed using tapped density tester Erweka SVM II (Langen, Germany).

Preparation of ASD: The Vacuum Compression Molding (VCM Essentials) type M-01-04-1 (MeltPrep GmbH, Graz, Austria) was used for the preparation of the ASD samples. 0.75 g of the PMs previously prepared were placed into a 25 mm diameter sample holder. The samples were heated at 165 ºC for 20 minutes at the vacuum, followed by cooling, obtaining transparent glasslike discs with well-defined geometry.

Rheological Behaviors: A Modular Compact Rheometer (Anton Paar GmbH, Graz, Austria) series 102e equipped with one set of 25 diameter parallel sandblasted plates was used to obtain viscosity curves. Measuring gap 0.8 mm, the samples were measured at 140 ºC obtaining 60 points (if possible) at a shear rate from 0.1 up to 1000 1/s. Data extrapolations were made using Excel Solver add-in.

Hot melt extrusion (HME): Co-rotating twin-screw extrusion was carried out using a Thermo Fisher Pharma 11 extruder (Thermo Electron GmbH, Karlsruhe, Germany). The extruder was equipped with a volumetric feeder (feeding rate 0.3 g/min) and with conveying screws and mixing elements, the rotation speed was set to 100 rpm. Processing temperatures were 140 °C in all seven zones, except for the first zone at 60 °C. The torque did not exceed 30% of the maximum allowed (6 N·m). The first 3 g of extrudates were discarded.

3. RESULTS AND DISCUSSION

P023

3.1. Flowability

CCX predominantly consists of needle-shaped crystals, whereas PVP/VA particles exhibit a distinctly rounded morphology, unlike the API (data not shown). Higher API content resulted in increased HR and CI values (Table 1), attributable to the needle-like particle morphology of CCX. All three PMs demonstrated markedly poor flowability.

Table 1. HR and CI of PMs

PMs (w/w %)	HR	CI (%)
30:70	1.65	39.6
50:50	1.73	42.1
70:30	1.74	42.6

3.2 Viscosity Curve extrapolation

Viscosity profiles were modelled using the Cross equation from viscosity curves (fig. 1), yielding extrapolated viscosity parameters (Table 2). The model predicts that extrusion at 140 °C will provide sufficient melt viscosity for the 30:70 (CCX:PVP/VA) formulation. For the 50:50 composition, optimal processing conditions may be achieved at reduced temperatures to maintain appropriate viscoelastic properties. The 70:30 formulation exhibited inadequate viscosity at 140 °C, resulting in excessive fluidity and unstable filament formation during extrusion.

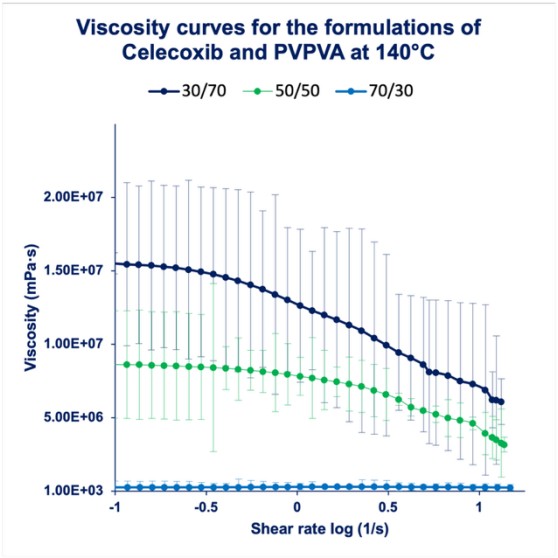

Figure 1. Viscosity curves at 140 ºC for all formulation ASDs;

Table 2. *Extrapolated viscosities of VCM ASD samples*

PMs (w/w %)	T (ºC)	Extrapolated viscosities (Pa·s)	
		2300 s^{-1}	21 000 s^{-1}
30:70	140	1740	462
50:50	140	320	280
70:30	140	14.7	12.5

3.3. Hot melt extrusion

The 30:70 (CCX:PVPVA) formulation demonstrated optimal extrusion parameters at 140 ºC, as evidenced by a practical torque value of 34% and the production of uniform, vitreous filaments, indicating appropriate melt viscosity and homogeneous dispersion. For the 50:50 formulation, while 140 ºC remained operationally acceptable (torque - 18%), thermal optimization through temperature reduction could improve torque performance. In contrast, the 70:30 formulation required additional temperature reduction to achieve viable processing conditions (torque - 10%), suggesting insufficient melt viscosity at the baseline temperature.

4. CONCLUSION

ASD of celecoxib and PVPVA was successfully created using HME and VCM techniques.

The experimental torque data closely aligns with the extrapolated viscosity predictions, but further experiments are required.

5. REFERENCES

1] 1. P. Saxena, P. K. Sharma, and P. Purohit, “A journey of celecoxib from pain to cancer,” Apr. 01, 2020, *Elsevier Inc.* doi: 10.1016/j.prostaglandins.2019.106379.

2. R. Iyer *et al.*, “Amorphous solid dispersions (ASDs): The influence of material properties, manufacturing processes and analytical technologies in drug product development,” *Pharmaceutics*, vol. 13, no. 10, Oct. 2021, doi: 10.3390/pharmaceutics13101682.

3. H. Patil, R. V. Tiwari, and M. A. Repka, “Hot-Melt Extrusion: from Theory to Application in Pharmaceutical Formulation,” *AAPS PharmSciTech*, vol. 17, no. 1, pp. 20–42, Feb. 2016, doi: 10.1208/s12249-015-0360-7.

P024

DEVELOPMENT AND IN VIVO EVALUATION OF CEFUROXIME-LOADED SELF-EMULSIFYING OILS AS A NOVEL FORM OF EYE DROPS

Katarzyna Krzeminska[1], Malgorzata Sznitowska[1], Zuzanna Wenta[2]

[1]Department of Pharmaceutical Technology, Faculty of Pharmacy, Medical University of Gdansk, Poland
[2]Master degree student, Department of Pharmaceutical Technology, Faculty of Pharmacy, Medical University of Gdansk, Poland

1. INTRODUCTION

This study aimed to develop and evaluate the in vivo ocular tolerance of a novel eye drops in form of self-emulsifying oil (SEO) formulation containing 5% (w/w) cefuroxime sodium (CEF), an antibiotic known for its limited stability in aqueous environment. Although SEO systems are typically investigated for their ability to enhance the solubility and bioavailability of active pharmaceutical ingredients [1], the primary objective of our work was to formulate SEO eye drops with water-labile antibiotics to improve their stability, a goal that has already been achieved [2]. An anhydrous SEO system, consisting of an oil and a surfactant, enabling suspension of the antibiotic and facilitating rapid dissolution upon contact with tear fluid through spontaneous emulsification [2]. In this study, homogenization parameters were optimized to obtain homogeneous suspensions which enabled the conduct of the in vivo ocular tolerance in male albino rabbits using a modified Draize eye irritation test. Despite the availability of alternative testing methods, animal studies remain indispensable for verifying the safety of ophthalmic formulations prior to their clinical application [3]. While previous studies have demonstrated the ocular safety of SEO-placebo and cyclosporine A-loaded SEO systems, SEO formulations incorporating antibiotics had not yet been evaluated in vivo, establishing the basis for the present investigation [4,5].

2. MATERIALS AND METHODS

2.1. Materials

Cefuroxime sodium (powder for injection) was sourced from MiP-Pharma (Chephasaar, St. Ingbert, Germany). Polyoxyethylene sorbitan monolaurate (Tween 20) was obtained from Sigma-Aldrich (Steinheim, Germany), while fractionated coconut oil (Miglyol 812) was purchased from Caesar & Loretz (Hilden, Germany). Sodium citrate was supplied by Stanlab (Lublin, Poland).

2.2. Homogenization of SEO-CEF

CEF and sodium citrate were micronized using a jet mill (LABOMILL, Laboratory Microniser FPS0357, Donau Lab, Poland) to achieve a particle size below 25 μm. The SEO-placebo was prepared by dispersing Tween 20 (5% w/w) into Miglyol using a magnetic stirrer (MR 3001K, Heidolph, Schwabach, Germany). To determine the homogenization parameters for the prepared SEO-CEF formulations, CEF (5% w/w) and sodium citrate (2% w/w) were incorporated into the SEO using either a high-shear homogenizer (Ultra-Turrax, operated at 3000–8000 rpm for 1–5 minutes) or an ultrasonic disintegrator (speed levels 1–5, operated for 10 seconds to 4 minutes). The homogeneity of the obtained suspensions was assessed based on visual and microscopic observations (Nikon Eclipse i50, Tokyo, Japan).

2.3. In vivo tolerance test

A single drop (50 μL) of the tested formulations- either SEO containing 5% cefuroxime sodium (SEO-CEF), 0.9% NaCl, SEO-placebo or a 5% CEF solution was administered directly onto six eyes of male New Zealand white rabbits. Ocular examinations assessing the changes in cornea, iris, and conjunctiva were conducted 30 minutes and 1 hour post-administration, based on the Draize eye irritation test scoring system. According to the results, the maximum average score (MAS) could reach up to 110 points [5].

3. RESULTS AND DISCUSSION

3.1. Optimization of homogenization parameters

Microscopic analysis confirmed the uniform distribution of particles in suspensions obtained

by homogenizing the systems using a high-speed homogenizer for 2 minutes at 5000 rpm, with ice cooling applied to ensure that the system temperature did not exceed 25°C during homogenization. In the case of ultrasound treatment, mixing the formulation for 15 seconds at level 1 proved sufficient to achieve uniform particle dispersion, however, cooling of the system was also necessary in this case. Both prolonged homogenization time and more intensive mixing when using the high-shear mixer, as well as ultrasonic homogenizer, resulted in agglomerate formation, even despite cooling, whereas a shorter homogenization time was insufficient to achieve a homogeneous suspension.

3.2. Results of in vivo tolerance

The administered formulations did not induce any visible alterations in the cornea or iris. Observed ocular reactions were limited to the conjunctiva and included hyperemia and noticeable redness. The mean Draize irritation score was 3.3 out of a possible 110 points, categorizing the SEO suspension as minimally irritating according to the established classification criteria [5].

4. CONCLUSION

Although further in vivo studies are necessary, the present results indicate that SEO suspensions possess significant potential as innovative ophthalmic preparations. Their physicochemical properties suggest they may offer an effective and modern approach to eye drop development, which will be confirmed in subsequent stages of in vivo research.

5. REFERENCES

[1] Rehman, F.U., et al., *Self-Emulsifying Drug Delivery Systems (SEDDS): Measuring Energy Dynamics to Determine Thermodynamic and Kinetic Stability*. Pharmaceuticals, 2022. 15.

[2] Krzeminska, K., et al., *Suspensions of antibiotics in self-emulsifying oils as a novel approach to formulate eye drops with substances which undergo hydrolysis in aqueous environment.* Drug Delierv, 2024. 31.

[3] Wilhelmus, K.R., et.al., The Draize eye test. Survey of Ophthalmology 2001. 45.

[4] Czajkowska-Kosnik, A., et.al., *Comparison of cytotoxicity in vitro and irritation in vivo for aqueous and oily solutions of surfactants.* Drug Development and Industrial Pharmacy, 2015. 41.

[5] Wolska, E., et al., *Microscopic and Biopharmaceutical Evaluation of Emulsion and Self-Emulsifying Oil with Cyclosporine.* Pharmaceuticals, 2023. 16.

ACKNOWLEDGMENT

The research is funded by a Medical Research Agency grant nr 2024/ABM/03/KPO/ KPOD.07.07-IW.07-0046/24-00.

P025

ENTERIC CAPSULES FOR INTESTINAL DELIVERY OF SELF-MICRO EMULSIFYING PELLETS CONTAINING VOLATILE NATURAL DRUGS

Gabriela Koutna[1], Katerina Kubova[1], Jan Kotoucek[2], Martina Urbanova[3], Larisa Janisova[3], Ivana Sedenkova[3], Jan Muselik[1], Jakub Vyslouzil[1], Miroslava Pavelkova[1], David Vetchy[1], Jiri Brus[3]

[1]Department of Pharmaceutical Technology, Faculty of Pharmacy, Masaryk University Brno, Czech Republic
[2]Department of Pharmacology and Toxicology, Veterinary Research Institute, Czech Republic
[3]Department of Structural analysis, Institute of Macromolecular Chemistry, Czech Academy of Sciences, CZ

1. INTRODUCTION

Over the past few decades, natural active ingredients have received growing attention across various scientific fields, particularly in pharmaceuticals. Monoterpenoid alcohols such as thymol and its isomer carvacrol, along with the phenolic compound eugenol, exhibit a wide range of biological activities and are considered promising candidates for the treatment of inflammatory bowel diseases. However, their hydrophobic nature, volatility, partial absorption in the stomach, and low bioavailability pose significant formulation challenges.

To address these limitations, stable self-microemulsifying drug delivery systems (SMEDDS), isotropic mixtures of oils and surfactants, sometimes combined with cosurfactants or cosolvents, can be incorporated into pellet-based systems (1) and encapsulated within commercially available enteric-coated hard capsules. The newly introduced Capsugel® Enprotect® capsules offer an innovative platform for targeted drug delivery to the small intestine (2). Despite this potential, interactions between volatile compounds in solidified SMEDDS and enteric capsules have not yet been investigated.

Therefore, this experimental study aims to evaluate the stability and *in vivo* performance of gastro-resistant capsules containing SMEDDS-based pellets loaded with thymol, carvacrol, and eugenol.

2. MATERIALS AND METHODS

2.1. Materials

SMEDDS components (Peceol™, Labrasol® ALF, Transcutol® HP) were provided by Gattefossé (FR). Medium-chain triglycerides (MCTs) were sourced from Fagron (CZ) and propylene glycol (PG) from Dr. Kulich Pharma (CZ). Carvacrol (C) and eugenol (E) were from Sigma-Aldrich (DE), and thymol (T) from Dr. Kulich Pharma (CZ). Pellet excipients included Neusilin® US2 (NEU**;** Fuji Chemicals, JP), chitosan (CH**;** JBICHEM, CN), and MCC (Avicel® PH 101, FMC, IE). Capsugel® Enprotect® capsules (Lonza, BE) were used for enteric delivery.

2.2. SMEDDS pellet formulation

Powder ingredients (MCC: NEU: CH ratio – 5:3:2) were wetted by SMEDDS mixture (60 g) containing 5% of each phytotherapeutic (w/w, 9.5% of Peceol™, 68.4% of Labrasol® ALF, 17.1% of Transcutol® HP) and water (75 g) was stepwise added into the mixture under constant stirring to ensure a high degree of homogenization and solidified into pellets by extrusion/spheronization method Pharmex 35T, Wyss & Probst, DE). The fractions 0.5 – 0.8 mm in the amount of 420 mg pellets were filled into enteric capsules (n = 3) (marked as CAP-T, CAP-C, and CAP-E.

2.3. Stability testing

Stability studies (time points 0, 3, 6, and 12 months; conditions 25 °C, 60 % RH and 40 °C, 75% RH) were carried out to evaluate phytotherapeutics content (Agilent, HPLC 1200 Series), *in vitro* dissolution testing (n = 3; 2 hours – pH 1.2, the test 6.8, Sotax AT-7 Smart, Sotax, CH) and FTIR of capsule samples CAP-T CAP-C, and CAP-E (3 and 6 months). A small section of the capsule shell's inner surface (in direct contact with the pellets) was cut and examined using attenuated total reflectance (ATR) mode on the diamond GoldenGate (Specac). The spectra were recorded with a resolution of 4 cm^{-1}, and 256 scans were

P025

accumulated for each measurement and compared with the empty Capsugel® Enprotect® capsules as a reference.

3. RESULTS AND DISCUSSION

3.1. Drug content and dissolution behaviour

The stability of drug content in enteric capsules filled with self-emulsifying pellets was evaluated under two storage conditions. At 25°C and 60% RH, the formulations remained stable over 12 months, with final drug contents of 98.8 ± 1.14% for thymol, 95.0 ± 0.79% for carvacrol, and 92.2 ± 0.54% for eugenol. Under accelerated conditions (40°C, 75% RH), after six months, the thymol content remained stable (101.5 ± 0.19%). However, there was a slightly greater loss of carvacrol (91.1 ± 4.42%) and eugenol (86.4 ± 1.20%) under stressed conditions due to the increased volatility of these compounds.

All enteric capsules containing self-micro emulsifying pellets demonstrated gastro-resistant behavior, with less than 10% of drug release during the first 120 minutes at pH 1.2, followed by rapid drug release upon transition to intestinal conditions (pH 6.8). At t = 0, more than 91.0% of the individual drugs were released within the first 60 minutes. At 25°C and 60% RH, a decline in drug release was observed over one year of stability testing, but all formulations achieved over 85% drug release within 120 minutes while maintaining similarity (f2 > 50). At 40°C and 75% RH, a further decrease in drug release was noted during six months of stability testing, with over 85% of the loaded drug released within 240 minutes.

3.2. FTIR analysis

Stability testing revealed that SMEDDS containing volatile phytotherapeutics can alter the internal structure of enteric capsules. FTIR analysis identified two key spectral changes (Figure 1). First, modifications in the secondary structure of hypromellose (internal structure polymer of enteric capsules) were observed, particularly in the carbonyl vibration band and hydrogen bonding, more prominently at elevated temperatures. Second, in formulations containing eugenol, spectral data indicated its gradual sorption into the polysaccharide matrix. In contrast, no significant spectral changes were noted for carvacrol and thymol. These results underscore the importance of considering–capsule interactions in formulation stability evaluations.

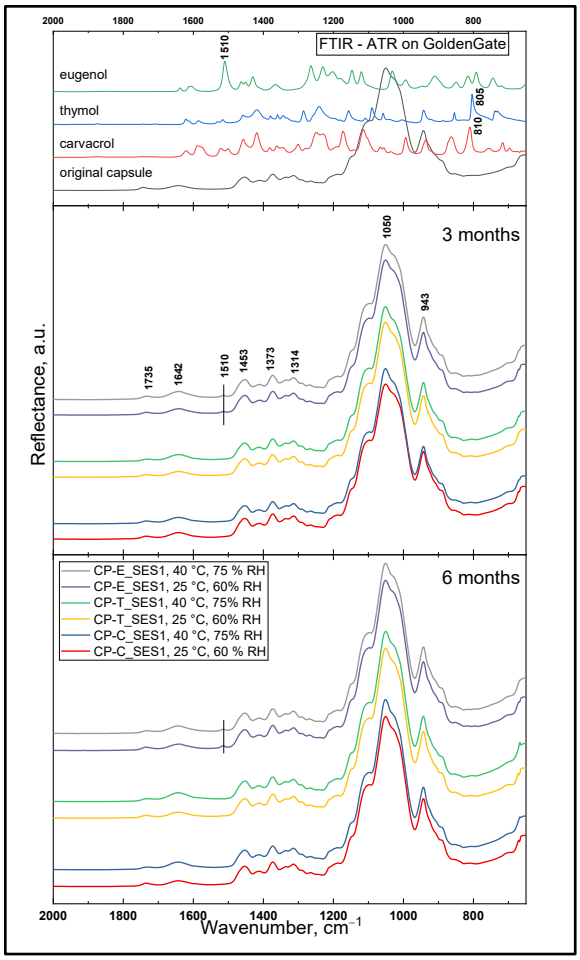

Figure 1. The FTIR spectra of the inner layer of the capsule shell for samples CAP-T, CAP-C, and CAP-E, stored under various conditions, compared with the spectra of individual natural drugs and the empty enteric capsule

4. CONCLUSION

Enteric capsules containing self-micro emulsifying pellets, stored under milder conditions, demonstrated promising potential for intestinal drug delivery of volatile natural compounds.

5. REFERENCES

1. Mandić, J., et al., *Overview of solidification techniques for self-emulsifying drug delivery systems from industrial perspective*. International Journal of Pharmaceutics, 2017, 533, 335–345.

2. Grimm, M. et al., *In Vivo Evaluation of a Gastro-Resistant Enprotect® Capsule under Postprandial Conditions.* Pharmaceutics, 2023, 15, 2576.

ACKNOWLEDGMENT

This work was supported by Czech Science Foundation (Grant No. GA 22-03187S).

P026

HIGH-ENERGY BALL MILLING FOR ENHANCED DISSOLUTION: FORMULATION AND OPTIMIZATION OF POSACONAZOLE AMORPHOUS SOLID DISPERSIONS

Agata Grzejdziak[1], Mateusz Kurek[2], Konstantinos Raftopoulos[3], Krzysztof Pielichowski[3], Aleksander Mendyk[2]

[1]Doctoral School of Medicinal and Health Sciences, Jagiellonian University Medical College, Krakow, Poland
[2]Chair of Pharmaceutical Technology and Biopharmaceutics, Faculty of Pharmacy, Jagiellonian University Medical College, Krakow, Poland
[3]Department of Chemistry and Technology of Polymers, Faculty of Chemical Engineering and Technology, Krakow University of Technology, Krakow, Poland

1. INTRODUCTION

The aqueous solubility of a drug substance is a critical property influencing its pharmaceutical availability and ultimately its bioavailability. Posaconazole (POS), practically insoluble in water and classified as BCS class II compound, served as the model drug in this study. Mechanical activation via planetary ball milling is an effective technique for enhancing the dissolution rate of poorly soluble compounds. Therefore, this study aimed to develop amorphous solid dispersions of POS with various polymers using ball milling to improve its dissolution rate.

2. MATERIALS AND METHODS

2.1. Materials

Posaconazole (POS, 99.5% purity, Wuhan ChemNorm Biotech Co., Ltd.) was used as a model drug. As a polymeric matrices for amorphous solid dispersions four polymers were used: two amorphous, i.e., Kollidon K30 (PVP, poly(vinylpyrrolidone), and Kollidon VA64 (KVA, poly(vinylpyrrolidone vinyl acetate)), both from BASF, and two semi-crystalline, i.e., Kollicoat IR (KIR, Macrogol poly(vinyl alcohol) grafted copolymer, BASF), and Parteck MXP (PXP, poly(vinyl alcohol), Merck KGaA).

2.2. Ball milling

Pure POS and mixtures of the drug and polymer in different ratios based on previous studies (1) (PVP, PXP and KIR drug polymer 1+1 w/w, and with KVA 0.3+0.7 w/w) in amount of 2 g was ground in a Fritsch Pulverisette 7 Premium Line planetary ball mill using different times from 20 to 110 min and different rotation speeds: from 400 to 550 rpm. During the process, optimal milling conditions leading to obtaining amorphous solid dispersions were selected.

2.3. X-ray Powder Diffraction (XRPD)

An XRPD analysis was performed using Brucker D2 Phaser to determine the molecular transformation of the drug from crystalline to amorphous state.

2.4. Intrinsic dissolution studies

In vitro intrinsic dissolution studies were carried out with Teledyne Hanson Vision G2 Elite 8 dissolution bath with rotation speed of 100 rpm at 37 ± 0.5 °C in 900 mL of pH 1.2 HCl solution. The compacts for the study were prepared in accordance with the requirements described in the monograph Ph. Eur. *2.9.29. Intrinsic dissolution*. Samples were taken at 5 min. intervals and absorbance was measured using a Shimadzu UV1800 spectrometer at $\lambda = 262$ nm.

3. RESULTS AND DISCUSSION

3.1. Ball milling

Milling the drug-polymer mixtures in the appropriate ratio using different milling times and rotational speeds allowed for the optimization of the process. For all series, grinding for 70 minutes at a rotational speed of 550 rpm proved to be the best for obtaining amorphous solid dispersions.

3.2. X-ray Powder Diffraction (XRPD)

An XRPD analysis was performed to assess the impact of the ball milling process on the molecular structure of the posaconazole and confirm the amorphous nature of the prepared

solid dispersions. As can be seen in Figure 1. all prepared systems were in amorphous form.

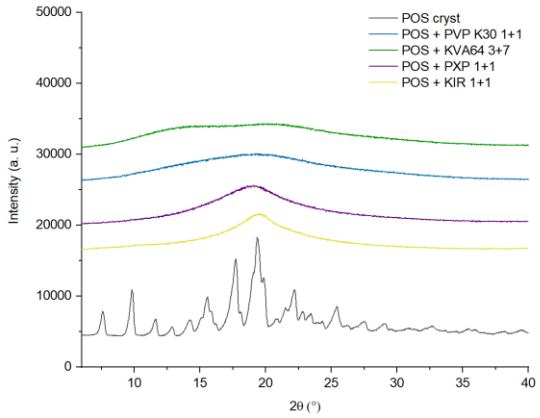

Figure 1. X-ray powder diffraction patterns of amorphous solid dispersions containing POS.

3.3. Intrinsic dissolution studies

Intrinsic dissolution studies were performed to investigate the influence of the amorphization process on the POS dissolution behaviour. Depending on the polymer used, the intrinsic dissolution rate (IDR) differed and was higher than for crystalline POS which was presented in Figure 2.

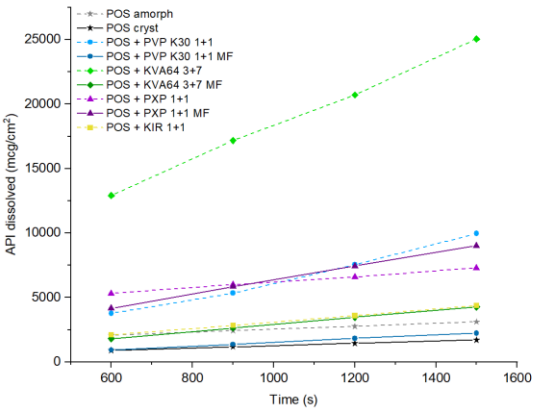

Figure 2. Posaconazole intrinsic dissolution profiles from prepared ASDs and pure drug compacts.

The fastest release of POS from amorphous solid dispersions was obtained from systems containing KVA. IDR was about 14.3 and was 5.3-fold higher than for the physical mixture of POS and the polymer. The process of grinding the active substance without polymer allowed to increase the dissolution rate by about 1.2 times. All values of IDR are shown in the Table 1.

Table 1. Intrinsic dissolution rates for prepared formulations.

Formulation	Intrinsic dissolution rate (μg/cm²/s)		Improvement factor
	processed	raw	
POS	1.1	0.9	1.2
POS + PVP	7.1	1.4	5.1
POS + KVA	14.3	2.7	5.3
POS + PXP	2.4	5.6	0.4
POS + KIR	2.6	-	-

The test could not be carried out for the physical mixture of POS + KIR because it disintegrated directly after immersion in the medium and fell out of the matrices.

4. CONCLUSION

Posaconazole ball milling seems to be an effective method of obtaining amorphous solid dispersions, which leads to an increase in the dissolution rate and thus to an improvement in the pharmaceutical availability of the API. Optimization of the milling process parameters allowed for a reduction in the process time, which have a beneficial effect on labor savings during the production of amorphous solid dispersions.

5. REFERENCE

1. Kramarczyk D, Knapik-Kowalczuk J, Kurek M, Jamróz W, Jachowicz R, Paluch M. *Hot Melt Extruded Posaconazole-Based Amorphous Solid Dispersions—The Effect of Different Types of Polymers*. Pharmaceutics. 2023 Mar 1;15(3).

ACKNOWLEDGMENT

This research was funded by grant no. N42/DBS/000410.

P027

APPLICABILITY OF BIOPOLYMERS OF AGROCULTURAL ORIGIN AS PHARMACEUTICAL EXCIPIENTS FOR PRODUCTION OF TABLETS BY DIRECT COMPRESSION METHOD

Jelena Čanji Panić[1], Nemanja Todorović[1], Aleksandra Ćoškov[1], Dušica Bosiljčić[2], Senka Popović[3], Mladena Lalić-Popović[1,4]

[1]Department of Pharmacy, Faculty of Medicine Novi Sad, University of Novi Sad, Serbia
[2]Pharmacy Institution Benu, Galenic Laboratory, Novi Sad, Serbia
[3]Department of Food Preservation Engineering, Faculty of Technology Novi Sad, University of Novi Sad, Serbia
[4]Center for Medical and Pharmaceutical Investigations and Quality Control (CEMPhIC), Faculty of Medicine Novi Sad, University of Novi Sad, Serbia

1. INTRODUCTION

Research for cost-effective and sustainable plant-based materials for pharmaceutical application has grown popular over the past years. Constant need for improvement of pharmaceutical formulation and therapeutic outcomes has created a need for novel pharmaceutical excipients [1,2]. Biopolymers derived from agricultural plants are gaining attention as potential excipients due to their biocompatibility, biodegradability, and diverse chemical and mechanical properties [2].
The aim of this study was to investigate the possibility of processing biopolymers - soy protein concentrate (SPC, soybean food derivate) and pumpkin oil cake (PuOC, *Cucurbita pepo L*. edible cold-pressed oil by-product) - as pharmaceutical excipients for tablet formulation obtained by direct compression method.

2. MATERIALS AND METHODS

2.1. Materials

Six tablet formulations were prepared, each one containing 0.5% magnesium stearate as lubricant, 1% colloid silicium-dioxide as glidant, 5% talc as antiadherent and 2% sodium starch glycolate as superdisintegrant. Ketoprofen was used as model drug and the dose was set at 25 mg per tablet. Two types of mixtures of microcrystalline cellulose (MCC) and α-lactose monohydrate (LAC) were used as diluents, one with 80% MCC and 20% LAC (MCC_{LAC}), and the other one with 80% LAC and 20% MCC (LAC_{MCC}). Biopolymers, SPC and PuOC, were donated by Faculty of Technology Novi Sad, Serbia. The type of diluent and biopolymer used in each formulation is shown in Table 1. Direct compression of the powders was done using a laboratory excenter press (Krosch, Germany).

Table 1. Tablet formulation composition in w/w %.

	LAC_{MCC}	MCC_{LAC}	SPC	PuOC
D1	ad 100	-	-	-
D2	-	ad 100	-	-
D3	ad 100	-	10	-
D4	ad 100	-	-	10
D5	-	ad 100	10	-
D6	-	ad 100	-	10

2.2. Flowability of the powder mixtures

The bulk and tapped density of the powder mixtures for tableting were tested in accordance with the 11th European Pharmacopoeia (Ph. Eur. 11) [3]. Jolting volumeter (J. Engelsmann AG, Germany) was used. Hausner ratio (HR) and Compressibility index (CI) were calculated. The angle of repose (α) was also determined in accordance with the Ph. Eur. 11 [3]. Diameter of the funnel used was 20 mm, positioned at a height of 2.4 cm above the work surface.

2.3. Pharmacopeial testing of the tablets

Uniformity of mass of single dose preparations, friability of uncoated tablets test performed in accordance with Ph. Eur. 11 [3]. Friability was tested on a standard drum device (Erweka TA, Germany), at 25 rpm for 4 min.

3. RESULTS AND DISCUSSION

Flowability characterisation of the powder mixtures depended greatly on the method of determination, as can be seen in Table 2 and 3. The difference in the results between the methods occurs because when evaluating flowability by bulk and tapped density, the propensity of the powder to distribute some

particles between others is important, while when determining angle of repose, tendency of particles to stack onto each other is crucial. Addition of SPC and PuOC increased angle of repose in formulations with higher proportions of MCC, D5 and D6 (Table 3).

Table 2. Powder mixture flowability evaluation based on the bulk and tapped densities

	HR	CI [%]	Flowability
D1	1.40	28.43	poor
D2	1.65	39.23	very very poor
D3	1.42	29.33	poor
D4	1.47	31.96	very poor
D5	1.66	39.86	very very poor
D6	1.55	35.38	very poor

Table 3. Powder mixture flowability evaluation based on angle of repose

	α [˚]	Flowability
D1	39.94	fair (aid not needed)
D2	39.29	fair (aid not needed)
D3	37.24	fair (aid not needed)
D4	39.94	fair (aid not needed)
D5	44.90	passable (may hang up)
D6	52.76	poor (must agitate, vibrate)

Despite differences in flowability of powder mixtures, all tablet formulations met the Pharmacopeial criteria for the Uniformity of mass of single dose preparations.

Figure 1. Friability of the tablets

Friability of the tablets was mainly influenced by the proportion of LAC. Formulations with higher proportions of LAC (D1, D3, D4) had higher friability (Figure 1). Presence of SPC and PuOC in the formulation seems to only slightly reduce tablet friability. Regardless, all tablet formulations showed friability <1%, which is in accordance with Pharmacopeial criteria for uncoated tablets.

4. CONCLUSION

This study has shown the possibility of SPC and PuOC to be processed as part of tablet formulation for direct compression method. Obtained tablets met the requirements of the Ph. Eur. 11 for uniformity of mass and friability. Further studies are needed to determine exact pharmaceutical role of these biopolymers, optimal proportion in the formulation, as well as their potential influence on the disintegration, dissolution and stability of the pharmaceutical dosage form.

5. REFERENCES

1. Garcia, K., et al., *Tobacco stalk nanofibrillated cellulose: An eco-friendly binder on fluidized bed granulation.* Journal of Drug Delivery Science and Technology, 2024. 102:106370.

2. Panda, J., et al., *Exploring Biopolymer for Food and Pharmaceuticals Application in the Circular Bioeconomy: An Agro-Food Waste-to-Wealth Approach.* Waste and Biomass Valorization, 2024. 15:5607–5637.

3. 11th European Pharmacopoeia, Council of Europe, Strasbourg, 2023.

ACKNOWLEDGMENT

This study was supported by the Ministry of Science, Technological Development and Innovation, Republic of Serbia (grant: 451-03-136/2025-03/ 200114).

P028

PHYSICOCHEMICAL CHARACTERIZATION OF CO-AMORPHOUS SYSTEMS FOR POTENTIAL APPLICATION IN FIXED-DOSE COMBINATION FORMULATIONS

Agata Nowak[1], Monika Rojewska[2] Janina Lulek[1] , Marcin Skotnicki[1]

[1]Industrial Pharmacy Division, Chair and Department of Pharmaceutical Technology, Poznan University of Medical Sciences, Poznan, Poland

[2]Institute of Chemical Technology and Engineering, Poznan University of Technology, Poznan (Poland)

1. INTRODUCTION

An active pharmaceutical ingredient (API) used in a solid dosage form can exist either in a crystalline or an amorphous state. The amorphous form is a high-energy state, differing from its crystalline counterparts in the lack of long-range molecular order and increased molecular mobility. Amorphous drug substances are increasingly applied in the design of solid pharmaceutical products due to their superior solubility and dissolution characteristics compared to crystalline materials [1]. Their main limitation is physical instability and an inherent tendency to recrystallize. To stabilize the amorphous phase, a co-amorphization process is employed, wherein the API is combined with either an excipient or another API. Intermolecular interactions between the API and the co-former contribute to the stabilization of the system [2]. Three model active pharmaceutical ingredients (APIs) from the antipsychotic drug class — amisulpride, sulpiride, and risperidone — were selected for the study due to their low solubility. These APIs exhibit significant potential for the development of fixed-dose combination (FDC) formulations. The primary objective was to obtain co-amorphous systems using the spray drying technique. The project aims to develop a strategy to ensure the physicochemical stability of the resulting structures, to investigate their thermal behavior and evaluate kinetic processes and to assess surface wettability.

2. MATERIALS AND METHODS

2.1. Materials

Amisulpride (AMI; crystalline; M = 369.5 g·mol^{-1}), sulpiride (SUL; crystalline; M = 341.4 g·mol^{-1}) and risperidone (RIS); crystalline; M = 410.5 g·mol^{-1}) were kindly obtained from *LEK-AM* Sp. z o.o. (Zakroczym, Poland).

2.2. Methods - Spray draying

Attempts were made to obtain co-amorphous AMI–RIS and SUL–RIS combinations. To obtain amorphous and co-amorphous materials in a 1:1 molar ratio, a Mini Spray Dryer B-290 (Büchi Labortechnik AG, Flawil, Switzerland) was used. Spray drying was performed using an API and API-API solutions in a solvent mixture of methanol and dichloromethane (1:1, v/v) at a concentration of 1% (m/v), at a drying temperature of 55 °C.

2.3. Thermogravimetric Analysis (TGA)

TGA curves were obtained using a TG 209 F3 Tarsus (Eric NETZSCH B.V. & Co. Holding KG; Selb, Germany). 10 mg of the sample was placed in a ceramic crucible and heated from 30 to 600 °C at 10 °C·min^{-1} rate under a nitrogen flow of 30 mL·min^{-1}.

2.4. Differential Scanning Calorimetry (DSC)

DSC curves were obtained using a DSC 214 Polyma (Eric NETZSCH B.V. & Co. Holding KG, Selb, Germany). 2 to 5 mg of sample were placed in a pierced aluminium crucible and heated/cooled from 30 to 195 °C at a rate of 10 °C·min^{-1}, under a nitrogen flow of 30 mL·min^{-1}.

2.5. Powder X-ray Diffraction (PXRD)

Powder X-ray diffractograms were obtained using a Bruker D2 PHASER (Bruker AXS GmbH, Karlsruhe, Germany).

2.6. Wettability test

Surface properties of the model materials, including wettability and surface free energy, are being investigated (Theta Litle 101, KSV

P028

Nima, Finland). For this purpose, contact angle measurements of the powders are planned using the sessile drop method (Sigma 701, KSV Nima,Finland).

3. RESULTS AND DISCUSSION

Differential scanning calorimetry (DSC) analysis of the spray-dried AMI and SUL revealed the presence of glass transition during the first heating cycle for amisulpride (T_g^{AMI} = 30.95 ± 0.05 °C, Δc_p = 0.809 ± 0.05 J·g^{-1}) and sulpiride (T_g^{SUL}= 56.55 ± 0.45 °C, Δc_p = 1.083 ± 0.004 J·g^{-1}). During the second heating, a single glass transition was also observed. (T_g^{AMI} = 40.74 ± 0.35°C, Δc_p = 0.35 ± 0.03 J·g^{-1} and T_g^{SUL} = 62.15 ± 0.07°C, Δc_p = 0.5 ± 0.01 J·g^{-1}). This results indicate amorphization of examined materials. The DSC curves of co-amorphous systems (Fig.1) shows a glass transition at the temperature of 43.3 ± 0.6 °C (Δc_p = 0.34 ± 0.02 J·g^{-1}) for AMI–RIS (Fig. 1) and 49.15 ± 0.15 °C (Δc_p = 0.768 ± 0.033 J·g^{-1}) for SUL-RIS. A single melting process occurs ($T_m^{AMI-RIS}$ = 123.33 ± 0.5 °C; $T_m^{SUL-RIS}$ = 176.8 ± 1.84 °C), therefore it is assumed that a co-crystal is formed during recrystallization. During the second heating, a single glass transition is observed (T_g^{AMI} = 38.15 ± 3.61 °C, Δc_p = 0.35 ± 0.02 J·g^{-1}; T_g^{SUL} = 46.05 ± 0.15°C, Δc_p = 0.354 ± 0.03 J·g^{-1}), suggesting molecular interactions between AMI and RIS; SUL and RIS. PXRD analysis of the spray-dried material confirmed the amorphization of the obtained systems. TGA was used to confirm the thermal stability and residual solvent. TGA examination excluded the presence of solvent in the resulting product. Based on the TGA results, thermal degradation occurs at AMI: 285.8 ± 3.2 °C; AMI–RIS: 262.25 ± 4.75 °C; SUL: 368.55 ± 18.25 °C; SUL–RIS: 358.45 ± 0.7 °C.

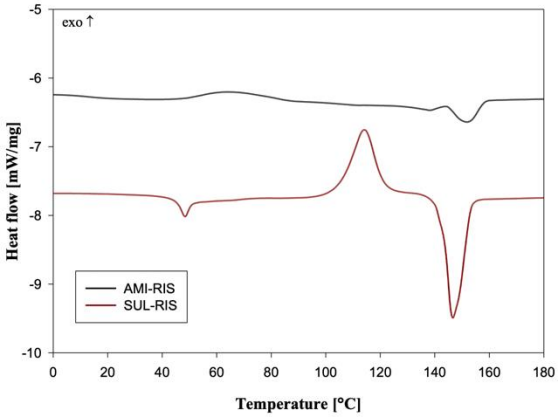

Figure 1. DSC curves (1st heating) for spray-dried: AMI-RIS and SUL-RIS (co-amorphous) samples.

4. CONCLUSION

The co-amorphous systems of AMI–RIS and SUL–RIS were successfully obtained and characterized. DSC confirmed the occurence of the single glass transitions in both systems, indicating the presence of homogeneous amorphous phases and suggesting strong molecular interactions between the drug components. The appearance of single melting points further supports the potential formation of co-crystals upon recrystallization. PXRD analysis verified the amorphous nature of the spray-dried materials. TGA revealed the absence of residual solvents in the products.

5. REFERENCES

[1] Hancock B.C., et al., “Characteristics and Significance of the Amorphous State in Pharmaceutical Systems,” *J Pharm Sci*, vol. 86, no. 1, pp. 1–12, Jan. 1997

[2] Dengale S. J., et al., “Recent advances in co-amorphous drug formulations,” *Adv Drug Deliv Rev*, vol. 100, pp. 116–125, May 2016,

P029

CRITICAL PROCESS PARAMETERS (CPPs) IDENTIFICATION AND PROCESS VALIDATION OF CETIRIZIN FILM COATED TABLETS 10 MG

Liljana Makraduli[1,2], Maja Gavriloska[1], Sevda Sofronievska[1], Marina Bakalinova[1], Natasha Churevski[1], Katerina Zafirova Georgievska[1], Jasna Bosnjakovska[1], Angelina Zimbakova[1], Vesna Tegova[3]

[1]Regulatory Affairs - Strategic Development, REPLEK, North Macedonia
[2]Faculty of Medical Sciences, Goce Delcev University, North Macedonia
[3]Quality Assurance, Replek Farm Ltd Skopje - REPLEK, North Macedonia

1. INTRODUCTION

Top priority of the pharmaceutical industries and the regulatory bodies is the quality, safety, and efficacy of drug products, accomplished with Quality by Design (QbD) approach and ICH Q8 (R2), ICH Q9, ICH Q10 guidelines [1, 3]. Drug product manufacturing should take the critical process phases/parameters (CPPs) into consideration in regards to level of their impact on product critical quality attributes (CQAs). Blend homogeneity and content uniformity are of primary importance, especially for dry mixing and direct compression [2].

2. MATERIALS AND METHODS

2.1. Materials

API: cetitizine dihydrochloride (Glochem Industries, India). Excipients: crospovidone and copovidone (BASF, Germany), cellulose microcrystalline and hypromellose (JRS Pharma, Germany), lactose monohydrate (Meggle, Germany), silica, colloidal anhydrous (Cabot, Belgium), talc and titanium dioxide (Merck, Germany), macrogol 6000 (Clariant, Germany), dimethicone (Dow Corning, USA), magnesium stearate (Mosselman, Belgium).

2.2. Method - manufacturing and equipment

Dry mixing and homogenization, tableting and film coating: high-shear mixer (VG 200 - Glatt, Germany), mixer-blender (Cyclop Miditumbler - Vima, Italy), tablet press (Unipress Diamond 20 - Manesty, Great Britain), film coater (XL-COTA - BOSCH, Great Britain).

2.3. Method - quality control and equipment

Dissolution test, Assay test, Uniformity of dosage units: VARIAN, Carry Win 50 UV-VIS Spectrophotometer (at 232 ± 2 nm).

3. RESULTS AND DISCUSSION

3.1. Critical process phases and critical quality attributes (CQAs) risk assessment

Risk assessment was used in identifying critical phases of the manufacturing process that have a significant impact on product critical quality attributes (CQAs) (Table 1).

Table 1. Critical process phases and level of impact on CQAs of the drug product

CQAs of drug product	**Critical process phases**		
	Mixing	Tableting	Film coating
Dissolution	low	low	medium
Assay	low	low	low
Content & Dosage units uniformity	medium	medium	low

Although cetirizine hydrochloride belongs to BCS class 1 (high solubility and permeability), the content uniformity and uniformity of tablet cores may be critical, because of the low dose of API and the dry mixing/ direct compression. The good content uniformity and uniformity of tablet cores usually result in a good content uniformity of the film coated tablet. But, the film coating process may influence the API dissolution if it is not properly performed.

3.2. Critical Process Parameters (CPPs)

The CPPs for each critical manufacturing process phase were identified and values for each parameter were set (Table 2).

Table 2. Set values for each CPP

Process Phase	**Critical Process Parameters**	**Set values**

Dry mixing, trituration	Mixer speed/ rpm Chopper speed/rpm Duration/ minutes	150 500 10
Dry mixing before lubrication	Speed/ rpm Duration/ minutes	16 10
Tableting	Pre-compress./ mm Compression/ mm Tool loading/ kN	min. 3.0 min. 1.0 max. 18
Film coating	Inlet air temp./°C Outlet air temp./°C Flow rate/ ml/min. Pan speed/ rpm Atomization p/ bar Spray pattern width pressure/ bar	53-58 40-42 150-300 4-7 1.8-2.2 2.0-2.4

3.3. Process validation

Table 3. Test results of 3 dry mixtures batches

Triturate **Assay:** 11.41% API (w/w) (10.84%-11.98%)
top 10.95%, middle 11.04%, bottom 11.38%
top 10.97%, middle 11.02%, bottom 11.08%
top 11.51%, middle 11.69%, bottom 11.38%
Dry mixture before addition of lubricant **Assay:** 7.78% API (w/w) (7.397%-8.175 %)
top 7.415%, middle 7.481%, bottom 7.653%
top 7.464%, middle 7.592%, bottom 7.489%
top 7.846%, middle 8.076%, bottom 7.906%

Table 4. Test results of 3 tablet cores batches

Dissolution: min 80% (Q) /tabl. expressed as % of the declared content in 45 minutes
start 96.12%, middle 96.56%, end 97.28%
start 98.69%, middle 94.90%, end 96.30%
start 93.23%, middle 94.96%, end 93.87%
Assay: 9.5 mg - 10.5 mg/tabl. or 95% - 105% of the declared content
start 95.99%, middle 96.77%, end 99.77%
start 99.48%, middle 97.15%, end 97.08%
start 100.87%, middle 102.45%, end 102.28%
Uniformity of dosage units: Acceptance value (AV) ≤ 15.0 (L1)
start 4.5, middle 4.5, end 4.5
start 5.5, middle 5.5, end 5.5
start 2.0, middle 2.0, end 2.0

Validation of the critical process phases was done. (Table 3, Table 4, Table 5)

Table 5. Test results - 1 film coated tabl. batch

Dissolution: min 80% (Q) /f. c. t. expressed as % of the declared content in 45 minutes
start 95.71%, middle 97.33%, end 96.14%
Assay: 9.5 mg - 10.5 mg/f. c. t. or 95% - 105% of the declared content
start 97.51%, middle 97.90%, end 100.87%
Uniformity of dosage units: Acceptance value (AV) ≤ 15.0 (L1)
start 4.5, middle 5.5, end 2.0

4. CONCLUSION

The CQAs, critical process phases and CPPs were identified. Risk levels were assessed. The test results for CQAs were within the specified limits. The successful traditional validation (EudraLex, Vol. 4, GMP guideline) of critical manufacturing process phases of Cetirizin film coated tablets 10 mg confirms that CQAs and CPPs were well identified.

5. REFERENCES

1. Khan, A., et al., *Quality by design - newer technique for pharmaceutical product development.* Intelligent Pharmacy, 2024, 2: 122-129

2. Makraduli, L., et al., *Improvement of content uniformity in low-dose powder blends: critical formulation and process variables.*Macedonian Pharmaceutical Bulletin, 2022, 68: 221 – 222

3. Ter Horst JP, et al., *Implementation of Quality by design (QbD) Principles in Regulatory Dossiers of Medicinal Products in the European Union (EU) Between 2014 and 2019.* Therapeutic Innovation & Regulatory Science 2021, 55(3):583-590

ACKNOWLEDGMENT

I express my sincere gratitude to my superiors and colleagues for the support and cooperation.

P030

INNOVATIVE APPROACH IN SUSTAINABLE MOISTURE-ACTIVATED DRY GRANULATION: EXCIPIENT AND PROCESS OPTIMIZATION FOR DIOSMIN 500 MG TABLETS

Roza Markovski[1], Anita Vasilevska[1], Malgorzata Strozyk[2], Chhanda Kapadia[3]

[1]IMCD, Germany
[2]IMCD, Polsk
[3]IMCD Group

1. INTRODUCTION

The objective of this study was to develop a robust, high-dose formulation for Diosmin 500 mg tablets using a sustainable and cost-efficient manufacturing approach, specifically, moisture-Activated Dry Granulation (MADG). Diosmin, a naturally occurring flavonoid present in citrus peels, is well recognized for its antioxidant and anti-inflammatory properties and is frequently used in the treatment of venous disorders such as haemorrhoids and chronic venous insufficiency-related leg ulcers.[1]

MADG presents several advantages over conventional wet granulation techniques. It enables a simplified manufacturing process by removing the need for a drying phase and making use of standard processing equipment. This results in lower material consumption, reduced energy requirements, and decreased labour input. Additionally, MADG's scalability makes it suitable for efficient production from pilot to commercial scale. These benefits position MADG not only as a sustainable and economical alternative to traditional methods, but also as a reliable process capable of achieving the desired bioavailability for high-dose formulations. [2]

2. MATERIALS AND METHODS

2.1. Materials

During the laboratory trials formulation development and optimization was done, using high shear mixer granulator. The added moisture was evenly distributed during mixing process, facilitated by microcrystalline cellulose, grade 200 LM and the other components.

Several water-absorbent excipients were tested based on their water absorption capacity and particle size. Cellulose microcrystalline (grade 200 LM) enhanced blend wettability by attracting more humidity and facilitating water distribution. Silica colloidal anhydrous improved blend flowability, reduced the surface charge of the active substance, and aided moisture distribution. For improvement of the blend cohesion, several binders such as different grades of povidone, copovidone and hydroxypropyl methylcellulose were evaluated. Hydroxypropyl methylcellulose (K100 LV) acted as a potent binder, enhancing water uptake and agglomeration. Croscarmellose sodium, an absorbent material, aided disintegration process through swelling.

Magnesium stearate provided better die lubrication and aided in the compression process. Flow ability of the final blend was evaluated using Carr index and Hausner ratio determination.

2.2. Methods

Tablet cores were compressed using standard laboratory rotary press machine. Critical quality attributes of the tablets such as tablet weight, resistance of crushing, friability and disintegration were assessed using standard laboratory in process control instruments. Dissolution testing was performed using dissolution apparatus type II, rotating paddle (900 ml 0.2N NaOH, 75 rpm). Drug release was evaluated using UV visible spectrophotometer at 268 nm wavelength, where Diosmin showed good absorbance when previously dissolved in 0.2 N NaOH.[3]

P030

3. RESULTS AND DISCUSSION

3.1. Results and Discussion

During the production process low amount of water as a granulation liquid (moisturization) was used (8%) which was accordingly calculated as a cumulative moisture with initial moisture of every single excipient. The powder blend, after preparation using MADG, exhibited a bulk density of 0.45 g/ml, tapped density of 0.60 g/ml, Carr's Index of 25%, and a Hausner ratio of 1.33, suggesting moderate powder flow. Friability of the produced tablets was 0.13% and the disintegration time was 3 minutes.

Experimental dissolution testing has showed drug release of not more than 40% for 3 hours.

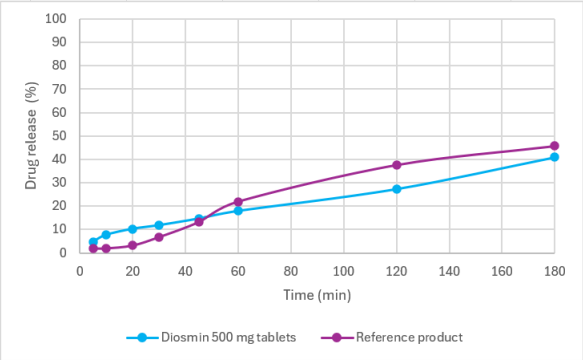

Figure 1. Dissolution test results of Diosmin 500 mg tablets and reference product (Dissolution conditions: 900 ml 0.2N NaOH, 75 rpm)

4. CONCLUSION

Moisture Activated Dry Granulation (MADG) represents a significant advancement in pharmaceutical formulation, particularly for heat and moisture-sensitive APIs. Experimental dissolution test for the MADG formulated tablet and market reference tablets formulated with wet granulation technique (Daflon 500 mg film-coated tablets) has shown that both formulations exhibit low release rate due to the Diosmin low solubility. As the pharmaceutical industry increasingly emphasizes sustainability, MADG is very promising alternative in shaping the future of formulation development.

5. REFERENCES

1. Branchet M-C, Gouhier-Kodas C, Verriere F, Jabbour V., Boisnic S., *Anti-inflammatory and antiradical effects of a 2% diosmin cream in a human skin organ culture as model,* Journal Cosmetology, 2018; 17: 848–854.
2. R. C. Garner, J. V. Garner, S. Grewgory, M. Whattam, A. Calam, D. Leong, *Comparison of the Absorption of Micronized (Daflon 500 mg) and Nonmicronized 14C-Diosmin Tablets After Oral Administration to Healthy Volunteers by Accelerator Mass Spectrometry and Liquid Scintillation Counting,* Journal of Pharmaceutical Sciences, Vol. 91, No. 1, January 2002
3. D. Srilatha, M. Nasare, B. Nagasandhya, V. Prasad, and P. Diwan, *Development and Validation of UV Spectrophotometric Method for Simultaneous Estimation of Hesperidin and Diosmin in the Pharmaceutical Dosage Form*, Volume 2013, Article ID 534830, 4 pages

ACKNOWLEDGMENT

The authors would like to thank Dioma for Diosmin and International Flavors and Fragrances Inc. (IFF) for providing excipient support.

P031

PURIFICATION TECHNIQUES FOR CONCENTRATING CANNABIS CRUDE EXTRACTS

Dejan Mihajlovski[1], Grozdana Leshevska[1], Nena Smiljanovska[1], Irena Slaveska Spirevska[2], Kristina Grncharovska[2]

[1]Production Department, Replek, North Macedonia
[2]Quality Control Department, Replek, North Macedonia

1. INTRODUCTION

The development of high-efficiency purification techniques and the optimization of operating conditions to enhance the yield, selectivity and quality of cannabis extracts, at the pilot scale are crucial steps for scaling up the industrial production of purified cannabis extracts. These methods include winterization, filtration and rotary evaporation and they are essential to isolate and concentrate the bioactive compounds in *Cannabis sativa*, such as cannabinoids (e.g., THC, CBD) and sometimes terpenes. These methods are used to achieve high purity and are essential for removal of undesirable plant materials, such as plant lipids, chlorophyll, waxes, fats, solvents, and other impurities, while maintaining safety and quality. [1]

2. MATERIALS AND METHODS

2.1. Materials

The cannabis extract used in this study was obtained from the Mataro Blue THC strain, produced at the Replek production plant using supercritical CO_2 technology. For the purification and concentration processes, analytical-grade ethanol (96%) was utilized. The winterization procedure was carried out using a Nuve model DF 490 refrigerator. Filtration of the extract was performed using a high-efficiency filtration machine model ApolloXstill manufactured by KNF. For the filtration process was used dedicated filter paper for ApolloXstill with varying pore sizes (20 µm, 10 µm, and 1 µm). Additionally, the solvent was removed using a Steroglass S.r.l. rotary evaporator (model Strike100). The analysis of the extracted crude was performed on Cannabis analyser Shimatzu HPLC prominence-i.

2.2. Methods

The preparation of the crude extract was done by dissolving it in 96% ethanol in a ratio of 1:3. The total amount of crude extract was divided into multiple stainless steel vessels and dissolved with 96% ethanol. The stainless steel vessels were placed in the refrigerator for winterization at a temperature of -60°C for 12 hours. The dissolved extract was subjected to active filtration for 1 hour with one layer of 20 µm filter paper. At the end of the process the total mass of the filtrate obtained was measured. The resulting filtrate was prepared for further concentration by rotary evaporation at a temperature of 70 °C, vacuum pressure of 150 mbar and it was applied gradual increase in the stirring speed in the range of 5 to 50 rpm. Rotary evaporation was performed in two one-hour intervals. Samples were collected after the first and second hour and then analyzed using HPLC.

The same procedure was performed with a 1:10 ratio of THC Crude extract diluted in 96% ethanol. The winterization and rotary evaporation processes were performed in the same manner as the previous probe. In the filtration process the only difference was using three layers of filtration paper, 20, 10 and 1 µm. At the end of the process, samples were collected and then properly analyzed.

3. RESULTS AND DISCUSSION

Before starting the filtration and concentration processes of the crude extract, an analysis of the initial samples was performed and the percentage of THC, CBD, and CBN was determined. The results are shown in the table.

Table 1. Initial cannabinoid content of crude extract

Cannabis extract THC- Mataro Blue	
Obtained results	66.08% THC 2.84% CBD 3.20% CBN

After the rotary evaporation process, from the first probe (1:3 ratio) the amount of 96% ethanol after first and second hour of evaporation was measured. The results of the analyzed samples are given in the table.

Table 2. Post-evaporation concentrations (1:3)

	After 1 h	After 2 h
Results	68.55 % THC 0.76% CBD	72.32% THC 0.96% CBD

The results of the sample collected from the second probe (1:10 ratio) are the following:

Table 3. Post-evaporation concentrations (1:10)

	After 1 h	After 2 h
Results	70.12 % THC 0.66% CBD	76.01 % THC 0.72% CBD

The final obtained result from probe 1 is 72.32% THC and from probe 2 is 76.01%.

3.2. Discussion

After receiving the results of the chemical analysis of the cannabis crude extract probe 1, it was noted that a certain amount of lipids and other components remained in the extract. The reason for this may be the use of one layer filter paper, which allows some of the fats present in the extract to pass through. The probes indicated that the usage of three layers of filtration paper (20, 10 and 1 μm) is more effective than the usage of one layer of filtration paper (20 μm). The filtration with one layer filter with pores of 20μm removes only larger particles. Finer filters (10μm and 1 μm) are used for further purification of the extract from the smaller particles. This process improves the quality of the final product by removing unwanted compounds like waxes, lipids and fats. [2]

Another reason for the higher presence of fats in the sample may be the dilution with ethanol. The sample-to-solvent ratio is a key parameter influencing the efficiency of cold ethanol filtration in cannabis processing. A comparison between 1:3 and 1:10 ratios revealed that the higher solvent volume (1:10) increased the concentration of THC. Additionally, the 1:10 ratio resulted in improved purification, likely due to more effective penetration of the solvent into the extract particles and better solubilization also, facilitating the removal of undesired constituents. [3]

4. CONCLUSION

This method is effective in purifying and concentrating cannabis crude extract. Factors that significantly affect the efficiency of the purification and concentration process are the amount of alcohol used to dilute the initial extract, and the type of filters used in the process itself. These factors need to be considered, when establishing the industrial production of purified cannabis extracts.

5. REFERENCES

1. Gonzalez, R. (2025, March 12). Cannabis Winterization Process: The complete guide. *Root Sciences*.https://www.rootsciences.com/blog/winterization-process-in-cannabis-extraction/
2. ErtelAlsop. (2019, September 12). *Proper cannabis filtration - ErtelAlsop – ErtelAlsop*. https://ertelalsop.com/proper-cannabis-and-cbd-oil-filtration-whitepaper/
3. Addo, P. W. et al. (2022). Cold ethanol extraction of cannabinoids and terpenes. *Molecules, 27*(24), 8780. https://doi.org/10.3390/molecules27248780

ACKNOWLEDGMENT

The authors would like to express their sincere gratitude to the team at Replek production plant for providing the cannabis crude extract and technical support during the purification process and to the analytical team for performing the analysis and providing the results.

P032

3D PRINTED POLYSACCHARIDE-BASED CAPSULES FOR COLON-SPECIFIC DRUG DELIVERY

Jan Muselík[1], Alena Komersová[2], Jan Elbl[1], Roman Svoboda[2], Kevin Matzick[2], Jana Macháčková[2], Marie Nevyhoštěná[2], Aleš Franc[1]

[1]Department of Pharmaceutical Technology, Masaryk University, Czech Republic
[2]Department of Physical Chemistry, University of Pardubice, Czech Republic

1. INTRODUCTION

Colonic drug delivery systems (CDDS) demonstrate significant potential for treatment of various diseases like ulcerative colitis, Crohn's disease or gastrointestinal stromal tumors [1]. Existing CDDS primarily rely on pH-dependent, time-delayed release, or microbiota-triggered mechanisms of release. However, individual patient variations in intestinal pH, transit times, and gut microflora can significantly impact the effectiveness of all these approaches, and hence the efficacy of CDDS. To mitigate the risks associated with CDDS relying on single release mechanism, dual systems have been developed [2]. Combination of 3D-printable polymers capable of time-triggered and microbiota-triggered release could offer a promising approach for colon-targeted drug delivery.

2. MATERIALS AND METHODS

2.1. Materials

Low glass transition HPMC suitable for HME process, available under the tradename Affinisol™ HPMC HME 15LV (DuPont, USA), was selected as the basic component for hot-melt filament extrusion. The input mixtures contained 10 wt.% or 20 wt.% of pectin from the citrus peel; the capsules were filled with caffeine (Sigma Aldrich, St. Louis, MO, USA).

2.2. Preparation of filaments and 3D printing process

Filaments were prepared by the hot-melt extrusion process using a single-screw extruder, the Noztek Touch (Noztek LTD, Shoreham-by-Sea, Great Britain), equipped with a 1.75 mm nozzle. Filaments were extruded at the temperature range of 140 – 145°C.

Capsules designed in Autodesk Fusion® 360 were exported into 3MF file. FDM 3D printers i3 MK3S+ (Prusa Research, Czech Republic) were used.

2.3. In vitro dissolution study

For dissolution testing of the capsules containing 100 mg of caffeine, SOTAX AT7 Smart was used (USP Apparatus II, 50 rpm, 37 ± 0.5 °C). First 0.9 L of acidic medium pH 1.2 for 120 min was used, then the dissolution medium has been changed to 0.9 L of FaSSIF (Biorelevant, UK). The amount of caffeine released from capsules was analyzed by automatic UV/Vis analysis (Perkin Elmer, Lambda 25, USA) at 275 nm. The dissolution test is characterized by lag time (average time to the release of 10 % of caffeine, n=6).

2.4. In vivo release testing

For *in vivo* release testing the 3D printed capsules were filled with 100 mg caffeine. In human study the release of caffeine from the 3D printed capsules into gastrointestinal tract and subsequently into the systemic circulation and saliva was tested. Four healthy human volunteers, aged 25 − 49 years (mean 35.4 years), BMI 22.2 − 31.0 (mean 25.4), were accepted in the trial. Blank saliva samples were collected and subsequently one test capsule was administered. Saliva samples were then obtained at 2, 6, 7, 8, 9, 10, 11, 12, 13, 14 and 16 hours after the capsule administration. Determination of caffeine assay in saliva samples was carried out using liquid chromatography (Agilent Technologies 1260, Germany) according to published method [3]. The purpose of the study was fully explained to all the volunteers, and they granted their permission to participate by signing a written informed consent. The experiment was approved by the ethics committee of Masaryk university (No. 129/2024).

3. RESULTS AND DISCUSSION

3D printed capsules utilizing a multiply release mechanism were prepared. The model and dimensions of the capsule is shown in Figure 1. The capsule's primary structure consisted of HPMC (a time-dependent release mechanism).

P032

The addition of selected natural polysaccharide (pectin citrus) ensured degradation by colonic bacteria (a microbiota-triggered release mechanism). Capsules for colon delivery should exhibit lag time long enough to ensure passing through stomach and small intestine. The lag time of drug dosage form for safety colon delivery should be at least 6-8 hours [4].

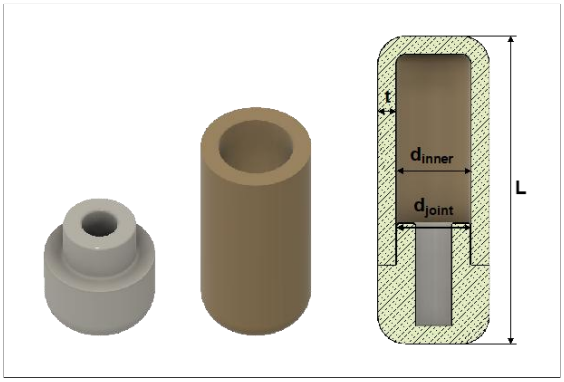

Figure 1. 3D models of capsules with measured parameters; t – thickness (1.8 mm), d_{inner} – inner diameter (6.0 mm), L – length (19.2), d_{joint} – diameter at the joint (5.8 mm)

3.1. Capsules lag time in vitro

The dissolution characteristics of 3D printed capsules were tested in a biorelevant medium. The capsules were first exposed to conditions in the GIT using acidic medium pH 1.2 for 120 min. After 120 minutes, capsules were moved to FaSSIF biorelevant medium. The detected lag time for the PECc10 sample was 648 ± 65 min and 532 ± 64 min for the PECc20 sample. In the biorelevant dissolution, the requirement for a lag time of at least 6-8 hours was met for these samples, which should ensure the delivery of the contents of the capsule to the colon environment.

3.3. In vivo release testing

The first-appearance time of caffeine into the saliva after the oral administration of tested capsules to human volunteers are shown in Table 1. The time, when the salivary caffeine concentrations exceeded the LOD value (0.06 µg/ml), was evaluated. The onset of drug absorption was found to be delayed, and the mean T_{lag} were 8.0 ± 1.6 hours for sample PECc10 and 8.8 ± 1.5 hours for sample PECc20. Based on the observed T_{lag} values, it can be assumed that both formulations don't release the drug into the stomach and small intestine. The delayed lag time in absorption followed by a measurable increase in caffeine salivary concentration demonstrates the disintegration of the system at the target site of the gastrointestinal tract (proximal colon).

Table 1. The first-appearance time (T_{lag}) of caffeine into the saliva after oral administration of capsules.

Sample	T_{lag} (hours)	
	Mean ± SD	**Min/Max**
PECc10	8.0 ± 1.6	6/10
PECc20	8.8 ± 1.5	8/10

4. CONCLUSION

3D printing of HPMC capsules with addition of citrus pectin has proven to be a suitable method for colonic drug delivery system manufacturing. This composition provides a dual release mechanism (time-triggered and microbiota triggered), which was confirmed by *in vivo* release testing in healthy volunteers.

5. REFERENCES

1. Charbe, N.B., et al., *Application of three-dimensional printing for colon targeted drug delivery systems.* Int J Pharm Investig, 2017. 7(2): 47-59.

2. Varum, F., et al., *A dual pH and microbiota-triggered coating (Phloral™) for fail-safe colonic drug release.* Int. J. Pharm., 2020. 583(15): 119379.

3. Zimová, L., et al., *The development and in vivo evaluation of a colon drug delivery system using human volunteers*. Drug Delivery, 2012. 19(2): 81-89.

4. Nandhra, G. K., et al., *Normative values for region-specific colonic and gastrointestinal transit times in 111 healthy volunteers using the 3D-Transit electromagnet tracking system: Influence of age, gender, and body mass index.* Neurogastroenterol. Motil., 2020. 32: e13734.

ACKNOWLEDGMENT

This work was supported by the Czech Science Foundation [GA 22-03187S] and by the Ministry of Education, Youth and Sports of the Czech Republic [SGS_2024_007].

P033

DEVELOPMENT TRENDS AND PATIENT EXPECTATIONS FOR PARENTERAL FORMULATIONS

Zsófia Németh[1], Ildikó Csóka[1]

[1]*Institute of Pharmaceutical Technology and Regulatory Affairs, University of Szeged, Szeged, Hungary*

1. INTRODUCTION

Parenterals are sterile products for the administration of active pharmaceutical ingredients through injection or infusion, ensuring direct drug delivery and high bioavailability. Parenteral therapies are driving advancements in healthcare and improving patient outcomes, as market reviews have found and predict that this transformative process will continue in the foreseeable future. Technological advancements, patient-centric approaches, and global market dynamic factors have, therefore, become as critical as the drug substance and its mechanism of action. Due to these recent trends, it now takes more than a promising molecule and a therapeutic target for new products to achieve favourable outcomes. [1]

This work analyses the latest formulation tendencies in the parenteral industry and the trends in the R&D sector, comparing them to the requirements and expectations of stakeholders, including patients, healthcare systems, and regulators, to highlight quality-driven development needs and opportunities.

2. MATERIALS AND METHODS

2.1. Materials

Up-to-date market reviews, industrial reports and scientific research papers for knowledge space building.

2.2. Method

Conducting a literature review to understand the current state-of-the-art and identifying gaps and challenges within the parenteral field. Applying the Quality by Design and Risk Assessment tools (QbD Lean Software®, QbDWorks LLC, USA) to evaluate the critical factors determining the sterile injectable therapeutics profile to be developed. [2]

3. RESULTS AND DISCUSSION

Parenteral administration is the second most common type of drug delivery after oral solids and liquids. The growing presence of biologics, technological innovations, regulatory requirements, and an emphasis on patient experience are reshaping the landscape of intravenous formulations. [3] The demand for parenteral products is continuously increasing as the overall pharmaceutical market expands and new therapies for the ageing population and treatments for chronic and rare diseases enter the pipeline. Patient-centric strategies are shifting the focus to the growth of at-home care and the rise of self-administration devices. [4]

4. CONCLUSION

An effective development sector must be committed to continuous improvement and emphasise integrating quality into the parenteral manufacturing process. The use of the QbD approach and compliance with requirements and needs are key components of a successful and effective development program.

Medical product design has shifted from presenting basic quality attributes, such as safety, efficacy, and potency, in a simple container. The sterile injectables of today carry a more complex profile and must offer a new approach to extending the value of the therapy to patients, while providing additional benefits.

5. REFERENCES

1. Kristin, B., *Parenteral Market Trends.* Contract Pharma, 2022. *www.contractpharma.com*, read: May 2025

2. Ergin, AD. & Uner, B. Quality by Design for Parenteral Formulations. In Jain, NK. & Bajwa, N. (Eds.), *Introduction to Quality by Design (QbD) From theory to practice* (pp. 217-242).

3. Clement, J., *The Evolving Landscape of Parenteral Drug Administration: Market Trends Shaping the Future.* Contract Pharma, 2024. *www.contractpharma.com,* read: May 2025

4. Peinovich, M., et al., *Parenteral medication use in hospital at home: Challenges and opportunities.* American Journal of Health-System Pharmacy, 2024. 81(15): e443-e453.

ACKNOWLEDGMENT

Project no TKP2021-EGA-32 has been implemented with the support provided by the Ministry of Culture and Innovation of Hungary from the National Research, Development and Innovation Fund, financed under the TKP2021-EGA funding scheme.

P034

ORALLY DISINTEGRATING TABLETS (ODTs) OF ADAPTOGENIC *RHODIOLA ROSEA* L. EXTRACT: DEVELOPMENT AND EVALUATION

Santa Niedra[1], Oxana Brante[1], Rihards Talivaldis Bagons[2], Austris Mazurs[1], Konstantins Logviss[1]

[1]Laboratory of Finished Dosage Forms, Faculty of Pharmacy, Rīga Stradiņš University, Latvia
[2]Department of Applied Pharmacy, Faculty of Pharmacy, Rīga Stradiņš University, Latvia

1. INTRODUCTION

Adaptogens, such as those present in *Rhodiola rosea* L., are natural substances that are considered to help the body adapt and form non-specific resistance to various external factors that can cause stress-related symptoms, including fatigue and weakness [1, 2]. Standardized extracts of *Rhodiola rosea* L. have been studied for neuroprotective activity, which may be important for patients suffering from mild to severe age-related neurodegenerative diseases. Due to the high prevalence of dysphagia in the geriatric population and a higher risk of choking in patients with a neurodegenerative diagnosis or cognitive impairment, it might be beneficial to replace traditional solid dosage forms with dosage forms that do not require swallowing whole tablets or capsules [3].

2. MATERIALS AND METHODS

2.1. Materials

Rhodiola rosea L. plant material (origin: Altai Republic, Russia) was obtained from Elpis Ltd. All reagents and analytical standards were of appropriate quality and analytical grade. Excipients were pharmaceutical grade received as complimentary samples from reputable manufacturers or procured through standard commercial procurement channels.

2.2. Extraction of *Rhodiola rosea* L.

Dried root and rhizome of *Rhodiola Rosea* L. were milled, using a blade cutting mill (SM 300, Retsch, Germany) and sieved with analytical sieves (AS 200-digit cA, Retsch, Germany). The fractional maceration (bismaceration) extraction was performed using ethanol at various concentrations (25%, 40%, 70%, 96%) as the extraction solvent. Different ratios of solid mass/extractant and maceration times were evaluated. The liquid extracts were concentrated via rotary evaporation (HemTron, India). Drying of the thick extract was done using two different methods: vacuum-drying (Lab Companion, South Korea) and freeze-drying (VaCo2, Zirbus, Germany).

2.3. Tableting

Orodispersible tablet (ODT) formulations were tableted using a benchtop compaction simulator (STYL'One Nano, Medelpharm, France).

2.4. Qualitative and Quantitative Analysis

Quantitative analysis of rosavin and salidroside in liquid extracts, dry extracts, and tablets was performed using HPLC-DAD (Vanquish CORE, Thermo Scientific, USA) at detection wavelengths of 254 nm and 220 nm, respectively. Chromatographic separation was achieved using a phenyl stationary phase (XBridge BEH Phenyl column, 150 × 4.6 mm, 2.5 µm, 145 Å; Waters, USA). Qualitative phytochemical profiling of the standardized extract was carried out using UHPLC-HRMS (Vanquish Flex system coupled with Orbitrap Exploris 120, Thermo Fisher Scientific) operated in both positive and negative ionization modes.

2.5. Physical Analysis of Tablets

Physical parameters of tablets were evaluated using a tablet tester (ST50, Sotax, Switzerland). Disintegration time of ODTs was measured using a disintegration tester (ZT 730, ERWEKA, Germany).

3. RESULTS AND DISCUSSION

3.1. Dry Extract

Quantitative analysis of the liquid extracts identified 70% ethanol as the most effective extractant for bismaceration, yielding the highest concentrations of rosavin (1.19%) and salidroside (0.49%). Both vacuum drying and lyophilization resulted in similar concentrations of these active compounds in the dry extracts (Table 1). However, the vacuum-dried extract was chosen for standardization due to a higher overall extract yield. The vacuum-dried extracts were pooled and standardized to 3% rosavin content and used in the formulations of ODTs.

Table 1. HPLC analysis results for dry extract.

Extract	Rosavin (%)	Salidroside (%)
Vacuum-dried extract	4.70	1.95
Lyophilized extract	4.66	1.93
Standardized vacuum-dried extract	3.02	1.70

Qualitative analysis by LC-MS revealed the presence of more than 50 compounds, including phenolic constituents such as flavonoids, flavonoid glycosides, cinnamic acid derivatives, and anthocyanidins.

3.2. Tablet Formulation

Formulations containing 100 mg of standardized extract and excipients such as croscarmellose, citric acid, dextrose, aspartame, talc, and magnesium stearate produced tablets with improved palatability. However, due to poor physical properties, the aspartame-free formulation (Batch R-14) was selected as the optimal formulation (Tables 2 and 3).

Table 2. ODT formulation, Batch R-14

Component	Content (%)
Extract	20.0
Dextrose	74.5
Citric acid	2.0
Croscarmellose	1.0
Talc	2.0
Magnesium stearate	0.5

Table 3. Physical characteristics of ODTs (Batch R14)

Test	Result
Weight (mg)	500
Extract (mg)	100
Diameter (mm)	11
Thickness (mm)	5
Hardness (N)	88.4
Disintegration time (min)	1:59

4. CONCLUSION

4.1. ***Rhodiola rosea* L. extract**: the standardized vacuum-dried *Rhodiola rosea* L. extract demonstrated suitability for the development of ODT formulations, offering high yield and consistent active compound content.

4.2. **ODT tablets**: Among 20 tested formulations, 3 demonstrated superior taste-masking and were selected for tablet preparation containing 100 mg of standardized extract. Formulations with slower disintegration times were associated with improved taste perception. Batch R-14, an aspartame-free formulation, showed the best adherence to the physical criteria.

5. REFERENCES

1. Tinsley, G.M., et al., *Rhodiola rosea as an adaptogen to enhance exercise performance: a review of the literature.* Br J Nutr, 2024. **131**(3): p. 461-473.
2. Wróbel-Biedrawa, D. and I. Podolak, *Anti-Neuroinflammatory Effects of Adaptogens: A Mini-Review.* Molecules, 2024. **29**(4).
3. Chinwala, M., *Recent Formulation Advances and Therapeutic Usefulness of Orally Disintegrating Tablets (ODTs).* Pharmacy, 2020. **8**(4): p. 186.

P035

PREDICTING POLYMER DRUG LOADING CAPACITY USING HANSEN SOLUBILITY PARAMETERS

Artūrs Paulausks[1], Artjoms Iljicevs[1], Konstantins Logviss[1], Liga Petersone[1]

[1]Laboratory of Finished Dosage Forms, Faculty of Pharmacy, Riga Stradins University, Latvia

1. INTRODUCTION

Nowadays lots of active pharmaceutical ingredients are poorly water soluble and/ or possess fast recrystallization, which in turn reduces drug bioavailability [1]. To address this problem, lots of solid amorphous dispersions have been developed [2]. Amorphous drug dissolves better and recrystalizes later because of absence of nucleation center. To achieve solid amorphous dispersion, various polymer-drug dosage forms are made. Not only that, but also drug delivery vehicles and implant devices are formulated as drug and polymer combinations [3]. Yet, finding new formulations might be time and resource consuming. Therefore, we aimed to establish predictive model for drug loading capacity in polymer to achieve amorphous drug phase. We used Hansen solubility parameters to achieve linear, predictive model for loading 13 model drugs into polylactic acid (PLA), as proof of concept.

2. MATERIALS AND METHODS

2.1. Materials

PLA was obtained from Alfa Chemistry (PL-PLA-A001). Model drugs of pharmaceutical grade: ketoprofen (Farmalabor), benzocaine (BLD Pharmatech GmbH), prednisolone (Sigma Aldrich), metronidazole (TCI), naproxen (Biosynth), ibuprofen sodium (Supelco), celecoxib (BLD Pharmtech), diclofenac sodium (Fagron), L-ascorbic acid (Sigma Aldrich), piracetam (Sigma Aldrich), paracetamol (Sigma Aldrich), lidocaine hydrochloride monohydrate (Biosynth), indomethacin (TCI). Solvents of analytical grade: chloroform, dichloromethane, 1,1-dichloroethane, aniline, tetrahydrofuran, acetonitrile, chlorobenzene, toluene, acetone, dimethyl formamide, ethyl acetate, methanol, dimethyl sulfoxide, formic acid, hexane, diethyl ether, triethyl amine, m-cresol, acetic anhydride, cyclohexyl chloride.

2.2. Hansen solubility parameters

Hansen solubility parameters were established using software *Hansen Solubility Parameters in Practice* (HSPiP v 6.0.04). PLA was subjected to solvents and results (dissolving/swelling graded as 1, no effect graded as 0) were entered into software and solubility parameters were calculated using genetic algorithm. For model drugs, Yamamoto molecular break (Y-MB) calculations were used. Model drugs were selected in such way to be with parameters close to PLA, far from it and in between.

2.3. Drug loading by solvent casting

Two grams of PLA was dissolved in 45 ml chloroform, 1ml of this solution was added to a pre-weighed amount of model drug and vortex mixed until dissolved. For drugs that didn't dissolve completely, 100 µl of THF was added. The solution was poured on glass slide and allowed to evaporate in fume hood and dry for 24 h.

2.4. HPLC analysis of drugs in PLA matrix

Sample weight of 20 mg was taken and dissolved in 1 ml chloroform, then 5 ml of methanol was added to crash out PLA. Samples were sonicated for 10 minutes, centrifuged. Liquid phase was filtered using 0.22 µm syringe filter and analysed. Chromatographic analysis was done using reverse phase chromatography system equipped with UV detector (ThermoFischer Vanquish, Germany). Three separate methods were developed to quantify all 13 drug molecules.

P035

2.5. XRD of drug loaded PLA samples

XRD analysis of samples was done in reflectance mode using MiniFlex 600-C (Rigaku Corporation, Japan), 2Θ range 3° - 90°, at 10°/min, step size 0.01°, lamp voltage 40kV, lamp current 15 mA, 1.25° divergence slit, Cu Kα radiation with Cu Kβx1.5 filter. Drug loaded samples were analyzed 24 h after making them.

3. RESULTS AND DISCUSSION

3.1. Hansen solubility parameters

Hansen solubility parameters for given PLA were established using 20 solvents in total, giving δD =18.9 δP = 8.0 δH = 7.6 ($\sqrt{MPa}$) with solubility sphere radius R = 6.6 and fit of the model 1.000, no wrong solvents in or out of the solubility sphere, which indicates well-established solubility parameters.

3.2. XRD of drug loaded PLA samples

Sample phase crystallinity was evaluated using XRD, it showed crystalline drug presence for samples which have been loaded to saturation point, while samples with lower drug load showed only amorphous PLA XRD pattern or in some cases crystalline PLA pattern.

3.3. Predictive model for drug loading capacity

Loading capacities for drugs were expressed as drug molecules volume in 1 gram of PLA, giving units of µl/g. Inverse square of total difference in solubility parameters between PLA and model drug was plotted against drug load capacity in order to linearize the data set. The data shows linear correlation between HSP's and loading capacity with R^2 value of 0,84 which indicates that this model predicts drug loading capacity of drugs for 84% of drugs used in this model (Fig. 1).

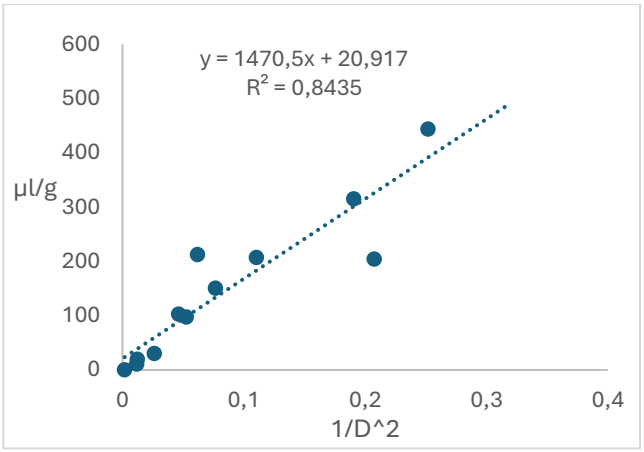

Figure 1. Drug loading vs solubility parameters.

4. CONCLUSION

To predict drug-polymer compatibility in order to formulate amorphous drug phase, Hansen solubility parameters have been used. Previously these calculations gave vague insight whether miscibility can be achieved, but with no means to predict drug loading capacity. This work presents way of establishing empirical model to predict drug loading capacity in polymer up until no more amorphous drug phase is possible using solvent casting method. For now, we show linear correlation of R^2 = 0.84, but to validate this model, more experiments with more drugs, polymers and loading methods needs to be done.

5. REFERENCES

1. Qiuyan Ran., et al, advances of combinative nanocrystal preparation technology for improving the insoluble drug solubility and bioavailability, crystals, 2022. volume 12 (9): 1200

2. Jagadeesh Babu N., et al, solubility advantage of amorphous drugs and pharmaceutical cocrystals, *crystal growth & design, 2011, vol 11 (7): 2662-2679*

3. Wiebke Kempin, et al, Assessment of different polymers and drug loads for fused deposition modeling of drug loaded implants, European Journal of Pharmaceutics and Biopharmaceutics, 2017, vol 115 : 84-93

P036

POLYMERIC CARRIER FOR VAGINAL ADMINISTRATION OF ANTIMICROBIAL PHYTOTHERAPEUTICS

Miroslava Pavelková[1], Lucie Pizúrová[1], Věra Vaibarová[2], Jakub Vysloužil[1], Kateřina Kubová[1], Jan Muselík[1]

[1]Department of Pharmaceutical Technology, Faculty of Pharmacy, Masaryk University, Brno, Czech Republic
[2]Department of Infectious Diseases and Microbiology, Faculty of Veterinary Medicine, University of Veterinary Sciences, Brno, Czech Republic

1. INTRODUCTION

Natural mucoadhesive polymers, such as sodium alginate, have garnered significant research attention for their beneficial properties in developing modern dosage forms, including vaginal drug delivery for infections treatment. Sodium alginate can form polymer hydrogel particles through external ionic gelation with safe cross-linking ions like Ca^{2+} [1].

These polymer carriers can serve as vehicles to incorporate biologically active natural substances derived from plant sources such as thymol, eugenol, and carvacrol. Their combinations may exhibit synergistic effects that hold promise in combating infectious diseases [2]. By integrating these substances into mucoadhesive polymers, we can leverage their effects when applied to mucous membranes. This study will explore the antimicrobial synergistic impact of these aforementioned phytotherapeutics against *Escherichia coli (E. coli)*.

2. MATERIALS AND METHODS

2.1. Materials

Sodium alginate (Alg; medium viscosity grade 5.0 – 40.0cps for 1% water dispersion) was used as polymer carriers (Sigma Aldrich, St. Louis, USA). $CaCl_2$ (Ca; Penta, Prague, CZE) was a crosslinking agent. To incorporate phytotherapeutics such as carvacrol (C), eugenol (E) and thymol (T), the polysorbate 80 (PS 80) was used. The bacterial strain used was *E. coli* (ATCC 25922).

2.2. Method of preparation

Seven different solutions were prepared for the study, namely 6% A solution with 1% PS 80 and thymol, eugenol, or carvacrol; 6% A solution with 1% PS 80 containing a combination of two or three drugs. They were extruded through a 0.22mm diameter needle into a 1M hardening solution of $CaCl_2$. Particles were allowed to harden for 1 hour at room temperature, then filtered and washed with purified water, followed by drying at 25°C in HORO – 048B drier (Dr. Hofmann GmbH, Ostfildern, Germany) for 24h. Sample characteristics are shown in Table 1.

Table 1. Formulation variables

Sample	Alg (%)	PS 80 (%)	Ca (M)	Phyto-therapeutics		
				C (%)	E (%)	T (%)
Alg_C	6	1	1	10	-	-
Alg_E	6	1	1	-	10	-
Alg_T	6	1	1	-	-	10
Alg_CE	6	1	1	5	5	-
Alg_ET	6	1	1	-	5	5
Alg_CT	6	1	1	5	-	5
Alg_CTE	6	1	1	3.33	3.33	3.33

2.3. Methods of evaluation

Morphological evaluation of the particles

The dried particles were evaluated by a spectroscopic microscope (Nikon SMZ 1500, C-PS 160) with a photo camera (TV Lens 0.55xDS), with an objective of 0.75. Factor sphericity and equivalent diameter were determined using the computer program NIS-Elements and expressed as average values and standard deviation (SD) from the 200 particles.

Content of phytotherapeutics

The drug contents were determined using an Agilent Technologies liquid chromatograph (HPLC 1200 Series) on a LiChrospher® 100 RP-18 column (particle size 5µm) at a wavelength of 274nm. The mobile phase consisted of 50% acetonitrile and 50% phosphoric acid (0.02M).

P036

Determination of minimal inhibition concentration (MIC) of phytotherapeutics and their mixtures against *E. coli*

To determine the MIC, individual substance and their combinations were tested using twofold dilutions in a microtiter plate (100 µL/well, in triplicate) with sufficient polysorbate 80. An overnight culture of *E. coli* cells was suspended in a Phosphate Buffered Saline (PBS), adjusted to OD_{600} 0.5 and further diluted in Cation Adjusted Müller-Hinton broth medium (CAMHB). Volume of 50 µl was transferred to each well of the microtiter plate to obtain final concentration $5x10^5$ CFU/ml. Plates were sealed using thermal adhesive sealing film and incubated for 16-20 hours at 37 °C. The MIC was visually assessed against a black background by identifying the first well that exhibited no turbidity, indicating bacterial growth inhibition.

3. RESULTS AND DISCUSSION

Morphological parameters, size and sphericity of particles are shown in Table 2. The observed nearly perfect sphericity is indicative of favorable properties for subsequent particle manipulation techniques.

Table 2. Morphological characteristics

Sample	Equivalent diameter ±SD [µm]	Sphericity factor ±SD
Alg_C	977.83 ±26.55	0.98 ±0.02
Alg_E	977.68 ±107.51	0.98 ±0.02
Alg_T	1078.20 ±57.29	0.98 ±0.04
Alg_CE	1023.21 ±38.00	0.98 ±0.02
Alg_ET	1258.53 ±100.39	0.98 ±0.07
Alg_CT	944.43 ±13.29	0.99 ±0.02
Alg_CTE	1291.75 ±46.93	0.97 ±0.02

The encapsulation method employed successfully achieved high content levels (in Table 3), making it suitable for further research.

Antimicrobial efficacy surveys of phytotherapeutics against *E. coli* showed synergistic interactions among nearly all active ingredient combinations, with the strongest effect observed when all three compounds were combined in a single sample. Results determination of MICs are shown in Table 4.

Table 3. Content of phytotherapeutics

Sample	Phytotherapeutic content [mg/g]		
	Carvacrol	Eugenol	Thymol
Alg_C	416.70 ±1.48	–	–
Alg_E	–	389.03 ±2.59	–
Alg_T	–	–	407.06 ±3.59
Alg_CE	214.51 ±1.51	210.90 ±1.43	–
Alg_ET	–	203.72 ±0.63	205.22 ±0.79
Alg_CT	229.61 ±5.52	–	230.67 ±6.01
Alg_CTE	136.85 ±0.62	133.89 ±0.72	134.65 ±1.88

Table 4. Determination of MIC

Phytoterapeutic	MIC against *E. coli* [mg/ml]
Carvacrol	2.5
Eugenol	3.9
Thymol	3.9
Carvacrol/Eugenol	4.0
Eugenol/Thymol	1.5
Carvacrol/Thymol	1.0
Carvacrol/Eugenol/Thymol	0.4

4. CONCLUSION

Satisfactory samples of hydrogel particles with phytotherapeutics, were synthesized. Using a triple combination of active ingredients shows promising therapeutic potential.

5. REFERENCES

1. Pavelková Miroslava, et al. *Assessment of Antimicrobic, Antivirotic and Cytotoxic Potential of Alginate Beads Cross-Linked by Bivalent Ions for Vaginal Administration.* Pharmaceutics, 2021, **13**(2): 165.

2. Yassine El Atki., et al. *Antibacterial Effect of Combination of Cinnamon Essential Oil and Thymol, Carvacrol, Eugenol, or Geraniol.* Journal of Reports in Pharmaceutical Sciences, 2020, 9(1): 104-109.

P037

THE FORMULATION PARAMETERS EFFECT ON THE PHYSICOCHEMICAL PROPERTIES OF ENTERIC-COATED CAPSULES FOR COLON-SPECIFIC DELIVERY OF HYDROPHILIC BIOMATERIALS

Sylvie Pavlokova[1], Nicole Fulopova[1], Katerina Bruckner[1], Ales Franc[1]

[1]Department of Pharmaceutical Technology, Faculty of Pharmacy, Masaryk University, Czech Republic

1. INTRODUCTION

The need for innovative drug delivery methods, particularly for the small and large intestines, is pressing today. This urgency is underscored by the demand for both local and systemic administration for conditions like ulcerative colitis, Crohn's disease, and colon cancer [1].

This research aims to design and evaluate an enteric-coated hard capsule dosage form for targeted delivery of biological materials, such as fecal microbiota transplant or live microbes, to the distal parts of the GIT. The capsules are designed to be internally protected against destruction by hydrophilic filling during passage through the digestive tract.

2. MATERIALS AND METHODS

2.1. Materials and samples

Hard gelatin (Ge) and DRcaps™ (DR) capsules based on HPMC and gellan were used to encapsulate a hydrophilic body temperature-liquefying gelatin hydrogel with caffeine or insoluble iron oxide mixture. Different combinations of polymers for the internal (INT) and external (EXT) coating were tested. INT: ethylcellulose (Etc), Eudragit® E (EuE), and polyvinyl acetate (PVA). EXT: Eudragit® S (EuS), Acryl-EZE® (Ac), and cellacefate (Ce). The EXT protects against the gastric environment, while the INT protects against the liquid hydrophilic filling during passage.

2.2. Physicochemical properties

Samples were evaluated for their physicochemical properties: thickness of INT/EXT coating determined using scanning electron microscopy (INT/EXT thickness), weight increment of INT/EXT coating (INT/EXT weight inc.), amount of API released after 120 and 360 min of dissolution (dis_120, dis_360), and disintegration time (disint. time).

2.3. Data analysis

The analysis of obtained data is primarily based on a combination of principal component analysis (PCA) and analysis of variance (ANOVA) outputs. As a multivariate technique, PCA examines interdependencies between formulation parameters (INT/EXT coating type, capsule type) and selected capsule characteristics. The software R, versions 4.2.1 and 3.6.0, was employed for data processing.

3. RESULTS AND DISCUSSION

The findings based on the statistical analysis of physicochemical features are presented here. More detailed information regarding this research is included in the published study [2].

3.1. Principal component analysis

A PCA visualization is presented in the scores plot (Fig. 1) and loadings plot (Fig. 2).

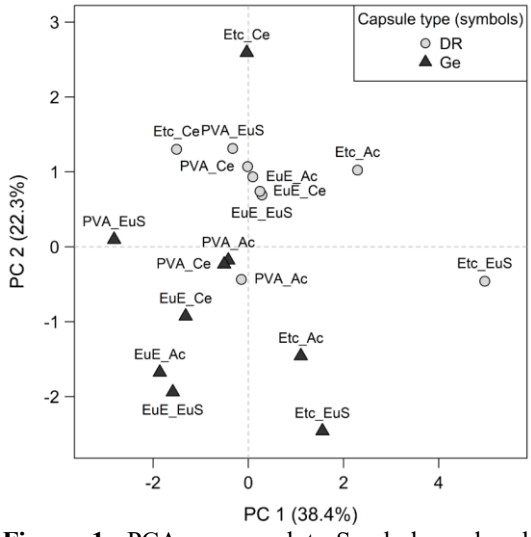

Figure 1. PCA scores plot. Symbols and colors differentiate the capsule type, and point labels differentiate the INT/EXT coating type.

P037

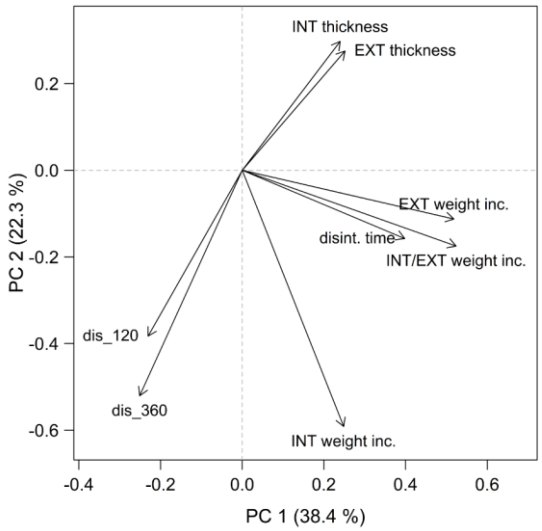

Figure 2. PCA loadings plot.

The influence of mean weight inc. of both coatings (INT/EXT) and capsule type was confirmed as statistically significant for the following values: INT/EXT thickness, EXT weight inc., disintegration time, and dis_360 ($p < 0.05$ for all cases). For dis_120, only the INT type plays a significant role ($p = 0.045$), while both coating types (INT/EXT) have a significant effect on the INT weight inc. ($p < 0.05$). Moreover, the ANOVA revealed a strong effect of interactions among the formulation parameters for almost all measured variables.

3.2. Effect of capsule type

Nevertheless, it can be stated that one noticeable correlational trend is present, namely the differentiation of samples based on capsule type (Fig. 1). In the upper part of the graph, DR_samples are located, while Ge_samples can be found in the lower part. When interpreting the connection with this direction in the loadings plot (Fig. 2), it can be said that DR_samples, compared to Ge_samples, have higher INT/EXT thickness and lower values of dis_120 and dis_360. The value of dis_360 is the most significant effect for differentiating samples according to the capsule type.

3.3. Effect of INT type

The differentiation of the samples based on the INT type is slightly noticeable in the direction of the first PC. PVA_samples and EuE_samples are located on the left side of the graph. At the same time, the Etc_samples are distributed more variably in space but rather in the right part of the graph (Fig. 1). EuE_samples and PVA_samples, compared to the Etc_samples, have lower disintegration time ($p < 0.001$), mainly due to the decisive difference between samples with a EuS EXT coating in both capsule types. Also, lower EXT and INT/EXT weight inc. ($p < 0.001$) were revealed for EuE/PVA compared to the Etc_samples. ANOVA also confirmed the same effect for INT weight inc. and INT/EXT thickness ($p < 0.05$ in all cases).

3.4. Effect of EXT type

Although the samples with different types of EXT coating are randomly distributed in space (Fig. 1), the ANOVA reveals the following trends: Ac > Eu/Ce for EXT thickness and Eu > Ce/Ac for disintegration time ($p < 0.05$ for both). Other influences are somewhat ambiguous, as interaction effects strongly influence them.

3.5. Samples with optimal properties

Regarding the requirement for a high disintegration time and a low percentage of the released amount of the substance at 120 and 360 min, an area with samples of desirable properties is located approximately in the upper right quadrant (Fig. 1). At the same time, the high INT/EXT thickness and EXT and INT/EXT weight inc. also correspond to this direction.

4. CONCLUSION

Innovative and easy capsule coatings offer significant potential for targeted drugs, especially FMT water suspension, to the GIT, preferably the colon. The administration method is robust and not considerably affected by the quantity of internal or external coatings, only by combining INT and EXT polymers. This method can be performed in regular laboratories without specialized individual and personalized treatment equipment, making it a practical and feasible method for drug delivery.

5. REFERENCES

1. Philip, A., et al., *Colon Targeted Drug Delivery Systems: A Review on Primary and Novel Approaches*. Oman Medical Journal., 2021, 25, 70–78.

2. Fulopova, N., et al., *Development and evaluation of innovative enteric-coated capsules for colon-specific delivery of hydrophilic biomaterials*. International Journal of Pharmaceutics, 2025. 668, 124991.

P038

USE OF MASS SPECTROMETRY FOR CHARACTERIZATION OF HEAT AND MASS TRANSFER DURING FREEZE-DRYING IN PROTECTIVE BAGS

Matija Pečnik[1], Pegi Ahlin Grabnar[1], Maja Bjelošević Žiberna[1], Biljana Janković[1,2], Klemen Kočevar[2]

[1]Faculty of pharmacy, University of Ljubljana, Slovenia
[2]Pharmaceutical development, Lek Sandoz d.d., Slovenia

1. INTRODUCTION

Characterizing heat and mass transfer, along with ensuring uniform thermal history during primary drying, is essential for achieving high-quality freeze-dried products. If the product temperature (T_p) exceeds critical thresholds, it can lead to structural defects such as collapse and result in excessive or inconsistent residual moisture levels in the final product. During scale-up or freeze-drying of toxic formulations in protective bags, inevitable alterations in the heat transfer coefficient (K_v) and total resistance (R_t) can significantly impact T_p, necessitating careful process control and optimization [1, 2].

$$R_t = \frac{(P_{ice} - P_{ch}) \times A_s}{\frac{dm}{dt}}$$

P_{ice} – equilibrium vapor pressure over ice; P_{ch} – chamber pressure; A_s – cross-sectional area of the vial

$$K_v = \frac{\Delta H_s \times \frac{dm}{dt}}{(T_s - T_p) \times A_s}$$

ΔH_s – heat sublimation of ice; T_s – shelf surface temperature; T_p – product temperature; A_s – cross-sectional area of the vial

The gravimetric approach—measuring individual vial weights—is the most precise method for determining sublimation mass flow (dm/dt). However, it is also time-consuming and invasive. Our goal is to develop a novel, less labor-intensive, yet sufficiently accurate technique for dm/dt determination while systematically assessing the impact of various permeable bag components on mass and heat transfer during sublimation [3].

2. MATERIALS AND METHODS

2.1. Materials

Lyoprotect® bags and stainless steel trays were provided by Teclen (Putzbrunn, Bayern, Germany). The bags consist of a PP-foil, seamlessly joined to an expanded-PTFE membrane layer, supported by a spun-bonded non-woven PP structure [1]. All sublimation tests were conducted using 20 mL type I borosilicate glass tubing vials partially sealed with igloo stoppers. Ultra-pure water was used for all experiments.

2.2. Freeze-drying

All experiments were conducted using Lyostar 3 (SP Scientific, Warminster, PA). Each run involved 65 vials, each filled with 7 mL of water, arranged on the middle shelf, surrounded by empty vials to ensure consistent thermal conditions. The liquid was frozen to -40°C overnight before primary drying at -5°C and 200 µbar for 7 hours. Four distinct experimental setups were tested in four iterations to analyze dm/dt, K_v, and R_t:

1. Vials placed directly on the shelf
2. Vials placed on stainless-steel tray
3. Vials placed on stainless-steel tray with single layer of PP-foil attached to the bottom of the tray
4. Vials placed on stainless-steel trays sealed in protective bags

2.3. Mass spectrometry

The mass of sublimated water was determined by weighing the entire tray before and after the test. Throughout the sublimation process, the water vapor concentration inside the chamber was continuously monitored using a mass spectrometer. The area under the curve from the spectrometer data was then correlated with the mass difference, allowing for the calculation of dm/dt under steady-state conditions.

2.4 Gravimetric approach

P038

Ten central vials were weighed before and after sublimation to determine water loss. Additionally, shorter sublimation tests were conducted to quantify the mass of sublimated water, before steady-state conditions were reached, enabling the calculation of sublimation dm/dt in steady-state conditions.

3. RESULTS AND DISCUSSION

3.1. Sublimation mass flow (dm/dt)

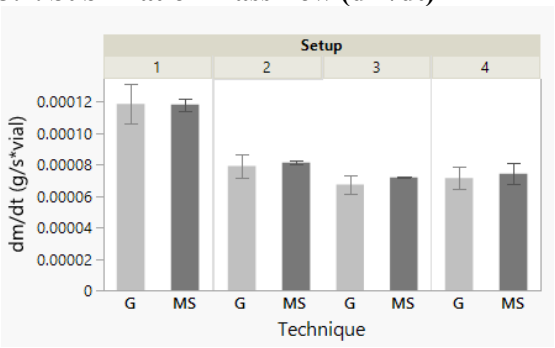

Figure 1. Mean and standard deviation for dm/dt versus setup (1-4) and technique (G-gravimetric approach / MS-mass spectrometry).

Mass flow measurements from both methods are comparable, though mass spectrometry yields slightly higher values due to inclusion of edge vials. Only setups #1 and #2 show significant differences to others, while #3 and #4 remain similar. This suggests that the tray is the primary factor limiting heat transfer during sublimation.

3.2. Heat transfer coefficient (K_v) and total resistance (R_t)

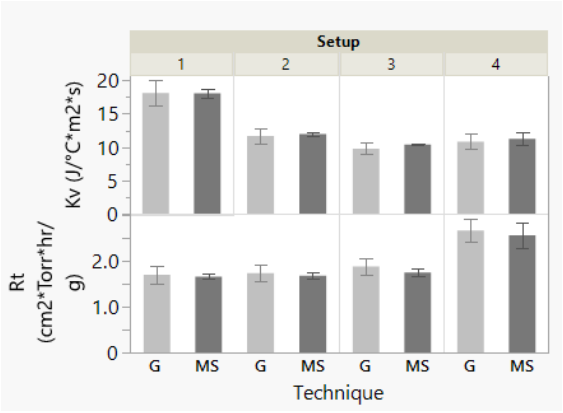

***F*igure 2**. Mean and standard deviation for K_v and R_t versus setup (1-4) and technique (G-gravimetric approach / MS-mass spectrometry).

Neither K_v nor R_t differ significantly across setups based on the determination method. In the gravimetric approach, K_v values for all setups differ significantly. Setup #4 unexpectedly shows higher values than #3, despite anticipated greater heat transfer in #3 due to additional heat radiation from the chamber and upper shelf. Chamberlain et al. found that higher vapor pressure in bags enhances heat transfer by improving water vapor conductivity over nitrogen or air. In mass spectrometry, setups #1, #2, and #3 show significant differences, while #4 does not differ significantly from #2 and #3, though a slightly higher response in #4 compared to #3 is observed.

Total resistance (R_t) consists of stopper resistance (R_s), dried product resistance (R_p), and chamber resistance (R_c) [1]. R_p is negligible with water, while R_s and R_c remain constant across setups. In the gravimetric approach, R_t differs significantly among #2, #3, and #4, with #1 comparable to #2 but distinct from #4. In mass spectrometry #1, #2, and #3 show no significant differences, whereas #4 stands out. The higher resistance in setup #4 is solely due to the bag's influence.

4. CONCLUSION

Mass spectrometry is sufficiently accurate to gravimetric approach in dm/dt determination while reducing the number of cycles. Trays hinder heat transfer, while Lyoprotect® bags significantly impact resistance.

5. REFERENCES

1. Chamberlain, R., et al., *Freeze-drying in protective bags: Characterization of heat and mass transfer.* European Journal of Pharmaceutics and Biopharmaceuticas, 2020. 154: 309-316.

2. Cherry, C. L. A., et al., *A novel approach to sterile pharmaceutical freeze-drying.* Pharmaceutical Development and Technology, 2014. 19(1): 7381.

3. Nail, S., et al., *Recommended Best Practices for Process Monitoring Instrumentation in Pharmaceutical Freeze-drying – 2017.* AAPS PharmSciTech, 2017. 18(7): 2379-2393.

ACKNOWLEDGMENT

This work was supported by the Slovenian Research Agency under grants P1-0189, and co-founded by Sandoz d.d.

P039

PREVENTING INSOLUBLE NICLOSAMIDE MONOHYDRATE FORMATION VIA FIVE NEW SOLVATES

Ilenia D'Abbrunzo[1], Veronica Rizzetto[1], Lara Gigli[2], Serena Bertoni[3], Michele R. Chierotti[4], Dritan Hasa[1], Beatrice Perissutti[1]

[1]*Department of Chemical and Pharmaceutical Sciences, University of Trieste, P.le Europa 1, 34127 Trieste, Italy*
[2]*Elettra-Sincrotrone Trieste, S.S. 14 Km 163.5 in Area Science Park, Basovizza–Trieste, Italy*
[3]*Department of Pharmacy and Biotechnology, University of Bologna, V. S. Donato 19/2, 40127 Bologna, Italy*
[4]*Department of Chemistry and NIS Centre, University of Torino, V. Giuria 7, 10125 Torino, Italy*

1. INTRODUCTION

Niclosamide (NCM), originally developed in the 1950s as an anthelmintic agent, has recently gained attention for its potential repurposing in diverse therapeutic areas, including antiviral, antibacterial, anticancer, and anti-inflammatory treatments [1-2]. However, its poor aqueous solubility and the tendency to convert into a highly insoluble monohydrate form hinder its clinical development and bioavailability [3]. One promising strategy to overcome these challenges is the formation of solvates, which can stabilize NCM in more soluble forms and prevent monohydrate conversion. Due to its planar molecular structure, NCM readily forms channel solvates stabilized by π-π stacking and strong hydrogen bonding with solvent molecules [4]. While several solvates and two monohydrates are already known [5-6], this study aimed to expand the solid-form landscape of NCM by screening 12 solvents through mechanochemical methods. Five new solvates were successfully obtained, each exhibiting unique interactions and stoichiometries. These were characterized using a range of solid-state analytical techniques and evaluated for physical stability, providing valuable insights into their potential for improving NCM formulation and therapeutic performance.

2. MATERIALS AND METHODS

2.1. Materials

NCM with a declared purity of 98-101% was used. Acetic acid (AA), 4-methylthetraydropyran (4-MTHP) hexane (HXN), methanol (MeOH), 2-pyrrolidone (2-PYR), dimethyl sulfoxide (DMSO), isopropanol (iPOH), Ethanol (EtOH), acetonitrile (ACN), ethyl acetate (EA), acetone (ACT) and benzyl alcohol (BENZOH) were of analytical grade.

2.2. Mechanochemical synthesis

The mechanochemical synthesis of NCM solvates was performed in Retsch MM400 vibrational mill (Retsch, Germany) equipped by two 25 mL stainless steel jars and one 10 mm Ø bead, respectively.

The milling frequency for each pathway was maintained at 25 Hz, the void volume in the jar was also kept constant (i.e., a total of 400 mg of powder per 25 mL jar) and the milling time was kept fixed (i.e., 60 min).

NCM was ground with above mentioned 12 different solvents using two different NCM-solvent molar ratios, i.e., 1:1 and 1:2. Based on the results obtained with the above-mentioned stoichiometries, additional molar ratios (i.e., 1:0.5, 1:1.5, 1:3) were used in limited cases.

For comparison purposes slurry bridging experiments (duration of 7 days) were conducted suspending NCM in the same solvents while stirring.

2.3. Characterization analyses

The solvates were characterized using a comprehensive solid-state analytical approach, including powder X-ray diffraction (PXRD), differential scanning calorimetry (DSC), thermogravimetric analysis (TGA), Fourier-transform infrared spectroscopy with attenuated total reflectance (FTIR-ATR), hot-stage microscopy (HSM), and (in selected cases) ^{1}H NMR and solid-state nuclear magnetic resonance (SS-NMR). Additionally, the solvates were subjected to compaction and storage at ambient temperature for six months and under humid conditions to assess their physical stability and potential conversion to the NCM monohydrate form. For the solvate obtained with 2-PYR, synchrotron powder X-ray diffraction data were collected.

P039

3. RESULTS AND DISCUSSION

Five out of the twelve solvents resulted in NCM solvates, in which the solvent was bound to NCM in different ways and with varying stoichiometry. This resulted in the discovery of five new solvates with solvents commonly used in the pharmaceutical field. Based on the above-mentioned extensive characterization of these compounds, the new systems were classified into two subgroups:

1) The first subgroup includes two equimolar stoichiometric solvates: niclosamide–dimethyl sulfoxide (NCM–DMSO) and the novel niclosamide–2-pyrrolidone (NCM–2-PYR). The latter represents a newly identified solid form, whose crystal structure has been solved here for the first time using synchrotron powder X-ray diffraction data. Lab-PXRD patterns are reported in Figure 1.

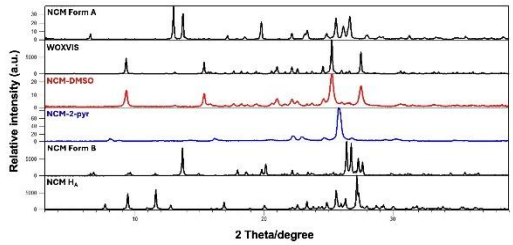

Figure 1. PXRD pattern of the stoichiometric solvates compared to known NCM solid forms.

2) The second subgroup consists of non-stoichiometric solvates, presumably isostructural channel solvates, given the similarity in PXRD and FTIR analyses. These include niclosamide-acetic acid (NCM-AA), niclosamide-acetone (NCM-ACT), and niclosamide-benzyl alcohol (NCM-BENZOH). These solvates both demonstrate low reproducibility in their formation and variable solvent content within the structure upon storage. This instability was confirmed by DSC, TGA and SS-NMR analyses, along with isostructurality evidenced through PXRD (figure 2) and FT-IR.

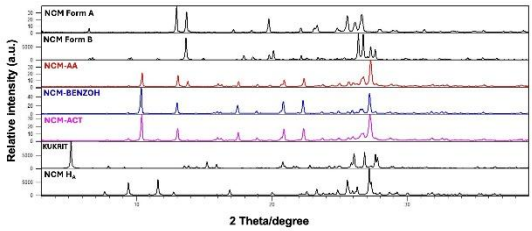

Figure 2. PXRD pattern of non-stoichiometric solvates compared to known NCM solid forms.

Importantly, all five NCM solvates were found to be stable for at least six months and resistant to conversion into the undesirable monohydrate form of NCM and to compression.

4. CONCLUSION

Through this experimental study, we expanded the solid-form landscape of niclosamide by identifying both stoichiometric and non-stoichiometric solvates, which not only offer several potential advantages for industrial applications in pharmaceutical formulation development but also effectively prevent the formation of the undesired monohydrate.

5. REFERENCES

1. Chen, W. et al. *Niclosamide: Beyond an Antihelminthic Drug.* Cell Signal 2018, 41, 89–96.

2. Xu, J et al. *Broad spectrum antiviral agent niclosamide and its therapeutic potential.* ACS Infect Dis 2020, 6, 909–915.

3. Van Tonder, E.C. et al. P*reparation and physicochemical properties of niclosamide anhydrate and two monohydrates*. Int J Pharm 2004, 269, 417–432.

4. Mann, J.E. et al. *Desolvation processes in channel solvates of niclosamide.* Mol Pharm 2023, 20, 5554–5562

5. Vuai, S.A.H. et al. *Cation–Π interactions drive hydrophobic self-assembly and aggregation of niclosamide in water.* Rsc Adv 2021, 11, 33136–33147, Doi:10.1039/D1ra05358b.

6. Sovago, I. et al. *Expanding the structural landscape of niclosamide: a high Z' polymorph, two new solvates and monohydrate Ha.* Acta Crystallogr C Struct Chem 2015, 71, 394–401

ACKNOWLEDGMENT

We thank Matteo Lusi (University of Limerick) for useful discussions.

P040

DEVELOPMENT OF AN INNOVATIVE DRY POWDER INHALER FOR SYSTEMIC DELIVERY OF AN ANTIPSYCHOTIC DRUG

Zsófia Ilona Piszman[1], Rita Ambrus[1], Petra Party[1]

[1]*Institute of Pharmaceutical Technology and Regulatory Affairs, University of Szeged, Hungary*

1. INTRODUCTION

Dry powder inhalers (DPIs) are an increasingly used system that allows targeted drug delivery directly into the lungs. Their use is non-invasive and environmentally friendly. Classically, inhalation systems have been used for the treatment of local diseases (e.g. cystic fibrosis, asthma) but in recent years, preparations with systemic effects have also emerged. Compared to oral administration, it has the advantage of avoiding a first pass effect and lower doses can reduce potential side effects, improving the overall quality of life of patients. DPI systems may be able to achieve rapid action using appropriate excipients and manufacturing techniques[1,2]. We aimed to develop a novel DPI system, which could potentially be used for the systemic treatment of schizophrenia.

2. MATERIALS AND METHODS

2.1. Materials

Chlorpromazine hydrochloride (CPZ), the active pharmaceutical ingredient was formulated with appropriate excipients: pullulan (PUL), leucine (LEU).

2.2. Preparation method

The optimized composition of the DPI was 65 mg of CPZ, 75 mg of PUL and 50 mg of LEU. The optimized parameters of the nano spray drying were the following: medium spray head, inlet temperature: 120 °C, spray: 100%, pump: 20%.

2.3. Investigation methods

The suitability of the prepared DPI for pulmonary delivery was verified by physico-chemical (laser diffraction, scanning electron microscopy), structural (X-ray powder diffraction, Fourier-transform infrared spectroscopy) and aerodynamic (Andersen cascade impactor) investigations. The optimized powder showed extra-fine particle size (<2 µm), spherical shape and high fine particle fraction (90 %).

3. RESULTS AND DISCUSSION

3.1. Particle size measurement

According to the laser diffraction-based analysis, the particle size (Dv50) of the DPI was under 2 µm. The targeted extra-fine particles were achieved. The particle size distribution (PSD) was monodisperse (<2), which contributes to the accurate dose delivery. The specific surface area (SSA) increased 10-fold.

Table 1. Particle size, PSD and SSA results.

Sample name	Dv50 (µm)	Span	SSA (m^2/g)
PM	50.7 ± 15.5	2.30 ± 0.42	0.54 ± 0.15
DPI	1.34 ± 0.03	1.61 ± 0.27	5.20 ± 0.12

3.3. X-ray powder diffraction (XRPD)

During the nano spray-drying process the initial crystalline materials become amorphous. The intensity of the characteristic peaks of CPZ decreased in the DPI sample, in contrast to the physical mixture (PM) and the raw materials (Figure 1.).

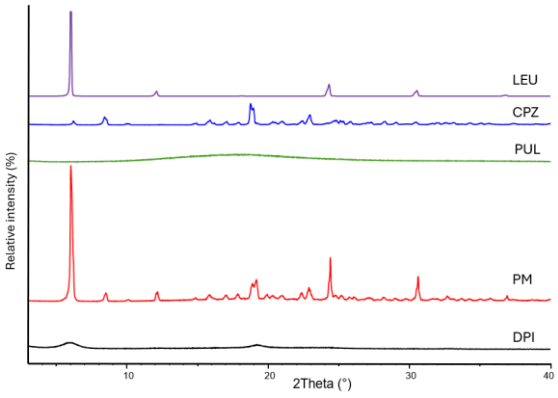

Figure 1. XRPD results

3.4. Fourier-transform infrared spectroscopy (FTIR)

To identify the molecular interactions occurring during spray drying, the initial materials, the

P040

PM and the DPI formulation were compared (Figure 2). All the characteristic peaks of CIP were detected in the DPI, indicating that the preparation process did not cause any structural changes.

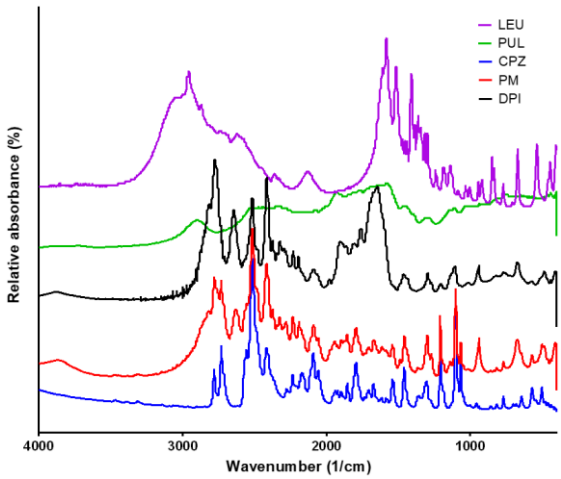

Figure 2. FTIR spectra

3.5. Scanning electron microscope (SEM)

The particles showed spherical morphology with moderately wrinkled surface (Figure 3.), which can be advantageous for aerosolization.

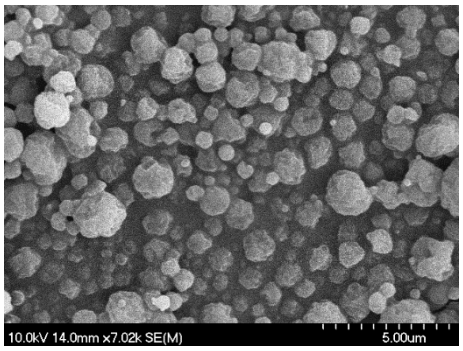

Figure 3. SEM picture of the DPI

3.6. Andersen cascade impactor (ACI)

High DPI deposition could be observed on stages 3 and 4, optimal for effective lung delivery, as well as in the inhaler device, due to the small particle size (Figure 4.). The exceptionally fine particle fraction (FPF) and small mass median aerodynamic diameter (MMAD) also indicate great aerodynamic properties. Emitted fraction (EF) is also preferable for pulmonary application (Table 2.).

Table 2. ACI results from the Inhalytix® softver

FPF (%)	MMAD (µm)	EF (%)
91.39 ± 10.84	1.94 ± 0.034	76.64 ± 2.10

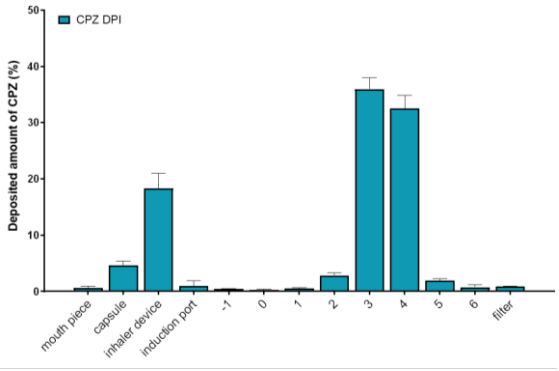

Figure 4. Distribution of the DPI in ACI device

4. CONCLUSION

We successfully developed a CPZ containing DPI and proved its suitability for pulmonary delivery. With optimal excipient composition and spray-drying production protocol we achieved small, spherical, amorphous particles with great aerodynamic properties. Further investigation is required to determine the dissolution and permeability profile of the DPI.

5. REFERENCES

1. Party, P.; et al. Development of extra-fine particles containing nanosized meloxicam for deep pulmonary delivery: in vitro aerodynamic and cell line measurements. European Journal of Pharmaceutical Sciences 2022, 176, 106247

2. Scherließ, R. et al. Particle engineering in dry powders for inhalation. European Journal of Pharmaceutical Sciences 2022, 172,

ACKNOWLEDGMENT

This work was supported by National Research, Development and Innovation Office, NKFIH OTKA K_146148; the National Academy of Scientist Education Program of the National Biomedical Foundation under the sponsorship of the Hungarian Ministry of Culture and Innovation. Project no TKP2021-EGA-32 has been implemented with the support provided by the Ministry of Culture and Innovation of Hungary from the National Research, Development and Innovation Fund, financed under the TKP2021-EGA funding scheme.

P041

EVALUATION OF CLEANING EFFICIENCY AFTER CONSECUTIVE BATCH PRODUCTION OF NIMESULIDE TABLETS IN VERTICAL GRANULATOR VG 200

Hristina Shavreska Dujovska[*1], Sanja Milosevic Krstevska[1], Natasha Milanovic[1], Elena Petrovska[1]

[1]Replek, Kozle 188, 1000 Skopje, North Macedonia

1. INTRODUCTION

In pharmaceutical manufacturing, cleaning validation is a regulatory and quality requirement that ensures the removal of product residues, cleaning agents and microbial contaminants from manufacturing equipement [1]. Traditionally, cleaning is performed after each batch, but with increasing focus on lean manufacturing and risk-based approaches, regulatory guidelines allow for extended cleaning intevals under validated conditions [2]. This study focuses on evaluating the cleaning procedure of Vertical Granulator VG 200 (GLATT) following the consecutive production of Nimesulide 100 mg tablets. Nimesulide (NSAID), was identified as the worst case product based on a risk assessment incorporating its solubility, cleanability, PDE value and batch size [3]. The purpose of this study was to determine whether partial cleaning between batches only with gross residue removal is sufficient to maintain microbiological and chemical cleanliness [4]. Additionaly, after how many consecutive batches the approved cleaning SOP remains effective.

2. MATERIALS AND METHODS

2.1. Materials

The evaluation of cleaning efficiency was performed on equipment vertical granulator VG 200 (GLATT). A total of 10 consecutive batches of Nimesulide 100 mg tablets were manufactured only with partial residue removal between batches. Sampling points were predetermined during initial equipment cleaning validation and include the mixer blade, inner lid, recipient surface and discharge outlet. After each batch were performed: swab sampling for API residues and swab sampling for microbiological contamination. Following the 10th batch, complete cleaning and disinfection was performed. First, absence of visible residues was confirmed by visual inspection, after which post-cleaning samples were taken to verify absence of API residues, absence of cleaning agents (COSA 90, 92), and microbiological contamination (Table 1.).

Table 1. Acceptance criteria and type of testing

Test Type	Acceptance criteria
Visual check- after complete cleaning	No visible residues of API/ cleaning agent
Residues of API after partial cleaning	≤525 ppm
Residues of API after complete cleaning	≤8 ppm
Residues of cleaning agent	≤18.15 ppm (COSA 90) ≤16,12 ppm (COSA 92)
Microbiological contamination	25 cfu/ 25 cm^2 (Signal limit) 50 cfu/ 25 cm^2 (Action limit)

2.2. Methods

API detection: UV-Visible spectrophotometry. (Apparatus: UV-VIS Spectrofotometer Shimadzu UV-1800 and UV-VIS Spectrofotometer Shimadzu UV-2600). Microbiology: Ph.Eur. 2.6.12, 2.6.13 – Total Viable Count Method. Cleaning agent: Conductivity & specific reagents per Ph.Eur. method and Ecolab validation data [5].

3. RESULTS AND DISCUSSION

Table 2. API residue levels (ppm) after each batch (swab sampling)

Batch	Mixer Impeller	Inner Lid	Recipient Surface	Discharge Surface
1	5.12	4.35	6.4	8.92
2	6.01	5.25	7.81	10.45
3	8.04	6.83	9.02	12.38
4	9.85	7.2	10.24	14.16
5	11.6	9.02	12.01	16.8
6	14.12	10.48	14.35	20.12
7	16.43	11.76	17.02	26.45
8	18.95	13.02	20.3	33.6
9	21.6	15.05	23.75	42.3
10	24.12	17.6	28.0	56.61

Table 3. Microbiological Results After Each Batch (CFU/25 cm^2)

Batch	Recipient Surface	Inner Lid
1–10	≤10	≤10

Table 4. Residues After Final Complete Cleaning and disinfection (Post-Batch 10)

Parameter	Location	Result
Visual check	All surfaces	No visible residues
API residue	All surfaces	≤0,81 ppm
Cleaning agent (COSA 90)	Discharge surface	8.5 ppm
Cleaning agent (COSA 92)	Inner lid	5.6 ppm
Microbiological contamination (Total Viable)	All surfaces	≤10 CFU/25 cm²

The results obtained through swab sampling after each batch demonstrate a gradual accumulation of API residues across all sampled surfaces (Table 2). Although all values remained well below the established **acceptance limit of** 525 ppm, the progressive increase in residue levels, particularly at the discharge surface which reached 56.61 ppm after batch 10, clearly indicates a residue buildup trend. This suggests that while partial cleaning between batches is effective in the short term, it may not be sufficient beyond a certain point (e.g., after batch 10), especially on more difficult-to-clean areas such as the discharge outlet. These findings support the importance of setting a validated maximum number of consecutive batches after which full cleaning must be performed to prevent potential contamination. Microbiological monitoring (Table 3) remained stable throughout all 10 batches, with total viable counts ≤10 CFU/25 cm² across both the recipient surface and inner lid. This suggests that partial cleaning was sufficient to control microbiological contamination within acceptable limits, with no action level breaches observed. Following complete cleaning and disinfection after batch 10 (Table 4), all chemical and microbiological parameters were well below their respective acceptance limits and the visual inspection confirmed the absence of visible residues across all surfaces.

4. CONCLUSION

The results of this study confirm that the applied partial cleaning strategy is effective in maintaining microbiological and chemical cleanliness of the vertical granulator VG 200 during the production of up to 10 consecutive batches of Nimesulide 100 mg tablets. Nevertheless, a clear upward trend in API residues, indicates that continued production beyond 10 batches without complete cleaning may lead to unacceptable buildup. The final complete cleaning and disinfection performed after the tenth batch, effectively reduced all residues to levels far below their respective acceptance criteria, reaffirming the reliability and adequacy of the cleaning procedure. Therefore, under the validated conditions, partial cleaning can be safely applied between batches, but must be followed by a complete cleaning after no more than 10 consecutive batches to ensure ongoing compliance with GMP standards and to mitigate the risk of contamination.

5. REFERENCES

1. European Commission. EudraLex Volume 4 – EU Guidelines to Good Manufacturing Practice, Part II & Annex 15: Qualification and Validation.
2. U.S. FDA. Guidance for Industry: Cleaning Validation – Questions and Answers (2021).
3. EMA. Risk Management Principles in Cleaning Validation - Questions and Answers. EMA/CHMP/CVMP/QWP/850374/2015, 20 November 2018
4. ISPE. Cleaning Validation Lifecycle – APQ Guide, 2021.
5. Ecolab. Cleaning Agent Residue Studies – Technical Bulletin, 2020.

ACKNOWLEDGMENT

Sincere gratitude to the management of Replek for providing access to the necessary data and equipment required for the completion of this study. The high level of professionalism and commitment of my colleagues played a significant role in the comprehensive evaluation of the cleaning efficiency following consecutive batch production.

P042

DEVELOPMENT AND CHARACTERIZATION OF RAPID-RELEASE METFORMIN GRANULES USING QbD PRINCIPLES

Maja Todeska, Martina Gjorgjevska, Daniel Velickovski, Dragana Petrusevska, Nikola Geskovski, Katerina Goracinova, Teodora Tasevska, Lina Livrinska, Maja Simonoska Crcarevska

Institute of pharmaceutical technology, Faculty of pharmacy, Ss. Cyril & Methodius University in Skopje, North Macedonia

1. INTRODUCTION

Metformin hydrochloride, a BCS Class III drug (high solubility, low permeability), is a first-line therapy for diabetes management. Despite limited clinical impact due to its permeability-limited absorption characteristics, dissolution timing may still be relevant due to metformin's narrow absorption window or exacerbation of GI side effects.

The objective of the study was to evaluate whether well-documented interactions between the binder, croscarmellose sodium (as disintegrant), and metformin hydrochloride (active substance) significantly affect granule characteristics at the specified concentrations and incorporation methods. The study aimed to determine how these interactions, particularly hydrogen bonding between components, influence critical granule properties such as particle size distribution, flow characteristics, compressibility, and disintegration behavior. Understanding these interactions is essential for risk analysis and management as well as for optimizing formulation parameters and ensuring consistent product performance in the final dosage form [2,3].

2. MATERIALS AND METHODS

2.1 Granule Preparation

Wet granulation was employed for the granule preparation. Metformin hydrochloride was kindly donated by Alkaloid AD, Skopje. As excipients Lactose (filler), Microcrystalline cellulose (binder/filler), Croscarmellose sodium and Sodium starch glycolate (superdisintegrants), Talc (lubricant) and Sucrose (taste masking) were used (Table 1). The API and excipients were dry-blended to ensure uniform distribution. A binder solution (Polyvinylpyrrolidone (PVP) (F1), Gelatin (F2) and Starch 1500 (F3) in purified water was gradually added under continuous mixing until a cohesive mass was formed. The wet mass was passed through a 2 mm sieve to form granules and dried at 50–60°C for approximately 60–90 minutes. After drying, regranulation was done to ensure uniform particle size.

Table 1. Composition of rapid-release metformin granule formulations

Component	F1 (g)	F2 (g)	F3 (g)
Metformin HCl	50	50	50
Lactose	27.25	27.25	27.25
Microcrystalline Cellulose	10	10	10
Croscarmellose Sodium	2.5	2.5	2.5
Sodium Starch Glycolate	5	5	5
Polyvinylpyrrolidone (PVP)	2.5	/	/
Gelatin	/	2.5	/
Starch 1500	/	/	2.5
Sucrose	2	2	2
Talc	0.75	0.75	0.75

2.2 Characterisation

Granules were evaluated according to the European Pharmacopoeia (Eur. Ph.) for moisture content, and their flow properties were assessed using Carr’s Index and Hausner ratio. The Metformin content was determined by UV/VIS spectroscopy following the method described in the British Pharmacopoeia (BP). Dissolution testing was performed according to the BP monograph for Metformin tablets, using

a basket apparatus with phosphate buffer pH 6.8 at 37 ± 0.5°C and a rotation speed of 100 rpm, with samples collected at 5, 10, 15, 20, 30, and 45 minutes. Vibrational spectroscopy analyses were conducted to assess potential chemical interactions between Metformin and the excipients. FTIR spectra were collected in the 4000–650 cm^{-1} range, while Raman spectroscopy (200-1800 cm^{-1}) was used to complement FTIR findings.

3. RESULTS AND DISCUSSION

QTTP for rapid-release Metformin granules was established to define patient-relevant quality attributes ensuring safety and efficacy. CQAs were identified as subsets of the QTPP based on regulatory guidelines and prior knowledge of Metformin properties and the wet granulation process. QRM was performed using an Ishikawa diagram, following ICHQ9 [3], to systematically identify and prioritize formulation and process variables potentially impacting the CQAs. The experimental results provided insights into the relationship between formulation variables and product performance, supporting the selection of optimal binder systems for rapid drug release and robust granule quality. Moisture content of the granules ranged from 1.61% to 2.68%, with the lowest value observed for the formulation containing PVP (F1) and the highest for the Starch 1500 formulation (F3). All values remained within acceptable limits, indicating efficient drying and low risk of granule instability. Formulation F2 (Gelatin) exhibited the best flowability, characterized by the lowest Carr's Index (6%) and Hausner ratio (1.06), corresponding to an "excellent" flow classification. In contrast, formulations F1 (PVP) and F3 (Starch 1500) showed Carr's Index values of 12% and Hausner ratios of 1.14, indicative of "good" flowability according to the Eur. Ph. criteria. The target Metformin content was 50%, and assay results confirmed uniform drug distribution across formulations, with measured contents of 50.90±1.25% (F1, PVP), 52.38±1.4% (F2, Gelatin), and 52.58%±1.63 (F3, Starch 1500). The F2 and F3 formulations released the entire Metformin content within 5 minutes, while F1 released 94.10±2.1% at 5 minutes and 98.16±2.5% at 10 minutes. Gelatin and Starch 1500 promote faster disintegration and rapid drug release while PVP's slightly delayed drug release most likely due to its stronger adhesive binding properties and possible water competition with croscarmellose sodium thus promoting a bit slower disintegration. The FTIR and Raman spectra were in accordance with literature data regarding the possible interactions among metformin and the used excipients [4].

4. CONCLUSION

This study applied Quality by Design (QbD) principles to develop rapid-release Metformin granules, focusing on the influence of binder type on formulation attributes. All three formulations (F1, F2, and F3) met the required criteria for moisture content, drug assay, and rapid drug release. Flowability, a critical factor for capsule filling, was optimal in the Gelatin formulation, F2, making it the most suitable for further development. While PVP (F1) and Starch 1500 (F3) formulations showed good drug release profiles, their flowability could be further optimized by adjusting the excipient composition.

5. REFERENCES

[1] Takasaki, H. et al., The importance of binder moisture content in Metformin HCl high-dose formulations prepared by moist aqueous granulation (MAG). *Results in Pharma Sciences*. 2015; 5: 1–7.

[2] ICHQ8(R2), 2009. Pharmaceutical development Q8(R2). ICH harmonized tripartite guideline.

[3] ICHQ9, 2005. Quality Risk Management Q9. ICH harmonized tripartite guideline.

[4] Balpande, H.M. et al., Compatibility study of metformin with pharmaceutical excipients. *International Journal of ChemTech Research, 2013*;.5(4): 1684-1693.

P043

MICRO- AND NANOPLASTICS IN MEDICINE: REGULATORY CONSIDERATIONS FOR DEVICES AND DRUG DELIVERY SYSTEMS

Bence Sipos[1], Petra Party[1], Gábor Katona[1], Rita Ambrus[1], Ildikó Csóka[1]

[1]*Institute of Pharmaceutical Technology and Regulatory Affairs, University of Szeged, Hungary*

1. INTRODUCTION

The environmental prevalence of micro- and nanoplastics (MNPs) has led to widespread scientific interest because of their suspected effects on human wellness. The discussion about the environmental persistence of micro- and nanoplastics has received more attention than their deliberate or accidental use in medical applications. Medical devices that include catheters, inhalers, syringes, and drug delivery systems contain MNPs, which create important questions about their compatibility with the body and their toxic effects and extended exposure dangers. The regulatory frameworks that govern MNPs in medical applications show significant gaps because they remain either incomplete or poorly developed. This poster investigates the existing knowledge about MNPs in healthcare practices while discussing new safety issues and emphasizing the necessity for specific science-based regulations that protect healthcare providers and their patients.

2. MATERIALS AND METHODS

2.1. Methodology

A structured review of European Union legal frameworks examined the regulatory environment surrounding micro- and nanoplastics (MNPs) in medical contexts. The REACH Regulation (EC No 1907/2006) was the main document studied because it regulates chemical use and proposes restrictions on microplastics that were added intentionally. The Medical Device Regulation (EU 2017/745) was studied for its requirements regarding safety assessments and material risk evaluations of devices that could contain or emit MNPs. The Directive 2001/83/EC on medicinal products was studied to understand its regulations about drug formulations and delivery systems that might use plastic-based carriers or coatings. The analysis of environmental laws included the Marine Strategy Framework Directive and the Single-Use Plastics Directive to assess their effects on healthcare plastic waste. The Classification, Labelling and Packaging (CLP) Regulation (EC No 1272/2008) was studied to determine how hazardous classifications would apply to MNPs. The scientific opinions from SCHEER and EFSA were included to understand the evolving safety assessments. The analysis of each document focused on direct mentions of micro- or nanoplastics as well as their implications for patient safety and material transparency requirements. The research findings were combined to determine regulatory deficiencies and the degree to which existing frameworks handle the distinctive risks of MNPs in medical and pharmaceutical fields. Analyzing multiple regulations offers a complete understanding of current oversight and identifies necessary advancements.

3. RESULTS AND DISCUSSION

The European Union lacks an integrated regulatory system for micro- and nanoplastics (MNPs) used in medical devices and pharmaceuticals. Recent proposals under REACH (EC No 1907/2006) intend to limit the deliberate inclusion of microplastics in products, yet such restrictions could affect future applications of polymer-based excipients and coatings, and carriers used in pharmaceutical and medical device manufacturing. REACH does not apply to medicinal products or medical devices because they fall under their regulatory systems. The Medical Device Regulation (EU 2017/745) requires device manufacturers to assess risks thoroughly for all materials within their products, including substances that degrade or emit substances during use. Although MNPs might fall under this regulation, the lack of a specific MNP reference creates inconsistent manufacturer and notified body approaches to these risks. The MDR emphasizes biological

safety and chemical characterization, and long-term biocompatibility, which relate to MNP concerns, although indirectly. The Directive 2001/83/EC for medicinal products demands safety assessments for every ingredient together with delivery systems, but it provides no particular guidance about polymeric particles, especially when they are at nano- or micro-scale dimensions. The CLP Regulation (EC No 1272/2008) controls substance classification and labelling, but standard plastics remain exempt from classification unless they demonstrate certain toxicity or persistence characteristics. The ongoing advancement of research could result in demands to change MNP classification due to increasing understanding of long-term toxic effects and accumulation patterns. The Marine Strategy Framework Directive, along with the Single-Use Plastics Directive, function as environmental regulations that decrease environmental contamination while promoting eco-friendly materials use, thus shaping healthcare product design and waste management practices. The health impacts of nanoparticle exposure concern both SCHEER and SCCS scientific committees because nanoparticles can enter the body through inhalation or ingestion, or skin contact. The absence of approved methods for detecting MNPs in medical matrices makes it challenging for regulatory agencies to enforce their rules. Risk assessment becomes complex because standard toxicological data on polymers and their sizes and exposure routes are not available. The regulatory guidelines for nanomaterials under REACH and MDR do not directly apply to polymeric nanoparticles, which creates uncertainty for regulatory interpretation. The medical industry lacks standard definitions for micro- or nanoplastics that would allow safety threshold establishment across the board. Manufacturers remain unclear about their responsibility to detect MNP risks independently or to wait for official regulatory instructions. The different regulatory approaches between products create difficulties for both obtaining market clearance and conducting post-market surveillance. The rising public and scientific interest in MNPs will likely drive future EU medical and chemical regulations to include specific requirements for their assessment process. The current regulatory oversight of MNPs in medical applications operates through piecemeal and precautionary measures instead of proactive action. A complete science-driven regulatory structure must be developed to prevent long-term risks from the use of MNPs in healthcare. Future regulatory standards for this evolving field depend on continuous research and standardized testing methods, and coordinated efforts between agencies.

4. CONCLUSION

The current EU regulations offer limited oversight of micro- and nanoplastics used in medical and pharmaceutical applications, yet they do not provide dedicated harmonized guidance for these materials. The healthcare industry requires regulatory frameworks to adapt to advancing scientific knowledge about MNP risks protecting patients and maintain product quality within the fast-evolving healthcare sector.

5. REFERENCES

1. Allan, J., et al., *Regulatory landscape of nanotechnology and nanoplastics from a global perspective.* Regulatory Toxicology and Pharmacology, 2021. 122:104885

2. Krishnan, K., *A Systematic Review on the Impact of Micro-Nanoplastics Exposure on Human Health and Diseases.* Biointerface Research in Applied Chemistry, 2023. 13(4):381

ACKNOWLEDGMENT

Project no. [2024-1.2.3-HU-RIZONT-2024-00032] has been implemented with the support provided by the Ministry of Culture and Innovation of Hungary from the National Research, Development and Innovation Fund, financed under the [2024-1.2.3-HU-RIZONT] funding scheme.

P044

MOLECULAR SIMULATIONS OF DRUG-SILICONE INTERACTION TO PREDICT SILICONE-OIL DEPLETION

Dimitra Škrekovski[1,2], Jure Cerar [2], Blaž Likozar[1]

[1]National Institute of Chemistry, Hajdrihova ulica 19, Ljubljana, Slovenia
[2]Novartis Pharmaceutical Manufacturing LLC, Kolodvorska cesta 27, Mengeš, Slovenija

1. INTRODUCTION

Pre-filled syringes (PFSs) are often the go-to choice for primary packaging for biological drugs due to their convenience for self-administration, especially when incorporated into autoinjectors. However, issues can arise if silicone oil (SO) used to lubricate the syringe barrel depletes into the solution, leading to syringe malfunction. The depletion is caused by interactions between SO and therapeutic proteins, which adsorb to the SO-liquid interface inside the syringe [1]. Protein aggregates form at the interface and subsequently detach, carrying SO particles along [1, 2, 3]. This results in an increased subvisible particle count, potentially rendering the drug product out of specification, while protein aggregates may reduce drug efficacy and increase the risk of an immunogenic response in patients [1, 3]. Due to limited testing scope in early phases of development, SO problems often go unnoticed until much later, when the primary packaging development begins. At that point mitigation of such issues becomes a challenging task, as any change in formulation would require significant redevelopment efforts. Currently, there is no accurate and reliable method of predicting these issues in early development stages. That's why the aim of our study is to identify the protein properties/surface descriptors that play a role in interactions with SO by using molecular modelling and simulations. Our goal is to develop a predictive model that will predict about possible SO-protein interactions already in early development, allowing to adapt and shift development strategy, saving both time and resources.

2. MATERIALS AND METHODS

In this study, we utilized molecular dynamics (MD) simulations to explore the interactions of various monoclonal antibodies (mAbs) at the SO – liquid interface. SO was modelled as a slab of polydimethylsiloxane (PDMS) molecules in contact with protein solution. Advanced simulation techniques such as umbrella sampling were utilized to simulate mAbs adsorption to the SO. These methods enable us to better understand the molecular interactions, and dynamic behaviors at the protein-SO interface, providing valuable insights into the underlying mechanism. Furthermore, these simulations allow us to calculate protein-SO interaction energies and correlate them with experimental data (e.g., microflow imaging, break-loose and gliding force measurements, and RapID) to validate our models.

3. RESULTS AND DISCUSSION

3.1. Predictive model formation

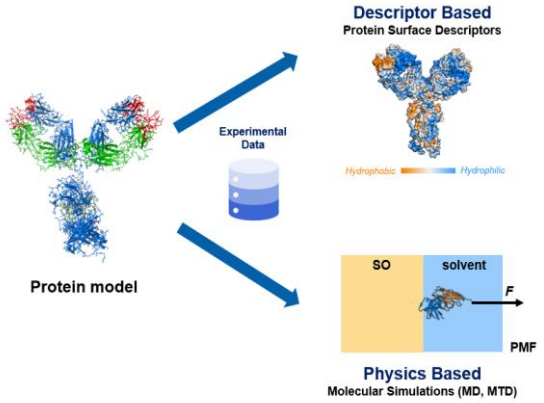

Figure 4. Schematic representation of predictive model creation workflow.

Our goal is to create a predictive model for possible SO-protein interactions in new drug candidates, based only on the protein's

properties. To form the prediction model, two different approaches will be tested (Figure 1); first, physics-based approach will be employed by studying the systems of interest with molecular dynamics simulations. For example, by calculating potential mean force required to pull the protein away from the SO surface and correlating that to experimental values. Secondly, once we gain a better understanding of the underlying mechanisms of protein-SO interactions, our model will be simplified by correlating protein surface properties responsible for the adsorption (e.g., hydrophobicity, charge distribution), even further reducing the time and computational resources needed for final result.

3.2. Proof of concept

The first stage of our work was to confirm whether the molecular simulations can capture the experimentally observed protein-SO interactions. We preformed MD simulations of three different mAbs with varying in their affinity to SO. Simulations of all three proteins were able to capture the experimentally observed effects. Therefore, we were able to confirm that molecular modelling approaches can sufficiently describe underlying physical phenomena of those systems and can be used as a tool to study SO-protein interactions.

4. CONCLUSIONS

In our work we were able to show the initial proof of concept, confirming that molecular modelling can be used to study SO depletion due to interactions with proteins in primary packaging. Further research efforts will be shifted towards finding possible correlations between experimental results and thermodynamic properties obtained with molecular simulations and generating reliable and accurate prediction model.

5. REFERENCES

1. Moll, F.A., et al., *The silicone depletion in combination products induced by biologics.* European Journal of Pharmaceutics and Biopharmaceutics, 2024. 203: 114418.

2. Saurabh, S., et al., *Adsorption of monoclonal antibody fragments at the water–oil interface: A coarse-grained molecular dynamics study,* APL Bioengineering, 2024. 8: 026128.

3. Dandekar, R., et al. *Monoclonal Antibody Aggregation near Silicone Oil−Water Interfaces*, Langmuir, 2021. 37: 1386-1398.

P045

DRY EMULSIONS AS 2D PRINTING PREFORMULATION: EFFECT OF BLANK INK MEDIA AND CARRIERS ON REDISPERSED PARTICLE SIZE

Barbara Sterle Zorec, Rok Dreu

Department of Pharmaceutical Technology, Faculty of Pharmacy, University of Ljubljana, Slovenia

1. INTRODUCTION

Due to the genetic influences on individual physiology and metabolism, personalized treatment is becoming increasingly important. In this context, various types of 2D printing technologies have been proposed that offer some potential solutions for personalized medication. Precise drug- on- demand deposition, the ability to consume multiple active ingredients in one product, and customization of individual drug assays are just some of the advantages that printing technologies offer over existing bulk manufacturing of pharmaceuticals [1].

In the present study, dry emulsions were prepared by spray drying as preformulations for 2D printing technology. The prepared dry emulsions were then redispersed in a different propylene glycol (PG)/water medium representing a printable ink formulation. Different dry emulsion carriers were used and their influence on the size of the redispersed particles was investigated, as this is one of the most important properties to avoid clogging of the printing nozzle with subsequent unsuccessful drug deposition. In addition, the one-month physical stability of such redispersed systems was evaluated.

2. MATERIALS AND METHODS

2.1. Materials

Simvastatin was kindly donated by Krka d.d., (Slovenia), Miglyol 812 (M812) was purchased from Sasol Germany GmbH, Germany, while 1-oleoyl-rac-glycerol (1OG) (technical grade ~ 40% (TLC)) and Tween® 20 (polyethylene glycol sorbitan monolaurate) were purchased from Merck, Germany. Lactose mesh 200, donated by Lek d.d. (Slovenia), nanocelullose (NCC, Cellu Force, Canada), maltodextrin DE 4.0-7.0 (MD, Sigma-Aldrich, USA) were used as carriers in spray drying experiments. PG (Sigma-Aldrich, ZDA) was used in redispersion experiments.

2.2. Emulsion preparation

1OG was heated to 40°C to obtain a clear liquid and mixed with M812 (9:1). Tween® 20 was added, followed by simvastatin (70 mg/g), then heated to 37°C and stirred until clear solution was obtained. Separately, the water phase was prepared by dissolving 30 w/w% of different carriers (lactose, lactose/NCC and MD) in purified water at 37°C. Three different emulsions were formed using an Ultra-Turrax mixer at 8,000 rpm (5 min) and 12,000 rpm (3 min), then homogenized with a high-pressure homogenizer APV 2000 (SPX Flow, ZDA) with five passes at 250 bar.

2.3. Dry emulsions preparation

Mini Spray Dryer (B-290, Büchi, Switzerland) was used to produce dry emulsions. A two-fluid nozzle with an orifice diameter of 1.4 mm and a cap orifice diameter of 2.20 mm was used. The optimal spray drying process parameters were as follows: drying gas volume flow rate of 38 m^3/h (100% aspiration rate); inlet temperature of 170 °C; spraying rate of 0,9 ml/min (30% of maximum peristaltic pump rotation) and flow meter spraying air (atomization gas flow rate) of 60 mm (742 L/h).

2.4. Redispersion of dry emulsions

Dry emulsions were dispersed in three different PG and water mixtures (10/90, 50/50, and 90/10% (V/V)). 100 mg of dry emulsion was weighed into a test tube by adding 20 mL of the selected blank ink medium. Samples were mixed using vortex for 2 min. The size of fresh and after one month of stability (25 °C, 40% RH and 40 °C, 45% RH) was measured by a laser diffraction (Mastersizer 3000, Malvern Instruments, Ltd., UK) using 300RF lens and Hydro EV unit. Their morphology was studied by a scanning electron microscopy using Supra 35 VP (Carl Zeiss, Germany).

P045

3. RESULTS AND DISCUSSION

3.1. Redispersion of dry emulsions

The use of different carriers for dry emulsions has a considerable influence on the size of the particles that are redispersed in different blank ink media. When lactose was used, the particles generally maintained similar median sizes (d50) except after being redispersed in a 90% (V/V) PG. Here the particle size is largest and increases with time and with increasing temperature and humidity during storage.

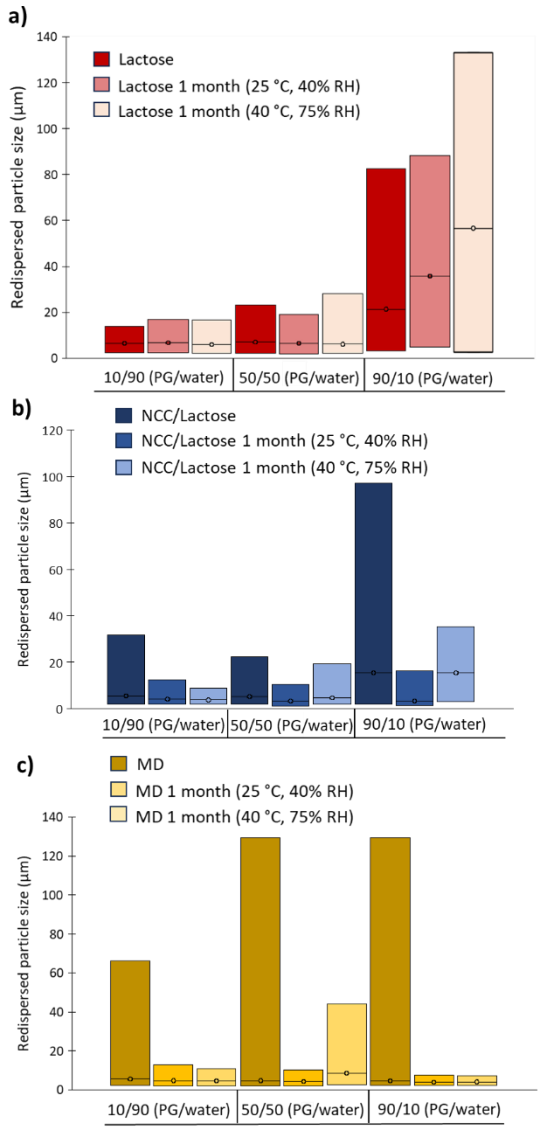

Figure 1. The size (d10 (lower boxplot line), d50 (middle boxplot line) and d90 (upper boxplot line)) of the redispersed particles directly after production and after one month of storage in different media, with a) lactose, b) NCC/lactose and c) MD as particle carrier.

When NCC/lactose is used, the d90 particle size tends to decrease over a one-month storage period, while the d50 and d10 values remain unchanged. This indicates that the smaller particles form clusters that gradually break down over time. A similar pattern is observed when MD is used as a carrier, regardless of the blank ink medium used. This observation is further supported by SEM analysis (Fig. 2), which shows that both NCC/lactose and MD particles initially form larger aggregates that break apart during storage.

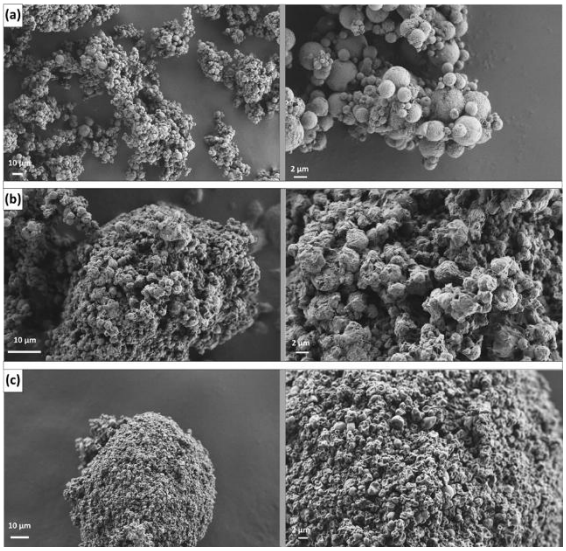

Figure 2. Morphology of particles containing (a) lactose, (b) NCC/lactose=25:75 %(w/w) and (c) MD (DE 4.0- 7.0) as dry emulsion carrier.

4. CONCLUSION

In the present study, dry emulsions were developed using three different particle carriers: Lactose, NCC/Lactose and MD. These carriers exhibited notable differences in particle morphology as well as in their redispersing behaviour in three blank ink media, each with unique surface tension and viscosity properties.

5. REFERENCES

1. Sterle Zorec, B., T*wo-dimensional printing of nanoparticles as a promising therapeutic method for personalized drug administration.* Pharmaceutical development and technology. 2023, Volume 28, p. 826-842.

ACKNOWLEDGMENT

The authors gratefully acknowledge the financial support provided by the Slovenian Research Agency (Program P1-0189).

P046

NIR HYPERSPECTRAL IMAGING FOR MONITORING OF DRUG CONTENT UNIFORMITY IN LIPID-BASED FORMULATION DEVELOPMENT

Elizabeta Atanaskova[1,2], Johannes Poms[2], Matthias Wolfgang[2], Carolina Alva[2], Nadia Mussner[2], Nikola Geskovski[1], Andreas Zimmer[3], Sharareh Salar-Behzadi[2,3]

[1]Ss. Cyril and Methodius University in Skopje, Faculty of Pharmacy, Institute of Pharmaceutical Technology, Skopje, Republic of North Macedonia
[2]Research Center Pharmaceutical Engineering GmbH, Graz, Austria
[3]University of Graz, Institute of Pharmaceutical Sciences, Department of Pharmaceutical, Technology and Biopharmacy, Graz, Austria

1. INTRODUCTION

Poor aqueous solubility is a critical challenge in pharmaceutical development. Lipid-based formulations offer flexibility in solubilizing of hydrophobic active pharmaceutical ingredients within the lipid matrix, leading to increased drug solubility and absorption from gastrointestinal tract, ultimately enhancing bioavailability. Ensuring uniform molecular distribution of the API throughout the production process of lipid-based formulations is essential for maintaining quality and performance. A rapid and precise in-process analytical techniques are needed to ensure consistent product quality. Near-infrared spectroscopy (NIR), a fast and non-destructive analytical tool, has been widely used to control various pharmaceutical processes. Hyperspectral imaging (HSI), an emerging technology that unlike conventional spectroscopy, provides a comprehensive spatial understanding of the formulation's chemical landscape, crucial for quality assessment and efficient development.

The current study introduces a novel application of near-infrared hyperspectral imaging (NIR-HSI) as a direct in-process control technique to produce a lipid-based formulation containing a model API belonging to BCS II compounds. Critical process parameters affecting product quality were optimized and verified using the developed and validated NIR-HSI method for API quantification and homogeneity analysis.

2. MATERIALS AND METHODS

2.1. Materials

Tetraglycerol partial esterified with palmitic and stearic acids (LipoGalen® PMF1684), di-, tri-, tertra, and hexaglycerol (PG2, PG3, PG4, and PG6) were kindly provided by IOI OLEO GmbH. Tetrahydrofuran, dimethylsulfoxide, 2-propanol, monobasic sodium phosphate, sodium phosphate dibasic and sodium lauryl sulphate were purchased from Sigma Aldrich (Austria).

2.2. Selection of lipid-base composition for API loading

The miscibility of different concentrations of PG2, PG3, PG4, and PG6 in molten LipoGalen® 1684 was visually evaluated to improve the wettability of the lipid. The potential phase separation was screened initially and after storage under accelerated conditions for two weeks. The visually stable mixture of LipoGalen® 1684 with 10 %w/w PG6 was selected as lipid-based system for API loading.

2.3. Determination of the theoretical API solubility in lipid-based system via differential scanning calorimetry (DSC)

The API solubility in the lipid base system of LipoGalen® 1684 and 10% PG6 was quantified vis DSC. Physical mixtures of 10%, 25%, 50%, 75% of API in lipid-based system, and 100% of pure API were prepared. Enthalpy of fusion (ΔHf) values against drug concentrations were plotted and extrapolated to $\Delta Hf=0$ to estimate

the drug's solubility in the lipid-based system [2].

2.4. Development and validation of NIR-HSI calibration model for API content analysis

The calibration set was composed of API ranging from 0% to 14% (in 2% steps), molecularly dispersed in the lipid-based system. The hyperspectral data from the samples was acquired using the EVK HELIOS EC32 push-broom hyperspectral imaging camera. Each sample of the calibration set was analyzed in triplicate and on both sides, resulting in a total of 48 hyperspectral data cubes used as the calibration dataset (Figure 5). The performances of the model were evaluated using coefficients of determination (R^2X and R^2Y), the root mean square error of calibration (RMSEC), the calibration BIAS, and the standard error of calibration (SEC).

3. RESULTS AND DISCUSSION

3.1. API Solubility in pre-selected lipid-based formulation determined via DSC

DSC analysis revealed the behaviour of the developed lipid-based formulation - as API concentration in the lipid-based system increased, the magnitude of the melting endotherm also grew, as a result of decreased concentration of dissolved drug in the lipid phase. By plotting the enthalpy of fusion (ΔHf) against the drug concentration and extrapolating to where ΔHf is zero, the maximum API solubility in the lipid matrix was determined to be 14%, which was then selected as the upper concentration limit for NIR-HSI model development.

3.2. Development and validation of NIR-HSI calibration model for drug content analysis

The developed NIR-HSI quantification model based on the 1st derivative pre-processed spectral data**,** demonstrated an excellent linearity and accuracy (R^2Y = 0.999, RMSEC = 0.084), while the low calibration BIAS and SEC values underscore its precision. The developed model enabled formulation optimization and identification of the critical production process parameters. In terms of formulation, incorporating hexaglycerol (PG6) enhanced the molecular distribution of API within the lipid base. To maintain a production temperature of 95 °C and extending the duration of the mixing process to 60 minutes were identified as critical parameters. These conditions promoted drug amorphization and uniform dispersion within the matrix, significantly reducing drug content variability from 16.58 % to 1.45 %.

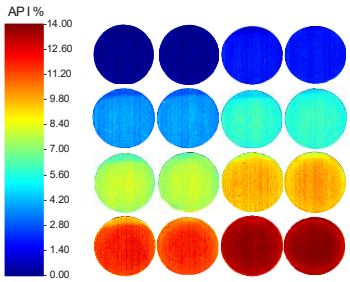

Figure 5. Concentration-mapped images: calibration data set.

4. CONCLUSION

Herein, we demonstrated the potential of NIR-HSI as a robust process analytical technology (PAT) tool for pharmaceutical development, particularly in ensuring consistent product quality of lipid-based systems.

5. REFERENCES

[1] Damle S. and Madankar C., *An overview on eco-friendly polyglycerol esters of fatty acid, synthesis and applications,* Tenside Surfactants Detergents, 2023, vol. 60, no. 6, 611-621.

[2] Gramaglia D., Conway B. R., Kett V. L., Malcolm R. K., and Batchelor H. K., *High speed DSC (hyper-DSC) as a tool to measure the solubility of a drug within a solid or semi-solid matrix*, International Journal of Pharmaceutics, 2005vol. 301, no. 1–2, 1–5.

ACKNOWLEDGMENT

The authors gratefully acknowledge the CEEPUS student mobility program for mobility grant provided through the CEKA PharmTech network which enabled this research. Special thanks to IOI OLEO GmbH for providing materials.

P047

STABILITY EVALUATION OF KETOCONAZOLE SHAMPOO: INFLUENCE OF pH AND ANTIOXIDANT ADDITION

Maja Todeska[1], Dobrinka Dimova[1], Natalija Dimovska[1]

[1]Research and Development Department, Replek, Republic of North Macedonia

1. INTRODUCTION

Ketoconazole is a widely used antifungal agent, it is an imidazole derivative, a weak base with two pKa: values 6.51 and 2.94. Product stability is an important issue in pharmaceutical industry. A thorough knowledge of the chemical and physical stability of drugs and dosage forms is critical in the development and evaluation of pharmaceuticals. Ketoconazole is chemically unstable, with oxidation and hydrolysis representing the main routes of its degradation. Further investigations are needed to improve the stability of ketoconazole in aqueous formulations and to explain how the pH of the shampoo, the addition of antioxidants, and other physicochemical parameters affect its stability. A combination of ionic and non-ionic surfactants has been shown to provide the most stable thixotropic system by optimizing interfacial film formation and molecular interactions. [1]

Given the widespread use of ketoconazole shampoos in treating dandruff and seborrheic dermatitis, ensuring their stability is essential for maintaining therapeutic efficacy and product shelf-life.

The aim of this study is to examine the stability of ketoconazole in relation to changes in the shampoo's pH and concentration of antioxidant to determine whether the addition of a stabilizer affects its stability.

2. MATERIALS AND METHODS

2.1. Materials

Ketoconazole, Sodium lauryl sulphate, disodium lauryl sulfosuccinate, Coconut diethanolamine, imidurea, hydrochloric acid, sodium hydroxide, sodium chloride, Butylated Hydroxytoluene. All materials were pharmaceutical grade.

2.2 Method of Preparation

For the purpose of the study, 2% ketoconazole shampoos were prepared using same preparation method. The formulations varied in pH, adjusted to 6.5, 7.5, and 8.5 by the addition of different concentrations of sodium hydroxide. Additionally, two 2% ketoconazole shampoos were prepared—one containing butylated hydroxytoluene (BHT) as an antioxidant, and one without BHT.

2.3. Stability Studies

Stability studies of ketoconazole shampoo were conducted in accordance with ICH guidelines. The shampoo samples were stored in stability chambers at 30 °C ± 2 °C / 65% RH ± 5% RH for a duration of 12 months. Samples were collected at intervals of: 0, 3, 6, 9, and 12 months for physical and chemical evaluation.[2]

2.4 In-Process Testing

The shampoo was examined to physical characteristics that influence the quality of the final product, including clarity, viscosity, uniformity, pH value, color intensity, and consistency.

3. RESULTS AND DISCUSSION

3.1. Physical Appearance and Visual Inspection

The shampoo was homogenous, uniform, clear, viscous liquid with a characteristic odor and an intense pink-orange color. During stability study there was no significant changes in physical evaluations.

3.2. Influence of pH on Ketoconazole Stability

The pH-stability of 2% ketoconazole is presented in Table 1. No visible changes were observed during this period. The most stable formulation was at pH 8.5 and formulation at pH 6.5 was the least stable, showing a 4.32% decrease in ketoconazole content compared to its initial concertation.

Table 1. Effect of pH on % Assay of Ketoconazole during Stability

Formulation	Initial Assay (%)	Initial pH	Final Assay (%)	Visual appearance
F1	99.78	8.5	100.84	No visual changes
F2	97.74	7.5	95.21	No visual changes
F3	101.37	6.5	96.99	No visual changes

3.4. Influence of Butylated Hydroxytoluene on the Stability of Ketoconazole Formulations

The formulation F1 was prepared with BHT, and the formulation F2 was prepared without BHT. The physical appearance of both formulations remained unchanged over a 12-month period. Both retained a homogenous, clear, and viscous liquid form with a characteristic odor and an intense pink-orange color. Minor reductions in pH and relative density were presented in Table 2. The assay of ketoconazole decreased by 2.03% in F1 and 3.59% in F2, indicating a gradual loss of active content over time (Figs.1).

Adding 0.1 % of butylated hydroxytoluene antioxidant does not seem to improve the stability of ketoconazole in the aqueous formulation particularly at pH 6.5.

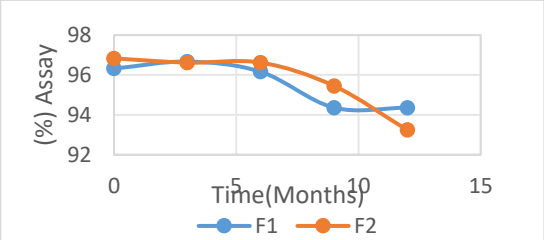

Figure 1. Effect of BHT on Assay of Kketoconazole during Stability.

Formulations	F1		F2	
Parameters	0 month	12 months	0 month	12 months
pH	6.47	6.05	6.50	6.08
Relative density	1.05	1.05	1.06	1.06
% Assay of Ketoconazole	96.32	94.36	96.83	93.24

Table 2. Effect of butylated hydroxytoluene levels on % Assay of Ketoconazole during Stability

4. CONCLUSION

The stability of ketoconazole in shampoo formulations was influenced by both pH and the presence of antioxidant. The formulation at pH 8.5 exhibited the highest stability, while the formulation at pH 6.5 showed the greatest degradation, with a 4.32% decrease in Ketoconazole content. The addition of 0.1% butylated hydroxytoluene (BHT) did not significantly enhance stability, particularly at lower pH. These findings suggest that optimizing the pH of formulation is more critical than addition of antioxidant for maintaining ketoconazole stability in Shampoo products.

REFERENCES

1. Skiba, M., Skiba-Lahiani, M., Marchais, H., Duclos, R., Arnaud, P. *Stability assessment of Ketoconazole in aqueous formulations*. International journal of pharmaceutics, 2000; 198(1): 1–6.

2. ICH Q1A (R2) S*tability testing of new drug substances and products*. Proceedings of the international conference on harmonisation, Geneva, 2003.

ACKNOWLEDGMENT

We would like to extend our gratitude to the colleagues from the Research and Development Department and the company Replek for their invaluable support and contributions to this study.

P048

SEMISOLID 3D PRINTING OF THIN FILMS: INFLUENCE OF LAYER CONFIGURATION AND POLYMER COMPOSITION ON FILM PERFORMANCES

Erna Turković, Ivana Vasiljević, Jelena Parojčić

[1]*Department of Pharmaceutical Technology and Cosmetology, University of Belgrade-Faculty of Pharmacy, Serbia*

1. INTRODUCTION

Semisolid 3D printing offers a versatile approach for preparing thin films with tailored drug loading and microstructural design. While such films are typically developed for immediate release to ensure rapid onset of action, especially in pediatric and geriatric populations, prolonged drug release is often preferred to maintain therapeutic levels and reduce dosing frequency [1]. This study investigates the influence of polymer composition and layer configuration on the mechanical and drug release performance of 3D printed thin films containing paracetamol as a model drug.

2. MATERIALS AND METHODS

2.1. Materials

Hydroxypropyl cellulose (Klucel™ GF, Ashland, USA - HPC) and hydroxypropyl methylcellulose (Methocel™ E4M, Chempoint, USA - HPMC) were used as film-forming polymers. Glycerol served as a plasticizer, and purified water was used as the solvent throughout the formulations. Paracetamol (≥98%, Sigma-Aldrich, USA - PAR) was employed as the model drug.

2.2. Thin film preparation

Dispersions were prepared by heating purified water and glycerol to 80 °C under continuous stirring. Paracetamol (2%) was added to the heated mixture for drug-loaded formulations. Once fully dissolved, the appropriate polymer (HPC or HPMC - 5%) was added gradually. The mixtures were rapidly cooled and stirred continuously on a magnetic stirrer at room temperature for 24 hours to ensure homogeneity and adequate swelling of the polymers. Digital models of the films were designed using Ultimaker Cura 4.13.0 (Ultimaker B.V., The Netherlands) and printed using the Ultimaker 2+ 3D printer via semisolid extrusion. Two shapes were designed: a square and a bone-shaped geometry (according to ISO 507-3 standard for mechanical testing). Printing was conducted layer-by-layer using pre-prepared dispersions. Print parameters included a layer - L height of 0.5 mm with either 3 or 6 total layers, and an infill density of 100% with a line pattern for internal structure. The first layer was printed at 5 mm/min to ensure proper adhesion to the print bed, while subsequent layers were printed at 10 mm/s. The build plate temperature was maintained at 20 °C throughout the process.

2.3. Sample characterization

Thermal properties of HPC and HPMC were analyzed using TGA (Netzsch TG 209F3) and DSC (Netzsch DSC 214 Polyma). Film mass was measured using an analytical balance, and thickness was recorded using a micrometer at five points per film (four corners and one center). Disintegration was tested using a modified method [2], where only the lower half of the film (with a 3 g magnet) was immersed in the water during vertical apparatus movement and the time of magnet detachment was recorded. Drug release was assessed using a flow-through cell (8 mL/min) with glass beads above and below the films. Mechanical testing was performed on a Shimadzu EZ-X universal testing machine (Shimadzu, Japan) at a speed of 5 mm/min until breakage. Tensile strength (TS), elongation at break (EB), and Young's modulus (YM) were calculated.

3. RESULTS AND DISCUSSION

3.1. Results and discussion

TGA confirmed high thermal stability of HPC and HPMC, with degradation onset at 340 °C and 330 °C, respectively well above processing temperatures. DSC showed a broad transition for HPC (265 °C) and no defined events for HPMC, indicating its amorphous nature. Both polymers were thermally suitable for semisolid 3D printing.

Table 1 summarizes the composition and structural characteristics of the prepared film samples, including measured mass - M, thickness - TH, and disintegration time - DT.

Table 1. Composition and properties of 3D printed film samples

P048

Samples	M (mg) ± SD	TH (ηm) ± SD	DT (s) ± SD
HPC 3L	56 ± 3	94 ± 2	64 ± 5
HPC 6L	110 ± 2	223 ± 11	153 ± 2
HPMC 3L	57 ± 3	98 ± 3	67 ± 7
HPMC 6L	135 ± 9	361 ± 9	671 ± 17
HPC/HPMC 3+3L Placebo	118 ± 8	310 ± 9	224 ± 12
Mix 6L Placebo	114 ± 5	295 ± 12	186 ± 14
HPC/HPMC 3+3L+PAR	163 ± 7	413 ± 10	224 ± 10
Mix 6L+PAR	166 ± 3	390 ± 12	182 ± 7

Increasing number of layers and incorporating paracetamol led to higher film mass (56–166 mg) and thickness (94–413 µm), with a corresponding increase in disintegration time (64–224 s). HPMC 6-layer films showed the longest disintegration, while 3-layer HPC films disintegrated the fastest. Disintegration time correlated with film thickness and composition, indicating that thicker, drug-loaded films disintegrated more slowly possibly due to reduced water penetration and increased matrix density.

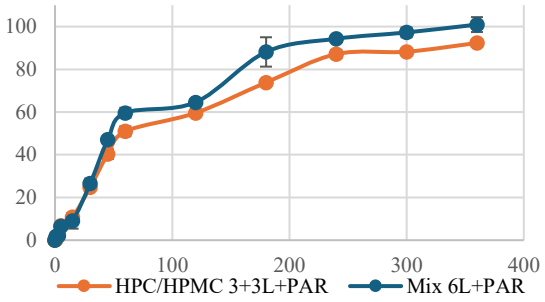

Figure 1. Drug release profiles of layered and mixed polymer films containing paracetamol.

Figure 1 shows that the PAR release from both film types showed a sustained profile over 6 hours. The mixed polymer films released ~100% of the drug, while the layered HPC/HPMC films (3+3 layers) released ~90% within the same time frame, indicating overall similar release behavior. The slight difference may suggest that, while both film types are suitable for prolonged delivery, polymer distribution affects release dynamics, with the more homogeneous matrix in the mixed film likely facilitating earlier drug diffusion. Table 2 shows the mechanical properties of the samples. HPMC 6-layer films showed the highest tensile strength (18.6 MPa) and stiffness (YM 718.2 MPa), while HPC 6-layer films were the most flexible (EB >700%). Mixed and layered placebo films had moderate strength (TS 7.4–8.9 MPa) and elongation (17.5–26.9%). Paracetamol reduced TS to 5.0–6.3 MPa and EB to 14.2–27.9%, suggesting that drug incorporation made the films weaker and less elastic.

Table 2. Mechanical properties of 3D printed samples

Samples	TS (MPa) ± SD	EB (%) ± SD	YM (MPa) ± SD
HPC 3L	3 ± 1	137 ± 5	18 ± 1
HPC 6L	n/a	>700	n/a
HPMC 3L	9 ± 1	7.9 ± 2	329 ± 21
HPMC 6L	19 ± 2	18 ± 2	718 ± 15
HPC/HPMC 3+3L Placebo	9 ± 2	18 ± 7	26 ± 5
Mix 6L Placebo	7 ± 3	27 ± 8.	15 ± 8
HPC/HPMC 3+3L+PAR	5 ± 1	14 ± 4	93 ± 15
Mix 6L+PAR	6 ± 1	28 ± 6	14 ± 1

*n/a – not applicable; sample exceeded the measurement capacity of the device

4. CONCLUSION

HPC- and HPMC-based 3D printed films exhibited distinct mechanical, disintegration, and release behaviors influenced by polymer type, layer configuration, and drug loading. HPMC enhanced film strength, while HPC contributed to flexibility. Increased thickness and drug content led to slower disintegration. Both mixed and layered designs achieved prolonged paracetamol release, confirming their potential for customizable drug delivery.

5. REFERENCES

1. Krause J, et al., 3D printing of orodispersible films via hot-melt extrusion: Personalized therapy for pediatric use. *European Journal of Pharmaceutics and Biopharmaceutics*, 2021, 158, 80–88.

2. Preis, M., e al., Comparative study on novel test systems to determine disintegration time of orodispersible films. Journal of Pharmacy and Pharmacology, 2014, 66, 1102-11.

ACKNOWLEDGMENT

This research was funded by the Ministry of Science, Technological Development and Innovation, Republic of Serbia through two Grant Agreements with University of Belgrade-Faculty of Pharmacy No 451-03-136/2025-03/ 200161 and No 451-03-137/2025-03/ 200161.

P049

EFFECT OF POLYMER CONCENTRATION AND MOLECULAR WEIGHT ON THE ELECTROSPINNING PROCESS

Luca Eva Uhljar[1], Adam Kajari[1], Rita Ambrus[1]

[1]Institute of Pharmaceutical Technology and Regulatory Affairs, University of Szeged, Hungary

1. INTRODUCTION

In solution-based electrospinning, nanofibers are fabricated from a charged polymer solution. The applied electric potential between the charged polymer solution and the grounded collector creates a strong electric field that is essential for the initiation and elongation of the polymer jet, ultimately leading to fiber formation (Fig. 1).

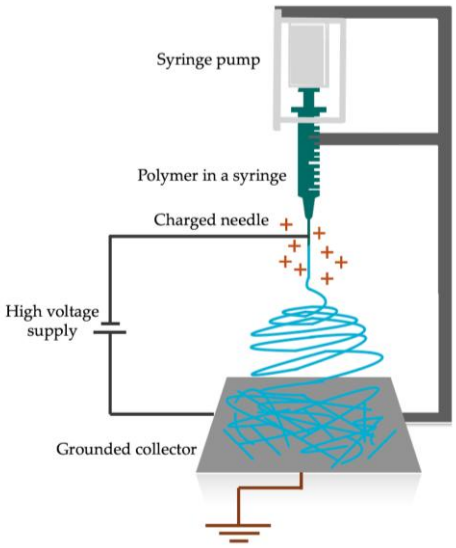

Figure 1. The electrospinning process with charged polymer solution and grounded collector [1].

To achieve a continuous fibrous structure, adequate entanglement of polymer chains is essential. Insufficient chain entanglement can result in the formation of beads, short fibers, or nanoparticles rather than uniform nanofibers [2]. Therefore, the concentration and the molecular weight of the fiber-forming polymer highly affect the nanofiber production and morphology.

This study aimed to investigate the electrospinnability of polyvinylpyrrolidone (PVP) solutions at varying concentrations and molecular weights.

2. MATERIALS AND METHODS

2.1. Materials

The used PVP powders (International Specialty Products, Inc. (ISP), Wayne, NJ, USA) were the following:

- Plasdone K-12 (Mw 3000 – 7000)
- Plasdone C-15 (Mw 10,000 – 16,000)
- Plasdone K-25 (Mw 30,000 – 40,000)
- Plasdone K-29/32 (Mw 45,000 – 58,000).

The solvent was 96% ethanol (Thermo Fisher Scientific Inc., Budapest, Hungary).

2.2. Solution preparation

Solutions of 70, 65 and 60 wt% for Plasdone K-12; 60, 50 and 40 wt% for Plasdone C-15; 50, 40 and 30 wt% for Plasdone K-25 and 40, 30, 20 and 10 wt% for Plasdone K-29/32 were prepared. Then the viscosity of the solutions was determined using a rotational viscometer (IKA Rotavisc me-vi viscometer, IKA-Werke GmbH & Co., Staufen, Germany).

2.3. Electrospinning

The nanofibers were fabricated using a Spincube electrospinning device (Spinsplit Kft., Budapest, Hungary). A 1 mL volume of PVP solution was pumped at a flow rate of 0.3 mL/h through a 22-gauge stainless steel needle positioned 17 cm from a stationary flat collector. The applied voltage was adjusted between 10 and 15 kV to ensure the formation of a stable polymer jet.

2.4. Scanning electron microscopy

The morphology of the electrospun fibers was examined by scanning electron microscopy (SEM; Hitachi S4700, Hitachi Scientific Ltd., Tokyo, Japan). The fiber diameter and distribution were determined using ImageJ 1.53a software (U.S. National Institutes of Health, Bethesda, MD, USA).

P049

3. RESULTS AND DISCUSSION

3.1. Solution viscosity

The two investigated properties, the molecular weight and concentration were related to the viscosity of the polymer solution (Fig. 2).

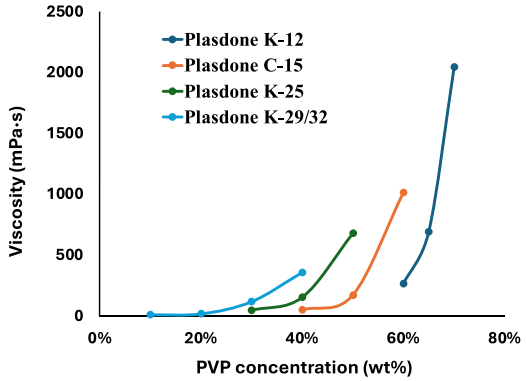

Figure 2. Viscosity of the PVP solutions.

3.2. Nanofiber fabrication

The results demonstrate that both the PVP concentration and the molecular weight played a crucial role in the production of nanofibers. Too high viscosity was disadvantageous as it led to the formation of thick, fragmented structures (Fig. 3.).

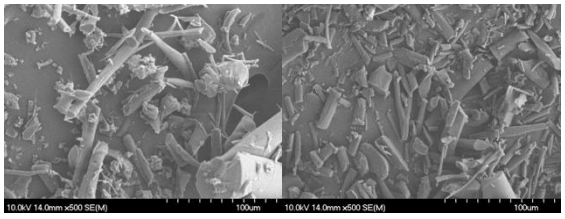

Figure 3. SEM images of the Plasdone K-12 65 wt% (690 mPa·s) and 70 wt% (2043 mPa·s) samples.

On the other hand, too low viscosity resulted in elongated beaded fibers or even spherical nanoparticles (Fig. 4). These results confirm that a suitable viscosity range is key for the successful fabrication of nanofibers.

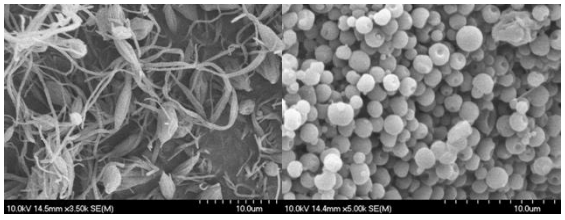

Figure 4. SEM images of the Plasdone K-29/32 30 wt% (114 mPa·s) and 10 wt% (7 mPa·s) samples.

Higher molecular weight PVPs, such as K-25 and K-29/32, provided nanofibers with better morphology (Fig. 5) whereas fiber formation was less consistent and more difficult to control when using lower molecular weight variants such as C-15 and K-12.

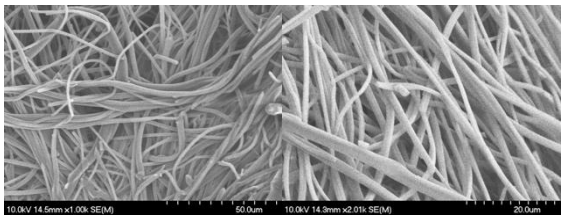

Figure 5. SEM images of the K-25 50% (678 mPa·s) and the K-29/32 40 wt% (353 mPa·s) samples.

3.3. Fiber diameter

The solution viscosity also affected the thickness of the fibers. From higher-viscosity solutions, microfibers were produced (Table 1).

Table 1. Viscosity and diameter of the PVP fibers

Sample name	Viscosity (mPa·s)	Diameter (nm)
K-25_40%	150	578 ± 93
K-29/32_40%	353	1372 ± 510
K-25_50%	678	1782 ± 436

4. CONCLUSION

Viscosity is a key factor for successful electrospinning. Since both polymer concentration and molecular weight affect viscosity, they must be carefully optimized to achieve the desired morphology and diameter.

5. REFERENCES

1. Uhljar, L.É., et al., *Electrospinning of Potential Medical Devices (Wound Dressings, Tissue Engineering Scaffolds, Face Masks) and Their Regulatory Approach.* Pharmaceutics, 2023. 15(2): 417.

2. Uhljar, L.É., et al., *Diclofenac-Loaded Orodispersible Nanofibers Prepared by Double-Needle Electrospinning.* Polymers, 2025. 17(9): 1262.

ACKNOWLEDGMENT

The work was supported by the TKP2021-EGA-32 project.

P050

BRIDGING ACADEMIA AND INDUSTRY IN PHARMACEUTICAL SCIENCES

PREPARING THE NEXT GENERATION FOR A REGULATED AND INNOVATION-DRIVEN EUROPEAN MARKET

Zoltán Ujhelyi

Faculty of pharmacy, Department of industrial, pharmaceutical technology, University of Debrecen

The pharmaceutical industry in Europe is rapidly evolving, shaped by scientific and technological advances, complex regulatory landscapes, and growing global competitiveness. In this context, higher education institutions have a responsibility to adapt and contribute more actively to the development of a future-ready pharmaceutical workforce as the newest department of the faculty of pharmacy, the department of pharmaceutical industrial technology has been established with the clear mission of becoming a key academic and professional hub for industrial pharmaceutical education and research. The department plays a vital role in the teaching of modern pharmaceutical technology and in conducting research and development activities closely aligned with industrial pharmaceutical manufacturing. Our goal is to provide students with high-quality, practice-oriented training that meets the current and future needs of the pharmaceutical industry. To this end, we maintain strong, active collaborations with both Hungarian and international industry partners. These partnerships foster scientific and technological innovation while offering real-world insight into the pharmaceutical product lifecycle. Special emphasis is placed on forming long-term, mutually beneficial collaborations with industrial stakeholders — partnerships that support the strategic goals of the faculty and the university, while simultaneously contributing to the sustainable development of the pharmaceutical sector. By integrating external expertise into our teaching and research activities, we aim to reduce the gap between academic knowledge and industry expectations. Incorporating an industrial mindset into pharmaceutical education is no longer optional — it is essential. Today's students must understand not only formulation science or process validation, but also the regulatory environment of gmp production, quality systems, and European marketing authorization pathways. Beyond technical skills, they must also be introduced to the fundamentals of pharmaceutical business models, innovation management, and the cost-efficiency logic behind modern drug development. Academic programs that mirror real-world challenges are fundamental in ensuring that pharmacy graduates are prepared to work in highly regulated, interdisciplinary environments. The department of pharmaceutical industrial technology is committed to nurturing this new generation — future professionals who will not only meet the high standards of the European pharmaceutical system but actively shape its evolution.

Building a stronger bridge between academia and industry is a strategic imperative. It ensures the relevance of pharmaceutical education, supports innovation, and most importantly, enables us to train competent, skilled, and adaptable professionals who are ready to contribute meaningfully to the health systems and pharmaceutical economies of Europe.

P051

FUNCTIONALITY-RELATED CHARACTERISTICS OF CO-PROCESSED EXCIPIENTS FOR EXTENDED DRUG RELEASE

Ivana Vasiljević, Erna Turković, Jelena Parojčić

Department of Pharmaceutical Technology and Cosmetology, University of Belgrade-Faculty of Pharmacy, Serbia

1. INTRODUCTION

Direct compression represents a favourable tablet manufacturing method but requires exceptional powder processability, especially at high drug loads. This limitation can be addressed using co-processed excipients (CPEs), which represent a combination of two or more excipients specifically processed to enhance physicochemical properties compared to their physical mixtures [1]. Although several hypromellose-based CPEs for extended-release (ER) tablets are available on the market, data on their performance and functionality-related characteristics remain limited [1]. The aim of this study was to evaluate CPEs for ER tablets, focusing on their flowability, tableting performance and dissolution, when high drug load is added.

2. MATERIALS AND METHODS

2.1. Materials

Two ER CPEs were used in this study: (1) RetaLac® (RL, Meggle Pharma) containing 50% milled alpha-lactose monohydrate and 50% hypromellose; (2) Pearlitol® CR-H (PL, Roquette) containing 30% D-mannitol and 70% hypromellose. Sodium stearyl fumarate (SSF, JRS Pharma) was used as a lubricant and caffeine (Fagron) as a model drug with high aqueous solubility. Dissolution medium contained monobasic potassium phosphate and sodium hydroxide (Sigma Aldrich).

2.2. Methods

In order to evaluate CPE performance, these excipients were tested: i) individually, and ii) in combination with either SSF (1%), CAF (50%) or both. Particle size analysis of CPE powders was measured by laser diffractometer (Anton Paar PSA 1190) and powder true density, used for solid fraction calculations, using gas pycnometer (Anton Paar Ultrapyc 5000). Powder flowability was estimated based on the Carr index and Hausner ratio calculations.

Powder samples were compressed by a single-punch laboratory tablet press (GTP series D) using compression loads of 125–500 kg, with the increment of 75 kg, i.e. compression pressure (CP) 44–174 MPa. The measured force-displacement curves were used to calculate detachment (DS) and ejection stress (EJ). The obtained compacts (100 mg, Ø 6 mm) were characterized regarding weight, thickness, diameter and hardness (Erweka TBH 125D). Subsequently, tensile strength (TS) and solid fraction (SF) were calculated and assessed using the compressibility (CP vs. SF), compactibility (SF vs. TS) and tabletability plots (CP vs. TS), with particular focus on CP and TS required for obtaining 0.85 solid fraction compacts. Samples for dissolution testing were prepared as Ø 13 mm tablets (500 mg) using eccentric tablet press (Erweka Korsch EK 0).

Dissolution test was performed in a modified rotating paddle apparatus (Erweka DT 126 light), with the addition of a disc on the bottom, to prevent tablet sticking. Paddle rotation speed was 50 rpm and 900 ml of phosphate buffer (pH 6.8) was used as the medium. The amount of CAF dissolved was determined using UV-VIS spectrophotometer (Thermo Scientific Evolution 300), at 273 nm.

3. RESULTS AND DISCUSSION

The investigated CPEs exhibited comparable particle size and narrow particle size distribution. Carr index of the investigated powder blends ranged from 23.8 (PL) to 27.7% (RL with 50% CAF), corresponding to passable to poor flowability. CPE flowability was not notably affected neither by the addition of CAF nor subsequent addition of SSF. This indicated that RL and PL exhibited high dilution capacity and compensated poor flowability of a high load of model drug.

Compression-related parameters of the investigated CPE blends are presented in Fig. 1. Generally, PL outperformed RL, but the CPE blends containing SSF and CAF exhibited comparable properties.

P051

RL exhibited high values of detachment (2.02–5.49 MPa) and, particularly, ejection stress (2.23–10.43 MPa). This indicates a need for lubricant addition, since ejection stresses lower than 3 MPa are recommended to prevent tablet capping or lamination [3]. PL exhibited lower detachment (1.16–3.90 MPa) and ejection stress values (1.02–2.13 MPa). Addition of SSF decreased detachment and ejection stress values, particularly in the case of RL.

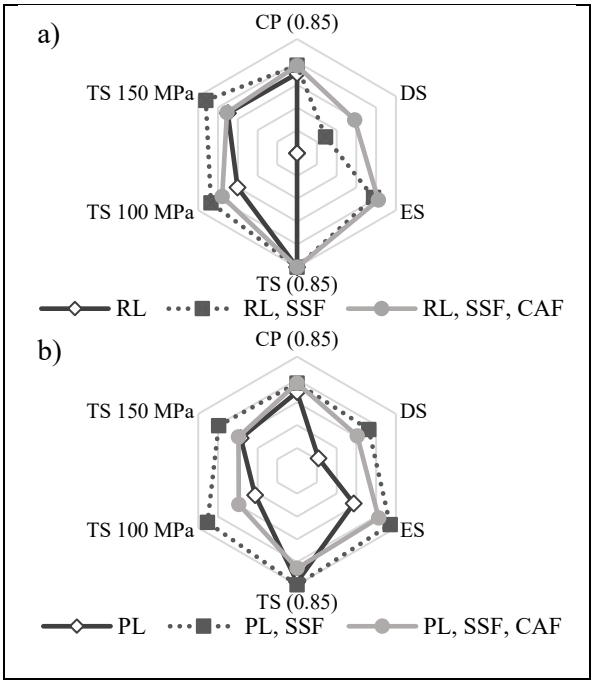

Figure 1. Compression-related parameters of the investigated CPEs: a) RL-blends b) PL-blends.

The investigated CPEs exhibited comparable compactibility and compressibility. CPE compacts with 0.85 solid fraction exhibited tensile strength higher than 2 MPa (2.65 and 2.25 MPa for RL and PL, respectively), which is considered acceptable for further processing. Tensile strength of compacts prepared from blends with CAF and SSF was 1.21 and 1.62 MPa (at 0.85 SF), indicating lower mechanical endurance. Addition of CAF and SSF enhanced CPE compressibility, i.e. lower compression pressure was required for obtaining compacts with high solid fraction (e.g. 0.85 SF obtained at ~174 MPa and ~97 MPa, for CPE powders and blends with CAF and SSF, respectively). Additionally, powder blends exhibited favourable tabletability to CPE powders, which may be attributed to CAF cohesiveness, promoting interparticulate binding.

The obtained CAF dissolution profiles from the ER tablets are exhibited in Fig. 2. The profiles followed the Korsmeyer-Peppas model ($R^2 > 0.9965$), suggesting the drug release mechanism governed by a combination of diffusion and polymer relaxation. The obtained profiles were similar, in spite of differences in the CPE composition (filler type and its solubility: lactose vs. mannitol; hypromellose content: 50 or 70%, i.e. 25 and 35% in the prepared compacts, for RL and PL, respectively). It may be postulated that somewhat higher solubility of mannitol compensated higher hypromellose content, while slower lactose dissolution may have moderated drug release in the RL matrix.

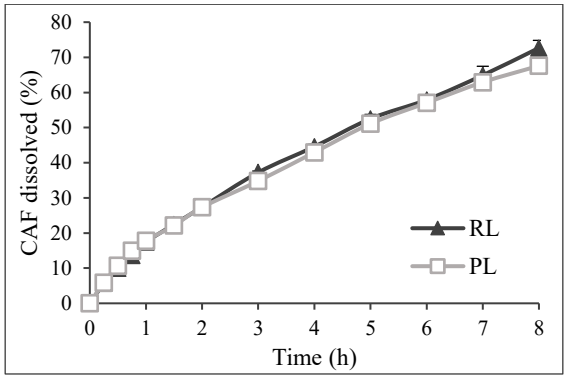

Figure 2. CAF dissolution profiles

4. CONCLUSION

The investigated CPEs, namely RetaLac® and Pearlitol® CR-H, exhibited comparable properties in terms of particle size, flowability and tableting behaviour, as well as drug dissolution. The addition of high load of model drug (50%) did not notably affect CPE properties, indicating their high dilution capacity, favourable for further processing.

5. REFERENCES

1. Li, Z, et al., *Composite Particles Based On Particle Engineering For Direct Compaction*. International Journal of Pharmaceutics, 2017. 519(1-2): 272-86.

2. Pitt, K.G., et al., *Compression prediction accuracy from small scale compaction studies to production presses*. Powder Technology, 2015. 270: 490-493.

ACKNOWLEDGMENT

This research was funded by the Ministry of Science, Technological Development and Innovation, Republic of Serbia through two Grant Agreements with University of Belgrade-Faculty of Pharmacy No 451-03-136/2025-03/ 200161 and No 451-03-137/2025-03/ 200161.

P052

TECHNOLOGICAL DEVELOPMENT OF BIOEQUIVALENT OMEPRAZOLE PRODUCT

David Vetchý[1], Gulzina Kumisbek[1], Jiří Zeman[1], Miroslava Pavelková[1], Kateřina Kubová[1]

[1]Department of Pharmaceutical Technology, Faculty of Pharmacy, Masaryk University, Czech Republic

1. INTRODUCTION

Proton pump inhibitors (PPIs) are the primary drugs used to treat acid-related diseases of the upper gastrointestinal tract due to their highly selective inhibitory effect on the acid-forming function of the stomach. The primary drug from the PPI group is omeprazole, which was synthesized in 1979 after discovering a unique enzyme, K+-stimulated ATPase, in parietal cells during experiments on the gastric mucosa [1]. In 2023, omeprazole was found to be the third most commonly prescribed chemical substance in England, with the drug listed on approximately 35 million prescriptions [2]. The localization of pharmaceutical drug production is one of Europe's primary strategies to ensure that the population has access to affordable and good-quality medicines. This study describes the technological development of bioequivalent delayed-release omeprazole.

2. MATERIALS AND METHODS

2.1. Active coating

In this step, omeprazole suspensions from two suspensions, IA and IB, were coated on inactive microcrystalline cellulose cores. Suspension IA was prepared by mixing the following ingredients: Omeprazole, lactose monohydrate, sodium lauryl sulfate, and di-sodium phosphate dodecahydrate in purified water. The second, IB, a solution of HPMC and HPC, was prepared by dispersing the components in purified water heated to 80 °C followed by slow cooling at room temperature for 3 hours.

Parts IA and IB were then mixed and sprayed onto inactive cores in fluidized bed coaters: Medipore, Czech Republic – for laboratory scale batches, Aeromatic-Fielder AG, Switzerland, FBD Bosch pilotlab L, Germany – for pilot scale batches.

2.2. Protective coating

The protective coating solution was prepared by gradually adding pre-weighed HPMC to the purified water while continuously stirring until completely dissolved and homogenized. After that, Solution was sprayed onto the active cores in fluidized bed coaters using the same parameters as used in step I, Active coating.

2.3. Enteric coating

First, a titanium dioxide suspension was prepared by adding a weighed amount of titanium dioxide to the purified water and mixing until being homogeneous. In order to obtain the dispersion for enteric coating, Eudragit L30-D55, PlasAcryl, and the prepared titanium dioxide suspension were added to weighed purified water with continuous stirring using an overhead stirrer for at least 120 minutes.

2.4. Dissolution study

Dissolution tests were performed according to the USP monograph by using the "Distek 2500" dissolution tester (USP type II apparatus with a paddle) at a stirrer rota-tion speed of 100 rpm and the dissolution medium temperature of 37.0 ± 0.5 ºC. An acid resistance test was performed in a dissolution medium of 500 ml of 0.1 M hydrochloric acid (HCl) pH 1.2 for 2 hours. After two hours, for the dissolution buffer stage, 400 mL of 0.235 M dibasic sodium phosphate was added to the 500 mL of 0.1 M hydrochloric acid medium in the vessel and adjusted, if necessary, with 2 M hydrochloric acid or 2 M so-dium hydroxide to the pH of 6.8 ± 0.05.

2.5. Bioequivalence study

The objective was to compare the rate and extent of absorption followed by a bio-equivalence assessment of the generic and Losec (originator) drugs after a single dose of each drug at a dose of 40 mg.

P052

3. RESULTS AND DISCUSSION

3.1. Active coating

Cellets®500 (500-710 µm) was changed to Cellets®700 (700-1000 µm) because of the small size of the pellets led to stick together.

3.2. Protective coating

The quantity of HPMC was increased from 7.97% to 8.67% to achieve a better protective layer.

3.3. Enteric coating

The quantity of Eudragit® L30-D55 was increased to achieve better enteric layers. The final qualitative and quantitative composition of the developed formulation is presented in Table 1.

Table 1. The final qualitative and quantitative composition in a capsule.

Components	Function	Quantity in mg
Omeprazole	API	40,00
Lactose monohydrate	Filler	34,00
Sodium lauryl sulfate	Solubilizer	1,20
Sodium pyrophosphate dodecahydrate	Buffer agent	5,20
HPMC	Film-former/ Binder	39,60
HPC	Film-former/ Binder	2,00
Cellets 700	Neutral Cores	285,24
Titanium dioxide	Colorant	2,00
Talc	Lubricant	0,80
Eudragit L30-D55 (dry matter)	Enteric coating agent	39,96
PlasAcryl (dry matter)	Anti-tacking /Plasticizer	6,80

3.4. Dissolution study

The amount of omeprazole released at pH 1.2 was evaluated at a single point in 120 minutes. The test and reference drugs released from 3.0% to 10.6% and 1.3% to 5.7% of the omeprazole, respectively. A comparison of dissolution profiles of the test drug and the reference drug Losec at pH 6.8 is shown in Fig 1.

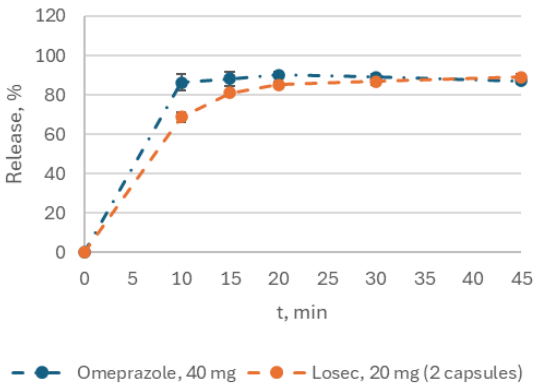

Figure 1. Comparison of dissolution profiles of the test drug and the reference drug Losec at pH 6.8.

3.3. Bioequivalence study

Fig. 2 shows the average pharmacokinetic profiles of omeprazole after the administration of the test and reference drugs.

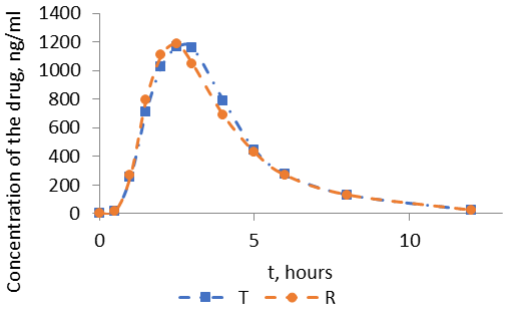

Figure 1. Averaged pharmacokinetic profiles of the test drug and the reference drug.

4. CONCLUSION

A bioequivalent delayed-release formulation of omeprazole has been developed for the market.

5. REFERENCES

1. Sachs G., *Proton pump inhibitors and acid-related diseases*. Pharmacotherapy, 1997, 17(1): 22-37

2. *Leading chemical substances dispensed in England in 2023, by number of items*. Available from: https://www.statista.com/statistics/378445/prescription-cost-analysis-top-twenty-chemicals-by-items-in-england// Accessed 25 Feb 2025.

P053

OPTIMIZATION OF RADIAL EXTRUSION WITH SPHERONIZATION USING ADVANCED EXPERIMENTAL DESIGNS

Aljoša Gradišek[1, 2], Klemen Korasa[1, 2]

[1]Krka d. d., Novo mesto, Slovenia
[2]Faculty of Pharmacy, University of Ljubljana, Slovenia

1. INTRODUCTION

Process Analytical Technology (PAT), as defined by the FDA is a system for designing, analyzing, and controlling manufacturing through real-time measurements of critical quality and performance attributes, ensuring final product quality. Among PAT tools, Design of Experiments (DoE) is essential for systematically exploring the effects of formulation and process variables on product properties [1]. PAT is especially valuable in complex operations like radial extrusion with spheronization, where precise control is essential for achieving consistent product quality. In development of new pharmaceutical dosage forms, formulation and process parameters are typically optimized in parallel, as they are often interdependent. The present study investigated the feasibility of using a Mixture–Process Variable DoE to simultaneously optimize both formulation composition and process parameters. To improve efficiency, a KCV (Kowalski–Cornell–Vining) design was employed, which supports key model terms while reducing the number of experimental runs compared to full factorial Cartesian designs. The goal was to develop and refine a carvedilol-based pellet formulation, intended for film coating, by identifying critical material attributes and process parameters using advanced experimental designs to ensure robust and reproducible manufacturing.

2. MATERIALS AND METHODS

2.1. Materials

Pellets were manufactured using carvedilol (Krka d. d., Novo mesto) as the model API. The excipients included microcrystalline cellulose (MCC; Avicel® PH-102; International Flavors & Fragrances Inc.; USA), lactose monohydrate (Granulac® 200; Meggle GmbH & Co. KG; Germany) and hydroxypropylmethyl-cellulose (HPMC; Pharmacoat® 606; Shin-Etsu; Japan). Purified water was used as a granulation liquid.

2.2. Preparation and evaluation of pellets

Wetted mass for extrusion was prepared by high shear granulation (HSM; Gea UltimaGral™ 25; GEA; Germany) of carvedilol, MCC, lactose monohydrate and HPMC with purified water. The mass was extruded and spheronized using a radial extruder and spheronizer (Gea NICA™ IPS25; GEA; Germany), then dried in a fluid bed dryer (GEA MP-1 S; GEA; Germany). The aim was to produce pellets with narrow particle size distribution, high sphericity, a high proportion of particles within the 0.63–1.00 mm range, and maximized process yield. Pellet characteristics were analyzed using a Camsizer XT image analyzer (Retsch Technology, Germany). Optimization was conducted in three phases. First, preliminary experiments to define feasible operating ranges of key process parameters. Second, a Plackett–Burman screening design to identify significant process parameters affecting critical quality attributes. Third, a combined Mixture–Process Variable DoE (KCV design) to simultaneously optimize the formulation and the process parameters that were defined as significant in the previous step. Experimental design and analysis were performed using Design Expert® version 13 (Stat-Ease, Inc., USA).

3. RESULTS AND DISCUSSION

3.1. Plackett-Burmann screening design

Based on the outcomes of preliminary experiments, the limits of key process parameters were established and used to construct a Plackett–Burman screening design comprising 11 factors. During the preliminary phase extrusion screen with openings of 0.8 × 0.7 mm was selected and used in all further experiments. The following factors were evaluated in the screening study: homogenization time (30–90 s), water quantity (40–70 mg/unit), spraying speed (75–150 g/min), impeller speed (200–425 rpm) and chopper speed (0–1000 rpm) during the spraying phase, kneading time (30–60 s), impeller speed (300–425 rpm) and chopper

speed (1500–3000 rpm) during the kneading phase, as well as spheronization time (60–240 s) and spheronization speed (200–800 rpm). The selected response variables were: width of particle size distribution, sphericity, proportion of pellets within the 0.63–1.00 mm size range, and process yield. Significant factors influencing each response were identified using automatic model term selection via forward selection, with a significance threshold of $p < 0.1$. The results are presented in **Table 2**. Three factors, water quantity, spheronization speed, and spheronization time, were found to have a significant impact on at least one response and were therefore selected for further optimization using the Mixture–Process Variable DoE.

Table 2. Significant factors in screening DoE.

Response	Significant factors
Width of particle size distribution	Water quantity ($p = 0.0006$) Spheronization speed ($p = 0.0123$)
Sphericity	Water quantity ($p = 0.0138$) Spheronization speed ($p < 0.0001$) Spheronization time ($p = 0.0485$)
Particle size 0.63–1.0 mm	Spheronization speed ($p < 0.0001$)
Process yield	Water quantity ($p = 0.0829$)

3.2. Mixture-Process Variable DoE (KCV design)

To simultaneously optimize both the formulation and process parameters, a 3 × 3 Mixture–Process Variable DoE (KCV design) was used (**Table 3**). The design included 29 experimental runs: 21 model points, 5 lack-of-fit points, and 3 center point replicates.

Table 3. Factors in KCV design.

Mixture components	Process parameter
MCC (40–50 mg)	Water quantity (40–70 mg)
Lactose monohydrate (24–38 mg)	Spheronization speed (400–800 rpm)
HPMC (2–6 mg)	Spheronization time (60–240 s)
Total = 80 mg	

Each response was initially analyzed individually. Numerical optimization was then performed to determine the optimal combination of formulation and process parameters. The objectives were to minimize the width of particle size distribution and maximize the sphericity, proportion of particles in desired size range and process yield. The most preferred solution with desirability score of 0.955 is presented in **Table 4**. The optimal solution favoured higher amounts of MCC, and lower amounts of lactose monohydrate and HPMC. At the higher levels of HPMC, especially when combined with high water content, pellet agglomeration was observed during spheronization. Lower water quantities led to increased fines formation, which explains the preference for higher water levels. Both spheronization time and speed were found to be optimal at intermediate values within their respective ranges.

Table 4. Most desirable solution from numerical optimization.

Factor	Optimal value
MCC	49.7 mg
Lactose monohydrate	28.3 mg
HPMC	2.0 mg
Water quantity	66.9 mg
Spheronization time	167 seconds
Spheronization speed	615 rpm

4. CONCLUSION

This study demonstrated the successful application of a Mixture–Process Variable DoE approach to simultaneously optimize formulation composition and process parameters for the development of carvedilol pellets. Key process variables, water quantity, spheronization speed, and time, were identified through a Plackett–Burman screening design, while formulation and process optimization was achieved using a combined experimental design. The approach enabled robust identification of critical factors and produced pellets with desirable quality attributes, including narrow size distribution, high sphericity, and high yield. These findings support the feasibility of integrated formulation–process development in line with PAT principles and highlight the potential of this strategy for future pharmaceutical product development.

5. REFERENCES

1. FDA. Guidance for Industry PAT — A Framework for Innovative Pharmaceutical Development, Manufacturing, and Quality Assurance, 2004.

ACKNOWLEDGMENT

This research has been supported by Krka, d. d., Novo mesto.

P054

DEVELOPMENT OF NON-DESTRUCTIVE METHOD FOR ASSESMENT OF CONTENT UNIFORMITY OF METOCLOPRAMIDE IN BUCCAL FILMS BASED ON NIR SPECTROSCOPY

Blaž Grilc[1], Odon Planinšek[1]

[1]Department of Pharmaceutical Technology, Faculty of Pharmacy, University of Ljubljana, Slovenia

1. INTRODUCTION

Film formulations intended for buccal application are not yet a widely integrated dosage form in pharmacy, although they were introduced decades ago. There are physiological and technological limitations that prevent their wider acceptance. This study focused on the technological aspects of buccal film preparation. Buccal films are usually produced by the solvent casting method, in which a viscous liquid containing a film composition is continuously casted on the moving liner. The thickness of the casting defines the dose of drug per surface area, which is a critical production parameter [1]. The issue of dose uniformity between films also depends on the drying process. When the drug content per film mass is expressed, the residual moisture in the film plays an important role. During the drying process, there is a risk of uneven evaporation of moisture, which leads to uneven mass of the films. The aim of this study was to develop a method for determination of drug concentration in the buccal films using NIR spectroscopy.

2. MATERIALS AND METHODS

2.1. Materials

The buccal film formulations contained sodium alginate polymer (Protanal 10/60, FMC BioPolymer, USA), xylitol (Xylisorb DC100, Roquette, France) as plasticiser and the drug metoclopramide hydrochloride monohydrate - MCP (Biosinth, Slovakia). Protective layer consisted of hydroxypropyl cellulose (Klucel ELF, Ashland, USA).

2.2. Preparation of buccal films

The solvent casting solution contained sodium alginate (3-5 %), xylitol (1-2 %) and MCP (0.8-1.4 %). Multiple combinations of ingredients were utilized to obtain films with various amounts of the drug. The solution was spread on a glass plate using applicator ZUA2000.S (Zehntner, Switzerland) at 1500 μm thickness. Films were dried in a convection dryer (SP -45, Kambič, Slovenia). The protective layer consisted of 20 % solution of HPC and was casted over the drug containing layer at thickness of 1000 μm. The bilayer film was dried at 40 °C for 60 min and cut in 20x30 mm size.

2.3. Transflectance NIR spectroscopy

The NIR spectroscopy of bilayer films were performed using NIR MPA (Bruker Optics, Germany) in reflectance mode. The films were placed over the measuring window of spectrometer and covered with flat aluminium weight that reflected the light back to the detector. The NIR spectra were obtained after 16 acquisitions at resolution of 16 cm^{-1} in the range from 12500 to 3600 cm^{-1}.

2.4. Drug content evaluation

The drug content in the films was evaluated using the classical approach of dissolving the films in water and determining the concentration of MCP in the solution. The absorbance was measured at 309 nm using a UV-Vis spectrometer (Carry 60, Agilent, USA). The spectra of all excipients were evaluated, and their absorbance range did not interfere with the measurement wavelength.

2.5 Preparation of the predictive model

The concentrations of MCP obtained by UV-vis spectroscopy were used as a reference value to calibrate the model for predicting drug content from NIR spectra. The prediction model was built with the use of Quant 2 chemometric module of software OPUS 8.1 (Bruker Optics, Germany). Total of 29 reference spectra was linked with the MCP concentration value on which the chemometric model was built. The optimal range of wavelengths was determined by cross-validation using the “leave one out” approach.

P054

3. RESULTS AND DISCUSSION

3.1. Challenges regarding formulation preparation

Buccal films based on sodium alginate have the structure of a gel. The polymer usually contains a certain amount of moisture to maintain its flexibility and shape. In our formulation, the water content in the films varied between 3.9-6.0% depending on the position of the film on the glass plate. The moisture content affects the mass and thickness of the film but should not affect the MCP dose per film. The fluctuating moisture content was the main concern for correct measurement using NIR spectrometry. Two aspects were in the foreground. Firstly, the NIR spectra are affected by the presence of water and secondly, the films with higher moisture content are thicker, so the light path through the sample is extended.

3.2. Selecting the optimal test samples for calibration model

Several batches of buccal films were prepared on a glass plate. The films were positioned in the shape of the matrix. The NIR spectra were obtained from all films, but the MCP content was determined by UV-Vis spectroscopy for only seven films per batch. To select the most representative films for content measurement, the samples were positioned on the diagonal of the matrix. In this way, the possible moisture gradient in the x- or y-direction of the matrix was compensated. The moisture gradients were present because the films were dried in the dryer with forced convection. The side of the glass plate closer to the heat source contained less moisture than the side facing the door of the dryer. To further minimize the error, the MCP content was normalized to the mass of the film.

3.3. Validation results of predictive model

The calibration of the model was performed by training with test data by randomly sampling one of the spectra as a test object. The optimal spectral range was determined by the cross-validation experiments in which the model showed the best fit to the test data. The spectral range finally chosen was between 7504 and 4248 cm^{-1}. The model was built on 408 spectral points and correlated with the measured concentration value. The optimal R^2 value was 0.998 with an RMSE of 0.076.

3.4. Concentration mapping of MCP in production batch

The validated model was used to analyze the spectra of each buccal film produced. The concentration map is shown as a contour plot in Figure 1. The results demonstrate that the MCP concentration can vary at the edges of the film batch, which was expected. In general, the buccal films at the edge of the batch are discarded as waste and only the formulations in the center of the batch are further used.

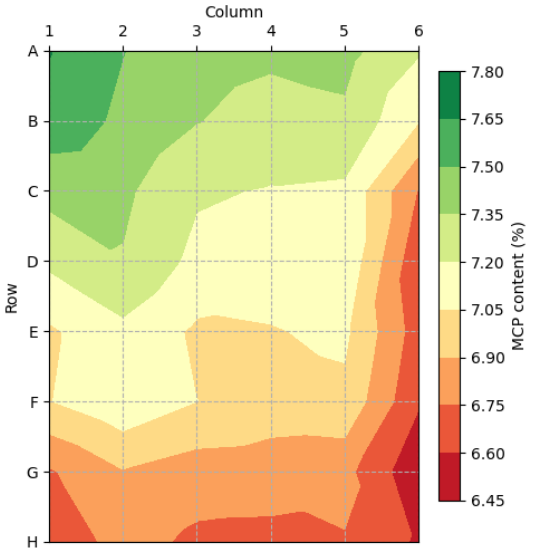

Figure 1. Concentration of MCP in bilayer buccal film batch presented as a contour map.

4. CONCLUSION

The use of NIR spectroscopy has been recognized as a useful method for determining MCP concentration in buccal bilayer films. Despite the variability in moisture and excipient content, the model showed high reliability. The measured precision was ±1.3%, which is acceptable for a non-destructive method. This method could serve as a process analytical tool for online quality control in the production of buccal films.

5. REFERENCES

1. Shipp, L.; Liu, F.; Kerai-Varsani, L.; Okwuosa, T.C. Buccal Films: A Review of Therapeutic Opportunities, Formulations & Relevant Evaluation Approaches. *J. Control. Release* **2022**, *352*, 1071–1092

ACKNOWLEDGMENT

The authors acknowledge financial support from the Slovenian research and innovation agency (research core funding, no. P1-0189)

P055

ADVANCED SKIN PERMEATION STRATEGY: NOVEL FORMULATIONS FOR LIDOCAINE DERMAL DELIVERY

Feria Hasanpour[1], Mária Budai-Szűcs[1], Anita Kovács[1], Péter Simon[2] Levente Törteli[2], Eszter Ducza[3] Adrienn Seres-Bokor[3], and Szilvia Berkó[1]

[1]Institute of Pharmaceutical Technology and Regulatory Affairs, University of Szeged, Hungary
[2]Institute of Pharmaceutical Chemistry, University of Szeged, Hungary
[3]Institute of Pharmacodynamics and Biopharmacy, University of Szeged, Hungary

1. INTRODUCTION

Effective topical dermal delivery of lidocaine requires overcoming the skin barrier and enabling drug passage into the nerve cells to block voltage-gated sodium channels. This process depends on balancing ionized and non-ionized forms of lidocaine or using suitable carriers and penetration enhancers. In this study, we explore two novel formulation strategies: a hydrophilic hydrogel system containing natural deep eutectic solvent (NADES) and a nanostructured lipid carrier (NLC) gel, using 2% lidocaine base. By comparing these distinct approaches with conventional ointment and hydrogel, we aim to optimize skin penetration, accelerate the onset of action, and enhance Local anesthetic and analgesic efficacy.

2. MATERIALS AND METHODS

2.1. Materials

Lidocaine was obtained from Sigma-Aldrich. Apifil (PEG-9 beeswax) and Miglyol® 812 N (caprylic/capric triglyceride) was gifted by Gattefossé (St. Priest, France) and Sasol GmbH (Hamburg, Germany) respectively. Kolliphor RH 40 (PEG-40 hydrogenated castor oil) was supplied by BASF SE Chemtrade GmbH (Germany). hydroxyethyl cellulose (HEC), sodium citrate (Na citrate), macrogol 400, and macrogol 1500 were obtained from Hungaropharma Ltd. (Budapest, Hungary**).** Natural deep eutectic solvent (NADES) mixtures were gifted from the Faculty of Technology, University of Novi Sad (Novi Sad, Serbia). Filtered and deionized water (Millipore Milli-Q, Milford, MA, USA) was used throughout the experiment.

2.2. Preparation and characterization of NADES gels

NADES was used in hydrogel formulations to increase the solubility and skin permeation of lidocaine. In terms of technological aspects, 3^2 full factorial design was used to optimize the pH of the formulation and concentration of NADES. The characterization of the optimized system was performed by XRD, Raman and NMR spectroscopy.

2.3. Preparation and characterization of NLC gels

NLCs containing lidocaine, based on 2^3 factorial design, were prepared and physicochemical properties of the formulations were investigated (particle size, zeta potential, crystallinity, encapsulation efficiency).

2.4. Biopharmaceutical investigations

Biopharmaceutical investigations, such as *in vitro* release tests (IVRT) and *in vitro* permeation tests (IVPT), were performed using vertical Fanz diffusion cell to evaluate the efficacy of dermal formulations compared with traditional ointment and hydrogel. The quantitative measurements were supported by qualitative Raman mapping which visualized the active ingredient in different skin layers.

2.5. *In vivo* tail flick experiments

The male Sprague-Dawley rats (300 to 330 g) were obtained and divided into the following groups (n = 6): 2% lidocaine containing groups: 1, NLC gel; 2, NADES gel; 3, ointment; 4, hydrogel; In the control groups (n = 6), rat tails were treated topically only with 250 µL of distilled water. The tail flick latency of rats was measured by the Tail Flick Unit - Thermal stimulation (Ugo Basile, Italy). 250 mg test samples were applied to two-thirds of the distal part of each rat tail, and the reaction time was measured at regular time intervals (0, 5, 10, 15, 30, 45, and 60 min) by exposing the analgesiometer to 35 IR radiation. The cutoff time for basal reaction was fixed at 20 s to prevent injury.

P055

3. RESULTS AND DISCUSSION

3.1. Evaluation of physicochemical properties of the systems

Both the optimized NADES gel and NLC gel formulations underwent comprehensive physicochemical and structural evaluations. The NADES gel, with pH of 4.46 and viscosity of 11212 mPa*s was selected. XRD analysis indicated lidocaine molecularly dispersed in the system. Further structural characterization using Raman and NMR spectroscopy verified the chemical stability of lidocaine in the NADES environment, even under acidic conditions [1]. Among the various NLC formulation one formulation was selected based on experimental design with a zeta potential of −44 mV, a particle size of 255 nm, and encapsulation efficiency of 94 % [2]. DSC and XRD analyses confirmed a dispersed lidocaine state within the NLC matrix. No signs of aggregation or phase separation were detected during storage, indicating structural stability appropriate for topical use.

3.2. Results of *in vitro* drug permeation

Both innovative formulations significantly improved lidocaine skin permeation and dermal deposition compared to conventional ointment and hydrogel. Raman spectroscopy mapping visualized deeper skin penetration for both innovative dermal drug delivery systems within 3 hours, as shown in Figure 1.

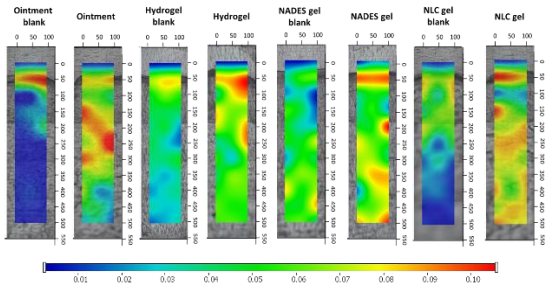

Figure 1. Raman correlation mapping of lidocaine penetration depth in skin layers: Comparison of reference ointment and hydrogel with NADES and NLC gel.

3.3. Results of *in vivo* studies

In vivo evaluation using the murine tail flick model confirmed the superior anaesthetic efficacy of NLC gel. The NLC gel produced prolonged and longer effects compare to other formulations (Fig. 2).

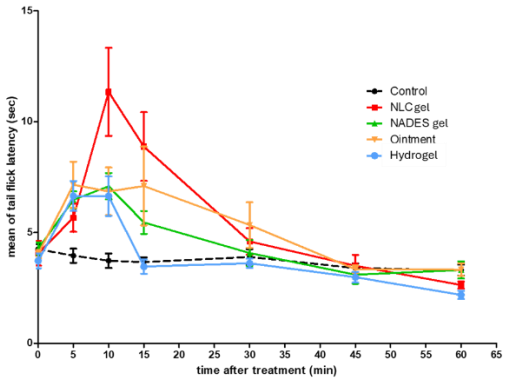

Figure 2. Results of tail flick test.

4. CONCLUSION

Physicochemical characterizations confirmed the stability of both systems. These findings demonstrated the effectiveness of NLC gel and NADES gel as advanced delivery systems for enhancing the skin permeation and biological effect of lidocaine.

5. REFERENCES

[1] Hasanpour, F. *et al.*, *The role of natural deep eutectic solvents in a hydrogel formulation containing lidocaine.* Pharmaceutics, 2025. 17(3): 324.

[2] Hasanpour, F. *et al.*, *Improvement of lidocaine skin permeation by using passive and active enhancer methods.* International Journal of Pharmaceutics, 2024. 660: 124377.

ACKNOWLEDGMENT

Project no. TKP2021-EGA-32 has been implemented with the support provided by the Ministry of Innovation and Technology of Hungary from the National Research, Development and Innovation Fund.

P056

COMPARISON OF BATCH AND CONTINUOUS WET GRANULATION OF A LOW DOSE POWDER MIXTURE, FOCUSSING ON THE PROPERTIES OF THE RESULTING GRANULES AND TABLETS

Zoran Lavrič[1], Eva Rotar Pucko[2], Rok Dreu[1]

[1]Department of Pharmaceutical Technology, Faculty of Pharmacy, University of Ljubljana, Slovenia
[2]Krka d. d., Novo mesto, Slovenia

1. INTRODUCTION

Continuous manufacturing has the potential to become the preferred manufacturing method of the future in pharmaceutical production as it offers many advantages, from increased efficiency, agility and flexibility in manufacturing to improved product availability and quality for patients [1]. However, there is a large gap between the theoretical advantages and the widespread acceptance of continuous manufacturing. This is because there is a lack of widespread awareness, knowledge and expectations about what continuous manufacturing is and how it should be planned, designed, developed and managed in an industrial environment to maximise its positive aspects. In order to increase acceptance, a detailed and easily understandable knowledge of such processes is required [2]. In this study, continuous wet granulation was compared with established batch processes, namely high shear granulation and fluidised bed granulation. The influence of the process type and the most important parameters of the granulation process on the granule and tablet properties was evaluated.

2. MATERIALS AND METHODS

2.1. Materials

The granules consisted of 63% fillers (lactose monohydrate mesh 200 - LM), 35% binders (30% microcrystalline cellulose Avicel PH101 - MCC, 5% polyvinylpyrrolidone K25 - PVP) and 2% of the model drug (tartrazine - TAR). Demineralised water was used as the granulating liquid. Before tableting, a lubricant (magnesium stearate – MgS) was added to make up 0.5% of the final tableting mixture.

2.2. Preparation of granules and tablets

The solid materials were weighed and then mixed in a 2-litre capsule of Bioengineering Inversina's Turbula mixer. The mixture was then transferred to one of the three granulators (twin-screw granulator (TSG) Leistritz ZSE 12 HP-PH, high-shear mixer (HSG) ProCept 4M8Trix or fluidised bed granulator (FBG) Glatt GPCG1) where the powders were granulated. Several samples were produced for all three devices, with the main process parameters being changed between samples. The properties of the granules were then determined. Lubricant was added to the granules and mixed in a Turbula mixer to produce the tableting mixture, which was then used to produce tablets on an IMA Killian SP300 single punch tableting press. The tablets were collected in fractions of 50 tablets from the beginning to the end of the tableting process.

2.3. Characterization of granules and tablets

The particle size distribution (sieve analysis, static light scattering), flow properties (bulk and tapped density, flowability 2.9.16 PhEur, dynamic angle of repose), morphology (SEM images), compressibility, tabletability, tablet hardness, friability, assay, uniformity of content and the tendency of the granules to segregate during tableting were measured or assessed.

3. RESULTS AND DISCUSSION

3.1. Properties of granules

The type of process and also changes in the process parameters influence the morphology of the granules and their size distribution. Of the three granulation methods FBG processing resulted in the smallest granules with the narrowest PSD, while high-shear processing resulted in the largest granules with the widest PSD, with twin-screw granules falling in between in terms of size and size distribution. In

terms of morphology FBD granulation resulted in the most irregular shaped granules, while high-shear granulation resulted in more consolidated granules with higher sphericity. Twin-screw granulation also resulted in more consolidated granules but with a greater length/width ratio, as shown in Figure 1.

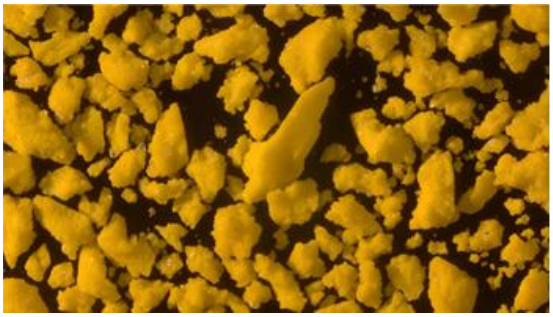

Figure 1. Optical microscope images of TSG granules.

The flowability also followed the same trend, with the FBG granules exhibiting poorer flowability than the granules produced with the HSG, while the flowability of the TSG granules was comparable to that of the HSG granules.

3.2. Compressibility and tabletabilty of granules

The type of granulation process used influences the tabletability (dependence of tensile strength on pressure) of the granules more than their compressibility (dependence of porosity on pressure) as shown in Figure 2.

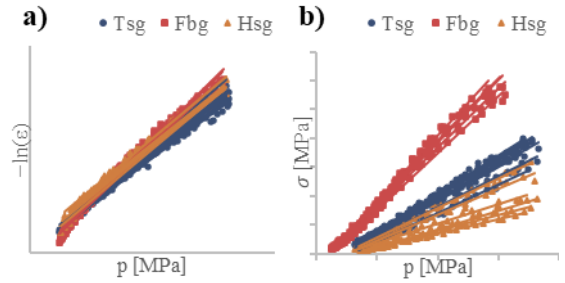

Figure 2. a) Compressibility and b) tabletability of granule mixtures.

3.3. Tablet properties

The characterisation of the tablet samples showed that the type of process had a significant influence on the mechanical properties, with the FBG tablets being the least friable, while the friability of the tablets made from TSG and HSG granules was comparable. Some tablet samples prepared from HSG granules did not pass the pharmacopeial friability test, as some of the tablets were broken during the test. Tablet mass variability was generally low (<1%) for all samples. Both uniformity of content and uniformity of dosage units met pharmacopeial requirements. The tendency of granules to segregate during tableting was also low (<5%) for all samples.

4. CONCLUSION

The choice of the type of granulation process and its process parameters has a significant influence on the morphology, particle size distribution and flowability of the granules and the resulting tablets. For the low-dose formulation used in the study, the application of optimised twin-screw granulation was an acceptable manufacturing process that ultimately resulted in robust granules and finished tablets.

5. REFERENCES

1. Portier, C., et al., *Continuous Twin Screw Granulation: A Review of Recent Progress and Opportunities in Formulation and Equipment Design.* Pharmaceutics, 2021. 13(5): 668

2. Kumar, A., et al., *Development of a process map: A step towards a regime map for steady-state high shear wet twin screw granulation.* Powder Technology, 2016. 300: 73-82.

ACKNOWLEDGMENT

This research was funded by the Slovenian Research Agency under grant number P1-0189.

P057

PREFORMULATION AND OPTIMIZATION OF NANOSTRUCTURED LIPID CARRIERS FOR DERMAL DELIVERY

Hristofor Lazov[1], Aleksandar Shkondrov[2], Krassimira Yoncheva[1], Marta Slavkova[1]

[1]Department of Pharmaceutical Technology with Biopharmacy, Faculty of Pharmacy, Medical University of Sofia, Bulgaria

[2]Department of Pharmacognosy, Faculty of Pharmacy, Medical University of Sofia, Bulgaria

1. INTRODUCTION

Current research focuses on various nanoparticulate systems - polymeric nanoparticles, solid lipid nanoparticles, and nanostructured lipid carriers (NLCs) - to improve drug delivery for poorly soluble and low-bioavailable drugs.

NLCs show potential for transdermal corticosteroid delivery, particularly for poorly water-soluble drugs like budesonide. These carriers are based on lipids with excellent dermal biocompatibility. Different compositional and experimental factors may affect the physicochemical properties of the nanocarrier. Thus, they should be optimized in regard to the loaded drug and intended administration route. NLCs offer numerous advantages over other lipid-based nanocarriers especially in terms of stability and loading capacity [1]. Therefore, in the present work we aimed at optimizing the NLC formulation for potential loading of budesonide and evening primrose oil to be used in the treatment of atopic dermatitis.

2. MATERIALS AND METHODS

2.1. Materials

Budesonide, Tween 20, Castor oil and Oleic acid were supplied from Sigma Aldrich. Lutrol F127 was purchased from BASF, Germany. Imwitor 900 K and Mygliol 812 N were kindly gifted by IOI Oleo GmbH, Hamburg, Germany. Precirol 5 ATO, Compritol 888 ATO, Gelucire 43/01 and Gelucire 50/13 were generously donated by Gattefosse, Saint-Priest, France. Evening primrose oil was of cosmeceutical grade.

2.2. Selection of components and optimal ratio between solid and liquid lipids

In the case of liquid lipids and surfactants (1% w/v aqueous solutions), an excess of the drug was mixed and incubated under agitation for 24 h at 37.0 ± 0.5°C. After centrifugation, the supernatant was mixed with methanol and spectrophotometrically evaluated at 245 nm.

In the case of the solid lipids, an increment of the molten lipid was added to a predetermined amount of drug and stirred until the drug was completely dissolved [2].

The lipid compatibility was tested by mixing and melting them in different ratios (9:1 to 5:5 w/w). A drop of the melt was placed on a glass slide with and without a cover slip. The mixture was rendered suitable if no lipid stains were evident on a filter paper immediately after preparation and after storage in climate chamber at 40°C and 65% RH. Additionally, light microscopy evaluation was performed with the help of Leica DM750 RH4K light microscope (Leica, Switzerland).

2.3. NLCs preparation and aqueous phase amount optimization

NLCs were prepared via melt ultrasonic nanoemulsification [2]. Molten solid and liquid lipids, in different ratios, were mixed with varying amounts of 1% Gelucire 50/13 solution. The aqueous phase was added incrementally under stirring, followed by 3 min pulse ultrasonication at 60% amplitude and cooling in an ice bath. Budesonide was added to the molten lipid mixture in amount 55mg/1g lipids.

2.3. NLCs characterization methods

The NLCs were characterized in terms of size, polydispersity index and zeta potential in 1:10 diluted aqueous samples with the help of ZetaSizer Nano ZS (Malvern Instruments, UK).

Surface morphology was evaluated by Transmission Electron Microscopy (JEOL, Japan). NLCs occlusion potential for the empty systems was in vitro evaluated based on a previously reported procedure [3].

Encapsulation efficiency and loading capacity were evaluated after separation of the

P057

nanodispersions with the help of a mini-column filled with Sephadex G50 (Pharmacia, Sweden). The eluate was freeze-dried, redissolved in a known amount of ethanol and determined with the help of HPLC methodology [3].

3. RESULTS AND DISCUSSION

3.1. Components selection

Based on the solubility data Imwitor 900 K (1.81 mg/g), Mygliol 812 N (103.17 μg/g) and 1% Gelucire 50/13 (148.83 μg/g) solution were used in the preparation of the NLCs.

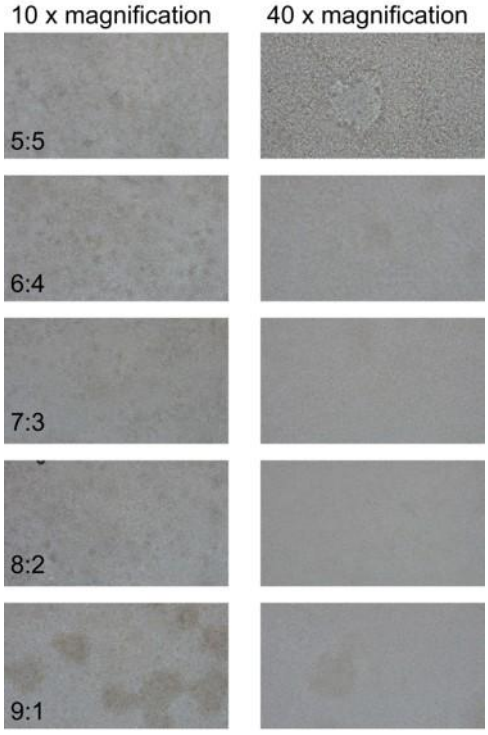

Figure 1. Light microscopy images for compatibility in different solid:liquid lipid ratios (w/w).

Three solid/lipid ratios were rendered miscible based on the performed studies, namely 7:3, 8:2 and 9:1.

3.2. NLCs preparation and aqueous phase amount optimization

Different batches were successfully prepared with varying the amount of surfactant solution. Their physicochemical parameters are presented in Figure 2. All samples had negative zeta potential ranging between -8.06 and -12.40 mV.

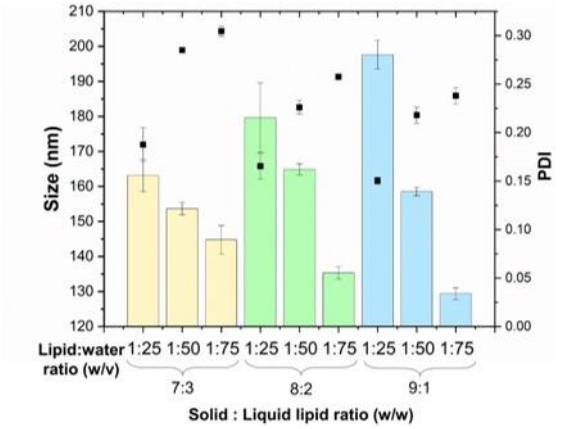

Figure 2. Particle size and PDI of the empty NLCs

3.3. Budesonide and/or Evening Primrose oil loading

Drug loaded nanocarriers were successfully prepared. Slight difference was observed in the size (171.4 – 177.6 nm), PDI (0.25 – 0.285) and zeta potential (-10.7mV to -13.7mV).

4. CONCLUSION

In the present work we reported a systematic optimization of NLCs as potential carriers for budesonide and/or evening primrose oil. The prepared NLCs had suitable characteristics in regard to size, zeta potential and occlusive properties for the therapy of atopic dermatitis.

5. REFERENCES

1. Jeitler, R. et al. *On the Structure, Stability, and Cell Uptake of Nanostructured Lipid Carriers for Drug Delivery*. Molecular Pharmaceutics, 2024, Vol 21(7), 3674-3683.

2. López KL. et al. *Solid Lipid Nanoparticles (SLN) and Nanostructured Lipid Carriers (NLC) Prepared by Microwave and Ultrasound-Assisted Synthesis: Promising Green Strategies for the Nanoworld*. Pharmaceutics, 2023, Vol. 15, 1333.

3. Slavkova M. et al. *Formulation of Budesonide-Loaded Polymeric Nanoparticles into Hydrogels for Local Therapy of Atopic Dermatitis.* Gels,. 2024 ;10(1), 79.

ACKNOWLEDGMENT

This work was funded by the Council of Medical Science by the Medical University of Sofia under project number 9643/27.11.2024

IOI Oleo GmbH, and Gattefosse are highly appreciated for donating free samples for this research.

P058

PRO-CEPT GRANULATOR AS AN EFFECTIVE TOOL IN DIFFERENT PELLETIZATION TECHNIQUE

Azza A. K. Mahmoud[1], Dániel Sebők[2], Ákos Kukovecz[2], Géza Regdon jr.[1], Katalin Kristó[1]

[1]Institute of Pharmaceutical Technology and Regulatory Affairs, University of Szeged, Hungary
[2]Department of Applied and Environmental Chemistry, University of Szeged, Hungary

1. INTRODUCTION

High-shear granulators is an important equipment that can be used to produce multiarticulate system with different techniques. It can be applied for direct production of pellet in only one steps that considered as economical alternative to other pelletization techniques that consume more time and cost. Although this process is simple and fast, it required an accurate optimization of all process parameters such as: granulating liquid volume, chopper speed, and impeller speed [1].

Moreover, it can be utilized in production of layered pellets in one step by loading drug in powder form or liquid form either solution or suspension dosage form on inert cellulose core. Additionally, it can affect in physical form of drug from through changing crystalline to amorphous form that improves physiochemical properties (solubility and dissolution) of drugs in final dosage form. However, this process requires appropriate temperature estimation to avoid recrystallization and ensure the forming of a uniform layer on pellet surface. This study aimed to prepare amlodipine besylate and hydrochlorothiazide pellets using different pelletization techniques with a high-shear granulator [2].

2. MATERIALS AND METHODS

2.1. MATERIALS

Hydrochlorothiazide and amlodipine besylate (Sigma- Aldrich, St.louis, MO, USA) while microcrystalline cellulose powder (MCC, Vivapur 102) was supplied from JRS Pharma (Patterson, NY, USA) and microcrystalline cellulose core were dedicated from Pharmatrans (Sanaq Ag, Basel, Switzerland).

Polyvinyl pyrrolidone (PVP) and mannitol were purchased from Hungaropharma Zrt. (Budapest, Hungary) and distilled water was applied as granulating liquid.

2.2. METHODS

Multiparticulate system loaded with amlodipine besylate and hydrochlorothiazide were prepared using different methods. The first method was applied in the direct pelletization method, in high-shear granulator (ProCept NV, Zelzate, Belgium) PVP solution was gradually added to the mixture of MCC and mannitol until spherical granules formed. After that the air-ventilated oven (Memmert GmbH+Co. KG, Büchenbach, Germany) was used in drying of resulting pellets then the obtained pellets were sieved and yield percent, sphericity, and hardness were determined. The optimum formulation was loaded with amlodipine besylate and hydrochlorothiazide.

In the layering method, inert cores composed of microcrystalline cellulose beads mixed with blend of both drugs in ProCept granulator to allow of formation of layer on spheres surface. After layering, the resulting pellet were characterized using high-resolution computed tomography (micro-CT) (TESCAN Group a. s., Brno, Czech Republic) and differential scanning calorimetry (DSC) (Mettler Toledo GmbH, Greifensee, Switzerland). After that dissolution behaviour of pellets was estimated in Erweka dissolution tester (Ereweka DT 700, Heusenstamm, Germany).

3. RESULTS AND DISCUSSION

3.1. Direct pelletization

Firstly, Quality by Design (QbD) concept was applied to determine all material attributes and process parameters that could affect the quality of the resulting pellets. Based on the risk estimation matrix and the Pareto chart, liquid addition rate, chopper speed, impeller speed, water volume and binder concentration were estimated as independent factors for DoE studies, whereas the process responses like

hardness, aspect ratio, and size distribution were determined as process responses as they had the highest severity scores.

According to screening design results, liquid addition rate fixed at 5 mL/minute as it had effect negatively on hardness and aspect ratio accompanied with increasing of size and porosity.

Central composite design was utilized to optimize the pelletization process and it included only factors that had significant effect on process such as impeller speed, chopper speed, binder concentration, and water volume. After that, the design space was constructed with constant water volume (55 ml) and binder amount (2 g) to obtain a yield percentage of more than 80%, a hardness of less than 35 N, and an aspect ratio of less than 1.2 (Figure 1).

The optimized formulation was prepared using 500 and 1500 rpm of impeller speed and chopper speed respectively. Adding amlodipine besylate and hydrochlorothiazide to this formulation did not significantly change the physical properties results of plain pellets except for the yield percentage of hydrochlorothiazide-containing pellets ($p<0.05$) which may be due to the hydrochlorothiazide hydrophobic nature that decreases the water-wetting effect on powder mixture and consequently reducing pelletization.

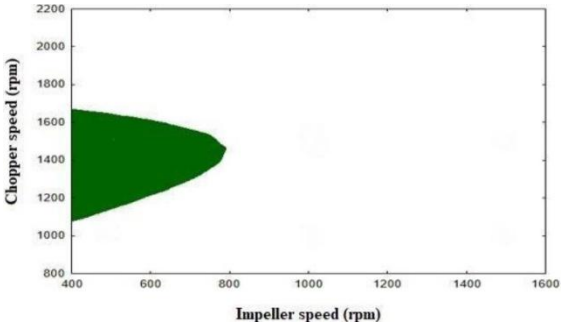

Figure 1. Design space for direct pelletization

3.2. Layering pelletization

According to micro-CT measurement, the pellet mean size increased by approximately 1.15-fold that revealed the layer formed on the pellets surface (Figure 2).

DSC results investigated crystalline amlodipine besylate changed to amorphous form while the crystallinity percent of hydrochlorothiazide reduced to a minimum value (3%) that mean it was not completely amorphized.

Moreover, hydrochlorothiazide and amlodipine besylate dissolution increased above two and one times respectively due to the minimization of the crystal lattice of two drugs due to the high mechanical force of the granulator related to high impeller speed used in the process.

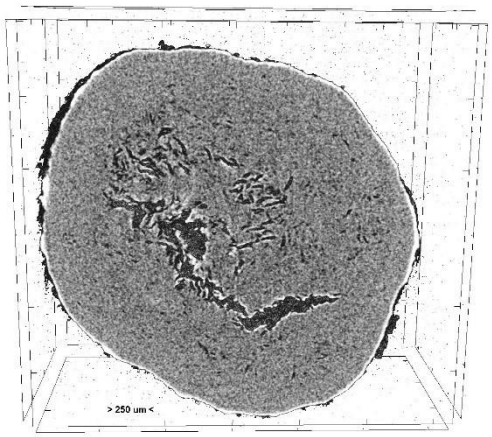

Figure 2. Micro-CT image of layered pellets

4. CONCLUSION

Using a high-shear granulator in direct pelletization leads to forming a spherical multiarticulate system with the required size, good mechanical properties, lower cost, and shorter operational time through good optimization of process parameters by QbD concept. On the other hand, performing layering techniques by high shear granulator led to form layered pellets in one step in addition to improving the physical form of the drugs loaded in pellets with significant enhancement of their release percents.

5. REFERENCES

1. Mahmoud, A. A. K., et al., Investigation of the Electrokinetic Potential of Granules and Optimization of the Pelletization Method Using the Quality by Design Approach. Pharmaceutics, 2024. 16(7): 848.

2. Kondo, K., et al., Solventless Amorphization and Pelletization Using a High Shear Granulator. Part I: Feasibility Study Using Indomethacin. European Journal of Pharmaceutics and Biopharmaceutics, 2022. 181: 147-158

P059

FROM BY-PRODUCT TO BIOACTIVE: BETAINE-UREA NADES EXTRACT OF BILBERRY LEAVES AS A NOVEL ANTI-AGING INGREDIENT

Milica Martinović[1], Ivana Nešić[1], Vanja Tadić[2], Ana Žugić[2], Nikola Krstić[3]

[1]Department of Pharmacy, Faculty of Medicine, University of Niš, Serbia
[2]Department for Pharmaceutical Research and Development, Institute for Medicinal Plant Research "Dr. Josif Pančić, Serbia
[3]Laboratory for Functional Genomics and Proteomics, Faculty of Medicine, University of Niš, Serbia

1. INTRODUCTION

The skin contains various enzymes whose regulation can significantly impact its condition. Tyrosinase plays a key role in melanogenesis, and its overactivity can lead to excess melanin accumulation and formation of spots and hyperpigmentation. Hyaluronidase, an enzyme that breaks down hyaluronic acid, is associated with skin dehydration and wrinkle formation, thus, its inhibition is considered important in preventing skin aging [1].

Bilberry (*Vaccinium myrtillus* L., Ericaceae) is a rich source of phenolic compounds with established anti-inflammatory, antioxidant, and metabolic benefits. While the fruit is traditionally used in medicine and cosmetics, the leaves are often discarded despite their high content of bioactive phytochemicals [2].

Aligned with main principles of Green Chemistry, such as waste reduction, the use of safer solvents, and renewable raw materials, this study explores the use of Natural Deep Eutectic Solvents (NaDES) as sustainable alternatives to conventional extraction solvents. Unlike traditional solvents, which may be toxic, volatile, and flammable, NaDES are considered inert, non-toxic, biodegradable, and environmentally friendly [3].

The aim of this study was to investigate the effect of NaDES on the anti-tyrosinase and anti-hyaluronidase activity of bilberry fruits and leaves extracts and to compare them with water and ethanol extracts. In addition, the aim was to evaluate whether these extracts could serve as novel, green ingredients for dermocosmetic applications.

2. MATERIALS AND METHODS

2.1. Materials

Plant materials used in the study were dried leaves and fruits of bilberry. All reagents used in the study for extract preparation or for conducting *in vitro* assays were purchased from Sigma-Aldrich.

2.2. NaDES preparation

NaDES were prepared by continuously heating and melting urea and betaine in 1:2 mol/mol ratio until clear liquid was formed, after which the 30% (v/v) of distilled water was added.

2.3. Extract preparation

Ultrasound-assisted extraction was conducted for 30 min at 50 °C in a sonication water bath. The plant material: solvent ratio was 1:20.

2.4. Determination of anti-tyrosinase activity

The spectrophotometric method based on measuring diphenolase activity of mushroom-derived tyrosinase using L-DOPA as a substrate was used. The absorbance of samples (As) and control (Ac) were measured at 492 nm. The tyrosinase inhibitory activity was calculated using equation

$$\%\ \text{tyrosinase inhibition} = \frac{Ac - As}{Ac} \times 100$$

The results were expressed as IC_{50} values (mg/mL).

2.5. Determination of anti-hyaluronidase activity

The anti-hyaluronidase activity of the extract was evaluated using a turbidimetric 45 minute method proposed by the Sigma-Aldrich protocol. This method is based on measuring the

P059

turbidity of undegraded hyaluronic acid, which is proportional to hyaluronidase inhibition. The absorbance of samples (As) and control (Ac) were measured at 600 nm. The percentage of inhibition was calculated using the following equation:

$$\%\ \text{hyaluronidase inhibition} = \frac{As}{Ac} \times 100$$

The results were expressed as IC_{50} values (mg/mL).

3. RESULTS AND DISCUSSION

3.1. Anti-tyrosinase activity

The results of *in vitro* anti-tyrosinase assay (Figure 1) showed that bilberry leaf extracts had higher anti-tyrosinase activity than fruit extracts. Although there were no statistically significant differences among fruit extract activities, the choice of solvent significantly affected leaves extract activity. The highest activity was observed in the betaine-urea NaDES leaves extract.

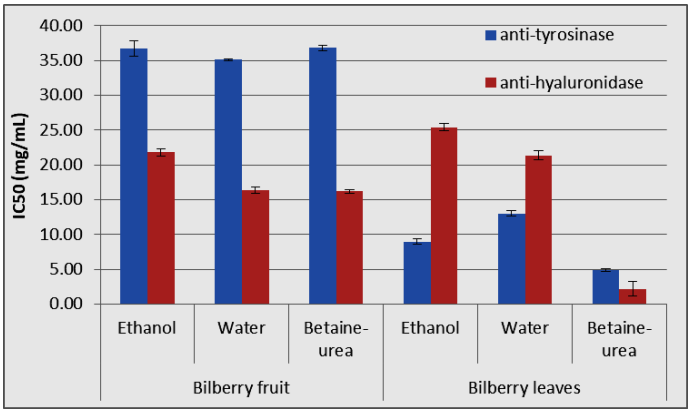

Figure 1. Anti-tyrosinase and anti-hyaluronidase activity (IC_{50} values) of tested bilberry fruits and leaves extracts prepared using NaDES as green extraction solvent and water and ethanol as conventional solvents

3.2. Anti-hyaluronidase activity

Similar results were observed in the anti-hyaluronidase assay (Figure 1), with the betaine-urea NaDES leaves extract demonstrating the best enzyme inhibitory effect. While betaine-urea fruit extract showed comparable anti-hyaluronidase activity to the water extract, it exhibited superior activity compared to the ethanol extract.

Previous studies have reported tyrosinase and hyaluronidase inhibitory activity in bilberry fruit extracts [4]. However, to the best of our knowledge, this is the first study to examine the use of betaine-urea as NaDES for extracting bilberry leaves and fruits and obtaining extracts with anti-age potential.

4. CONCLUSION

This study demonstrates that bilberry leaf extract obtained using betaine-urea NaDES exhibits strong anti-tyrosinase and anti-hyaluronidase activities, highlighting its potential as a sustainable, anti-aging ingredient for dermocosmetic applications.

5. REFERENCES

1. Cruz, A. M. et al. *In Vitro Models for Anti-Aging Efficacy Assessment: A Critical Update in Dermocosmetic Research.* Cosmetics, 2023. 10 (2): 66.

2. Tadić, V. M. et al. *Old Plant, New Possibilities: Wild Bilberry (Vaccinium myrtillus L., Ericaceae) in Topical Skin Preparation*. Antioxidants, 2021. 10(3): 465.

3. Hikmawanti, N. P. E., Ramadon, D., Jantan, I. & Mun'im, A. *Natural Deep Eutectic Solvents (NADES): Phytochemical Extraction Performance Enhancer for Pharmaceutical and Nutraceutical Product Development*. Plants, 2021. 10 (10): 2091.

4. Studzińska-Sroka, E. et al. *Anti-Aging Properties of Chitosan-Based Hydrogels Rich in Bilberry Fruit Extract*. Antioxidants, 2024. 13 (1): 105.

ACKNOWLEDGMENT

Ministry of Science, Technological Development, and Innovation of the Republic of Serbia, grant numbers: 451-03-137/2025-03/200113 and 451-03-136/2025-03 / 200003.

P060

IN VITRO AND IN SILICO CHARACTERISATION OF THEOPHYLLINE NOVEL CO-SPRAY-DRIED POWDER FOR INHALATION

Lomass Soliman, Petra Party, Rita Ambrus

Institute of Pharmaceutical Technology and Regulatory Affairs, Faculty of Pharmacy, University of Szeged, Hungary

1. INTRODUCTION

Dry powder inhalers (DPIs) are leading inhaled products; however, their development requires formulation optimization. The performance of DPIs is influenced by material properties, particle size, inhaler design, and patient factors. Future DPI choices consider technology versus affordability in the evolving inhaler market [1]. Fine micro-sized carriers, specifically, spray-dried combinations of saccharides and amino acids, are being explored to enhance the stability, dispersibility, and aerodynamic profile of DPIs. Therefore, this work presents a novel formulation and comprehensive investigation of theophylline (TN) using a combination of raffinose or trehalose with amino acids as fine co-spray-dried carriers, aimed at improving the pulmonary delivery of low-dose TN (10 mg) for asthma treatment [2, 3].

2. MATERIALS AND METHODS

2.1. Materials

Theophylline anhydrous (TN) (Hungaropharma Ltd.), raffinose pentahydrate (Rf) (Tokyo Chemical Industry Co., Ltd.), trehalose dihydrate (Tr) (Sigma Aldrich Chemie GmbH), l-leucine (Lc) (Molar Chemicals Kft.), glycine (Gl) (VWR International LCC).

2.2. Preparation

200 mL stock solutions of the respective components of each formulation (TN + Tr or Rf + Lc and/or Gl) were prepared in ethanol 10%, with ultrasound sonication and magnetic stirring (200 rpm, 40 °C, 30 min). Microparticles were produced using a Büchi B-191 mini spray dryer. The formulation's composition was adjusted based on preliminary experiments to optimize the yield, TN-saccharide ratio, and the intended dose of TN, as described in detail through our previous studies [2, 3]. Spray-dried TN (SD-TN) was also prepared for comparison with the developed DPIs containing fine carriers.

2.3. Characterisation

Rigorous assessment is crucial to determine the formulation properties and ensure effective lung deposition. The characterization methods employed included particle size distribution analysis by laser diffraction (Malvern Mastersizer 2000), structural analysis using X-ray powder diffraction (XRPD), and morphology assessment utilizing scanning electron microscopy (SEM). Additionally, in vitro and in silico aerodynamic investigations were conducted using the Andersen cascade impactor (ACI), aerodynamic particle counter (APC), and stochastic lung model. The solubility in simulated lung fluid (SLF), in vitro drug release, and diffusion of TN were also assessed [2, 3].

3. RESULTS AND DISCUSSION

3.1. Structure, Morphology, and Particle Size

A partially amorphous structure was detected after spray drying of the developed samples (crystallinity index: 38.5% - 45.2% for TN-Tr-Lc and TN-Rf-Lc-Gl, respectively) (Fig. 1A). However, the raw materials revealed high crystallinity indices (94.3% - 97.6%). Moreover, SEM screening exhibited spherical and hollow microparticles with suitable particle size characteristics for inhalation (within a 1-5 µm range for respirable particles) (Fig. 1B).

3.2. Solubility, Dissolution, and Diffusion

TN solubility in SLF was significantly enhanced (TN: 15, TN-Tr-Lc: 312, and TN-Rf-Lc-Gl: 205 mg/mL) (Fig. 1C). Furthermore, rapid drug release was recorded since approximately 100% of the embedded dose was

released within up to 5 minutes. Moreover, the in vitro permeability of TN was remarkably improved (~2.4-fold) in TN-Tr-Lc and TN-Rf-Lc-Gl compared to raw TN (Figure 1D). This enhanced physicochemical performance is attributed to the micronization upon spray drying and the incorporation of water-soluble excipients.

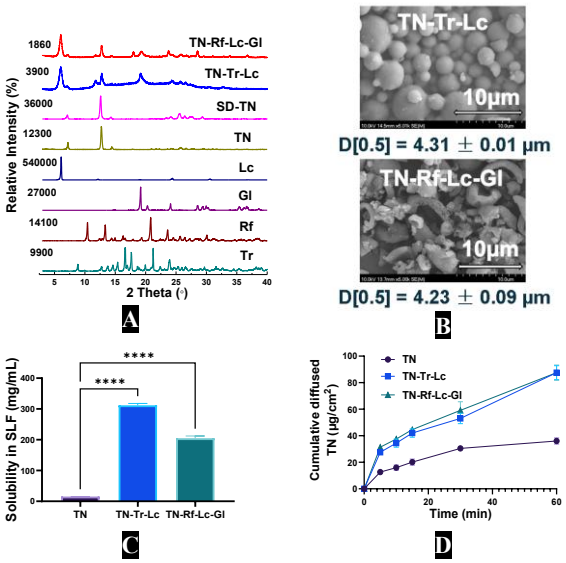

Figure 1. XRPD patterns (A), morphology and particle size (B), solubility (C), and in vitro diffusion (D) characteristics of the developed DPIs.

3.3. Aerodynamic Performance

The in vitro aerodynamic measurements (ACI and APC) revealed that the fine particle fraction (FPF: particles < 5µm) of TN-Tr-Lc and TN-Rf-Lc-Gl is 43% and 48%, respectively, with aerodynamic particle size within the optimal range (1-5 µm) for deep lung administration. Fig. 2 demonstrates the simulated in silico deposition pattern of SD-TN, TN-Tr-Lc, and TN-Rf-Lc-Gl utilizing the in vitro aerodynamic data. A total lung deposition of TN co-spray-dried powders was recorded (36% and 40%, respectively) compared to 18% for SD-TN.

4. CONCLUSION

Raffinose and trehalose combined with low-concentration amino acids showed promising results as fine micro-sized carriers for DPIs via co-spray-drying. Developing a co-spray-dried respirable powder featuring theophylline with these combined fine carriers was successful,

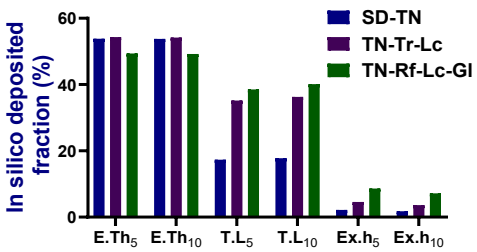

Figure 2. In silico aerodynamic investigation of SD-TN, TN-Tr-Lc, and TN-Rf-Lc-Gl.

demonstrating significant improvements for targeting asthma symptoms by optimizing particle size and shape for deep lung delivery. Enhanced solubility, dissolution, and diffusion contributed to favourable physicochemical characteristics. Aerodynamic assessments indicated improved deep lung delivery. This approach provides an effective inhalation treatment for TN, potentially reducing the required dose and systemic side effects.

5. REFERENCES

1. Morton, D.A., & Barling, D. *Developing dry powder inhaler formulations*. Journal of aerosol medicine and pulmonary drug delivery, 2024, 37(2), 90-99.

2. Party, P., et al. *Optimization, in vitro, and in silico characterization of theophylline inhalable powder using raffinose-amino acid combination as fine co-spray-dried carriers*. Pharmaceutics, 2025, 17, 466.

3. Soliman, L., et al. *Enhanced pulmonary delivery of spray-dried theophylline: investigation of the trehalose and amino acid combinations as innovative fine carriers*. European journal of pharmaceutical sciences, 2025, 209, 107109.

ACKNOWLEDGMENT

This work was supported by project No. TKP2021-EGA-32 and NKFIH OTKA K_146148 project.

P061

A KNOWN DRUG IN A NEW FORMULATION - A LONG WAY TO PHARMACEUTICAL PRODUCT

Malgorzata Sznitowska[1], Marzena Jamrogiewicz[2], Anna Roszkowska[3], Tomasz Bączek[3]

[1]Department of Pharmaceutical Technology, Medical University of Gdansk, Poland
[2]Department of Physical Chemistry, Medical University of Gdansk, Poland
[3]Department of Pharmaceutical Chemistry, Medical University of Gdansk, Poland

1. INTRODUCTION

Some antibiotics, due to their low stability in water, are used in ophthalmology only as pharmacy compounded preparations. We have developed anhydrous eye drops in the form of an antibiotic suspension (VAN - vancomycin sodium and CEF - cefuroxime HCl) in a self-emulsifying oil (SEO) [1]. The SEO carrier is well tolerated, as demonstrated in studies on rabbit eyes [2, 3]. After application, the suspension will immediately transform into an emulsion, with the antibiotic dissolved. The long-term stability of antibiotics in this form was proven and patent was granted [4].
Presentation of the research actually performed and the planned further stages of work required to implement the preparation for industrial production and clinical practice is the aim of this submission.

2. MATERIALS AND METHODS

2.1. Materials and method of preparation

The suspensions were compounded aseptically using sterile ingredients. The SEO carrier was prepared by mixing Miglyol 812 (fractionated coconut oil; Caesar & Loretz, Hilden, Germany) with Tween 20 (polysorbate; Sigma Aldrich, Steinheim, Germany) at concentration of 5% w/w followed by sterile filtration. Micronized CEF and VAN powders for injection (MIP-Pharma, St. Ingbert, Germany) at concentration of 5% w/w and sodium citrate (2% w/w; Stanlab, Lublin, Poland) were added and the suspension was homogenized.

2.2. Tests before scale-up

Two stages of industrial-scale production were selected as critical: sterilization of SEO and homogenization of the suspension. Different materials of 0.22 μm membranes were used for filtration and microscopic (SEM) examination of the filters was performed in order to confirm compatibility. Homogenization was performed using ultrasound, high-shear and glass ball homogenizers and stability of antibiotics was analyzed using HPLC-MS method.

2.3. Choice of the container

Bottles with droppers offered by different manufacturers were tested for compatibility with the product in the long term (25°C) and accelerated (40°C and 60°C) storage conditions. Besides the microscopic examination of the package material, mechanical tests of the packages were performed using a texture analyser. Physical parameters of the product (viscosity, rheology, agglomeration) of the product were evaluated and assay for antibiotics was done. Moeover, the material of the containers was analysed using DSC and IR techniques.

2.4. In vivo tolerance

The antibiotics in SEO and in aqueous solutions are tested on swine eyes. Reaction is evaluated using a Draize test scores. The residence time of a drug on the eye surface is evaluated by collecting tear fluid and determination of antibiotic present.

2.5. Choice of the antibiotic supplier

The search was done for the commercial source of the active substances for future production. The requirements were: particle size, sterility and CEP (Certificate of European Pharmacopoeia). Documentation received is used to prepare “Substance” 3S section of the registration documents in CTD format.

3. RESULTS AND DISCUSSION

3.1. Compatibility of SEO with filters

It was confirmed that among the filters tested only those recommended for oils were suitable. Durapore (Millipore) allows filtration with the least applied force (120 Ns). Surfactant in SEO is increasing the flow through the filter. Microscopic analysis did not show any difference in a surface structure of the filters after contact with SEO.

3.2. Method of homogenization

Homogenization of antibiotic suspension in a high-shear homogenizer (Ultra-Turrax) was optimized in time and intensity for VAN-SEO, but CEF-SEO suspension was very sensitive to the increase of temperature during the process. Homogenization in a planetary centrifugal mixer (Thinky ARE 250) with glass balls in the container was more effective and safer for the product.

3.3. Compatibility with container

The interaction of SEO with polyethylene material was observed at 60°C but no changes in the spectroscopic and microscopic analysis were detected in lower storage temperatures.

3.4. Choice of API supplier

Two European and four Asian suppliers of CEF (precipitated or lyophilized) with CEP were identified. VAN for large-scale production may be purchased from two European and two Chinese manufacturers. Suitability for production of the sterile ocular suspension will be confirmed using antibiotics from at least two sources.

3.4. In vivo study

Preliminary results were performed in rabbits but further experiments are in progress on pigs. The experimental phase is in preparation with the application to the Bioethical Committee. Novel formulations will be compared with aqueous solutions. Each formulation will be administered to the eye of eight animals. The next step will be an experiment on naturally infected eyes. Positive results from these tests will let to apply for registration the CEF suspension as veterinary medicinal product and to continue the project with GMP production for clinical study in humans.

4. CONCLUSION

Despite the great practical value of the idea and the proposed simple technology the conducted experiments and their continuation are required to attract the serious attention of an industrial partner. Even if the obtained results are satisfactory, the future manufacturer will still have to face an expensive clinical research and to find or create a GMP production site (Fig. 1). The project indicates that already at the stage of scientific research there is a need to plan research that is as close as possible to the conditions of production and fulfillment of the registration requirements.

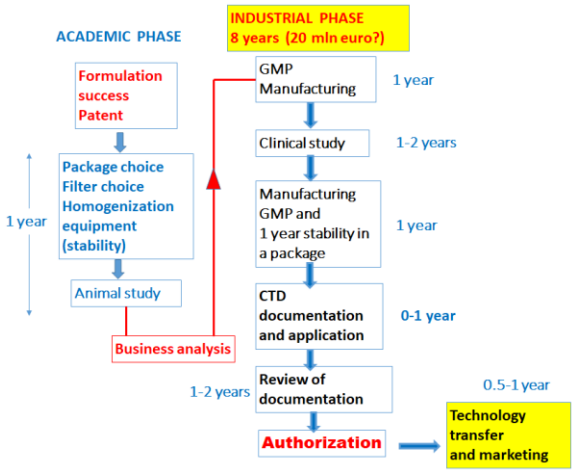

Figure 1. Medicinal product development – time and costs after a successful academic research phase

5. REFERENCES

1. Krzeminska, K., et al., *Suspensions of antibiotics in self-emulsifying oils as a novel approach to formulate eye drops with substances which undergo hydrolysis in aqueous environment.* Drug Deliv, 2024. 31.
2. Wolska, E., et al., *Microscopic and biopharmaceutical evaluation of emulsion and Self-Emulsifying Oil with cyclosporine.* Pharmaceuticals, 2023. 16.
3. Czajkowska-Kosnik, A., et.al., *Comparison of cytotoxicity in vitro and irritation in vivo for aqueous and oily solutions of surfactants.* Drug Development and Industrial Pharmacy, 2015. 41.
4. Sznitowska, M., et al., *Self-emulsifying pharmaceutical composition in the liquid form, containing as the active substance a drug substance unstable in an aqueous environment.* 2025. European Patent EP3917498.

ACKNOWLEDGMENT

The research is funded by a Medical Research Agency grant nr 2024/ABM/03/KPO/ KPOD.07.07-IW.07-0046/24-00.

P062

A NOVEL APPROACH FOR LOADING DRUGS INTO 3D-PRINTED TABLETS USING PAN COATING AND MICROSYRINGE-BASED TECHNIQUES

Yusra Ahmed[1], Tamás Sovány[1]

[1]*University of Szeged, Institute of Pharmaceutical Technology and Regulatory Affairs, Szeged, Hungary*

1. INTRODUCTION

Drug incorporation into filaments can be achieved in Fused Deposition Modeling (FDM), either by hot melt extrusion (HME) or impregnation. With HME, the drug and polymer are first melted together and then extruded using a heated nozzle. On the other hand, impregnation involves immersing either filament or printed objects in a highly concentrated drug solution, allowing the drug to diffuse into the material. Despite its simplicity, impregnation has some disadvantages, including the requirement for high drug concentrations, long process times, and the possibility of drug degradation during the process [1] to overcome this disadvantage, loading drug into 3D-printed tablets using an deposition of active pharmaceutical ingredient (API) solution with electronic syringe or by controlled spraying of liquid droplets with pan coating may be novel, automated, accurate, and reproducible alternatives for loading. They are high-speed, automated and well controllable process, resulting in reduced material losses. This project aimed the comparison of loading methods to produce paracetamol containing polylactic acid (PLA) based FDM printed tablets.

2. MATERIALS AND METHODS

2.1. Materials

PLA filaments were purchased from Formlabs (Somerville, Massachusetts, USA), paracetamol was kindly gifted by Gedeon Richter Plc. (Budapest Hungary), hydroxypropyl-methyl-cellulose (HPMC, Pharmacoat 606, Shin-Etzu, Japan was used as thickening agent of the pan coating solution. Other materials used were reagent grade.

2.2. 3D-printing

A Bambulab A1 FDM printer (Bambu Lab Co., Ltd., Shenzhen, China) was used to print plain tablets with a honeycomb infill shape and two different infill percentages (30% and 60%).

2.3. Loading of paracetamol solution

A ProCepT 4M8 Pancoat drum coater, (ProCepT, Belgium) was used to spraying of paracetamol solution on the 3D printed tablets, while for microsyringe loading, the automatic syringe system of a Dataphysics OCA 20 device (Dataphysics, Germany) was used.

2.4. Characterization of paracetamol printed tablets

To determine the drug loading%, the tablets were placed in pH 5.8 phosphate buffer solution and stirred on magnetic stirrer for two hours then the absorbance was measured by UVVIS spectrophotometer (ThermoScientific Genesys, Waltham, MA, Usa) at wavelength of 243 nm. The mechanical properties were determined with a friability tester (Erweka, Langen, Germany). Drug-carrier interactions and drug distribution were analysed with Avatar 330 FT-IR spectrometer and DXR Raman microscope (both ThermoScientific, Waltham, MA, USA) Finally, morphology studies before and after loading were conducted using a scanning electron microscope (SEM) (Hitachi S4700, Hitachi Scientific Ltd., Tokyo, Japan).

3. RESULTS AND DISCUSSION

3.1. 3D-printing

Fig. 1 depicts the design of a plain tablet made with FDM and PLA filaments. The tablets were designed in a honeycomb shape with two distinct infill percentages (30% and 60%).

P062

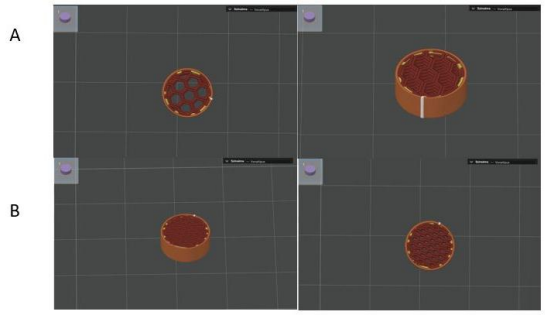

Figure 1. 3D representation of the printed solid dosage forms: (A) 30% Honeycomb (B) 60% Honeycomb infill.

To ensure printing consistency, the plain tablet's diameter and height were estimated. FDM has low variability (RSD < 1) in diameter and height, indicating high printing reproducibility [2].

3.2. Characterization of paracetamol printed tablets

More than 85% loading was achieved for two different infill percentages in both loading techniques.

Friability was determined to estimate the tablet's mechanical resistance to abrasion, capping, and chipping during manufacturing, packaging, and transportation. In case of pan coating loading technique the paracetamol tablets met USP standards with a weight loss of less than 1%; however, for the microsyringe loading technique, friability% was more than 1%, which may be due to drug loss from the tablet surface.

No appearance or disappearance of peaks was observed in FT-IR analysis, indicating drug-polymer compatibility. Raman mapping showed that the API was distributed mainly on the surface of tablets.

Fig. 2 depicts the tablets' appearance before and after loading by scanning electron microscope, which revealed a smooth surface with minor printing defects. However, these defects were not evident to the human eye and are hence unlikely to impair patient compliance

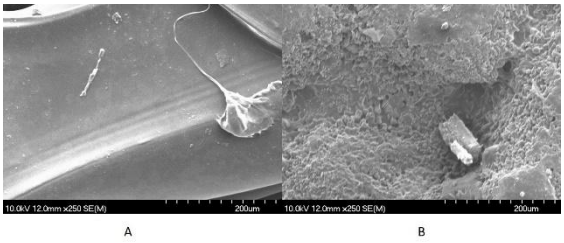

Figure 2. SEM images of the printed tablets: (A) before loading (B) after loading.

4. CONCLUSION

This study successfully demonstrates the integration of Fused Deposition Modeling (FDM) and pan coating or microsyringe method as a novel strategy for producing paracetamol tablets. The use of PLA filaments and honeycomb infill structures ensured high printing reproducibility and mechanical integrity. Pan coating enabled efficient drug loading, achieving over 85% incorporation with minimal material loss. The final tablets exhibited acceptable mechanical properties and met USP friability standards, indicating suitability for pharmaceutical use. This combined approach offers a promising, automated, and scalable method for fabricating personalized drug delivery systems.

5. REFERENCES

1. Ahmed, Yusra., et al., Advances in Loading Techniques and Quality by Design for Fused Deposition Modeling in Pharmaceutical Production: A Systematic Review. Pharmaceuticals, 2024. 17(11): 1496.

2. Junqueira, Laura Andrade., et al., Coupling of fused deposition modeling and inkjet printing to produce drug loaded 3D printed tablets. Pharmaceutics, 2022. 14(1):159.

ACKNOWLEDGMENT

The authors would like to thank Krisztián Kovács for the help with the 3D printing process.

P063

THERMAL EVALUATION OF RESVERATROL-POLYMER MIXTURES WITH MESOPOROUS CARRIERS FOR MELT GRANULATION

Pia Berglez[1], Barbara Sterle Zorec [1], Odon Planinšek [1], Alenka Zvonar Pobirk [1]

[1]Department of Pharmaceutical Technology, University of Ljubljana Faculty of Pharmacy, Slovenia

1. INTRODUCTION

Amorphous solid dispersions (ASD) are one of the approaches to increase water solubility and dissolution rate of poorly soluble drugs [1]. ASD can be formed by incorporating a drug into a suitable polymer-solid carrier system using, e.g., melt-based methods [2]. While melt granulation is a suitable method for preparing ASDs [3], differential scanning calorimetry (DSC) serves as a useful tool for pre-formulation screening as it can confirm the amorphous state of the active substance and possible interactions between active substance and excipients [1]. Resveratrol (RSV) is a natural, poorly water-soluble active ingredient with low oral bioavailability, which may benefit from formulation in ASDs. Hydrophilic polymers used in ASDs can protect antioxidants from recrystallization and enhance their dissolution rate [1]. Additionally, adding mesoporous carriers may further stabilize the amorphous state of both the polymer and the antioxidant [4].

In present work, we aimed to demonstrate the use of DSC as a pre-formulation screening tool in the development of RSV-loaded ASDs prepared by manual melt granulation using different types of polymers and mesoporous carriers.

2. MATERIALS AND METHODS

2.1. Materials

RSV, a polyphenolic antioxidant, was obtained from Biosynth (Slovakia). For formulation screening with DSC, three polymers and two mesoporous carriers were selected: hypromellose acetate succinate (HPMC AS) AQOAT® medium melting point (MMP) and low melting point (LMP) from Shin-Etsu Chemical Co. (Japan) were donated from HARKE Pharma GmbH, Polyethylene glycol (PEG) 6000 was donated from Lek d.d. (Slovenia), and Eudragit® EPO was obtained from Evonik (Germany). Mesoporous carrier Syloid® 244 FP, obtained from Grace (Germany), and Neusilin® US2 from Fuji Chemical Industries Co. (Japan), were employed as solid carriers in various ratios relative to RSV and the polymer.

2.2. Physical mixtures preparation

Physical mixtures of RSV, polymers, and mesoporous carriers were prepared in an Inversina 2 L 3D mixer (Bioengineering AG, Switzerland) by mixing for 8 minutes in the ratios presented in Table I.

Table I. Composition of physical mixtures for RSV with polymers and solid carriers.

Carrier	RSV (%)
HPMC AS LMP or MMP	10–90
Eudragit® EPO	10–90
PEG 6000	10–90
PEG 6000 and Neusilin® (ratio 1:1)	20–50
PEG 6000 and Syloid® (ratio 1:1)	20–50

2.3. Manual melt granulation

Physical mixtures containing 20 % and 40 % RSV loadings were transformed into solid dispersions by manual melt granulation. RSV was slowly added to molten polymer in a mortar over a hot water bath. When the homogeneous mixture was obtained, the mesoporous solid carrier was added and the final mixture was cooled on a tray to room temperature.

P063

2.4. Differential scanning calorimetry

Thermal properties of RSV, polymers, mesoporous carriers, physical mixtures, and prepared solid dispersion samples were evaluated using a differential scanning calorimeter DSC1 with STARe 16.20 software (Mettler Toledo, Switzerland). Between 5–10 mg of a sample was weighed in a 40 µL aluminium pan and sealed. DSC curve was measured from 25 to 320 °C, with a heating rate of 10 K/min, in an inert atmosphere under a nitrogen flow of 50 mL/min.

3. RESULTS AND DISCUSSION

After DSC analysis of physical mixtures, PEG 6000 was identified as the best polymer for preparation of ASD with RSV. Based on the DSC heating curves, active ingredient loadings of up to 40 % were identified as appropriate as no or minimal melting peak was detected, indicating a formation of a molten mixture with PEG 6000 during heating. In contrast, HPMC AS and Eudragit® demonstrated limited applicability due to their thermal degradation or instability above 260 °C, which is a melting point of RSV.

For a proof-of-concept, PEG 6000 loaded with 20 % and 40 % RSV was heated and mixed with either Syloid® or Neusilin®.

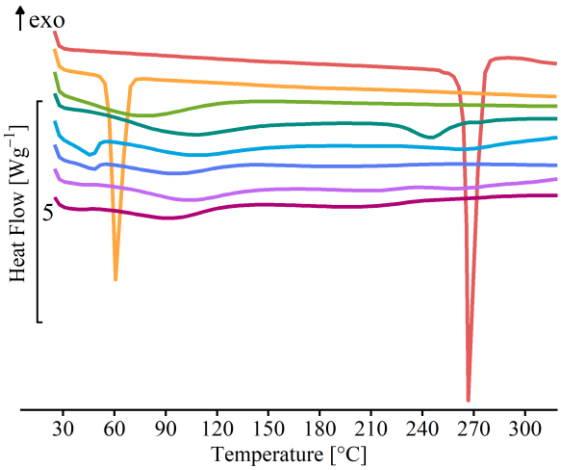

Figure 1. DSC curves of raw materials and ASDs. Legend: ■ RSV ■ PEG ■ Syloid® ■ Neusilin® ■ SD20-RSV/PEG:NEU ■ SD20-RSV/PEG:SYL ■ SD40-RSV/PEG:NEU ■ SD40-RSV/ PEG:SYL

DSC analysis of all four formulations revealed the absence of RSV melting peak, as seen on Fig. 1, indicating successful amorphization presumably by pore-filling and molecular dispersion mechanisms. The relatively low melting point of PEG 6000 enabled the formation of a molten phase at moderate temperatures, which likely eased the melting of resveratrol and its incorporation into the pores of the mesoporous carriers.

4. CONCLUSION

In this proof-of-concept study, we successfully utilized DSC as a tool for screening raw materials and optimizing the component ratios to obtain amorphous state of resveratrol in solid dispersion formulations prepared via manual melt granulation. These findings establish a basis for scaling up the preparation of solid dispersions using hot-melt extrusion methods and for the further evaluation of amorphous solid dispersions consisting of a drug, polymer, and mesoporous carrier.

5. REFERENCES

1. Han G., et al. *Optimization and evaluation of resveratrol amorphous solid dispersions with a novel polymeric system*. Mathematical Biosciences and Engineering, 2022. 19(8):8019–34.

2. Rumondor A.C.F., et al. *Effects of Polymer Type and Storage Relative Humidity on the Kinetics of Felodipine Crystallization from Amorphous Solid Dispersions*. Pharmaceutical Research, 2009. 26(12):2599–606.

3. Bhujbal S.V., et al. *Pharmaceutical amorphous solid dispersion: A review of manufacturing strategies*. Acta Pharmaceutica Sinica B, 2021. 11(8):2505–36.

4. Kovačević M., et al. *The comparison of melt technologies based on mesoporous carriers for improved carvedilol dissolution.* European Journal of Pharmaceutical Sciences, 2024. 202(2024):106880.

ACKNOWLEDGMENT

The authors acknowledge financial support from the Slovenian Research Agency (Research Core Funding, No. P1-0189).

P064

THE IMPACT OF TERMINAL STERILISATION ON THE CHEMICAL AND PHYSICAL STABILITY OF GLASSY DRUG MICRONEEDLES

Mohamed Elkhashab[1], Ziad Sartawi[2], Denis Lynch[3], Abina Crean[1], Waleed Faisal[2], Sonja Vucen[1]*

[1]SSPC, School of Pharmacy, University College Cork, Cork, T12 K8AF, Ireland
[2]ArrayPatch Ltd, Euro Business Park, Little Island, Cork, T45 FX94, Ireland
[3]ABCRF, School of Chemistry, University College Cork, Cork, T12 YN60, Ireland

1. INTRODUCTION

Microneedle array patches (MAPs) containing glassy drug microneedle structures, composed entirely of active pharmaceutical ingredients (APIs), enable high drug dosing intradermally (Elkhashab et al., 2025; Sartawi et al., 2023). During administration, MAPs disruption of the skin barrier can pose a risk of microbial skin invasion leading to a clinically significant infection (Dul et al., 2025). To minimise this risk, strategies that control bioburden during MAP manufacturing, followed by terminal sterilisation can be applied. This study investigates drug microneedle chemical and physical stability following exposure of MAPs to clinically relevant sterilization conditions. The impact of two sterilization methods (gamma irradiation and ethylene oxide (EtO)) on the chemical and physical integrity of MAPs composed of glassy itraconazole (ITZ) and zolmitriptan (ZMT) microneedles was investigated.

2. MATERIALS AND METHODS

2.1. Materials

ITZ and ZMT were supplied by Kemprotec (UK). Standard analytical reagents and neonatal porcine skin were used for characterization and penetration studies.

2.2. Fabrication

Each API was melted above its melting point and moulded into polydimethylsiloxane (PDMS) arrays, cooled and microneedle structures removed to form MAPs.

2.3. Sterilisation

Sterilisation was performed via gamma irradiation (25 kGy, Co-60) and EtO (50°C, 60% RH, 3 h exposure). Samples were sealed to prevent ingress of external humidity.

2.3. Sterility testing

Sterility testing was conducted in accordance with European Pharmacopoeia regulations (European Pharmacopoeia. 10th Ed. 2019) using direct inoculation into fluid thioglycolate medium (FTM) and soybean-casein digest broth (TSB), incubation at 32°C and 22°C, respectively, for 14 days. Tests included positive and negative controls for accuracy.

2.4. Stability Assessment

Post-sterilization, MAPs were evaluated for chemical stability using RP HPLC and LC-MS to quantify API degradation and impurity profiles and ^{1}H NMR to determine chemical structural integrity.
Microneedle physical stability was determined by visual analysis of morphology and appearance combined with porcine skin penetration assessment.

3. RESULTS AND DISCUSSION

3.1. Sterility Analysis

No microbial growth was observed during testing of ITZ and ZMT MAPs.

3.2. Morphology and Appearance

Post EtO exposure and gamma radiation the ITZ MAPs retained their geometric structure. However, immediately post gamma radiation the ITZ MAPs exhibited a temporary discoloration (greyish green) (Fig. 1).

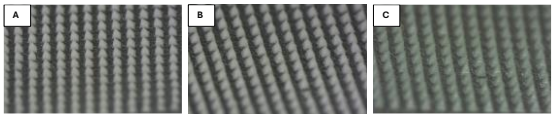

Figure 1. ITZ MAP before and after sterilisation. (A) Control ITZ MAP before sterilisation. (B) ITZ MAP after ethylene oxide sterilisation. (C) ITZ MAP after gamma irradiation.

In contrast, post EtO exposure and gamma radiation the ZMT MAP lost their geometrical structure (Fig. 2).

P064

Figure 2. ZMT MAP before and after sterilisation. (A) Control ZMT MAP before sterilisation. (B) ZMT MAP after EtO sterilisation. (C) ZMT MAP after gamma irradiation.

3.2. Chemical Stability

ITZ showed good chemical stability post sterilisation by both techniques with >98% recovery determined by RP-HPLC and minimal degradation (~0.27%) detectable by LC-MS.

In contrast, ZMT crystalline raw material and cooled molten samples showed extensive degradation upon exposure to EtO (61% and 93% recovery for the crystalline and cooled molten samples respectively). LC-MS analysis identified hydroxyethylated derivative degradants (m/z 332, 376, 420) (Fig. 3).

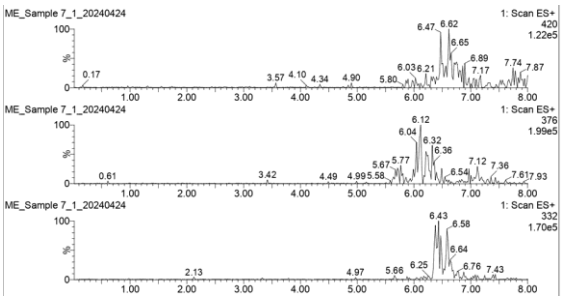

Figure 3. ES+ scan of ZMT crystalline form post EtO sterilisation showing degradation products with molecular weight of 420, 376 and 332 g/mol

^{1}H NMR spectroscopy confirmed the structural stability of ITZ following both sterilization methods. In contrast, ZMT post sterilisation exhibited distinct impurity signals in both aliphatic and aromatic regions, consistent with hydroxyethylation and indole ring modification. These changes were significantly reduced in the cooled-molten form compared to the crystalline form, attributed to lower reactivity due to a reduced surface exposure.

3.3. Skin penetration assessment

ITZ MAPs retained a high penetration efficiency (>80%) post sterilisation as determined by ex-vivo skin penetration studies. ZMT MAPs lost penetration capability following sterilization due to severe microneedle structural deformation, despite a high pre-sterilization penetration efficiency (Fig.4.).

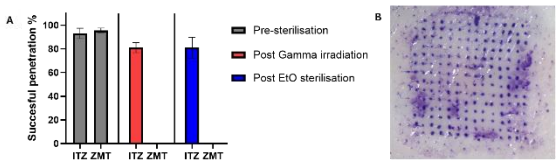

Figure 4. skin penetration efficiency of the ITZ and ZMT MAPs pre and post sterilisation. (A) Data represent the mean ± SD of the percentage of successful penetration pre-sterilisation and post gamma irradiation and EtO sterilisation. (B) Representative image of skin penetration showing stained perforations following MAP application.

4. CONCLUSION

ITZ and ZMT were successfully sterilised by both EtO exposure and gamma irradiation. ITZ MAPs tolerated both sterilisation methods with a minor reversible impact on ITZ colour. ZMT, however, exhibited extensive chemical and physical instability with EtO-induced hydroxyethylation and partial melting following gamma radiation. The results underscore the importance of determining drug-specific compatibility with sterilization protocols during the development of pharmaceutical MAPs and other medical device-drug combination products.

5. REFERENCES

Council of Europe. European Pharmacopoeia. 10th ed. Strasbourg: Council of Europe; 2019. Sterility; p. 191.

DUL, Maria *et al.* White paper: Understanding, informing and defining the regulatory science of microneedle-based dosage forms that are applied to the skin. **Journal of Controlled Release**, v. 378, p. 402–415, 10 Feb. 2025.

ELKHASHAB, Mohamed *et al.* Glassy Drug Microneedle Array Design: Drug Glass-Forming Ability and Stability. **Molecular Pharmaceutics**, v. 22, p. 1373–1383, 3 mar. 2025.

SARTAWI, Ziad *et al.* Glass Microneedles: A Case Study for Regulatory Approval Using a Quality by Design Approach. **Advanced Materials**, p. 2305834, 21 nov. 2023.

ACKNOWLEDGMENT

This research has emanated from research conducted with the financial support of Enterprise Ireland Commercialization Funds, Grant Numbers: CF-2020-1482-I and CF-2022-1974, and Taighde Éireann – Research Ireland, under Grant Number 12/RC/2275_P2.

P065

VISCOSITY AND INJECTION FORCE OF MONOCLONAL ANTIBODY FORMULATIONS FOR SUBCUTANEOUS ADMINISTRATION: EFFECTS OF CONCENTRATION

Maja Bjelošević Žiberna, Monika Prašnikar, Pegi Ahlin Grabnar

University of Ljubljana, Faculty of Pharmacy, Department of Pharmaceutical Technology, Ljubljana, Slovenia

1. INTRODUCTION

In recent years, the use of monoclonal antibody (mAb) therapies in the form of subcutaneous injections has increased significantly, owing to their numerous advantages over other parenteral administration routes. However, the volume of solution that can be administered subcutaneously is limited to a maximum of 2 mL, necessitating the formulation of highly concentrated mAb solutions (>100 mg/mL). Such high concentrations can lead to increased viscosity of the formulation and reduced stability of biological macromolecules. In addition to requiring optimisation of the manufacturing process, these formulations also demand high injection forces to deliver the solution into the subcutaneous tissue, which potentially affecting the suitability of pre-filled syringes for self-administration [1, 2].

The objective of this study was to investigate the impact of mAb concentration on formulation viscosity, followed by the examination of glide force, which is a mimic for *in vivo* injection force.

2. MATERIALS AND METHODS

2.1. Materials

The model IgG mAb was obtained from Novartis d.o.o. (Slovenia). Sucrose was from Merck (Germany). Polysorbate 80 was from J.T. Baker (USA). Ultra-pure water was from a Milli-Q purification system (Bedford, MA, USA).

2.2. Methods

Sample preparation

The mAb stock solution was obtained by concentrating it to approximately 200 mg/mL using ultra-centrifugal filter units with 50 kDa MWCO pore size. For final formulation, mAb stock solution was mixed with the water solution of the excipients (200 mM sucrose, 20 mM histidine and 0.2 mg/mL polysorbate 80) in a ratio 1:2, respectively, and concentrated to the target mAb concentration. At the end, the pH of the formulation was adjusted to 6.00±0.05, filtered through 0.22 µm PVDF filters and stored at 4 °C until further use.

Viscosity

Viscosity was measured at 25 °C on a microfluidic viscometer/rheometer-on-a-chip (mVROC; RheoSense, USA). A chip with a 2 mm × 13 mm rectangular slit and a 50-µm-deep microfluidic channel was used. Rheological behaviour of the solutions was evaluated within the shear rates of 960–3960 s^{-1}. Viscosity measurements were conducted under shear rate determined by the software, based on a constant flow rate criterion.

Determination of glide force

The flow performance of the solutions through a syringe and needle was assessed using a TA.XTplusC texture analyser (Stable Micro Systems Ltd, UK) fitted with a universal syringe rig. The test speed was kept constant at 5 mm/s, and the target mode force was set in the range of 2000–3500 g (19.6–34.3 N).

3. RESULTS AND DISCUSSION

3.1. Rheological behaviour of sucrose solution and mAb formulation

By varying the shear rate, the viscosity of sucrose solution and mAb formulation remained almost constant, with changes less than 0.1 mPa·s, indicating Newtonian behaviour. Consequently, single-point viscosity

measurements were deemed adequate for subsequent analyses.

3.2. Viscosity of sucrose solutions

Protein drugs are typically unstable in aqueous environment, therefore, a stabiliser (most commonly sucrose) is often added to such formulations. In this context, we aimed to evaluate the effect of increasing sucrose concentration on the viscosity of aqueous solutions. As shown in Fig. 1, the viscosity of solution increased with the concentration of sucrose. Although the increase was not pronounced up to a concentration of 200 mM, which corresponds to the concentration in the tested formulation, we assumed that the addition of sugar to the mAb formulation further contributes to the crowding effect and altering protein-protein interactions.

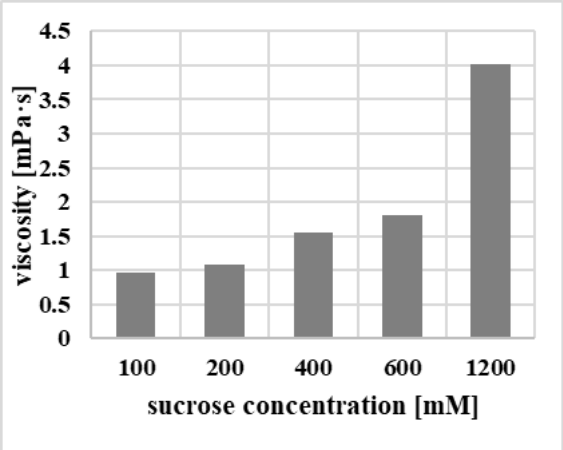

Figure 1. Effect of increasing sucrose concentration on the viscosity of aqueous solutions.

3.3. Viscosity and injection force of mAb formulations

Viscosity measurements revealed that formulations with higher mAb concentration exhibit increased viscosity (Fig. 2). Namely, the threshold of 20 mPa·s, considered as upper limit for pain-free subcutaneous administration was exceeded at the mAb concentration between 50 and 100 mg/ml. Closely related to viscosity is the injection force required for administration of mAb therapeutics. Fig. 2 illustrates the relationship between viscosity and glide force (the force required to keep the syringe plunger moving), showing that increasing mAb concentration was associated with a corresponding increase in the injection force. At the highest tested mAb concentration, the glide force exceeded the target threshold of 20 N, which may compromise patient comfort during therapy.

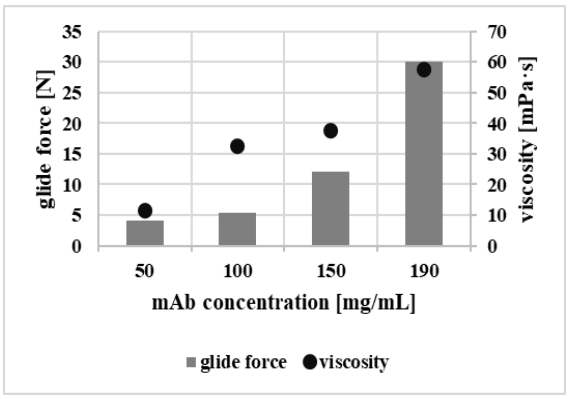

Figure 2. Viscosity and glide force of tested formulations as a function of mAb concentration.

4. CONCLUSION

Our study highlights formulation bottlenecks associated with the subcutaneous delivery of mAb. One of the promising strategies for overcoming this challenge is the incorporation of excipients which can effectively lower formulation viscosity and improve its injectability.

5. REFERENCES

1. Bjelošević, M., et al., *Effects of monoclonal antibody concentration and type of bulking agent on critical quality attributes of lyophilisates.* Drug Delivery Science and Technology, 2021. 63:102510.

2. Prašnikar, M., et al., *The search for novel proline analogs for viscosity reduction and stabilization of highly concentrated monoclonal antibody solutions.* International Journal of Pharmaceutics, 2024. 655:124055.

ACKNOWLEDGMENT

The authors acknowledge financial support by the Slovenian Research and Innovation Agency, research core funding No. P1-0189 and grant L1-3160 co-financed by Novartis d.o.o.

P066

CHARACTERIZATION OF ATORVASTATIN CALCIUM LIQUISOLID TABLETS PREPARED WITH NEUSILIN® US2 AND SYLOID® XDP 3050 AS CARRIES

Teodora Glišić[1], Isidora Spasojević[1], Sofija Stanković[1], Svetlana Ibrić[1], Jelena Parojčić[1], Ivana Aleksić[1]

[1]Department of Pharmaceutical Technology and Cosmetology, University of Belgrade – Faculty of Pharmacy, Serbia

1. INTRODUCTION

Atorvastain calcium (ATC) is a BCS class II drug known for its low absolute bioavailability (12%), which is due to its poor solubility in gastrointestinal fluids [1]. The technology of liquisolid systems (LSS) has been shown to improve the bioavailability of a number of poorly soluble drugs, primarily due to the increased surface area available for dissolution and the presence of the hydrophilic liquid vehicle, resulting in faster drug release [2]. The aim of this study was to investigate the possibility of using the LS technique to improve the dissolution rate of ATC. Two novel porous excipients with high absorption capacity were selected as carriers to formulate LS tablets with high liquid phase content and suitable mechanical properties as well as acceptable disintegration times and improved dissolution rate.

2. MATERIALS AND METHODS

2.1. Materials

Syloid® XDP 3050 (mesoporous silicon dioxide, Grace GmbH, Germany) and Neusilin® US2 (magnesium aluminometasilicate, Fuji Chemical Industry Co, Ltd., Japan) were chosen as carriers, while colloidal silicon dioxide (Evonik Industries AG, Germany) was used as the coating material. Polyethilene glycol 400 (PEG 400, Fagron, Netherlands) was used as the solvent for the model drug ATC. Crosscarmellose sodium (Primellose®, DFE Pharm, Germany) and sodium stearyl fumarate (PRUV®, JRS PHARMA, Germany) were added as superdisintegrant and lubricant, respectively.

2.2. LSS Preparation and Tableting

The liquid phase containing 2% ATC in PEG 400 was mixed with the carrier using a mortar and pestle in a ratio previously determined for each carrier. The coating material (ratio of carrier to coating material = 30), the superdisintegrant (5%) and the lubricant (1%) were added sequentially and mixed. The LS tablets (100 mg) were compressed on an instrumented tablet press (GTP D series, Gamlen Tableting Ltd, UK) with 6 mm punches at a compression load of 500 kg and compression speed of 60 mm/min.

2.3. LSS Characterisation

The breaking force of the LS tablets was measured with a hardness tester (Erweka TBH 125D, Germany) and used to calculate the tensile strength.

The disintegration time was measured in a disintegration time tester (Erweka ZT52, Erweka, Germany) with distilled water at 37 °C.

The dissolution tests were carried out in a mini paddle apparatus (modified DT600, Erweka, Germany) using 250 ml phosphate buffer (pH 6.8) at 37 °C and a mini paddle rotation speed of 75 rpm. The amount of ATC released was determined by UV spectroscopy at 241 nm. Dissolution tests were also performed on directly compressed (DC) tablets of the same composition, but without PEG 400.

X-ray powder diffraction (XRPD, Ultima IV X-ray diffractometer, Rigaku, Japan) was performed to analyse the physical state of ATC in LSS.

3. RESULTS AND DISCUSSION

3.1. Tensile Strength

The obtained LS tablets showed satisfactory mechanical properties with tensile strength values higher than 1.5 MPa despite high liquid loads. Formulation LS-N with carrier Neusilin® US2 achieved tensile strength of 1.8 MPa at the liquid phase content of 54.7 %.

P066

3.2. Disintegration Time

The LS tablets of both formulations disintegrated in less than four minutes. The disintegration time appeared to be influenced by the mechanical properties of the LS tablets, as the LS-N tablets, which have a higher tensile strength, had a slightly longer disintegration time than the LS-S formulation, which contained the carrier Syloid® XDP 3050.

3.3. Dissolution Studies

The results of dissolution testing (Fig. 1) show that ATC was completely released from the LS tablets irrespective of the carrier used, while only around 70 % ATC was released from DC tablets.

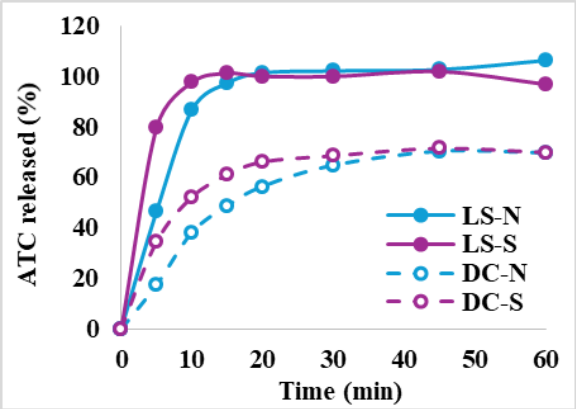

Figure 1. Dissolution profiles of LS and DC tablets; labels N and S indicate the use of carrier Neusilin® US2 and Syloid® XDP 3050, respectively.

It can be observed that the application of the LS technique improves both the extent and the rate of ATC release. For both LS and DC tablets, the carrier Syloid® XDP 3050 appeared to promote faster drug release compared to Neusilin® US2. More than 80% of the drug was released from LS-S in the first 5 minutes. The faster drug release from LS-S tablets could be due to the lower tensile strength and shorter disintegration time observed for these tablets. Although the drug release from formulation LS-N was slightly slower than that from formulation LS-S, more than 80% of the drug was released in the first 10 minutes, indicating that both formulations exhibited rapid drug release and meet the United States Pharmacopoeia recommendations on dissolution testing of ATC uncoated tablets.

3.4. X-ray Powder Diffraction

The XRPD results showed the disappearance of distinctive ATC peaks in the LS formulations, indicating that the drug is no longer in crystalline form and is dissolved in PEG 400. The significantly improved dissolution of ATC from LS tablets can thus be attributed to the drug being molecularly dispersed in PEG 400.

4. CONCLUSION

The ATC LS tablets prepared with both of the investigated carriers showed satisfactory mechanical strength and disintegration time. The use of LS technology led to an improvement in the dissolution rate of ATC, with complete drug release achieved in less than 20 minutes.

5. REFERENCES

1. Prabhu, P., et al., *Dissolution enhancement of atorvastatin calcium by co-grinding technique*. Drug delivery and translational research, 2016. 6: 380-391.

2. Aleksić, I., et al., *Liquisolid systems as a novel approach in formulation and manufacturing of solid dosage forms: Challenges and perspectives*. Archives of Pharmacy, 2022. 72(6): 521-545.

ACKNOWLEDGMENT

This research was funded by the Ministry of Science, Technological Development and Innovation, Republic of Serbia through two Grant Agreements with University of Belgrade-Faculty of Pharmacy No 451-03-136/2025-03/ 200161and No 451-03-137/2025-03/ 200161.

P067

IN VITRO NASAL DEPOSITION PROFILES OF DONEPEZIL-LOADED CHITOSAN-BASED THERMOGELLING SYSTEM: CONVENTIONAL vs. BI-DIRECTIONAL DELIVERY

Mirna Perkušić[1], Laura Nižić Nodilo[1], Cvijeta Jakobušić Brala[1], Ivan Pepić[1], Dijana Zadravec[2], Livije Kalogjera[3], Anita Hafner[1]

[1]*Department of Pharmaceutical Technology, University of Zagreb Faculty of Pharmacy and Biochemistry, Croatia*
[2]*Department of Diagnostic and Interventional Radiology, University Hospital Center Sestre Milosrdnice, University of Zagreb School of Dental Medicine, Croatia*
[3]*ORL/HNS Department, University Hospital Center Sestre Milosrdnice, Croatia*

1. INTRODUCTION

Oral administration of donepezil is often associated with gastrointestinal side effects and limited brain delivery. Nasal route has emerged as a promising alternative, enabling direct and efficient transport of the drug to the brain, *via* olfactory and trigeminal nerves, innervating olfactory and/or respiratory regions of nasal cavity [1, 2]. Innovative nasal formulations, such as thermoresponsive *in situ* gelling systems, offer significant potential for nasal drug administration [3]. To ensure efficient delivery to the regions of interest, nasal deposition studies need to be performed as a crucial part of formulation development. Conventional nasal delivery relies on a unidirectional spray, while bi-directional delivery refers to breath-powered nasal administration where, during exhalation, elevation of the soft palate separates the nasal and oral cavity, allowing airflow to enter through one nostril toward the nasopharynx and exit through the other [4].

In this work we evaluated and compared *in vitro* nasal deposition profiles of donepezil-loaded chitosan-based thermogelling system upon conventional and bi-directional delivery, to screen the impact of nasal delivery mode on donepezil brain targeting efficiency.

2. MATERIALS AND METHODS

2.1. Materials

A thermogelling chitosan-based formulation for nose-to-brain delivery of donepezil was developed using low molecular weight chitosan (C; Sigma-Aldrich, Germany) and β-glycerophosphate (B; Biosynth Ltd., Slovakia) as the gelling agent. Chitosan solution (1.5%, *w/w*) was slowly added to β-glycerophosphate solution (49%, *w/w*) at 4 °C in a 1.6:1 volume ratio. Donepezil (D; Carbosynth Ltd., UK) was then incorporated into the resulting C-B solution. In the final formulation (DCB), the concentrations of D, C, and B were 0.30, 9.23, and 188.00 mg mL^{-1}, respectively.

2.2. Methods

Nasal deposition studies were performed using a multi-sectional 3D-printed nasal cast obtained from a CT scan of a 62-year-old patient. The protocol was approved under identification code EP-9941/19-3, Class: 643-02/19-01/02; Registry number: 251-62-03-19-43. Prior to the administration of the sample, the model was evenly coated with a thin layer of a Sar-gel® indicator paste to visualise the deposition pattern and prevent dripping. The fractional spray deposition pattern was determined gravimetrically. Each experiment was performed in duplicate. The formulation was delivered into the model using an Aptar VP7 spray pump, equipped with the 232 NE actuator.

For conventional delivery of DCB formulation, the VP7 pump was inserted into the right nostril, while the left nostril was blocked. The device was actuated at an angle 0˚ from the vertical plane, and 75˚ angle from the horizontal plane (AAH). The model was connected to the respiratory pump to simulate breathing, with inspiratory flow rate (IFR) of 0 L min^{-1} and 30 L min^{-1}.

In order to simulate bi-directional drug administration, the respiratory pump was connected to the left nostril. Airflow through the nasal cavity was simulated with the following settings on the respiratory pump: inhaled air

volume of 700 mL, inhalation to exhalation ratio at 25:75, at 35 breaths per minute. The set breath rate corresponds to a flow of 30 L min^{-1}. The DCB formulation was sprayed into the free (right) nostril. The passage to the oral cavity was sealed with parafilm to simulate the raising of the soft palate during exhalation, creating a closed system. The device was actuated at an angle 0° from the vertical plane, and 60° and 75° AAH.

3. RESULTS AND DISCUSSION

Results of the nasal deposition of DCB formulation using conventional and bi-directional delivery methods are presented in Table 1.

Table 1. Results of *in vitro* nasal deposition studies.

DCB	OR (%)	TR (%)	S (%)	AR (%)	Recovery (%)
Bi-Directional (75 ˚ AAH)	5,8 ± 5,2	49,9 ± 1,9	29,1 ± 5,2	13,8 ± 3,6	98,4 ± 5,5
Bi-Directional (60 ˚ AAH)	2,7 ± 1,3	54,0 ± 0,2	35,6 ± 1,6	4,0 ± 2,6	96,2 ± 2,1
Conventional (75 ˚ AAH, 0 L min^{-1} IFR)	71,8 ± 0,8	10,5 ± 2,1	10,2 ± 0,6	5,0 ± 0,4	97,5 ± 2,2
Conventional (75 ˚ AAH, 30 L min^{-1} IFR)	35,0 ± 3,4	41,4 ± 1,0	19,0 ± 5,2	0,9 ± 0,5	96,3 ± 9,1

All values are mean ± SD (n=2). DCB – donepezil chitosan β-glycerophosphate formulation; OR – olfactory region; TR – turbinate region; S – septum; AR – anterior region; AAH – angle of administration from the horizontal plane; IFR – inspiratory flow rate.

For both methods of DCB formulation delivery, relatively low fraction of applied dose was deposited in the anterior region, i.e. in front of the nasal valve. Bi-directional delivery resulted in higher turbinate and septum deposition, and lower olfactory deposition, compared to conventional nasal delivery. AAH in bi-directional delivery did not influence the nasal deposition pattern. It is possible that bi-directional airflow dragged the formulation away from the olfactory region, leading to greater deposition in the turbinate area. Fraction of the drug dose deposited in the turbinate region can be directly delivered to the brain by trigeminal nerve. However, it is also at disposal for systemic absorption [5]. Drug deposited in olfactory region can be more efficiently delivered directly to the brain by olfactory and trigeminal nerve, assigning this region as preferable [5]. In line with this, it may be concluded that, in case of donepezil loaded thermogelling system, conventional mode of nasal delivery was superior to bi-directional. The optimal delivery mode among tested refers to conventional spray administration at a 75° AAH without inhalation (0 L min^{-1}).

4. CONCLUSION

Administration of the DCB formulation by both conventional and bi-directional method demonstrated strong potential for deposition beyond the nasal valve, e.g. to the regions of interest. Given the critical role of olfactory deposition in nose-to-brain drug delivery, conventional (unilateral) mode is confirmed as the optimal method for delivering the developed *in situ* gelling donepezil system.

5. REFERENCES

1. Djupesland, P.G., et al., *The Nasal Approach to Delivering Treatment for Brain Diseases: An Anatomic, Physiologic, and Delivery Technology Overview.* Therapeutic Delivery, 2014. 5: 709-733.

2. Agrawal, M., et al., *Nose-to-Brain Drug Delivery: An Update on Clinical Challenges and Progress towards Approval of Anti-Alzheimer Drugs.* Journal of Controlled Release, 2018. 281: 139 - 177.

3. Agrawal, M., et al., *Stimuli-Responsive In Situ Gelling System for Nose-to-Brain Drug Delivery.* Journal of Controlled Release, 2020. 327: 235 - 265.

4. Liu, Y., et al., *Bi-directional nasal drug delivery systems: A scoping review of nasal particle deposition patterns and clinical application.* Laryngoscope Investigative Otolaryngology, 2023. 6: 1484 – 1499.

5. Laffleur, F., Bauer, B. *Progress in nasal drug delivery systems.* International Journal of Pharmaceutics, 2021. 607: 120994.

ACKNOWLEDGMENT

This work has been supported in part by Croatian Science Foundation under the project UIP-2017-05-4592, European Social Fund under the Croatian Science Foundation project DOK-2020-01-2473.

P068

NEBULIZATION STUDY OF TOCILIZUMAB IN SINGLE STAGE GLASS IMPINGER, A PHARMACOPEIAL IN-VITRO MODEL OF THE HUMAN PULMONARY SYSTEM

Juraj Piestansky[1,2], Patricia Jackliakova[1], Paula Cermakova[1], Miroslava Spaglova[1]

[1]Department of Galenic Pharmacy, Faculty of Pharmacy Comenius University, Slovakia
[2]Institute of Neuroimmunology, Slovak Academy of Sciences, Slovakia

1. INTRODUCTION

Biopharmaceuticals, including monoclonal antibodies (mAb) represent the innovative tool in therapeutic strategies for various acute and/or chronic life-threating diseases. The typical delivery route of such drugs is based on intra venous (i.v.), sub cutaneous (s.c.), or intra muscular (i.m.) application. However, such delivery routes do not possess suitable safety profile especially in cases of diseases affecting respiratory tract [1]. The main disadvantages of the aforementioned delivery routes are: the impossible self-medication, possible induction of haemolysis, severe adverse effects (organ toxicity), necrosis, and sloughing the tissues in case of extravasation of some drugs, etc. Therefore, it is necessary to investigate alternative and more effective delivery routes of the biopharmaceuticals.

Inhalation delivery route is a non-invasive technique allowing administration of drugs both locally and systematically. Inhalation drug delivery of biologics offers several advantages – lower concentration of the biologics is applied what can finally results in lower price of the final product with the same or better therapeutic effect, specific targeted respiratory system intervention with possible local or systemic therapeutic effect, possible self-medication (no need of skilled medical staff for application).

The aim of this work was to investigate the possibility of mAb tocilizumab to be applied by inhalation delivery route. We also studied, using a pharmacopeial in-vitro human pulmonary system model, into which compartments of the respiratory tract tocilizumab could be delivered.

2. MATERIALS AND METHODS

2.1. Materials

Sodium phosphate dibasic, sodium phosphate monobasic, sodium chloride (p.a. quality), methanol, and water of LC quality were obtained from Merck (Darmstadt, Germany). BEH 450 SEC Protein Standard Mix was purchased from Waters (Milford, MA, USA). The drug Tyenne® was obtained from a local drug store. Single Stage Glass Impinger was obtained from Westech Scientific Instruments (Essex, UK) and the nebulizer PARI eFlow® was purchased from PARI Pharma (Gräfelfing, Germany).

2.2. Size-exclusion chromatography (SEC)

All of the analyses were carried out on the chromatographic apparatus Acquity UPLC H-Class equipped with a quaternary gradient pump, autosampler, and column thermostat (Waters, Prague, Czech Republic). The UHPLC apparatus was coupled with the UV-detector (Waters), which was set at a constant wavelength of 280 nm. The chromatographic separation was carried out using an Acquity UPLC® BEH450 SEC column (2.5 µm, 4.6 x 150 mm). As a mobile phase, 25 mM phosphate buffer (pH 6.8) with addition of 250 mM NaCl was used. The flow rate of the mobile phase was set at 0.3 mL/min. During all of the analyses the column temperature was maintained at room temperature. The injection volume was 10 µL.

2.3. Single Stage Glass Impinger – nebulization test

The nebulization test was performed with the pharmacopeial in-vitro model of human pulmonary system. The test procedure was composed of following steps: 1) introduction of prescribed amount of water (LC quality) into upper and lower impingement chambers; 2) connection of all component parts of the apparatus and connection of a suitable pump fitted with a filter to the outlet of the apparatus; 3) adjustment of the air flow through the apparatus to 60 L/min; 4) introduction of 5 mL of the tocilizumab (2 mg/mL) into the reservoir of the nebuliser; 5) fitting the mouthpiece and its connection by an adapter to the device; 6) switching on the pump of the apparatus and

P068

after 10 s switching on the nebuliser (Figure 1); 7) after 60 s, switching off the nebuliser, waiting 5 s ad then switching off the pump; 8) dismantling the apparatus and washing the inner surface of selected impinger chambers; 9) analysis of the collected samples by SEC-UV.

Figure 1. Nebulisation of the mAb tocilizumab (drug Tyenne®) during the Single Stage Glass Impinger test.

3. RESULTS AND DISCUSSION

In our study, the possibility of inhalation delivery route of mAb (here, tocilizumab) was investigated. Nebulization of mAb seem to be a promising tool for such type of mAb delivery. According to the availability of nebulization devices at the market, we selected to realize a nebulization study with the use of a vibrating-mesh nebulizer (PARI eFlow). This device was connected to the Single Stage Glass Impinger, a pharmacopeial in-vitro model of the human pulmonary system. The presence of the nebulized mAb tocilizumab (c = 2 mg/mL) was investigated in the collected samples from each particular compartment of the in-vitro model apparatus by the SEC-UV method (Figure 2). As can be seen, the presence of tocilizumab in upper chamber of the apparatus (representing upper respiratory tract) and also in lower chamber of the apparatus (representing lower respiratory tract, lungs) confirmed effective formation of suitable particles accessible the demanded part of the respiratory tract.

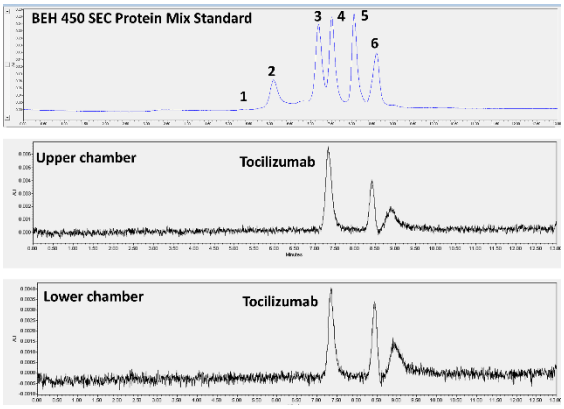

Figure 2. Representative chromatograms obtained from the SEC-UV analysis of BEH450 SEC Protein Mix Standard (upper trace), nebulised sample collected from the upper chamber (middle trace), and nebulised sample collected from the lower chamber (lower trace). 1 – thyreoglobulin dimer (MW = 1440 kDa), 2 – thyreoglobulin monomer (MW = 660 kDa), 3 – IgG (MW = 150 kDa), 4 – bovine serum albumin (MW = 66.4 kDa), 5 – myoglobin (MW = 17 kDa), 6 – uracil (MW = 112 Da).

4. CONCLUSION

It is expected that the best route for inhaled administration of mAb (here, tocilizumab) into the body is nebulization. There are several types of inhalation devices, however, not all types of them are suitable for mAb. Jet nebulizers could cause degradation of protein drugs due to the presence of a partition with very small holes, while ultrasonic nebulizers heat up to some extent, which could have a bad effect on stability. The most suitable is the use of membrane nebulizers, such as the PARI eFlow system. Thanks to this system, we managed to get a portion of the undegraded tocilizumab (drug Tyenne®) to the lowest part of the pharmacopeial airway model, representing the lungs. These results are very promising, however further research is needed.

5. REFERENCES

1. Parray, H.A., et al., *Inhalation monoclonal antibody therapy: a new way to treat and manage respiratory infections.* Applied Microbiology and Biotechnology, 2021. 105(16-17): 6315-6332.

ACKNOWLEDGMENT

This work was supported by the Slovak Research and Development Agency under Contract no. APVV-23-0508.

P069

THE INFLUENCE OF PEGYLATION ON THE PASSIVE LOADING OF RISPERIDONE IN NANOEMULSIONS

Jelena Đoković, Tamara Radosavljević, Snežana Savić

Department of pharmaceutical technology and cosmetology, Faculty of pharmacy, University of Belgrade, Serbia

1. INTRODUCTION

Passive loading is a material-saving approach that allows a maximum loadable amount of drug to be incorporated into a nanoparticle system [1,2]. PEGylation is a strategy to extend the circulation time of parenterally administered formulations by using hydrophilic PEG chains to coat the particles, thereby inhibiting the adsorption of serum opsonins and the subsequent rapid removal of the particles from the circulation [3]. The aim of this work was to determine the effects of PEGylated phospholipid on the passive loading of risperidone, a poorly water-soluble psychopharmacological agent, in nanoemulsions (NEs) for parenteral use.

2. MATERIALS AND METHODS

2.1. Materials

Medium-chain triglycerides (MCT) were purchased from Fagron GmbH & KG (Barsbüttel, Germany). Soybean oil (SO), soybean lecithin (SL), sodium oleate (SOl) and PEG2000-DSPE were generously gifted by Lipoid GmbH (Ludwigshafen, Germany). RSP was kindly donated by Zdravlje Actavis (Leskovac, Serbia). Polysorbate 80 (P80), bovine serum albumin (BSA) and butylhydroxytoluene (BHT) were purchased from Sigma-Aldrich Co. (St. Louis, MO, USA), while glycerol (Gly) was provided by Merck KGaA (Darmstandt, Germany).

2.2. The preparation of nanoemulsions

The NEs were prepared using the hot high pressure homogenization technique. For the non-PEGylated formulation (F1), the oil phase (MCT (16 %, w/w), SO (4 %, w/w), SL (2 %, w/w) and BHT (0.05 %, w/w)) and the aqueous phase (Gly (2.25 %, w/w), P80 (2 %, w/w), SOl (0.03 %, w/w) and highly purified water to 100 %, w/w) were prepared separately and heated to 50 ˚C, then mixed and first processed on the rotor-stator homogenizer (11000 rpm for 1 minute), and finally on the high-pressure homogenizer (EmusiFlex C3) for 10 discontinuous cycles at 800 bar. The PEGylated NE (F2) was prepared in the same way, with the addition of 0.3 % (w/w) PEG2000-DSPE to the aqueous phase.

2.3. Passive loading of risperidone

To determine the maximum loading of risperidone in the NEs and the time required to achieve this, risperidone was added in excess to 1 ml of both F1 and F2 and mixed for 8 days in Eppendorf tubes, which were tested for risperidone loading at regular intervals (after 1, 2, 3, 4 and 8 days) after the undissolved drug had been removed by centrifugation. Subsequently, the selected optimal amount of risperidone was added to 10 ml of F1 and F2 and mixed to achieve complete loading. These formulations were used for further analyses. The concentration of risperidone was determined spectrophotometrically at 280 nm after dilution in isopropanol.

2.4. Physicochemical characterization

Droplet size (Z-ave), polydispersity index (PDI), zeta potential (ZP), pH and conductivity were measured for both F1 and F2, before and after the addition of risperidone.

2.5. Protein interactions

To assess the influence of risperidone loading on the PEGylation efficacy, risperidone-loaded F1 and F2 were incubated for 24 h in 30 mg/ml BSA in PBS (pH 7.4), as well as pure PBS for controle. Droplet size (Z-ave) and droplet size distribution (PDI) were measured regularly during this time to detect protein binding.

2.6. In vitro release

The release of risperidone from the NEs was assessed using the direct dialysis bag technique. The dialysis tubes/bags were filled with 2 mL of the NE sample (donor phase) and placed in a flask containing 200 mL of dissolution medium (PBS pH 7.4 : methanol, 80:20, v/v) at 37 °C.

3. RESULTS AND DISCUSSION

3.1. Maximum loadability

P069

The maximum concentration of risperidone in the nanoemulsions varied between 1.5 and 2.5 mg/ml during the test period. However, there were no significant differences between F1 and F2, indicating that PEGylation did not interfere with the uptake of risperidone into the nanoemulsion droplets. For further analysis, risperidone-loaded F1 and F2 were prepared by adding 15 mg risperidone to 10 ml of F1 or F2 and mixing overnight (250 rpm) on an orbital shaker to achieve a final concentration of 1.5 mg/ml.

3.2. Physicochemical characterization

After the period of incubation there were no signs of undissolved risperidone in either NE. Fig. 1 shows that the addition of risperidone led to an increase in droplet size and size distribution (F1R and F2R compared to F1 and F2, respectively), indicating binding of risperidone to the droplets. The ZP value did not change significantly with the addition of risperidone in F1, but did in F2, indicating a different localisation of the drug in the droplet. Interestingly, both pH and conductivity values increased after the addition of risperidone, which requires further investigation into its precise localisation and possible interactions with the other components of the NEs. However, the obtained results show that the F1R and F2R have satisfactory properties for parenteral use.

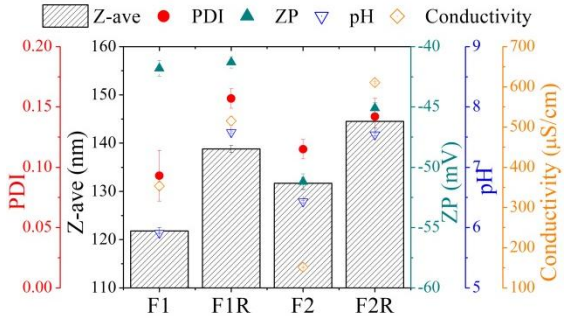

Figure 1. Physicochemical properties of NEs before and after passive encapsulation.

3.3. Protein interactions

It was observed that Z-ave and PDI remained unchanged for both F1R and F2R after incubation in pure PBS for 24 hours, suggesting that any changes in these parameters after incubation with BSA-rich PBS were due to the presence of protein. As expected, Z-ave and PDI increased significantly in F1, reflecting a lack of steric protection. Interestingly, droplet size did not change drastically for F2, suggesting that passive loading of risperidone did not adversely affect the PEG coating around the droplets.

3.4. In vitro release

The in vitro release data (Fig. 2) show similar release patterns between the two formulations, with PEGylated formulation F2 showing a higher percentage of release, indicating a different localisation of risperidone compared to F1, possibly in the PEGylated coating. The release data were best described by the Weibull model, indicating complex release patterns.

Figure 2. In vitro release of risperidone

4. CONCLUSION

PEGylation did not interfere with the passive

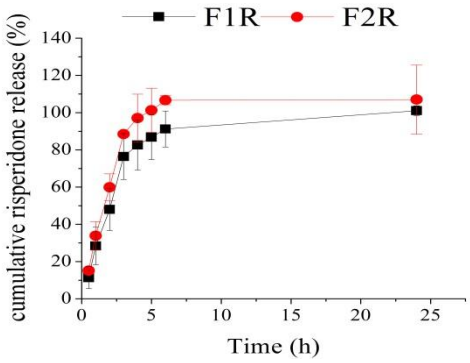

encapsulation of risperidone in the nanoemulsion droplets, which is a good technique for the preparation of risperidone-loaded NEs.

5. REFERENCES

1. Rosenblatt, K. M., Bunjes H., *Evaluation of the drug loading capacity of different lipid nanoparticle dispersions by passive drug loading.* European Journal of Pharmaceutics and Biopharmaceutics, 2017. 117: 49-59.

2. Göke, K., Bunjes H., *Carrier characteristics influence the kinetics of passive drug loading into lipid nanoemulsions.* European Journal of Pharmaceutics and Biopharmaceutics, 2018. 126: 132-139.

3. Elsewedy, H. S. et al., *Brucine PEGylated nanoemulsion: In vitro and in vivo evaluation.* Colloids and Surfaces A, 2021. 608: 125618

ACKNOWLEDGMENT

This research was financially supported by the Ministry of Science, Technological Development and Innovation of the Republic of Serbia through Contracts Nos. 451-03-136/2025-03/200161 and 451-03-137/2025-03/200161.

P070

LOW ENERGY NANOEMULSIONS WITH CITRUS ESSENTIAL OILS: FORMULATION DEVELOPMENT AND ANTIOXIDANT ACTIVITY

Ana Gledović[1], Tamara Jekeli[1], Aleksandra Janošević Ležaić[2], Danica Bajuk-Bogdanović[3], Snežana Savić[1]

[1]Department of Pharmaceutical Technology and Cosmetology, University of Belgrade, Faculty of Pharmacy, Serbia

[2]Department of Physical Chemistry and Instrumental Methods, University of Belgrade, Faculty of Pharmacy, Serbia

[3]University of Belgrade, Faculty of Physical Chemistry, Serbia

1. INTRODUCTION

Nowadays, there is a great demand for natural cosmetic products and pharmaceuticals produced from renewable bio-resources [1,2]. A striking example of such popular raw materials is citrus essential oils (EOs), which are known for their characteristic refreshing scent and flavour, but are also currently being investigated as potential antioxidant, antimicrobial and anti-inflammatory actives [1-3]. Due to their volatility and sensitivity to heat, light and air, there is a need for innovative formulations such as nanoemulsions (NEs) to address these issues [3,4]. Therefore, the aim of this study was to develop stable nanoemulsions suitable for topical applications with different citrus EOs and to evaluate their antioxidant activity.

2. MATERIALS AND METHODS

2.1. Materials

The following 6 citrus essential oils from the *Rutaceae* family were tested: *Citrus aurantium bergamia* – bergamot, *Citrus limon* – lemon, *Citrus aurantifolia* – lime, *Citrus aurantium dulcis* – sweet orange, *Citrus nobilis* – mandarin orange, and *Citrus paradisi* – grapefruit peel oil. Polyglycerol-10 laurate (P10L) was used as the main surfactant, glyceryl caprylate (GC) as cosurfactant (both certified for natural cosmetics) and/or phenoxyethanol/ethylhexyl glycerine (PE) as a preservative/cosurfactant, ethylhexyl stearate (ES) as carrier oil, while water phase of the NEs' was ultra-pure water.

2.2. Nanoemulsion preparation and optimisation

EO-loaded NEs were prepared by using the low energy phase inversion composition (PIC) method at room temperature as previously described [4]. The influence of surfactant-to-emulsion (SER), surfactant-to-oil (SOR) ratio and the influence of EO and cosurfactant addition on the NE formation and properties was evaluated by varying their concentration, while the oil phase content was kept at 10 wt.%.

2.3. Nanoemulsion characterisation

NEs were confirmed visually and by dynamic light scattering – DLS (Z-average droplet size and polydispersity index – PDI), pH value and conductivity measurements. All stable NEs were kept at room temperature (RT) and retested, up to 3 months.

2.4. Raman spectroscopy of EOs

Raman spectra of the citrus EOs were recorded to confirm their major components responsible for bioactivity (with DXR Raman microscope, excitation wavelength 780 nm).

2.5. Antioxidant activity of EOs and EO-loaded nanoemulsions

Two antioxidant assays were performed: DPPH test in lipophilic medium (methanol) and ABTS test in aqueous medium (PBS buffer).

3. RESULTS AND DISCUSSION

3.1. Formulation optimisation

It was found that optimal SOR value is 1, and minimal SER value was 8 to 10, and the optimal concentration of EO was 1 wt.% for all citrus EO-loaded NEs. Although the EO-loaded NEs had significantly lower droplet sizes (Z-ave ~ 37 – 46 nm) than the blank NE (~169 nm) they quickly showed signs of instability, such as fast increase of droplet sizes and creaming (especially blank NE, sweet orange, mandarin orange and grapefruit EO-loaded NEs). Formulation optimisation was achieved by adding 0.5 wt.% of GC and 0.5 wt.% of PE, which significantly improved the stability of NEs loaded with bergamot, lime or lemon EO (Table 1).

P070

Table 1. Optimised EO-loaded NEs - results of DLS measurements after 3 months of storage at RT.

NE	Z-ave	PDI
Bergamot EO	48.91 ± 0.208	0.076 ± 0.008
Lime EO	45.10 ± 0.731	0.068 ± 0.005
Lemon EO	43.11 ± 0.172	0.089 ± 0.017

3.2. Raman spectroscopy of EOs

The Raman spectra of the citrus EOs are dominated by limonene bands (with characteristic peaks observed at 1680, 1645, 1435, and 760 cm^{-1}) (Figure 1).

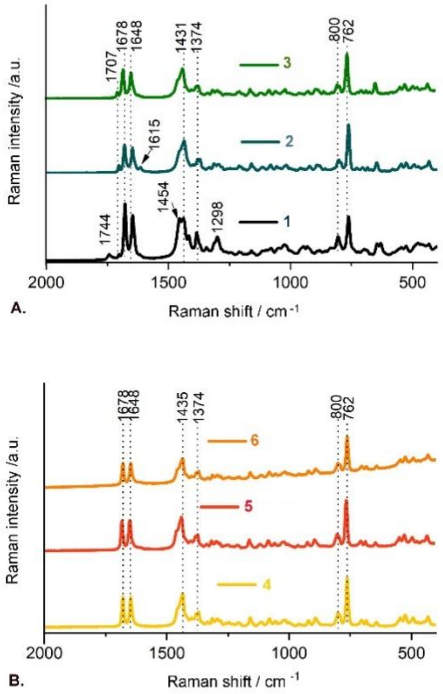

Figure 1. Raman spectra of the citrus EOs: **A**. 1- lemon, 2- lime, 3- bergamot and **B:** 4- grapefruit, 5- sweet orange, 6- mandarin orange.

Therefore, these citrus EOs were classified in two different groups: A. medium limonene group (≤45–70%), and B. high limonene content group (≤99%). In addition, the spectra of lemon, lime and bergamot also exhibited bands of other relevant molecules for the EOs' antioxidant activity (i.e., linalool, linalyl acetate, citral). The obtained results were generally in line with the product specifications.

3.3. Antioxidant activity of EOs and EO-loaded nanoemulsions

The tested EOs scavenged ABTS free radical in the following order: sweet orange ~ mandarin orange (≥95%), lime (~68%), grapefruit (~64%), lemon (~56%) and bergamot (~47%), at 6µL/mL test concentration. On a contrary, the tested EOs were much less effective DPPH radical scavengers, since only lime and lemon EO showed moderate activity at 5x higher test concentrations (~42% and ~38%, respectively). Optimized NEs with bergamot, lime or lemon EO also scavenged the ABTS radical (~28%, ~42% and ~19%, respectively).

4. CONCLUSION

Based on the obtained results it was concluded that bergamot, lime and lemon EOs are more suitable for development of cosmetic nanoemulsions for antioxidant skin protection.

5. REFERENCES

1. Guzmán, E., Lucia, A., *Essential Oils and Their Individual Components in Cosmetic Products*. Cosmetics, 2021, 8: 114.

2. Li, Y. et al., *The Chemical Composition and Antibacterial and Antioxidant Activities of Five Citrus Essential Oils*. Molecules, 2022, 27: 7044.

3. Liu, T. et al., *Preparation, Characterization, and Antioxidant Activity of Nanoemulsions Incorporating Lemon Essential Oil.* Antioxidants, 2022, 11: 650.

4. Gledović, A. et al. Low Energy Nanoemulsions as Carriers for Essential Oils in Topical Formulations for Antioxidant Skin Protection: Hemijska Industrija, 2022, 76 (1): 29-42.

ACKNOWLEDGMENT

This research was funded by the Ministry of Science, Technological Development and Innovation, Republic of Serbia through two Grant Agreements with University of Belgrade-Faculty of Pharmacy No 451-03-136/2025-03/ 200161 and No 451-03-137/2025-03/ 200161.

P071

PREPARATION OF LIQUID CRYSTALLINE NANOPARTICLES USING A LOW-ENERGY METHOD: FORMULATION OPTIMISATION

Mirjam Gosenca Matjaž[1], Monika Prašnikar[1], Mercedes Vitek[1], Janez Mravljak[2], Andrej Jamnik[3], MatijaTomšič[3]

[1]*Department of Pharmaceutical Technology, University of Ljubljana, Faculty of Pharmacy, Slovenia*
[2]*Department of Pharmaceutical Chemistry, University of Ljubljana, Faculty of Pharmacy, Slovenia*
[3]*Department of Physical Chemistry, University of Ljubljana, Faculty of Chemistry and Chemical Technology, Slovenia*

1. INTRODUCTION

Liquid crystalline nanoparticles (LCNPs) such as cubosomes and hexosomes, are promising drug delivery systems that combine the structural order of liquid crystalline mesophases with the benefits of nanodelivery systems. Their unique internal nanostructure enables the encapsulation of hydrophilic, hydrophobic, and amphiphilic drugs, offer protection for sensitive drugs and provide sustained release, which is especially valuable for drugs with short half-lives, such as peptides [1,2]. Preparation of LCNPs mainly includes top-down and bottom-up methods, which differ primarily in energy requirements. Bottom-up methods use lower energy and require a hydrotrope, such as ethanol (EtOH), to facilitate nanoparticle formation. While this approach is more sustainable and better suited for encapsulating fragile drugs, it often results in polydisperse systems [3]. In this study, we investigate the influence of formulation variations on the glycerol monooleate (GMO)-based LCNP formation, with the aim to optimise a bottom-up preparation of LCNPs for the encapsulation of peptide drugs.

2. MATERIALS AND METHODS

2.1. Materials

Peceol™ (32.0–52.0% GMO) was donated by Gattefosse, France and Monomuls® 90-O 18 (97.7% GMO) was a gift from BASF, USA. Kolliphor® (poloxamer 407) and EtOH (96%) were purchased from Sigma-Aldrich Chemie GmbH, USA and Pharmachem, Slovenia, respectively.

2.2. Preparation of nanoparticles

Nanoparticles were prepared using a bottom-up hydrotrope method [1,3]. GMO and EtOH were mixed in various ratios in a glass vial, and poloxamer 407 was added. Buffer (phosphate or acetate) was added dropwise using a syringe and needle under magnetic stirring (1000 RPM). The dispersion was then stirred for 2 hours in a closed vial at room temperature or in a water bath.

2.3. Particle size and polidispersity

Particle size and polydispersity index (PDI) was measured by dynamic light scattering method (Zetasizer Ultra, Malvern Panalytical, UK).

2.4. Ultra-high-performance liquid chromatography coupled to high-resolution mass spectrometry (UHPLC-HRMS)

UHPLC-Q-Orbitrap HRMS analysis of lipids was performed on an UltiMate 3000 UHPLC Systems (Thermo Scientific™) system coupled with an Q Exactive™ Plus Hybrid Quadrupole-Orbitrap™ Mass Spectrometer (Thermo Scientific™).

2.5. Small angle X-ray scattering (SAXS)

SAXS measurements were performed using a modified Kratky-type camera (Anton Paar) equipped with a Göbel mirror, a line-collimation system, and a Mythen 1K detector (Dectris). Samples were measured in 1 mm quartz capillary at 25 °C for 15 minutes.

3. RESULTS AND DISCUSSION

Two lipids were considered for LCNPs preparation, namely low GMO content Peceol™ and high GMO content Monomuls®. Besides, Peceol™ contained a significant proportion of oleic acid diester (t_R 45.3 min), whereas Monomuls® 90-O 18 contained only oleic acid monoester (t_R 30.5 min). Both materials also contained trace amounts of palmitic and stearic acid monoesters (t_R 29.7 min and 32.3 min, respectively) (Fig. 1).

P071

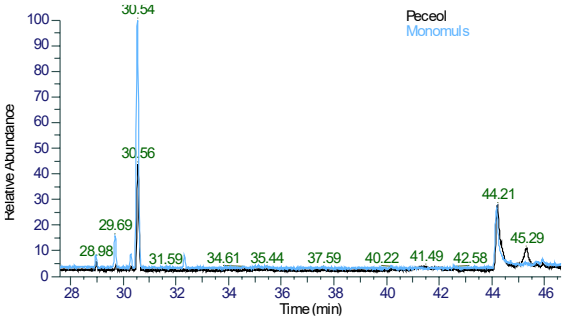

Figure 1. Total ion chromatogram (TIC) of Peceol™ (black line) and Monomuls® 90-O 18 (blue line).

Initial experiments using Peceol™ (GMO content<52.0%) yielded nanoparticles with promising size (~170 nm) and low PDI (<0.18) across a broad pH (5.5–7.4) and temperature range (25–45 °C), indicating robust formulation reproducibility. GMO, EtOH and poloxamer 407 ratios significantly affected the nanoparticle size and PDI. A GMO:EtOH ratio of 1:1 and 2:1 enabled formation of nanoparticles below 200 nm with PDI below 0.20, while at a 3:1 ratio, the nanoparticles had a higher PDI. The experiments showed that the formulation with 5% GMO, 5% EtOH and 1.42% poloxamer 407 yielded low PDI (<0.14) and a reproducible nanoparticle size (~170 nm), which did not change significantly after 28 days of storage at room temperature. However, for these nanoparticles SAXS analysis showed a broad scattering peak lacking narrow peaks characteristic of lyotropic liquid crystalline mesophases (Fig. 1). Therefore, we assumed that the dispersion was likely an emulsified microemulsion rather than LCNPs.

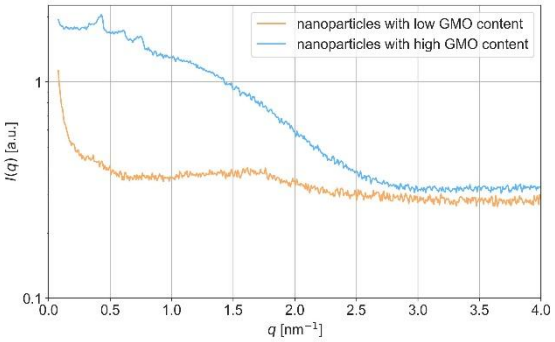

Figure 2. SAXS analysis of nanoparticles with low and high GMO content lipids.

Switching to Monomuls® 90-O 18 with 97.7% GMO resulted in successful cubosome formation as confirmed by SAXS, showing characteristic Bragg peaks of Im$\bar{3}$m cubic phase (Fig. 2). However, applying the same bottom-up hydrotrope method resulted in suboptimal nanoparticle quality, i.e. large average particle size (475 nm) and a high PDI (0.55). An increased ethanol content (GMO:EtOH=1:1) disrupted the formation of the liquid crystalline mesophase, while adding GMO (≥20%) to dispersion led to gelation, further indicating instability of LCNP formation under these conditions.

4. CONCLUSION

This study demonstrates that the formation of LCNPs via a bottom-up hydrotrope method is highly dependent on the lipid's characteristics and the precise balance of formulation parameters. While low-content GMO with diesters also present (Peceol™) enabled the formation of nanoparticles with favorable size and polydispersity, SAXS analysis revealed the absence of an internal liquid crystalline order, indicating the formation of emulsified systems rather than genuine LCNPs. In contrast, high-content GMO in the form of monoesters (Monomuls® 90-O 18) enabled the formation of LCNPs with well-defined cubic phase Im$\bar{3}$m. Further refinement of the method will focus on reducing LCNP size and PDI to develop a robust system for peptide drug encapsulation and sustained subcutaneous delivery.

5. REFERENCES

1. Yaghmur, A., et al., *Recent advances in drug delivery applications of cubosomes, hexosomes, and solid lipid nanoparticles.* Acta Pharm Sin B, 2021. 11(4):871-85.
2. Vitek, M., et al., E*xploiting the potential of in situ forming liquid crystals: development and in vitro performance of long-acting depots for peptide drug thymosin alpha 1 subcutaneous administration.* Drug Delivery, 2025. 32(1):2460708.
3. Spicer, P.T., et al., *Novel Process for Producing Cubic Liquid Crystalline Nanoparticles (Cubosomes).* Langmuir, 2001. 17(19):5748–56.

ACKNOWLEDGMENT

This work was supported by the Slovenian Research and Innovation Agency under Research core Funding No. P1-0189 and Grant No. L1-3160.

P073

OLEOYL-HYALURONATE NANOPARTICLES FOR ENHANCED STABILITY AND SKIN PENETRATION OF ENCAPSULATED COENZYME Q10

Martin Juhascik [1], Ondrej Zidek [1], Jana Polaskova [1], Frantisek Ondreas [1]

[1]Contipro a.s,, Dolní Dobrouč, Czech Republic

1. INTRODUCTION

The skin, the body's largest organ, acts as a critical barrier against environmental stressors. Chronic exposure to UV radiation, oxidative stress, and air pollution accelerates skin aging by impairing barrier function, leading to fine wrinkles, reduced elasticity, pigmentation irregularities, and diminished skin tone [1]. These effects are driven by extracellular matrix degradation, including reduced levels of collagen and decreased hyaluronic acid (HA) content. Coenzyme Q10 (CoQ10) is a lipophilic, vitamin-like compound naturally present in the human body, playing a vital role in mitochondrial electron transport and acting as a potent antioxidant. Furthermore, it stimulates collagen synthesis [2]. However, its extreme lipophilicity limits its skin penetration, posing a challenge for effective dermal delivery [3]. In this study, we developed a novel solution-based drug delivery system by encapsulating CoQ10 within oleoyl hyaluronate-based carriers (O-HAQ10) and investigating the influence of processing parameters on loading capacity, particle size, long-term stability and skin penetration.

2. MATERIALS AND METHODS

2.1. Materials

O-HA (Mw = 12,000 g/mol) was provided by Contipro a.s. CoQ10 was acquired from Selco Wirkstoffe Vertriebs GmbH. Pentylene glycol (PG) was bought from Gimex s.r.o. Other chemicals were sourced from Lach-Ner s.r.o. and Pharmasal.

2.2. Carrier Preparation

O-HA solution was prepared by dissolving it in water overnight. CoQ10 dissolved in isopropanol was added dropwise to the O-HA solution. The mixture was evaporated on a rotary vacuum evaporator, replenished with water, and PG was added. The final solution was filtered through a 1 μm glass filter to form O-HAQ10.

2.3. Characterization

Particle size and zeta potential were measured using a Zetasizer Nano-ZS. Cryo-SEM was used to analyze particle morphology. CoQ10 concentration was determined using high-performance liquid chromatography.

3. RESULTS AND DISCUSSION

3.1. Influence of Preparation Temperature

Four preparation temperatures were assessed: 34°C, 40°C, 55°C, and 65°C. Temperature variations did not significantly affect the loading capacity of CoQ10 up to 55°C; however, a sharp decrease was observed at 65°C. Temperature variations influenced particle size, with higher temperatures correlating with larger particle sizes due to the thermal behavior of CoQ10.

3.2. Loading Capacity and Batch Size

Batch size, O-HA concentration, and CoQ10 loading concentration were systematically varied. Initial 10 mL batches targeted a CoQ10 loading capacity of 2.0–3.3 g L^{-1}, yielding a cumulative average loading capacity of approximately 2.83 g L^{-1}. Larger batch sizes of 100 mL and 500 mL showed enhanced encapsulation efficiencies, reaching 96% for 100 mL batches and 92% for 500 mL batches compared to 81% in 10 mL batches.

3.3. Particle Size and Zeta Potential

Particle size plays a critical role in topical drug delivery, with smaller particles generally facilitating enhanced skin penetration. Particles prepared in 10 mL batches exhibited larger sizes compared to those produced in 100 mL and 500 mL batches. The particle size in these batches varied between 240 and 295 nm, further confirmed by cryogenic scanning electron microscopy (**Fig. 1**). Zeta potential values remained below -44 mV, achieving a high degree of colloidal stability.

P073

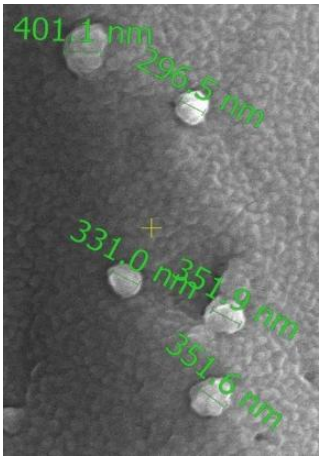

Figure 1. Image acquired using Cryo-SEM depicting O-HAQ10 with particle size range 296–401 nm.

3.4. Long-Term Stability

Stability studies were performed at 25°C (1 year) and 40°C (6 months) using three batches. Key parameters monitored included CoQ10 concentration, microbial stability, and colloidal stability. Long-term CoQ10 concentration trends showed 89 % retention of CoQ10 after 6 months at 40°C and an 92 % retention after one year at 25°C. Microbial counts remained below 5 CFU, confirming sufficient preservation efficacy.

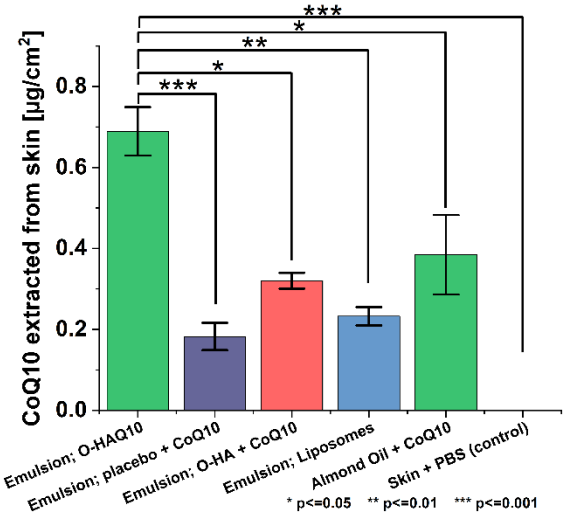

Figure 2. Comparative analysis of CoQ10 skin penetration from control emulsions, including an emulsion with dissolved CoQ10, an emulsion containing non-encapsulated CoQ10 and O-HA, and a commercially available liposomes with encapsulated CoQ10, solution of CoQ10 in almond oil. PBS was used as a negative control to detect potential CoQ10 in the skin. Data are presented as mean ± SEM (n = 4).

3.5. *In Vitro* Skin Penetration

Three independent batches of O-HAQ10, prepared according to the same protocol, were assessed for skin penetration in FDA-certified Franz diffusion cells, with a maximum detected CoQ10 concentration of 0.33 µg/cm² in the extracted tissue. Incorporating O-HAQ10 in a water-in-oil emulsion system enhanced CoQ10 cutaneous penetration. Emulsions incorporating O-HAQ10 carriers significantly increased skin penetration compared to control emulsions (**Fig. 2**).

4. CONCLUSION

In this study a stable solution-based carrier system of CoQ10 in O-HA was successfully developed, optimizing key formulation parameters to achieve high encapsulation efficiency, colloidal stability, and enhanced skin penetration. The optimal preparation temperature (34°C) minimized structural alterations, while larger batch sizes (100 mL and 500 mL) achieved encapsulation efficiencies up to 96%. Long-term stability assessments confirmed the robustness of the carrier, maintaining 91% of the initial CoQ10 concentration after 12 months at 25°C and 89% after 6 months at 40°C. *In vitro* skin penetration studies revealed that the application of O-HAQ10 carriers incorporated into water-in-oil emulsions significantly improved skin penetration compared to commercial liposomes and unencapsulated CoQ10 in emulsion or O-HAQ10 carriers.

5. REFERENCES

1. Parrado, C. et al., *Environmental Stressors on Skin Aging. Mechanistic insights.* Frontiers in pharmacology, 2019. 10: 759.

2. Pastor-Maldonado, C. J., et al., *Coenzyme Q10: novel formulations and medical trends.* International Journal of Molecular Sciences, 2020. 21(22): 8432.

3. El-Leithy, E. S., et al., *Validation and application of Vierordt's spectrophotometric method for simultaneous estimation of tamoxifen/coenzyme Q10 in their binary mixture and pharmaceutical dosage forms.* asian journal of pharmaceutical sciences, 2016. 11(2), 318-325.

P073

PREPARATION OF A DRY FORMULATION OF ALBUMIN NANOPARTICLES FOR QUERCETIN DELIVERY

Klemen Kirbus[1,2], Lovro Žiberna[2], Petra Kocbek[1]

[1]*Department of Pharmaceutical Technology, Faculty of Pharmacy, University of Ljubljana, Slovenia*
[2]*Department of Biopharmacy and Pharmacokinetics, Faculty of Pharmacy, University of Ljubljana, Slovenia*

1. INTRODUCTION

Albumin nanoparticles represent a promising approach for parenteral application of poorly water-soluble drugs, due to the intrinsic ligand-binding domains for various endogenous and exogenous molecules within the albumin molecule. They are also biocompatible, biodegradable and can enhance stability of loaded drugs [1]. Their intrinsic ability for passive and active targeting via albumin receptors (e.g. secreted protein acidic and rich in cysteine (SPARC) and glycoprotein 60), which are overexpressed in cancer and inflamed tissues [2], further enhances their value in targeted delivery of antioxidants and anti-inflammatory agents to such regions [1].

Thus, the aim of our study was to develop a freeze-dried formulation of rapidly reconstitutable albumin nanoparticles loaded with quercetin, a flavonol exhibiting antioxidant, anti-inflammatory and vasoprotective properties.

2. MATERIALS AND METHODS

Albumin nanoparticles were prepared from bovine serum albumin (Glentham Life Sciences, UK) by desolvation method [3]. First, an albumin solution (100 mg/mL) was prepared in ultra-pure water, followed by controlled addition of ethanol (3 mL/min) while stirring, which caused precipitation of albumin and formation of nanoparticles. Quercetin (Biosynth, Slovakia) loading was performed during desolvation step, as it was dissolved in the ethanol used for desolvation of albumin. Nanoparticles were stabilized by cross-linking the amine residues in albumin molecules with glutaraldehyde. The prepared nanoparticles were purified by two cycles of centrifugation (21000 g, 12 min, 5°C) to remove the excess of cross-linking agent and change the dispersion medium. The sediment was redispersed in an aqueous solution of sucrose (2% (w/v)) and mannitol (2% (w/v)), which were used as cryoprotectants in the freeze-drying process. The obtained dispersion was frozen (−18 °C) and freeze-dried (Christ Beta 1-8K freeze dryer; primary drying: −6 °C, 0.630 mbar, 20 h; secondary drying: 25 °C, 0.160 mbar, 4 h).

The nanoparticle size and size distribution were evaluated by dynamic light scattering and their surface charge was measured by laser Doppler anemometry (Zetasizer Ultra, Malvern Panalytical). The time required for reconstitution of nanoparticles from freeze-dried formulations and their physical stability during drying were also evaluated. The morphology of the freeze-dried product was visualized by scanning electron microscopy. The cytotoxicity of nanoparticles was evaluated on the cell line EA.hy926 using a resazurin-based assay [4] after 3 h and 24 h exposure to nanoparticle dispersions (0.1–1 mg/mL).

3. RESULTS AND DISCUSSION

Desolvation of albumin yielded the largest nanoparticles (BNP (173 ± 4) nm) in the absence of quercetin. Dissolution of quercetin in ethanol (1 mg/mL) used for desolvation resulted in a smaller nanoparticle size (QNP1 (154 ± 2) nm). The purification of nanoparticles by two cycles of centrifugation resulted in more homogenous BNP dispersion, while the size distribution of QNP formulations remained unchanged (Fig. 1). This could be attributed to losses of smaller nanoparticles with the removed supernatant, as has been described in the literature [3]. All freeze-dried NP

formulations reconstituted in ≤ 10 s after the addition of purified water. Average hydrodynamic size of quercetin-loaded nanoparticles after freeze-drying was slightly increased contrary to unchanged average particle size in case of quercetin-free nanoparticles, which could be attributed to the formation of aggregates. The size distribution, shown as polydispersity index, was below 0.1 for all investigated nanoparticle formulations, suggesting highly monodisperse nanoparticle populations even after reconstitution (Fig. 1).

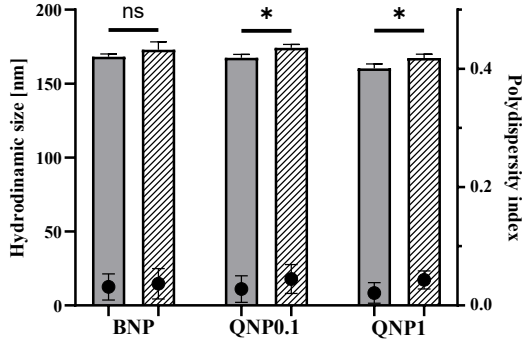

Figure 1. Average hydrodynamic size (columns) and polydispersity index (dots) of quercetin-free albumin nanoparticles (BNP) and albumin nanoparticles prepared with 0.1 mg/mL (QNP0.1) and with 1 mg/mL (QNP1) quercetin solution before (solid grey) and after freeze-drying (dashed white). Student t-test was used to compare two groups. Data shown are mean ± SD (n = 3), ns, non-significant; *, $p < 0.05$.

The zeta potential of nanoparticles in purified water was low, with values around −20 mV for all prepared formulations. It remained unchanged also after reconstitution of freeze-dried QNP formulations, but the absolute value of zeta potential decreased after reconstitution of the quercetin-free nanoparticles. The minimal changes in average nanoparticle size, size distribution and surface charge during freeze-drying indicate that the process used is suitable for the preparation of dry formulation of albumin nanoparticles.

Furthermore, the prepared nanoparticles had no adverse effects on cell viability after a 3 h incubation, as the viability of cells, treated with quercetin-free or quercetin loaded nanoparticles in concentrations of up to 1 mg/mL was comparable to the viability of untreated control. After 24 h incubation cell viability decreased in case of QNPs, while cells incubated with BNPs exhibited no significant change in cell viability, indicating good biocompatibility of the prepared nanodelivery system. Furthermore, the viability of cells treated with all investigated nanoparticle formulations was above 80 % after incubation with 1 mg/mL of nanoparticles for 24 h. The decrease in cell viability observed in case of QNPs may indicate a high intracellular quercetin delivery, as high intracellular quercetin concentrations correlate with cytotoxic effects.

4. CONCLUSION

We developed lyophilized, quercetin-loaded albumin nanoparticle formulations, which exert minimal cytotoxicity and can be reconstituted rapidly. Furthermore, the method used for nanoparticle preparation was shown to be highly reproducible. Based on the results obtained, our future work will focus on determining the antioxidant properties of quercetin-loaded nanoparticles in various *in vitro* cell-based assays.

5. REFERENCES

1. Spada, A., et al., *The Uniqueness of Albumin as a Carrier in Nanodrug Delivery.* Molecular pharmaceutics, 2021. 18(5): 1862-1894.

2. Ji, Q., et al., *GP60 and SPARC as albumin receptors: key targeted sites for the delivery of antitumor drugs.* Frontiers in Pharmacology, 2024. 15.

3. Langer, K., et al., *Human serum albumin (HSA) nanoparticles: Reproducibility of preparation process and kinetics of enzymatic degradation.* International Journal of Pharmaceutics, 2008. 347(1-2): 109-117.

4. Dragar, Č., et al., *Bioevaluation methods for iron-oxide-based magnetic nanoparticles,* International Journal of Pharmaceutics, 2021. 597: 120348.

ACKNOWLEDGMENT

This research was funded by the Slovenian Research and Innovation agency (program codes P1-0420, P1-0189, P3-0067).

P074

DEVELOPMENT AND OPTIMIZATION OF ELECTROSPUN NANOFIBERS FOR DERMAL APPLICATION OF VITAMIN A ACETATE

Tanja Potrč, Žane Temova Rakuša, Robert Roškar, Petra Kocbek

Faculty of Pharmacy, University of Ljubljana, Slovenia

1. INTRODUCTION

Vitamin A and its derivatives, collectively known as retinoids, play well-established roles in skin physiology, including the regulation of epidermal cell differentiation, keratinization, and immune response, thus they are widely used topically for treatment of various dermatological conditions such as psoriasis, photoaging, ichthyosis, and certain forms of acne. Nowadays, they are often used also in cosmetics as anti-aging and skin-rejuvenating agents. Due to teratogenicity and local adverse reactions such as skin erythema, dryness, itching, peeling, and blistering, the clinical use of retinoic acid is limited [1] and therefore, retinoid precursors such as retinol esters, retinol, and retinal are commonly used in topical formulations. However, the vitamin A derivatives, such as vitamin A-acetate (vit. A-ac), are chemically unstable, especially when exposed to light, oxygen, and elevated temperatures, leading to loss of therapeutic efficacy, and increased risk of skin irritation and phototoxicity [2]. To overcome these challenges and to enhance stability of vit. A-ac. in the product for dermal application, we developed nanofiber (NF)-based formulation.

2. MATERIALS AND METHODS

2.1. Materials

Vit. A-ac. (99.8%) and tocopherol (vit. E, 97.3%) were purchased from Carbosynth (Berkshire, UK). HPLC-grade acetonitrile, ethanol (96%), butylhydroxytoluene (BHT, 99.0%), polyethylene oxide (PEO, Mw = 400,000) and poloxamer 407 were purchased from Sigma-Aldrich (Steinheim, Germany). Ultra-pure water was obtained through a Milli-Q water purification system A10 Advantage (Millipore Corporation, Bedford, MA, USA).

2.2. Methods

The initial polymer solution was prepared by dissolving PEO and poloxamer 407 in weight ratio 1:1 in 96% (v/v) ethanol (formulation F1). The mixture was stirred using a magnetic stirrer for 30 min at 60 °C, followed by additional 24 h stirring at room temperature [3]. Stock solutions of vit. A-ac., BHT and vit. E were prepared in 96% (v/v) ethanol. Just prior to the electrospinning, the polymer solution was mixed with an adequate amount of vit. A-ac. solution with or without an antioxidant, namely only vit. A-ac. (0.5 wt%) (formulation F2), vit. A-ac. with BHT (0.5 wt% each) (formulation F3), and vit. A-ac. with vit. E (0.5 wt% each) (formulation F4).

The polymer solutions were electrospun immediately after preparation using an electrospinning device in a horizontal configuration (Spinbox® system, Bioinicia, Spain). Each sample was loaded into a 5 mL plastic syringe (Chirana, Slovakia) that was placed in the syringe pump, which was equipped with a metal needle (Bioinicia, Spain; outer diameter 0.7 mm). The needle was connected to a high-voltage generator (15 kV) and positioned 15 cm from a grounded collector wrapped in aluminum foil. Electrospinning was conducted at a polymer solution flow rate of 1.77 mL/h for 75 min at room temperature and relative humidity ≤ 35%.

The morphology of electrospun products was examined by scanning electron microscopy (SEM; Supra35 VP, Carl Zeiss, Germany). Electrospun products were mounted on metal studs with double-sided conductive tape (diameter, 12 mm; Oxford Instruments, UK) and imaged at an accelerating voltage of 1 kV using a secondary electron detector. The diameters of at least 100 nanofibers (NFs) were measured on representative SEM images using ImageJ (v1.53e) software (National Institutes of Health, USA), and the average NF diameter along with the standard deviation was calculated.

The content of vit. A-ac. in NFs was determined by a validated method using Agilent HPLC Series 1100/1200 instrument (Santa Clara, USA) equipped with a UV detector. Chromatographic analysis was performed on a reversed-phase C18 column with a mobile phase consisting of acetonitrile and water in an

isocratic elution mode at a flow rate of 1 mL/min. Detection was carried out at 325 nm.

The effect of light on the stability of vit. A-ac. in the prepared NF was assessed in accordance with the ICH Q1B guideline. After preparation, the NFs were stored in a climatic chamber with a light module (Memmert HPP260eco, Germany) at 25 °C, Vit. A-ac. content in NFs was determined by HPLC method prior light exposure and after 5 days of light treatment.

3. RESULTS AND DISCUSSION

3.1. Morphology of the electrospun products

The SEM images revealed formation of uniform electrospun NFs without beads (Fig. 1). The average diameter of electrospun NFs was between 178 ± 52 nm and 213 ± 161 nm. The incorporation of vit. A-ac. (F2), vit. A-ac. with BHT (F3) and vit. A-ac. with vit. E (F4) did not importantly affect the NF morphology compared to the pure PEO/P407 NFs (F1).

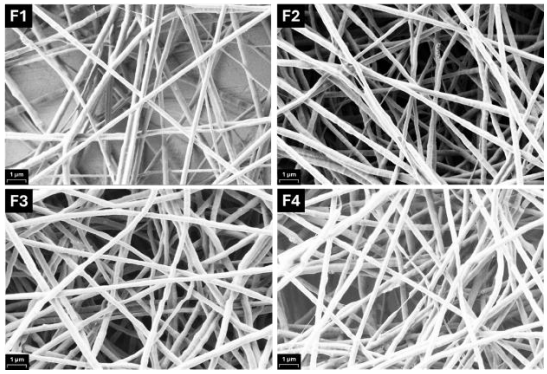

Figure 1. Representative scanning electron microscopy images of the pure PEO/P407 nanofibers (F1), PEO/P407 nanofibers loaded with vit. A-ac. (F2), PEO/P407 nanofibers loaded with vit. A-ac and BHT (F3) and PEO/P407 nanofibers loaded with vit. A-ac. and vit. E (F4).

3.2. Vitamin A-acetate loading efficiency

Vit. A-ac. loading efficiency was determined based on vit. A-ac. content of the NFs just after their preparation and the theoretical vit. A-ac. content in NFs (Table 1). The results revealed that the vit. A-ac. loading efficiency was significantly higher in the NF formulation supplemented with vit. E, indicating a stabilising effect of vit. E on vit. A-ac. during the electrospinning process.

Table 1. Vitamin A-acetate loading efficiency in nanofibers.

Formulation	Vit. A-ac. loading efficiency (%)
F2	41.2-58.7
F3	59.0-72.9
F4	84.2-104.2

3.3. Influence of light exposure on the stability of vitamin A-acetate in nanofibers

The results of the forced degradation photostability study demonstrated that light exposure has a significant impact on the stability of vit. A-ac. Over the 5-days exposure of NFs to light vit. A-ac. completely degraded in contrast to the vit. A ac. in the control NF samples, which were stored protected from light under the same conditions. These findings indicate that the NFs represent a promising advanced delivery system for Vit. A-ac; however, packaging to assure effective protection of the NFs from light is essential to assure stability vit. A-ac. in NFs.

4. CONCLUSIONS

The incorporation of vit. A-ac. along with vit. E into polymer NFs was shown to be a promising strategy for stabilizing vit. A-ac. during electrospinning, offering advanced delivery systems for the treatment of various dermatological conditions and cosmetic applications. Further studies are required to ensure the long-term stability of vit. A-ac. within the NFs, either through the use of appropriate packaging or by incorporation of additional stabilizing excipients.

5. REFERENCES

1. Motamedi M, Chehade A, Sanghera R, Grewal P. *A Clinician's Guide to Topical Retinoids.* Journal of Cutaneous Medicine and Surgery, 2022. 26: 71–8.

2. Milosheska D, Roškar R. *Use of Retinoids in Topical Antiaging Treatments: A Focused Review of Clinical Evidence for Conventional and Nanoformulations.* Advances in Therapy, 2022. 39: 5351-5375.

3. Dragar Č, Roškar R, Kocbek P. *The Incorporated Drug Affects the Properties of Hydrophilic Nanofibers.* Nanomaterials, 2024. 14(11): 949.

ACKNOWLEDGMENT

This research was funded by the Slovenian Research and Innovation agency (program codes P1-0420 and P1-0189).

P075

IN VITRO AND EX VIVO STUDIES ON THE ABSORPTION AND DISTRIBUTION OF β-CYCLODEXTRIN-POLYMER

Réka Révész[1,2,5], István Lekli[3], Ildikó Bácskay[2,4], Ádám Haimhoffer[2]

[1]Doctoral School of Pharmaceutical Sciences, University of Debrecen, Hungary
[2]Department of Pharmaceutical Technology, Faculty of Pharmacy, University of Debrecen, Hungary
[3]Department of Pharmacology, Faculty of Pharmacy, University of Debrecen, Hungary
[4]Institute of Healthcare Industry, University of Debrecen, Hungary
[5]Department of Industrial Pharmaceutical Technology, Faculty of Pharmacy, University of Debrecen, Hungary

1. INTRODUCTION

Cyclodextrin polymers are becoming more and more widely used because of their advantages. For native cyclodextrins, much information is available on their *in vitro, ex vivo* or *in vivo* bioavailability or intracellular distribution, but much less information is available on modified, soluble or insoluble cyclodextrin polymers [1,2]. We aimed to study the β-CD polymer penetratioon in several models.

2. MATERIALS AND METHODS

2.1. Materials

Fluoresncence labelled β-CD polymer was purchased from Cyclolab. All other reagents were purchased from Sigma Aldrich Kft. (Budapest, Hungary) in analytical grade.

2.2. In vitro permeability study

The *in vitro* permeability of CD polymer was investigated using an in-line cell apparatus. Four different pore size membranes were used for the measurements. 500 µl of pH 5.5 phosphate buffer was chosen as the acceptor phase and 1 ml of 1 m/m% fluorescently labelled CD polymer solution as the donor phase. Subsequently, 200 µl of the acceptor phase was taken off after 30, 60, and 120 min, and replenished with 200 µl of pure buffer. The cyclodextrin polymer content of the samples was measured by fluorescence spectrophotometry.

2.3. In vitro absorption study

For the permeability studies, cell monolayers were grown on inserts in 12-well plates. 250,000 cells/insert were used to create monolayers. Caco-2, HaCaT and TR146 monolayers were used for experiments. Fluorescently labelled CD polymer was dissolved in Hank's balanced salt solution (HBSS) at a concentration of 1 m/m %. Cell monolayers were washed with HBSS, and the solutions of beta-CD-polymer were put onto the apical surface of cell layers, it was 500 µl. Samples were taken after 30, 60 and 120 min from the basal side of the cell layers, it was 500 µl and replenished with 500 µl pure HBSS. The cyclodextrin polymer content of the samples was measured by fluorescence spectrophotometry.

2.4. Ex vivo permeability study

Ex vivo permeability studies were performed using a Franz diffusion apparatus. Isolated porcine ear and isolated rat intestinal and buccal tissue were used in the experiment as a membrane. Hank's balanced salt solution was chosen as acceptor phase. 500 µl/cm^2 of a 1 m/m% fluorescently labelled cyclodextrin polymer solution was added on the tissues. During the experiment, samples were taken from the acceptor phase after 30, 60, and 120 min. respectively and measured by fluorescence spectrophotometry.

3. RESULTS AND DISCUSSION

P075

3.1. In vitro permeability study

From the results of our in vitro permeability study, less than 1% of the polymer penetrated the 3.5 kDa and 10 kDa membranes in 2 hours and approximately 1% of the polymer penetrated the 50 kDa membrane. On the 4500 kDa membrane, a much larger amount of polymer, nearly 30%, penetrated in 2 hours (eg.as Fig.1).

3.2. In vitro absorption study

Based on the results of our in vitro absorption study, we found that the least amount of polymer was absorbed through the TR146 monolayer, about 3%, and a little more, 4.5%, was absorbed through the Caco-2 monolayer in 2 h. The highest amount of polymer was absorbed through the HaCaT monolayer, about 10% in 2 h (eg. as Fig.2).

3.3. Ex vivo permeability study

Based on our ex vivo permeability assays, the polymer permeated through the buccal and intestinal tissues in nearly equal amounts, approximately 0.25%, in 2 hours. For skin, 0.4% of polymer was absorbed in 2 hours (eg. as Fig.3).

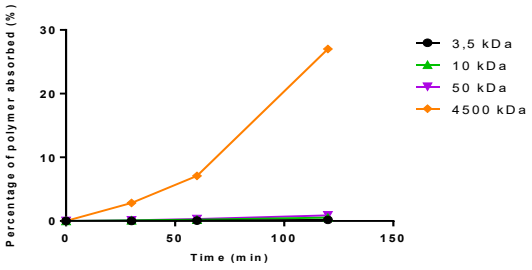

Figure 1. Polymer absorption on membranes.

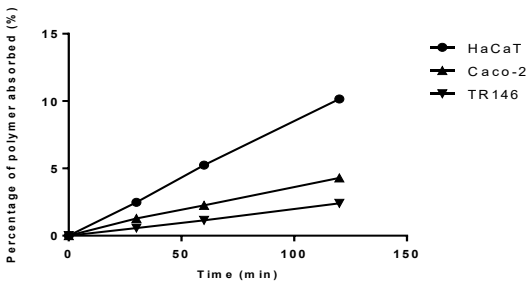

Figure 2. Polymer absorption on monolayers.

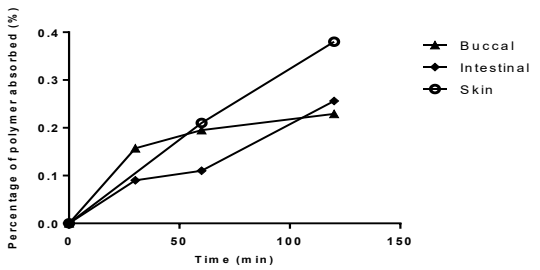

Figure 3. Polymer absorption on tissues.

4. CONCLUSION

Our results show that different pore sizes affect the penetration of the polymer. For different cell lines the penetration rate is different. In the ex vivo model system, differences in polymer permeation between different tissue types were also observed. The polymer penetration through tissues showed a linear correlation with the in vitro results for intestinal tissue and skin tissue, but a non-linear correlation for buccal tissue.To summarize the results, β-CD polymers are good penetration enhancers, which can penetrate into themselves to a certain extent.

5. REFERENCES

1. Haimhoffer, Á., et al., *Cyclodextrins in Drug Delivery Systems and Their Effects on Biological Barriers* Scientia Pharmaceutica, 2019., 87

2. Kubota, Y., et al., *Absorption, Distribution and Excretion of β-Cyclodextrin and Glucosyl-β-cyclodextrin in Rats.* Biological and Pharmaceutical Bulletin, 1996. 19 (8): 1068-1072.

ACKNOWLEDGMENT

Project no. TKP2021-EGA-18 has been implemented with the support provided by the Ministry of Culture and Innovation of Hungary from the National Research, Development and Innovation Fund, financed under the TKP2021-EGA funding scheme. Supported by the EKOP-24-4 University Research Scholarship Program of the Ministry for Culture and Innovation from the source of the National Research, Development and Innovation Fund.

P076

PRODUCTION OF LIPID-POLYMER HYBRID NANOPARTICLES WITH TUNABLE DIAMETER USING HERRINGBONE MICROMIXER: IMPACT OF FORMULATION AND PROCESS PARAMETERS

Tanja Ilić[1], Jelena Đoković[1], Ivana Pantelić[1], Bojan Marković[2], Sonja Vučen[3], Abina Crean[3], James M. Cook[4], Miroslav Savić[5], Snežana Savić[1]

[1]Department of Pharmaceutical Technology and Cosmetology, University of Belgrade–Faculty of Pharmacy, Serbia
[2]Department of Pharmaceutical Chemistry, University of Belgrade–Faculty of Pharmacy, Serbia
[3]University College Cork – School of Pharmacy, Cork, Ireland
[4]Department of Chemistry and Biochemistry, University of Wisconsin–Milwaukee, United States
[5]Department of Pharmacology, University of Belgrade–Faculty of Pharmacy, Serbia

1. INTRODUCTION

To overcome the fundamental difficulty of delivering drugs to the brain, a novel approach based on nanoparticle-mediated transport through the brain lymphatic vasculature after subcutaneous administration has recently been disclosed [1]. The nanoparticle delivery to the lymphatic system is primarily determined by size (10-100 nm) and surface functionality [2]. Among the existing nanocarriers, lipid-polymer hybrid nanoparticles (LPHNPs) are promising for targeted drug delivery, combining the positive features of polymeric and lipid nanoparticles. However, the conventional bulk methods, commonly used to produce LPHNPs, are associated with low reproducibility and limited size control [3]. Therefore, we aimed to explore suitability of a novel microfluidic device based on herringbone micromixer to develop PEGylated LPHNPs as carrier for GL-II-73, a positive allosteric modulator of α5GABAA receptors, suitable for lymphatic system targeting. The effects of process (total flow rate (TFR) and flow rate ratio (FRR)) and formulation parameters (concentration of polymer/lipids, lipid/GL-II-73 to polymer mass ratio) on critical quality attributes were investigated.

2. MATERIALS AND METHODS

2.1. Materials

GL-II-73 was synthesized at University of Wisconsin—Milwaukee. The following excipients were used: soybean lecithin and DSPE-PEG2000 (Lipoid GmbH, Germany), poly(D,L-lactide-co-glycolide) (inherent viscosity 0.1-0.3 dl/g, average Mw 5-27 Ka) (Ashland Inc., Poland), acetone and ethanol (Sigma-Aldrich GmbH, Germany)) and ultrapure water.

2.2 Microfluidic synthesis of LPHNPs

The commercially available device TAMARA (Inside Therapeutics, France) was used for the microfluidic synthesis of LPHNPs. PLGA (2.5 to 20 mg/ml) was dissolved in acetone. Lecithin/DSPE–PEG2000 (molar ratio 7:3) were dissolved in 4% ethanol aqueous solution (20% to 70% of polymer weight). To determine maximal loading capacity of LPHNPs, GL-II-73 at 100% of the polymer weight was dissolved into the PLGA/acetone solution before precipitation. The FRR was set to 10:1 or 3:1, while TFR was varied from 2 to 8 mL/min. Residual acetone and free molecules were removed by Amicon Ultra-4 ultrafiltration (10 kDa) (Millipore, MA). GL-II-73 concentration in filtrate and resuspended LPHNPs was determined by LC-MS.

2.3. Characterization of LPHNPs

Particle size (Z-ave), size distribution (PDI) and zeta potential of the prepared LPHNPs were analysed using Zetasizer Nano ZS90 (Malvern Instruments, UK). In vitro release testing was performed using the direct dialysis method with a mixture of phosphate buffer pH 7.4 and ethanol 96% v/v as a receptor medium. At selected intervals, GL-II-73 concentration was determined by LC-MS.

3. RESULTS AND DISCUSSION

To control particle size, in the first part of this study, we tested the effect of process parameters (TFR and FRR) on the size and dispersity of blank PEGylated LPHNPs. With increasing the TFR, we observed a trend towards decreasing particle size with increasing size distribution at both FRR tested (Fig.1). Decreasing the flow rate of aqueous phase compared to organic solution (FRR 3:1) increased particle size and zeta potential.

P076

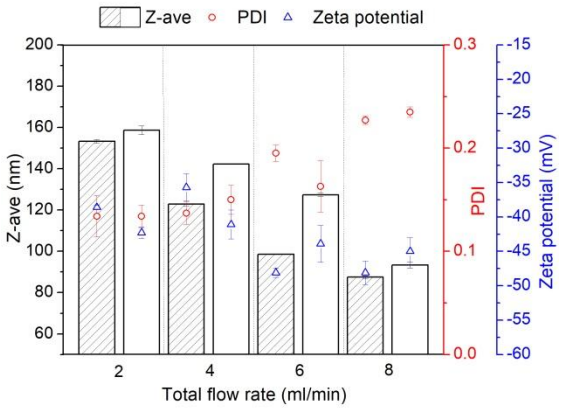

Figure 1. The effect of TFR on critical quality attributes of LPHNPs prepared with 10 mg/ml PLGA at different FRR (10:1 grey bar, 3:1 white bar)

The end results of investigating the lipid/polymer mass ratio revealed that 20% of the lipid/polymer mass ratio was required to form sub-100 nm. Further increase of lipid content was accompanied with the particle size increase. When the polymer concentration was increased from 2.5 to 20 mg/ml in acetone (with corresponding increase in added lipids), we also observed a trend of increasing particle size from 62 to 150 nm with a corresponding increase in ZP from -35 mV to -55 mV.

Table 1. LPHNP particle size and encapsulation efficacy (EE) for GL-II-73

Sample	Z-ave (nm)	PDI	EE %
$F_{(10)}$10:1	103.0±0.4	0.219±0.008	40.20
$F_{(10)}$3:1	93.4±1.5	0.235±0.005	44.73
$F_{(20)}$10:1	147.9±3.2	0.172±0.008	44.73
$F_{(20)}$3:1	172.9±3.7	0.187±0.010	56.62

Interestingly, the incorporation of GL-II-73 into the selected formulations prepared with different PLGA concentrations (10 mg/ml and 20 mg/ml) and at different FRR (10:1 and 3:1) (Table 1) did not affect the system properties compared to the corresponding blank samples (almost unchanged particle size and ZP were observed). Moreover, the encapsulation efficiency of GL-II-73 directly depended on the content of PLGA polymer in the formulation. In vitro release testing proved the sustained release of GL-II-73 from the tested LPHNPs over 24 hours (no premature release of GL-II-73 was detected), which proves that the lipid layer on the particle surface restricts the release of the incorporated compound.

4. CONCLUSION

This study suggests that the microfluidic approach based on a herringbone micromixer enables the production of GL-II-73-loaded LPHNPs with sub-100 nm size, high loading efficiency and sustained release profile, making them promising for the lymphatic system targeting.

5. REFERENCES

1. Ramos-Zaldívar, H.M., et al. The Cervical and Meningeal Lymphatic Network as a Pathway for Retrograde Nanoparticle Transport to the Brain. International Journal of Nanomedicine, 2024. 9: 10725-10743.

2. Maisel, K., et al. Nanotechnologies for Physiology-Informed Drug Delivery to the Lymphatic System. Annual Review of Biomedical Engineering. 2023. 8;25: 233-256.

3. Rouco, H., et al. Screening strategies for surface modification of lipid-polymer hybrid nanoparticles. International Journal of Pharmaceutic 2022. 624:121973. doi: 10.1016/j.ijpharm.2022.121973. Epub 2022 Jul 8. PMID: 35811041.

ACKNOWLEDGMENT

This research was supported by the Science Fund of the Republic of Serbia, grant no. 17811, *Development of an innovative platform consisting of lipid-polymer hybrid nanoparticles and microneedles for targeted brain delivery of novel GABAkines favored by reverse transport – MiNe2Brain.*

P077

NANOEMULSIONS LOADED WITH CW-02-79-PHOSPHOLIPID COMPLEX: LINKING EPR SPECTROSCOPY-ANALYZED INTERFACIAL PROPERTIES WITH PHYSICOCHEMICAL STABILITY

Tijana Stanković[1], Tanja Ilić[1], Vassiliki Papadimitriou[2], Georgios Sotiroudis[2], Jelena Đoković[1], Ines Nikolić[3], James M. Cook[4], Miroslav Savić[5], Snežana Savić[1]

[1]Department of Pharmaceutical Technology and Cosmetology, Faculty of Pharmacy, University of Belgrade, Serbia

[2]Institute of Chemical Biology, National Hellenic Research Foundation, Greece

[3]Section of Pharmaceutical Sciences, Faculty of Science, University of Geneva, Switzerland

[4]Department of Chemistry and Biochemistry, University of Wisconsin - Milwaukee, United States

[5]Department of Pharmacology, Faculty of Pharmacy, University of Belgrade, Serbia

1. INTRODUCTION

To address the undesirable physicochemical properties, such as low solubility of the novel patent-protected ligand CW-02-79 in aqueous and oily media, phospholipid complex-based nanoemulsions containing CW-02-79 were successfully developed as a promising lipid-based delivery system [1]. However, despite its potential impact, the influence of the drug-phospholipid complex on the interfacial architecture is still insufficiently investigated. Previous studies have highlighted the impact of nanoemulsions' interfacial properties on their in vivo behavior by modulating interactions with plasma proteins, blood and immune cells and biological barriers, ultimately affecting circulation time, biodistribution and efficacy. On the other hand, the stabilizing layer also governs the physical stability of the formulation [2]. Therefore, we aimed to gain a deeper insight into the interfacial properties and localization of the phospholipid complex within the intricate structure of lipid-based systems and linking these findings to their impact on long-term physicochemical stability.

2. MATERIALS AND METHODS

2.1. Materials

CW-02-79 was synthesized at the Department of Chemistry and Biochemistry University of Wisconsin—Milwaukee, USA. The following excipients were used: soybean lecithin and DSPE-PEG2000 (Lipoid GmbH, Germany), DSPE-PEG2000-mannose (Biopharma PEG Scientific Inc., USA), castor oil and medium chain triglycerides (Fagron, Greece), glycerol (Merck, Germany), polysorbate 80, butylhydroxytoluene and 5- and 16-doxyl stearic acid free radical (5-DSA and 16-DSA, respectively (Sigma-Aldrich GmbH, Germany)) and ultrapure water.

2.2. Electron paramagnetic resonance (EPR) spectroscopy

ERP spectroscopy using two spin probes 5- and 16-DSA, was applied to investigate interfacial properties and the localization of the CW-02-79-phospholipid complex (CW_{PC}) encapsulated in tested nanoemulsions. Measurements were performed with Bruker EMX EPR spectrometer operating in the X-band (9.8 GHz) with a flat aqueous quartz sample cell. The results were expressed by the rotational correlation time (τR), the order parameter (S), and the isotropic hyperfine coupling constant (αN).

2.3. Stability monitoring of nanoemulsions

Undecorated and PEGylated nanoemulsions with different concentrations of DSPE-PEG2000 with/without DSPE-PEG2000-mannose were prepared as previously described by Stanković et al. [1]. To examine the stability of nanoemulsions after six months of storage at 25 °C, physicochemical characterization was performed in terms of droplet size (Z-ave), polydispersity index (PDI), zeta potential (ZP), pH value, electrical conductivity (EC) and osmolality.

2.4. Scanning electron microscopy (SEM)

SEM analysis was utilized in order to take a glance at the morphology of the samples stored for six months at 25 °C using Thermal Field Emission Scanning Electron Microscope JSM-7001F (Jeol Ltd., Japan).

3. RESULTS AND DISCUSSION

The EPR spectra of 5-DSA and 16-DSA were analyzed to estimate CW_{PC} localization and to deeply investigate interfacial properties in both

P077

undecorated and PEGylated nanoemulsions. Despite the differences in interfacial composition, the spectra obtained with 16-DSA showed no relevant alteration in interfacial properties upon CW_{PC} addition. Otherwise, it affected the movement of 5-DSA by increasing the τR values, indicating its localization at the surfactant interface, between the hydrophobic chains and the hydrophilic polar heads, probably due to the phospholipid complex being formed by CW-02-79 and soybean lecithin. The stabilizing effect of CW_{PC} on all tested nanoemulsions was also observed.

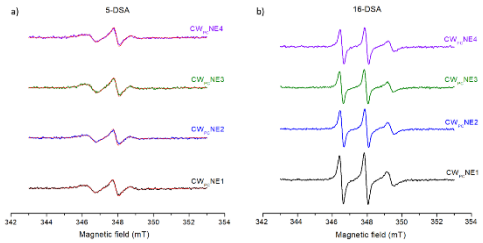

Figure 1. EPR spectra of the nanoemulsions with a) 5-DSA and b) 16-DSA spin probe. (Experimental spectra of 5-DSA are plotted with solid lines and corresponding simulated with short dotted red line).

Based on these findings, the influence of PEGylation on the interfacial properties was investigated. PEGylation with DSPE-PEG2000 in different concentrations at 0.2% ($CW_{PC}NE2$), 0.3% ($CW_{PC}NE3$) and combination with 0.2% DSPE-PEG2000 and 0.1% DSPE-PEG2000-mannose ($CW_{PC}NE4$) resulted in higher τR values with the most pronounced effect observed with $CW_{PC}NE3$, when compared to undecorated nanoemulsion ($CW_{PC}NE1$). This indicates reduced mobility of 5-DSA due to the increased interfacial rigidity, which suggests an improved stabilization and tightening of the interfacial layer. Interestingly, the addition of DSPE-PEG2000-mannose resulted only in a slight increase in τR value compared to the corresponding sample prepared only with DSPE-PEG2000 ($CW_{PC}NE2$), possibly due to the reduced fluidity caused by the additional steric hindrance provided by mannose. The values of S and αN did not change with the addition of CW_{PC} and PEGylation of the nanodroplets' surface, respectively, indicating that the interphase flexibility and the local polarity were not significantly affected.

These interphase investigations are supplemented by measurements of key attributes after six months of storage at 25 °C. The results confirmed the presence of nanodroplets with a narrow size distribution, a relatively high surface charge, pH and osmolality values within acceptable ranges for parenteral use, as shown in Figure 2. In the case of surface decoration with PEGylated phospholipids as well as brain-targeting ligand (DSPE-PEG2000-mannose), minor changes in the physicochemical parameters were observed compared to $CW_{PC}NE1$, whereby the stability was still preserved regardless of the interfacial composition.

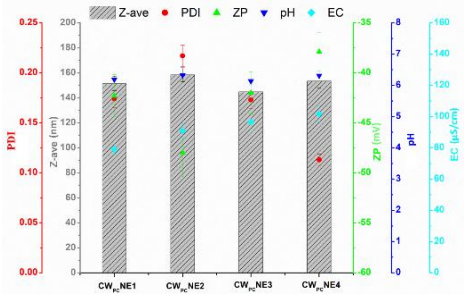

Figure 2. The physicochemical parameters of the nanoemulsions after six months of storage.

These results are supported by SEM analysis, which revealed that the nanodroplets were spherical and smooth, with no evidence of droplet collapse or coalescence. The absence of morphological changes indicates the presence of a robust interfacial layer in all tested nanoemulsions, which is consistent with the previously obtained results.

4. CONCLUSION

Although minor variations were observed in interfacial properties, these did not affect the stability of the nanoemulsions; however, further evaluation of interfacial phenomena will be conducted through hemocompatibility testing.

5. REFERENCES

1. Stanković, T., et al., Pharmaceutics, 2025. 17(2): 232,https://doi.org/10.3390/pharmaceutics17020232

2. Đoković, J., et al., J. Mol. Liq., 2024. 404: 124888, https://doi.org/10.1016/j.molliq.2024.124888

P078

ATOMIC FORCE MICROSCOPY AND RHEOLOGICAL MEASUREMENTS - VALUABLE TECHNIQUES FOR DESCRIBING MICROSTRUCTURAL ORGANIZATION OF IBUPROFEN NANOEMULGELS

Anđela Tošić[1], Danijela Randjelović[2], Branka Ivković[3], Snežana Savić[1], Ivana Pantelić[1]

[1]Department of Pharmaceutical Technology and Cosmetology, University of Belgrade-Faculty of Pharmacy, Serbia
[2]Institute of Chemistry, Technology and Metallurgy, National Institute of the Republic of Serbia, University of Belgrade, Serbia
[3]Department of Pharmaceutical Chemistry, University of Belgrade-Faculty of Pharmacy, Serbia

1. INTRODUCTION

Nanoemulsion gels, by definition, are composed of nanoemulsion droplets inside the polymeric gel network [1]. The internal organization of the polymeric gelling agents and nanodroplets in a 3D gel network can directly affect the release of the loaded drug substance [2].

The aim of this study was to investigate and visualize the microstructure of nanoemulgels produced with three different gelling agents and to test how it affects the release kinetics of ibuprofen as a model active substance.

2. MATERIALS AND METHODS

2.1. Materials

Carbomer 980 (Carbopol® 980) was purchased from Lubrizol (USA). Xanthan gum (VANZAN® NF-C) was purchased from Vanderbilt Minerals, LLC (USA). Polyacrylate crosspolymer-6 (Sepimax Zen) was kindly donated from Seppic (France). Sodium benzoate and trometamol were purchased from Sigma Aldrich (USA). Ultrapure water was obtained via a Genpure apparatus (TKA Wasseranfbereitungssysteme, Germany).

2.2. Preparation of nanoemulsion gels

Nanoemulsion was prepared by emulsion phase inversion method, and transformed into nanoemulgels directly by swelling the gelling agent with the nanoemulsion. Labelling of the formulations is represented in Table 1.

2.3. Atomic Force Microscopy (AFM)

Nanoemulgels were diluted in ultrapure water (1:2000 V/V) and one drop of solution was dried in a vacuum for 2 h prior to analysis. Micrographs are recorded with an NTEGRA Prima Atomic Force Microscope (NT-MDT, Russia) in intermittent-contact mode.

Table 1. Type of the used gelling agent for gelation of the nanoemulsion.

	Gelling agent (1% *m/m*)
NEG_C980_d	Carbomer 980
NEG_XG_d	Xanthan gum
NEG_SZ_d	Polyacrylate crosspolymer-6

2.4. Rheological analysis

A rotational rheometer (Rheolab MC 120, Paar Phisica, Germany) equipped with a cup/plate measuring system (diameter 50 mm, angle 1°) was used. The test was conducted under continuous shear conditions at 20 ± 0.1 °C, with a controlled shear rate from 0 to 200 s^{-1}, in triplicate.

2.5. In vitro release testing (IVRT)

The test was conducted using Franz diffusion cells coupled with a polycarbonate membrane with a pore diameter of 0.4 μm, under infinite dosing conditions. Samples were collected at predefined time points (after 1, 2, 4, 6, and 8 h), and the ibuprofen concentration in the receptor medium was estimated by a validated HPLC method.

3. RESULTS AND DISCUSSION

3.1. AFM

AFM analysis provided valuable insight into the morphology and topography of the nanoemulgels. 3D topography of formulation NEG_C980_d (Fig. 1) clearly shows densely packed clusters of carbomer 980, as well as small-diameter spherical structures representing

preserved nanoemulsion droplets containing ibuprofen. Micrographs of the formulation NEG_XG_d indicate extended and very porous 3D organization, while sample NEG_SZ_d exhibits characteristic densely packed spherical structures of both polymer and nanoemulsion droplets. This analysis indicates that the nanoemulsion droplets are located both within and on the surface of the gel network and that the direct gelation process did not lead to degradation of their structure.

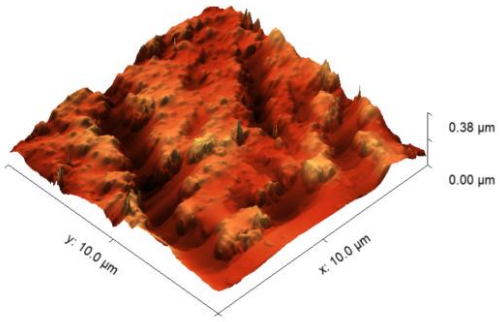

Figure 6. 3D topography of the formulation NEG_C980_d.

3.2. Rheological analysis

All formulations exhibit non-Newtonian, shear-thinning, thixotropic behavior, as evidenced by flow curves and viscosity vs. shear rate curves (Fig. 2).

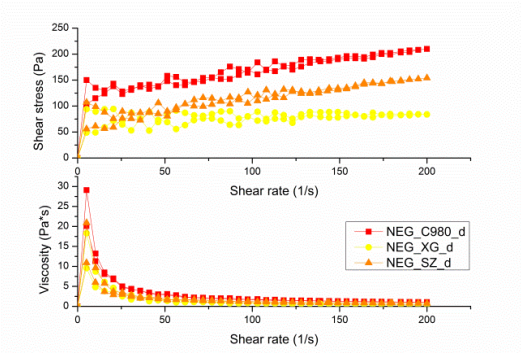

Figure 2. Flow curves (upper graph) and viscosity vs. shear rate profiles (down graph).

This behavior is typical for topical semisolid formulations and indicates that the formulation could be easily squeezed out of the tube and simply spread at the site of application. The highest viscosity was exhibited by NEG_C980_d, while the lowest viscosity was observed for the sample NEG_XG_d, which was in agreement with the findings obtained by AFM.

3.3 IVRT

The release rate in the first 8 h of the experiment followed the rank order: NEG_XG_d > NEG_SZ_d > NEG_C980_d. The differences in the 3D organization, shown by AFM, significantly influence the release of ibuprofen from the nanoemulgels. A porous structure of nanogel with xanthan gum allowed the free movement of ibuprofen after release from the oil core, while the compact matrix in nanogel with carbomer 980 significantly slowed down the release. In addition to nanoemulgel structure, viscosity also played an important role, as both viscosity and release rate followed identical rank orders.

4. CONCLUSION

This study showed that, after adequate sample preparation, AFM can successfully provide visualisation of the internal organization of the nanoemulsion gels' 3D matrix. When further combined with rheological measurements, microstructure of these complex formulations was successfully described, revealing potential of the novel Polyacrylate crosspolymer-6. Carbomer 980 produces nanoemulgels with the densely packed network, while xanthan gum produces porous, low-viscosity gel.

5. REFERENCES

1. Donthi, M.R., et al., Nanoemulgel: A Novel Nano Carrier as a Tool for Topical Drug Delivery. Pharmaceutics, 2023. 15(1): 164.

2. Ojha, B., et al., Nanoemulgel: A Promising Novel Formulation for Treatment of Skin Ailments. Polymer Bulletin, 2022. 79(8): 4441–4465.

ACKNOWLEDGMENT

This research was funded by the Ministry of Science, Technological Development and Innovation, Republic of Serbia through two Grant Agreements with University of Belgrade-Faculty of Pharmacy No 451-03-136/2025-03/ 200161, No 451-03-137/2025-03/ 200161, and No 451-03-136/2025-03/200026.

P079

PHYSICOCHEMICAL AND RHEOLOGICAL EVALUATION OF THYMOL-LOADED VESICULAR PHOSPHOLIPID GELS

Željka Vanić[1], Sabina Keser[1], Marica Jozić[2], Magda Vodolšak[1], Zora Rukavina[1]

[1]Department of Pharmaceutical Technology, University of Zagreb Faculty of Pharmacy and Biochemistry, Croatia
[2]Healthcare Facility Pharmacy Slavonski Brod, Croatia

1. INTRODUCTION

Thymol, one of the main compounds of thyme essential oil, has shown potential for the treatment of various skin disorders/diseases due to its multiple activities comprising antimicrobial, anti-inflammatory and antioxidative effects [1]. However, thymol also increases skin permeability and porosity, acting as a penetration enhancer [2], which can consequently lead to difficulties in its localization within the skin. These limitations as well as its poor solubility in water can be overcome by incorporating thymol into a vesicular phospholipid gel (VPG), a novel semisolid dermal vehicle consisting of tightly packed phospholipid vesicles (liposomes) [3]. Accordingly, the aim of this research was to prepare thymol-VPGs (T-VPGs) and evaluate the influence of (phospho)lipid composition and process parameters on their physicochemical and rheological properties.

2. MATERIALS AND METHODS

2.1. Materials

Lipoid S100, i.e., a soybean lecithin containing ≥ 94% phosphatidylcholine (SPC), was obtained from Lipoid GmbH (Ludwigshafen, Germany). Thymol and cholesterol were purchased by Sigma-Aldrich (St. Louis, USA).

2.2. Preparation of T-VPGs

SPC (9.6 g), with or without cholesterol (1 g) was added to a solution of thymol (0.5 g) in propylene glycol (1 g). The mixture was dispersed in water (18.9 g) during continuous magnetic stirring (500 rpm, 60 min) at room temperature or at 50 ˚C (preparation with cholesterol). The hydrated mixtures were then homogenized in a Microfluidizer LM20 (Microfluidics, USA) at 500 bars in one cycle to form T-VPGs. The amount of SPC in T-VPG containing cholesterol was 8.6 g.

2.3. Characteristics of T-VPG Liposomes

Size and zeta potentials of T-VPGs were determined on a Zetasizer Ultra (Malvern Panalytical, Malvern, UK) [3]. Prior to the measurements, T-VPGs were converted to T-VPG liposomes by dispersing VPG in water (1:30) on a magnetic stirrer (600 rpm, 30 min).

2.4. Rheometry of T-VPGs

Viscosity and amplitude sweep profiles of T-VPGs were determined on a Modular Compact Rheometer MCR 102 (Anton Paar GmbH, Austria) utilizing RheoCompass™ software. The system was fitted with a cone-plate measuring system (CP25, 25 mm diameter) with gap set at 0.102 mm for viscosity testing or parallel-plate measuring system (PP25, 25 mm diameter) with gap set to 1 mm for amplitude sweep tests. Viscosity tests were performed in the shear rate range from 0.01 to 1000 s^{-1}, while amplitude range was set from 0.01 to 100 %, with an angular frequency of 10 s^{-1} [4]. The measurements were performed in triplicate at 25 and 32 ˚C (viscosity) or 32 ˚C (amplitude sweep).

3. RESULTS AND DISCUSSION

3.1. Physicochemical Properties of T-VPG Liposomes

High-pressure homogenization method enabled preparation of T-VPGs with mean diameters of the liposomes between 140 and 150 nm, which is consistent with the previous study [3]. Zeta potentials of T-VPG liposomes were very slightly negative and influenced by the physicochemical properties of SPC. The composition of T-VPGs affected encapsulation of thymol in T-VPG liposomes. Significantly higher encapsulation efficiency (62 %) was achieved in the nanoformulation composed only

P079

of SPC (Table 1) due to higher phospholipid content.

Table 1. Characteristics of T-VPG liposomes

Parameter	SPC/T-VPG	SPC/Ch/T-VPG
MD (nm)	143.5 ± 3.9	147.9 ± 0.5
PDI	0.42 ± 0.04	0.23 ± 0.01*
ZP (mV)	-2.3 ± 0.35	-6.0 ± 0.5
EE (%)	62.1 ± 3.8	53.0 ± 3.3*

Ch, cholesterol; EE, encapsulation efficiency; MD, mean diameter; ZP, zeta potential; SPC, soybean phosphatidylcholine; T, thymol; VPG, vesicular phospholipid gel. The results are mean ± S.D. (n=3). *Significantly different compared to SPC/T-VPG ($p < 0.05$).

3.2. Viscosity of T-VPGs

The results presented in Fig. 1 demonstrate that both T-VPGs exhibited non-Newtonian behavior, typical for pseudoplastic systems. The viscosity of the prepared T-VPGs depended on the shear rate, with viscosity decreasing as the shear rate increased, regardless of the temperature at which the sample was measured. Moreover, the viscosity was affected by the concentration of SPC in the nanoformulations. Hence, T-VPG containing cholesterol (SPC/Ch/T-VPG) was less viscous than T-VPG without cholesterol (SPC/T-VPG).

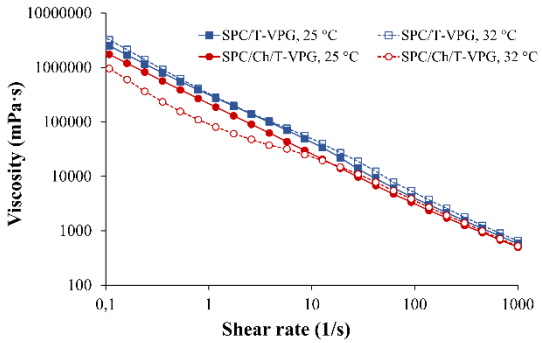

Figure 1. Viscosity profiles of T-VPGs.

3.3. Amplitude Sweep Profiles of T-VPGs

T-VPGs displayed storage modulus (G′) greater than loss modulus (G″), indicating a viscoelastic solid-like structure of both VPGs (Fig. 2). The linear viscoelastic region (characterized by a constant plateau where G′ and G″ remain unaffected by shear strain), was observed in the region from approximately 0.05 to 1 %. SPC/T-VPG have shown significantly higher values of G′ and G″ than SPC/Ch/T-VPG ($p < 0.05$) because of the higher concentration of SPC in the nanoformulation.

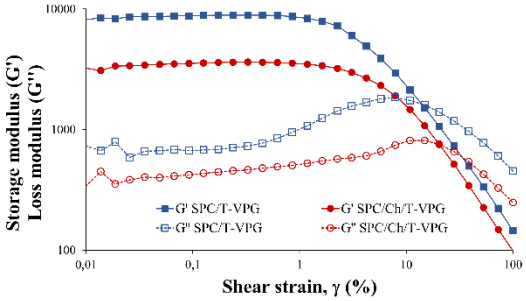

Figure 2. Amplitude sweep curves of T-VPGs.

4. CONCLUSION

The high-pressure homogenization method yielded T-VPGs enabling high loading of thymol in neutral liposomes of mean diameters less than 150 nm. Appropriate rheological properties, suitable for dermal administration, were obtained by both T-VPGs.

5. REFERENCES

1. Najafloo, R., et al., *A mini-review of Thymol incorporated materials: Applications in antibacterial wound dressing*. Journal of Drug Delivery Science and Technology, 2020. 60: 101904.
2. Pham, Q.D., et al., *Chemical penetration enhancers in stratum corneum - Relation between molecular effects and barrier function*. Journal of Controlled Release, 2016. 232: 175-187.
3. Keser, S., et al., *Vesicular phospholipid gels: A new strategy to improve topical antimicrobial dermatotherapy*. International Journal of Pharmaceutics, 2024. 667(Pt B):124931.
4. Rukavina, Z., et al., *Azithromycin-loaded liposomal hydrogel: a step forward for enhanced treatment of MRSA-related skin infections*. Acta Pharmaceutica, 2023. 73: 559–579.

ACKNOWLEDGMENT

This work was supported by a project entitled “Drug delivery nanosystems for topical application” at the University of Zagreb, Croatia.

P080

NANOFIBER PHYSICAL PROPERTIES INFLUENCE IMMUNE CELL BEHAVIOUR

Anže Zidar[1], Špela Zupančič[1], Julijana Kristl[1], Matjaž Jeras[2]

[1]*Department of Pharmaceutical Technology, Faculty of Pharmacy, University of Ljubljana, Slovenia*
[2]*Department of Clinical Biochemistry, Faculty of Pharmacy, University of Ljubljana, Slovenia*

1. INTRODUCTION

Electrospun nanofibers are promising materials in biomedical applications, such as drug delivery, tissue regeneration, and wound healing [1, 2]. However, their immunological safety remains poorly understood. This study explores how nanofiber physical properties — specifically diameters, interfibrillar pore sizes, and mat thicknesses — affect the metabolic activity, proliferation, and viability of peripheral blood mononuclear cells (PBMCs), under both homeostatic and inflammatory conditions [3].

2. MATERIALS AND METHODS

2.1. Materials

Poly(ε-caprolactone) (PCL), poly(ethylene oxide) (PEO), low molecular weight chitosan (CS), polyvinylpyrrolidone (PVP) and zein, all from Sigma-Aldrich (Steinheim, Germany); sodium alginate (ALG) from FMC BioPolymer (Haugesund, Norway); phytohemagglutinin-L (PHA-L), from Roche (Basel, Switzerland); CytoTox 96® Non-Radioactive Cytotoxicity Assay (the LDH test) and CellTiter 96® Aqueous One Solution Cell Proliferation Assay both from Promega (Madison, WI, USA); and ProLongTM Gold antifade reagent with DAPI from Thermo Fisher (Eugene, OR, USA).

2.2. Methods

Nanofibers were produced using climate-controlled electrospinning, by adjusting the polymer concentration, collector voltage and time of spinning to obtain different diameters, pore sizes and math thicknesses respectively. PBMCs were cultured on nanofibers for 72 h under unstimulated and PHA-L stimulated conditions. Relative metabolic activity (RMA) was determined by MTS assays, cytotoxicity by LDH release, while fluorescence microscopy was used to assess cell proliferation and penetration.

3. RESULTS AND DISCUSSION

Electrospun nanofibers were prepared using four polymers with distinct surface chemistries: hydrophobic PCL, negatively charged ALG, positively charged CS, and protein-based zein, the last three blended with suitable co-polymers to enable electrospinning. These polymers were selected to represent a broad spectrum of chemical characteristics influencing immune cell interactions. To investigate the impact of physical properties on immunological safety, we varied three key nanofiber attributes: diameters (56–926 nm), pore sizes (0.06–7.5 μm²), and mat thicknesses (5–148 μm).

3.1. Nanofiber Diameter

Variation in nanofiber diameter had a minimal effect on PBMC activity in most nanofiber mats. Notably, only zein nanofibers showed a statistically significant positive correlation between diameter and RMA. This may reflect their higher surface-driven cell activation, suggesting immunogenic potential. Other tested polymers (PCL, ALG, and CS) exhibited negligible or no correlation (Figure 1).

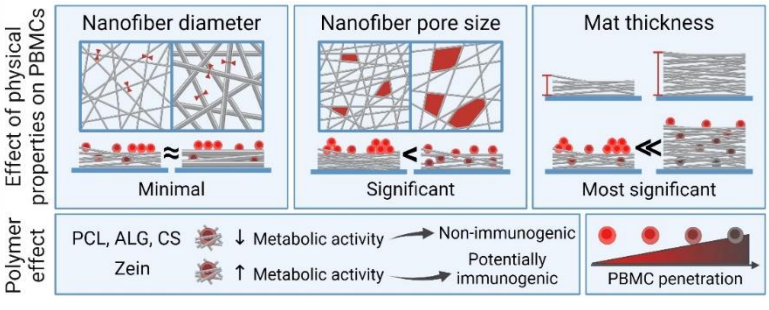

Figure 7. The impacts of nanofiber diameter, nanofiber pore size and mat thickness on PBMC penetration and activation.

3.2. Nanofiber Pore Size

Interfibrillar pore size had a more pronounced effect. In PCL, ALG, and CS nanofibers, larger pore sizes correlated with decreased RMA, likely due to deeper cell penetration and entrapment which reduced proliferation. In contrast, zein nanofibers with larger pores increased PBMC activity (Figure 1), further highlighting their potential to activate cellular immune responses. This suggests that pore size plays a significant role, influencing both cell infiltration and immune activation.

3.3. Nanofiber Mat Thickness

Mat thickness was the most influential factor. Thicker mats allowed deeper PBMC penetration, reduced proliferation, and significantly lowered metabolic activity without inducing cytotoxicity in PCL, ALG, and CS nanofibers. Zein mats, however, maintained or even increased RMA in thicker mats, likely due to greater immune cell activation potential despite reduced proliferation (Figure 1).

Fluorescent imaging confirmed that cell density and clustering were significantly reduced in thick mats, with more cells found deeper in the structure (Figure 2). Also the experiment where we cultured the same number of cells on nanofibers and rinsed them from the nanofiber surface showed that more cells remained in thicker nanofiber mats suggesting they penetrated deeper and got entrapped in the mat.

4. CONCLUSION

Among the physical properties examined, mat thickness and pore size had the strongest impact on immune cell behavior, while nanofiber diameter had limited effect. Thicker and more porous mats modulated immune responses through cell entrapment and/or activation. Zein nanofibers showed signs of immunogenicity and should be investigated further. These findings offer an insight into the design of safer nanofiber-based biomedical materials.

5. REFERENCES

[1] A. Zidar, Š. Zupančič, J. Kristl, M. Jeras, Development of a novel in vitro cell model for evaluation of nanofiber mats immunogenicity, International Journal of Pharmaceutics 650 (2024) 123696.

[2] J. Pelipenko, P. Kocbek, J. Kristl, Nanofiber diameter as a critical parameter affecting skin cell response, Eur. J. Pharm. Sci. 66 (2015) 29-35.

[3] A. Zidar, Š. Zupančič, J. Kristl, M. Jeras, Impact of polycaprolactone, alginate, chitosan and zein nanofiber physical properties on immune cells for safe biomedical applications, Int. J. Biol. Macromol. 282 (2024) 137029.

ACKNOWLEDGMENT

Supported by Slovenian Research Agency (Grant No. P1-0189, P3-0310, J3-3062, J7-4418) and European Regional Development Fund (Grant C333-19-952061 EATRIS-TRI.si).

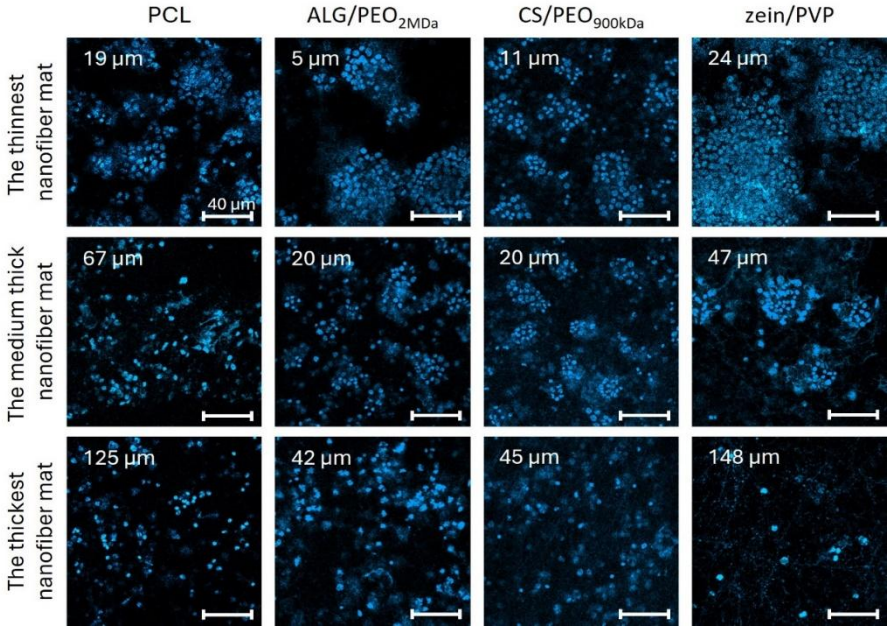

Figure 8. Proliferation of PHA-L activated PBMCs, cultured for 72 h on differently thick nanofiber mats (thickness noted in upper left corners) made of PCL, ALG/PEO_{2MDa}, CS/PEO_{900kDa}, and zein/PVP. Cells were stained with DAPI. Scale bars on each individual image represent 40 µm.

P081

EXENDIN-4-FUNCTIONALIZED NANOEMUSLIONS FOR TARGETED DRUG DELIVERY

Nataša Holler[1], Bernd Gesslbauer[1], Ilse Letofsky-Papst[2], Claudia Mayrhofer[2], Andreas Zimmer[1]

[1]Institute of Pharmaceutical Sciences, Pharmaceutical Technology & Biopharmacy, University of Graz, Austria
[2]Graz University of Technology, Centre for Electron Microscopy Graz, Graz, Austria

1. INTRODUCTION

Nanocarriers for targeted drug delivery currently represent one of the most actively researched areas in the pharmaceutical sciences. Our research focuses on the development of peptide-directed nanoemulsions (NEs). For peptide model, a 39 amino acids long GLP-1 receptor agonist exendin-4 is used. GLP-1 agonists are considered promising pharmacological agents in metabolic syndrome disorders such as type 2 diabetes mellitus, obesity and metabolic dysfunction-associated liver disease (MASDL). GLP-1 receptor is a G-protein coupling receptor and is prone to a rapid internalization in response to various agonists. [1] It is expressed in the pancreas, lung, brain, kidney, liver, as well as in muscle and adipose tissue. [2] The uptake of the drug carrier was tested on 3T3-L1 mouse preadipocyte cell line, which is a commonly used tool for study of the subcellular pathways involved in preadipocytic cell differentiation. [3]

2. MATERIALS AND METHODS

Firstly, the raw nanoemulsions were prepared using high-pressure homogenization. Here, we tested different emulsifiers (egg lecithin Lipoid ® E80, E PC S, and E80 SN) in different concentrations, and we were adjusting the oily phase by using various oils and LCT:MCT ratios. The best candidates in terms of the particle size distribution and zeta potential were further used for preparation of peptide-directed nanoemulsions. To design the drug carrier, the exendin-4 was coupled to the PEG end of a pegylated phospholipid chain by a click-chemistry reaction. This enables the attachment of the peptide to the surface of the oil droplets within the nanoemulsion. The selected raw nanoemulsion was mixed with the lyophilized peptide conjugate to prepare an exendin-4 nanoemulsion (see Figure 1).

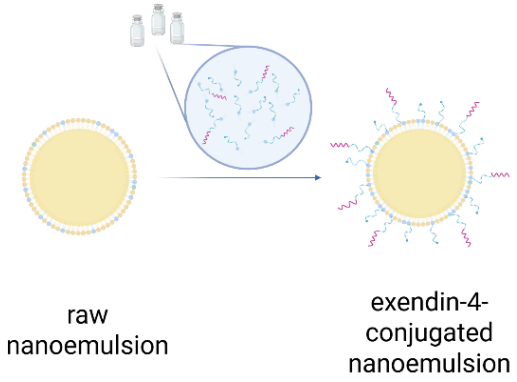

Figure 1. Preparation of the exendin-4-functionalized nanoemulsion by mixing the raw nanoemulsion with the lyophilized reaction product (exendin-4-PEG(2000)-DSPE).

To track changes in the characteristics of the obtained product and inspect the product stability, particle size distribution and zeta potential were measured again immediately after preparation, after 7 days, and after one month of preparation. Furthermore, the cellular uptake of the designed nanocarrier was measured. According to the literature, the GLP-1 receptor is expressed in the 3T3-L1 cells. [4] We compared the uptake in the 3T3-L1 cells prior to and after the differentiation to the mature adipocytes. As control, a pegylated nanoemulsion (PEG NE) was used. This differed from the ex-4 NE only in the absence of the peptide on the surface of the oil droplets.

3. RESULTS AND DISCUSSION

3.1. Size and charge

The preparations proved to be stable over the set period of time. As expected, the droplet size increased after conjugation (see Table 1).

P081

Table 1. Size and charge comparison of the raw nanoemulsion containing 1% E80SN as emulsifier prior to and after conjugation with DSPE-PEG(2000) and DSPE-PEG(2000)-exendin-4 (n=3, ±SD).

	Size [nm]	PdI	Charge [mV]
raw NE	*166,8±1,8*	*0,10±0,01*	*-45,0±0,7*
PEG NE	*175,5±2,2*	*0,12±0,02*	*-56,9±1,4*
ex-4 NE	*175,3±1,1*	*0,11±0,01*	*-41,4±0,4*

3.2. Uptake studies

Measurements of cellular uptake over time are presented in Figure 2. The uptake was confirmed with both, undifferentiated and differentiated cells, and for both types of nanoparticles. However, higher uptake levels were observed in cells treated with the exendin-4 nanoemulsion. Microscopic images (see Figure 3) showing mature 3T3-L1 adipocytes after 30 minutes of incubation with comparing nanoemulsions also confirm the internalization of the oil droplets.

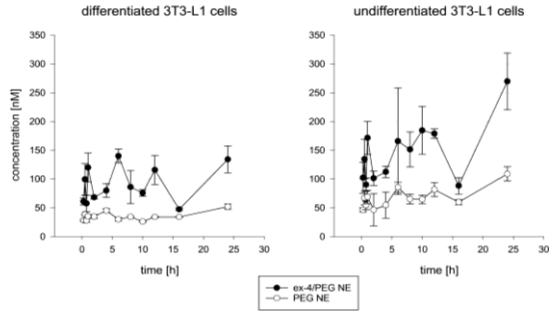

Figure 2. Cellular uptake over 24 hours (n=3, ±SD). Both nanoemulsions were diluted in the same way, so that the final peptide concentration is 500nM.

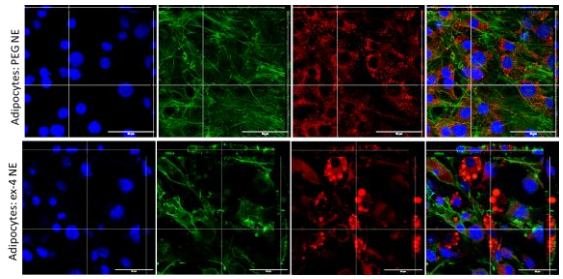

Figure 3. Images obtained from confocal microscope (Leica Microsystems, Germany). Before imaging, cells were fixed in 4% formaldehyde and stained with F-actin-phalloidin (Alexa Fluor ™488, green) and Hoechst stain (blue).

4. CONCLUSION

Our findings demonstrate that the uptake patterns observed in 3T3-L1 fibroblasts were significantly different and that the uptake rates were higher when the peptide was present on the surface of the oil droplets. This tendency is even more pronounced after the fibroblasts are fully differentiated to the mature adipocytes. This suggests a specific or a receptor-mediated uptake. Subsequent studies will focus on exploring the significance of this specific type of uptake using receptor antagonists and different endocytosis inhibitors.

5. REFERENCES

1. Roed, S. N. et al., *Real-time trafficking and signaling of the glucagon-like peptide-1 receptor.* Molecular and Cellular Endocrinology, 2014. 382(2): 938–949.

2. Müller, T. D. et al., *Glucagon-like peptide 1 (GLP-1*). Molecular Metabolism, 2019. 30: 72–130.

3. Dufau, J., et al., *In vitro and ex vivo models of adipocytes*. American Journal of Physiology - Cell Physiology, 2021. 320(5): 822–841.

4. Chen, J., et al., *GLP-1/GLP-1R Signaling in Regulation of Adipocyte Differentiation and Lipogenesis.* Cellular Physiology and Biochemistry, 2017. 42(3): 1165–1176.

ACKNOWLEDGMENT

We would like to thank to the Phospholipid Research Center (PRC) for sponsoring our master students (Project number AZI-2021-096/1-1) and to the Lipoid GmbH for providing the egg-lecithins used in this research.

P082

METRONIDAZOLE-LOADED POLY(E-CAPROLACTONE) NANOFIBERS: A FORMULATION ASSESSED BY EUROPEAN PHARMACOPOEIA QUALITY CRITERIA

Špela Zupančič[1], Maruša Vrčon[1], Robert Roškar[1], Julijana Kristl[1]

[1]*Faculty of Pharmacy, University of Ljubljana, Slovenia*

1. INTRODUCTION

Electrospun nanofibers are promising carriers for local drug delivery due to their high surface area, porosity, and capacity for controlled drug release. Their potential is especially relevant for treating vaginal infections, where localized delivery of antimicrobials enhances efficacy and patient compliance. Despite extensive scientific research on nanofibers, regulatory or legislative publications are scarce. As single-dose pharmaceutical forms, their use must align with pharmacopeial standards [1]. This study aimed to develop and evaluate poly(ε-caprolactone) (PCL) nanofibers loaded with metronidazole (MTZ), a widely used antimicrobial, with emphasis on how the collection method affects key quality parameters defined by Ph. Eur. 11.7.

2. MATERIALS AND METHODS

2.1. Materials

Metronidazole (MTZ) and poly(ε-caprolactone) (PCL, MW 80 kDa), both from Sigma-Aldrich (China, UK, or USA); glacial acetic acid (100%), formic acid (98–100%), potassium dihydrogen phosphate, sodium hydroxide, methanol, and acetonitrile, all from Merck (Finland or USA).

2.2. Electrospinning of Nanofiber Mats

PCL (15% w/w) and MTZ (5% w/w) were dissolved in a 3:1 (w/w) mixture of acetic and formic acid. Electrospinning was performed using a Fluidnatek LE-100 instrument (BioInicia, Spain) under ambient conditions (21 °C, 35% RH). The flow rate was set at 500–900 µL/h with a 15–21 kV applied voltage. The nozzle-to-collector distance was 15 cm, and the collector voltage was set to –5 kV. Samples were collected either on a stationary plate or a rotating drum, with the nozzle moving along x- and y-axes (plate) or only x-axis (drum) at 12 mm/s (Table 1).

Table 5. The collection parameters of three samples.

Sample name	Collector	Movement in x-axis direction (mm)	Movement in y-axis direction (mm)
P1	Plate	/	0–300
P2	Plate	110–190	0–290
D	Drum	110–190	/

To evaluate the effect of residual solvents, a portion of each nanofiber mat was dried at 45 °C for at least 38 hours.

2.3 Evaluation of Nanofiber Mats

Nanofiber morphology was analyzed using scanning electron microscopy (SEM, Zeiss Supra 35 VP). Layer thickness was measured at center and edge areas using a stereo microscope (Olympus SZX12). Nanofiber mats were sectioned into 1.5 × 1.5 cm units (2.25 cm²) for testing.

Nanofibers were evaluated according to Ph. Eur. 11.7: Uniformity of mass of single-dose preparations (2.9.5), Uniformity of content of single-dose preparations (2.9.6), and Uniformity of dosage units (2.9.40). MTZ was quantified via validated UPLC (Waters Acquity) at 320 nm.

Residual solvent content was analyzed by HPLC (Agilent 1100/1200) before and after drying, following ICH Q3C guidelines. *In vitro* drug release was conducted in phosphate buffer (pH 7.4, 37 °C), and samples were analyzed by UPLC (Acquity UPLC, Waters Corp., USA). Statistical analysis was performed using OriginPro® 2019.

P082

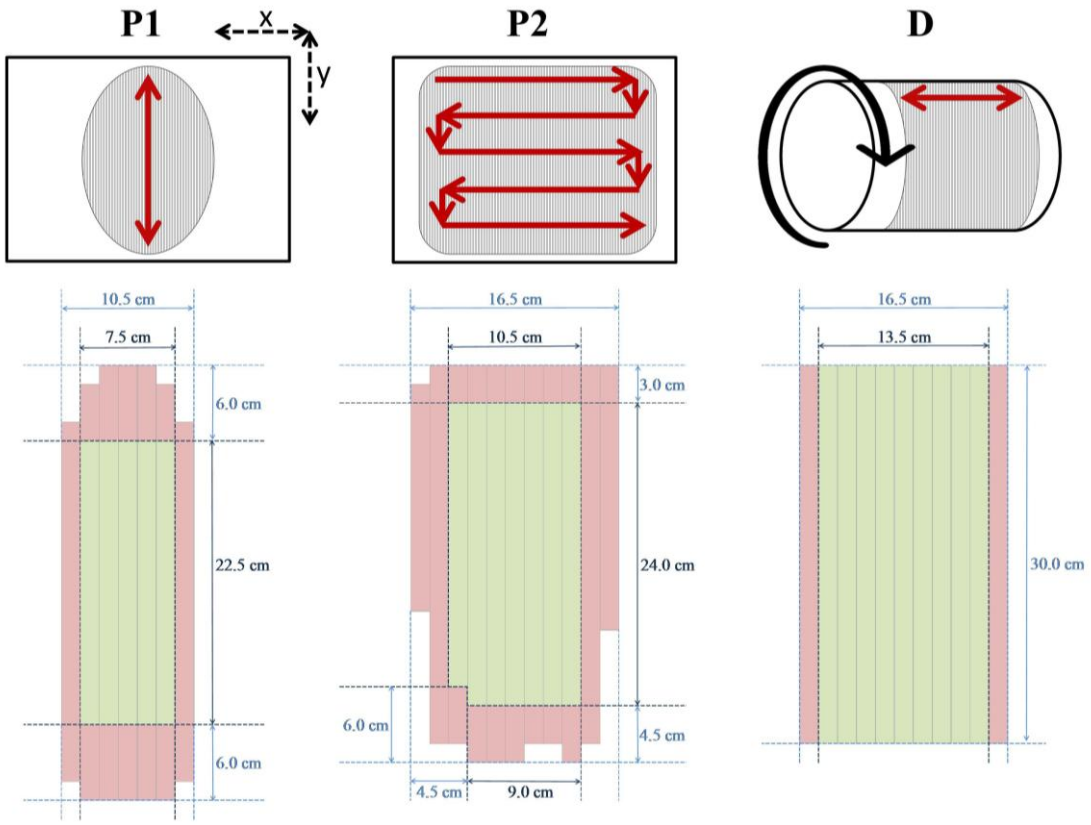

Figure 9. Scheme of nozzle movement (red arrows) above different collectors during electrospinning process of samples (grey area) (a) plate (P1), (b) plate (P2), and (c) drum (D). Dimensions of the nanofiber layers in samples that comply with the pharmacopoeial requirements for the uniformity of mass in single-dose preparations along longitudinal sections are marked in green, while those that do not meet the criteria are shown in red.

3. RESULTS AND DISCUSSION

SEM analysis confirmed the successful formation of smooth, bead-free nanofibers with average diameters around 300 nm, regardless of the collector type. Different collection setups significantly affected the geometry and homogeneity of the nanofiber mats. All nanofiber mats exhibited edge thinning; however, drum-collected samples provided a larger usable area with more uniform central regions. The central 13.5 cm section of drum-collected mats (405 cm^2) fully met the Ph. Eur. 2.9.5 mass uniformity criteria. In plate-collected samples, compliant zones were also identified after excluding the outermost regions. All tested units, regardless of collection method, complied with content uniformity (2.9.6) and dosage unit uniformity (2.9.40) requirements. Residual solvent analysis showed 0.2% formic and 0.04% acetic acid in undried nanofibers, both well below the 0.5% Ph. Eur. threshold for class 3 solvents. Drying further reduced these levels below the limit of detection. Dried nanofibers released MTZ more slowly than undried ones (95% released after 13 vs. 5 days), likely due to increased hydrophobicity after solvent removal.

4. CONCLUSION

This study demonstrated that PCL nanofibers can be produced by electrospinning to meet Ph. Eur. requirements for single-dose pharmaceutical forms when appropriate collection strategies are applied. The rotating drum collector ensured better homogeneity and uniformity of mass across the mat, while residual solvents were safely removed by controlled drying. These findings underscore the importance of both collection method and post-processing in developing acceptable nanofiber-based dosage forms.

5. REFERENCES

[1] J. Pelipenko, P. Kocbek, J. Kristl, Nanofiber diameter as a critical parameter affecting skin cell response, Eur. J. Pharm. Sci. 66 (2015) 29-35.

ACKNOWLEDGMENT

Supported by Slovenian Research Agency (Grant No. P1-0189, J7-4418) and University of Ljubljana Start-up Research Programme (SN-ZRD/22-27/0510).

P083

TARGETING CANCER CELLS BY THE MACROPINOCYTOSIS OF CYCLODEXTRINS

Ferenc Fenyvesi[1], Csenge Urgyán[1], Katalin Réti-Nagy[1], Ágnes Rusznyák[1], Ildikó Bácskay[2]

[1]Department of Molecular and Nanopharmaceutics, University of Debrecen, Hungary
[2]Department of Pharmaceutical Technology, University of Debrecen, Hungary

1. INTRODUCTION

The ability of cyclodextrins to form complexes with various biomolecules is widely used in biological studies. It was also revealed, that cyclodextrins can enter the cell by endocytosis, by which a new cellular delivery route was opened and applied in cholesterol storage disorders [1]. The endocytosis of cyclodextrin derivatives on different cell lines has not been studied and compared yet. Our aim was to characterize the physicochemical properties of fluorescein-, and rhodamine-labelled derivatives and test the endocytosis of fluorescein-labelled hydroxypropyl-beta-cyclodextrin (FITC-HPBCD) and random methyl-beta-cyclodextrin (FITC-RAMEB) in different cancer cell lines. Finally, an attempt was made to find physicochemical and biological attributes, that affect endocytosis.

2. MATERIALS AND METHODS

FITC-HPBCD and FITC-RAMEB were purchased from Cycloab Ltd. (Hungary). Octanol-water partition coefficient was determined, and molecular association was measured by dynamic light scattering (DLS). Cancer cell lines were cultured by regular passaging. The cellular uptake of the fluorescent cyclodextrins was studied by flow cytometry.

3. RESULTS AND DISCUSSION

Octanol-water partition coefficient and molecular association was determined, and significant differences were revealed among the fluorescent derivatives of HPBCD and RAMEB. Rhodamine labelling had more pronounced effect on the molecular association, and lipophilicity of the molecules, therefore these derivatives were not used in cellular experiments. Cancer cell lines showed major differences in the endocytosis of the cyclodextrins and interestingly the uptake of HPBCD and RAMEB was different in the tested cell lines (Fig 1). The expression of KRAS protein and its role in the endocytosis of cyclodextrins is under investigation as well as the *in vivo* tumour uptake of the radiolabelled derivatives.

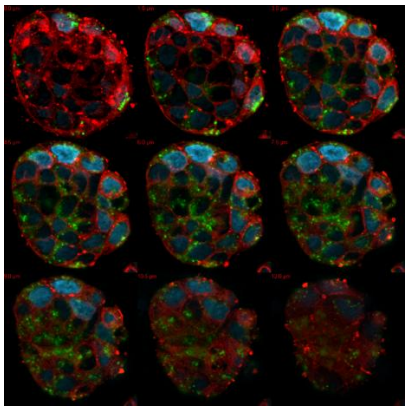

Figure 1. FITC-RAMEB accumulation in Caco-2 cells [2] (green: FITC-RAMEB; blue: cell nucleus; red: cell membrane).

4. CONCLUSION

The results show the applicability of cyclodextrins in targeting various types of cancer via the endocytic pathway.

5. REFERENCES

1. Rosenbaum, A.I., et al., *Endocytosis of beta-cyclodextrins is responsible for cholesterol reduction in Niemann-Pick type C mutant cells. Proceedings of the National Academy of Sciences, 2010, 107(12):5477-82.*

2. Fenyvesi, F., et al., *Fluorescently Labeled Methyl-Beta-Cyclodextrin Enters Intestinal Epithelial Caco-2 Cells by Fluid-Phase Endocytosis.* PLoS ONE, 2014. 9(1): e84856.

P083

ACKNOWLEDGMENT

The research project was supported by OTKA K-147308 research grant of the National Research Development and Innovation Office, Budapest, Hungary.

Project no. TKP2021-EGA-18 has been implemented with the support provided by the Ministry of Culture and Innovation of Hungary from the National Research, Development and Innovation Fund, financed under the TKP2021-EGA funding scheme

P084

GENTAMICIN-LOADED CHITOSAN NANOPARTICLES EMBEDDED IN NANOCELLULOSE WOUND HEALING NANOCOMPOSITE

Lina Livrinska[1], Marija Petrushevska[1], Nikola Geškovski[1], Urška Jančič[2], Vineta Vuksanović[3], Beti Djurdjic[1], Maja Simonoska Crcarevska[1], Selestina Gorgieva[2]

[1]Faculty of Pharmacy, Ss. Cyril and Methodius University in Skopje, N. Macedonia
[2]Faculty of Mechanical Engineering, University of Maribor, Slovenia
[3]Center for medical microbiology, Institute of Public Health of Montenegro, Montenegro

1. INTRODUCTION

Surgical site infections remain a persistent healthcare challenge, accounting for a significant proportion of hospital-acquired infections. They severely disrupt the wound healing process and prolong the postoperative recovery. Current strategies for their prevention mainly include preoperative antiseptic measures and antibiotic prophylaxis. However, the systemic administration of antibiotics poses the risk of systemic toxicity and adverse effects, often leading to disrupted gut microbiome. Hence, approaches utilizing local antimicrobial treatment, including advanced biomaterials, have gained interest. This study aims to develop and characterize a composite wound dressing made from bacterial nanocellulose (*BNC*) scaffold impregnated with gentamicin-loaded nanoparticles (*GNPs*) as a potential postoperative wound treatment [1].

2. MATERIALS AND METHODS2.1. Materials

Medium molecular weight chitosan, tripolyphosphate and gentamicin sulfate were purchased from MerckMilipore. For the cell culture studies, Dulbecco's Modified Eagle's medium (DMEM) purchased from Lonza, USA, was used as cell culture medium, supplemented with 10% Fetal bovine serum (FBS) – Sigma Aldrich, Germany, and 1% pen-strep solution (Sartorius, Germany).

2.2. Preparation of the GNPs and GNPs-impregnated BNC scaffolds

Chitosan nanoparticles were synthesized using the ionic gelation method, with sodium tripolyphosphate as a crosslinker. For the *GNPs*, gentamicin sulfate was dissolved in the chitosan solution prior to sonication. The *BNC* was produced using the *K. melomenusus* AV436^T bacteria strain, as previously described [2]. The obtained *BNC* scaffolds were impregnated with empty nanoparticles (*BNC-NP*), gentamicin-loaded NPs (*BNC-GNP*) and gentamicin sulfate solution (*BNC-GS-Sol*) by simple deposition of the suitable dispersion/solution onto the *BNC* scaffolds placed in plate wells. Three different concentrations were prepared for each formulation.

2.3. Physico-chemical characterization

Particle size, particle size distribution and zeta potential of the *GNPs* were determined using dynamic light scattering (DLS) analysis (*Nano-ZS, Malvern Instruments, UK*). FTIR (*Cary 630 FTIR spectrometer, Agilent, Germany*) and Raman spectroscopy (*ATR 3000 portable Raman spectrometer, Optosky, China*) were employed to analyze the structural and chemical properties of both the nanoparticles and *BNC* scaffolds. Morphology of obtained nanocomposites and inclusion pattern were assessed by means of SEM (microscope Supra 35 VP, Carl Zeiss, Jena, Germany). XRD diffractograms were acquired for all samples as well (*D2 X-ray diffractometer, Bruker Siemens, Germany*).

2.4. *In vitro* cell culture studies

For the in vitro studies, human fibroblasts (BJ cells) derived from neonatal male skin, were used. Briefly, cell viability and cell attachment studies were conducted. Cell cytotoxicity was assessed using the MTT assay, while the attachment was visualized using SEM microscopy.

2.5. Antimicrobial activity

Antimicrobial activity was tested against *Klebsiella pneumoniae* bacteria using the well-diffusion method. The diameter of the inhibition zones surrounding both nanoparticles' wells and nanoparticles-impregnated nanocellulose scaffolds were measured in millimeters after incubation at 37 °C for 24 h.

3. RESULTS AND DISCUSSION

3.1. Optimization of NPs and physico-chemical characterization

Three formulation parameters were optimized to produce *NPs* with favourable particle size (80.07 ± 2.2) and particle size distribution (0.192 ± 0.02). FTIR and Raman spectroscopy confirmed successful ionic crosslinking between chitosan and TPP and efficient encapsulation of gentamicin, evidenced by shifted characteristic bands. The spectra of *BNC* revealed no structural changes upon impregnation with *NPs*. XRD analysis revealed characteristic cellulose peaks 2θ = 15° and 22.5°, confirming that all samples maintained their fundamental nanocellulose crystalline structure.

3.2. *In vitro* studies

All formulations demonstrated viability exceeding the 70% threshold set by ISO-10993-5, indicating good biocompatibility and potential safety for biomedical applications. As for the cell attachment, the micrographs reveal distinct patterns of fibroblast BJ cells attachment and morphology on nanocellulose substrates. A clear trend is visible across the concentration series. As concentration increases from 5 to 15 in all sample types (*G, NP, GNP*), there is a noticeable reduction in the number of attached cells. Despite these concentration-dependent effects, it's important to note that cell-nanocellulose interactions persist.

3.3. Antimicrobial activity

One-way ANOVA with significance level set at $p<0.05$ showed a statistically significant difference in mean inhibition zones among the formulations ($p<0.001$). Subsequently, a post-hoc Tukey's HSD revealed no statistically significant difference between the *GS-solution* and *BNC-GNPs* ($p=0.970$). For both *BNC-GNP* and *GS-solution* a significantly larger inhibition zones were measured in comparison with *GNP* and *BNC-GS-sol* ($p<0.001$).

4. CONCLUSION

GNP-BNC nanocomposites were developed with promising potential as a wound dressing for preventing surgical site infections and promoting healing. Optimal NPs showed nm-size and charge sufficient to avoid the stability issues and promote dispersibility. The composite scaffolds exhibited strong antimicrobial activity against *Klebsiella pneumoniae,* maintained scaffold integrity as shown in the FTIR and Raman spectra and supported fibroblast adhesion without significant cytotoxicity effects.

5. REFERENCES

1. Josyula, A. et al. *Engineering biomaterials to prevent post-operative infection and fibrosis* Drug Delivery and Translational Research, 2021. 11(4): 1675–1688.

2. Gorgieva, S. et al. *Production efficiency and properties of bacterial cellulose membranes in a novel grape pomace hydrolysate by Komagataeibacter melomenusus AV436T and Komagataeibacter xylinus LMG 1518*. International Journal of Biological Macromolecules, 2023. 244, 1–16.

ACKOWLEDGEMENT

Part of this research was funded by Slovenian research agency ARIS, project BI-ME/21-22-002, P2-0118/0795, N2-0388.

P085

REACTIVE OXYGEN SPECIES-REGULATED CONJUGATES BASED ON POLY(JASMINE) LACTONE FOR SIMULTANEOUS DELIVERY OF DOXORUBICIN AND DOCETAXEL

Jyoti Verma[1], Vishal Kumar[1,2], Carl-Eric Wilen[2], Jessica M. Rosenholm[1] and Kuldeep K. Bansal[1,2]

[1]Pharmaceutical Sciences Laboratory, Faculty of Science and Engineering Åbo Akademi University, Finland.
[2]Laboratory of Molecular Science and Engineering, Faculty of Science and Engineering, Åbo Akademi University, Finland.

1. INTRODUCTION

In recent years, massive attempts have been made to develop nanosized drug delivery carriers (NCs) capable of effectively delivering drugs precisely to diseased areas. The major goals of NC-based cancer therapy include minimizing drug leakage in off-target areas and stimulating sufficient drug release within the tumor. However, in most cases, premature drug release from NCs diminished their advantages. Polymer–drug conjugates are capable of inhibiting premature drug release in cancer therapy, thereby ensuring minimal side effects caused by chemotherapeutic agents [1]. However, their widespread use is limited due to their non-selectiveness and slow drug release, leading to poor efficacy. In cancer therapy, it is essential to selectively release cytotoxic agents into the tumor to prevent the adverse effects associated with anticancer drugs. Nevertheless, the incorporation of stimulus-sensitive characteristics in NCs could be a potential solution, enabling near-complete drug release in response to a stimulus associated with a specific disease symptom [2]. Thus, in this study, a stimuli sensitive polymer–drug conjugate was synthesized for selective drug release.

2. MATERIALS AND METHODS

2.1. Materials

Poly(ethylene glycol) methyl ether (mPEG, Mn = 5.0 KDa), 1,5,7-triazabicyclo [4.4.0]dec-5-ene (TBD) (98%), mercaptopropionic acid (99%), dimethoxy-2-phenylacetophenone (99%), triethylamine (TEA) (≥99.5%), N-(3-dimethylaminopropyl)-N′-ethylcarbodiimide (EDC) (≥97%), 4-(dimethylamino) pyridine (DMAP) (≥99%), N-hydroxysuccinimide (NHS) (≥99.5%), HPLC grades methanol (≥99.9%), acetone (≥99.8%), deuterated dimethyl sulfoxide (DMSO-d6), deuterated chloroform (CDCl3), THF, DMF, DCM, Diacetyldichlorofluorescein (DCFH-DA), Paraformaldehyde (PFA) and hexane were purchased from Sigma-Aldrich, Finland. Jasmine lactone (≥97%) was purchased from Lluch Essence, Spain. Doxorubicin (>99%) and Docetaxel (>99%) were purchased from LC Laboratories, USA. Chlorine e6 (Ce6) (≥90%) was purchased from Cayman Chemical, USA. Resazurin, 1,3-Diphenylisobenzofuran (DPBF) were purchased from TCI Europe Pvt. Ltd. VECTASHIELD (mounting medium with DAPI) was purchased from Vector Laboratories, Inc. Burlingame, CA.

2.2. Method

In the present study, we synthesized stimuli-responsive NCs to deliver DOX and DTX simultaneously in a controlled manner at the tumor region. We conjugated doxorubicin (DOX), docetaxel (DTX), and chlorin e6 (Ce6) to the hydroxy-terminated poly(jasmine lactone) (mPEG-b-PJL-OH) polymer, resulting in the formation of mPEG-b-PJL-Ce6-TK-DOX-DTX conjugates, further referred to as PJL-DOX-DTX. We synthesized DOX-TK and DTX-TK separately before adding them to the reaction. The synthesized conjugates were incorporated into self-assembled micelles (PJL-DOX-DTX micelles) using the nanoprecipitation method, and characterization was performed by analysing the drug loading, size, and in vitro drug release utilizing DLS and UV spectrophotometry [3]. We also conducted in vitro reactive oxygen species ($^1O_2$) generation and TK linker cleavage using DBPF, intracellular ROS generation using DCFH+DA, and cell cytotoxicity studies using the Alamar blue assay.

P085

3. RESULTS AND DISCUSSION

Doxorubicin (DOX) and docetaxel (DTX) were conjugated onto novel poly(jasmine lactone) based copolymer via a thioketal (TK) linker. In addition, a photosensitizer (chlorin e6) was attached to the polymer, which served as a reactive oxygen species generator to cleave the TK linker. The conjugate is readily self-assembled into micelles less than 100 nm in size. Micelles demonstrate a notable increase in their ability to cause cell death when exposed to near-infrared (NIR) light on MDA-MB-231 breast cancer cells. The increase in cytotoxicity is higher than that observed with the combination of free DOX and DTX (Fig. 1). The accumulation of DOX in the nucleus after release from the micelles (laser irradiation) was also confirmed by confocal microscopy (Fig. 2). In the absence of light, micelles did not show any toxicity while the free drugs were found toxic irrespective of the light exposure.

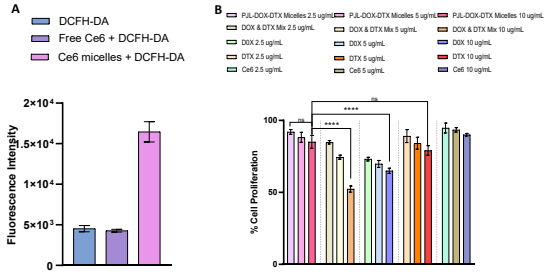

Figure 1. DCFH-DA fluorescence intensity post treatment with Ce6 micelles and free Ce6 in MDA MB-231 cells after 3 h incubation and laser irradiation. (B) Percentage cell proliferation inhibition study of DOX, DTX, mixture of DOX-DTX, Ce6, and PJL-DOX-DTX micelles (2.5, 5, 10 μg mL−1 with respect to DOX) on Vero H10 cell lines after 48 h incubation. ns, $p \geq 0.05$, ****, $p < 0.0001$.

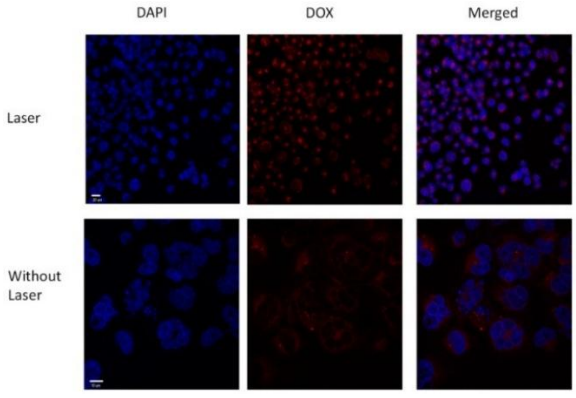

Figure 2. CLSM images of PJL-DOX-DTX micelles internalized in MDA-MB-231 cells after 12 h incubation with or without laser treatment. Cells were treated with 400 ng mL−1 equivalent concentration of DOX. Cell nucleus was stained with DAPI (blue), while DOX inherent red fluorescence was used to detect PJL-DOX-DTX micelles. Scale bar—20 μm (laser) and 10 μm (without laser).

4. CONCLUSION

The study successfully conjugated two anticancer drugs, DOX and DTX, onto a poly(jasmine lactone) block copolymer using an ROS-sensitive TK linker. The photosensitizer Ce6 was added to accelerate drug cleavage in the presence of NIR light. The conjugate self-assembled into 100 nm micelles, which showed higher cytotoxicity in cancer cells compared to free drugs. However, basic analytical tools failed to determine the exact amount of drug loading in the micelles, indicating the potential of the developed formulation in reducing side effects. Future work will focus on developing analytical methods and approaches to accurately calculate drug content.

5. REFERENCES

1. Thakor, P.; et. al., Polymer–drug conjugates: recent advances and future perspectives. drug discovery today 2020(25): 1718–1726.
2. Monteiro, P.F.; et. al., Reduction-responsive polymers for drug delivery in cancer therapy—is there anything new to discover? Wires nanomedicine Nanobiotechnology. 2021(13): e1678.
3. Bansal, K.K.; et. al., Evaluation of solubilizing potential of functional poly(jasmine lactone) micelles for hydrophobic drugs: a comparison with commercially available polymers. International Journal of polymeric material. Polymer Material. 2023(72): 1272–1280

ACKNOWLEDGMENT

J.V. and V.K. acknowledge the funding support provided by the National Overseas Scholarship, Ministry of Social Justice and Empowerment, Government of India for her personal PhD scholarship. Parts of the research used the Research Council of Finland Research Infrastructure “Printed Intelligence Infrastructure” (PII-FIRI). Electron microscopy imaging was performed in the Electron Microscopy Laboratory, Institute of Biomedicine, University of Turku. Confocal microscopy was performed at the Cell Imaging and Cytometry Core, Turku Biosciences Centre, Finland, with the support of Biocentre Finland.

P086

EVALUATION OF IN VIVO NOSE-TO-BRAIN DELIVERY OF FAVIPIRAVIR-LOADED ASPASOMES

Maryana Salamah[1,2], Balázs Volk[3], István Lekli[4], István Bak[4], Alexandra Gyöngyösi[4], Ildikó Csóka[1], György Tibor Balogh[5,6], Gábor Katona[1]

[1]*Institute of Pharmaceutical Technology and Regulatory Affairs, University of Szeged, Hungary.*
[2]*Institute of Pharmacodynamics and Biopharmacy, University of Szeged, Hungary.*
[3]*Directorate of Drug Substance Development, Egis Pharmaceuticals Plc., Budapest, Hungary.*
[4]*Department of Pharmacology, University of Debrecen, Hungary.*
[5]*Department of Pharmaceutical Chemistry, Semmelweis University, Hungary.*
[6]*Center for Pharmacology and Drug Research & Development, Semmelweis University, Hungary.*

1. INTRODUCTION

Neurotropic viruses, including RNA viruses, can invade the central nervous system (CNS) through the nasal epithelium, blood-brain barrier (BBB) or peripheral nerves, causing meningitis and several neurodegenerative diseases [1]. Intranasal administration of antiviral drugs, such as favipiravir (FAV), is a promising approach to overcome the bioavailability challenges and reduce the systemic adverse effects [2]. Lipid nanoparticles with amphiphilic materials, such as ascorbyl palmitate (AP), are considered a suitable antiviral drug carrier to enhance the BBB penetration and reach the site of infection in sufficient concentrations [3,4].

The aim of this study was to develop FAV-loaded aspasome formulations (FAV-ASPs) to improve the poor solubility and CNS penetration of FAV.

2. MATERIALS AND METHODS

2.1. Materials

FAV was provided by Egis Pharmaceuticals Plc. (Budapest, Hungary). Ascorbyl acid-6-palmitate (AP), sorbitan monostearate (Span® 60), cholesterol (CH) were purchased from Sigma Aldrich Co. Ltd. (Budapest, Hungary).

2.2. Preparation of FAV-ASP formulations

A modified film hydration method was employed for the preparation of FAV-ASPs [4]. Varying ratio of AP/Span® 60 with a fixed amount of CH, were dissolved in chloroform. A fixed amount of FAV was solubilized in methanol. Then, FAV solution was subsequently mixed with the lipid solution in a round-bottom flask, and the organic solvents were evaporated using a rotary vacuum evaporator. Finally, the thin lipid film was hydrated with phosphate-buffered saline (PBS, pH 7.4).

2.3. Characterization

FAV-ASPs were characterized in term of particle size distribution and zeta potential, encapsulation efficiency, droplet size distribution, *in vitro* permeability and release rate, and *in vivo* permeability.

3. RESULTS AND DISCUSSION

3.1. Nasal Applicability

The four prepared formulations showed homogeneous nanosized particles and adequate zeta potential. ASP1, ASP2 and ASP3 were suitable to cross the olfactory region and reach the brain (Z-average < 300 nm). Only ASP1 and ASP3 demonstrated EE% > 50%, while ASP1 demonstrated Dv50 < 200 µm, hence, we selected ASP1 for further investigations (Fig 1).

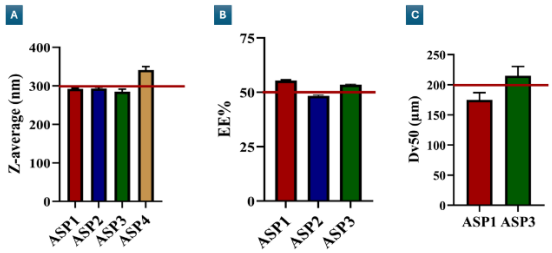

Figure 1. Z-average (A), EE% (B), Dv50 (C) for the developed formulations.

3.2. *In vitro* permeability and release rate

BBB-PAMPA results indicated that ASP1 had a significantly higher passive transport of FAV through the porcine brain polar lipid extract (Fig 2A&B). Moreover, ASP1 demonstrated a significantly higher release rate than FAV

suspension due to increase the surface area and its hydrophilic properties (Fig 2C).

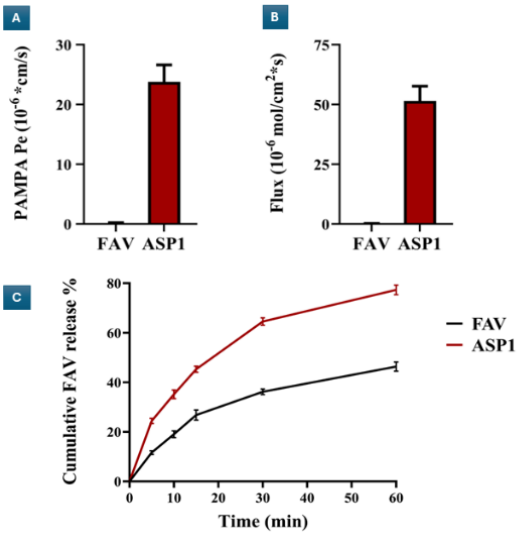

Figure 2. Permeability (A) and flux (B) results of BBB-PAMPA, Cumulative *in vitro* release profile at nasal conditions (C). Results are expressed as means ± SD (n = 4).

3.3. *In vivo* permeability

The capacity of ASP1 to deliver FAV to the CNS via the intranasal route was evaluated using Sprague–Dawley rats. The results demonstrated that FAV was detected in both plasma and CSF samples after a single nasal dose (Fig 3). ASP1 showed higher $t_{1/2}$ value compared to pure FAV (Table 1), which could be attributed to the impact of AP in reduce the elimination rate and extend the duration in the systemic circulation. Furthermore, The evaluation of CSF samples demonstrated a significant increase in FAV concentration of ASP1 compared to pure FAV (p-value < 0.05).

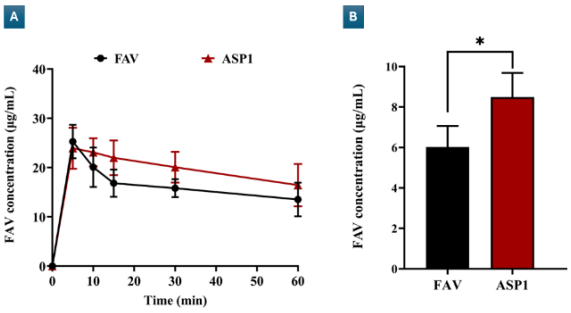

Figure 3. Plasma concentration–time profile (A) and The concentration of FAV in CSF (B) after 1 hour of nasal administration. Results are expressed as means ± SD (n = 4).

Table 1. Pharmacokinetic (PK) data of pure FAV and ASP1. Results are expressed as means ± SD (n = 4).

PK parameters	FAV	ASP1
C_{max} (µg/mL)	26.3 ± 7.4	27.1 ± 6.9
T_{max} (min)	7.5 ± 2.9	7.5 ± 2.9
$t_{1/2}$ (min)	127.5 ± 103.6	226.4 ± 337.1
MRT (min)	185.2 ± 153.7	329.9 ± 486.1
F%	—	124.5 ± 5.3

4. CONCLUSION

ASPs could be promising drug carrier for intranasal delivery systems to improve solubility, avoid first-pass metabolism, and decrease systemic adverse effects.

5. REFERENCES

1. Klein, RS., et al., *Neuroinflammation During RNA Viral Infections.* Annual Review of Immunology, 2019. 37(1): 73-95.

2. Kakinen, A., et al., *Brain Targeting Nanomedicines: Pitfalls and Promise.* International Journal of Nanomedicine, 2024. 19: 4857-4875.

3. Xinchen, Y., et al., *Lipid-Based Nanoparticles via Nose-to-Brain Delivery: A Mini Review*. Frontiers in Cell and Developmental Biology, 2023. 11: 01-08.

4. Khalil, RM., et al., *Development of Tizanidine Loaded Aspasomes as Transdermal Delivery System: Ex-Vivo and in-Vivo Evaluation*. Journal of Liposome Research, 2021, 31(1): 19-29.

ACKNOWLEDGMENT

This work was supported by Project no. TKP2021-EGA-32 implemented with support provided by the Ministry of Culture and Innovation of Hungary from the National Research, Development and Innovation Fund, financed under the TKP2021-EGA funding scheme.

P087

EXPLORING HPMC OLEOGELS FOR SIMULTANEOUS DELIVERY OF BCS CLASS I AND CLASS II DRUGS

Katarina Bolko Seljak, Mirjana Gašperlin

Department of Pharmaceutical Technology, Faculty of Pharmacy, University of Ljubljana, Slovenia

1. INTRODUCTION

Co-delivery can enhance patient adherence by reducing pill burden, and may also enable synchronized drug release for optimal pharmacological effect [1]. However, formulating oral systems that can simultaneously deliver drugs with divergent solubility profiles, such as those classified as Biopharmaceutics Classification System (BCS) Class I (high solubility, high permeability) and Class II (low solubility, high permeability), poses significant challenges.

We propose hydroxypropyl methylcellulose (HPMC)-based oleogels as a novel, biocompatible, and sustainable platform that addresses these issues by combining the lipid-mediated solubilization of poorly soluble amlodipine with polymer-controlled release for highly soluble atorvastatin. This approach allows for simultaneous management of blood pressure and lipid levels, improving overall cardiovascular outcomes.

2. MATERIALS AND METHODS

2.1. Materials

Amlodipine besilate (AML) and atorvastatin calcium (ATV) were donated by Krka, d.d. (Novo Mesto, Slovenia). HPMCs used in this study were Methocel K100 Premium LV EP, Methocel K15M Premium EP, and Methocel K4M Premium EP (Colorcon, Harleysville, PA, USA). Lipid phase was Capmul MCM EP (Abitec Corporation, Columbus, OH, USA) or olive oil (A.C.E.F, Fiorenzuola d'Arda, Italy), while Tween 20 (Sigma Aldrich, Burlington, MA, USA) was used as surfactant. All other chemicals used were laboratory grade.

2.2. Oleogel preparation

To prepare HPMC oleogels, indirect oleogelation was performed. Firstly, HPMC was dissolved in water with the addition of water soluble AML. Subsequently, water was removed by the freeze-drying process. The resulting HPMC/AML cake was then crushed into flakes. Subsequently, oil with dissolved ATV phase was absorbed onto the flakes to produce final HPMC oleogel drug delivery system and loaded into hard gelatin capsule.

2.3. Rheological measurements

A rotational test was conducted using a rheometer (Physica MCR301¸Anton Paar, Austria) equipped with a cone-and-plate sensor system (25°C, max. compressive force 40 N); followed by amplitude and frequency sweep.

2.4. *In vitro* lipolysis

pH stat *in vitro* lipolysis was carried as described in our previous work [2]. Simultaneous detection of both APIs was performed with Agilent 1100 Series HPLC, equipped with LiChrospher® 100 RP-18 column at 25 ± 0.5°C with mobile phase (acetonitrile:50 mM KH_2PO_4 (60:40, V/V)) flow set at 1.0 ml/min and detection at 240 nm.

3. RESULTS AND DISCUSSION

3.1. Indirect oleogelation of HPMC

Among the tested oleogelators, HPMC with the highest molecular weight and lowest viscosity (Methocel K100 Premium LV) proved to be the most suitable, particularly as a 2% (w/w) aqueous solution. This formulation yielded stable foams after homogenization and showed optimal porosity following lyophilization, compared to 1% and 3% (w/w) solutions of the same HPMC and other, more viscous HPMC types.

Owing to its amphiphilic nature, freeze dried flakes of 2% HPMC solutions successfully absorbed up to~95 % of its weight in oil phase, whether olive oil or Capmul MCM EP, the latter composed of medium chain mono- and diglycerides.

3.2. Rheological characteristics

Different oil phases were absorbed onto HPMC and evaluated for their rheological behaviour. Rheological analysis demonstrated that the HPMC oleogels exhibited pseudoplastic and

P087

viscoelastic behavior, with olive oil-based gels showing higher viscosity than those with Capmul MCM EP. The addition of Tween 20 to the oil phase reduced the viscosity of all investigated oleogels [data not shown].

3.3. Final formulation and *in vitro* digestion

Due to poor solubility of ATV in olive oil, Capmul MCM (with or without Tween 20) was selected as liquid phase of final HPMC oleogel formulations (Table 1).

Table 1. Composition of final HPMC oleogel compositions.

Composition	*Oleogel 1*	*Oleogel 2*
HPMC K100	25 mg	24.96 mg
AML	10 mg	10 mg
Tween 20	/	16.52 mg
Capmul MCM EP	548.33 mg	548.33 mg
ATV	10 mg	10 mg

Oleogels were further evaluated using *an in vitro* lipolysis model simulating gastrointestinal conditions. ATV release from HPMC oleogel reached plateau after 10 minutes, as the gel released the oil phase immediately after disintegration of hard capsule containing oleogel (Figure 1). Unfortunately, only approx. 65% ATV was released after 30 minutes, as the oil digestion during *in vitro* lipolysis caused loss of ATV solubilization capacity.

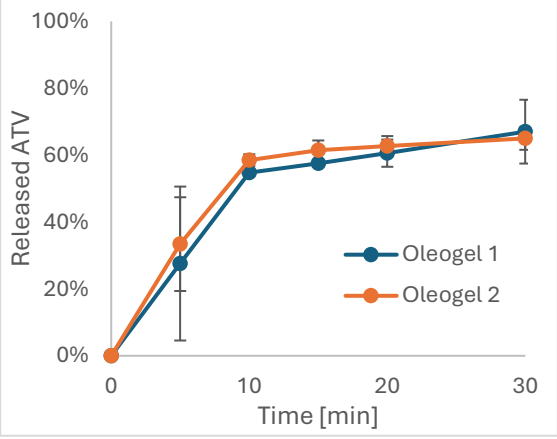

Figure 1. Percentage of released ATV during *in vitro* lipolysis [n=3].

This was not the case for AML, where almost complete release was achieved after 30 minutes of *in vitro* lipolysis (Figure 2).

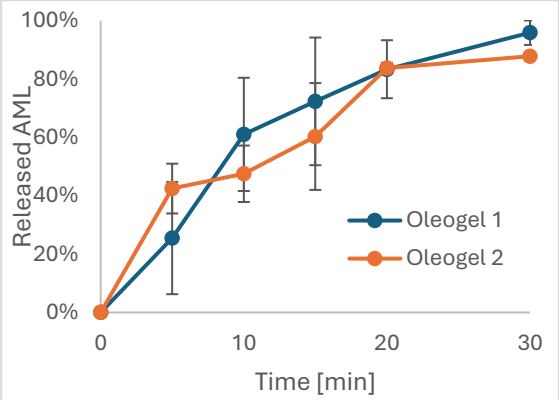

Figure 2. AML release from HPLC oleogel during *in vitro* lipolysis [n=3].

Nevertheless, as both formulations exhibited similar behaviour during *in vitro* lipolysis, no advantage of Tween 20 addition to the HPMC oleogel was demonstrated.

4. CONCLUSION

HPMC-based oleogels represent a promising novel drug delivery system capable of accommodating drugs with varying solubility and release profiles due to their biphasic structure, combining a hydrophilic polymer matrix with a lipophilic phase. Their ability to be formulated without surfactants offers a significant advantage over conventional lipid-based systems such as SMEDDS, potentially reducing gastrointestinal irritation and toxicity while maintaining effective drug solubilization and release.

5. REFERENCES

1. Janczura M, Sip S, Cielecka-Piontek J. *The Development of Innovative Dosage Forms of the Fixed-Dose Combination of Active Pharmaceutical Ingredients*. Pharmaceutics. 2022. 14(4):834.

2. Bolko Seljak K, Ilić IG, Gašperlin M, Zvonar Pobirk A. *Self-microemulsifying tablets prepared by direct compression for improved resveratrol delivery.* International Journal of Pharmaceutics. 2018. 548(1):263-275.

ACKNOWLEDGMENT

The authors acknowledge financial support from the Slovenian Research Agency (research core funding, No. P1-0189).

P088

EVALUATION OF DUAL ANTIOXIDATIVE AND ANTIBACTERIAL POTENTIAL OF 2'-HYDROXYCHALCONES

Valentina Gocić[1], Jelena Zvezdanović[2], Jelena Lazarevic[3*]

[1]Faculty of Medicine, University of Niš, Serbia
[2]Faculty of Technology, University of Niš, Serbia
[3]Department of Chemistry, Faculty of Medicine, University of Niš, Serbia

1. INTRODUCTION

The spread of multidrug-resistant strains of pathogenic bacteria is a growing problem constantly requiring innovations in treatment strategies. Agents with antibacterial properties that also act as antioxidants have sparked interest in recent years as antioxidative activity can attenuate oxidative stress damage during bacterial infection, which is of particular interest in chronic conditions often associated with the presence of drug-resistant bacteria, such as cystic fibrosis [1,2]. In addition, dual-acting agents, instead of two molecules with different activities, are presented with a single pharmacokinetic profile which may enhance the therapeutic efficacy and reduce adverse effects [2].

Chalcones (1,3-diphenylprop-2-en-1-ones) are compounds widely present in natural sources with a variety of documented pharmacological activities [3].

In this work, we have synthesized three 2'-hydroxychalcone derivatives and evaluated their antibacterial and antioxidative activity with the purpose of finding dual-acting molecules. Antioxidative activity was evaluated in terms of inhibition of lipid peroxidation (LP), a useful target for assessment of oxidative stress. All compounds were subjected to an *in silico* study to predict their physicochemical, pharmacokinetic and toxicological profile.

2. MATERIALS AND METHODS

2.1. Synthetic procedure

To a solution of 2'-hydroxyacetophenone (2 mmol) in 96% ethanol (4 ml), 20% aqueous solution of potassium hydroxide (4 ml) was added dropwise, followed by the addition of the corresponding benzaldehyde (2 mmol). The reaction mixture was stirred at room temperature and monitored by thin layer chromatography (TLC). After the completion of the reaction, the reaction mixture was cooled at 0 ºC and 10% hydrochloric acid was added until the formation of precipitate. Crude product was purified by recrystallisation or column chromatography. Obtained compounds were characterized by NMR experiments and their purity was confirmed by high performance liquid chromatography (HPLC).

2.2. Evaluation of antibacterial activity

Antibacterial activity was tested *in vitro*, against a panel of laboratory control strains: two Gram-positive (*Bacillus subtilis* ATCC 6633 and *Staphylococcus aureus* ATCC 6538) and two Gram-negative (*Escherichia coli* ATCC 8739 and *Salmonella typhimurium* ATCC 14028), using the disc diffusion assay recommended by NCCLS.6 2.3 [4].

2.3. Evaluation of LP inhibitory activity

Inhibition of LP process was measured by thiobarbituric acid - malondialdehyde (TBA-MDA) assay. Trolox was used as standard [5].

2.2. *In silico* study

Physicochemical and pharmacokinetic properties of obtained compounds were calculated using SwissADME online platform. Toxicological properties in terms of their potential to cause mutagenic, tumorigenic, irritating, and/or reproductive effects were predicted using OSIRIS Property Explorer.

3. RESULTS AND DISCUSSION

3.1. Synthesis of chalcone derivatives

P088

2'-Hydroxyhalcones **1-3** (Fig.1) were obtained in crystal form with purity above 95.0%, determined by HPLC.

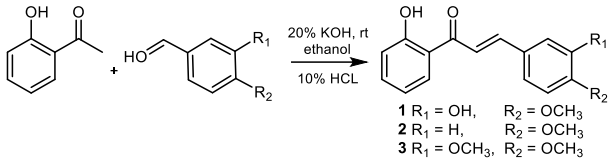

Figure 1. Synthesis of chalcones **1-3**.

3.2. Antibacterial activity of compounds 1-3

According to the results of the preliminary *in vitro* antibacterial evaluation (Table 1), in tested concentrations (1 mg/cm^3) all chalcones have affected the growth of the Gram-negative strains, with compound **1** being the most active and the only compound to inhibit the growth of Gram-positive bacteria *S. Aureus*. All chalcone derivatives expressed weaker antibacterial activities in comparison to tetracycline.

Table 1. The antibacterial activity of compounds **1-3** (diameters of growth inhibition zones measured in mm) and of positive control (antibiotic tetracycline).*

Comp.	1	2	3	Tetracycline
B. Subt.	na**	na	na	32.1±0.5
S. Aureus	11.0±0.2	na	na	32.1±0.5
E. Coli	19.1±0.1	18.0±0.2	18.0±0.3	32.1±0.5
S. Typhi.	19.3±0.1	18.0±0.1	18.0±0.3	32.1±0.5

*Mean value ± SD (in mm) **not active in tested concentrations

3.3. Antioxidative activity of compounds 1-3

Results of the LP inhibitory potential of synthesized compounds (Table 2) showed that compound **1** expressed antioxidative activity, as opposed to compounds **2** and **3** that expressed prooxidative activity in tested concentrations (1 mg/cm^3).

Table 2. LP inhibition activity of compounds **1-3.**

Comp.	1	2	3	Trolox
LP inhibition (IC_{50})*	2.2±0.2	Prooxidative activity	Prooxidative activity	0.005±0.001

*Mean value ± SD (in mg/cm^3)

3.3. Results of the *in silico* study

All compounds were predicted to have good oral bioavailability and high gastrointestinal absorption. Only compound **2** was predicted with high risk for irritating effects and medium risk for reproductive effects.

4. CONCLUSION

In this research, compound **1**, bearing the additional phenolic moiety in the chalcone structure, stands out as the only dual-acting agent expressing both antibacterial and antioxidative effects, accompanied by favourable *in silico* predicted physicochemical, pharmacokinetic, and toxicological profile. In the quest for novel structures to address the bacterial resistance, compound **1** could represent a starting point for further research for unconventional antibacterial drugs.

5. REFERENCES

1. Gangwar, B., et al., *Antioxidant phytochemicals as novel therapeutic strategies against drug-resistant bacteria*. In *Importance of Oxidative Stress and Antioxidant System in Health and Disease*; Suna Sabuncuoğlu, S., Yalcinkaya, A., Eds.; IntechOpen: London, UK, 2023.

2. Martelli, G., et al., *Antibacterial and antioxidant activities for natural and synthetic dualactive compounds*. European Journal of Medicinal Chemistry, 2018. 158: 91-105.

3. Okolo, E.N., et al., *New chalcone derivatives as potential antimicrobial and antioxidant agent*. Scientific Reports, 2021. 11: 21781.

4. NCCLS Performance Standards for Antimicrobial Disk Susceptibility Test, 6th ed., National Committee for Clinical Laboratory Standards, approved standard: P. A. Wayne, M100- S9, 19971-5.

5. Lazarević, J., et al. *Lipid peroxidation inhibition study: A promising case of 1, 3-di ([1, 1'-biphenyl]-3-yl) urea.* Chemico-Biological Interactions, 2020. 326: 109137.

ACKNOWLEDGMENT

The work was funded by the Ministry of Science, Technological Development and Innovation of Serbia (Projects 451-03-137/2025-03/200113 and 451-03-136/2025-03/200113).

P089

POLYMERIC CARRIERS FOR SPRAY-DRIED MICROPARTICLES WITH POTENTIAL FOR SUSTAINED PULMONARY RELEASE

Hana Hořavová[1]

[1]*Department of Pharmaceutical Technology, Faculty of Pharmacy, Masaryk University Brno, Czech Republic*

1. INTRODUCTION

Inhalation is a non-invasive route of drug administration, particularly effective for respiratory diseases, allowing for high local drug concentrations and reduced systemic effects. Recently, there has also been growing interest in using pulmonary administration for systemic effects due to lung tissue's large surface area, rich blood supply, ability to bypass liver metabolism, or limited enzymatic activity [1].

The complex branching of the respiratory tree requires specific conditions to be met for inhaled formulations to effectively reach their intended target area. The deposition of these formulations is primarily influenced by the size and shape of the particles, as well as the patient's inhalation technique [2]. However, lung defense mechanisms like mucociliary clearance or alveolar macrophage activity can limit the duration of their effects after a rapid onset of action of inhaled formulations [3, 4].

This work aimed to prepare inhalable microparticles designed for sustained release using various polymers as carriers. Spray drying was employed as the method for particle preparation. The resulting particles possessing properties suitable for inhalation were loaded with a model drug to evaluate their release profile.

2. MATERIALS AND METHODS

2.1 Materials

The materials used in this work were: mannitol (MAN; Roth, DE), sodium alginate (ALG), chitosan (CHIT) and polyvinyl alcohol (PVA) (Sigma–Aldrich, DE), carbomer (CARB; Fagron, CZ), leucine (GymBeam, DE), colistin-sulphate (Hebei Shengxue Dacheng Pharmaceutical Co., CN).

2.2 Preparation of microparticles

Before spray drying, aqueous solutions of each carrier were prepared in two concentrations as indicated in Table 1. Leucine was added to each solution to serve as an aerosolization enhancer, constituting 20% of the solid content by replacing an equivalent amount of the carrier (in the case of MAN_20% and PVA_20% it was only 6% due to the limited water solubility of leucine). To dissolve chitosan, 1% acetic acid was used instead of water. These solutions were then subjected to spray drying.

Spray drier LabPlant SD-06 (equipped with 1 mm nozzle, 215 x 800 mm drying chamber and cyclone separator) was utilized for microparticle preparation. The following parameters were set: inlet temperature 140 °C, feed rate 8 ml/min, air speed 3,5 m/s, nozzle pressure 3 bars.

After evaluation, selected samples were prepared in the same manner, with the addition of the model drug colistin-sulfate, which constituted 10% of the solid content, replacing an equivalent amount of the carrier.

2.3 Evaluation

The resulting powders were evaluated using various methods including density and flow properties determination, optical and electron microscopy, or residual moisture measurement. The key parameters assessed for inhalable particles were geometrical median size (D50) determined by laser diffraction and mass median aerodynamic diameter (MMAD) along with the fine particle fraction (FPF) determined by aerodynamic particle sizer.

Drug-loaded samples were subjected to a dissolution test using acceptor compartments of Franz dissolution cells. The samples were placed on the surface of 20 ml of phosphate-buffered saline (pH 7.4) tempered to 37 °C. Aliquots of 1 ml were taken at intervals of 0.5, 1, 2, 3, 5, and 8 hours after the sample application. The amount of drug released was quantified using high-performance liquid chromatography (HPLC).

P089

3. RESULTS AND DISCUSSION

The resulting values of the measured parameters are presented in Table 1. In most cases, the D50 value increased with higher concentration, except for the alginate sample that exhibited a greater tendency for aggregation when spray-dried from a diluted solution. The same trend was consistent across all samples for MMAD. Particles with an MMAD of around 5 µm can effectively be deposited in the deep lungs, indicating that most carriers show good potential for pulmonary delivery. Larger particles (5–10 µm) can still reach the tracheobronchial region. The high viscosity of the PVA_20% solution led to the formation of fibril structures. Despite the large particle size of PVA_5%, this sample demonstrated good aerodynamic properties due to its low bulk density. The sugar carrier displayed a smooth surface morphology, while the polymeric carriers exhibited some surface roughness, which may be advantageous for aerosolization.

Table 1. Resulting particle properties

Sample	D50 ± SD (µm)	MMAD ± SD (µm)	FPF (%)
MAN_5%	5.53 ± 0.25	5.29 ± 0.13	42.02
MAN_20%	9.17 ± 0.41	7.62 ± 0.39	14.83
CHIT_0.5%	4.64 ± 0.37	4.86 ± 0.22	54.21
CHIT_2%	7.29 ± 0.82	7.25 ± 0.77	22.66
ALG_1%	7.48 ± 0.16	5.72 ± 0.09	32.39
ALG_3%	5.77 ± 0.05	6.40 ± 0.36	22.85
CARB_0.5%	5.25 ± 0.32	3.74 ± 0.58	61.88
CARB_1%	5.86 ± 0.33	5.15 ± 0.79	55.57
PVA_5%	10.04 ± 0.16	5.24 ± 0.53	42.27
PVA_20%	14.43 ± 3.21	7.77 ± 1.90	20.42

CARB_0.5% displayed excellent aerodynamic properties, but the drug addition resulted in poor dispersion and its elimination from further testing. In the 8-hour dissolution test, key differences emerged in the first 3 hours (Fig. 1). Mannitol served as a reference carrier, achieving 90% drug release in 30 minutes with no retardation. Polyvinyl alcohol showed similar results. Chitosan released about 60% in 30 minutes and reached saturation after 3 hours. Alginate was the slowest, releasing only 40% after 30 minutes and gradually reaching complete release at the 3-hour mark. Greater retardation might be achieved by ionic gelation of these polymers.

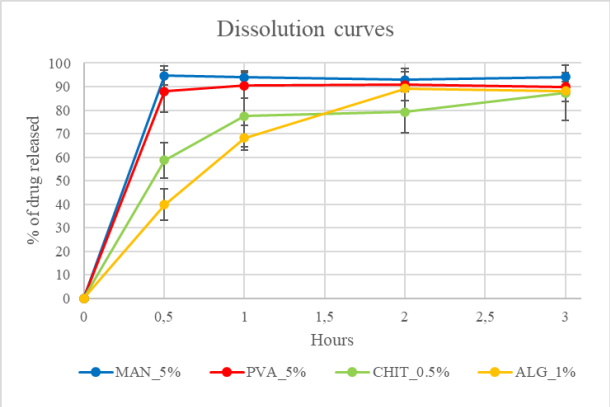

Figure 1. Release profiles of colistin-sulphate from chosen carriers

4. CONCLUSION

Spray drying has been shown to be an effective method for producing particles with good aerodynamic properties and high potential for pulmonary deposition. It was observed that a higher dilution of the input dispersion results in the production of finer particles. Among the polymers tested, only chitosan and sodium alginate demonstrated the ability to sustain the release of colistin-sulfate within the first three hours.

5. REFERENCES

1. Patil, J. S., et al., *Pulmonary drug delivery strategies: A concise, systematic review*. Lung India, 2012. 29(1): 44–49.
2. Darquenne, Ch., *Deposition Mechanisms*. Journal of Aerosol Medicine and Pulmonary Drug Delivery, 2020. 33(4): 181–185.
3. Misra, A., et al., *Recent advances in liposomal dry powder formulations: preparation and evaluation*. Expert Opinion on Drug Delivery, 2009. 6(1): 71–89.
4. Ghanem, R., et al., *The (re)emergence of aerosol delivery: Treatment of pulmonary diseases and its clinical challenges*. Journal of Controlled Release, 2025, 379: 421–439.

ACKNOWLEDGMENT

Aerodynamic measurements were performed at the Faculty of Mechanical Engineering of Brno University of Technology.

P090

THE ROLE OF PHARMACISTS IN OPTIMIZING PHARMACOTHERAPY AND IMPROVING CLINICAL OUTCOMES

Sonja Icheva Doneva[1], Marija Taleska Velkovski[2], Ljuba Karanakov[3]

[1]Regulatory Affairs Department, ReplekFarm Ltd Skopje, North Macedonia,
[2]Strategic Development Department, Replek AD Skopje, North Macedonia,
[3]Regulatory Affairs Department, Replek AD Skopje, North Macedonia,

1. INTRODUCTION

The global trend of population aging signifies a major demographic shift with profound implications for healthcare systems worldwide. While increased life expectancy reflects substantial public health progress, it is also associated with a growing burden of chronic and degenerative diseases, leading to higher rates of multimorbidity in older adults. This often necessitates polypharmacy, which presents complex challenges including adverse drug reactions, medication-related complications, and escalating healthcare costs. Age-related physiological changes further complicate pharmacotherapy by altering drug metabolism and response. Despite the well-documented prevalence of multimorbidity, the importance of optimizing pharmacological treatment in this population remains underemphasized.

2. MATERIALS AND METHODS

2.1. Materials

A comprehensive literature search was conducted using electronic databases, including PubMed, MEDLINE, and EMBASE, to identify studies and reviews related to the role of pharmacists in optimizing pharmacotherapy and the associated benefits on clinical outcomes.

2.2. Method

The focus was broad and not restricted to any single drug class, specific disease, or healthcare setting. This approach allowed for the inclusion of diverse perspectives on the role of the pharmacists for medication optimization, encompassing general principles and multidisciplinary strategies applicable across various clinical contexts. In addition to the electronic search, a manual review of was performed to identify additional relevant sources. This method ensured a comprehensive and diverse representation of strategies aimed at improving clinical outcomes in older populations.

3. RESULTS AND DISCUSSION

3.1. Global Population Aging

According to the United Nations *"World Population Prospects 2024"*, the global population is projected to increase from 8.2 billion in 2024 to approximately 10.3 billion by the mid-2080s, before experiencing a gradual decline to around 10.2 billion by 2100 (Fig 1). This demographic shift is accompanied by significant aging; the number of individuals aged 65 and older is expected to double over the next 30 years, reaching 203 million by 2054 and comprising 23% of the total population. These trends underscore the need for policies that address the challenges and opportunities associated with an aging global populace [1].

3.2. Comprehensive Medication Reviews

The optimization of pharmacotherapy in older adults is essential to address the challenges posed by multimorbidity and polypharmacy, which can lead to adverse drug events and increased healthcare costs. Pharmacists are integral to this optimization process, employing various strategies to enhance medication safety and efficacy [2]. One key strategy is comprehensive medication review (CMR), where pharmacists systematically assess patients' medication regimens to identify and resolve issues such as drug interactions and therapeutic duplications. This approach has been shown to reduce inappropriate prescribing and medication-related problems, thereby improving patient outcomes [3].

3.3. Collaborative care

Collaborative care is another cornerstone of effective pharmacotherapy optimization. Pharmacists work closely with physicians, nurses, and other healthcare providers to tailor treatment plans that align with clinical guidelines and individual patient needs [4]. This interdisciplinary approach ensures that pharmacological decisions are holistic, evidence-based, and patient-centered.

3.4. Monitoring and follow-up

Monitoring and follow-up are also critical in ensuring the long-term success of pharmacotherapy. Pharmacists track patient responses to medications and collaborate with other providers to make necessary adjustments. This ongoing evaluation helps maintain therapeutic effectiveness while minimizing the risk of complications.

3.5. Implementation of clinical guidelines and tools

Pharmacists utilize evidence-based tools such as the Beers Criteria and STOPP/START criteria to guide appropriate prescribing for older adults [5]. These resources help identify potentially inappropriate medications and support safer prescribing practices tailored to the geriatric population.

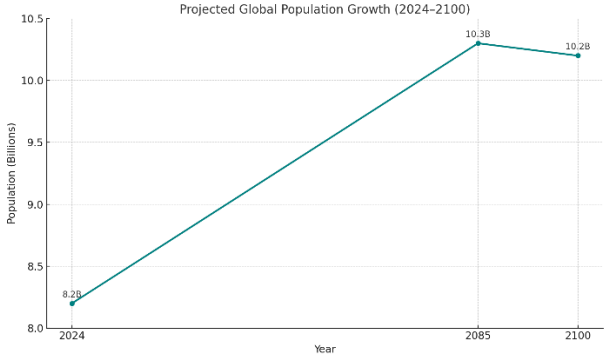

Figure 1 The projected global population growth from 2024 to 2100, showing a peak around 2085 followed by a slight decline.

4. CONCLUSION

Pharmacists play a pivotal role in optimizing pharmacotherapy, particularly in the care of older adults who often present with complex medication regimens due to multimorbidity and polypharmacy. As medication experts, pharmacists are uniquely positioned to identify, prevent, and resolve drug-related problems, thereby enhancing medication safety and therapeutic effectiveness. As the healthcare landscape continues to evolve, the integration of pharmacists into patient care teams will be vital to meeting the complex medication needs of aging populations and ensuring high-quality, effective, and safe healthcare delivery.

5. REFERENCES

1. United Nations, Department of Economic and Social Affairs., *World Population Prospects 2024: Summary of Results*. 2024. UN DESA/ POP/ 2024/TR/NO. 9.

2. Lee, JK., et al., *Optimizing pharmaco-therapy in elderly patients: the role of pharmacists.* Integrated Pharmacy Research and Practice. 2015.11:101-11.

3. Salm, C., et al., *Over-and under-prescribing, and their association with functional disability in older patients at risk of further decline in Germany–a cross-sectional survey conducted as part of a randomised comparative effectiveness trial.* 2022. BMC geriatrics, 22(1) 564.

4. Monzón-Kenneke, M., et al.,*Pharmacist medication review: An integrated team approach to serve home-based primary care patients.* 2021. PLoS One.16(5):e0252151.

5. Gavazova, E., et al., *Managing polypharmacy through medication review tools–pros and cons.* 2024. Folia Medica, 66(2), 161-170.

ACKNOWLEDGMENT

I would like to express my sincere gratitude to Replek AD and Replek Farm Ltd. Skopje for their invaluable support and collaboration during this research. Their commitment to innovation and excellence in pharmaceutical manufacturing significantly contributed to the success of this study.

P091

OPTIMISATION OF PHARMACOTHERAPY WITH ORAL MEDICINES IN ADULT HOSPITALISED PATIENTS WITH IMPAIRED SWALLOWING

Julija Komac[1], Brigita Mavsar Najdenov[2], Mojca Kerec Kos[1]

[1]Faculty of Pharmacy, University of Ljubljana, Slovenia
[2]Jesenice General Hospital, Slovenia

1. INTRODUCTION

Dysphagia is defined as an impairment of swallowing that leads to an abnormal delay in the transit of a liquid or solid bolus from the oral cavity to the stomach. It can be acute or chronic, intermittent or persistent. The proportion of people with dysphagia increases with age and it is estimated that 60% of older adults in nursing homes suffer from occasional dysphagia. Swallowing disorders are also common after a stroke, in Parkinson's disease, dementia, etc. [1].

If oral feeding via the normal physiological route is not recommended, is not feasible or does not meet the body's nutritional needs, patients receive nutrients via an enteral tube or stoma directly into the stomach or small intestine. In these patients, medicines are also administered via enteral feeding tubes [1].

The aim of the retrospective study was to evaluate the appropriateness of prescribed oral medicines in adult hospitalised patients with swallowing impairment. We also evaluated the role of the clinical pharmacist in optimising pharmacotherapy in this group of patients.

2. MATERIALS AND METHODS

2.1 Clinical study

We conducted a retrospective clinical study in which we included adult patients with swallowing difficulties (dysphagia or enteral feeding tubes) who were hospitalised in the Internal Medicine Department of the Jesenice General Hospital between 2021 and 2023. Another inclusion criterion was that the patient had at least one prescription oral medicine in solid dosage form. The study was approved by the Medical Ethics Committee of the Jesenice General Hospital.

2.2. Data collection and analysis

The following data was obtained from the hospital's medical documentation:

- basic patient data (gender, age, body mass index)
- patient health status data (number and type of comorbidities, laboratory results related to kidney function)
- type of enteral feeding tube
- number and types of prescribed oral medicines during and after hospitalisation

We were interested in the suitability of the prescribed oral dosage forms for patients with swallowing difficulties. The possibility of changing the dosage form (splitting, crushing tablets, opening hard capsules or dissolving tablets or capsules) was checked in Summary of Product Characteristic and in different professional information sources [2-5].

Moreover, the pharmacotherapy of some patients included in our study was reviewed by a clinical pharmacist as part of a pharmacotherapy review. We were interested in type of recommendations made by the clinical pharmacist to optimise pharmacotherapy in these patients and how often the recommendations were accepted by the treating physician.

3. RESULTS AND DISCUSSION

151 patients were included in the study (median age 75 years, 54.3% male, median length of hospitalisation 11 days). They had several concomitant diseases (median 8, range 2-19). Almost half of the patients (47.0%; 71/151) had a percutaneous endoscopic gastrostomy, followed by patients with a nasogastric tube (48/151; 31.8%) and patients with dysphagia without an enteral feeding tube (32/151; 21.2%).

During hospitalisation, patients received 88.6% (1050/1185) of their oral medicines in solid dosage forms and 11.4% (135/1185) in liquid dosage forms. The median number of oral solid dosage forms per patient was 7 and the median number of oral liquid dosage forms was 1. It is noteworthy that 73/151 (48.3%) patients were not prescribed an oral liquid dosage form during their hospitalization. Of the oral solid dosage forms prescribed to patients during hospitalisation, just over half (53.7%; 564/1050) were suitable for crushing (opening) and dispersing, while 75.5% (793/1050) were suitable for dispersing only. Contrary to expectations, patients were very rarely prescribed orodispersible tablets, chewable tablets and sublingual tablets — with a relative frequency of ≤ 0.2% — although these are suitable for patients with dysphagia. Possible reasons for their less frequent prescribing could be the higher cost compared to regular tablets/film-coated tablets, an unpleasant taste or the unavailability on the Slovenian market.

Due to staff shortages in the hospital, the clinical pharmacist only conducted a pharmacotherapy review for 25.2% of patients included in the study (38/151). The pharmacist provided 251 instructions on the correct administration of medicines via enteral feeding tube and suggested 161 interventions to optimise pharmacotherapy. The most common interventions were substitution of a dosage form (48.4%; 78/161), drug substitution (32.3%; 52/161) and a change in administration (timing of dosing, adjustment regarding the food intake). The interventions were frequently related to solid dosage forms with modified release and soft capsules.

The physicians accepted 67/161 (41.6%) of proposed interventions. They accepted all recommendations for adding a new medicine, reducing the dose and changing the route of administration, more than half of the suggestions for discontinuation of the medicine, but less than half of the other suggested interventions. Reasons for not considering pharmaceutical interventions could include insufficient awareness of the importance of the dosage form in ensuring the safety and efficacy of drug treatment, physicians' heavy workloads and their reliance on their own clinical judgement.

Patients whose physicians accepted the majority of the clinical pharmacist's recommendations were discharged with a significantly higher number of oral solid dosage forms suitable for crushing (opening) and dispersing than for whom the clinical pharmacist had not reviewed pharmacotherapy (Mann-Whitney U-test, $p < 0.05$).

4. CONCLUSION

Prescribing and administration errors associated with oral solid dosage forms could be avoided if a pharmacist was involved in the comprehensive healthcare management of patients with impaired swallowing. Namely, with their knowledge of potential changes in the drug pharmacokinetics and pharmacodynamics, pharmacists can advise healthcare professionals on optimal pharmacotherapy.

5. REFERENCES

1. Wilkinson JM, Codipilly DC, Wilfahrt RP. *Dysphagia: Evaluation and Collaborative Management*, American family physician, 2021, 103 (2): 97-106.

2. White R, Bradnam V: *Handbook of Drug Administration via Enteral Feeding Tubes White*, Pharmaceutical Press, 3rd edition, Pharmaceutical Press, London, 2015.

3. *NHS Guidelines For The Administration Of Medicines to Adults via Enteral Tubes Within NHS Grampian*. [https://www.nhsgrampian.org/globalassets/foidocument/foi-public-documents1---all-documents/Guide_EnteralTubeA.pdf]

4. *NHS Neemmc guidelines for tablet crushing and administration via enteral feeding tube.* [https://www.stch.org.uk/wp-content/uploads/pct-version-neemmc-guidelines-for-tablet-crushing-april-2012.pdf]

5. Bischoff SC, Austin P, Boeykens K, et al. *ESPEN guideline on home enteral nutrition. Clinical Nutrition, 2020, 39(1):5-22.*

ACKNOWLEDGMENT

The authors acknowledge the financial support from the Slovenian Research Agency (research core funding No. P1-0189).

P092

ASSESSMENT OF HYDROXYL RADICAL SCAVENGING ACTIVITY OF SELECTED 4-METHYL SUBSTITUTED COUMARINS

Katarina Milosavljević[1], Jelena Lazarević[2]*

[1]Faculty of Medicine, University of Niš, Serbia
[2]Department of Chemistry, Faculty of Medicine, University of Niš, Serbia

1. INTRODUCTION

Hydroxyl radicals (•OH) are increasingly recognized as being tightly regulated to maintain cellular homeostasis under physiological conditions. However, when •OH levels become excessive or when cellular antioxidant defenses are compromised, they can initiate free radical chain reactions by interacting with and damaging proteins, lipids, and nucleic acids. •OH is known as the most reactive of all the reduced forms of dioxygen and has been implicated, either directly or indirectly, in a wide range of pathological conditions, including Parkinson's disease, rheumatoid arthritis, cardiovascular diseases, and cancer [1].

Coumarins (2H-1-benzopyran-2-ones) are naturally occurring phenolic compounds characterized by structural diversity and a broad spectrum of biological activities, including antioxidant, anti-inflammatory, anticancer, and anticoagulant effects [2].

This study aims to evaluate the •OH scavenging potential of four synthetic coumarin derivatives and includes *in silico* predictions of their physicochemical, pharmacokinetic, and toxicological properties.

2. MATERIALS AND METHODS

2.1. Synthetic procedure for the preparation of 4-methyl coumarin derivatives

Coumarins **1**–**4** were synthesized via Pechmann condensation, as previously reported by our research group [3]. The identities of pure compounds **1**–**4** were confirmed by ^{1}H and ^{13}C NMR. Purity (>95%) was verified by HPLC analysis.

2.2. Hydroxyl radical scavenging assay

The hydroxyl radical scavenging capacity of synthesized coumarin derivatives **1**–**4** was assessed using a modified method by Halliwell et al. (1987) [4], involving Fenton-reaction-induced degradation of 2-deoxyribose (2-DR), followed by derivatization with thiobarbituric acid (TBA).

2.3. *In silico* study

Physico-chemical and pharmacokinetic properties of the obtained coumarin derivatives **1**–**4** were evaluated using SwissADME online platform. Toxicological profiles, including mutagenic, tumorigenic, irritant, and reproductive effects were predicted using the OSIRIS Property Explorer.

3. RESULTS AND DISCUSSION

3.1. Results

Four coumarin derivatives were synthesized according to previously reported procedures.

The hydroxyl radical scavenging activity of coumarins **1**–**4** and the standard BHA was evaluated using the 2-DR assay. This assay measures the ability of the tested compounds to inhibit hydroxyl radical-mediated degradation of deoxyribose in an *in vitro* system that consists of Fe^{3+}-EDTA-ascorbate and H_2O_2. The scavenging capacity of the compounds against •OH is directly correlated with their antioxidant activity. The obtained results are presented in Table 1.

Table 1. Synthesized coumarin derivatives **1**-**4** along with the results of the 2-DR assay.

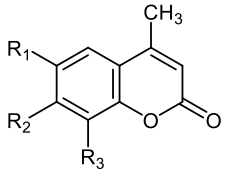

	R_1	R_2	R_3	IC_{50}(μg/mL)
1	H	OH	H	21.5 ± 0.08
2	H	OCH_3	H	23.2 ± 0.13

3	OH	OH	H	34.1 ± 0.11
4	H	OH	OH	84.2 ± 0.34

The results indicated that all compounds **1**–**4** demonstrated radical scavenging activity at the tested concentrations (50–250 μg/mL). Based on IC_{50} values, compounds **1** and **2** exhibited better inhibition compared to compounds **3** and **4**, which showed weak radical scavenging activity. These results were compared with the standard BHA (IC_{50} = 15.2 μg/mL), which proved to be more effective than the tested compounds.

All four compounds **1**–**4** are predicted to have favorable oral bioavailability and high gastrointestinal absorption. Toxicological predictions indicate they are non-mutagenic, non-tumorigenic, and non-irritant, but may pose a high risk of reproductive toxicity.

3.3. Discussion

Our results partially align with Payá et al. (1992) [5], who studied •OH scavenging in two *in vitro* systems. In the H_2O_2-$FeCl_3$-ascorbate system (rapid •OH generation), similar to ours, 7-hydroxy- (**1**) and 7-methoxy-4-methylcoumarin (**2**) showed no significant inhibition at 100μM, while 6,7-dihydroxy- (**3**) and 7,8-dihydroxy-4-methylcoumarin (**4**) inhibited deoxyribose degradation [5]. In contrast, in our study (50–250 μg/mL), compounds **1** and **2** showed activity comparable to BHA, whereas compounds **3** and **4** had weaker effects. Interestingly, in the $FeCl_3$-EDTA-H_2O_2 system (slow •OH generation), compounds **1** and **2** reduced •OH levels, while compounds **3** and **4** showed pro-oxidant effects [5]. These results suggest that •OH scavenging depends not only on compound structure but also on experimental conditions.

In our earlier work [3], compounds **3** and **4** inhibited lipid peroxidation, whereas **1** and **2** were inactive below 100 μM and showed pro-oxidant effects at higher concentrations. Notably, this trend was reversed in the •OH scavenging assay, where compounds **1** and **2** were more active, supporting the concept of radical-type-dependent (anti)oxidant activity.

4. CONCLUSION

Four synthetic 4-methylcoumarin derivatives were evaluated for their *in vitro* •OH scavenging activity. Compounds **1** and **2** showed the strongest inhibitory effects and favorable predicted physicochemical, pharmacokinetic and toxicological profiles, except for a potential risk of reproductive toxicity. Further optimization is needed to identify analogues with improved safety profiles.

5. REFERENCES

1. Cheng, FC., et al., *Hydroxyl radical in living systems and its separation methods*. Journal of Chromatography B, 2002. 781(1-2): 481-496.
2. Borges, F., et al., *Simple coumarins and analogues in medicinal chemistry: occurrence, synthesis and biological activity.* Current medicinal chemistry, 2005. 12: 887-916.
3. Ilić, K., et al., *Synthesis and evaluation of lipid peroxidase inhibition of 4-methyl substituted coumarins*. Macedonian Pharmaceutical Bulletin, 2023. 69(suppl 1): 269-270.
4.Halliwell, B., et al., *The deoxyribose method: a simple "test-tube" assay for determination of rate constants for reactions of hydroxyl radicals*. Analytical Biochemistry, 1987. 165(1): 215-219.
5. Payá, M., et al., *Interactions of a series of coumarins with reactive oxygen species: scavenging of superoxide, hypochlorous acid and hydroxyl radicals*. Biochemical pharmacology, 1992. 44(2): 205-214.

ACKNOWLEDGMENT

The work was funded by the Ministry of Science, Technological Development and Innovation (Projects 451-03-137/2025-03/200113 and 451-03-136/2025-03/200113).

P093

EVALUATION OF THE MUCOADHESIVE PROPERTIES OF OLOPATADINE EYE DROPS: INFLUENCE OF POLYMER COMBINATION

Anđelka Račić[1], Veljko Krstonošić[2], Danina Krajišnik[3]

[1]*Department of Pharmaceutical Technology and Cosmetology, Faculty of Medicine, University of Banja Luka, Bosnia and Herzegovina*

[2]*Department of Pharmacy, Faculty of Medicine, University of Novi Sad, Novi Sad, Serbia*

[3]*Department of Pharmaceutical Technology and Cosmetology, University of Belgrade-Faculty of Pharmacy, Serbia*

1. INTRODUCTION

Mucoadhesion is a useful strategy to improve ocular availability by introducing polymers into the composition of liquid ophthalmic preparations. These polymers increase the viscosity of tear-film and utilize their bioadhesive properties to reduce drainage, prolong retention time at the application site, and improve therapeutic efficacy. Since low-viscosity mucoadhesive solutions are more comfortable than high-viscous ones, mucoadhesion is preferred over a simple increase in viscosity [1]. Investigating the mucoadhesive behavior of a formulation is crucial for understanding and simulating the *in vivo* interaction with ocular tissues. Therefore, a number of *in vitro*, *ex vivo*, and *in vivo* methods have been developed to evaluate and characterize bioadhesive ophthalmic dosage forms [2]. The aim of the present study was to evaluate mucoadhesive properties of olopatadine eye drops containing hydroxypropyl guar gum (HPG) and sodium hyaluronate (SH) alone or in combination using different *in vitro* methods.

2. MATERIALS AND METHODS

2.1. Materials

Olopatadine hydrochloride (OLO) was received as a gift sample from Hemofarm A.D. (Serbia). HPG was purchased from Ashland Inc.; SH was a kind gift from Sandream Impact LLC (USA). Mucin (from porcine stomach, type II) was purchased from Sigma-Aldrich (USA).

2.2. Preparation and characterization of OLO eye drops

The eye drops (Table 1) were prepared at room temperature by mixing polymer solutions, excipients and aqueous solutions of OLO [3].

2.3. Mucoadhesion measurements

Polymer–mucin interactions were evaluated by measuring the zeta potential at 34 °C using a Zetasizer Nano ZS90. Changes in zeta potential values indicated potential interactions between the polymer and mucin.

The mucoadhesive strength was measured with an EZ-LX texture analyzer (Shimadzu, Japan) using mucin discs. The maximum force required to detach the mucin disc from the eye drop sample represents the mucoadhesive force (mN), while the area under the force-time curve was estimated as work of adhesion (mJ).

2.4. Rheological measurements

Rheological analyses of the viscous eye drops were carried out by HAAKE MARS rheometer (Thermo Scientific, Karlsruhe, Germany) equipped with a cone-plate C35 2°/Ti measuring system. Flow curves were determined using a coaxial cylinder measurement system, for the shear rate from 0.001 to 150 1/s at 20 °C and 34 °C (with addition of simulated tear fluid).

Table 1. Compositions of the tested eye drops.

Composition (% m/V)	Sample label		
	F1	F2	F3
OLO	0.1	0.1	0.1
HPG	0.25	-	0.25
SH	-	0.4	0.4
NaCl	q.s.	q.s.	q.s.
Na_2HPO_4	0.5	0.5	0.5
BAC	0.01	0.01	0.01
Water, purified	q.s. ad 100 ml	q.s. ad 100 ml	q.s. ad 100 ml

3. RESULTS AND DISCUSSION

3.1. Mucoadhesion measurements

The addition of vehicle F2 (SH) to the mucin dispersion (–7.8 ± 0.8 mV) led to significant increase in the negative zeta potential (–25 ± 0.2 mV). This change is attributed to the anionic properties of SH and the high density of carboxyl groups in its polymer structure. In contrast, mixing vehicle F3 (SH and HPG) with mucin resulted in only a slight increase in zeta

P093

potential compared to the native mucin dispersion (–0.41 ± 0.2 mV).

The highest values for mucoadhesive force (5.05 ± 0.21 mN) and work of adhesion (0.021 ± 0.004 mJ) were determined for the formulation containing the polymer combination (Figure 1) [3].

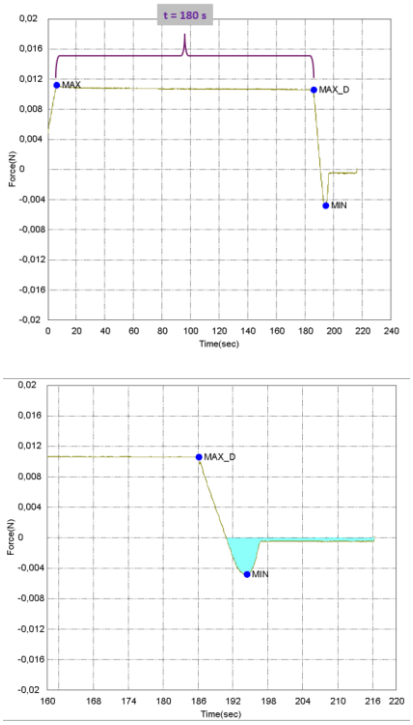

Figure 1. The detachment force vs. time plot during measurement procedure: a) during the entire measurement, b) during the second half of the measurement.

3.1. Rheological measurements

The formulation with polymer combination showed pseudoplastic behaviour (Figure 2). It provides a high viscosity at rest when the eye is open, while the viscosity decreases under the mechanical shear exerted by blinking. This formulation exhibited the highest viscosity due to synergistic interactions between polymers which significantly contribute to its rheological characteristics [3].

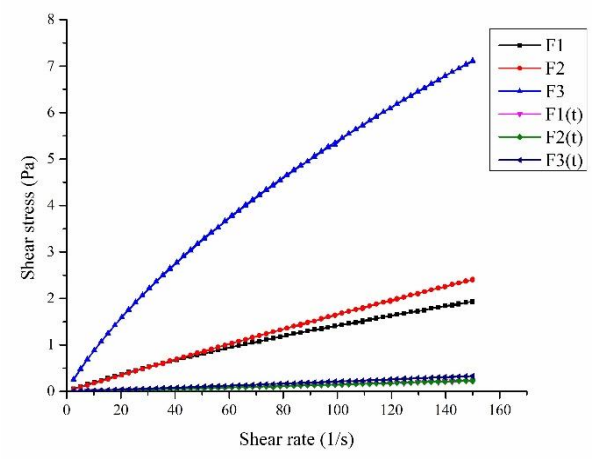

Figure 2. Flow curves of the tested eye drops

4. CONCLUSION

Formulation F3 exhibited desirable pseudoplastic behaviour, i.e. high viscosity at rest for prolonged precorneal residence time, resulting in an optimal balance between mucoadhesion and rheological properties. The evaluation of the mucoadhesive properties of viscous ophthalmic preparations by different techniques is important for the assessment of their functional properties and the expected therapeutic effect.

5. REFERENCES

1. Di Colo, G., et al., Selected polysaccharides at comparison for their mucoadhesiveness and effect on precorneal residence of different drugs in the rabbit model. Drug Development and Industrial Pharmacy, 2009. 35(8): 941-949.

2. Bassi da Silva, J., et al., A critical review about methodologies for the analysis of mucoadhesive properties of drug delivery systems. Drug Development and Industrial Pharmacy, 2017. 43: 1053-1070.

3. Račić, A., et al. Stability and Efficacy of Mucoadhesive Eye Drops Containing Olopatadine HCl: Physicochemical, Functional, and Preclinical In Vivo Assessment. Pharmaceutics, 2025. 17: 517

ACKNOWLEDGMENT

This research was funded by the Western Balkans Mobility Scheme—A POLICY ANSWERS Pilot Program; Grant Agreement No 101058873. Also, the research was funded by the Ministry of Science, Technological Development and Innovation, Republic of Serbia through two Grant Agreements with University of Belgrade-Faculty of Pharmacy No 451-03-136/2025-03/200161 and No 451-03-137/2025-03/200161.

P094

SUSTAINED CLINDAMYCIN DELIVERY USING MICROSPONGES: A PROMISING STRATEGY FOR ORODENTAL INFECTIONS

Dushko Shalabalija, Natasa Draskovic, Lina Livrinska, Nikola Geskovski, Marija Glavas Dodov, Ljubica Mihailova

Institute for Pharmaceutical Technology, Faculty of Pharmacy, Ss. Cyril and Methodius University in Skopje, N. Macedonia

1. INTRODUCTION

Clindamycin (CM), classified as a lincosamide antibiotic, is extensively utilized in managing orodental infections. Its effectiveness arises primarily from its robust activity against anaerobic bacteria and a significant number of Gram-positive cocci, including *Streptococcus* spp. and *Staphylococcus aureus*, making it a preferred option in dentistry [1]. Conventional formulations of CM, however, often encounter limitations such as low patient compliance due to the dosages required, burst release profiles that can lead to suboptimal therapeutic levels, and potential adverse systemic effects. In this sense, recent advancements in drug delivery systems have emerged as a solution, particularly focusing on the use of microsponge-based systems. The microsponge technology facilitates the sustained release of CM, allowing it to act directly at infected sites while reducing side effects associated with higher systemic concentrations [2]. Given these advantages, the aim of this study was to develop and characterize clindamycin hydrochloride (CM-HCl)–loaded microsponges, which were afterwards, evaluated in terms of particle size, particle size distribution, encapsulation efficiency, and *in vitro* release characteristics.

2. MATERIALS AND METHODS

2.1. Materials

Ethyl cellulose (EC), poly(vinyl alcohol) (PVA) and Chitosan, low molecular weight were purchased from Sigma Aldrich (St. Louis, USA). CM-HCl was kindly donated by Phytofarm, North Macedonia. All other reagents used were of analytical or pharmaceutical grade.

2.2. Preparation of CM-HCL-loaded microsponges

Initially, a primary water-in-oil (W/O) emulsion was formed by dropwise addition of the aqueous internal phase consisted of CM-HCl (0.4%) into an EC solution in dichloromethane (DCM). Emulsification was carried out at ambient temperature using high shear homogenization (9500 rpm, 5 min; Ultra-Turrax T25, IkaWerke, Germany). The primary emulsion was then added dropwise into an external aqueous phase containing PVA to form a secondary water-in-oil-in-water (W/O/W) emulsion under the same homogenization conditions. Subsequently, the system was stirred (40 °C, 500 rpm) until complete evaporation of DCM, yielding hardened microsponges. Five different formulations (A–E) were prepared, differing in polymer composition (Table 1).

Table 1. Composituon od microsponges formulations.

Formulation	Chitosan (%)	EC (%)	PVA (%)
A	–	0.33	0.2
B	0.4	0.33	0.2
C	0.4	0.5	0.2
D	–	0.33	0.4
E	–	0.33	0.15

2.3. Particle size and particle size distribution analysis

Determination of the mean particle size (d50) and particle size distribution (span) was conducted using laser diffraction analysis (Mastersizer 2000, Hydro 2000S, Malvern Instr. Ltd., UK) at a stirrer speed of 1750 rpm, RI of 1.52 and absorption coefficient of 0.1.

2.4. Determination of encapsulation efficiency

Encapsulation efficiency (EE) was determined indirectly. The samples underwent centrifuging (Rotofix 32 - Hettich Zentrifugen, Germany) in Vivaspin 20 ultrafiltration cuvettes, 1 000 000 MWCO units (Sartorius, Germany) (20 min, 1000 rpm). The resulting filtrate was analyzed using validated pharmacopeial HPLC method (LiChroCART 250-4.6 mm, Purospher_ STAR RP-18c end capped 5 µm column).

P094

2.5. *In vitro* drug release

The release profile of CM-HCl from microsponges was studied using membrane dialysis method (MEMBRA-CEL dialysis tubing; Serva Feinbiochemica GmbH, Germany). The receptor phase consisted of phosphate buffer pH 7.4, maintained at 37 ± 0.5 °C and stirred at 50 rpm under sink conditions. Aliquots of 5 mL were withdrawn at 1, 2, 4, 8, and 24 hours and replaced with fresh buffer. CM-HCl concentration was quantified using the aforementioned HPLC method.

3. RESULTS AND DISCUSSION

3.1. Particle size, encapsulation efficiency, and release profile

As shown in Table 2, all formulations were characterized with D_{50}<6 **µm** and uniform particle size distributions (span<6) which implies on the physical formulation stability as well as better contact with the mucosal membranes in the oral cavity, thus resulting with efficient treatment of the local infections. Chitosan-containing formulations (B, C) achieved higher EE (>78%), probably due to the possible physical entrapment of CM-HCl as well as the formed hydrogen bonds with chitosan NH_2 molecules [3]. As shown in Figure 1, all formulations exhibited sustained CM-HCl release over 24 hours (35.76-100%), with varying profiles depending on polymer composition. Therefore, the complex interactions and bonds formed between the drug and EC, PVA and chitosan can strongly influence the morphological and surface properties, porosity of the micro-delivery system and thus, the mechanism, release kinetics as well as the extent of drug release.

Table 2. Overview of encapsulation efficiency and particle size parameters for formulations A–E.

Formulation	d_{50} (µm)	Span	EE (%)
A	3.368	4.083	48.19
B	4.759	4.327	78.32
C	4.877	1.9	93.86
D	3.13	1.759	90.57
E	5.981	1.947	87.11

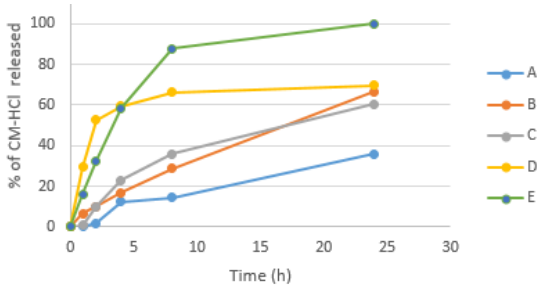

Figure 1. . *In vitro* release profile of formulations A-E in a period of 24 h.

4. CONCLUSION

Clindamycin HCl-loaded microsponges were successfully prepared with uniform size distribution, high EE and prolonged CM-HCl release profile. However, further investigation on the impact of consisting polymers interactions on the physic-chemical and biopharmaceutical performance of the microsponges in order to obtain optimal formulation. Overall, the EC–chitosan–PVA microsponge system offers a promising strategy for controlled, localized delivery of clindamycin in orodental applications.

5. REFERENCES

1. Bogacz, M., et al., *Evaluation of drug susceptibility of microorganisms in odontogenic inflammations and dental surgery procedures performed on an outpatient basis*. Biomed Research International, 2019: 1-12.

2. Kaur, M., et al., *Microsponge: a review*. Journal of Drug Delivery and Therapeutics, 2024. 14(6): 294-297.

3. Słota, D., et al., *Targeted Clindamycin Delivery Systems:Promising Options for Preventing and Treating Bacterial Infections Using Biomaterials.* International Journal of Molecular Sciences, 2024. 25(8): 4386

P095

CHONDROITIN SULFATE-FUCOIDAN SYNERGY IN 3D CANCER MODELS

Eva Nováková[1,2,3], Jozef Zima[2], Miroslava Špaglová[2], Martina Labudová[1,3], Miroslava Šupolíková[1,2]

[1]Comenius University Bratislava, Faculty of Natural Sciences, Department of Microbiology and Virology, Bratislava, Slovakia
[2]Comenius University Bratislava, Faculty of Pharmacy, Department of Galenic Pharmacy, Bratislava, Slovakia
[3]Biomedical Research Center of the Slovak Academy of Sciences, Institute of Virology, Bratislava, Slovakia

1. INTRODUCTION

Spheroids, a widely used 3D model, self-organize into heterogenous aggregates that mirror tumor microenvironments, making them ideal for evaluating therapeutic efficacy [1]. Glycosaminoglycans like chondroitin sulfate (CS) and marine-derived fucoidan (F) exhibit immunomodulatory and antitumor properties [2]. Their potential synergy in disrupting tumor progression is explored here using NIH3T3 and Hepa1c1c7 spheroids. By quantifying live, apoptotic, and necrotic cells post-treatment, this study aims to uncover combinatorial effects that could inform targeted cancer therapies.

2. MATERIALS AND METHODS

2.1. Materials

The Hepa1c1c7 cell line is a stabilized adherent cell line derived from C57L mouse hepatocellular carcinoma (ATCC CRL-2026™). The NIH3T3 fibroblast cell line is a stabilized adherent cell line derived from mouse embryonic tissue (ATCC CRL-1658™). Chondroitin sulfate (99%) was from Gnosis Bioresearch (Desio, Italy). Fucoidan (70%) was from KangCare Biotech (Nanjing, China). RIPA lysis solution was from MGP (Bratislava, Slovakia). Trypsin-EDTA solution, propidium iodide, and annexin V were from Lambda Life (Bratislava, Slovakia). DMEM culture medium was from Viagene (Bobrov, Slovakia). Agarose and phosphate buffer saline (PBS) were from Biotech (Bratislava, Slovakia).

2.2. Spheroid Treatment and Analysis

On day 3 of culture, spheroids from NIH3T3 and Hepa1c1c7 cells were treated with chondroitin sulfate (CS), fucoidan (F), or their combination (CS+F) diluted in DMEM at 1:1, 1:2, and 1:4 ratios (Table 1). Controls received PBS. Every few days, 100 µL of medium was removed and replaced with fresh treatment. Spheroids were monitored under a 50x inverted microscope (Zeiss Axiovert 40 CFL) and imaged with ProView software. Spheroid areas were measured using ImageJ. Treatments were applied three times over a 10-day period. Results represent averages from three independent experiments.

Table 1. The concentration of fucoidan (F) and chondroitin sulfate (CS).

Dilution in DMEM	CS (mmol/L)	F (mmol/L)	CS+F (mmol/L)
1:1	0.0620	0.0920	0.0620 0.0920
1:2	0.0310	0.0460	0.0310 0.0460
1:4	0.0155	0.0230	0.0155 0.0230

2.3. Spheroid processing

Spheroids were transferred from a 96-well plate to a microtube, washed with PBS, and lysed with 30 µL RIPA solution for 15 minutes with gentle mixing. After centrifugation at 14,000 rpm for 15 minutes, the supernatant was collected for analysis.

2.4. Flow cytometry

Spheroids were transferred to a rounded-bottom 96-well plate, washed with PBS, and treated with trypsin-EDTA to dissociate cells. Cells were then resuspended, fixed, and stained with propidium iodide for viability and annexin V for apoptosis. Analysis was performed using the Guava® EasyCyte™ Plus flow cytometer.

3. RESULTS AND DISCUSSION

3.1. Treatment and growth analysis

Hepa1c1c7 spheroids: Most growth occurred with the CS+F combination (0.0155 mmol/L CS

P095

+ 0.023 mmol/L F, 1:4 dilution). F alone at 0.092 mmol/L (1:1) showed minimal size change compared to control.

NIH3T3 spheroids: Similar trends were observed, with the greatest increase in spheroid area following combined CS+F treatment. F at 0.092 mmol/L (1:1) reduced spheroid size.

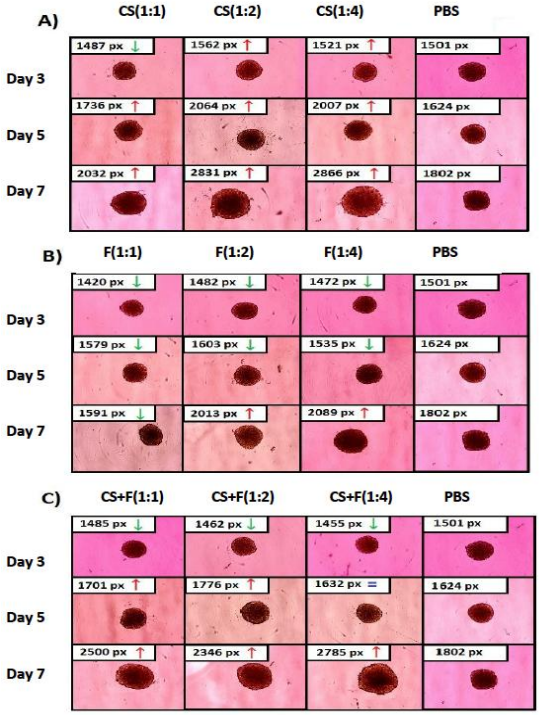

Figure 1. Spheroids from the Hepa1c1c7 tumor cell line after treatment with A) chondroitin sulfate (CS), B) fucoidan (F), C) the combination of chondroitin sulfate and fucoidan (CS+F) at 50x magnification. Day 3 – first addition of substances; Day 7 – last addition of substances. Up arrow (↑) – spheroids that increased their area compared to control spheroids; Down arrow (↓) – spheroids that decreased their area compared to control spheroids; Equal to (=) – spheroids that have approximately the same area compared to control spheroids.

3.2. Flow cytometry

The results demonstrate the synergistic effect of CS+F at selected concentrations, promoting favorable outcomes in spheroid cell viability (see Table 2). Tumor cells often have dysregulated growth signals and may also be more sensitive to the inhibitory effects of certain compounds, leading to antiproliferative outcomes when treated with CS or F [3]. Their molecular weight and specific composition can significantly influence its biological activity.

Table 2. Quantitative representation of cells in spheroids prepared from the NIH3T3 cell line compared to Hepa1c1c7 cell line evaluated by flow cytometry (5000 cells).

	NIH3T3 cell line			
	Living cells (%)	Apoptotic cells (%)	Dead cells (%)	Necrotic cells (%)
CS	66.43 ± 4.43	20.98 ± 1.03	9.79 ± 0.52	2.80 ± 0.18
F	13.53 ± 3.60	38.72 ± 4.09	1.50 ± 0.17	46.25 ± 2.97
CS+F	28.30 ± 1.65	19.10 ± 1.05	24.23 ± 5.28	28.37 ± 1.78
PBS	31.57 ± 3.81	32.67 ± 10.05	4.61 ± 0.50	31.15 ± 6.46
	Hepa1c1c7 cell line			
CS	29.18 ± 3.69	29.57 ± 18.29	3.89 ± 0.55	37.36 ± 5.97
F	49.65 ± 4.77	27.66 ± 6.83	9.93 ± 0.25	12.75 ± 1.25
CS+F	41.52 ± 3.76	31.50 ± 6.55	19.84 ± 5.80	7.14 ± 0.83
PBS	50.00 ± 8.15	33.22 ± 2.52	7.09 ± 0.67	9.69 ± 0.45

4. CONCLUSION

The use of CS in cancer is controversial; while some studies show it promotes tumor cell growth, modified forms may have anticancer effects requiring further research [4]. Our study found that F significantly inhibited tumor spheroid growth, and combined treatment with CS enhanced this effect. Flow cytometry showed dead tumor cells increased from 7.09% (control) to 19.84% with both agents. The data provide a foundational basis for developing an oleogel formulation incorporating the studied active ingredients.

5. REFERENCES

1. Anu Varshini, A.M., et al., *New frontiers in anti-cancer drug testing: The need for a relevant In vitro testing model.* NAM Journal, 2025. 1:1-19

2. Wang, Y., et al., *Biological activities of fucoidan and the factors mediating its therapeutic effects: a review of recent studies.* Marine Drugs, 2019. 17(3):183.

3. Bittkau, K.S., et al., *Comparison of the Effects of Fucoidans on the Cell Viability of Tumor and Non-Tumor Cell Lines*. Marine Drugs, 2019;17:441.

4. Asimakopoulou, A.P., et al., *The biological role of chondroitin sulfate in cancer and chondroitin-based anticancer agents.* In Vivo, 2008.22:385–9.

ACKNOWLEDGMENT

The project was realized with the financial support of the grant VEGA 1/0146/23.

P096

HEMOADSORPTION OF MEROPENEM, PIPERACILLIN AND VANCOMYCIN TO CYTOSORB®: *IN VITRO* STUDY

Sara Kenda[1], Tomaž Vovk[2]

[1]*General hospital dr. Franc Derganc Nova Gorica, Slovenia*
[2]*University of Ljubljana, Faculty of Pharmacy, Slovenia*

1. INTRODUCTION

Antibiotics are widely used drugs, and their use in intensive care units can be up to 10 times higher than in other departments. The pharmacokinetic and pharmacodynamic properties of antibiotics are altered in critically ill patients, making therapy optimization very difficult. However, critically ill patients may also be treated with dialysis, extracorporeal membrane oxygenation or even hemoadsorption, which can make drug dosing even more difficult [1]. The elimination of inflammatory mediators in patients with sepsis is crucial to achieve better circulatory stability of patients and thus better survival. The CytoSorb® hemoadsorber has recently been used for this purpose. It is a porous, biocompatible polymer with specific properties that enable it to bind many hydrophobic molecules with a molecular weight of up to 55 kDa (the size of most cytokines). However, it has also been shown to bind low molecular weight compounds [2]. The aim of the present study was to determine the *in vitro* binding of selected antibiotics to the Cytosorb®. In addition, we developed and validated a simple analytical method for determination of selected antibiotics.

2. MATERIALS AND METHODS

The *in vitro* study was performed with bovine blood obtained from a local slaughterhouse. The study was approved by the Administration for Food Safety, Veterinary Sector and Plant Protection of the Republic of Slovenia (authorisation number U34453-63/2023/3). To mimic the septic conditions in blood, albumin concentration and hematocrit were adjusted to 20 g/L and 30 %, respectively. In the experiment, we tested the binding of three different antibiotics, meropenem (MER), piperacillin (PIP) and vancomycin (VAN), to the CytoSorb®. To 100 mL of blood with adjusted albumin concentration and hematocrit, antibiotic was added at its maximum therapeutic concentration (MER = 16 mg/L, PIP = 80 mg/L and VAN = 20 mg/L), followed by the addition of 0, 0.1 or 1 g of CytoSorb®. The blood was mixed at 190 rpm, incubated at 37°C and blood samples were taken at fixed time intervals to determine albumin [3] and antibiotic concertation (Figure 1). In addition, hemoglobin was determined in the plasma and blood samples and the values obtained were used to assess hemolysis [4]. The range of the developed analytical method for antibiotic determination was between 1.0 µg/mL to 75 µg/mL for MERO and PIP and between 1.0 µg/mL to 100 µg/mL for VAN. The lower limit of quantification was 1 µg/mL. The inter- and intra-day bias and precision were within 15 %.

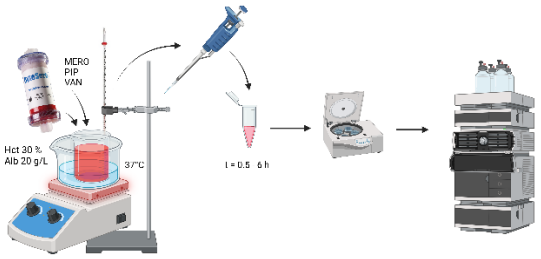

Figure 1. Schematic presentation of the *in vitro* study.

3. RESULTS AND DISCUSSION

The *in vitro* model was designed to mimic the blood characteristics of patients with sepsis (hematocrite 30% and albumin concentration 20g/L). In a similar *in vitro* study conducted by C. König and colleagues, antibiotics were dissolved in saline, albumin solution or reconstituted blood [5]. The prepared solutions were pumped through the CytoSorb® cartridge. We believe that our *in vitro* model better matches the septic conditions in patients' blood. In addition, our *in vitro* model is much simpler and therefore easier to use for determining the binding of drugs to CytoSorb® *in vitro*, as it requires only small amounts of CytoSorb® and blood. The chosen conditions of the *in vitro* model allowed to follow the binding process for

6 hours, which corresponds to the conditions used in clinical practise. The hemolysis at the beginning of the experiment was 0.3% and the final hemolysis after six hours was 0.6%, confirming that hemolysis did not affect the experimental results. Albumin levels decreased by 19% after the 2-hour of CytoSorb® addition, confirming significant binding of albumins to CytoSorb®. The kinetics of binding of antibiotics to CytoSorb® is shown in Figure 2. The binding process for MERO was negligible regardless of the mass of the CytoSorb®. In contrast, PIP and MERO bind significantly only at 1 g of hemoadsorbent. Since the CytoSorb® cartridge contains approximately 325 g of hemoadsorbent beads, our *in vitro* results indicate that the CytoSorb® cartridge would bind approximately 919 mg ± 272 mg of PIP and 1070 mg ± 210 mg VAN, while the bound amount of MERO on the CytoSorb® cartridge would be negligible. Therefore, our results suggest that patients treated with the CytoSorb® and receiving concomitant antibiotic therapy with VAN or PIP should receive higher antibiotic doses to compensate for the binding of the antibiotic to the CytoSorb®.

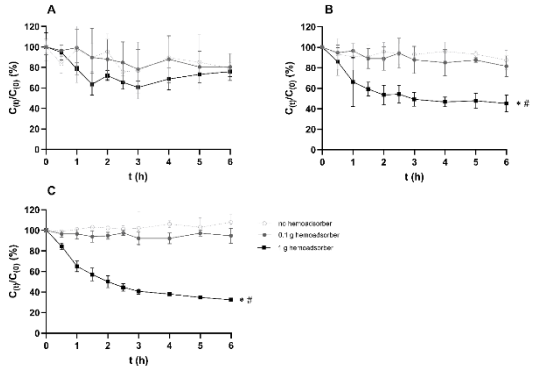

Figure 2. Hemoadsorption of antibiotics to CytoSorb®

A MERO, B PIP, C VAN, symbols ∗ and # indicates significant difference between experiments with no adsorbent and 1 g of CytoSorb® and between 0.1 g and 1 g of CytoSorb®, respectively.

4. CONCLUSION

The developed *in vitro* method shows that PIP and VAN, in contrast to MERO, bind to the CytoSorb®. For this reason, we conclude that it is necessary to replace VAN and PIP during simultaneous treatment with CytoSorb®. We therefore recommend the use of therapeutic drug monitoring and further investigations in critically ill patients.

5. REFERENCES

1. Abdul-Aziz MH, et al., Antimicrobial therapeutic drug monitoring in critically ill adult patients: a Position Paper. Intensive Care Medicine, 2020.46(6):1127-1153.

2. CytoSorb Therapy: Evidence in septic and vasoplegic shock. 1st Edition. PDF.; Retrieved from https://cytosorbents.com/wp-content/uploads/2019/02/Sepsis_booklet_B1086R01EN2019_interaktiv.pdf.

3. Leonard PJ, Persaud J, Motwani R. The estimation of albumin by BCG dye binding on the Technicon SMA 12-60 analyser and comparison with HABA dye binding technique. Clina Chima Acta, 1971.35(2):409-12.

4. Frenchik MD, McFaul SJ, Tsonev LI. A microplate assay for the determination of hemoglobin concentration. Clina Chima Acta 2004.339(1-2):199-201.

5. König C, et al. In vitro removal of anti-infective agents by a novel cytokine adsorbent system. The International Journal of Artificial Organs. 2019.42(2):57-64.

P097

MUCOADHESIVE FILMS EMBEDDED WITH DEXAMETHASONE LOADED NANOSTRUCTURED LIPID CARRIERS FOR ORAL LICHEN PLANUS TREATMENT

Ljubica Mihailova, Matej Nikolovski, Metodi Naumovski, Magdalina Petrushevska, Teodora Tasevska, Marija Glavas Dodov, Dushko Shalabalija

Institute for Pharmaceutical Technology, Faculty of Pharmacy, Ss. Cyril and Methodius University in Skopje, N. Macedonia

1. INTRODUCTION

Oral lichen planus (OLP) is a chronic, immune-mediated inflammatory disorder of the oral mucosa, predominantly driven by T-cell-mediated immune responses. Clinically, OLP manifests in several forms, including reticular, erosive, atrophic, and ulcerative variants, all of which can induce pain, discomfort, and significantly compromise patients' quality of life. Although traditionally regarded as a benign condition, OLP carries a recognized risk of malignant transformation into oral squamous cell carcinoma. Current therapeutic approaches primarily involve corticosteroid administration - topically, orally, or via intralesional injection, in order to attenuate inflammation and alleviate symptoms. Among these, topical dexamethasone (DEX) is the most commonly employed treatment. However, conventional topical therapies are hindered by limitations such as rapid clearance from the mucosal surface, leading to suboptimal therapeutic efficacy [1]. To address these shortcomings, innovative drug delivery systems are under investigation. Notably, bioadhesive films incorporating DEX-loaded nanostructured lipid carriers (NLCs) have demonstrated considerable potential. These formulations offer sustained and localized drug release, enhanced mucosal adherence, and improved drug bioavailability. The integration of NLCs facilitates prolonged therapeutic action, consistent dosing, and an improved safety and efficacy profile. Therefore, the aim of this study is development and characterization of mucoadhesive films embedded with dexamethasone-loaded NLCs, with the objective of enhancing current treatment modalities for OLP.

2. MATERIALS AND METHODS

2.1. Materials

Phospholipone 90H (PL90H) was supplied from Phospholipid, Germany, while Tween 80and oleic acid (OA) were obtained from Sigma Aldrich (St. Louis, USA). Sodium alginate (SA, viscosity of 15.00–20.00 cps) was purchased from Sigma Aldrich, USA and sodium carboxymethyl cellulose (NaCMC, average molecular weight of 250,000) was contributed from Acros Organics, Belgium. DEX glycerol and calcium chloride were purchased from Alkaloid, N. Macedonia.

2.2. Preparation of NLCs

The NLC formulations, were prepared using the solvent evaporation technique, previously described by Mihailova et al. (2022), with slight modification. In summary, the oil phase was consisted of a 1:1.15 (w/w) mixture of PL90H (solid lipid) and oleic acid (liquid lipid), dissolved in ethanol. To this mixture, 100 mg of DEX was incorporated under continuous magnetic stirring at 250 rpm (Jenway, UK) and maintained at 60 °C. Subsequently, the lipid phase was gradually introduced into the aqueous phase, which was preheated to 60 °C and contained 3% Tween 80. The process continued until complete ethanol evaporation was achieved. Obtained lipid emulsions were homogenized with ultra-turrax for 5 min at 6500 rpm and were left in a refrigerator at 2-8 °C for 24 h.

2.3. Mean particle size and particle size distribution of NLCs

The mean particle size (D_{50}) and particle size distribution (SPAN) of the prepared NLCs were analysed using laser diffraction (Mastersizer 2000, Hydro 2000S, Malvern Instruments Ltd., UK) under controlled conditions, including a stirring speed of 1750 rpm, with the refractive index and absorption index of the NLs set to 1.348 and 0.001, respectively.

2.4. Encapsulation efficacy of NLCs

The absolute quantity of DEX encapsulated within the nanostructured lipid carriers (NLs) was determined indirectly by quantifying the amount of unencapsulated DEX, where NLCs dispersions were subjected to centrifugation using a Rotofix 32 centrifuge (Hettich Zentrifugen, Germany) at 4500 rpm, 25 °C for 15 minutes, across four consecutive cycles, utilizing Vivaspin 20 ultrafiltration units with a molecular weight cut-off (MWCO) of 100,000 Da (Sartorius, Germany). The resulting supernatant was collected and analysed by spectrophotometer at 243 nm wavelength (Darmstadt, Germany).

2.5. Preparation of mucoadhesive films

The films were prepared by mixing pre-weighed amounts of SA and NaCMC in a 3.5:1 ratio (w/w) in distilled water using a magnetic hotplate stirrer (3h, 300 rpm, 60 °C, IKA Plate RCT Digital, IKA Werke, Germany). Once fully dissolved, 1% glycerol, 0.5 mL and 1 mL of 4% $CaCl_2$ solution were added, followed by continuous stirring overnight. After complete dissolution of the $CaCl_2$, 1g of 10% DEX solution (F1) or NLCs (F2) were incorporated and 5 g of each hydrogel formulation was poured into Petri dishes with a 5 mm diameter.

2.5. *In vitro* release study

The cumulative release of DEX from F1 and F2 was evaluated using dialysis tubing (MEMBRA-CEL®, MWCO 7000, RC, Serva Feinbiochemica GmbH, Germany), where each film was placed into 30 mL of phosphate buffer (pH 7.4) and incubated at 37 ± 1 °C with continuous stirring at 200 rpm. At predetermined time points (1, 2, 4, 6, 8, 24 and 48 h), 5 mL aliquots of the release medium were withdrawn and analysed. The concentration of DEX released from the formulations was quantified using a validated spectrophotometric method (243 nm, Darmstadt, Germany).

3. RESULTS AND DISCUSSION

The prepared NLCs formulation was characterized D_{50}<180 nm which indicates on the facilitated penetration of the NLCs into the mucosal surface and potentially deeper tissue layers. The narrow unimodal distribution (SPAN<2) ensures the homogeneous drug delivery and reduced aggregation risk thus improving the overall stability and performance of the drug in biological environments. Additionally, the high DEX encapsulation efficacy (>90%) is indicator of therapeutically potent formulation. From Fig. 1 it can be observed that both mucoadhesive film formulations showed prolonged release of DEX over the period of 48 h (75%). Additionally, the formulation with DEX loaded NLCs (F2) was characterized with slower release in the first 6h compared to the formulation containing free DEX in the film matrix (F1), probably due to the dual barrier effect where the DEX release is governed by both: diffusion from the lipid nanocarrier and subsequential diffusion through the mucoadhesive polymeric film matrix [2].

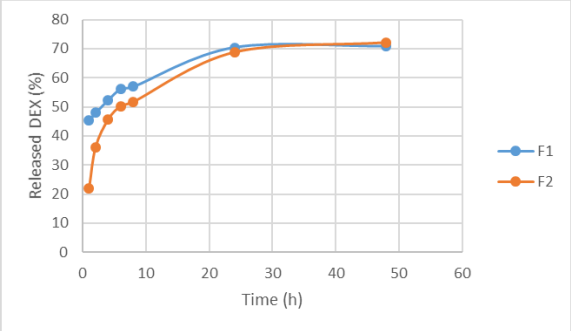

Figure 1. *In vitro* release profile of DEX from mucoadhesive films (F1 and F2)

4. CONCLUSION

In conclusion, the controlled slow initial release from mucoadhesive films embedded with DEX loaded NLC can be beneficial for sustained therapeutic effect, especially in conditions like OLP, where longer exposure to the drug at the mucosal site is desirable, leading to prolonged therapeutic effects, improved safety profile, and enhanced patient compliance.

5. REFERENCES

1. Park, S.Y., et al., *Factors affecting treatment outcomes in patients with oral lichen planus lesions: a retrospective study of 113 cases.* Journal of Periodontal and Implant Science, 2018. 48(4): 213-223.
2. Sodata, P., et al., *Optimization of Mucoadhesive Film Reinforced with Functionalized Nanostructured Lipid Carriers (NLCs) for Enhanced Triamcinolone Acetonide Delivery via Buccal Administration: A Box–Behnken Design Approach.* Sci, 2025. 7(22).

P098

MICROPARTICLES IN FISH REPRODUCTION: PREPARATION, EVALUATION AND STABILITY STUDY

Jakub Vysloužil[1], Jan Muselík[1], Kateřina Kubová[1], Sylvie Pavloková[1], Lucie Pizúrová[1] Miroslava Pavelková[1]

[1]Masaryk University Brno, Faculty of Pharmacy, Department of Pharmaceutical Technology, Brno, Czech Republic

1. INTRODUCTION

Poly(lactic-co-glycolic acid) (PLGA) is a widely used biodegradable FDA approved polymer for parenteral administration, extensively studied for peptide delivery. In the last decades, PLGA systems have also received a great interest in veterinary medicine [1]. A potential field for PLGA particles use can be seen in intensive fish aquacultures, where they could serve as carriers for the treatment and prevention of wide range of diseases or for production yield increase [2]. Control of reproductive function in fish can be achieved by several ways. However, the final stage of gametogenesis and synchronization may require use of exogenous hormonal addition. Hormonal supplementation has focused on the use luteinizing hormone (LH) or synthetic gonadoliberin agonists (GnRHa) [3]. An administration of these substances in form of conventional parenteral solution means repeated administration and fast enzymatic drug degradation. Therefore, their incorporation into PLGA microparticle carriers could bring numerous advantages, such as higher efficacy, stress reduction, lower mortality and higher stability of active substances. The aim of this study was to design and prepare PLGA particles suitable for parenteral administration of alarelin acetate and their subsequent characterization including stability study.

2. MATERIALS AND METHODS

2.1. Materials

Alarelin acetate (APExBIO), PLGA Resomers® RG 203, RG 504, RG 653, RG 753 (Evonik), poly(vinyl alcohol) (PVA, Mw 31 000 – 50 000; 98 – 99% hydrolyzed (Sigma Aldrich). All other materials were of analytical grade and were used without further purification.

2.2. Sample preparation

Microparticles were prepared using w1/o/w2 emulsion. For w1, 10 mg of alarelin acetate were dissolved in 1.5 g of gelatine solution of 2.5/5/10% concentration. Exactly 800 mg of appropriate Resomer® were dissolved in 5 ml of dichloromethane (oil phase). Prepared phases were pre-mixed on vortex and homogenized (Ultra-Turrax T25, Ika Werke, Germany) at 11000 or 22000 rpm. Resulting w1/o emulsion was pre-mixed on homogenizer with 12 g of 1% PVA solution to create concentrated double emulsion w1/o/w2. Concentrated emulsion was then poured at once to 200 g of 0.1% PVA/2.0% NaCl. Resulting w1/o/w2 emulsion was stirred for 2 hours. Formed particles were collected through centrifugation, re-suspended in purified water and lyophilized. Each sample was prepared from four runs. Totally 24 samples were prepared.

2.3. Sample evaluation

The microparticle surface morphology and size estimation was examined with scanning electron microscopy (SEM; MIRA3, Tescan Orsay Holding, Czech Republic) equipped with secondary electron detector.

To determine the drug content, to the appropriate weight of particles 10 ml of acetone were added. After mixing, 10 ml of phosphate buffer solution were added. A small amount of solution was filtered through a 0.45 μm pore size filter into a sample vial. Subsequently, alarelin acetate content was measured on HPLC (Agilent 1100, USA) involving NUCLEODUR 100-5 CN-RP (150 mm x 4.6 mm, 5 μm) column. Binary mixture of acetonitrile:20mM H_3PO_4 (16:84, v/v) was used as a mobile phase at the flow rate of 0.8 ml/min with temperature set at 30 °C, injected sample volume of 20 μl and detection wavelength of 220 nm.

In vitro release testing (time course 7 days) was performed in agarose gel (2%). 50 mg of microparticles were placed into a vial, fixed in agarose gel and after gel solidifying, 5 ml of phosphate buffer solution pH 7.4 was added. The buffer was sampled (2.0 ml) regularly in 4, 24, 48, 72, 96 and 168 hrs, and completely replaced with fresh medium after sampling. All

P098

measurements were performed six times. Alarelin concentration was quantified by HPLC method described above. Stability study was performed in three conditions: stability box at 25 °C and 60% humidity, refrigerator (2 – 8 °C) and freezer box (-30 °C). Drug content and dissolution profiles were observed in 1, 3, 6 months.

3. RESULTS AND DISCUSSION

During preparation several features were employed to ensure higher yield. Gelatine in the internal water phase w1 served for increase of the density core. This also helped to create spherical particles with defined shape. Pre-mix of w1/o emulsion on vortex was used to reduce losses of the oil phase stuck to the vessel bottom during the emulsification. Fine emulsion ensured by homogenization was important also to provide particles suitable for parenteral administration.

All 24 samples were successfully prepared. Higher homogenization speed showed lower particle size but also strikingly lower encapsulation efficiency (EE), usually at similar yield values. This hints at drug loss during the preparation at higher homogenization speed. For this reason, the stability studies were performed with selected samples prepared at lower homogenization speed. PCA plot revealed that the dependence between the amount of gelatine and DL and EE is not linear and the best DL and EE are achieved at 5% gelatine. Tab. 1 shows EE, DL and yield results for a 5% gelatine/lower homogenization speed subset. Noticeable was lower yield in samples prepared from Resomer® RG 504 (33.02% to 58.2%). In overall, the yield was lowered by sample collection before the freeze-drying process. In this regard, the best results yielded PLA (RG 203) samples (71.85 to 81.02%). The stability study revealed that the best stability of the dissolution profile possessed the RG 504 polymer (Figure 1). The other tested polymer RG 653 showed remarkable differences when compared to default time 0 profile.

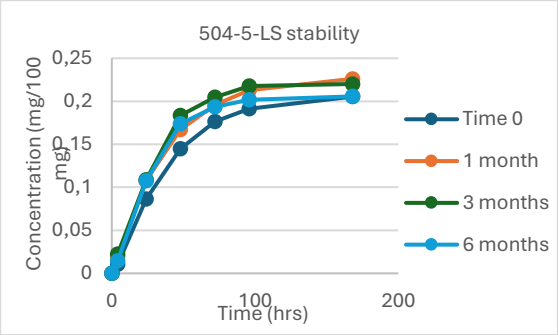

Figure 1. Stability of 504-5-LS in 6 months (-30 °C)

Table 1. Samples prepared with 5% gelatine and 11 000 rpm homogenization speed characterization.

Sample	Yield(%)	EE (%)	DL (%)
203-5-LS	76.03	53.80±3.19	0.40±0.04
504-5-LS	33.02	41.99±3.10	0.47±0.04
653-5-LS	63.71	56.55±4.05	0.64±0.05

4. CONCLUSION

Microparticles with content of encapsulated GnRHa alarelin acetate were successfully prepared. Particle size was found to be suitably small for parenteral administration by injection and it was possible to easily resuspend the particles as well. Effect of homogenization speed and gelatine concentration was observed. Resomer® RG 504 was found the most suitable in terms of stability of the dissolution profile.

5. REFERENCES

1. Bilhalva, A. F., et al., Utilization of biodegradable polymers in veterinary science and routes of administration: a literature review, Journal of Applied Animal Research, 2017. 46: 643-649.

2. Yun, S, et al., Efficacy of PLGA microparticle-encapsulated formalin-killed Aeromonas hydrophila cells as a single-shot vaccine against A. hydrophila infection, Vaccine, 2017. 35: 3959-3965.

3. Mylonas, C. and Zohar, Y. Controlling fish reproduction in aquaculture, New Technologies in Aquaculture (book). 2009. 109-142.

ACKNOWLEDGMENT

This experimental work was realized by support of NAZV (Ministry of agriculture of Czech Republic) project number QK1810221

P099

PHYSICS BASED SURFACE PATCH ANALYSIS FOR PREDICTION OF HYDROPHOBIC CONTRIBUTION TO VISCOSITY OF MABS

Benjamin Knez[1], Miha Ravnik[2], Mitja Zidar[1]

[1]Novartis d.o.o., Verovškova 57, 1000 Ljubljana, Slovenia
[2]Faculty of Mathematics and Physics., Jadranska 19, 1000 Ljubljana, Slovenia

1. INTRODUCTION

Protein-based therapeutics, such as monoclonal antibodies (mAbs), have become increasingly prominent in the pharmaceutical industry. They are often administered subcutaneously to enable patient self-dosing. However, high-concentration formulations required for such administration are prone to elevated viscosity, which can complicate injection and delay drug development. Traditional viscosity assessments rely on resource-intensive wet-lab experiments, which are often impractical in early drug development. As a result, there is a growing shift toward computational predictive models [1], also utilizing machine learning (ML), but most focus on electrostatics and largely overlook hydrophobic interactions.

We present a physics-based, *in silico* method to predict the hydrophobic contribution to mAb solution viscosity. We developed a novel surface patch analysis algorithm capable of identifying and quantifying hydrophobic regions on protein surfaces. We applied this algorithm to a dataset of monoclonal antibodies and calculated the interaction energies between hydrophobic patches. This allowed for the definition of a threshold interaction energy that distinguishes between low- and high-viscosity candidates.

Importantly, the method reveals not only the significance of hydrophobicity but also how neighbouring “electrostatic guard” patches can modulate protein self-association under different solution conditions. While validated on mAbs, the framework is broadly applicable to any protein format, making it a versatile tool for early-stage biopharmaceutical screening and formulation design.

2. MATERIALS AND METHODS

2.1. Protein material and experimental methods

Nine mAbs were formulated at 150 mg/mL, pH 6.0, 220 mM sucrose, prepared with and without 100 mM NaCl to assess electrostatic screening effects. Viscosity measurements were conducted at 25 °C using a microfluidic viscometer (RheoSense VROC).

2.2. Computational details

The amino acid sequences of all mAbs were used to construct the 3D structure of each antibody's Fv region, which were then grafted onto a model IgG1 template.

The surface patch identification algorithm was developed in-house. Hydrophobicity was quantified using the Spatial Aggregation Propensity (SAP) score [2], and electrostatics using the Spatial Charge Map (SCM) score [3], calculated per atom and projected on the solvent excluded surface.

2.3. Hydrophobic interaction calculation

We calculated patch interactions using the hydrophobic interaction potential equation, introduced by Donaldson et al. [4]. Principal component analysis (PCA) was used to identify the interaction plane between the patches.

3. RESULTS AND DISCUSSION

3.1. Patch-patch interaction calculation for mAbs

We propose that the dominant way the hydrophobic effect influences the solution viscosity is due to the attractive force between two hydrophobic patches on two different

proteins. As the hydrophobic interaction potential is developed for planar surfaces, we identify the interaction surface as the projection of the patch to the best-fit plane of the patch, translated to the maximum point along the normal vector (Fig. 1)

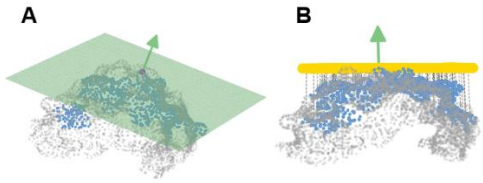

Figure 1. Use of PCA to identify the (A) best-fit plane (green) shifted to pass through the patch's highest point along the normal vector and (B) side view of the patch, showing the interaction surface (yellow).

3.2. Experimental dataset

We observed a strong correlation between the calculated patch-patch hydrophobic interaction energies and the measured viscosities (electrostatic interactions screened using 100 mM NaCl). Antibodies with interaction energies stronger than approximately –3 k_BT consistently exhibited high viscosities (more than the arbitrary threshold of 15 cP), whereas those with weaker interactions remained below this threshold (Fig. 2). Notably, this cutoff aligns well with previously established limits for the onset of weak, reversible protein-protein interactions [5].

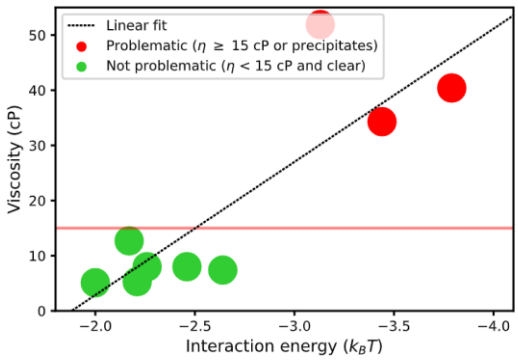

Figure 2. Viscosity plotted with respect to the interaction energy.

3.3. Electrostatic guard

We found that closely bordering electrostatic patches modulate how hydrophobic patches influence viscosity. In some antibodies, addition of salt screens the repulsive electrostatic effect of the positively charged patch with the predominantly positively charged antibody surface, allowing for the hydrophobic interaction to dominate and increase viscosity. This "electrostatic guard" highlights the coupled influence of charge and hydrophobicity on protein behaviour.

4. CONCLUSION

In this work, we introduced a high-throughput, physics-based computational method for predicting the hydrophobic contribution to protein solution viscosity. Designed for early application in the drug research and development pipeline, our approach enables more efficient resource investment and provides a generalizable alternative to many existing ML–based models, making it theoretically applicable to any protein format.

5. REFERENCES

1. Goswami S.., et al., *Developments and challenges for mAb-based therapeutics.* Antibodies, 2013. 2(3): 452-500.

2. Chennamsetty N., et al., *Design of therapeutic proteins with enhanced stability.* Proceedings of the National Academy of Sciences, 2009. 106(29): 11937-11942.

3. Agrawal N., et al., *Computational tool for the early screening of monoclonal antibodies for their viscosities.* MAbs, 2016. 8(1): 43-48.

4. Donaldson S.H., et al., *Developing a general interaction potential for hydrophobic and hydrophilic interactions.* Langmuir, 2015. 31(7): 2051-2064.

5. Hofmann .J.L., et al., *Ultra-weak protein-protein interactions can modulate proteome-wide searching and binding.* BioRxiv, 2022. 2022-09.

P100

THE INFLUENCE OF *DUNALIELLA* EXTRACT AND WATER BRINE FROM SEČOVLJE SOLINE ON SKIN HYDRATION AND BARRIER FUNCTION

Alenka Zvonar Pobirk[1], Mercedes Vitek[1], Maja Bjelošević Žiberna[1], Katarina Bolko Seljak[1], Neli Glavaš[2], Eylem Atak[3], Daniel Bosch[3], Katja Klun[3], Ana Rotter[3], Mirjam Gosenca Matjaž[1]

[1]University of Ljubljana, Faculty of Pharmacy, Slovenia
[2]SOLINE Pridelava soli d. o. o., Portorož, Slovenia
[3]Marine Biology Station Piran, National Institute of Biology, Piran, Slovenia

1. INTRODUCTION

Healthy barrier function of epidermis is essential for preventing excessive water loss through the skin (known as transepidermal water loss – TEWL). It also hinders penetration of xenobiotics and microorganisms and contributes to UV protection. Properties of stratum corneum, the uppermost layer of the epidermis, specifically its hydration level and pH, the composition and organization of extracellular lipids, functionality of corneodesmosomes, appropriate content of natural moisturizing factor, and a well-functioning endogenous antioxidant network, all considerably contribute to the skin's barrier function (1).

While brine is known to positively affect the skin due to the large presence of minerals, plant extracts are commonly incorporated in skincare products as active ingredients. Algae extracts from the genus *Dunaliella* are widely used in cosmetics and dietary supplements due to its high content of bioactive compounds. The main constituents contributing to its skin beneficial effects are β-carotene, phytoene and phytofluene as colorless carotenoids, essential fatty acids, and glycerol (2). Anti-glycation, anti-inflammatory, and anti-aging properties of *Dunaliella* extracts, particularly under conditions of high UV exposure, were confirmed by Havas et al. (3).

The aim of the present study was to compare the efficacy of conventional hydrophilic cream (HC) and formulation based on lamellar liquid crystals (LLCs), both containing *Dunaliella* extracts isolated in the Sečovlje salt pans (Slovenia) during 2 weeks usage. All formulations and their unloaded counterparts were tested on the lower forearm skin of 15 healthy volunteers – both alone and following application of water brine from the Sečovlje salt pans used as skin tonic.

MATERIALS AND METHODS

2.1. Materials

LLCs are composed of Lipoid S-100 (Lipoid GmbH, Germany), Montanov 68 (Tovarna Organika), flaxseed oil (A.C.E.F., Italy), bidistilled water andvitamin E. Hydrophilic cream (HC) was composed of glycerol (Farmalabor, Italy), Creammaker® wax (MakingCosmetics Inc, USA), mandel oil (A.C.E.F, Italy), cetyl alcohol (Milnica, Slovenia), Gelmaker®EMU (MakingCosmetics Inc, USA), Cosgard (Tovarna Organika, Slovenia), and bidestilled water. *Dunaliella* extract was prepared by National Institute of Biology (Piran, Slovenia) and incorporated in 120 mg / 100 g ratio. Water brine Lepa Vida was from Piranske soline, Slovenia.

Tewameter® TM 300, Corneometer® CM 825, Skin pH meter® PH 905, and Mexameter® MX 18, (all from Courage+Khazaka electronic GmbH, Germany) were used for evaluation of skin parameters before (t=0) and upon 1 and 2 week(s) of testing.

The study protocol was approved by the National Medical Ethics Committee of the Republic of Slovenia (approval numbers 0120-573/2024-2711-4 and 0120-9/2024-2711-3).

3. RESULTS AND DISCUSSION

P100

3.1. Effect on skin hydration and barrier function

Positive influence of water brine on skin barrier function was confirmed as a decrease in TEWL values was observed upon 2 weeks usage of water brine as tonic (Fig. 1). No considerable change in the skin pH or erythema index were observed, which is in line with the improvement of the skin's barrier function. Nevertheless, lower hydration values were detected when water brine was applied as the sole skin-care regimen.

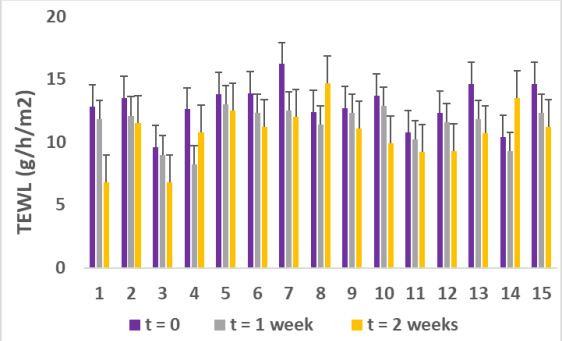

Figure 1. The influence of water brine on TEWL before (t=0) and after 1 and 2 week(s) of its usage as skin tonic on lower forearm.

Consequently, the usage of water brine with subsequent application of HC and LLCs with and without *Dunaliella* extract was also tested. Thereby the advantages of water brine used as tonic were merged with skin hydration effect of skin care formulations (Table 1). The moisturizing activity of formulations was tested by measuring stratum corneum hydration in addition to TEWL, skin pH, and erythema index. Application of HC, with and without algae extract, resulted in significantly increased hydration of stratum corneum. This effect was slightly less pronounced when water brine was first applied, however its usage is justified by its TEWL lowering effects. No significant effect on skin hydration was observed for LLCs samples. This was contrary to our expectations, as preliminary *in vitro* testing on pig˙s ear skin also resulted in improved skin hydration and lower TEWL values, which were in the same range upon applying either LLCs or HC with and without *Dunaliella* extract. In addition, significant improvement of skin barrier function as well as skin hydration was also observed when testing flaxseed and hempseed oil-based LLCs on healthy volunteers (1).

Table 1. Skin hydration values measured as Corneometer® CM 825 arbitrary units (a.u.) before and after 1 and 2-week(s) usage of unloaded HC and LLCs, and their Dunaliella extract loaded counterparts used alone (HCa; LLCa) or after prior application of water brine (HCa+b, LLCa+b).

Sample	t = 0	t = 1 week	t = 2 weeks
HC	31,7 ± 3,4	45,4 ± 3,6	53,0 ± 2,9
HCa	30,2 ± 2,6	42,8 ± 2,2	49,5 ± 2,9
LLC	31,6 ± 2,2	31,0 ± 1,7	32,2 ± 1,6
LLCa	33,4 ± 2,5	29,8 ± 2,1	32,8 ± 1,9
HCa+b	31,3 ± 3,2	36,9 ± 2,2	44,1 ± 1,8
LLCa+b	31,9 ± 2,8	29,7 ± 1,3	32,9 ± 1,8

4. CONCLUSIONS

To fully exploit the beneficial effect of water brine on the skin's barrier function, it should be best used together with emollients like conventional creams or novel delivery systems as LLCs, with or without algae extract, posing skin hydrating effect. In the future the UV-protective activity of cosmetic products with *Dunaliella* extract should also be tested to unlock its full skin care potential.

5. REFERENCES

1. Vitek, M. and Gosenca Matjaž, M., *Clinical application of hempseed or flaxseed oil-based lyotropic liquid crystals : evaluation of their impact on skin barrier function.* Acta Pharm, 2024. 74(2): 301–13.

2. Rotter, A., et al., *Marine cosmetics and the blue bioeconomy: From sourcing to success stories.* iScience, 2024. 12: 111339.

3. Havas, F., et al., A *Dunaliella salina Extract Counteracts Skin Aging under Intense Solar Irradiation Thanks to Its Antiglycation and Anti-Inflammatory Properties*. Mar. Drugs, 2022. 20(2): 104.

P101

ENABLING ADVANCED TOPICAL DRUG DELIVERY EVALUATION: A COMPARATIVE STUDY OF MICRODIALYSIS AND OPEN FLOW MICROPERFUSION SAMPLING EFFICIENCY

Laura Wiltschko[1,2], Simon Schwingenschuh[2], Peter Reisenegger[2], Stephanie Eder[1], Manfred Bodenlenz[2], Eva Roblegg[1], Thomas Birngruber[2], Reingard Raml[2]

[1]University of Graz, Institute of Pharmaceutical Sciences, Pharmaceutical Technology & Biopharmacy, Graz, Austria

[2]HEALTH – Institute for Biomedical Research and Technologies, Joanneum Research Forschungsgesellschaft mbH, Graz, Austria

1. INTRODUCTION

The development of advanced drug formulations, particularly topical delivery systems such as microneedles has highlighted the need for novel technologies capable of measuring local drug concentrations continuously and in real-time. However, accurately quantifying pharmacologically active drug concentrations within target tissues remains a challenge. Accordingly, the lack of relevant data continues to limit our understanding of pharmacokinetic/ pharmacodynamic (PK/PD) relationships at the site of action [1]. Microdialysis (MD) and open flow microperfusion (OFM) are two advanced, minimally invasive technologies that enable continuous and time-resolved sampling of interstitial fluid (ISF) in various tissues. Both technologies provide valuable opportunities for biopharmaceutical testing of novel drug formulations under *in vivo* and *ex vivo* conditions, as they offer direct measurements within the tissue and allow closer insight into the unbound, pharmacologically active drug fraction [1]. However, in MD and OFM, ISF samples obtained are diluted, resulting in the recovery of only a fraction of the true drug concentration in the tissue. This fraction is referred to as the relative recovery (RR) [2]. Translating these measured concentrations to actual tissue concentrations is challenging, especially for highly protein bound drugs. This comparative study of MD and OFM therefore aims to investigate how variations in perfusate composition, specifically the addition of binding proteins such as human serum albumin (HSA), impact the RR *in vitro* and *ex vivo*. This will help us to optimize dermal PK/PD studies [3].

2. MATERIALS AND METHODS

2.1. Model Drugs

Four drugs with varying degrees of protein binding were selected: metronidazole ($f_{(bound)}$ = -4.97 ± 10.92%), lidocaine ($f_{(bound)}$ = 9.61 ± 2.75%), methylprednisolone ($f_{(bound)}$ = 80.91 ± 1.69%) and diclofenac ($f_{(bound)}$ = 99.99 ± 2.78%).

2.2. *In vitro* MD and OFM

The *in vitro* setups involved two distinct models to simulate different diffusive resistances: 1) *In vitro* MD calibration in a stirred solution, 2) MD and OFM in an *in vitro* agar gel model with increased matrix viscosity compared to the stirred solution. For each model, four different HSA concentrations in the surrounding matrix (0, 1, 2, 4%) were tested, simulating the ISF protein concentration and four perfusates with different protein concentration (0, 1, 2, 4%), resulting in a total of 16 setups. RR were measured, and the impact of perfusate composition on the accuracy of drug sampling was evaluated.

2.3. *Ex vivo* MD and OFM

The same perfusate compositions (0, 1, 2, 4% HSA) were tested *ex vivo* in dermal tissue to translate the *in vitro* observed sampling effects to the actual target tissue.

3. RESULTS AND DISCUSSION

3.1. Impact of Perfusate Composition on Drug Sampling

In the *in vitro* solution model, highly and moderately protein-bound drugs like diclofenac and methylprednisolone exhibited a significant increase in RR when perfusates containing HSA were used (Fig. 1). For diclofenac a fivefold increase was observed when comparing

P101

perfusates with 0% HSA versus 4% HSA. This indicates that HSA influences the concentration gradient for protein-bound drugs, potentially enhancing their RR. Accordingly, it is important to consider the perfusate composition in *in vitro* MD experiments to achieve more accurate sampling profiles translatable to *ex vivo*.

3.2. Impact of Diffusion Resistance on Drug Sampling

Using the agar gel model, the influence of HSA on RR was less pronounced compared to the *in vitro* solution, likely due to increased diffusion resistance in the gel. The gel's higher viscosity and tortuosity reduced the ability of drugs to diffuse into the perfusate, emphasizing the need to consider diffusion resistance when interpreting data from more complex tissue matrices. This also points to the importance of matching the sampling technology to the tissue environment, as different sampling technologies may perform better in certain matrices. Tailoring MD and OFM protocols to account for these factors can improve the sampling process, improving the precision of drug concentration measurements and supporting better therapeutic decisions.

3.3. *Ex vivo* dermal Drug Sampling

In the ex vivo human skin model, the drug sampling with both MD and OFM was less sensitive to variations in HSA concentration compared to in vitro conditions. This highlights a key limitation of using in vitro RR values for extrapolating to *ex vivo* or *in vivo* drug concentrations. Notably, OFM achieved the highest RR when the perfusate protein content closely matched physiological ISF protein levels. Moreover, due to its membrane-free exchange interface, OFM enabled sampling of higher concentrations of protein-bound drugs than MD, suggesting that it may be particularly advantageous for monitoring highly protein-bound compounds. These findings suggest that careful optimization of perfusate composition and sampling parameters is essential for improving the accuracy of local drug concentration measurements, ultimately contributing to more effective and individualized pharmacotherapy strategies.

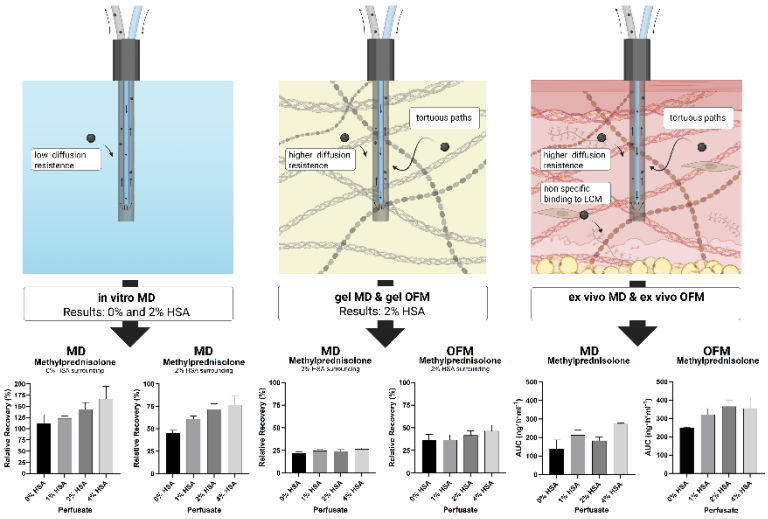

Figure 1. Exemplarily results of the RRs of the moderately protein bound methylprednisolone in the three different models, including the in vitro MD in a stirred solution, MD and OFM in an in vitro agar and MD and OFM in ex vivo dermis.

4. CONCLUSION

Our detailed evaluation of in vitro an *ex vivo* sampling efficiency of MD and OFM helps to select an appropriate combination of sampling technologies and perfusate composition in *ex vivo* and *in vivo* PK/PD studies of topical drug formulations. For both sampling methods a perfusate composition similar to the ISF protein concentration can be suggested to obtain stable sampling. Moreover, special attention should be paid when comparing sampling between various tissues with different diffusive resistances as well as *ex vivo/in vivo* and *in vitro* setups.

5. REFERENCES

1. Holmgaard, R. et al., Comparison of open-flow microperfusion and microdialysis methodologies when sampling topically applied fentanyl and benzoic acid in human dermis ex vivo., Pharm Res 29 (2012)

2. Bodenlenz, T. et al, Comparative Study of Dermal Pharmacokinetics Between Topical Drugs Using Open Flow Microperfusion in a Pig Model, Pharm Res 41 (2024)

3. Wiltschko, L. et al, Impact of protein binding on drug sampling by microdialysis and open flow microperfusion, Journal of Drug Delivery Science and Technology (2025) (in press)

P102

EXTENDING ANALYSIS OF PARETO OPTIMALITY TO THE ANTIBODY-ANTIGEN INTERFACE

Tadej Medved[1,2], Goran Miličić[1], San Hadži[2]

[1]*Biologics Drug Product Development, Novartis LLC, Slovenia*
[2]*Faculty of Chemistry and Chemical Technology, University of Ljubljana, Slovenia*

1. INTRODUCTION

A constant challenge in the field of biologics drug product development is the multi-objective optimization of various developability properties, such as conformational, colloidal and chemical stability. Optimization of these properties should not compromise the function of the molecule, which in the case of antibody-based therapeutics is the binding to the target antigen [1]. The binding process can be considered as a trade-off between two underlying thermodynamic contributions observed in the form of enthalpy and entropy. Structural characteristics of the binding interface that define whether binding is enthalpically or entropically driven are still not completely understood. Understanding the structural features that define the thermodynamic driving force of high-affinity binding could in turn guide the optimization of developability properties without detrimental effect to antibody's primary function.

To this end, we expanded the Pareto Task Inference method [2], which has already been applied to biological entities under selective pressure determined by performance at two or more biologically relevant tasks. Under the Pareto theory of optimality [2, 3], entities that have withstood selective pressure by optimizing such trade-offs are distributed inside low-dimensional polytopes ("Pareto fronts") in a high-dimensional space defined by relevant features, and the vertices of these polytopes correspond to "archetypes", specific feature combinations from which the relevant tasks can be inferred [3].

As a proof of concept, we determined Pareto-optimal trade-offs between camelid single-chain antibodies (nanobodies) bound to their respective antigens and correlated those with the enthalpic-entropic compensation associated with antigen binding, while also assessing the distributions of structural features that could pose a higher developability risk.

2. MATERIALS AND METHODS

2.1. Dataset preparation

Our dataset was comprised of 67 unique nanobody-antigen interfaces found in published crystal structures, with the additional requirement of available experimentally measured K_d and ΔH_b of binding measured via ITC.

2.2. Feature calculation

Each interface was assigned a vector of handcrafted structural features sorted into 3 distinct groups: **1)** specific contact features (H-bonds, salt bridges, vdW interactions), **2)** geometric features (buried surface area, interface curvature, shape complementarity), and **3)** physicochemical features (electrostatic and chemical complementarity, flexibility at the interface). All features were normalized by the interface area and highly correlated pairs of features with a Spearman $\rho > 0.7$ were removed.

2.3. Pareto Task Inference

A custom version of the existing Pareto Task Inference [2] algorithm was used to find putative Pareto-optimal trade-offs between the interface structural features. Briefly, the high-dimensional feature set was reduced to 2 or 3 dimensions with PCA, and putative Pareto fronts were fitted with the Sisal and MVSA [2] algorithms. The statistical significance of each fit was assessed with the t-ratio test [2, 3], which compared the tightness of fit of the chosen polytope against 10,000 reshuffled datasets. The significance cutoff p-value was set to 0.05. Enrichments of individual features and thermodynamic measurements were computed for each putative archetype by Spearman correlation between the feature value and the Euclidean distance from the corresponding archetype in principal component space. Only statistically significant ($p \leq 0.05$) enrichments after FDR correction, as well as a Spearman ρ above the cutoff value 0.3, were considered in the final analysis.

3. RESULTS AND DISCUSSION

P102

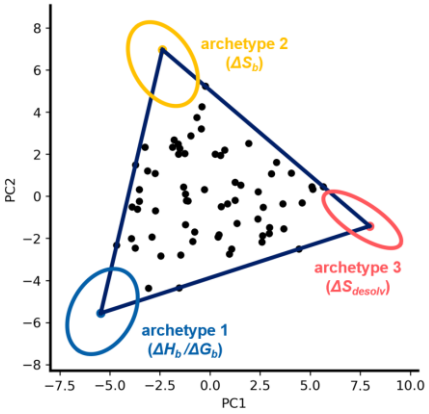

Figure 1. Statistically significant Pareto front (dark blue) with 3 archetypes (vertices) in principal component space of nanobody-antigen interface features. The convex hull of dataset is shown in red, and the vertex positional errors (95 % CI) are depicted as ellipses and colored corresponding to their vertices.

Our approach identified a statistically significant fit (p = 0.01, t-ratio = 1.25) of a triangular Pareto front in the space defined by the first 2 principal components (Fig. 1). The three putative archetypes were first annotated by calculating enrichments of the experimental ΔH_b, ΔS_b, ΔG_b and the normalized enthalpicity $\Delta H_b/\Delta G_b$ as well as the theoretically calculated desolvation entropy ΔS_{desolv}. The latter was estimated from the change in polar and nonpolar solvent accessible surfaces. For the first archetype, we observed significant enrichment of $\Delta H_b/\Delta G_b$ (ρ = -0.336) and annotated it as the **enthalpy** archetype. The second archetype was enriched in ΔS_b (ρ = -0.385) as well as ΔH_b (ρ = -0.392), highlighting a favourable entropic contribution at the expense of the binding enthalpy, and was subsequently termed the **entropic** archetype. The third archetype was enriched only in ΔS_{desolv} (ρ = -0.626) and was termed the **hydrophobic entropy** archetype. ΔG_b, however, was not enriched at any archetype, leading us to postulate that the observed Pareto front is a reflection of three different strategies of achieving high binding affinity, as all nanobodies within the dataset maintain a K_d in the sub-micromolar range. We also determined the physicochemical feasibility of the above enrichments by analysing which interface features are coenriched or depleted at the same archetype. The **enthalpy** archetype was enriched in density of polar contacts, H-bonds, and secondary structure propensity, showing that the interfaces at this archetype are conformationally constrained with a greater optimization of specific contacts. The **entropy** archetype was enriched in the interface B-factor value as well as depleted in the density of heavy-atom contacts and secondary structure propensity – interfaces at this archetype typically consist of more flexible loops, and the prevailing strategy appears to be minimization of the conformational entropic penalty incurred upon binding. The **hydrophobic entropy** archetype is likewise explained by coenrichments of normalized hydrophobic interface area and the density of nonpolar contacts, pointing to interface desolvation as the main driver of binding in this case.

4. CONCLUSION

We have identified a Pareto-optimal trade-off between interface features of single chain antibodies and their three possible thermodynamic strategies of achieving high binding affinity. The archetypes, however, are not equivalent in terms of other developability properties – the **hydrophobic entropy** archetype, for example, is enriched in hydrophobic interface patches which could result in increased aggregation risk or polyspecificity. For such proteins, the Pareto front could be used in the future as an additional constraint for rational redesign – both as a reference for mutations that could guide the protein closer to another archetype with better developability criteria, and as a cutoff ensuring that any proposed mutants retain optimal-like interface properties that would be less likely to impact their affinity, reducing the attrition rate in candidate reengineering or selection.

5. REFERENCES

1. Zhang, W., et al., *Developability assessment at early-stage discovery to enable development of antibody-derived therapeutics.* Antibody therapeutics, 2023. 6(1): 13-29.
2. Hart, Y., et al., *Inferring biological tasks using Pareto analysis of high-dimensional data*. Nature Methods, 2015. 12(3): 233-235.
3. Shoval, O., et al. *Evolutionary Trade-Offs, Pareto Optimality, and the Geometry of Phenotype Space*. Science, 2012. 336(6085): 1157-1160.

ACKNOWLEDGMENT

The authors acknowledge financial support from Novartis LLC and thank colleagues at both Novartis and the Faculty of Chemistry and Chemical Technology, UL for their invaluable contributions.

P103

EVALUATION OF TETRACOSACTIDE PEPTIDE IN GALENIC FORMULATIONS FOR RAPID ADRENOCORTICOTROPHIC HORMONE STIMULATION TEST

Aleksandra Bračko[1], Janez Ilaš[2]

[1]*Hospital Pharmacy of University Medical Centre Maribor, Slovenia*
[2]*Faculty of Pharmacy, University of Ljubljana, Slovenia*

1. INTRODUCTION

In Slovenian hospitals and outpatient clinics, tetracosactide solution with a concentration of 5 µg/ml is most often prepared in a glass vial. In 2016, the Central Pharmacy of the University Medical Centre Maribor started with the aseptic preparation of tetracosactide solution filled in syringes at the request of hospital departments. The industrial drug was diluted in sodium chloride solution under aseptic conditions. The reason for its widespread use lies in its simple execution using a pre-filled syringe containing precisely 1 µg of tetracosactide solution. Until the year 2016, we prepared a 5 ml solution with a concentration of 5 µg/ml in glass vials. Based on a literature data we set a shelf life of three months from the date of production for the solution filled in plastic syringe. The solution in glass vials has a shelf life of four months (1). We wanted to confirm this shelf life with several analytical methods.

2. MATERIALS AND METHODS

We stored the sample solution of tetracosactide with a concentration of 5 µg/ml, filled in glass and plastic containers, for five months under various conditions. We performed the analysis using the Qubit 4 fluorometer, the Bradford method and method based on ultra-high-performance liquid chromatography coupled to high-resolution mass spectrometry (UHPLC–HRMS).

The first two relatively simple methods, Qubit 4 fluorometer, the Bradford method, did not provide the desired results. We assume that these methods were not sensitive enough for our sample with a concentration of 5 µg/ml. In the end, we used the UHPLC-HRMS analysis, which proved to be sensitive and highly selective.

3. RESULTS AND DISCUSSION

First, we focused on the identification of our peptide and its main impurities. Using the Protein Deconvolution program (2), we identified the molecule of tetracosactide and its 11 impurities. The peptide molecule has eight basic centers in its structure, so both tetracosactide and each impurity were differently charged in an acidic medium, specifically +3, +4, +5, +6, +7, and +8. The distribution of similarly charged molecules of tetracosactide and impurities among the samples is very similar, with the highest proportion represented by molecules with a charge of +6.

In the final part, a quantitative evaluation of all the acquired signals followed. We utilized two specific programs, Thermo FreeStyle and Thermo Xcalibur (3, 4), to integrate the signals and obtain important data about the area under the curve (AUC). Based on the obtained results and certain professional articles (1), we concluded that the solution of tetracosactide remains stable for at least 127 days in a glass container stored in the refrigerator and in darkness, as the AUC of tetracosactide dropped to 99%. However, the solution in a plastic container stored under the same conditions remains stable for 66 days, with an AUC of 83% for tetracosactide on that day. Among impurities, the highest proportion was represented by impurity with mass +16 (tetracosactide sulfoxide), and oxidation led to the formation of several other impurities with masses: +32, +48, and +64.

P103

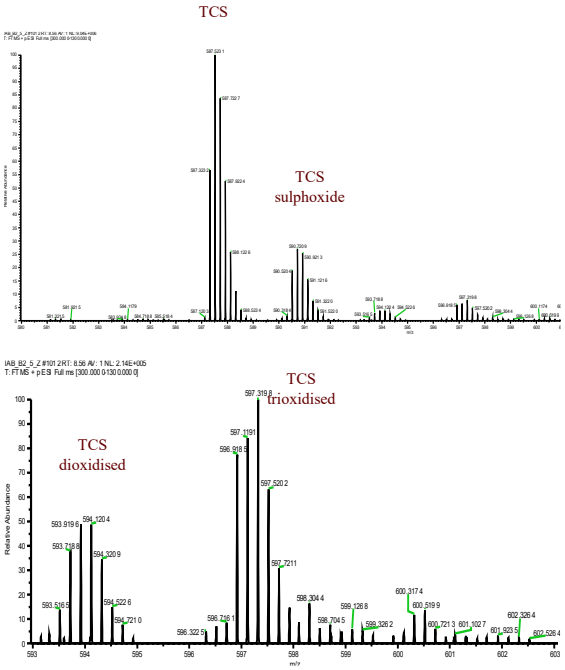

Figure 1.: Tetracosactide (TCS) and its impurities with a charge +5 analyzing with HRMS,

4. CONCLUSION

To perform a rapid ACTH test, it is sufficient to load the patient with 1 µg of TCS. The article describes pharmacopoeial method for the evaluation of TCS and describes the use of state-of-the-art analytical methods that could potentially be used to evaluate TCS final preparations.

5. REFERENCES

1. Dickstein G, Shechner C, Nicholson W.E, Rosner I, Shen-Orr Z, Adawi F, Lahav M. Adrenocorticotropin Stimulation Test: Effects of Basal Cortisol Level, Time of Day, and Suggested New Sensitive Low Dose Test. Journal of Clinical Endocrinology 1991; 72; 773-778.

2. TermoFisher Scientific. Protein Deconvolution. User Guide, 2014. Dostopno dne 10.05.2023 na: https://assets.thermofisher.com/TFS-Assets/CMD/manuals/Man-XCALI-97576-Protein-Deconvolution-30-User-ManXCALI97576-A-EN.pdf.

3. TermoFisher Scientific. Freestyle Software Support. Dostopno dne 20.5.2023 na: https://www.thermofisher.com/si/en/home/technical-resources/technical-reference-library/mass-spectrometry-support-center/liquid-chromatography-mass-spectrometry-software-support/freestyle-software-support/freestyle-software-support-getting-started.html.

4. TermoFisher Scientific. Xcalibur Data Acquisition and Interpretation Software. Dostopno dne 20.5.2023 na: https://www.thermofisher.com/si/en/home/industrial/mass-spectrometry/liquid-chromatography-mass-spectrometry-lc-ms/lc-ms-software/lc-ms-data-acquisition-software/xcalibur-data-acquisition-interpretation-software.html.

P104

GREEN SILICA-BASED HPLC METHOD FOR QUANTIFICATION OF CEPHALEXIN IN CAPSULES USING DIMETHYL ISOSORBIDE AS A BIO-RENEWABLE SOLVENT

Aleksandra Damjanoska[1,2], Stefan Radevski[2], Cveta Dolikjoska Trajkova[2], Katerina Brezovska[1], Jasmina Tonikj-Ribarska[1], Natalija Nakov[1]

[1]Institute of Applied Chemistry and Pharmaceutical Analysis, Faculty of Pharmacy, Ss Cyril and Methodius University in Skopje, Republic of North Macedonia

[2]Manufacturing Technical Operations, ALKALOID AD, Republic of North Macedonia

1. INTRODUCTION

In response to the growing demand for sustainable analytical practices [1], there has been a notable shift towards greener methodologies in analytical chemistry. Conventional high-performance liquid chromatography (HPLC) often relies on hazardous organic solvents, which pose environmental and health risks. The adoption of alternative, more sustainable approaches is thus becoming essential. This silica-based method [2], leveraging dimethyl isosorbide (DMI) as a bio-renewable solvent, presents an innovative solution. DMI is a versatile, eco-friendly solvent that significantly reduces the reliance on toxic organic solvents. The methodology closely aligns with per aqueous liquid chromatography (PALC), a technique that prioritizes water-based solvents for enhanced environmental safety [3]. This study presents the development of a green HPLC method for the quantitative determination of cephalexin in cephalexin capsules.

2. MATERIALS AND METHODS

2.1. Materials

DMI (≥99%, BioRenewable, ReagentPlus®) was sourced from Sigma Aldrich. Methanol (HPLC grade, ≥99%), Acetonitrile (HPLC grade, ≥99%), Heptane-1-sulfonic acid sodium salt (LiChropur™ for ion pair chromatography), Triethylamine (≥99%), and ortho-Phosphoric acid 85% (EMSURE® for analysis) were from Merck KGaA Darmstadt, Germany. The cefalexin in-house secondary reference standard and the formulation analyzed (Cefalexin 500 mg hard capsules), were supplied by Alkaloid AD Skopje.

2.2. Conventional in-house method

The chromatographic separation was conducted on an XTerra RP-18 column (150 mm × 4.6 mm, 5 µm). The mobile phase consisted of a pH 3.0 buffer, methanol and acetonitrile in a volume ratio of 85:5:10 (% v/v/v). The flow rate was maintained at 1.0 mL/min, with an injection volume of 20 µL. Detection was performed at a wavelength of 254 nm and the column was operated at ambient temperature. The method was developed in-house and validated according to ICH Q2 guidelines [4].

2.3. Green method using DMI as an eluent

The chromatographic separation was conducted on a Silica Spherisorb column (250 mm × 4.6 mm, 5 µm). The mobile phase consisted of a 0.5% acetic acid solution and DMI in a volume ratio of 90:10 (% v/v). The flow rate was maintained at 1.5 mL/min, with an injection volume of 5 µL. Detection was performed at a wavelength of 254 nm and the column was operated at 50°C.

3. RESULTS AND DISCUSSION

The approach utilized in the green method is innovative, as it replaces the conventional toxic non-polar mobile phases with an eco-friendly mobile phase composed of 90% diluted acetic acid (0.5% v/v) and DMI as a bio-renewable organic solvent. This change aligns with the principles of green chemistry, offering a more sustainable solution for chromatographic analysis without compromising the efficiency or reliability of the results.

Table 1. Comparison of chromatographic performance between conventional and green method for determination of cephalexin in Cefalexin capsules.

Parameter	Conventional Method	Green Method
Retention Time (RT) (minutes)	6.9	5.5
Total Runtime (minutes)	12	8

P104

Capacity Factor (k')	3.2	1.9
Column Backpressure (bar)	174	194
Theoretical Plates (N)	3251	9126
Symmetry Factor (As)	1.3	1.2

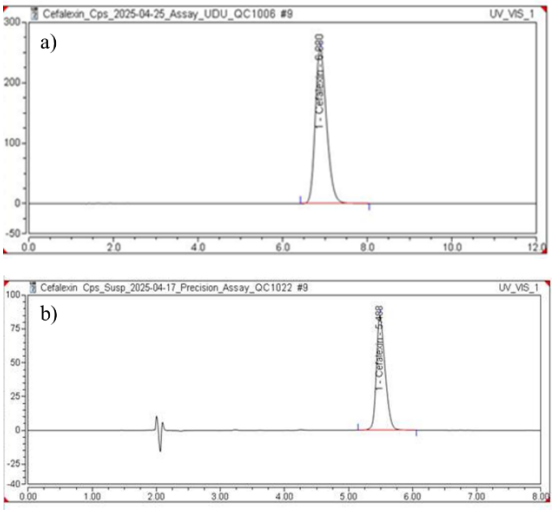

Figure 1. Chromatograms of a sample solution obtained with: a) conventional method, b) green method.

The obtained results demonstrate significant improvements in chromatographic performance and environmental sustainability with the green method, compared to the conventional method (Table 1, Figure 1). Notably, the green method yields a shorter retention time compared to the conventional method. This reduction contributes to enhanced sample throughput, allowing for faster analysis and, consequently, a decrease in solvent consumption and overall resource usage. Additionally, the total runtime is shorter in the green method compared to the conventional, further reinforcing its efficiency. The capacity factor (k') for the green method is lower, indicating faster migration of analytes through the stationary phase. This could be attributed to the unique properties of the polar stationary phase used in the green method, which allows for more efficient separation, despite the lower k' value. However, the column efficiency, measured by the theoretical plates (N), is significantly higher in the green method compared to the conventional method, demonstrating a more effective separation process. While the column backpressure in the green method is slightly higher than in the conventional method, the difference is minimal and does not affect the method's applicability. This increase is likely due to the higher flow rate used in the green method, but it remains within acceptable limits for the silica column. The symmetry factor (As) for both methods is similar, with the green method showing a slight improvement over the conventional method, which suggests comparable peak shapes and thus equivalent accuracy and reproducibility of results.

4. CONCLUSION

The method using DMI as a bio-renewable, non-toxic solvent in conjunction with a silica column demonstrates reliable analytical performance while significantly reducing the negative environmental impact and analyst exposure to toxic reagents. Given the widespread use of cephalexin and the increasing emphasis on green chemistry, this method offers a practical and eco-conscious alternative for routine pharmaceutical quality control.

5. REFERENCES

1. Shaaban, H., et al., New Insights into Liquid Chromatography for More Eco-Friendly Analysis of Pharmaceuticals. *Anal. Bioanal. Chem.*, 2016, 408(25): 6929–6944.

2. Sobańska, A. W., et al., Emerging or Underestimated Silica-Based Stationary Phases in Liquid Chromatography. *Crit. Rev. Anal. Chem.*, 2020: 1–25.

3. Santos, A. L. R., Carvalho, G. O., Faria, A. M., et al., Per-Aqueous Liquid Chromatography Stationary Phase with Poly(Ethylene Oxide-Co-Dimethylsiloxane) Immobilized on Mesoporous Aluminized Silica Support. *Microporous Mesoporous Mater.*, 2023, 356: 112608.

4. ICH Harmonised Guideline: Validation of Analytical Procedures Q2(R2); Final Version, 1 November 2023.

ACKNOWLEDGMENT

The authors acknowledge the pharmaceutical company ALKALOID AD Skopje, R. North Macedonia for their support and provision of resources for this research.

P105

REALISTIC SIMULATIONS OF GASTRIC EMPTYING VARIABILITY ON A POPULATION LEVEL USING COMPASS™ SOFTWARE

Dorota Danielak[1], Michał Romański[2], Maciej Winiarski[3], Grzegorz Banach[1], Jadwiga Paszkowska[1], Marcela Staniszewska[1], Michał Smoleński[1], Justyna Dobosz[1], Grzegorz Garbacz[1]

[1]Physiolution Polska, 74 Piłsudskiego St., 50-020 Wrocław, Poland

[2]Department of Physical Pharmacy and Pharmacokinetics, Poznan University of Medical Sciences, Poznań, Poland

[3]Institute of Low Temperature and Structure Research, Polish Academy of Sciences, Wrocław, Poland

1. INTRODUCTION

The performance of the immediate-release (IR) oral dosage form may depend on the variability of gastric emptying (GE). Under fasting conditions, GE may be described by the rate the gastric fluid flows out of the stomach (k_{GE}) and the timing of the "housekeeping wave" (GET). Maximum plasma drug concentrations (C_{max}) or area under the time-concentration curve (AUC) may differ, depending on the k_{GE} and GET combinations. For example, rapid k_{GE} = 14 1/h and early GET = 0.25 h would lead to a higher C_{max} than when the gastric emptying was slow (k_{GE} = 3 1/h and GET = 2 h). However, some of these combinations are more probable than others, and some distinct types of GE patterns were proposed [1]. To address this, we developed a novel module for the COMPASS software [2]. Its novelty is introducing the prevalence of the GE emptying patterns on a population level, as proposed earlier [1].

We describe the working principles of the module using two ritlecitinib formulations as an example: one 100 mg capsule (Reference) vs. two 50 mg capsules (Test). In the virtual bioequivalence trial, these formulations were assessed as bioequivalent [3].

2. MATERIALS AND METHODS

2.1 Software

COMPASS is a Python-based tool with an intuitive user interface, and its performance was evaluated earlier [2]. It allows a straightforward translation of the in vitro dissolution profiles to reliable PK simulations. In the interface, the user provides the values of effective permeability (P_{eff}), volumes of distributions (V1/F, V2/F), and clearances (CL/F, Q/F). In the novel module, the user defines the study group size and respective between-subject variabilities (BSV). The algorithm creates virtual subjects with varying PK parameter values, and assigns them to one of the four GE types: "Sprint", "Average", "Tight, or "Lazy" (Table 1).

Table 1. COMPASS GE motility types

GE type	k_{GE} [1/h]	GET [h]	Prevalence [%]
Sprint	3 - 14	≤ 0.25	27
Tight	3	0.25 < & ≤ 0.75	22
Average	3 - 14	0.25 < & ≤ 0.75	31
Lazy	2	0.75 < & ≤ 2	20

2.2. Dissolution and PK data

Dissolution data were taken from the literature [3]. PK parameters and the whole workflow, including dissolution curve fitting, were the same as described earlier by Danielak et al. [2].

2.3. GE motility patterns module setup

Simulations were performed for 100 virtual subjects. The BSV was set to the values reported previously [1].

3. RESULTS AND DISCUSSION

3.1. Influence of GE patterns on predicted PK profiles

"Sprint" and "Average" motility patterns led to the highest predicted ritlecitinib plasma concentrations for both Reference and Test products (Fig. 1).

P105

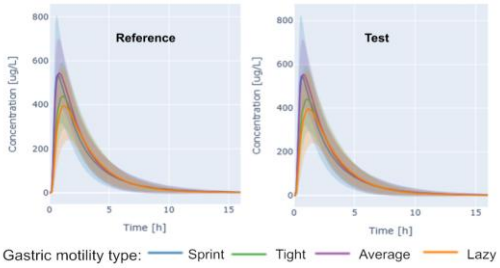

Figure 1. Influence of GE patterns on ritlecitinib plasma profiles for Reference and Test products (n = 100).

3.2. Variability of predicted C_{max} and AUC

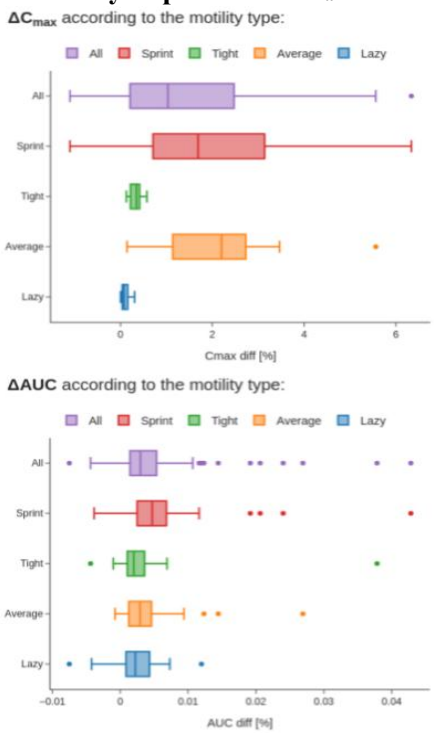

Figure 2. Relative C_{max} and AUC differences between Test and Reference products (n = 100).

Fig 2. shows the relative differences of C_{max} and AUC pooled for all 100 virtual subjects ("All") and split into GE motility types. The "Average" motility type produced the highest median ΔC_{max}, but the greatest differences (over 6%), were observed for the "Sprint" type. For AUC the differences were negligible, due to good and complete ritlecitinib absorption from the intestine. Table 2 shows that the mean predicted C_{max} was similar to the observed one. The differences for AUC and T_{max} can be attributed to a small study group size.

3.3. Comparison with the standard COMPASS output

Fig 3. compares how the standard COMPASS module and the novel one evaluate the influence of GE. The standard module systematically analyzes 100 combinations of k_{GE} and GET (visualized as a 3D plane) without weighting their probabilities for a subject with typical PK parameters. The novel module focuses on the physiologically plausible k_{GE} and GET combinations and includes the BSV of the PK parameters.

Table 2. Comparison of the observed (n = 6) [4] and simulated (n=100) ritlecitinib PK parameters. For C_{max} and AUC, data are shown as geometric means with a geometric CV. For T_{max} data are shown as medians with range.

Source	C_{max} [µg/L]	AUC_{inf} [µg*h/L]	T_{max} [h]
Observed	647.7 (24)	1085 (23)	0.5 (0.5 - 0.617)
Simulated	500.6 (37.4)	1404 (35.7)	1 (0.5 - 3.5)

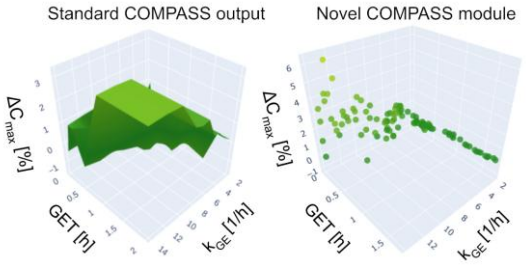

Figure 3. C_{max} similarity evaluation with the standard COMPASS module vs. the novel GE variability module (n = 100).

4. CONCLUSION

The novel COMPASS module realistically simulates the endpoint PK parameters and their variabilities, including physiologically plausible k_{GE} and GET combinations.

5. REFERENCES

1. Romański M, et al. More Than a Gut Feeling─A Combination of Physiologically Driven Dissolution and Pharmacokinetic Modeling as a Tool for Understanding Human Gastric Motility. Mol Pharm. 2024;21:3824–37.
2. Danielak D, et al. Compare and PASS − Fast screening of oral dosage forms for bioequivalence probability with the COMPASS software. Int J Pharm. 2025;670:125123.
3. Saadeddin A, et al. Virtual Bioequivalence Assessment of Ritlecitinib Capsules with Incorporation of Observed Clinical Variability Using a Physiologically Based Pharmacokinetic Model. AAPS J. 2024;26:17.
4. Center for Drug Evaluation and Research. 215830Orig1s000, Multidiscipline review Available from:https://www.accessdata.fda.gov/drugsatfda_docs/nda/2023/215830Orig1s000MultidisciplineR.pd

P106

MONITORING THE EFFECT OF POLYVINYLPYRROLIDONE ON THE PRECIPITATION BEHAVIOUR OF A MODEL DRUG

Tjaša Felicijan[1], Marija Bogataj[1]

[1]*University of Ljubljana, Faculty of Pharmacy, Department of Biopharmaceutics and Pharmacokinetics, Slovenia*

1. INTRODUCTION

Generating and maintaining a supersaturated state is one of the methods often used in drug formulation to overcome challenges related to poor aqueous solubility of drugs [1]. The concentrations of the dissolved drug that exceed solubility in the supersaturated state should be maintained long enough for the absorption to occur and, therefore, influence the bioavailability. Due to the high tendency for drug precipitation from a supersaturated state, the "parachute" approach is frequently applied, where the excipients added into the supersaturating drug delivery systems delay or inhibit drug precipitation [2]. Precipitation can be inhibited thermodynamically by increasing drug solubility or kinetically by adding a polymer that can influence drug nucleation or crystal growth [3].

Several mechanisms of precipitation inhibition by polymers were described in the literature, and the effect of polymers is often drug-specific. Therefore, this study aimed to assess the influence of polyvinylpyrrolidone on the precipitation behavior of a model drug, diclofenac sodium. Within this work, the precipitation of the selected model drug from a supersaturated solution was induced by pH shift and monitored by UV-Vis spectroscopy and laser diffraction method.

2. MATERIALS AND METHODS

2.1. Fundamentals of precipitation experiment

A model drug, diclofenac sodium (DF-Na, Merck KGaA, Germany), was dissolved in purified water without or with added polymer, polyvinylpyrrolidone (PVP, Kollidon® 17 PF, BASF, Germany). The concentration of the drug in the aqueous solution was 200 mg/L, while the concentration of the polymer was 0.003% or 0.1% (m/V%). The drug precipitation in experiments was initiated by the pH-shift method, i.e., by adding 1 M HCl, prepared from Titrisol® concentrate (Merck KGaA, Germany), in a suitable volume to obtain a final HCl concentration of 0.001 M.

2.2. UV-Vis spectroscopy measurements

The precipitation experiments were performed in a beaker with 100 mL of drug or drug/polymer solution, stirred at 100 rpm with a magnetic stirring bar. After acidification, inducing drug precipitation, absorption spectra were measured at different time points using the fiber optic dip probe with a 5 mm path length attached to a UV-Vis spectrophotometer (Cary 60, Agilent Technologies, USA). The spectra were obtained in a wavelength range from 800 to 200 nm with a wavelength step of 2 nm and a measurement speed of 800 nm/min. The concentration of the dissolved drug was calculated from the absorbances at the drug's maximum wavelength (276 nm), corrected by the absorbances at a wavelength of 400 nm. Such correction was used to mitigate the effect of particles on the obtained UV-Vis spectra.

2.3. Particle size analysis

100 mL of DF-Na solution in purified water without or with polymer was poured into the beaker of the Mastersizer S laser diffraction instrument with a 300RF lens (Malvern Panalytical, UK). The solution was stirred constantly at a rate of 1200 rpm. Precipitation was induced by solution acidification. The volume distribution of particle sizes was then obtained from measurements at predetermined time points using the pre-set combination of refractive indexes: 1.596, 0.100, and 1.330, and the material density of 1.4 g/mL.

3. RESULTS AND DISCUSSION

The concentrations of the dissolved drug in experiments without or with added polymer are presented in Figure 1.

P106

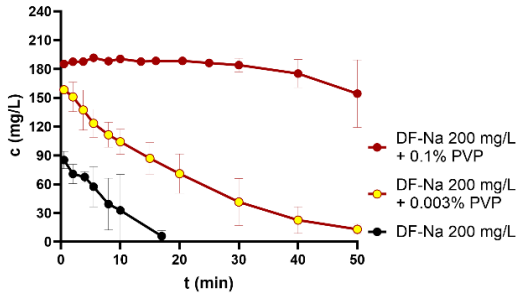

Figure 1. The concentration of the dissolved drug in experiments without and with added PVP. The average of three replicates and standard deviations are presented.

The dissolved drug concentration decreased fast after precipitation was initiated in an experiment without polymer, and the amount of dissolved drug decreased continuously during the experiment. The addition of PVP decreased the precipitation rate, and the inhibitory effect of PVP was concentration-dependent. At 0.1% PVP, the dissolved drug concentration decreased only minimally within the first 40 minutes of the experiment compared to the initial drug concentration.

Furthermore, precipitation behavior was also monitored by measuring particle size using the laser diffraction method, and the particle size distributions are presented in Figure 2.

Fast precipitation in experiments without added polymer was also observed from the particle size analysis. At early times, the main peak in volume distribution was observed at nanometer sizes. During the experiment, the peak at nanometer sizes decreased, whereas a peak at micrometer sizes appeared and subsequently increased. However, such a typical transition was not observed in experiments with added PVP, where the particle size distribution was more heterogeneous at all time points, and the changes in particle size distribution occurred over a longer period of time.

4. CONCLUSION

The inhibitory effect of PVP on precipitation from DF-Na supersaturated solution was observed from UV-Vis spectra as well as from the particle size analysis.

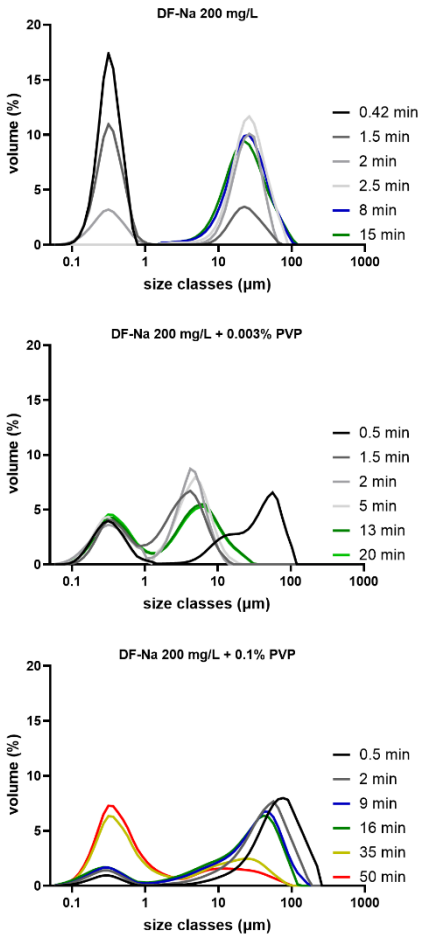

Figure 2. Particle size distributions in experiments without or with added PVP. The volume distributions at selected time points of a single replicate at each condition are presented.

5. REFERENCES

1. Williams, H.D., et al., *Strategies to address low drug solubility in discovery and development*. Pharmacological Reviews, 2013. 65(1): 315–499.
2. Guzmán, H.R., et. al., *Combined use of crystalline salt forms and precipitation inhibitors to improve oral absorption of celecoxib from solid oral formulations*. Journal of Pharmaceutical Sciences, 2007. 96(10): 2686–702.
3. Xu, S. et. al., *Drug precipitation inhibitors in supersaturable formulations*. International Journal of Pharmaceutics, 2013. 453(1): 36–43.

ACKNOWLEDGMENT

The authors acknowledge the Slovenian Research Agency for financial support (grant number P1-0189).

P107

EVALUATION OF THE THIAMINE CONTENT IN EXTRACTS OF *VERBASCUM* SPECIES

Maja Grigorov[1], Slavica Sunarić[2], Dragana Pavlović[1]

[1]Department of Pharmacy, Faculty of Medicine, University of Niš, Niš, Serbia
[2]Department of Chemistry, Faculty of Medicine, University of Niš, Niš, Serbia

1. INTRODUCTION

The genus *Verbascum* L., whose species are commonly known as "mullein", is one of the largest genera of the family Scrophulariaceae [1]. The Committee on Herbal Medicinal Products at the European Medicines Agency (HMPC/EMA) recommends the use of *Verbasci flos* from *V. thapsus* L., *V. densiflorum* Bertol. (*V. thapsiforme* Schrad) and *V. phlomoides* L. flowers for respiratory disorders [2]. However, folk medicine recommends the use of the entire aerial parts of *Verbascum* species for the treatment of skin inflammations, wounds, and other dermatological problems [3]. Since all these activities are related to the chemical constituents of the plants, many different compounds have been identified in *Verbascum* species [3]. However, we have not found any literature data about their vitamin content.

Thiamine, also known as vitamin B1, is an essential nutrient that is important for the proper functioning of the nervous system, heart and muscles as well as for general health [4]. Therefore, its content in different plant extracts could contribute to the health effects of these products. Hence, we aimed to determine the thiamine content in different extracts of three *Verbascum* species.

2. MATERIALS AND METHODS

2.1. Materials

The leaves of *Verbascum* species were collected in summer near Bosilegrad, Southeast Serbia. The extracts were prepared from the dried material (**Fig. 1**) by percolation with 50% ethanol or distilled water according to European Pharmacopeia 11.0 (2022) [5]. Approximately 0.1 g of the dry extracts were dissolved in 2 mL of 96% ethanol and 0.5 mL of distilled water. 1 mL of the obtained liquid extract was derivatized with 400 µL 1% potassium ferricyanide in a 15% sodium hydroxide mixture. After vortex mixing, the insoluble precipitate was removed by centrifugation. An aliquot of the resulting supernatant was filtered through a cellulose membrane syringe filter prior to HPLC analysis.

2.2. Method

The Agilent Technologies 1200 Series apparatus (Santa Clara, CA, USA) with fluorescence detector was used for the detection and quantification of thiamine. The separation was performed on Zorbax Eclipse plus C18 solvent saver analytical column (3.0 mm × 150 mm, 3.5 µm) at 30 °C. The mobile phase consisting of 40.0% (v/v) methanol and 60.0% (v/v) 0.005 M NH_4Ac (pH 5.0) was pumped isocratically. The fluorescence detector was programmed to an excitation wavelength of 370 nm and an emission wavelength of 435 nm (optimal wavelengths for thiochrome). Identification was performed with a standard and the chromatograms were recorded under the same conditions.

Figure 1. Dried leaves of *Verbascum* species

3. RESULTS AND DISCUSSION

According to our results, thiamine was detected in four out of six extracts tested. Thiamine was not detected in the ethanol extracts of *Verbascum niveum* (VNE) and *Verbascum phlomoides* (VPE). The amounts detected

ranged from 0.44 µg/g to 2.34 µg/g of dry extract, with the highest amount detected in *Verbascum phlomoides* water extract (VPH) and the lowest in *Verbascum niveum* water extract (VNH). Of the three species tested, *Verbascum speciosum* was the only one that contained thiamine in both extracts, ethanol and water, with the water extract (VSH) containing a higher amount.

The idea is to use these extracts to prepare creams for topical application (as mullein is traditionally used for skin problems). As vitamins are increasingly recommended for better skin, hair and nails, the vitamins in the mullein extracts could contribute to their positive effects on the skin and skin appendages.

Table 1. Thiamine content in µg/g of dry extract

Sample	VNE	VSE	VPE	VNH	VSH	VPH
Thiamine content	/	0.93	/	0.44	1.80	2.34

[1]**VNE** – *V. niveum* ethanol extract, [2]**VSE** – *V. speciosum* ethanol extract, [3]**VPE** – *V. phlomoides* ethanol extract, [4]**VNH** – *V. niveum* aqueous extract, [5]**VSH** – *V. speciosum* aqueous extract, [6]**VPH** – *V. phlomoides* aqueous extract

4. CONCLUSION

This work pointed out thiamine is present in most of the extracts tested. However, the vitamin content in mullein extracts still needs to be investigated in more detail.

5. REFERENCES

1. Stan, R.L., Vicaș, L.G., Hangan, A.C., et al. *Antitumor effect of Verbascum phlomoides L. on ehrlich carcinoma tumor cells*. Studia Universitatis "Vasile Goldiş", Seria Ştiinţele Vieţi, 2019; 29(1):6-12.

2. European Medicinal Agency (EMA). Assessment report on *Verbascum thapsus* L., *V. densiflorum* Bertol. (*V. thapsiforme* Schrad) and *V. phlomoides* L., flos. Committee on Herbal Medicinal Products, 2018, London, UK.

3. Angeloni, S., Zengin, G., Sinan, KI., et al. *An insight into Verbascum bombyciferum extracts: Different extraction methodologies, biological abilities and chemical profiles*. Industrial Crops and Products, 2021. 161:113201.

4. Bozic, I., Lavrnja, I. *Thiamine and benfotiamine: Focus on their therapeutic potential*. Heliyon, 2023. 9(11):e21839.

5. Ph.Eur. 11. European Pharmacopeia. 11th Edition. European Directorate for the Quality of Medicines and Healthcare. Council of Europe, 2022, Strasbourg.

ACKNOWLEDGMENT

Botanical identification was performed by Prof. Bojan Zlatković (Faculty of Science and Mathematics, University of Niš). The voucher specimens are kept in the herbarium of the Faculty of Science and Mathematics, University of Niš (Herbarium codes: *V. phlomoides* – 14506, *V. niveum* - 14615, *V. speciosum* – 14616).

This research was supported by the Ministry of Science, Technological Development and Innovation of the Republic of Serbia (No. 451-03-136/2025-03/200113 and 451-03-137/2025-03/200113).

P108

COVID-19 PATIENT DERIVED LYMPHOBLASTOID CELL LINES AS AN ALTERNATIVE TO WHOLE BLOOD FOR COMPOUND SCREENING

Luka Hiti[1], Maša Kandušer[1], Tijana Markovič[1], Tilen Burnik[1], Mitja Lainscak[2,3], Emil Pal[2], Jerneja Farkaš Lainščak[2,4], Irena Mlinarič-Raščan[1]

[1]Faculty of Pharmacy, University of Ljubljana, Slovenia
[2]General Hospital Murska Sobota, Slovenia
[3]Faculty of Medicine, University of Ljubljana, Slovenia
[4]National Institute of Public Health, Slovenia

1. INTRODUCTION

Cytokine storm, a COVID-19 complication, is a life-threatening systemic inflammatory syndrome involving the uncontrolled secretion of cytokines, which in severe cases leads to systemic organ failure and death [1].

We present here a novel in vitro cell model for evaluating the potential of compounds in decreasing the secretion of cytokines: immortalised B-lymphocytes, known as lymphoblastoid cell lines (LCL cells).

LCLs are immortalised B-lymphocyte derived cell lines. They are produced by transfecting isolated donor B lymphocytes with Epstein-Barr virus (EBV) [2]. Empirically, we found they secrete various cytokines, and can for that reason be used as an alternative to an established in vitro model of cytokine release, whole blood [3].

2. MATERIALS AND METHODS

2.1. Materials

Dexamethasone, trametinib, tanzisertib, and adezmapimod (all Sigma–Aldrich) were dissolved in DMSO.

Donor blood samples of convalescent COVID-19 patients were obtained as part of the clinical study approved by the Slovene National Medical Ethics Committee (0120-496/2022/6).

2.2. LCL Cells Generation

Peripheral blood mononuclear cells (PBMCs) were isolated from whole blood samples obtained from donors using density gradient centrifugation. To establish lymphoblastoid cell lines (LCLs), PBMCs were transformed by infection with Epstein-Barr virus (EBV). Following infection, cells were cultured in RPMI 1640 medium supplemented with 10–10% foetal bovine serum (FBS), L-glutamine, and antibiotics. Cyclosporin A was added at a final concentration of 400 ng/mL to inhibit T-cell proliferation and support B-cell outgrowth. Cultures were maintained at 37°C in a humidified incubator with 5% CO_2 and monitored regularly for cell clumping and growth. LCL cells typically emerged within 2–3 weeks and were expanded for downstream experiments.

2.3. Cytokine Secretion Assay

The production of cytokines was analysed as described previously [3,4]. Briefly, cells were pre-treated for 1 h with the non-cytotoxic concentration of the compound of interest and activated by 100 ng/ml LPS (whole blood) or 0.5 mM ionomycin and 3.33 ng/ml PMA (LCL cells) and incubated for 24 h. The resting, untreated cells and the LPS or ionomycin/PMA activated cells were used as controls. Cytokine production was assessed by BD Cytometric Bead Array (CBA) Human Inflammatory Cytokine kit (Contents: IL-1β, IL-6, IL-8, IL-10, IL-12, TNFα and) using AttuneNext flow cytometer.

3. RESULTS AND DISCUSSION

3.1. Lymphoblastoid Cell Lines and Whole Blood Exhibit Similar Cytokine Modulation

Our results on a selected set of compounds, including dexamethasone, indicate that the trend of cytokine secretion suppression is comparable between whole blood and human LCLs (Fig. 1). The most promising candidates for drug repurposing were identified as MAPK inhibitors (trametinib, a registered drug; and tanzisertib and SB203580, two research compounds).

P108

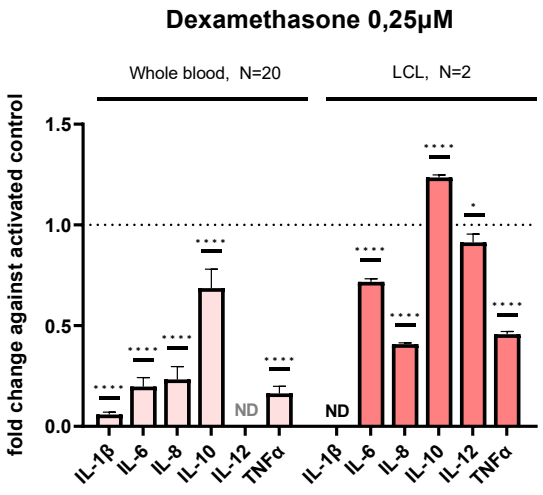

Figure 1. Cytokine profiles for dexamethasone (0,25 µM) in fold change against untreated activated cells. Cytokine production was assessed on twenty whole blood and two LCL samples. Bars above columns represent SEM, *p ≤ 0.05, **p ≤ 0.01, ***p ≤ 0.001, ****p ≤ 0.0001, using Dunnett's test. ND – not detected.

3.2. LCL Biobank Preparation

To cover different phenotypes, we have prepared a biobank of human LCLs derived from 71 convalescent COVID-19 donors with differing severity of disease. Human LCLs were generated from fresh lymphocytes isolated from blood samples donated for this purpose by consenting adults (Fig. 2).

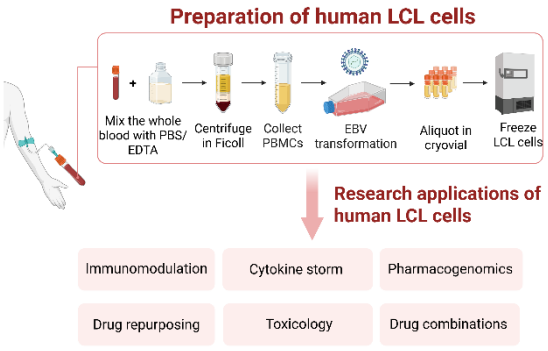

Figure 2. Lymphoblastoid cell lines (LCLs) preparation through B lymphocyte Epstein-Barr virus (EBV) transfection and their applications in biomedical research.

4. CONCLUSION

Our results on a selected set of compounds indicate that the trend of cytokine secretion suppression is comparable between whole blood and human LCLs. This supports the use of human LCLs as a suitable *in vitro* cell model and as a good personalised medicine platform for cytokine-release related compound screening.

5. REFERENCES

1. Hiti, L, et. al., *The immunopathogenesis of a cytokine storm: The key mechanisms underlying severe COVID-19*. Cytokine & Growth Factor Reviews 2025;82:1–17.

2. Hui-Yuen J, et al., *Establishment of Epstein-Barr virus growth-transformed lymphoblastoid cell lines. Journal of Visualized Experiments*, 2011 Nov 8;(57):3321.

3. Markovič, T., et al., *Characterization of human lymphoblastoid cell lines as a novel in vitro test system to predict the immunotoxicity of xenobiotics*. Toxicology Letters, 2015. 17;233(1):8-15

4. Remick, et. al,. *Whole-Blood Assays for Cytokine Production*. Evans, T.J. (eds) Septic Shock Methods and Protocols. Methods in Molecular Medicine™, vol 36. Humana Press.

ACKNOWLEDGMENT

This work was supported by the Slovenian Research Agency (Grant no. P1-0208), by the Ministry of Higher Education, Science and Innovation and the European Regional Development Fund (OP20.05187 RI-SI-EATRIS), by the Network of Research Infrastructure Centers of University of Ljubljana - MRIC UL (I0-E011-2022), and by REMEDi4ALL Project (under Grant agreement no. 101057442).

P109

EXTRACTABLES AND LEACHABLES IN PHARMACEUTICAL MANUFACTURING PROCESSES: A USP <665> PERSPECTIVE

Pija Košir[1,2], Žane Temova Rakuša[1], Tina Trdan Lušin[2], Robert Roškar[1]

[1]Faculty of Pharmacy, Aškerčeva cesta 8, 1000, Ljubljana, Slovenia
[2]Lek Pharmaceuticals, d.d., Verovškova cesta 57, 1000, Ljubljana, Slovenia

1. INTRODUCTION

With the rise of biopharmaceuticals, the industry has shifted from traditional stainless-steel equipment to single-use (SU) systems mainly made of plastics and elastomers. While SU systems offer flexibility and efficiency, they also introduce new risks, particularly the potential for extractables and leachables (E&L) to migrate into drug products (DP) during liquid process streams. Extractables are substances or chemical entities, extracted from a test article by an extraction medium under exaggerated laboratory test conditions, including temperature, duration, extraction process and dimensions of contact. Leachables are substances that actually migrate from the test article under real manufacturing conditions [1]. Plastic SU components contact liquid process streams at multiple manufacturing stages and can persist throughout the process, leading to accumulation in the DP, which poses potential risks to product stability, quality and patient safety.

2. MATERIALS AND METHODS

A comprehensive review of regulatory and compendial guidelines on E&L testing was conducted, including: USP monographs <1665> (2022) and <665> (effective 2026) for evaluating E&Ls from plastic manufacturing process components, <1663> (2015) and <1664> (2024) addressing E&Ls from packaging and delivery systems, as well as the ICH Q3D Elemental Impurities (2022) and Q3E Extractables and Leachables (2020) guidelines. Key databases for scientific articles and data on E&L were also reviewed: ELSIE database, containing safety information and controlled extraction study data on E&Ls, PubMed and Science Direct databases, as well as industry best practices compiled in *Product Quality Research Institute* (PQRI), *BioPhorum Operations Group* (BPOG) and *Bio-Process Systems Alliance* (BPSA).

3. RESULTS AND DISCUSSION

3.1. Designing and implementing E&L studies according to the USP <665>

USP <665> *Plastic Components and Systems Used to Manufacture Pharmaceutical Drug Products and Biopharmaceutical Drug Substances and Products*, effective May 1, 2026, is currently the key monograph establishing a comprehensive framework for the qualification of SU manufacturing components that come into contact with pharmaceutical process streams. The main novelty with USP <665> is the shift to a standardized, risk-based framework for qualifying plastic components in pharmaceutical manufacturing including consistent extraction protocols. Previously, E&L testing varied widely and lacked clear regulatory guidance. The monograph is already being widely applied retroactively across drug development, not only to new DPs, but also to products already on the market. This will help manufacturers avoid regulatory delays and costly rework ahead of its enforcement in 2026.

3.2. Scope of testing

E&L testing applies to all plastic components in the DP's process stream (Fig. 1.).

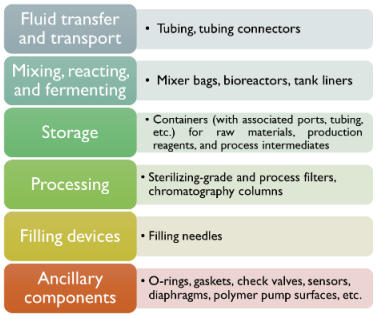

Figure 1. Grouping of plastic components in the drug products' process stream requiring E&L testing.

Glass, metal and stainless-steel materials are generally excluded since they do not release significant organic extractables. However, rubber-based elastomers require qualification due to their potential to leach compounds [1,2]. The physical state of a process stream influences its interaction with components, with liquids and semisolids posing higher leaching risks than solids or gases. Due to limited contact, transfers involving solids or gases are minimal and typically restricted to volatiles, so components exposed only to these streams are generally exempt from E&L testing [1,2].

3.3. Study workflow

A risk-based framework of E&L studies (Fig. 2) categorizes SU systems components into low, moderate or high risk based on material sensitivity, DP characteristics (e.g., pH, formulation) and contact conditions (e.g., temperature, duration). Low-risk components may not need additional evaluation if supported by supplier data or previous assessments, while medium- and high-risk components require identification through extraction studies under stress conditions (e.g., high temperatures, harsh solvents) [2–4]. Leachables studies typically involve targeted analysis based on extractables data to identify specific compounds of concern and are performed under actual manufacturing conditions to determine which extractables migrate into the DP. Samples are collected throughout the manufacturing process [1,4].

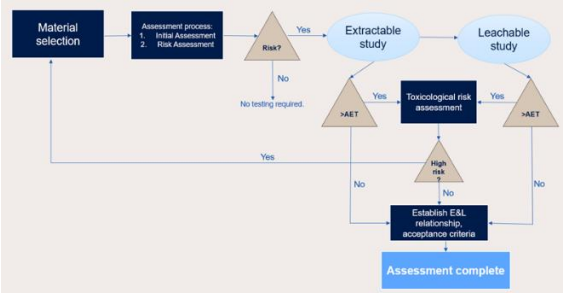

Figure 2. E&L assessment workflow.

The PQRI established the Safety Concern Threshold (SCT), which sets levels below which leachables are considered too low to pose any significant safety risks. Compounds above the SCT must be identified and assessed. The SCT varies by delivery system: 0.15 µg/day for orally inhaled and nasal DPs and 1.5 µg/day for parenteral DPs. The SCT is converted into the Analytical Evaluation Threshold (AET) using product-specific parameters, and any compound exceeding the AET requires further toxicological assessment [4].

Best practices for USP <665> implementation

To address common E&L study challenges, it's essential to perform early extractables profiling, monitor leachables during manufacturing process and use AET calculations to support toxicological evaluations. Close collaboration with suppliers to obtain detailed material information and prioritizing testing on high-risk components enhances effectiveness. Establishing strong extractable-to-leachable correlations minimizes redundant testing and facilitates control strategies [1,4].

4. CONCLUSION

The retroactive application of USP <665> plays a crucial role in ensuring the quality and safety of pharmaceuticals and biopharmaceuticals manufactured using SU systems. Compliance enables manufacturers to minimize risks, maintain product integrity, meet regulatory requirements and strengthen their industry reputation. Nonetheless, despite increasing attention, publicly available data on this topic remains scarce, underscoring the importance of ongoing research.

5. REFERENCES

1. Jenke D. Extractables and Leachables: Characterization of Drug Products, Packaging, Manufacturing and Delivery Systems, and Medical Devices. 1st ed. Wiley; 2022.
2. USP: <665>Plastic Components and Systems Used to Manufacture Pharmaceutical Drug Products and Biopharmaceutical Drug Substances and Products (to be official).
3. USP: 〈1665〉 Characterization and Qualification of Plastic Components and Systems Used to Manufacture Pharmaceutical Drug Products and Biopharmaceutical Drug Substances and Products (2022).
4. BioPhorum. Best practices guide for evaluating leachables risk from polymeric single-use systems used in biopharmaceutical manufacturing. 2021.

P110

SMALL PRESSURE, BIG IMPACT: QUANTIFICATION OF GASTROINTESTINAL MOTILITY FORCES FOR BIORELEVANT DISSOLUTION TESTS IN THE FED STATE

Janja Zabukovnik[1,2], Grzegorz Garbacz [3], Igor Locatelli [1]

[1]University of Ljubljana, Faculty of pharmacy, Aškerčeva cesta 7, 1000 Ljubljana, Ljubljana, Slovenia
[2]Panakea, Cesta v Gorice 2b, Ljubljana, Slovenia
[3]Physiolution Polska, ul. Piłsudskiego 74, 50-020 Wrocław, Poland

1. INTRODUCTION

A comprehensive understanding of the digestive system is crucial for pharmaceutical development. The gastrointestinal tract (GIT), constantly in motion, requires deeper insight into its contractile processes. Traditional methods focus on high-pressure effects on dosage forms, but evidence shows that even minor, sustained GIT contractions significantly influence drug release and absorption. Biorelevant tests simulating such conditions yield more accurate predictions of drug behavior *in vivo*. They enhance understanding of how contractions affect disintegration, dissolution, and release. While past studies emphasized high pressures, overlooking frequent small contractions gives an incomplete picture [1, 2]. Thus, grasping the full spectrum of GIT motility forces is vital for advancing drug development. Therefore, the aim of this study was to investigate and quantify contraction force intensity and duration across different GIT parts in the fed state.

2. MATERIALS AND METHODS

2.1. SmartPill® telemetry capsule study

The GIT motility forces data (pressure profiles) were obtained from the previously published study by Koziolek *et al.* in 2015 [1]. A SmartPill® telemetry capsule was administered to 19 participants to monitor intragastric pH and pressure profiles after consuming a high-fat, high-calorie breakfast (964 kcal).

2.2. Signal analysis of contraction data

The raw data of GIT motility forces (pressure data) were processed using R Studio, Clarity Chromatography Software, and MS Excel. The motility forces were analysed according to categories of magnitude of contractions. Subsequently, the following pressure size classes were created:

- 15 mbar $\leq x <$ 25 mbar,
- 25 mbar $\leq x <$ 50 mbar,
- 50 mbar $\leq x <$ 100 mbar,
- 100 mbar $\leq x <$ 150 mbar,
- 150 mbar $\leq x <$ 200 mbar,
- 200 mbar $\leq x <$ 300 mbar,
- and $x \geq$ 300 mbar.

The data processing was conducted in three phases. In the preliminary phase, data was prepared under R software environment (R Studio) and imported into Clarity Chromatography Software (version 8.7.1.19) due to the structural similarity between raw pressure data and chromatograms. Peak integration procedure in Clarity allowed accurate calculation of peak areas, which were then re-imported into the R software environment for further analysis.

3. RESULTS AND DISCUSSION

The main results of this study show that smaller magnitude contractions (up to 100 mbar) are significantly more frequent than larger ones (above 100 mbar). The most frequent magnitude contractions were observed between 15 and 50 mbar. The highest intensities were observed in the stomach, within the range of 15 to 25 mbar. In the small bowel, the most frequent contractions were observed to occur within the range of 25 to 50 mbar, while those above 50 mbar were rare. Similarly, in the colon, contractions between 25 and 50 mbar are the most prevalent.

Contractions above 150 mbar are rare in all regions, although they are pronounced at the pylorus.

P110

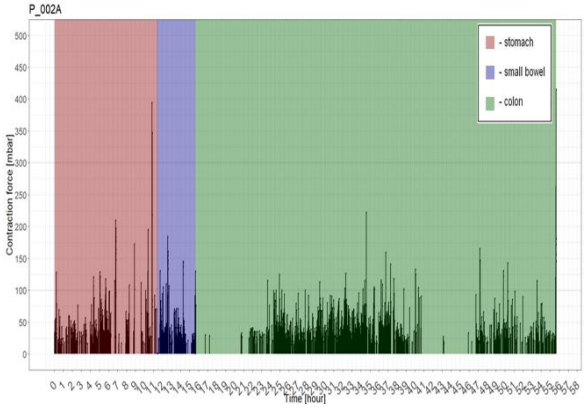

Figure 1. Example of GIT motility force in different parts of the GIT for a specific participant.

The analysis of contraction intensities per hour revealed that contractions within the range of 15 to 50 mbar are the most frequent, with the highest durations observed in the colon. The graphical representation of the data provides a clear illustration of the prevalence of smaller contractions (Fig. 2). A comparison of the participant profiles revealed notable discrepancies in the duration of capsule retention across different regions of the GIT. Some participants retained the capsule in the stomach for up to 20 hours, while others did so for only 4 hours.

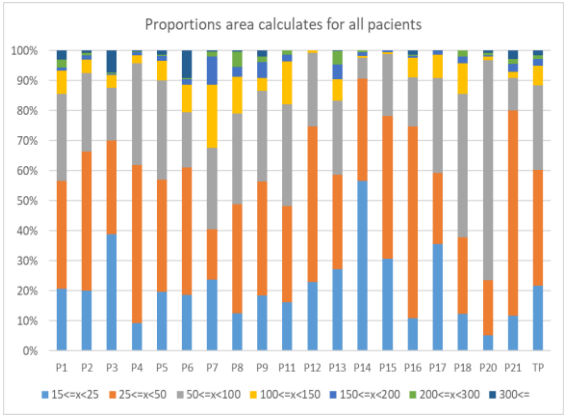

Figure 2. The prevalence of contraction intensity by pressure size class.

4. CONCLUSION

Our study revealed that small contractions (up to 100 mbar) are more common than large contractions (above 100 mbar), with the most common being in the range between 15 and 50 mbar, especially in the stomach. Contractions between 25 and 50 mbar predominate in the small intestine and large intestine. Contractions above 150 mbar are rare throughout the digestive tract, although they are more pronounced at the pylorus. Our assessment of the frequency of minor contractions in the gastrointestinal tract provides a solid foundation for the future development of more representative biorelevant dissolution test devices.

5. REFERENCES

1. Koziolek, M., et al., *Intragastric pH and pressure profiles after intake of the high-caloric, high-fat meal as used for food effect studies.* J. Control. Rel., 2015. 220: 71–78.
2. Schneider, F., et al., *In vitro simulation of realistic gastric pressure profiles.* Eur. J. Pharm. Sci., 2017. 107: 71–77.
3. Staniszewska, M., et al., *A Rational Approach to Predicting Immediate Release Formulation Behavior in Multiple Gastric Motility Patterns: A Combination of a Biorelevant Apparatus, Design of Experiments, and Machine Learning.* Pharmaceutics, 2023. 15(8): 2056.
4. Romański, M., et al., *More Than a Gut Feeling - A Combination of Physiologically Driven Dissolution and Pharmacokinetic Modeling as a Tool for Understanding Human Gastric Motility.* Mol. Pharm., 2024. 21(8): 3824–3837.

ACKNOWLEDGMENT

We thank professor Werner Weitschies' research group at the University of Greifswald Institute of Pharmacy for sharing the raw data from the SmartPill® telemetry capsule study used in our analysis.

P111

INHALED MICRO- AND NANOPLASTICS IN THE RESPIRATORY SYSTEM: CURRENT EVIDENCE AND METHODOLOGICAL CHALLENGES

Petra Party[1], Bence Sipos[1], Gábor Katona[1], Ildikó Csóka[1], Rita Ambrus[1]

[1]*Institute of Pharmaceutical Technology and Regulatory Affairs, University of Szeged, Hungary*

1. INTRODUCTION

Microplastics (MPs) and nanoplastics (NPs), which are synthetic solid particles with a diameter of 1 µm–5 mm and <1 µm, respectively, have emerged as a significant environmental and public health issue. Humans are inevitably exposed to MPs and NPs *via* inhalation from various sources. Recent studies indicate that inhaling airborne MPs and NPs could potentially damage the human respiratory system (Figure 1.). As the particle size ranges are various, their deposition are in different regions of the respiratory tract. Larger particles are often eliminated by the clearance mechanisms, but smaller particles may accumulate in the lungs. The primary mechanism through which MPs and NPs exert their harmful effects is associated with the induction of oxidative stress, inflammation, and pulmonary fibrosis [1,2]. The deposition, and possible health effects of inhaled MPs were studied in this work, with a focus on the available *in vitro, in vivo* and *in silico* characterization methods to identify research gaps through comparative analysis of findings and methodological limitations across studies.

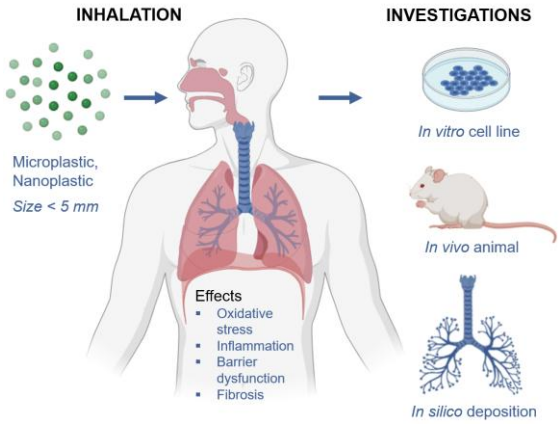

Figure 1. The effects of NP and MP exposure on the human body, and the investigation methods to understand the mechanisms behind them.

2. MATERIALS AND METHODS

2.1. Methodology

This literature review was conducted using a systematic approach to identify and analyse relevant studies on inhaled MPs, NPs and their effects on the respiratory system. Studies employing various experimental models and computational simulations were reviewed.

3. RESULTS AND DISCUSSION

3.1. *In vitro* methods

In vitro cell line studies play a crucial role in understanding the cellular mechanisms underlying MPs' toxicity. Research involving human bronchial epithelial cells (BEAS-2B) and human lung epithelial A549 cells has demonstrated that MPs and NPs cause ROS production, inflammation, cellular and tissue damage. This may lead to pulmonary barrier dysfunction and chronic obstructive lung disease (COPD) [3–5]. There are more physiologically relevant *in vitro* models representing the lung (MucilAir™) to study membrane passage of various MPs, which shows higher *in vitro-in vivo* translatability compared to conventional models [6]. Using a lung-on-a-chip technique the structural features and key functions of the alveolar-blood barrier can be accurately simulated while integrating multiple immune cells. The system allows the alveolar-capillary barrier, various cells, tissue-tissue interfaces, and vascular perfusion to be integrated to model the characteristics of lung *in vitro* [7].

3.2. *In vivo* investigations

Animal models have extended the understanding of the impacts of MPs beyond cellular responses, investigating their pharmacokinetics and systemic effects. Mice and rat models are frequently used to test the exposure of MPs. Inhaled plastics can lead to the activation of immune pathways, leading to increased lung inflammation. Studies show that inhalation of MPs leads to particle accumulation in lung tissues, resulting in physiological damage, which potentially extends to other

organs [8]. The analysis of bronchoalveolar lavage fluid (BALF) and histopathological analysis of the lung tissue can be used to reveal lung inflammation and lung injury and fibrosis [9,10]. There are studies investigating the effect of MPs in asthmatic mice, where the exposure escalated asthma symptoms by increasing mucus production and inflammatory cell infiltration [11].

3.3. *In silico* studies

The application of *in silico* modelling provides a novel framework for understanding how MPs are transported and deposited within the human respiratory system. Using computational fluid dynamics, researchers have simulated airflow patterns and the deposition of MPs in the airways, revealing insights on the behaviour of inhalable particles [12,13]. Differences were observed in deposition patterns for MPs and NPs across varying breathing rates. Moreover, larger MPs displayed a tendency for rapid deposition in the upper airways, whereas smaller NPs exhibited a higher likelihood of escape or reaching deeper airway generations. Shape is a also a crucial factor, non-spherical particles have a propensity for deeper lung penetration compared to spherical ones [14].

3.4. *Limitations*

While studies have begun to characterize size distributions of airborne MPs and NPs, there remains a noticeable gap regarding the variability of shape and size. There is a limited understanding of the biological effects stemming specifically from different types of plastics and their additives. Existing studies often lack longitudinal data, focusing instead on short-term exposure. Moreover, MPs in the atmosphere often co-exist with other pollutants, and the combined effects on health outcomes remain largely unexplored.

4. CONCLUSION

The combination of *in vitro, in vivo*, and *in silico* methodologies has enriched the knowledge surrounding the impacts of inhaled MPs and NPs on the respiratory system. Evidence suggests that MPs can induce inflammation, and cellular damage, with systemic implications that necessitate further investigation.

5. REFERENCES

1. Chen, C.Y., et al. *Exploring the potential and challenges of developing physiologically-based toxicokinetic models to support human health risk assessment of microplastic and nanoplastic particles*. Environ. Int. 2024, 186, 108617
2. Saha, S.C. et al. *Effect of microplastics deposition on human lung airways: A review with computational benefits and challenges.* Heliyon 2024, 10, e24355
3. Jeon, M.S. et al. *Polystyrene microplastic particles induce autophagic cell death in BEAS-2B human bronchial epithelial cells.* Environ. Toxicol. 2023, 38, 359–367
4. Yang, S. et al. *In vitro evaluation of nanoplastics using human lung epithelial cells, microarray analysis and co-culture model.* Ecotoxicol. Environ. Saf. 2021, 226, 112837
5. Woo, J.H. et al. *Polypropylene nanoplastic exposure leads to lung inflammation through p38-mediated NF-κB pathway due to mitochondrial damage.* Part. Fibre Toxicol. 2023, 20, 1–17
6. Donkers, J.M. et al. *Advanced epithelial lung and gut barrier models demonstrate passage of microplastic particles.* Microplastics and Nanoplastics 2022, 2. 6.
7. Yang, S. et al. *Sentinel supervised lung-on-a-chip: A new environmental toxicology platform for nanoplastic-induced lung injury*. J. Hazard. Mater. 2023, 458, 131962
8. Tomonaga, T. et al. *Investigation of pulmonary inflammatory responses following intratracheal instillation of and inhalation exposure to polypropylene microplastics.* Part. Fibre Toxicol. 2024, 21, 1
9. Danso, I.K. *Pulmonary toxicity assessment of polypropylene, polystyrene, and polyethylene microplastic fragments in mice.* Toxicol. Res. 2024, 40, 313–323
10. Li, X. et al. *Intratracheal administration of polystyrene microplastics induces pulmonary fibrosis by activating oxidative stress and Wnt/β-catenin signaling pathway in mice.* Ecotoxicol. Environ. Saf. 2022, 232, 113238
11. Lu, K. et al. *Detrimental effects of microplastic exposure on normal and asthmatic pulmonary physiology.* J. Hazard. Mater. 2021, 416, 126069
12. Islam, M.S. et al. *How microplastics are transported and deposited in realistic upper airways?* Phys. Fluids 2023, 35
13. Riaz, H.H. et al. Breathing in danger: Mapping microplastic migration in the human respiratory system. Phys. Fluids 2024, 36,
14. Huang, X. et al. *Transport and deposition of microplastics and nanoplastics in the human respiratory tract*. Environ. Adv. 2024, 16

ACKNOWLEDGMENT

Project no. [2024-1.2.3-HU-RIZONT-2024-00032] has been implemented with the support provided by the Ministry of Culture and Innovation of Hungary from the National Research, Development and Innovation Fund, financed under the 2024-1.2.3-HU-RIZONT funding scheme.

P112

HIGHLY SENSITIVE AND RAPID LC-HRMS METHOD FOR DETERMINATION OF *N*-NITROSO-FOLIC ACID IN FOOD SUPPLEMENTS

Timeja Planinšek Parfant, Žane Temova Rakuša, Robert Roškar

Department of Biopharmaceutics and Pharmacokinetics, University of Ljubljana, Faculty of Pharmacy, Slovenia

1. INTRODUCTION

N-nitrosamines (NA) are potentially highly carcinogenic compounds that have recently been detected in trace amounts in pharmaceuticals [1,2]. Therefore, the European Medicines Agency (EMA) has set acceptable intake (AI) limits for multiple NAs, including *N*-nitroso-folic acid (NFA) (1500 ng/day), which can be formed by a reaction between folic acid (FA) and sodium nitrite [3]. FA, a water-soluble B-complex vitamin, plays a vital role in numerous biochemical processes, including RNA/DNA synthesis, cell division, and amino acids metabolism. Since insufficient levels can lead to various health complications, the European Food Safety Authority (EFSA) recommends 330 µg of folates daily for adults, and 600 µg for women before and during pregnancy, obtainable from dietary sources or food supplements (FS) [4]. Consequently, FA supplementation is common, especially during pregnancy, due to its essential role in foetal development. Despite the growing trend of NA detection in pharmaceuticals, NAs in FS remain neglected, highlighting the urgent need for the development of an analytical method suitable for routine control to ensure the safety of FSs and thus reduce risks to human health.

2. MATERIALS AND METHODS

2.1. Reagents and chemicals

Reference FA and NFA standards were obtained from Carbosynth and TRC, respectively. MeOH was purchased from Honeywell. Formic acid, NaOH solution and LC-MS grade MeOH were obtained from Merck. Ultra-pure water (MQ) was obtained through an Adrona Connect LT purification system. FSs containing FA in different dosage forms were purchased on the Slovenian market.

2.2. LC-HRMS method

A Kinetex F5 100 × 4.6 mm, 2.6 µm particle size column (Phenomenex, USA) at 40 °C with gradient elution at 0.65 mL/min using 0.1% formic acid and MeOH were used on a UHPLC UltiMate 3000 coupled to a Q Exactive™ Plus Orbitrap mass spectrometer, equipped with HESI and operated in positive mode (Thermo Scientific, USA). The injection volume was 5 µL. The extracted ion chromatogram of NFA was obtained based on *m/z* 471.1372 with a mass extraction window of ± 5 ppm, while full-scan (*m/z* 100.0–600.0) was recorded.

2.3. Method validation

The method was validated following USP general chapter <1469> Nitrosamine impurities [5] in terms of specificity, linearity, accuracy, precision, recovery, LOQ and sample stability. It was performed with a blank FS, which was spiked with a calibration or QC solution prior to the extraction and prepared according to the sample preparation procedure.

2.4. Method application

Six commercially available mono-vitamin FSs containing 200–1000 µg of FA in the form of tablets, capsules, and solution were analysed. The FS declared daily dose was transferred into a 100 mL volumetric flask (capsules and the solution dosage form were directly placed, while tablets were crushed, and homogenized). 10 % MeOH in 1 mM NaOH was used as the extraction solvent. The samples were mixed for 10 min with a magnetic stirrer, followed by sonication (15 min) and filtration through an RC filter with 0.2 µm pore size and analysed by LC-HRMS. All samples were prepared in triplicate.

3. RESULTS AND DISCUSSION

3.1. LC-HRMS method development

LC-HRMS was used due to high specificity and sensitivity. In order to prevent matrix interferences, the optimal separation between FA and NFA was achieved with a Kinetex F5 column and gradient elution program (Fig. 1). MS parameters were optimized to improve the sensitivity of the method and 5 µL was selected as injection volume, due to improved sensitivity and no matrix effect was observed.

P112

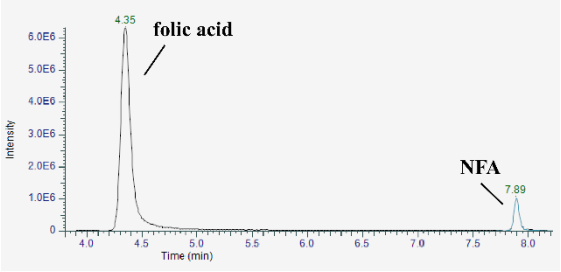

Figure 10. Representative chromatogram of separation between folic acid and N-nitroso-folic acid (NFA).

3.2. Sample preparation development

For accurate determination of NFA content in FSs, FA must be completely dissolved in the extracted samples. As FA solubility increases in alkaline solutions, different solvents of 0.1–10 mM NaOH containing 0–40% MeOH were tested during the development of the extraction procedure. The extraction proved to be the most efficient using 1 mM NaOH containing 10% MeOH, which provided complete dissolution of the FSs in 100 mL of extraction solvent, while observing no matrix effect. Furthermore, the mixing and sonication times were optimized for complete dissolution of FA and extraction of NFA. FSs completely dissolved within 10 min of mixing combined with 15 min of sonication.

3.3. Method validation

The method was validated according to USP and was proved to be specific and linear (R^2 = 0.998) in the concentration range 0.5–50 µg/L, which is equivalent to 50–5000 ng of NFA per FS unit. Accuracy (< 15%) and precision (< 10%) were well within acceptance criterion (< 30%, ≤ 25%, ≤ 30% for accuracy, repeatability and intermediate precision, respectively). The acceptance criterion for LOQ (signal-to-noise ratio > 10:1) and recovery (70–130%) was achieved. Furthermore, the samples remained stable in the autosampler for at least one day.

3.4. Method application

The method was successfully applied to real FS samples to assess the NFA content. NFA was detected in four FSs, three of which contained NFA above the LOQ ranging from 71.1 to 202.1 ng/daily dose (Table 1). In FSs that contained less than 400 µg of FA, NFA was not detected, whereas in FSs with detected NFA, a positive correlation was observed between FA and NFA content. All samples contained NFA below the AI limit (1500 ng/day).

Table 1. NFA content in analysed FSs.

Sample	Dosage form	FA content [µg]	NFA content [ng]
S1	Tablets	1000	202.1
S2	Tablets	400	71.1
S3	Solution	200	< LOD
S4	Tablets	400	2.0*
S5	Tablets	800	88.9
S6	Capsules	300	< LOD

*estimated value since the measurement was below LOQ.

4. CONCLUSION

A highly sensitive, accurate and rapid analytical method for the determination of NFA in FSs containing FA was developed. The method was fully validated and was applied to commercially available FSs. Four of the six analysed FSs contained NFA above LOQ. Since the NFA contents were below 1500 ng, all FSs met the regulatory requirements for NFA content. Despite this, these findings are still concerning, as the FSs containing FA are predominantly used by pregnant women, a particularly vulnerable population. Therefore, strict quality control of NFA in such products and implementation of effective NA mitigation strategies are crucial to minimize potential health risks. The developed analytical method thus enables routine quality control of NFA in such products, providing a valuable tool for ensuring FSs safety.

5. REFERENCES

1. Planinšek Parfant T, Roškar R., *A comprehensive approach for N-nitrosamine determination in pharmaceuticals using a novel HILIC-based solid phase extraction and LC-HRMS.* Talanta, 2025. 282: 126752.

2. Planinšek Parfant T, et al., *A robust analytical method for simultaneous quantification of 13 low-molecular-weight N-Nitrosamines in various pharmaceuticals based on solid phase extraction and liquid chromatography coupled to high-resolution mass.* European Journal of Pharmaceutical Sciences, 2024.192: 106633.

3. EMA, *Questions and answers for marketing authorisation holders/applicants on nitrosamine impurities in human medicinal products*, 2025.

4. EFSA, *Scientific Opinion on Dietary Reference Values for folate.* EFSA Journal, 2014. 12(11):1-59.

5. USP-NF. *<1469> Nitrosamine Impurities.* Usp-Nf. 2020

P113

DEVELOPMENT OF CHROMATOGRAPHIC METHODS FOR THE DETERMINATION OF BOVINE IMMUNOGLOBULIN G

Nika Kržišnik[1], Robert Roškar[1]

[1]*Department of Biopharmaceutics and Pharmacokinetics, University of Ljubljana, Faculty of Pharmacy, Slovenia*

1. INTRODUCTION

Whey is increasingly recognized for its unique and rich composition, especially for its content of functional proteins with proven health benefits [1]. Among these, immunoglobulin G (IgG) is the predominant immunoglobulin, accounting for about 90% of the total immunoglobulin content in whey [1,2]. Bovine IgG has been shown to bind to numerous human allergens and pathogens, preventing infections and inflammation, particularly in the gastrointestinal and respiratory tract [1,3]. Its resistance to intestinal degradation allows effective supplementation with colostrum or in nutraceuticals containing purified IgG [1–3]. Given the limited regulation in the field of food supplements, the main objective of our work was to develop robust chromatographic methods for the quality control of IgG-containing products.

2. MATERIALS AND METHODS

2.1. Reagents and chemicals

Reference standards of bovine IgG and other whey proteins were purchased from Sigma-Aldrich. HPLC-grade acetonitrile was purchased from Honeywell. All mobile phases and sample solutions were prepared with ultrapure water obtained using an Adrona SIA water purification system. All other chemicals used were of analytical grade.

2.2. Methods

Various ion-exchange, size-exclusion, affinity, and reversed-phase chromatographic columns from four manufacturers were tested (Agilent, Phenomenex, BIA Separations, and Waters). An Agilent 1100/1200 HPLC system with a diode array detector was used.

3. RESULTS AND DISCUSSION

Our work focused on the development of selective and complementary chromatographic methods based on different separation mechanisms for the determination of IgG in various samples that may also contain other important whey proteins, including lactoferrin, α-lactalbumin, β-lactoglobulin, bovine serum albumin, and lactoperoxidase. Given the different isoelectric points of selected whey proteins, it was hypothesized that IgG (pI 5.5–8.3 [3]) could be selectively separated from other whey proteins using ion exchange chromatography. Both cation and anion exchange columns (CiMAC, BIA Separations) were evaluated in the pH range of 6–8. Contrary to expectations, IgG was not retained on any of the columns tested under these conditions.

IgG has the highest molecular weight (150–161 kDa [3]) among the selected whey proteins, which is why it was assumed that separation could be achieved using a size-exclusion chromatographic method. Although the developed method successfully separated IgG from other whey proteins, due to the potential instability and aggregation of other whey proteins (e.g. bovine serum albumin; Fig. 1) and the possible presence of other proteins, this method does not provide sufficient selectivity for product quality control, especially for complex samples such as colostrum.

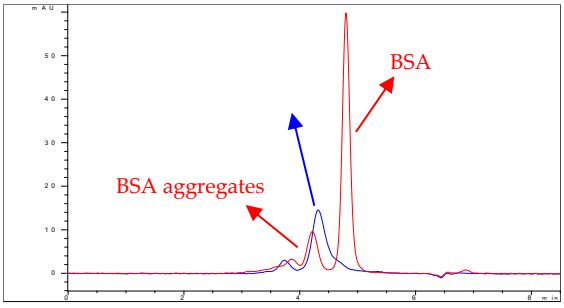

P113

Figure 1. Optimized size-exclusion method: chromatograms showing the co-elution of bovine serum albumin aggregates and IgG.

Development continued with reversed-phase chromatographic methods which proved to be the most challenging as the separation of IgG from other whey proteins or the appropriate chromatographic peak shape for IgG was difficult to achieve. Different stationary phases were tested (C3, C8, polyphenyl). We found out that high column temperatures (≥70 °C) are required for IgG elution. The separation of IgG from other whey proteins was achieved only on a BioResolve RP mAb column (Waters), with the addition of formic acid in the mobile phase and – atypically – methanol as an organic modifier. However, the method is not suitable for quantification, as the IgG is eluted in a broad and poorly defined peak (Fig. 2).

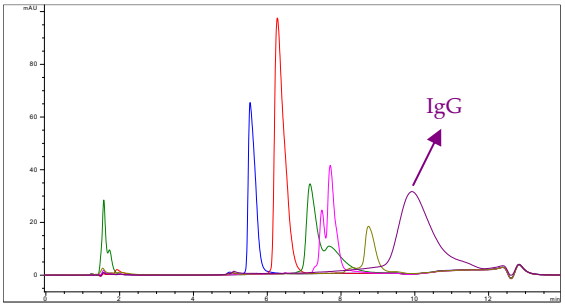

Figure 2. Optimized reversed-phase chromatograms of IgG and other selected whey proteins on BioResolve RP mAb column.

Affinity chromatography was also evaluated using an r-Protein G column (BIA Separations), which specifically binds to the Fc region of IgG antibodies. Among all methods tested, this approach showed the highest selectivity for IgG, as other whey proteins were not retained on the column (Fig. 3). An optimal peak shape was achieved using 75 mM phosphate buffer with addition of 300 mM NaCl (pH 7.4) as the binding mobile phase and 5% acetic acid as the eluting mobile phase.

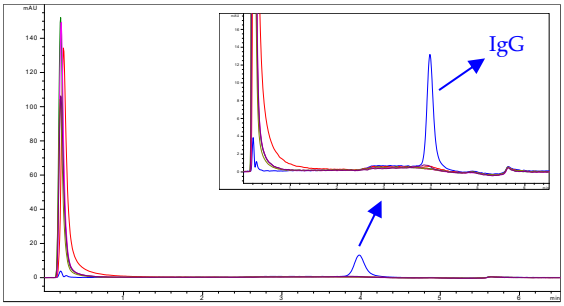

Figure 3. Affinity chromatography on r-Protein-G column: chromatograms of IgG and other whey proteins.

4. CONCLUSION

The development of a robust analytical method is essential for the quality control of IgG in complex samples. Among the tested approaches, affinity chromatography using an r-Protein G column provided the best results in terms of selectivity and peak shape. Future work will focus on the integration of mass spectrometry to enable more reliable and selective quantification of IgG in complex matrices.

5. REFERENCES

1. Ostertag, F., et al., *Enrichment of Lactoferrin and Immunoglobulin G from Acid Whey by Cross-Flow Filtration.* Foods, 2023. 12(2163): 1–15.

2. Tsermoula, P., et al., *WHEY - The waste-stream that became more valuable than the food product.* Trends in Food Science & Technology, 2021. 118: 230–241.

3. Heidebrecht, H. J., et al., *Isolation of biofunctional bovine immunoglobulin G from milk- andcolostral whey with mixed-mode chromatography at lab and pilotscale.* Journal of Chromatography A, 2018. 1562: 58–68.

ACKNOWLEDGMENT

This research was co-funded by Slovenian Research Agency, grant number [P1 0189] and by Support of Research and development projects (TRL 3–6): LAKTIKA.

P114

EXPLORING MUCOADHESION OF LATANOPROST EYE DROPS: A COMPARATIVE STUDY OF MEASUREMENT TECHNIQUES

Maša Safundžić Kučuk[1], Željko Agić[1], Anđela Nosić[2], Jelena Štimac[2], Laura Nižić Nodilo[2], Anita Hafner[2], Jasmina Lovrić[2]

[1]Research and Development, JGL d.d., Croatia

[2]Department of Pharmaceutical Technology, University of Zagreb Faculty of Pharmacy and Biochemistry, Croatia

1. INTRODUCTION

Mucoadhesion is a physicochemical property that significantly affects the behavior of formulations administered to the ocular surface. In this study, three specific methods were used to determine the mucoadhesive properties of latanoprost (LAT) eye drops with sodium hyaluronate (NaHA): texture profile analysis (TPA), rheological synergism, and dynamic light scattering (DLS) [1]. TPA determines mucoadhesive properties based on mechanical force between formulation and mucin. Rheological synergism measures how the interaction with mucin affects the formulation flow properties. DLS is used to measure the size distributions of mucins and of the mucin mixed with formulation.

2. MATERIALS AND METHODS

2.1. Materials

The LAT eye drops were prepared with Kolliphor® RH40 (BASF), sodium dihydrogen phosphate monohydrate, disodium phosphate anhydrous, sodium chloride and purified water. Kolliphor RH40 was dissolved in water (26–28 °C), stirred until clear, and cooled to ~20 °C. LAT (Yonsung Ltd.) was added with stirring (600 rpm, 80 min). A buffered bulk with sodium phosphates, sodium chloride, and 0.4% (*w*/*w*) NaHA (Contipro Ltd., M_w grade 950 or 820 kDa) was prepared separately. The solutions were mixed under controlled stirring (1000 rpm), rinsed, and brought to final volume.

2.2. Mucoadhesion studies based on mechanical force determination

A tensile test was performed with a TA.XTplus C Texture Analyser (Stable Micro Systems) equipped with a 1 cm cylindrical probe. Filter paper, cut into a circular shape matching the probe diameter, was attached to the probe and soaked with 50 µL of a porcine mucin type II (Sigma Aldrich) dispersion in STF (10% *w*/*v*). The formulation (100 µL) was pipetted onto the platform and brought into contact with mucin-soaked filter paper for 120 s, after which the probe with filter paper was raised at a speed of 0,10 mm/s. Peak force (N), work of adhesion (N·sec), debonding distance (mm), and area (N·mm) were measured in 5 parallel measurements. The measurements were performed at 34 °C.

2.3. Mucoadhesion studies based on rheological synergism

Zero shear viscosity of formulations mixed with a dispersion of mucin (3 %, *w*/*v*) and the corresponding controls was determined at 34 °C using an MCR 102 rheometer (Anton Paar Instruments) equipped with a cone-plate measuring device (CP 50-1, trim position 102 µm). Samples were subjected to pre-shear at a rate of 0.1 s^{-1} for 30 s, followed by a shear rate sweep, 1 s^{-1} to 15 000 s^{-1}. Rheological synergism was calculated as the ratio between the zero-shear viscosity of the mixture ($\eta_{0,mix}$) and the theoretical sum of the individual zero-shear viscosities of the sample ($\eta_{0,sample}$) and mucin ($\eta_{0,mucin}$).

2.4. Mucoadhesion studies based on DLS

A mucin type II dispersion (1%, *v*/*v*) was prepared by diluting a 10% (*w*/*v*) mucin dispersion in simulated tear fluid (STF). Eye drop formulations were mixed with the prepared mucin dispersion or STF at a ratio of 30:7 (*v*/*v*) and stirred (300 rpm) for 30 minutes at room temperature. The particle size, polydispersity index and zeta potential were determined using a Zetasizer Ultra (Malvern Instruments).

3. RESULTS AND DISCUSSION

3.1. The main properties of LAT formulations

Prepared formulations present LAT micellar solutions with micelle size raging between 15

P114

and 20 nm, suitable for ophthalmic administration in form of eye drops.

3.2. Mucoadhesive properties of LAT eye drop formulations determined by TPA, rheological synergism and DLS

Comparative study of three mucoadhesion measurement techniques revealed positive impact of NaHA on mucoadhesive properties of LAT formulation (Fig.1 and 2, Table 1).

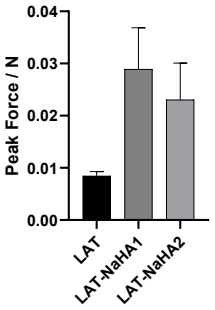

Figure 1. Determination of peak force (N) of LAT formulations (mean ± SD; n = 5).

The increase in mucoadhesion was more pronounced in the LAT formulation prepared with NaHA of higher molecular weight (950 vs 820 kDa). LAT-NaHA1 formulation was characterized by the highest peak force (Fig. 1), the largest increase in particle size when mixed with mucin (Fig. 2) and the strongest rheological synergism among the formulations compared.

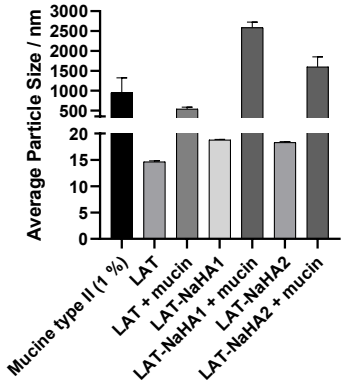

Figure 2. Average particle size (nm) of mucin, LAT formulations and mucin mixed with LAT formulation (mean ± SD; n = 3).

Table 1. Rheological synergism of LAT formulations with mucin. Viscosity (η_0) of mucin dispersion is 3.96 m·Pas.

Sample	$\eta_{0,sample}$ (m·Pas)	$\eta_{0,mix}$ (m·Pas)	Rheological synergism
LAT-NaHA1	8.58	22.03	1.76
LAT-NaHA2	5.51	14.87	1.57

Formulations with NaHA exhibited higher zero-shear viscosity in the mixtures than the theoretical sum, indicating positive rheological synergism (Table 1). This suggests interaction between components and potential mucoadhesive behavior.

The combination of techniques to measure mucoadhesion provided a comprehensive approach to understanding the mucoadhesive properties of the LAT formulation.

4. CONCLUSION

Combined *in vitro* mucoadhesion studies contributed to the targeted development of the mucoadhesive LAT eye drop formulation.

5. REFERENCES

1. Woertz C. et al. *Assessment of test methods evaluating mucoadhesive polymers and dosage forms: An overview*. European Journal of Pharmaceutics and Biopharmaceutics 2013. 85 (3): 843-853.

ACKNOWLEDGMENT

This work was supported by the National Recovery and Resilience Plan of the Republic of Croatia under the project *Collaborative research and development of an innovative product for the treatment of glaucoma and related ocular surface diseases – GlauCollab* (project code: NPOO.C3.2.R3-I1.04.0013) and by the European Regional Development Fund under the project FarmInova (KK.01.1.1.02.0021). GlauCollab project is led by Jadran-Galenski laboratorij d.d. in collaboration with the University of Zagreb Faculty of Pharmacy and Biochemistry.

P115

METHOD SUITABILITY VALIDATION FOR DETERMINATION OF MICROBIOLOGICAL PURITY OF METRONIDAZOLE+CLOTRIMAZOLE (500+200) mg PHARMACEUTICAL PREPARATION FOR VAGINAL USE

Damjan Shushleski[1], Marjan Velkovski [1], Irena Slaveska Spirevska[1], Silvana Ristevska [1], Ivana Karchicka [1], Anica Dimovska[1]

[1]Quality Control Department, Replek Farm, Skopje, North Macedonia

1. INTRODUCTION

The development and validation of analytical methods are essential components of drug discovery and pharmaceutical product development.

Metronidazole, nitroimidazole-class antimicrobial, is widely used to treat anaerobic bacterial and protozoal infections, including those affecting the vaginal tract [1]. Clotrimazole, an imidazole derivative, is a broad-spectrum antifungal commonly indicated for the treatment of vaginal fungal infections [2].

However, the antimicrobial activity of this combination therapy can interfere with microbiological testing by inhibiting the growth of test microorganisms. Such suppression may compromise the accuracy of microbial purity assessments, particularly during microbial limit testing of non-sterile pharmaceutical products.

Therefore, it is essential to perform method suitability validation to confirm that the analytical method can detect viable microorganisms in the presence of antimicrobial substances. Analytical method validation is critical to ensuring the reliability of microbiological quality control procedures and compliance with pharmacopeial requirements.

2. MATERIALS AND METHODS

2.1. Materials

During the method validation, standard microbiological laboratory equipment was utilized, including a Class II A biosafety cabinet, Binder microbiological incubators set at two temperature ranges (20–25 °C and 30–35 °C), a Bunsen burner, filtration apparatus, orbital shaker, and sterile glassware suitable for microbiological use.

For the validation process, 10 g of the Metronidazole + Clotrimazole (500 mg + 200 mg) vaginal pessary was accurately weighed using a Kern analytical balance. A pharmacopoeia diluent, supplemented with neutralizing agents—Buffered Sodium Chloride-Peptone Solution (pH 7.0) containing 3% Polysorbate 80, 0.3% Lecithin, and 0.1% Histidine—was selected as the dissolution and dilution medium for preparing the culture suspensions.

The membrane filtration method was employed using sterile PVDF membrane filters (0.45 µm pore size) and a 0.9% Sodium Chloride solution as the rinsing fluid. All nutrient media used during the validation were ready-to-use and sourced from BioMérieux, Oxoid, and Merck, ensuring compliance with quality standards.

The validation incorporated a panel of standard test microorganisms, as specified by the current European Pharmacopoeia for method suitability testing. These included: *Pseudomonas aeruginosa* ATCC 9027, *Bacillus subtilis* ATCC 6633, *Staphylococcus aureus* ATCC 6538, *Candida albicans* ATCC 10231, *Aspergillus brasiliensis* ATCC 16404 [3].

2.2. Method

To assess antimicrobial activity and validate the test method, a challenge test was performed using the specified microorganisms. The membrane filtration method with a 1:100 product dilution (secondary suspension) was validated as suitable for quantitative determination of TAMC and TYMC (Ph. Eur. 2.6.12, 5-2-1), and for qualitative testing of the absence of Staphylococcus aureus, Pseudomonas aeruginosa, and Candida albicans (Ph. Eur. 2.6.13, 4-4, 4-5, 4-7).

Inoculum levels ranged from 10 to 100 CFU/mL, and all tests were conducted in duplicate. Incubation times and temperatures were medium-dependent: TSA (30–35°C, 3 days), SDA (20–25°C, 5 days), TSB (30–35°C, 24h), CTRA and MSA agars (30–35°C, 24h).

Post-incubation, microorganism recovery in the presence of the product was compared to controls prepared in Pharmacopoeial diluent (pH 7.0) supplemented with neutralizing agents. Recovery percentages were within the acceptable range of 50–200%, and Recovery Factors (RF) met the requirement that counts must not differ from controls by more than a factor of 2 [3].

3. RESULTS AND DISCUSSION

3.1. Results and Discussion

The selected test method for determining microbiological purity must closely replicate the conditions of the proposed microbial limit test, including sample preparation procedures, types of media and diluents, and incubation parameters. To verify the method's suitability, it is essential to demonstrate that the proposed procedure can effectively recover viable microorganisms potentially present in the product. This is achieved by challenging the method with representative microorganisms as specified by the European Pharmacopoeia.

Our results indicate that the product, Metronidazole + Clotrimazole (500 mg + 200 mg) vaginal pessary, exhibits notable antimicrobial activity against Candida albicans, a recommended test organism. When using the primary suspension (1:10 dilution), the observed Recovery Factor exceeded the acceptable threshold (RF > 2), indicating microbial inhibition by the product. However, the use of a secondary suspension (1:100 dilution) successfully neutralized this antimicrobial effect, as evidenced by microbial growth comparable to the control, thereby confirming the elimination of antimicrobial interference and the method's suitability for use.

Additionally, a product negative control was performed to assess any inherent bioburden that could potentially interfere with microbial recovery during the challenge study [3].

4. CONCLUSION

The product Metronidazole + Clotrimazole (500 mg + 200 mg) vaginal pessary exhibits significant antimicrobial activity against the test microorganism *Candida albicans* when using a Pharmacopoeial diluent (pH 7.0) supplemented with neutralizing agents for the preparation of the primary suspension (1:10 dilution). This antimicrobial effect was neutralized in subsequent dilutions prepared with the same diluent and neutralizers.

In comparison with the control, positive microbial growth was observed in the secondary suspension (1:100 dilution), indicating that the antimicrobial activity of the product was effectively neutralized at this dilution. The secondary suspension demonstrated no interference from the product on microbial growth, with all tested microorganisms exhibiting compliant Recovery Factor values (≤2), in accordance with validation criteria.

5. REFERENCES

1. Löfmark S, Edlund C, Nord CE. Metronidazole is still the drug of choice for treatment of anaerobic infections. Clin Infect Dis. 2010 Jan 01;50 Suppl 1:S16-23

2. Crowley PD, Gallagher HC. Clotrimazole as a pharmaceutical: past, present and future. J Appl Microbiol. 2014 Sep;117(3):611-7.

3. European Pharmacopoeia 10th Edition. (2020).

P116

SETTING CLEANING VALIDATION ACCEPTANCE LIMITS AND DEVELOPING HPLC METHOD FOR DETERMINATION OF BENZYDAMINE RESIDUES ON MANUFACTURING EQUIPMENT

Irena Slaveska Spirevska[1], Katerina Kochova[1], Kristina Grncharoska[1], Elena Petrovska[1],

[1]Replek Farm Ltd., Kozle 188, 1000, Skopje, N. Macedonia

1. INTRODUCTION

Benzydamine is a locally acting nonsteroidal anti-inflammatory drug (NSAID) with local anaesthetic and analgesic properties. The most common pharmaceutical dosage forms of the drug are a liquid mouthwash, oromucosal spray and pastilles.

Toxicological properties of benzydamine are well known due to its extended therapeutical use in humas and no special hazards for humans have been observed. Preclinical studies have not reported any no observed effect level/no observed adverse effect level (NOEL/ NOAEL) values [1].

When formulated as a pastille, each unit contains 3 mg of benzydamine hydrochloride. The lowest recommended dose of benzydamine hydrochloride is 3 mg. Therefore, the lowest observed effect level/lowest observed adverse effect level (LOEL/LOAEL) of 3 mg/day is used for calculation of permitted daily exposure (PDE) [2].

In accordance with ICH Q3C, the procedure for determination of PDE described in Guideline on "Setting health-based exposure limits for use in risk identification in the manufacture of different medicinal products in shared facilities" (EMA 2014), the obtained value for PDE was 0.03 mg/day [2][3].

For setting maximum allowable carryover (MACO) limit for benzydamine residues on manufacturing equipment, as a next product was selected the product with the highest maximum daily dose as the worst-case scenario. The obtained MACO value of 580 mg or 4.12 ppm (below the 10-ppm), ensure the safe value. Furthermore, the limit per surface area of manufacturing equipment and in the analyzed sample were calculated, with the obtained values 2.53 µg/cm^2 and 2.53 ppm, respectively [4].

The objective of this study was to develop and validate a sensitive reversed-phase high performance liquid chromatography (RP-HPLC) method for detecting benzydamine residues in swab samples as part of the cleaning validation process.

2. MATERIALS AND METHODS

2.1. Instrumentation and equipment

Chromatography was performed using a Shimadzu Nexera XR UPLC system equipped with a quaternary low-pressure gradient (LPG) pump, with degasser, autosempler, column oven, controller and a photodiode array (PDA) detector, controlled by Lab Solutions software. Additional equipment included a semi-micro analytical balance Mettler Toledo XRP10, TP690/H ultrasonic bath, and a Mettler Toledo S213 pH/conductivity meter. Ultrapure water was produced using a Simplicity UV system. Syringe filters (0.45 µm, regenerated cellulose) were obtained from Agilent Technologies (USA).

2.2. Chemical and reagents

The reagents that have been used are diethylamine, methanol, 85% o-phosphoric acid and acetonitrile purchased from Carlo Erba. Reference standard Benzydamine hydrochloride BPCRS, was supplied by the European Directorate for the Quality of Medicines (EDQM). Textwipe 714 A Swabs (Large Alpha Swab) were used for direct sampling.

2.3. Chromatographic conditions

Separation was achieved on a LiChrospher RP Select B 125 mm, 4.0 mm, 5 µm column, at 30°C, using isocratic elution, with flow rate 1.1 mL/min. The injection volume was 20 µL and detection wavelength was 232 nm. The mobile phase consisted of a mixture of 20 volumes of methanol, 25 volumes of acetonitrile and 55 volumes of 0.4 %(v/v) diethylamine with the pH adjusted to 3.0 using phosphoric acid. A 1:1 (v/v) mixture of Methanol and water pH 3.0 adjusted with phosphoric acid was used as diluent.

3. RESULTS AND DISCUSSION

The validation of the RP-HPLC method was conducted in accordance with the criteria specified in the International Conference on Harmonization (ICH) guideline for validation of analytical procedures [5]. Selectivity testing showed no interference from the blank swab sample at the retention time of Benzydamine. Recovery studies and spiking tests were conducted on a stainless-steel plate to confirm the suitability of the direct sampling procedure for determination of Benzydamine residues on equipment surface by spiking standard solutions of Benzydamine at three concentration levels: 5 µg/mL, 25 µg/mL and 30 µg/mL. The achieved swab recovery factor of 0.729 (72.88 %) was applied as a correction factor in the cleaning validation results.

The linearity of the method was demonstrated through seven concentrations, in the range from 40 µg/mL to 2.5 µg/mL with the correlation coefficient value (R^2) was 0.9999. The limit of detection (LOD) and limit of quantification (LOQ) were determined by using series of linearity solutions and were found to be 0.01 µg/mL and 0.04 µg/mL, respectively. The precision of the system was also evaluated at the LOQ level, and the obtained RSD value was less than 5 %.

4. CONCLUSION

The HPLC method was developed and validated for determining residual amounts of benzydamine after the cleaning procedure demonstrating sensitivity, linearity, accuracy and precision. The established limits are practical, achievable, and ensure product quality and patient safety and minimize the risk of cross contamination. Based on the validation results, the method is suitable for determination of benzydamine residues in swab samples from manufacturing equipment, and the proposed limits can be applied for routine cleaning validation procedures

5. REFERENCES

1. National Center for Biotechnology Information. PubChem Compound Summary for CID 12555, Benzydamine. https://pubchem.ncbi.nlm.nih.gov/compound/Benzydamine. Accessed May 14, 2025.
2. International Conference on Harmonization, 2024. Impurities guideline for residual solvents Q3C (R9). ICH, Geneva, Switzerland.
3. EMA/CHMP/CVMP/SWP/169430/2012. European Medicine Agency (EMA) (2014). Guideline on setting health-based exposure limits for use in risk identification in the manufacture of different medicinal products in shared facilities
4. LeBlanc Destin A., 2000. Validated Cleaning Technologies for Pharmaceutical manufacturing. Interpharm Press, Denver, Colorado, US.
5. International Conference on Harmonization, 2005. Validation of analytical procedures: Text and methodology Q2(R1). ICH, Geneva, Switzerland.

P117

CHIRAL SEPARATION BY HPLC OF PEPTIDE SULFOXIDES CONTAINING OXIDIZED METHIONINE IN THEIR SEQUENCE

Lucian-Mihai Stănescu[1], Corina-Cristina Aramă[1], Gabriela Chirițoiu[2], Ștefana Petrescu[3], Cristian V.A. Munteanu[2]

[1]*University of Medicine and Pharmacy, Carol Davila, Faculty of Pharmacy, Analytical chemistry department, Bucharest, Romania*

[2]*Department of Bioinformatics and Structural Biochemistry, Institute of Biochemistry of the Romanian Academy (IBRA), Bucharest, Romania*

[3]*Department of Molecular Cell Biology, Institute of Biochemistry of the Romanian Academy (IBRA), Bucharest, Romania*

1. INTRODUCTION

Chiral separations of peptides derived from D and L amino acids are analytical methods developed for compounds with asymmetric C-atom. The biological activity of the stereoisomers may differ and it is important to develop optimum method of separation [1].

In other cases, the sulphur atom may be chiral, for the peptides containing methionine (Met) oxidized to sulfoxides. These compounds have different activity compared to native, unoxidized peptides [2], but it is not known if the biological activity and the efficacity of optical isomers differ.

Our aim is to separate the isomers using a chiral chromatographic technique for future possible biological use. Peptides containing at least an oxidized methionine residue were separated using liquid chromatography coupled with UV-Vis and circular dichroism (CD) detection. The sequence of the collected fractions was confirmed by mass spectrometry (MS).

2. MATERIALS AND METHODS

2.1. **Materials**

Various nonapeptides containing oxidized methionine residues were analyzed using reverse phase chiral liquid chromatography using a chromatograph equipped with CD and UV detection, followed by MS analysis.

2.2. Method-HPLC-CD analysis

The absolute configuration (*R* and *S*) was attributed to each optic isomer by HPLC analysis, using a stationary phase derived from cellulose. The separated fractions were collected and purified. For each peptide racemic, stability was verified for two conditions.

3. RESULTS AND DISCUSSION

In chiral HPLC analysis, we obtained separation of some racemic sulfoxide peptides with different sequences, containing one oxidized methionine, when chaotropic agents were added to the mobile phase. The stability of the racemic mixtures was verified during a month of storage at -20°C and 4°C

4. CONCLUSION

The obtained results demonstrate that the workflow is suitable for the isolation and purification of stereoisomers with high optical purity. Each of them is stable at -20 °C without further interconversion. Future studies will extend to other Met-containing peptides. The collected fractions may be used in cell cultures in order to verify if different biological effect can be attributed to each stereoisomer.

5. REFERENCES

1. Ali I. et al, Advances in chiral separations of small peptides by capillary electrophoresis and chromatography Journal of Separation Science, 2014 (00): 1–20

2. Chirițoiu G. et al, Methionine oxidation selectively enhances T cell reactivity against a melanoma antigen, iScience, 2023 (26): 107205

P117

ACKNOWLEDGMENTS

Funding was received through grant PN-IV-P8-8.3-ROMD-2023-0100, and by “Carol Davila” University of Medicine and Pharmacy Bucharest, Romania Contract no. 33PFE/30.12.2021 funded by the Ministry of Research and Innovation within PNCDI III, Program 1—Development of the National RD system, Subprogram 1.2—Institutional Performance—RDI excellence funding projects.

P118

DETERMINATION OF SEDIMENTATION RATE IN MEDROXYPROGESTERONE ACETATE INJECTABLE SUSPENSION

Ema Šolić[1], Petra Golja Gašparović[1], Ivana Mijakovac[1], Marjana Dürrigl[1]

[1]PLIVA Croatia Ltd, Research and Development, member of Teva, Zagreb, Croatia, Zagreb, Croatia

1. INTRODUCTION

Many pharmaceutical products are aqueous suspensions of a water-insoluble active ingredient in the presence of excipients. Their sedimentation characteristics are of significant importance in formulation research because they determine the compactness of the sediment during storage and thus the resuspendability of the suspension. In fact, the homogeneity of a suspension after shaking affects the amount of active ingredient that is present in a given dose, and hence its efficacy [1]. In this study the characterization of sediments was exemplified by using aqueous suspensions of medroxyprogesterone acetate (MPA), a derivative of progesterone . The sedimentation properties of these model of pharmaceutical suspensions were manipulated by adjusting the particle size distribution and by the addition of polyethylene glycol (PEG). The latter has been reported to have a concentration and molecular weight dependent effect on sedimentation properties, which may be ascribed to depletion or bridging flocculation [1]. Polymer-induced flocculation with high molecular weight polymer proceeds through particle bridging mechanism. Bridging flocculation occurs when high molecular weight polymer molecules adsorb simultaneously on more than one particle, a phenomenon that can produce large flocs [2]. This phenomenon is desired in terms of easier resuspendability of suspensions.

2. MATERIALS AND METHODS

2.1. Materials

Different formulations of MPA injectable suspensions were evaluated, as seen in Table 1.

Table 1. Physical characteristic of tested samples.

Sample	API* PSD Dx (90) / µm	Amount of PEG 3350 (mg/ml)
0	9	20
1	30	20
2	30	20 (1/2 the amount of API)
3	30	10 (1/2 the amount of all the excipients)
4	30	10
5	30	40

*API – Active pharmaceutical ingredient, PSD – particle size distribution

2.2. Method

2.2.1. Sediment rate determination at 1g

Sedimentation rate was examined with an instrument LUMiFuge (LUM GmbH, Berlin, Gemany) which speeds up the separation of dispersions by using centrifugal force, hence sees the results of destabilizing processes far faster than visual observation. The experiment was conducted on 4 formulations (Sample 0, 1, 2 and 3) at 3 different rotational speeds: 200, 500 and 1000 rpm. Based on experimental values of velocity and relative centrifugal acceleration (RCA) a linear equation was obtained and sedimentation rate at 1g was extrapolated.

2.2.2. Sediment height determination

Sedimentation rate at 500 rpm and the height of the sediment were examined for 3 different formulations, as seen in Table 1 (formulation 1, 4 and 5).

P118

3. RESULTS AND DISCUSSION

3.1. Sediment rate determination at 1g

The results for Sample 1 are presented in Table 2 and in Figure 1. The sedimentation rates extrapolated to 1g for all tested samples are shown in Table 3.

Sample 0 with smaller PSD showed slower sedimentation rate than Sample 1 with higher PSD, which is in accordance with the law of gravity. Sample 2 had smaller viscosity due to the reduced amount of API by half, therefore sedimented faster than Sample 1. Sample 3 had half the amount of all components, hence showed the highest sedimentation rate due to the lowest viscosity.

Table 2. Velocity and RCA results at different rotational speeds for Sample 1.

Rotational speed (rpm)	RCF (g)	Velocity (µm/s)	RCA (g)
200	6	2.3	5.1
500	36	15.1	31.4
1000	144	52.4	125.6

RCF = Relative Centrifugal Force

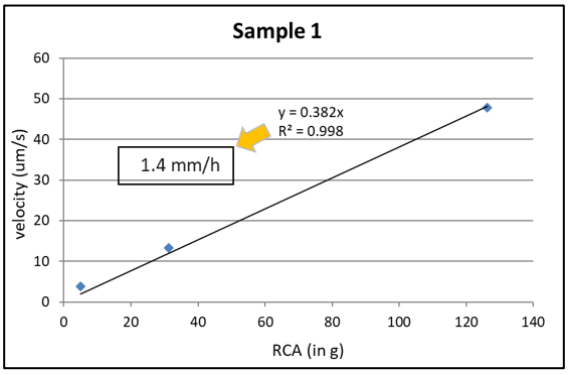

Figure 1. Graphic representation of linear independence between velocity and RCA for Sample 1.

Table 3. Sedimentation speed results at 1g for all tested samples.

Sample	Sedimentation rate (mm/h)
0	0.7
1	1.4
2	3.1
3	3.8

3.2. Sediment height determination

Some studies suggest that in the presence of a large amount of high molecular weight PEG, a percolating structure is possibly obtained with the polymer forming a backbone, providing significant enhancement to flocculation [1]. The homogenous flocculated network becomes slowly compressed under the effect of gravity [1]. In accordance with that theory, the results presented in Table 4. show that reduction of amount of PEG resulted in lower sediment height, which implies that API particles weren't that flocculated and sediment was more compressed than in Sample 5, which contained more PEG and, therefore, less compressed sediment due to higher flocculation of API particles. Results also imply that there's a negative correlation between sedimentation velocity and sediment height.

Table 4. Velocity at 500 rpm and sediment height

Sample	Velocity at 500 rpm (µm/s)	Sediment height (mm)
1	15.0	13
4	16.1	12
5	12.2	14

4. CONCLUSION

In summary, this method allowed the determination of sedimentation rate and sediment height as a part of characterization of physical properties of an injectable suspension, the important parameters which may impact on administered dose and, therefore, facilitating optimal drug product development.

5. REFERENCES

1. Wuxin, Z., *Sedimentation and resuspendability evaluation of pharmaceutical suspensions by low-field one dimensional pulsed field gradient NMR profilometry,* Pharmaceutical Development and Technology, 2013; 18(4)

2. Hogg, R., *Bridging flocculation by polymers,* KONA Powder and Particle Journal No.30, 2013.

ACKNOWLEDGMENT

Special credits to the whole R&D MPA team.

P119

STABILITY-INDICATING HPLC-UV ANALYTICAL METHOD FOR FOLATES IN MEDICINES AND FOOD SUPPLEMENTS

Žane Temova Rakuša, Robert Roškar

Faculty of Pharmacy, University of Ljubljana, Slovenia

1. INTRODUCTION

Folate is a generic term for a group of essential micronutrients that are part of the B-complex family of water-soluble vitamins. Under the current European Union legislation, three specific folate forms are authorized for use in food supplements (FS): pteroylmonoglutamic acid, commonly known as folic acid, (FA), and the calcium and glucosamine salt of 5-methyl-tetrahydrofolic acid (5-MTHF) [1]. The 5-MTHF is the metabolically active folate form, which is involved in several physiological processes, including the synthesis of DNA and RNA and the functioning of the methionine cycle. As folate is essential for DNA replication and cell division, folate deficiency mostly affects rapidly proliferating tissues such as bone marrow, which can lead to megaloblastic anaemia. Since folate deficiency is associated with abnormalities in both foetuses (neural tube defects) and mothers (anaemia, peripheral neuropathy), its supplementation is especially important during pregnancy [2]. Recent research indicates that supplementation with 5-MTHF is more effective than FA, as it circumvents the need for enzymatic activation, which is often impaired due to the high prevalence of genetic polymorphisms in the general population [3]. Consequently, the use of 5-MTHF in FS has gained increasing popularity in recent years. However, their analytics are running behind, as there is currently no published analytical method for the simultaneous determination of both 5-MTHF and FA in FS and medicines. Furthermore, 5-MTHF is known to exhibit significantly lower stability compared to folic acid; yet, specific and quantitative data regarding its stability remain limited in the scientific literature. Therefore, this study aimed to develop a simple stability-indicating analytical method, using common analytical equipment based on liquid chromatography, suitable for both stability evaluation of 5-MTHF and FA and the quantification of their content in various matrices, including fortified foods, FS, and medicines.

2. MATERIALS AND METHODS

2.1. Materials

FA (97.8%) and 5-MTHF (98.1%) were purchased from Carbosynth (Berkshire, UK). HPLC-grade methanol was purchased from Sigma-Aldrich (Steinheim, Germany). Sodium dihydrogen phosphate monohydrate was obtained from Merck (Darmstadt, Germany). Ultra-pure water was obtained through a Milli-Q water purification system A10 Advantage (Millipore Corporation, Bedford, MA, USA).

2.2. HPLC (High-Performance Liquid Chromatography) Analysis

An Agilent UHPLC Infinity 1290 instrument (Agilent Technologies, Santa Clara, CA, USA), equipped with a diode array detector and an EZChrom acquisition system was used. The chromatographic separation was performed on a reversed-phase XSelect CSH C18 (150 × 4.6 mm, 3.5 µm particle size column (Waters Corporation, Milford, MA, USA) at 40 °C with a gradient elution mode consisting of a phosphate buffer solution and methanol. The detection wavelength was 287 nm.

2.3. Forced degradation study

The forced degradation study was performed following the ICH guidelines Q1A (R2) [4], by exposing 5-MTHF and FA individual standard solutions to daylight (photodegradation), elevated temperature (60 °C for thermal degradation), 0.1 M sodium hydroxide (alkaline degradation), 0.1 M hydrochloric acid (acidic degradation) and 0.3% H_2O_2 (oxidation) for 24 and 48 hours.

2.3. Method Validation

The method was validated following the ICH guidelines Q2(R2) [5] in terms of specificity, linearity, range, quantitation and detection limit. Accuracy, precision, and sample stability were determined based on three different quality control samples (QC) in triplicates.

P119

2.4. Method application: assay of food supplements

The developed method was applied to 5-MTHF and FA assay determination in commercial FS, available in Slovenia, in various dosage forms (capsules, tablets, powders, sprays, and oral drops).

3. RESULTS AND DISCUSSION

3.1. Method development and forced degradation study

The developed stability-indicating HPLC-UV method was found suitable for the separation and accurate quantification of both 5-MTHF and FA, as their chromatographic peaks are symmetric and properly baseline separated (Fig. 1). The degradation products formed in the forced degradation study did not interfere with any of the chromatographic peaks, proving the stability-indicating nature of the method. The obtained results from the forced degradation study indicated that 5-MTHF is significantly less stable than FA, showing considerable degradation under all stress conditions, whereas FA was found most susceptible to degradation under oxidative and acidic conditions.

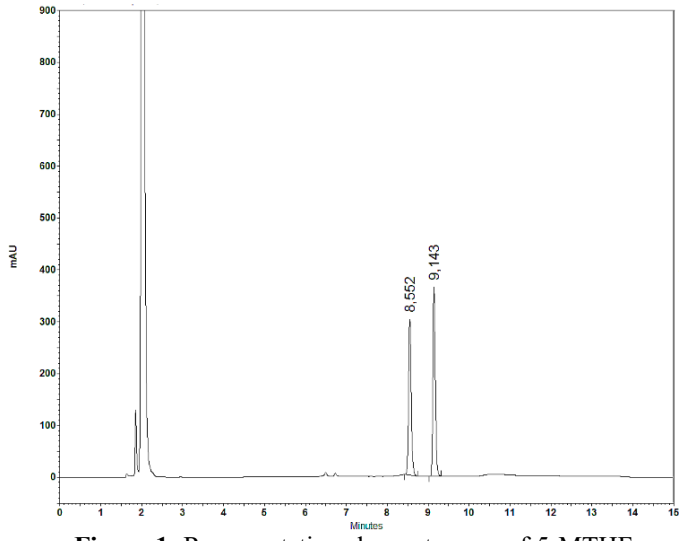

Figure 1. Representative chromatogram of 5-MTHF (retention time 8.6 min) and FA (retention time 9.1 min) at 287 nm.

3.2. Method validation

The method was successfully validated, proving its specificity, linearity (R^2>0.999) over the selected concentration range (1-10 mg/L), precision (RSD ≤ 5%), accuracy (100 ± 5%), and sample stability (100 ± 5%) and sufficiently low quantitation and detection limit for their analysis in FS.

3.3. Method application: assay of food supplements

The obtained results for 5-MTHF and FA contents in the tested FS confirm the applicability of the method for their routine assay analysis. The assay results were further evaluated in accordance with the *European Commission's (EC) Guidance Document for Competent Authorities on the Control of Compliance with EU Legislation* (Table 1), which establishes a tolerance range of 80% to 150% of the labelled claim [6]. Accordingly, FA and THFA contents falling within this range were considered compliant with the EC Guidance Document (coloured green in Table 1).

Table 1. FA and 5-MTHF assay in the tested FS.

	FS 1	FS 2	FS 3	FS 4	FS 5	FS 6	FS 7	FS 8	FS 9	FS 10
Product		tablets			capsules		powders		spray	oral drops
FA										
5-MTHF										

Green colour – contents within, red – above, and orange – below the acceptable tolerances, provided by the EC (80-150% of the labelled claim).

4. CONCLUSION

The developed method represents a step forward in folate analysis, enabling the analysis of both FA and the newer and active folate form 5-MTHF with a single sample preparation and chromatographic run and is applicable for both their stability evaluation and their assay in fortified foods, FS, and medicines.

5. REFERENCES

1. Directive 2002/46/EC of the European Parliament and of the Council. OJ L 183, 2002, 51–57.
2. EFSA Panel on Dietetic Products, Nutrition and Allergies. Scientific Opinion on Dietary Reference Values for folate. EFSA J. 2014;12:3893.
3. Vidmar Golja M, et al. *Folate Insufficiency Due to MTHFR Deficiency Is Bypassed by 5-Methyltetrahydrofolate.* J Clin Med. 2020;9:2836.
4. ICH Stability Testing of New Drug Substances and Products Q1A(R2). 2003.
5. ICH Validation of analytical procedures Q2(R2). 2023.
6. European Commission. Guidance Document for Competent Authorities 2012. Available from: https://assets.publishing.service.gov.uk/government/uploads/system/uploads/attachment_data/file/212935/EU-Guidance-on-Tolerance.pdf

P120

SODIUM METABISULFITE AS AN ANTIOXIDANT AND PRESERVATIVE USED IN FORMULATION OF THE MEDICINAL PRODUCTS: DEVELOPMENT OF THE ANALYTICAL METHOD FOR THE ASSAY OF SODIUM METABISULFITE IN SOL ORAL SOLUTION FORMULATION

Justyna Wolniarska[1], Justyna Dąbrowska[1], Tatsiana Krautsova[1], Magdalena Łysiak[1], Daniel Nosal[1], Łukasz Przybyło[1], Joanna Rząsa[1]

[1]R&D Department, Adamed Pharma S.A., Poland

1. INTRODUCTION

Sodium Metabisulfite (E223) can be used both as an antioxidant and/or as a preservative for the medicinal product formulations. In oral, parenteral and topical formulations is used at concentration of 0.01 – 1.0% w/v, in acidic preparations.

Properties: It has the chemical formula $Na_2S_2O_5$, and its molecular mass is 190.1 g/mol. Colourless, crystals or white to creamy white crystalline powder, has the odour of sulfur dioxide, pH for a 5.0% aquas solution is 3.5 – 5.0. In water, is immediately converted to sodium and bisulfite ions. Soluble 1: 1.2 in water, freely soluble in glycerin, slightly soluble in ethanol. [1]

For each antioxidant and antimicrobial preservative, the application should contain:
• reason for inclusion and justification of level of inclusion
• proof of safety and efficacy
• the method of control in medicinal product
• levels on storage of broached and unbroached containers
• details on the labelling of the medicinal product [2]

Table 1. Labelling requirements for Sodium metabisulfite used for the medicinal products

Name	Route	Threshold	Information for the Package Leaflet
Sulphites including metabisulphites	Oral Parenteral Inhalation	Zero	May rarely cause severe hypersensitivity reactions and bronchospasm

Allergy to sulfite is estimated to occur in 5 – 10% of asthmatics, thus warrant on the package and patient leaflet is mandatory, as presented in Table 1. [1],[3]

Requirements in the release and shelf-life specification are established according to guidelines ICH Q6A, 3AQ11a and experimental data.[4], [5]

2. MATERIALS AND METHODS

2.1. Scope of work

The analytical method was developed and validated to determine the content of Sodium Metabisulfite in the oral solution formulation. The analytical method had to be specific for Sodium Metabisulfite be well separated from the active substance and its impurities. Different diluents were tested to obtain symmetrical and reproducible peak of Sodium Metabisulfite.

2.2. Sample diluent

Sodium metabisulfite is soluble in water, therefore water was first used as a sample diluent. The peak shape was good, but the stability of the solution was poor.

The next solvent, which was used as diluent, was phosphate buffer (diammonium hydrogen phosphate solution (4 mg/ml)). Three different

pH (pH 7.0, pH 7.2 and pH 7.5) of phosphate buffer were tested.

3. RESULTS AND DISCUSSION

3.1. Results and Discussion

The best peak shape was achieved with the phosphate buffer pH 7.0 and it was decided that this solution will be used as a sample diluent.

The peak shape was worse when a different HPLC system was used. Therefore, the phosphate buffer pH 7.0 was mixed with methanol in volumetric ratio 8:2.

Sodium metabisulfite is an inorganic compound that in an aqueous environment is transformed into sodium hydrosulfite with oxidizing properties. Due to the chemical nature of sodium metabisulfite, specific HPLC analysis elements were used, such as:

- use of tetrabutylammonium hydrogen sulphate salt in mobile phase A to generate an ion pair with sodium hydrogen sulphite during analysis,

- a diamine hydrogen phosphate buffer with pH = 7.0 was used in the solvent to stabilize sodium hydrosulfite against decomposition into sulfur dioxide, which occurs in an acidic environment,

- Kinetex Biphenyl column in a size typical for UHPLC analyses, due to the low affinity of the tetrabutylammonium hydrosulfate ion pair with sodium hydrosulfite to typical stationary phases, the instrumental analysis conditions were selected so that the column operating pressure oscillated around 2000 psi.

4. CONCLUSION

The medicinal product release specifications should include a content determination test with acceptance criteria and limits for each antioxidant and antimicrobial preservative present in the formulation.

The developed method for determining sodium metabisulfite assay is in line with the requirements as well as is optimal from the quality control's point of view.

5. REFERENCES

1. Sheskey, PJ, et al, *Sodium metabisulfite,* Handbook of Pharmaceutical Excipients 8th Edition, 2017

2. A guideline on excipients in the dossier for application for marketing authorisation of a medicinal product Doc. Ref. EMEA/CHMP/QWP/396951/2006, Revision 2, 2008

3. Annex to the European Commission guideline on Excipients in the labelling and package leaflet of medicinal products for human use (SANTE-2017-11668), Revision 4, 2024

4. ICH Q6A, Test procedures and acceptance criteria for new drug substances and new drug products: chemical substances, 2000

5. ICH 3AQ11a, Specifications and control tests on the finished product, 1992

ACKNOWLEDGMENT

Project is co-financed from the EU funds under the European Regional Development Fund;

Project title: „Development and implementation of a new generation drug in the form of an easily applicable oral solution used to eradicate nicotine addiction” POIR.01.02.00-00-0072/18-00

P121

3D PRINTED SETUPS FOR IMAGING AND DRUG RELEASE TESTING

Piotr Kulinowski[1*], Wojciech Kulinowski[1], Wiktor Hudy[1], Mateusz Kuprianowicz[2], Bartłomiej Milanowski[2], Martyna Nyga [2], Przemysław Dorożyński[3], Ewelina Baran[1], Grzegorz Banach[4], Grzegorz Garbacz[4]

[1]Institute of Technology, Pedagogical University of Cracow, Kraków, Poland
[2]GENERICA Pharmaceutical Lab, Regionalne Centrum Zdrowia Sp. z .o.o., Poland
[3]Faculty of Pharmacy, Jagiellonian University Medical College, Kraków, Poland
[4]Physiolution Polska Sp. z o.o., Wrocław, Poland

1. INTRODUCTION

Garbacz et al. proposed the *pHysio-grad®* device [1], which has been successfully used in several studies. It has also been integrated with the *Revolver* apparatus (Physiolution Polska Sp. z o.o., Poland) [2]. The magnetic resonance imaging (MRI) technique has been proven to be a valuable tool for studying drug delivery systems [3]. The first approach to customize drug release devices using fast prototyping techniques has been presented by Dorożyński et. al [4]. Therefore, the study aimed to design and evaluate 3D printed setups serving as an extension for the *Revolver* apparatus, offering fixtures for various drug delivery systems (DDS), enabling drug release testing, and *in situ* imaging of "working" dosage forms.

2. MATERIALS AND METHODS

2.1. Materials (drug delivery systems)

Various dosage forms were prepared, including, among others, a floating system (a gelatin capsule filled with a mixture of HPMC and metronidazole) and Ropinirole HCl buccal tablets composed of sodium alginate, Pluronic F-127, and magnesium stearate.

2.2. Design, 3D printing, and metrology

The setup's models were designed using Inventor 2023 (Autodesk, United States). They were printed using Photon D2 resin printer and standard resin (Hongkong Anycubic Technology CO., Hong Kong). Printed setup geometry was measured using an optical 3D profilometer VR-5000 (Keyence, Belgium).

2.4. Drug release

Drug release profiles from DDS positioned in the 3D printed setups of the flow-through cells were obtained using the Revolver apparatus working in a closed loop configuration (Fig. 1) [1, 2]. The amount of released APIs was determined using validated RP-HPLC-UV methods.

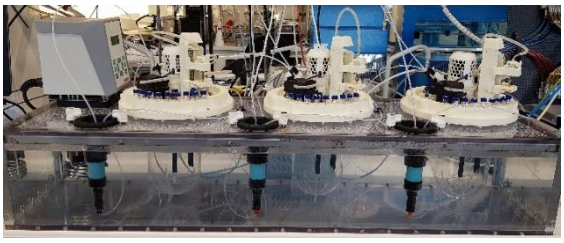

Figure 1. The Revolver apparatus in closed loop configurations with flow-through cells (three units) and a peristaltic pump.

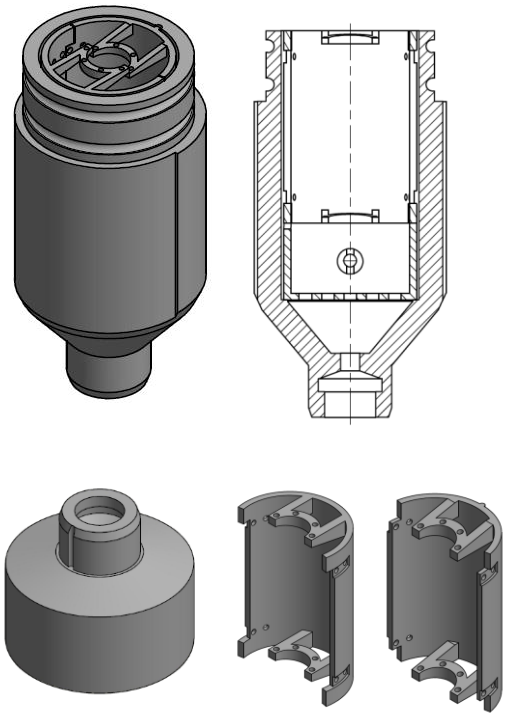

Figure 2. Example of the setup for floating dosage form imaging/drug release.

2.2. Magnetic resonance imaging

MRI was performed using a 9.4 T MRI research scanner (Biospec 94/20, Bruker BioSpin MRI

GmbH, Ettlingen, Germany). Two imaging sequences were used: multi-echo spin-echo (MSME) and a three-dimensional version of UltraShort Echo Time (UTE3D).

3. RESULTS AND DISCUSSION

All setups were designed as modifications of USP4 flow through cell and consisted of corpus, cap, and interchangeable inserts. The cell designed for floating DDS is presented in Fig. 2. The drug release results for floating and buccal DDS are shown in Fig. 3. UTE3D imaging results for floatin and buccal DDS are presented in Fig. 4 and Fig. 5 respectively. Buccal DDS are shown using two contrasting variants (spin-echo MRI at 1st and 19th echo).

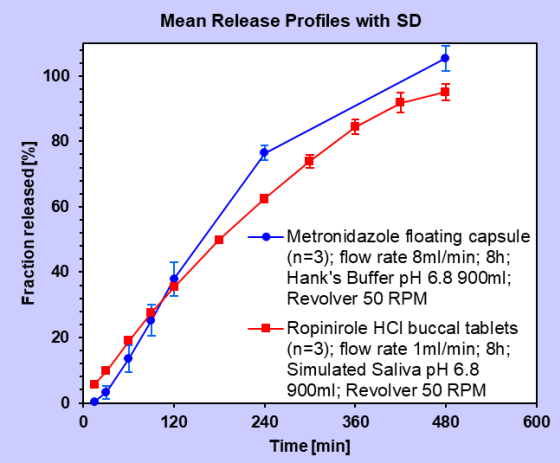

Figure 3. APIs release profiles from floating and buccal DDS.

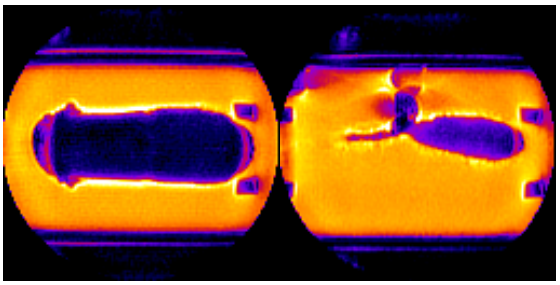

Figure 4. Floating DDS immediately after immersion (left) and after 2h (right) imaged using UTE3D.

4. CONCLUSION

The study demonstrated that the designed 3D-printed setups can be effectively used as extensions for the Revolver apparatus, offering flexibility in adaptability—providing dedicated configurations for various drug delivery systems (DDS), including floating systems, modified-release matrix systems, buccal systems, wound dressings, intravaginal matrix systems, and implantable devices—and enabling both drug release testing and imaging experiments.

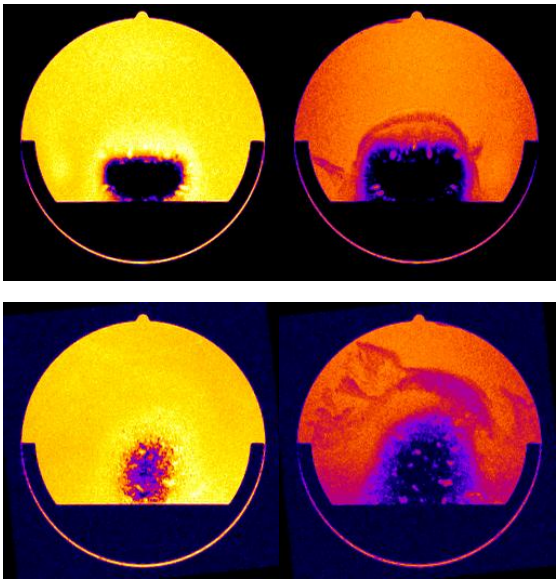

Figure 5. Buccal DDS immediately after medium immersion at 1st (upper row, left) and 19th echo (upper row, right), and after 4h 1st (lower row, left) and 19th echo (lower row, right), imaged using MSME.

5. REFERENCES

1. Garbacz, G., Kołodziej, B., Koziolek, M., Weitschies. W., Klein, S., 2014. *A dynamic system for the simulation of fasting luminal pH-gradients using hydrogen carbonate buffers for dissolution testing of ionisable compounds*. Eur J Pharm Sci. 51, 224-31

2. Milanowski B. & Kuprianowicz M., *Application of a novel Revolver apparatus for a biorelevant dissolution test of ropinirole sustained release tablets*, Macedonian pharmaceutical bulletin, 2023:69 (Suppl 1) 241 – 242

3. Kulinowski, P. & Dorożyński, P. *Applications of MRI to Study Controlled Drug Release Formulations: From Model Formulations Toward the Understanding of Drug Products Behavior.* In: Mantle, M. D. & Hughes, L. P. (eds.) *Magnetic Resonance and its Applications in Drug Formulation and Delivery*. Royal Society of Chemistry, 2024

4. Dorożynski P., Jamroz W., Węglarz W.P., Kulinowski W., Zaborowski M., Kulinowski P., *3D Printing for Fast Prototyping of Pharmaceutical Dissolution Testing Equipment for Nonstandard Applications*, Dissolution Technologies 2018:25(4) 48-53.

ACKNOWLEDGMENT

This work was supported by the Polish National Centre for Research and Development (NCBR), grant number POIR.04.01.04-00-0142/17.

P122

ASSESSMENT OF CHANGES IN TOTAL HEMISPHERICAL REFLECTANCE AND EMISSIVITY OF PARACETAMOL AND VITAMIN C EFFERVESCENT TABLETS STORED UNDER STRESS CONDITIONS

Michał Meisner[1,2], Szulc-Musioł Beata[3], Sarecka-Hujar Beata[2]

[1]Doctoral School of the Medical University of Silesia in Katowice, Faculty of Pharmaceutical Sciences in Sosnowiec, Poland

[2]Department of Basic Biomedical Science, Faculty of Pharmaceutical Sciences in Sosnowiec, Medical University of Silesia in Katowice, Poland

[3] Department of Pharmaceutical Technology, Faculty of Pharmaceutical Sciences in Sosnowiec, Medical University of Silesia in Katowice, Poland

1. INTRODUCTION

Effervescent tablets are a solid dosage form that offers ease of administration similar to liquid forms, making them suitable for people with swallowing difficulties, including children and the elderly. They offer a longer shelf life and greater resistance to adverse conditions compared to liquid drugs [1,2].

Dissolving effervescent tablets before administration may result in a milder effect on the gastrointestinal tract and may enhance absorption of active substances due to increased permeability in the presence of carbon dioxide. The stability of pharmaceutical products, guided by standards such as those of the International Council for Harmonization (ICH), is crucial to ensuring therapeutic efficacy and safety. Traditional methods of monitoring drug stability are often destructive and time-consuming.

New methods, such as hemispherical directional reflectance and spectral emissivity, are being investigated for rapid, non-destructive assessment of pharmaceutical stability [3–5].

In the study, new spectral techniques, i.e., total hemispherical reflectance (THR) and emissivity, were investigated to assess the changes in effervescent tablets containing paracetamol and vitamin C under stressful conditions.

2. MATERIALS AND METHODS

Effervescent tablets were divided into two groups; the first group of tablets was exposed to UV radiation at 26°C for 3 and 7 days in an aging chamber, while the second group was not stressed. For each tablet, the THR parameter across seven spectral bands (from 335 nm to 2500 nm) was assessed with the SOC410 Reflectometer as well as directional (20° and 60° angles) and hemispherical thermal emissivity (1.5–21.0 μm) using an ET100 Emissometer.

3. RESULTS AND DISCUSSION

Hemispheric directional reflectance quantifies the proportion of incoming light reflected by a surface in a specific direction, relative to the total light striking it from above at a defined angle θi. By analysing and aggregating both directly reflected and diffusely scattered light, this measurement enables the calculation of light absorption by the surface.

Reflectance values typically fall within the range of 0 to 1, but, for certain highly reflective or glossy surfaces, reflectance values can exceed 1.

For the spectral ranges, i.e., UV (335-380 nm), visible light ranges (400-540nm, 480-600nm, 590-720nm) and IR light bands (700-1100nm, 1000-1700nm and 1700-2500 nm) THR was lower for tablets exposed to UV radiation for 3 and 7 days by approx. 25-35% compared to non-exposed tablets (Figure 1).

P122

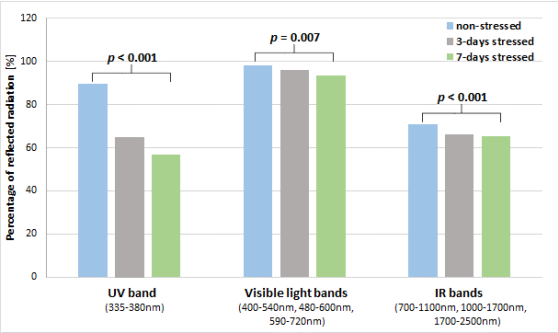

Figure 1. Percentage of reflected radiation for the spectral range of UV, and the cumulative visible and IR ranges

Tablets stressed under UV for 7 days exhibited higher emissivity (εH = 0.934 ± 0.003) across all spectral ranges, compared to non-stressed tablets (εH = 0.920 ± 0.002, $p < 0.001$). Directional emissivity at 60° (ε60) also increased significantly in stressed tablets (0.939 ± 0.004 vs. 0.931 ± 0.004 for non-stressed tablets).

The changes in analyzed spectral parameters may result from photodegradation that concerned tablets under UV radiation. Some specific photoproducts may be formed during such an exposure, although the exact mechanism is not understood.

4. CONCLUSION

UV radiation significantly alters the emissivity and reflectance profiles of effervescent tablets with paracetamol and vitamin C, with stressed tablets showing elevated emissivity and reduced reflectance. The study demonstrated the potential of emissivity and reflectance measurements as rapid, non-destructive tools for pharmaceutical stability testing, offering advantages over conventional destructive methods.

5. REFERENCES

1. Patel SG, Siddaiah M. *Formulation and evaluation of effervescent tablets: a review*. J Drug Deliv Ther. 2018; 8: 296-303.

2. Aslani A, Sharifian T. *Formulation, characterization and physicochemical evaluation of amoxicillin effervescent tablets*. Adv Biomed Res. 2014; 3: 209.

3. Sih SS, Barlow JW. *Emissivity of powder beds*. 6th Solid Free Fabr Symp. 1995; 402-408.

4. Szulc-Musioł B, Duda P, Meisner M, Sarecka-Hujar B. *Hyperspectral and Microtomographic Analyses to Evaluate the Stability of Quercetin and Calcium Effervescent Tablets Exposed to Heat and Ultraviolet Radiation*. Processes. 2024; 12.

5. Błoński B, Wilczyński S, Hartman-Petrycka M, Michalecki Ł. *The Use of Hemispherical Directional Reflectance to Evaluate the Interaction of Food Products with Radiation in the Solar Spectrum*. Foods. 2022; 11(13): 1974.

ACKNOWLEDGMENT

The was funded by the Medical University of Silesia in Katowice (Poland) within the projects: BNW-1-062/N/3/F and BNW-2-042/N/3/Z.

P123

APPLICATION OF SODIUM ALGINATE SPHEROIDS FOR COLON-SPECIFIC DELIVERY OF PREDNISOLONE ACETATE

Aleksandra Ćoškov[1], Nemanja Todorović[1], Doroteja Arbutina[1], Dušica Bosiljčić[2], Jelena Čanji Panić[1], Nataša Milošević[1], Mladena Lalić-Popović[1,3]

[1]Department of Pharmacy, Faculty of Medicine Novi Sad, University of Novi Sad, Serbia
[2]Pharmacy Institution Benu, Galenic Laboratory, Novi Sad, Serbia
[3]Centre for Medical and Pharmaceutical Investigations and Quality Control (CEMPhIC), Faculty of Medicine Novi Sad, University of Novi Sad, Serbia

1. INTRODUCTION

The European Pharmacopoeia defines spheroids as spherical granules with a typical particle size range of 200 μm to 2.8 mm, which may be prepared by any suitable method [1]. Regulatory guidelines favor disintegrating dosage forms with multiple units of pellets over single unit non-disintegrating dosage forms in the development of delayed release products. These formulations exhibit more predictable and generally shorter gastric residence time, and are associated with a lower risk of dose dumping and/or erratic concentration profiles [2].

Inflammatory bowel disease (IBD) is a chronic inflammation of the gastrointestinal tract, with the two main forms being ulcerative colitis and Crohn's disease [3]. IBD is a major health issue, with a 2019 study estimating that approximately 4.9 million people worldwide suffer from the disease [4]. Glucocorticoids are the drugs of choice in the treatment of Crohn's disease, and they also play an important role in managing moderate to severe ulcerative colitis. Achieving site-specific delivery of active pharmaceutical ingredients (API) to the colon remains a significant challenge in pharmaceutical formulation.

The aims of this research are focused on formulation of alginate spheroids with prednisolone acetate for controlled delivery, detailed characterization of the prepared formulations and detection of formulation factors that contribute to release modification.

2. MATERIALS AND METHODS

2.1. Materials

Spheroids were formulated using sodium alginate and calcium chloride anhydrous, with prednisolone acetate as the API. Spheroids were encapsulated in white, size 0 gastro-resistant capsules. Dissolution media were prepared with sodium lauryl sulfate (SLS) and 35% hydrochloric acid. The Spectroquant® Calcium Test was employed for the quantitative determination of calcium ions. Distilled water obtained at the Department of Pharmacy, Faculty of Medicine, Novi Sad, was used in all experiments.

2.2. Methods

Prednisolone acetate spheroids (A1-4) were prepared using 2% and 2.5% sodium alginate solutions and varying needle diameters via extrusion. The mass of spheroids containing 30 mg of API was filled into gastro-resistant capsules, while the control capsule was filled with pure substance. The contents of prednisolone acetate and calcium, loss on drying, flow properties, dissolution tests, *FTIR* and *in silico* predictions of regional absorption were determined. The simulation of gastrointestinal absorption was performed using the GastroPlus™ software (Simulations Plus, Lancaster, CA, USA).

3. RESULTS AND DISCUSSION

The prepared spheroid formulations have a similar composition. The flowability of the prepared formulations, determined by the Compressibility Index and Hausner ratio, is excellent in pharmacopoeial terms.

In vitro dissolution testing showed that during 120 minutes in an acidic medium (0.1 M HCl), none of the formulations released prednisolone acetate (Figure 1), confirming gastro-resistant properties. With a change in the pH of the medium (to 0.5% SLS), the release of prednisolone acetate from gastro-resistant capsules filled with pure prednisolone acetate begins almost immediately, and up to the 150 minutes the active substance is released rapidly, after which the release has a more continuous

course (Figure 1). Statistical analysis showed that the release profiles of prednisolone acetate from the prepared spheroids differ significantly compared to the pure substance. Spheroids with encapsulated prednisolone acetate start releasing the API with a shorter time lag. Formulation A1 showed the fastest release, likely due to the lower sodium alginate concentration (2%) and smaller needle diameter (0.5×25 mm) used in its preparation. Among all formulations (A1–A4), A1 released the full API in the shortest time. Additionally, no statistically significant difference was observed between the release profiles of formulations A2 and A3.

FTIR analysis showed no significant shifts in the main absorption bands of pure prednisolone acetate and no new bands, indicating the absence of chemical interaction between the active substance and the polymer.

The *in silico*–predicted regional absorption indicates no absorption is expected in the stomach or duodenum. The most significant absorption is expected in the ascending colon, which is 47.80 - 52.30% for formulations A1-A4. This is precisely the area of targeted drug action, and the above predictions are extremely positive for the further development of formulations of this type.

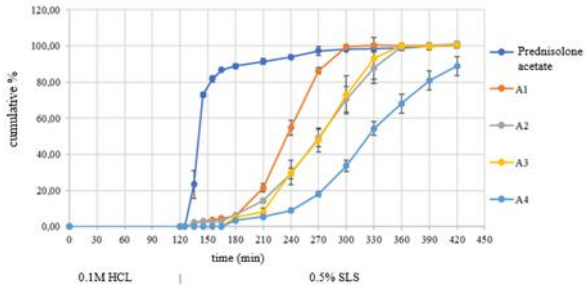

Figure 1. In vitro dissolution rate of prednisolone acetate from formulated spheroids.

4. CONCLUSION

Spheroids derived from sodium alginate have demonstrated the ability to deliver prednisolone acetate in a controlled manner. The most important formulation factors are sodium alginate concentration and needle diameter. Increasing these parameters leads to the formation of particles that are more resistant to simulated conditions in the gastrointestinal tract. Managing these factors during formulation could lead to safer and more effective glucocorticoid therapy.

5. REFERENCES

1. European Directorate for the Quality of Medicines & HealthCare (EDQM). 2019. *European Pharmacopoeia*, 11th edition. Strasbourg: Council of Europe.

2. European Medicines Agency. 2014. *Guideline on quality of oral modified release products*. Available from: https://www.ema.europa.eu/en/documents/scientific-guideline/guideline-quality-oral-modified-release-products_en.pdf (Accessed: 13 May 2025).

3. Anbazhagan, A.N., et al., *Pathophysiology of IBD associated diarrhea*. Tissue Barriers, 2018. 6(2): e1463897.

4. Wang, W.R., et al, *Global, regional and national burden of inflammatory bowel disease in 204 countries and territories from 1990 to 2019: a systematic analysis based on the Global Burden of Disease Study 2019*. BMJ Open, 2023. 13(3): e065186.

ACKNOWLEDGMENT

This research was supported by the Ministry of Science, Technological Development and Innovation of the Republic of Serbia (project 451-03-136/2025-03/200114).